THE HONG KONG
POLYTECHNIC UNIVERSITY
香港理工大學
Pao Yue-kong Library
包玉剛圖書館

Copyright Undertaking

This thesis is protected by copyright, with all rights reserved.

By reading and using the thesis, the reader understands and agrees to the following terms:

1. The reader will abide by the rules and legal ordinances governing copyright regarding the use of the thesis.
2. The reader will use the thesis for the purpose of research or private study only and not for distribution or further reproduction or any other purpose.
3. The reader agrees to indemnify and hold the University harmless from and against any loss, damage, cost, liability or expenses arising from copyright infringement or unauthorized usage.

IMPORTANT

If you have reasons to believe that any materials in this thesis are deemed not suitable to be distributed in this form, or a copyright owner having difficulty with the material being included in our database, please contact lbsys@polyu.edu.hk providing details. The Library will look into your claim and consider taking remedial action upon receipt of the written requests.

Pao Yue-kong Library, The Hong Kong Polytechnic University, Hung Hom, Kowloon, Hong Kong

http://www.lib.polyu.edu.hk

LONG-TERM PERFORMANCE OF FRP BARS AND FRP-REINFORCED SEAWATER SEA-SAND CONCRETE BEAMS IN REAL MARINE ENVIRONMENTS

ZHANG JUNJIE

PhD

The Hong Kong Polytechnic University

2025

The Hong Kong Polytechnic University

Department of Civil and Environmental Engineering

Long-Term Performance Of Frp Bars And Frp-Reinforced Seawater Sea-Sand Concrete Beams In Real Marine Environments

ZHANG Junjie

A Thesis Submitted in Partial Fulfilment of the Requirements for the Degree of Doctor of Philosophy

June 2025

CERTIFICATE OF ORIGINALITY

I hereby declare that this thesis is my own work and that, to the best of my knowledge and belief, it reproduces no material previously published or written, nor material that has been accepted for the award of any other degree or diploma, except where due acknowledgement has been made in the text.

_____ (Signed)

ZHANG Junjie (Name of student)

To My Family

ABSTRACT

As coastal cities increasingly rely on resilient marine infrastructure to address the challenges posed by climate change and rising sea levels, the demand for sustainable construction materials has become more urgent. However, the construction industry faces significant challenges due to the scarcity of river sand and freshwater resources, as well as the issue of chloride-induced steel corrosion in concrete. In this context, a new type of reinforced concrete structure, composed of corrosion-resistant fibre-reinforced polymer (FRP) bars and seawater sea-sand concrete (SSC) (termed FRP-SSC structure) has been deemed as a promising solution due to its environmental and economic benefits. While existing accelerated aging test data on the durability of FRP bars, FRP bars embedded in concrete, and SSC suggests that FRP-SSC structures can be expected to be highly durable in marine environments, there remains a critical need to investigate their long-term performance and deterioration mechanisms under real-world conditions.

Against this background, this thesis presents an in-depth study aimed at the investigation of long-term performance of FRP bars and FRP-reinforced SSC (FRP-SSC) beams after prolonged exposure to real marine environments. The PhD project consists of three parts, each addressing specific aspects of the durability performance of glass FRP (GFRP) bars, GFRP bar-to-SSC bonded joints, and GFRP-SSC beams.

Following a comprehensive review and systematic analysis of existing research on the durability of FRP bars, FRP bar-to-concrete bonded joints, and FRP-reinforced concrete beams (based on three newly assembled databases containing over 15200 specimens),

the first part of this thesis investigated the residual tensile properties of two batches of GFRP bars after exposure to different marine environmental conditions, including atmospheric, splash, tidal, and underwater zones, for up to four years. The results indicated that the GFRP bars conditioned in tidal and underwater environments exhibited a significant decrease in tensile strength compared to those exposed to atmospheric and splash environments. Besides, the bar size effect on the long-term tensile performance of GFRP bars was revealed. Based on these experimental findings, along with a critical review and assessment of existing models, a refined prediction model that incorporates a time-dependent correction factor was proposed, demonstrating enhanced accuracy in predicting their long-term tensile performance of GFRP bars under tidal exposure.

The second part of this thesis focused on the bond durability between GFRP bars and SSC. Direct pullout tests were conducted on two series of GFRP bar-to-SSC bonded joints exposed to various marine environmental conditions over a period of four years. The test results revealed that the failure mode, shapes of bond stress-slip curves and bond strength of the specimens exhibited minimal changes after prolonged field exposure. However, specimens subjected to tidal conditions experienced a notable reduction in bond stiffness, with retention decreasing to approximately 64% after four years. Additionally, a time-dependent bond stress-slip model for GFRP bars in SSC was developed based on the modified BPE (mBPE) model, and its reliability was validated against the experimental data, showing satisfactory agreement and predictive capability.

In the final part of this thesis, the flexural performance of two series of GFRP-SSC beams was experimentally investigated under four-point bending after field exposure to different marine environments. The results showed that long-term field exposure did

not affect the failure modes and load-deflection behavior of the specimens, regardless of sustained loading conditions. While specimens exposed to atmospheric and splash environments exhibited no significant changes in flexural capacity over the exposure period, those subjected to tidal conditions exhibited a noticeable reduction in load carrying capacity, with retention stabilizing at approximately 90% after four years, accompanied by increased crack widths and decreased crack numbers. These changes were attributed primarily to the deterioration of bond stiffness between GFRP bars and SSC. To simulate the flexural behavior of these beams, a finite element (FE) model accounting for the deterioration of bond stiffness between FRP bars and SSC was developed, which demonstrated the capability to accurately predict the long-term flexural performance of GFRP-SSC beams under tidal conditions, particularly in terms of load-deflection responses and crack patterns.

LIST OF PUBLICATIONS

Refereed journal papers from the dissertation:

1. **Zhang, J. J.**, Yang, J. L.* and Yu, T.* (2026) "Durability of FRP bars and FRP-reinforced concrete beams: A critical review of accelerated aging tests and performance insights." *Composites Part B: Engineering.* 308: 112965.

Other referred journal papers during Ph.D. Study:

1. Chen, G. M., Dan, T. S., Ma, X. Z., **Zhang, J. J.***, and Xiong, Y. (2025). "Fire resistance and residual compressive behavior of FRP-concrete-steel double-skin tubular columns with ECC or FRP grid-reinforced ECC layers". *Journal of Composites for Construction*. (Accepted)

2. Chen, G. M., Gan, R. X., **Zhang, J. J.***, Hou, W., and Zhang, Y. X.* (2025). "FRP spiral strip-confined concrete circular columns with ECC jackets: Fire resistance and post-fire compressive behavior". *Engineering Structures*. 337: 120503.

3. Chen, G. M., Fu, M. Q., **Zhang, J. J.***, Lin, G.*, Chen, J. P., and Jiang, T. (2023). "FRP spiral strip-confined concrete columns: Stress-strain behavior and size effect." *Structures*. 57: 105223.

4. Zhang, L. W., **Zhang, J. J.**, Chen, G. M.* and Lin, G.* (2023). "Flexural behavior of hybrid FRP-recycled aggregate concrete-steel hollow beams." *Journal of Constructional Steel Research*. 200, 107650.

5. Wu, B., Yang, X., **Zhang, J. J.**, Chen, G. M.* and Zhao, X. Y. (2022). "Recycled lump concrete-filled FRP tubular columns: Axial compressive behavior and size effects." *Construction and Building Materials*. 352, 129000.

Conference papers:

1. **Zhang, J. J.**, Jiang, C., Zhang, Y. W., Yu, T.* and Teng, J. G.* (2024) "Long-term bond performance of GFRP bars in seawater sea-sand concrete: Field exposure tests." *The 10th Conference of Asian Concrete Federation (ACF)*, 15-18 August, Ulaanbaatar, Mongolia (Abstract).

2. **Zhang, J. J.** and Yu, T.* (2024) "On developing a time-dependent bond stress-slip model for GFRP bars in seawater sea-sand concrete." *9th Asia-Pacific Conference on Fiber Reinforced Polymers in Structures (APFIS-2024)*, 8-11 December, Adelaide, Australia (Abstract).

3. Lin, G.* and **Zhang, J. J.** (2023). "Concrete Filled FRP Tubular Columns Containing Recycled Concrete Lumps: Current Research and Future Work." *International Symposium of the International Federation for Structural Concrete (fib Symposium 2023)*, 5-7 June, Istanbul, Turkey. 350: 1168-1176.

ACKNOWLEDGEMENTS

First and foremost, I would like to express my deepest appreciation to my chief supervisor, Prof. Tao Yu, whose generous support, enlightening guidance, rigorous training and advanced expertise have been invaluable in shaping my research and academic growth. I truly appreciate his encouragement and all his contributions to make my PhD journey enriching and joyful.

My heartfelt gratitude also goes to my co-supervisors, Prof. Guang-Ming Chen, from South China University of Technology, and Dr. Guan Lin, from Southern University of Science and Technology, for their continues supports and guidance before and during my PhD study.

I extend my thanks to many past and current colleagues at The Hong Kong Polytechnic University, who offered tremendous help in many ways during my PhD study. In particular, I wish to express my sincere thanks to Dr. Jun-Long Yang for his valuable suggestions and constructive comments on my research, as well as his assistance in revising part of my thesis, which have greatly enhanced the quality of my work. I would also like to express my gratitude to all those who made valuable contributions to various aspects of the field exposure tests presented in this thesis, including Dr. Cheng Jiang, Dr. Yi-Wen Zhang, Dr. Jun-Jie Zeng, Dr. Zhi-Hao Hao, Ms. Yu-Yi Ye and Mr. Zhen-Xiong Wang. In particular, I am especially grateful to Dr. Cheng Jiang and Dr. Yi-Wen Zhang for their significant contributions, as detailed in Chapter 3.

Thanks also go to Dr. Chun-Wa Chan, Dr. Yu Xiang, Dr. Kai-Cheng Liu, Dr. Le Huang, Dr. Zhi-Yu Xia, Mr. Po-Chang Liu, Mr. Dong Han, Mr. Jia-Jie Cai, Mr. Rui-Long Li,

Mr. Jia-Ming Zhu, Ms. Chu-Ying Cui, Ms. Yan-Ran Meng, Mr. Yun-Hong Luo, Ms. Xi Li, Mr. Pan-Deng Zheng, Mr. Ze-Yu Gao, Ms. Yi-Fei Wang, Mr. Zheng-Ze Liu, Dr. Zhi-Hang Xue, Dr. Yan-Qin, Dr. Ran Deng and Mr. Zhe Zhang, whose collaboration and companionship have made this journey not only productive but also enjoyable.

The experimental investigations presented in Chapters 3, 5 and 6 were largely carried out at Guangdong University of Technology. Many thanks must go to Dr. Jun-Jie Zeng, Dr. Jie-Kai Zhou, Prof. Yong-Chang Guo, Mr. Xiao-Dong Mo, Mr. Gen-Quan Zhong, and Mr. Zhen-Xiong Wang for their assistance and support throughout my research.

I gratefully acknowledge The Hong Kong Polytechnic University for offering the research facilities and financial support during my PhD study.

Last but certainly not least, I am deeply appreciative of my family, whose love, understanding, support and encouragement have been a constant source of strength and motivation to overcome the challenges throughout my PhD journey.

CONTENTS

CERTIFICATE OF ORIGINALITY ..... **I**

ABSTRACT ..... **III**

LIST OF PUBLICATIONS ..... **VI**

ACKNOWLEDGEMENTS ..... **VIII**

CONTENTS ..... **X**

LIST OF TABLES ..... **XV**

LIST OF FIGURES ..... **XVIII**

LIST OF ACRONYMS ..... **XXV**

NOTATION ..... **XXVIII**

CHAPTER 1 INTRODUCTION **1**

1.1 BACKGROUND 1

1.2 DURABILITY OF FRP BARS AND FRP-REINFORCED CONCRETE BEAMS 4

1.3 OBJECTIVES AND LAYOUT OF THE THESIS 6

CHAPTER 2 LITERATURE REVIEW **10**

2.1 INTRODUCTION 10

2.2. EXPERIMENTAL DATABASES 16

2.3 BARE FRP BARS 21

2.3.1 Single Environmental Effect 21

2.3.2 Coupled Effects of Environmental and Loading Conditions 36

2.4 FRP BARS EMBEDDED IN CONCRETE 39

2.4.1 Tensile Strength, Interlaminar Shear Strength and Transverse Shear Strength....41
2.4.2 Bond Strength....45
2.4.3 Relationship Between the Durability of ILSS and BS of FRP Bars....52
2.5 FRP-REINFORCED CONCRETE BEAMS....54
2.5.1 Saline Condition....54
2.5.2 Coupled Effects of Environmental and Loading Conditions....60
2.5.3 Other Conditions....66
2.6 CONCLUDING REMARKS....71
CHAPTER 3 LONG-TERM TENSILE PERFORMANCE OF GFRP BARS IN REAL MARINE ENVIRONMENTS....74
3.1 INTRODUCTION....74
3.2 EXPERIMENTAL PROGRAM....78
3.2.1 Materials....78
3.2.2 Field Exposure Stations....79
3.2.3 Specimen Preparation and Test Method....83
3.3 RESULTS AND DISCUSSION....86
3.3.1 Surface Characteristic Observations....86
3.3.2 Failure Modes....87
3.3.3 Variations in Tensile Properties of GFRP Bars....89
3.4 CONCLUSIONS....99
CHAPTER 4 PREDICTION MODEL FOR DURABILITY OF FRP BARS....101
4.1 INTRODUCTION....101
4.2 EXISTING PREDICTION MODELS FOR DURABILITY OF FRP BARS....102
4.2.1 Empirical Models Based on Arrhenius Theory....102

4.2.2 *fib* Bulletin 40 (2007) Model 105
4.2.3 Prediction Models Based on Environmental Reduction Factor (ERF) 107
4.3 EXPERIMENTAL DATABASE 109
4.3.1 Bare GFRP Bars 110
4.3.2 Concrete-Embedded Unstressed GFRP Bars 110
4.3.3 Concrete-Embedded Stressed GFRP Bars 111
4.4 PERFORMANCE OF EXISTING MODELS FOR DURABILITY OF FRP BARS 113
4.4.1 Arrhenius Empirical Model 113
4.4.2 *fib* Bulletin 40 (2007) Model 126
4.4.3 Huang and Aboutaha's (2010) Model 141
4.4.4 Comparison Between Existing Models 151
4.5 PROPOSED PREDICTION MODEL 154
4.6 CONCLUSIONS 159
CHAPTER 5 LONG-TERM BOND PERFORMANCE BETWEEN GFRP BARS AND SEAWATER SEA-SAND CONCRETE IN REAL MARINE ENVIRONMENTS 162
5.1 INTRODUCTION 162
5.2 EXPERIMENTAL PROGRAM 164
5.2.1 Materials 164
5.2.2 Design and Preparation of Pullout Specimens 166
5.2.3 Field Exposure Conditions 168
5.2.4 Test Procedure 170
5.3 RESULTS AND DISCUSSION 171

5.3.1 Visual Observations 171
5.3.2 Failure Modes 172
5.3.3 Bond Stress-Slip Curves 174
5.3.4 Bond Strength 182
5.3.5 Bond Stiffness 184
5.4 TIME-DEPENDENT BOND STRESS-SLIP MODEL 186
5.5 CONCLUSIONS 192
CHAPTER 6 LONG-TERM FLEXURAL PERFORMANCE OF GFRP-REINFORCED SEAWATER SEA-SAND CONCRETE BEAMS IN REAL MARINE ENVIRONMENTS 194
6.1 INTRODUCTION 194
6.2 EXPERIMENTAL PROGRAM 196
6.2.1 Materials 196
6.2.2 Design and Preparation of FRP-SSC Beam Specimens 196
6.2.3 Sustained Load 198
6.2.4 Field Exposure Conditions 199
6.2.5 Instrumentation and Test Set-Up 201
6.3 RESULTS AND DISCUSSION 202
6.3.1 Appearance Observations 202
6.3.2 Long-Term Deflections of FRP-SSC Beams with Sustained Load 203
6.3.3 Failure Modes 207
6.3.4 Load-Midspan Deflection Curves 212
6.3.5 Cracking Load and Flexural Capacity 216
6.3.6 Crack Width and Distribution 224
6.4 CONCLUSIONS 226

CHAPTER 7 NUMERICAL SIMULATION OF GFRP-REINFORCED SEAWATER SEA-SAND CONCRETE BEAMS SUBJECTED TO MARINE ENVIRONMENTS 228

7.1 INTRODUCTION 228

7.2 FINITE ELEMENT MODELING 229

7.2.1 General 229

7.2.2 Material Properties 230

7.2.3 Bond Behavior Between FRP Bars and SSC 232

7.2.4 Numerical Results 234

7.3 VERIFICATION OF FE MODEL FOR LONG-TERM FLEXURAL PERFORMANCE OF FRP-SSC BEAMS 236

7.4 CONCLUSIONS 242

CHAPTER 8 CONCLUSIONS 243

8.1 INTRODUCTION 243

8.2 LONG-TERM TENSILE PERFORMANCE OF GFRP BARS 244

8.3 LONG-TERM BOND PERFORMANCE OF GFRP BARS IN SEAWATER SEA-SAND CONCRETE 245

8.4 LONG-TERM FLEXURAL PERFORMANCE OF GFRP-REINFORCED SEAWATER SEA-SAND CONCRETE BEAMS 246

8.5 FUTURE RESEARCH 248

REFERENCES 251

APPENDIX A DATABASE FOR ACCELERATED AGING TESTS 279

APPENDIX B DATABASE FOR FIELD EXPOSURE TESTS 505

LIST OF TABLES

Table 3.1 Plan of field exposure tests 77

Table 3.2 Physical and mechanical properties of GFRP bars provided by manufacturer 79

Table 3.3 Environmental characteristics of different exposure zones 81

Table 3.4 Test matrix of GFRP bar specimens 84

Table 3.5 Tensile properties of 6-mm GFRP bars exposed at Station I 96

Table 3.6 Tensile properties of 10-mm GFRP bars exposed at Station I 97

Table 3.7 Tensile properties of 10-mm GFRP bars exposed at Station II 98

Table 4.1 Influencing parameters adopted in *fib* Bulletin 40 (2007) 106

Table 4.2 Correction factors (CFs) required for long-term predictions using different types of aging tests [Dong et al. (2017b)] 109

Table 4.3 FET database for model assessment 112

Table 4.4 Coefficients of regression equations based on Arrhenius empirical model for bare GFRP bars 115

Table 4.5 Coefficients of regression equations based on Arrhenius empirical model for concrete-embedded unstressed GFRP bars 121

Table 4.6 Coefficients of regression equations based on Arrhenius empirical model for concrete-embedded stressed GFRP bars 124

Table 4.7 Coefficients and predicted results based on *fib* Bulletin 40 (2007) model for bare GFRP bars 128

Table 4.8 Coefficients and predicted results based on *fib* Bulletin 40 (2007) model for concrete-embedded unstressed GFRP bars 135

Table 4.9 Coefficients and predicted results based on *fib* Bulletin 40 (2007) model for

concrete-embedded stressed GFRP bars 138
Table 4.10 Coefficients and predicted results based on Huang and Aboutaha's (2010) model for bare GFRP bars 143
Table 4.11 Coefficients and predicted results based on Huang and Aboutaha's (2010) model for concrete-embedded unstressed GFRP bars 148
Table 4.12 Coefficients and predicted results based on Huang and Aboutaha's (2010) model for concrete-embedded stressed GFRP bars 150
Table 4.13 Assessment of tensile strength retention ratio (R_{pre}/R_{test}) 152
Table 4.14 Key information of bare GFRP bars used in the selected studies 156
Table 4.15 Comparison between the test and predicted results 157
Table 5.1 Mix proportions of SSC 166
Table 5.2 Test matrix of pullout specimens 169
Table 5.3 Pullout test results of Series I specimens 180
Table 5.4 Pullout test results of Series II specimens 181
Table 5.5 Parameters of prediction model for specimens in T-I zone 190
Table 6.1 Physical and mechanical properties of GFRP bars provided by manufacturer . 196
Table 6.2 Test matrix of beam specimens 200
Table 6.3 Key test results of Series I specimens (w/o sustained load) 209
Table 6.4 Key test results of Series II specimens (w/ sustained load) 211
Table 6.5 Compressive strength of SSC cores drilled from beam specimens 220
Table 6.6 Flexural stiffness of Series I specimens (w/o sustained load) 222
Table 7.1 Comparison between the test and predicted results 239
Table A1 AAT database for tensile properties of FRP bars 280
Table A2 AAT database for shear properties of FRP bars 380
Table A3 AAT database for flexural properties of FRP bars 455

Table B1 AAT database for bond properties of FRP bars in concrete 465

Table C1 AAT database for flexural behavior of FRP-reinforced concrete beams.....497

Table D1 FET database for tensile properties of FRP bars 506

Table D2 FET database for shear properties of FRP bars 509

Table D3 FET database for flexural properties of FRP bars 512

Table E1 FET database for bond properties of FRP bars in concrete.....513

Table F1 FET database for flexural behavior of FRP-reinforced concrete beams 514

LIST OF FIGURES

Fig. 1.1 Corrosion of Steel Reinforcement (extracted from https://gharpedia.com/blog/causes-of-corrosion-of-reinforcement-steel/) 2

Fig. 1.2 Four types of FRP bars (Dong and Wu 2019) 2

Fig. 1.3 Deterioration mechanism of FRP-reinforced concrete beams under saline conditions (Chang et al. 2022) 5

Fig. 2.1 Distribution of test parameters in three assembled databases 20

Fig. 2.2 Effect of alkaline concentration on the durability of bare GFRP bars..... 24

Fig. 2.3 Effect of fiber type on the durability of bare FRP bars under alkaline conditions 26

Fig. 2.4 Effect of diameter on the durability of bare GFRP bars under alkaline conditions 28

Fig. 2.5 Effect of saline solution on the durability of bare GFRP bars 30

Fig. 2.6 Effect of fiber type on the durability of bare FRP bars under saline conditions 31

Fig. 2.7 Effect of water on the durability of bare GFRP bars 33

Fig. 2.8 Effect of fiber type on the durability of bare FRP bars under water conditions 34

Fig. 2.9 Effects of WD cycles, FT cycles, acid solution immersion and UV radiation on the durability of bare GFRP bars 35

Fig. 2.10 Coupled effects of environmental and loading conditions on the durability of bare FRP bars 37

Fig. 2.11 Tensile strength retentions of bare FRP bars with different stress levels under the same alkaline condition..... 38

Fig. 2.12 Comparison of mechanical properties between bare FRP bars and concrete-embedded FRP bars under the same condition 40
Fig. 2.13 Comparison of mechanical properties between bare and concrete-embedded FRP bars immersed in different solutions 43
Fig. 2.14 Coupled effects of environmental and loading conditions on the durability of concrete-embedded FRP bars 44
Fig. 2.15 Comparison of tensile strength retentions for concrete-embedded FRP bars with different stress levels 45
Fig. 2.16 Effect of surface treatment on the durability of bond strength of GFRP bars under saline conditions 47
Fig. 2.17 Effects of fiber and resin types on the durability of bond strength of ribbed FRP bars under saline conditions 48
Fig. 2.18 Effect of alkaline concentration on the durability of bond strength of GFRP bars under alkaline conditions 49
Fig. 2.19 Effect of fiber type on the durability of bond strength of FRP bars under alkaline conditions 50
Fig. 2.20 Effect of surface treatment on the durability of bond strength of GFRP bars under water conditions 51
Fig. 2.21 Effect of concrete type on the durability of bond strength of GFRP bars 52
Fig. 2.22 Comparison between interlaminar shear strength of bare FRP bars and their corresponding bond strength under alkaline conditions 53
Fig. 2.23 Comparison between interlaminar shear strength of bare FRP bars and their corresponding bond strength under saline conditions 54
Fig. 2.24 Comparison between interlaminar shear strength of concrete-embedded FRP bars and their corresponding bond strength under alkaline and saline conditions

..... 54
Fig. 2.25 Failure modes of FRP-reinforced SWSSC beams under saline conditions (Dong et al. 2018c, 2020; Su et al. 2022) 56
Fig. 2.26 Load-deflection curves of FRP-reinforced concrete beams after saline conditions 56
Fig. 2.27 Ultimate load and bond strength retentions 57
Fig. 2.28 Ultimate load and corresponding deflection retentions of FRP-reinforced concrete beams under saline conditions 59
Fig. 2.29 Deterioration mechanism of FRP-reinforced concrete beams under saline conditions (Chang et al. 2022) 60
Fig. 2.30 Load-deflection curves of FRP-reinforced concrete beams with sustained load 61
Fig. 2.31 Load-deflection curves of FRP-reinforced concrete beams with sustained load after water solution conditioning 62
Fig. 2.32 Load-deflection curves of FRP-reinforced concrete beams with sustained load in saline solution 65
Fig. 2.33 Ultimate load retentions of conditioned FRP-reinforced concrete beams with sustained load 66
Fig. 2. 34 Load-deflection curves of FRP-reinforced concrete beams under water immersion. 68
Fig. 2.35 Ultimate load and concrete strength retentions under water immersion 69
Fig. 2.36 Load-deflection curves of FRP reinforced concrete beams under freeze-thaw cycling conditions 71
Fig. 3.1 Concrete casting for field exposure tests 77
Fig. 3.2 Close-up view of different batches of GFPR bars 78

Fig. 3.3 Field exposure stations 80
Fig. 3.4 Variations of temperature and relative humidity in Xiangzhou (Zhuhai City) and Xiashan (Zhanjiang City) districts during exposure period (obtained from https://www.qweather.com/) 81
Fig. 3.5 Specimen preparation and test set-up 85
Fig. 3.6 Surface characteristics of GFRP bars exposed in different exposure zones 87
Fig. 3.7 Failure modes of GFRP bars exposed in different exposure zones 89
Fig. 3.8 Tensile strength variations of GFRP bars in different field exposure conditions 92
Fig. 3.9 Elastic modulus variations of GFRP bars in different exposure conditions 94
Fig. 3.10 Comparison of tensile properties of different-sized GFRP bars 95
Fig. 4.1 Relationship between RH correction factor and relative humidity (adapted from Huang and Aboutaha 2010) 108
Fig. 4.2 Comparison between FET result and prediction curves based on Arrhenius empirical model for bare GFRP bars 120
Fig. 4.3 Comparison between FET results and prediction curves based on Arrhenius empirical model for concrete-embedded unstressed GFRP bars 123
Fig. 4.4 Comparison between FET results and prediction curves based on Arrhenius empirical model for concrete-embedded stressed GFRP bars 126
Fig. 4.5 Tensile strength retention curves based on *fib* Bulletin 40 (2007) model for bare GFRP bars 132
Fig. 4.6 Comparison between FET results and predictions based on *fib* Bulletin 40 (2007) model for bare GFRP bars 133
Fig. 4.7 Tensile strength retention curves based on *fib* Bulletin 40 (2007) model for concrete-embedded unstressed GFRP bars 136

Fig. 4.8 Comparison between FET results and predictions based on *fib* Bulletin 40 (2007) model for concrete-embedded unstressed GFRP bars 136
Fig. 4.9 Tensile strength retention curves based on *fib* Bulletin 40 (2007) model for concrete-embedded stressed GFRP bars 140
Fig. 4.10 Comparison between FET results and predictions based on *fib* Bulletin 40 (2007) model for concrete-embedded stressed GFRP bars 140
Fig. 4.11 Comparison between FET results and predictions based on Huang and Aboutaha's (2010) model for bare GFRP bars 146
Fig. 4.12 Comparison between FET results and predictions based on Huang and Aboutaha's (2010) model for concrete-embedded unstressed GFRP bars 149
Fig. 4.13 Comparison between FET results and predictions based on Huang and Aboutaha's (2010) model for concrete-embedded stressed GFRP bars 151
Fig. 4.14 Tensile strength retention ratio by different prediction models for GFRP bars 154
Fig. 4.15 Correction factor αT value versus exposure time 159
Fig. 4.16 Comparison between FET results and model predictions 159
Fig. 5.1 Two batches of GFRP bars used in this chapter 164
Fig. 5.2 Grading curve of sea-sand 165
Fig. 5.3 Schematic diagram and preparation of pullout specimens (unit: mm) 167
Fig. 5.4 Specimens in different exposure zones 169
Fig. 5.5 Test set-up 170
Fig. 5.6 Appearance characteristics of specimens exposed in different zones 172
Fig. 5.7 Typical bond failure surface 173
Fig. 5.8 Bond stress-slip curves of pullout specimens 179
Fig. 5.9 Bond strength variations of pullout specimens in different exposure conditions

.....183
Fig. 5.10 Bond stiffness variations of pullout specimens in different exposure conditions 186
Fig. 5.11 Curve fittings of specimens subjected to tidal condition 189
Fig. 5.12 Characteristic curve of the proposed time-dependent bond stress-slip model 189
Fig. 5.13 Comparison between predicted and test bond stress-slip curves 191
Fig. 6.1 Details and preparation of FRP-SSC beam specimens 198
Fig. 6.2 Sustained loading system 199
Fig. 6.3 Specimens exposed in splash zone (S-I) 200
Fig. 6.4 Test set-up (unit: mm) 201
Fig. 6.5 Visual appearance of field-exposed specimens 203
Fig. 6.6 Measuring method for residual deflection 204
Fig. 6.7 Long-term deflections of FRP-SSC beams with sustained load 206
Fig. 6.8 Failure modes 208
Fig. 6.9 Load-midspan deflection curves of Series I specimens 214
Fig. 6.10 Load-midspan deflection curves of Series II specimens 215
Fig. 6.11 Changes in cracking load of Series I specimens 216
Fig. 6.12 Effect of environmental exposure on flexural capacity 218
Fig. 6.13 Preparation procedures for SSC cores 219
Fig. 6.14 Comparison between the load carrying capacity of Series I specimens and the compressive strength of SSC cores 219
Fig. 6.15 Changes in flexural stiffness of Series I specimens 221
Fig. 6.16 Comparison between retention of flexural stiffness and bond stiffness 223
Fig. 6.17 Effect of sustained load on flexural capacity 224

Fig. 6.18 Load-maximum crack width curves 225
Fig. 6.19 Crack distribution of exposed specimens (left: 24-month; right: 48-month) 225
Fig. 7.1 Comparison of experimental and numerical load-midspan deflection curves for representative specimens 235
Fig. 7.2 Comparison of experimental and numerical crack patterns for a selected specimen 236
Fig. 7.3 Load-midspan deflection curves for specimens with different exposure durations: test results versus numerical predictions..... 238
Fig. 7.4 Comparison between predicted and test results: ultimate load and the corresponding mid-span deflection..... 239
Fig. 7.5 Comparisons between predicted and experimental crack patterns for FRP-SSC beam specimens with exposure durations of 24 and 48 months..... 241

LIST OF ACRONYMS

2D	two-dimensional
AAE	average absolute error
AAT	accelerated aging tests
AE	abrasion and erosion
AFRP	aramid fiber-reinforced polymer
BFRP	basalt fiber-reinforced polymer
BS	bond strength
CDP	concrete damage plasticity
CE	concrete-embedded
CF	correction factor
CFRP	carbon fiber-reinforced polymer
COV	coefficient of variation
DIC	digital image correlation
DL	design life
EP	epoxy resin
ERF	environmental reduction factor
FE	finite element
FET	field exposure tests
FM	flexural elastic modulus
FRP	fiber-reinforced polymer
FS	flexural strength
FT	freeze-thaw

GFRP	glass fiber-reinforced polymer
GRC	glass fiber-reinforced concrete
HH	high humidity
HS	high salinity
HSC	high-strength concrete
HT	high temperatures
ILSS	interlaminar shear strength
IMMR	immersion
LT	low temperature
LVDT	linear variable differential transformer
MARH	mean annual relative humidity
MAT	mean annual temperature
MMRH	mean monthly relative humidity
MMT	mean monthly temperature
NC	normal concrete
OG	organic growth
PE	polyester resin
RH	relative humidity
RT	room temperature
SD	standard deviation
SL	sustained load
SLS	serviceability limit state
SSC	seawater sea-sand concrete; sea-sand concrete in Chapter 2
SWC	seawater concrete
SWSSC	seawater sea-sand concrete in Chapters 2 and 4

TF	temperature fluctuations
TM	tensile elastic modulus
TS	tensile strength
TSF	time shift factor
TSS	transverse shear strength
ULS	ultimate limit state
UV	ultraviolet radiation
VE	vinylester resin
WD	wet-dry
WP	wave pressure

NOTATION

A	constant of material and degradation process
A_f	nominal cross-sectional area of an FRP bar
a	fitting parameter in Eqs. (4.4) and (4.5)
a_1	fitting parameter in Eq. (5.7b)
a_2	fitting parameter in Eq. (5.8b)
b	fitting parameter in Eqs. (4.4) and (4.5)
b_1	fitting parameter in Eq. (5.7b)
b_2	fitting parameter in Eq. (5.8b)
C	solution ion concentration
c_1	constant in Eq. (7.3a)
c_2	fitting parameter in Eq. (5.8b); constant in Eq. (7.3a)
D	diffusion coefficient
d_a	maximum aggregate size
d_b	diameter of an FRP bar; nominal diameter of an FRP bar in Eq. (5.1)
E_a	activation energy of material
E_c	elastic modulus of concrete
E_f	tensile elastic modulus of an FRP bar
f_c	compressive strength of concrete
f_{fk0}	characteristic value of tensile strength obtained from short-term tests
$f_{fk1000h}$	characteristic value of tensile strength after 1000-hour exposure
f_t	tensile strength of concrete
f_u	ultimate tensile stress of an FRP bar

G_F	fracture energy
K	simplified bond stiffness
K_0	initial bond stiffness
K_b	bond stiffness
k	degradation rate
k_0, k_1	degradation rates at temperatures of T_0 and T_1
L_c	distance between the end of embedded bar and the point of attachment of the two loaded end LVDTs
l_a	actual bonded length
M_u	ultimate moment of an FRP-reinforced concrete beams
N	number of data points
n_H	correction factor for relative humidity
n_{mo}	exponent for moisture influence
n_{SL}	exponent for service life influence
n_T	exponent for temperature influence
n_d	exponent for bar diameter influence
P	applied pullout force
P_{cr}	cracking load of an FRP-SSC beam
P_{fp}	first peak load of an FRP-SSC beam
P_{max}	maximum load of an FRP-SSC beam
P_{pre}	predicted ultimate load of an FRP-SSC beam
P_{test}	test ultimate load of an FRP-SSC beam
p	fitting parameter in Eq. (5.5)
R	universal gas constant
R^2	coefficient of determination

R_{10} standard reduction of tensile strength in percent per logarithmic decade

$R_{pre,i}$ predicted value for the *i*th data point

$R_{test,i}$ test value for the *i*th data point

r_0 radius of an FRP bar

s_L average readings obtained by the two LVDTs at the loaded end

s_c elastic elongation of an FRP bar

s_l relative slip at the loaded end

s_m loaded end slip at ultimate bond strength

s_{m0} initial loaded end slip at ultimate bond strength

s_r slip corresponding to residual bond strength

T temperature

T_{AT} mean annual temperature

T_g glass transition temperature

T_{MT} mean monthly temperature

t aging time

t_0, t_1 time required for the mechanical property to reach a given retention value at temperatures of T_0 and T_1

w_{cr} crack opening displacement corresponding to the status of the complete release of tensile stress or fracture energy

w_t crack opening displacement

Y retention of FRP mechanical property

Y_K retention of bond stiffness after field exposure

Y_s retention of loaded end slip at ultimate bond strength after field exposure

Y_∞ retention of FRP mechanical property at aging time of infinity

α correction factor for concrete-wrap; fitting parameter in Eq. (5.4); an

	experimentally obtained coefficient standing for the initial tangent modulus in Eq. (7.2)
α_T	time-dependent correction factor for additional effects of tidal conditions
δ_{cr}	midspan deflection at cracking load of an FRP-SSC beam
δ_{fp}	midspan deflection at first peak load of an FRP-SSC beam
δ_{max}	midspan deflection at maximum load of an FRP-SSC beam
δ_{pre}	predicted midspan deflection at ultimate load of an FRP-SSC beam
δ_{test}	test midspan deflection at ultimate load of an FRP-SSC beam
ε	compressive strain of concrete
ε_p	experimentally obtained compressive strain corresponding to compressive strength of concrete
η	correction factor for temperature fluctuation
η_E	environmental strength reduction factor in Eq. (4.11)
$\eta_{E,pre}$	predicted tensile strength retention
$\eta_{E,test}$	test tensile strength retention
$\eta_{env,t}$	environmental strength reduction factor in Eq. (4.9)
ρ	slope of Arrhenius regression line of the single logarithmic model
σ	compressive stress of concrete
σ_p	experimentally obtained compressive strength of concrete
σ_t	tensile stress normal to the crack direction
τ	fitting parameter in Eqs. (4.6) and (4.7); average bond stress in Eq. (5.1)
τ_0	bond strength obtained from control specimens
τ_{max}	ultimate bond strength
τ_r	residual bond strength

Δ_1 tensile strength reduction after 1-year experimental exposure

CHAPTER 1
INTRODUCTION

1.1 BACKGROUND

Marine infrastructure plays a crucial role in the development and sustainability of many coastal cities worldwide. As global warming leads to predicted sea level rise, the significance of marine infrastructure is expected to increase in response to climate change. However, the scarcity of river sand and freshwater resources for concrete production has posed a considerable challenge for the construction industry worldwide for several decades. On one hand, the overconsumption of river sand has not only raised environmental concerns but has also severely affected riverine ecosystems, floodplains, and navigation. On the other hand, the substantial consumption of freshwater, coupled with high transportation costs, presents critical challenges for the construction sector. To mitigate these problems, the use of sea sand and seawater as substitutes for river sand and freshwater in concrete production has emerged as a promising alternative, gaining acceptance globally. However, due to the presence of chlorides in seawater sea-sand concrete (SSC), chloride-induced corrosion of steel reinforcement in concrete would inevitably be caused (see Fig. 1.1) (Wang et al. 2019; Li et al. 2024).

In this context, SSC structures reinforced with fiber-reinforced polymer (FRP) bars (termed FRP-SSC structures), which was first proposed by Teng et al. (2011) and subsequently promoted internationally by Teng (2014), have attracted world-wide research interests over the past decade owing to its environmental and economic benefits (Selicato et al. 2015; Xiao et al. 2017; Zhao et al. 2021). Currently, the most

widely utilized FRP bars are primarily composed of a variety of fibers (e.g., glass, carbon, basalt, aramid), which are impregnated with different resin matrices (e.g., epoxy, vinylester, polyester) (see Fig. 1.2).



Fig. 1.1 Corrosion of Steel Reinforcement (extracted from https://gharpedia.com/blog/causes-of-corrosion-of-reinforcement-steel/)



(1) GFRP (2) CFRP

(3) AFRP (4) BFRP

Fig. 1.2 Four types of FRP bars (Dong and Wu 2019)

Existing research has revealed that FRP bars possess exceptional durability in marine environments, experiencing only minimal deterioration even after prolonged exposure (Robert and Benmokrane 2013; Benmokrane et al. 2016; Nishizaki et al. 2016; Ruiz Emparanza et al. 2022). While accelerated aging test results raised concerns regarding the durability of glass FRP (GFRP) bars in the alkaline environment of concrete, researchers have found no evidence of significant degradation in GFRP bars embedded in real concrete structures, such as bridges and wharfs, even after many years of service (Mufti et al. 2007b; Gooranorimi and Nanni 2017; Benmokrane et al. 2018; Al-Khafaji et al. 2021; Ramanathan et al. 2021).

Moreover, SSC has demonstrated good durability over a long period, as the effects of sea sand and seawater primarily influence the early strength development of concrete due to their high chloride content (Otsuki et al. 2014; Xiao et al. 2017). Consequently, existing accelerated aging test data on the durability of FRP bars, FRP bars embedded in concrete, and SSC generally suggest that FRP-SSC structures can be expected to be highly durable, even in marine environments. Nevertheless, significant deterioration of FRP-SSC structures might still occur due to various factors, including the coupled effects of environmental exposure and mechanical loading, as observed in some existing accelerated aging tests (AAT) (Almusallam and Al-Salloum 2006; Dong et al. 2018a; Fergani et al. 2018b). This situation necessitates research focused on the long-term performance of FRP-SSC structures, addressing aspects from the material level to the component level, to ensure their safe and reliable application in practice.

1.2 DURABILITY OF FRP BARS AND FRP-REINFORCED CONCRETE BEAMS

A large amount of research has been carried out on the durability of FRP bars and FRP-reinforced concrete beams under controlled laboratory conditions (i.e., AAT studies). These studies have systematically investigated the effects of various environmental factors, including water, alkaline solutions, saline solutions, acidic solutions, elevated temperatures, ultraviolet radiation, freeze-thaw cycles, and wet-dry cycles, as well as their combinations (Tannous and Saadatmanesh 1998; Micelli and Nanni 2004; Chen et al. 2007; Al-Salloum et al. 2013; Hassan et al. 2016; Dong et al. 2018c; Ali et al. 2019; Manalo et al. 2020). Additionally, the coupled effects of simulated environmental conditioning and sustained loading on the durability of FRP bars and FRP-reinforced concrete beams have been extensively examined (Benmokrane et al. 2002; Almusallam and Al-Salloum 2006; Laoubi et al. 2006; Wu et al. 2015; El-Hassan et al. 2018; Fergani et al. 2018a; Fergani et al. 2018b; Chang et al. 2021; Chang et al. 2022). Generally, the durability of FRP bars is inherently complicated, as the degradation of their mechanical properties is governed by multiple factors simultaneously, including the fibers, resin and fiber-resin interface (Chen et al. 2007; Kamal and Boulfiza 2011; Robert and Benmokrane 2013; Wang et al. 2017b; Fergani et al. 2018a). Similarly, the degradation processes in FRP-reinforced concrete beams are complex due to the interactions among the FRP bars, the concrete matrix, and the bar-concrete interface, as shown in Fig. 1.3 (Chang et al. 2022).

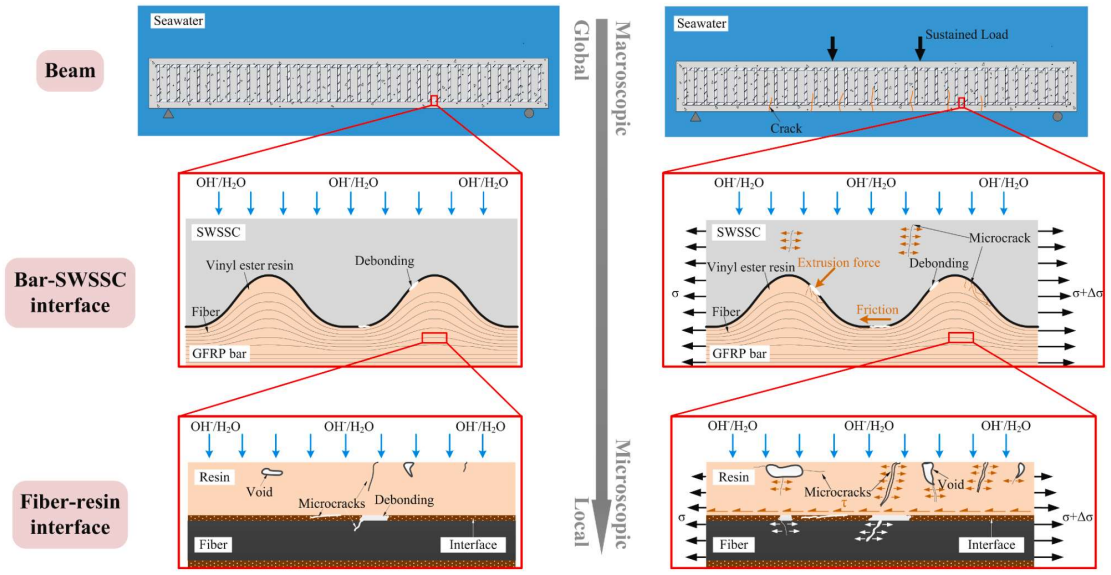


Fig. 1.3 Deterioration mechanism of FRP-reinforced concrete beams under saline conditions (Chang et al. 2022)

In contrast to AAT, research focusing on the durability of FRP bars and FRP-reinforced concrete beams under natural conditions [referred to as field exposure tests (FET)] is notably limited (Al-Salloum et al. 2013; Esmaeili et al. 2020; Kychkin et al. 2021; Morales et al. 2021; Ramanathan et al. 2021; Chen et al. 2022). This scarcity of studies can be attributed to the significantly longer durations and higher costs associated with such studies.

A critical concern is that the severe exposure conditions employed in AAT, such as immersion in aggressive solutions at elevated temperatures, may not accurately reflect the deterioration mechanisms of FRP bars and FRP-reinforced concrete beams in the actual environmental conditions they encountered during their service life. To be more specific, laboratory settings often fail to adequately simulate factors such as temperature fluctuations, ultraviolet radiation, high humidity, and wet-dry cycles, which may lead to highly conservative conclusions drawn from AAT regarding such durability issues.

Despite the limited research on FET, existing studies have demonstrated significant discrepancies between the results obtained from AAT and those from FET (Al-Salloum et al. 2013; Morales et al. 2021). These findings highlight the necessity of conducting FET on both FRP bars and FRP-reinforced concrete beams, which is essential for clarifying their deterioration mechanisms under real world conditions and improving the reliability of durability assessments for FRP bars and FRP-reinforced concrete beams in practical applications.

1.3 OBJECTIVES AND LAYOUT OF THE THESIS

Against the above background, the present PhD research project focuses on the long-term performance and deterioration mechanisms of FRP bars and FRP-SSC beams in real marine environments. The primary objectives of this thesis are structured at both the material and component levels, as follows:

(1) To clarify the effects of various parameters on the durability of FRP bars, FRP bar-to-concrete bond, and FRP-reinforced concrete beams based on existing AAT data;

(2) To investigate the durability performance and deterioration mechanisms of GFRP bars, GFRP bar-to-SSC bonded joints, and GFRP-SSC beams after long-term exposure to various marine environmental conditions;

(3) To establish a conversion relationship between AAT and FET results, thereby developing a reliable prediction model for the long-term performance of GFRP bars in marine environments;

(4) To propose a time-dependent bond stress-slip model for GFRP bars in SSC;

(5) To develop a numerical model for the long-term flexural performance of GFRP-SSC beams, incorporating the deterioration of bond stiffness between GFRP bars and SSC.

This thesis consists of three parts comprising a total of eight chapters, each addressing specific aspects of the long-term performance of GFRP bars (Chapters 3 and 4), GFRP bar-to-SSC bonded joints (Chapter 5), and GFRP-SSC beams (Chapters 6 and 7). A summary of each chapter is provided below.

Chapter 2 presents a comprehensive review on the durability of FRP bars (both bare and concrete-embedded), FRP bar-to-concrete bonded joints, and FRP-reinforced concrete beams subjected to various environmental conditions (e.g., solution immersion, wet-dry cycles, freeze-thaw cycles, high temperatures, UV radiation) and/or loading conditions (i.e., with and without sustained load). Critical parameters (including fiber type, resin type, bar diameter, bar surface treatment, concrete type, exposure environment, and aging duration) influencing the durability issues are systematically investigated based on three AAT databases collected in this study, containing over 15200 specimens.

In Chapter 3, an overview of the FET programs and the two field exposure stations involved in the research project is first presented, detailing the types of exposure zones and their corresponding environmental characteristics. This is followed by the results of an experimental program involving two batches of GFRP bars exposed to different marine environmental conditions (i.e., atmospheric, splash, tidal and underwater zones) for up to four years. The residual tensile properties of the GFRP bars after various field exposure durations were investigated, along with the effect of bar diameter on their

long-term tensile performance.

To bridge the gap between AAT and FET for the durability of GFRP bars, Chapter 4 proposes a refined prediction model that incorporates the additional effects of tidal conditions based on the experimental results presented in Chapter 3. The chapter begins with a comprehensive review of existing prediction models developed for durability of FRP bars, followed by a systematic assessment of three widely used models using the AAT and FET databases introduced in Chapter 2. The proposed model is shown to provide accurate predictions for the GFRP bars subjected to tidal conditions.

Given the critical importance of the long-term bond performance of the FRP bar-to-SSC interface for the durability of FRP-SSC beams, Chapter 5 presents the results of direct pullout tests conducted on two series of GFRP bar-to-SSC bonded joints after up to four years of field exposure in different marine environmental zones. Additionally, a time-dependent bond stress-slip model for GFRP bars in SSC is proposed based on the modified BPE (mBPE) model (Cosenza 1996), and the accuracy of the proposed model is assessed.

Chapter 6 focuses on an experimental study of the long-term performance of GFRP-SSC beams subjected to marine environments for up to four years. Two series of beam specimens were prepared and tested under four-point bending, with the examined variables including the type of exposure zone, the exposure duration, and the presence of sustained load. The flexural performance was evaluated by analyzing failure modes, load-midspan deflection response, cracking load, flexural capacity, and crack width and distribution. Besides, the deterioration mechanisms of the GFRP-SSC beams under tidal conditions are revealed.

Based on the experimental findings from Chapters 5 and 6, a numerical investigation into the long-term flexural performance of GFRP-SSC beams subjected to tidal conditions is presented in Chapter 7. Simplified bond stiffness values, determined from the pullout test results in Chapter 5, are first proposed for finite element (FE) modeling to simulate the behavior of undegraded GFRP-SSC beams. Subsequently, the deterioration of bond stiffness, based on the time-dependent bond stress-slip model for GFRP bars in SSC, is incorporated into the FE modeling of GFRP-SSC beams after prolonged exposure to marine environments. The numerical results demonstrate good agreement with the experimental results in Chapter 6 in terms of load-deflection responses and crack patterns.

The thesis concludes with Chapter 8 by summarizing the main findings from the preceding chapters with further research needs also being highlighted.

CHAPTER 2
LITERATURE REVIEW

2.1 INTRODUCTION

Chloride-induced corrosion of conventional steel reinforcement in concrete structures is of great concern to industrial and research communities worldwide. Due to the prominent features such as high strength-to-weight ratio, superior corrosion resistance and electrical insulation properties, FRP bars have been considered as one of the most promising and cost-effective solutions to this issue, especially in harsh environmental conditions (e.g., offshore and coastal areas). Currently, commonly used FRP bars are mainly composed of various fibers (e.g., glass, carbon, basalt, aramid) impregnated with different resin matrices (e.g., epoxy, vinylester, polyester), leading to the fact that their mechanical properties are primarily governed by three different components: fiber, matrix and fiber/matrix interface. The key mechanical properties of FRP bars can be summarized as follows: (1) Tensile strength (TS) and tensile elastic modulus (TM) are fiber-dominated properties that depend mainly on the fiber volume fraction of FRP bars (ACI 2015); (2) Transverse shear strength (TSS) is a matrix-dominated property, since the fibers cannot resist the shear force acting on a plane perpendicular to the fiber direction (fib 2007); (3) Interlaminar shear strength (ILSS), which is primarily governed by the bond between fibers and matrix, is a fiber/matrix interface-dominated property (Benmokrane et al. 2015); (4) Flexural strength (FS) and flexural elastic modulus (FM) are matrix-dominated properties because the flexural failure of FRP bars correlates to the properties of resin matrix (Wang et al. 2022); (5) Bond strength (BS) at

the FRP bar-to-concrete interface is considered a fiber/matrix interface-dominated property, particularly when the FRP bars are embedded in high-strength concrete (Nepomuceno et al. 2021).

To determine the aforementioned mechanical properties of FRP bars, existing studies have adopted the following standard test methods:

(1) Most researchers utilized tensile tests to assess the TS and TM of FRP bars according to American standard ASTM D7205 (ASTM 2021), while a limited number of studies followed alternative standards, including ASTM D3916 (ASTM 2016b), Chinese standard GB/T 26743 (GB/T 2011), Japanese standard JSCE E531 (JSCE 1995a), and Canadian standard CSA S806 (CSA 2021);

(2) Short-beam shear tests following ASTM D4475 (ASTM 2016a) were commonly used to measure the apparent horizontal shear strength (i.e., ILSS) of FRP bars;

(3) Transverse shear tests as per ASTM D7617 (ASTM 2017) were employed by most studies to obtain the TSS of FRP bars;

(4) Three-point flexural tests in accordance with ASTM D4476 (ASTM 2014) were the most common method to determine the FS and FM of FRP bars;

(5) Direct pullout tests according to ASTM D7913 (ASTM 2020) or Method B3 in ACI 440.3R (ACI 2012) were the most commonly used approaches for assessing the BS of FRP bars.

For a safe and confident use of FRP bars in practice, extensive research has been conducted through accelerated aging tests (AAT) to evaluate the long-term performance of FRP bars and FRP-reinforced concrete beams under different environmental conditions [e.g., water, alkaline solutions, saline solutions, acidic solutions, high

temperatures (HT), ultraviolet (UV) radiation, freeze-thaw (FT) cycles, wet-dry (WD) cycles, and their combinations] (Tannous and Saadatmanesh 1998; Micelli and Nanni 2004; Bakis et al. 2007; Chen et al. 2007; Kamal and Boulfiza 2011; Al-Salloum et al. 2013; Robert and Benmokrane 2013; El Refai et al. 2015; Hassan et al. 2016; Ali et al. 2019; Dong et al. 2020; Lu et al. 2020a; Manalo et al. 2020; Kazemi et al. 2022; Lu et al. 2023b; Wang et al. 2023a) as well as loading conditions (i.e., with and without sustained load) (Benmokrane et al. 2002; Laoubi et al. 2006; Wu et al. 2015; El-Hassan et al. 2018; Fergani et al. 2018a; Chang et al. 2021; Lu et al. 2022). Currently, the most frequently used method for accelerating corrosion is to increase the temperature within a specific environment, while ensuring that it remains below the glass transition temperature (T_g) of FRP bars.

In general, the durability of FRP bars is rather complicated since the degradation of mechanical properties is likely to be dominated by the fibers, resin and fiber-resin interface simultaneously, as stated above (Chen et al. 2007; Kamal and Boulfiza 2011; Robert and Benmokrane 2013; Wang et al. 2017b; Fergani et al. 2018a; Lu et al. 2020c). Micelli and Nanni (2004) demonstrated that the durability of FRP bars subjected to alkaline solutions was significantly influenced by the resin type, which is subsequently confirmed by Benmokrane et al. (2017a); however, no obvious degradation was observed in the conditioned FRP bars after undergoing simulated environmental cycles. Chen et al. (2007) found that FRP bars were more sensitive to continuous immersion in solutions than WD cycling exposure, while FT cycles had negligible effects on their degradation. Benmokrane et al. (2020b) reported that carbon FRP (CFRP) bars exhibited the highest resistance to alkaline environments, followed by basalt FRP (BFRP) and glass FRP (GFRP) bars, and Wang et al. (2017b) found that GFRP bars exhibited superior durability compared to BFRP bars under alkaline conditions.

Additionally, Wang et al. (2023a) observed that GFRP bars immersed in a saline solution possessed higher residual tensile strength than those immersed in water and alkaline solutions for up to 360 days, which aligns with the findings of Al-Salloum et al. (2013). Furthermore, existing studies indicated that the application of sustained load could amplify the detrimental effects on the long-term durability of FRP bars, especially for those conditioned at elevated temperatures, compared to single environmental exposure (Almusallam and Al-Salloum 2006; Wu et al. 2015; Wang et al. 2018).

Apart from the degradation of the mechanical properties of FRP bars alone, the bond performance of FRP bar-concrete interface after exposure is also critical for the durability of FRP-reinforced concrete structures. Extensive studies have been carried out to investigate bond durability under various environmental conditions and material parameters (Bakis et al. 2007; El Refai et al. 2015; Hassan et al. 2016; Kazemi et al. 2022; Xiong et al. 2022). Zheng et al. (2020) found that GFRP bars manufactured with vinylester resin possessed better performance in aggressive environments than those made with epoxy resin. Similar tests were performed by Altalmas et al. (2015) and their findings indicated that the trend of the bond-slip responses was detected to be irrelevant to the type of aqueous solution, which is consistent with the observations made by Zheng et al. (2020). However, Dong et al. (2016a) concluded that sand-coated FRP bars exhibited superior bond durability to that of ribbed bars under seawater exposure, indicating the correlation between bond degradations and bar surface treatment. Yan et al. (2017) reported that the durability of GFRP bar-concrete pullout specimens subjected to FT cycles in an alkaline-saline solution was generally poorer than those conditioned in individual FT cycles. In addition to normal concrete (NC), Dong's research group (Dong et al. 2016b; Dong et al. 2018a; Dong et al. 2018b) found that the

BS degradation of FRP bars in seawater sea-sand concrete (SWSSC) in a seawater immersion environment was more severe than that in a WD cycling condition, while Chang et al. (2021) reported that more significant BS degradation was detected in FRP-SWSSC interfaces under the coupled effects of seawater immersion and sustained load, especially for FRP bars with a small diameter.

To better understand the long-term structural behavior of FRP-reinforced concrete beams in aggressive environments, some efforts have been made in this field. Rajput and Sharma (2017) indicated that the aggressive environments (WD cycling in a 45℃ saline solution and continuous immersion in a 60℃ alkaline solution) had little impact on the flexural strength of GFRP-reinforced concrete beams after 30-day exposure. However, Tannous and Saadatmanesh (1999) concluded that the strength loss of FRP bars in concrete beams might depend more on exposure time rather than solution type, and thus, more significant stiffness loss and bending capacity degradation were observed for the GFRP-reinforced concrete beams after two years of exposure to saline solutions. Besides, Dong et al. (2018c, 2020) found that environmental exposure could change the failure modes of BFRP-reinforced SWSSC beams from concrete crushing to shear failure after seawater immersion or WD cycling, which indicated the decreased contributions of FRP stirrups to shear resistance. In order to mitigate this negative effect, Su et al. (2022) developed the carbon nanotube-modified BFRP material to be used as shear reinforcement in SWSSC beams and their test results showed that this novel type of FRP bars was effective in suppressing the shear failure caused by the bond degradation after exposure to seawater WD cycling. Moreover, the coupled effects of sustained load and environmental exposures on the bending performance of FRP-reinforced concrete beams have also been studied; however, there was no consensus regarding this issue based on the limited existing research (Laoubi et al. 2006; Dong et

al. 2018a).

It should be noted that most existing studies on the durability of FRP bars and FRP-reinforced concrete beams have been conducted using AAT rather than field exposure tests (FET) since the former method consumes much less time. Using the available AAT results, several models based on Arrhenius relation (Nelson 2009) have been proposed to predict the long-term mechanical properties of FRP bars (Tannous and Saadatmanesh 1998; Bank et al. 2003; Huang and Aboutaha 2010; Davalos et al. 2011; Robert and Benmokrane 2013; Wu et al. 2015; Dong et al. 2017b). Therefore, it is essential to clarify the durability performance of FRP bars and FRP-reinforced concrete beams under accelerated aging exposure, as this will facilitate the establishment of a conversion relationship between AAT and FET. However, the existing AAT results seem to be highly scattered due to differences in inherent material properties (e.g., fiber type, resin type, manufacturing process), environmental conditions (e.g., solution type, solution concentration, exposure temperature), as well as loading conditions (i.e., stress level). Consequently, reaching a consensus based on a limited number of studies may prove challenging. Thus, a comprehensive database is urgently needed to examine the degradation law of FRP bars and FRP-reinforced concrete beams under accelerated aging conditions.

In this chapter, the durability of FRP bars, FRP-concrete bonded joints and FRP-reinforced concrete beams was assessed based on three assembled AAT databases derived from open literature. Various parameters (including fiber type, resin type, bar diameter, bar surface treatment, concrete type, exposure environment, aging duration, etc.) that affect the degradation of mechanical properties of FRP bars and flexural behavior of FRP-reinforced concrete beams were systematically investigated, aiming to

give a comprehensive review that spans from the material level (FRP bars) to the component level (FRP-reinforced concrete beams), thereby providing a solid foundation for future research. Note that the durability assessment only considered test results obtained from AAT, where the test specimens were exposed to simulated environments at ambient and/or elevated temperatures, with or without sustained load, for a specified duration.

2.2. EXPERIMENTAL DATABASES

The AAT results for over 13200 FRP bars, 1800 FRP bar-concrete bonded joints and 200 FRP-reinforced concrete beams, from more than 4300 tests published in the existing literature, have been collected and the resulting three databases are presented in Tables A1-A3, B1 and C1, respectively (see Appendix A). Besides, three corresponding FET databases have been collected for reference, as detailed in Tables D1-D3, E1 and F1, respectively (see Appendix B). To ensure the reliability and consistency of the results in these databases, several filtering criteria were adopted as follows:

- Only commonly used FRP bars [i.e., aramid FRP (AFRP), BFRP, CFRP and GFRP bars] were included in the three databases, with only thermosetting resin matrices [i.e., (modified) epoxy, (modified) vinylester and (modified) polyester resin matrices] being considered. Additionally, only specimens made with normal concrete (NC), high-strength concrete (HSC) and seawater and/or sea-sand concrete (SWC, SSC, SWSSC) were included in the databases of FRP bar-concrete bonded joints and FRP-reinforced concrete beams, while those made with fiber-reinforced concrete, lightweight aggregate concrete, coral aggregate concrete, recycle aggregate concrete, etc., were excluded.

- To avoid the changes in the degradation mechanism of FRP bars caused by elevated temperatures above the T_g of resin matrix, test results obtained at conditioning temperatures higher than 80°C were ignored.

- Individual or coupled effects of the following environmental conditions were included during the database collection:

  - Alkaline solution immersion (IMMR),
  - Acid solution immersion (IMMR),
  - Saline solution/ (simulated) seawater immersion (IMMR),
  - Water immersion (IMMR),
  - NC/SWSSC solution immersion (IMMR),
  - Concrete-embedded condition for FRP bars,
  - Wet-dry cycles (WD),
  - Freeze-thaw cycles (FT),
  - Sustained load (SL),
  - Ultraviolet radiation (UV),
  - Room temperature (RT),
  - High temperature (HT),
  - Low temperature (LT),
  - Relative humidity (RH),
  - Pre-cracks for FRP-reinforced concrete beams.

It can be seen from the Tables (A1-A3, B1 and C1) in Appendix A that each database consists of the most critical information for each specimen, including FRP type, bar manufacturer and diameter, resin type, concrete type, environmental condition, exposure duration, and key test results. In this study, retention was defined as the

average value of the test results for several identically conditioned specimens expressed as a percentage of that for unconditioned ones. Note that the unconditioned specimens without environmental exposure and time aging effects were denoted “control” specimens, while those without environmental exposure but with time aging effects were denoted “reference” specimens, especially for the FRP bar-concrete bonded joint and FRP-reinforced concrete beam specimens. The overall distribution of the above-mentioned parameters in each database is shown in Fig. 2.1, where the proportion of specimens within selected ranges is also presented in diagrams versus the main test parameters to quantify these differences and identify research needs. It is evident that, in the three databases, the majority of specimens used FRP bars made with glass (58~62%) and basalt (23~34%) fibers, while fewer tests were conducted on FRP bars made with aramid (approximately 1%) and carbon (6~18%) fibers. It is important to note that a significant proportion of studies (18%) adopted CFRP bars as internal reinforcements for FRP-reinforced concrete beams, which may result from the superior tensile properties of CFRP bars in prestressed applications (Sen et al. 1999).

Regarding resin type, the overwhelming majority of the studies adopted vinylester resin-based FRP bars (43.1~53.3%) due to their excellent durability, followed by epoxy resin-based ones (18.4~31.6%). Another noteworthy finding is that FRP bars with a small diameter (e.g., smaller than 13 mm) were commonly used in the selected studies, with percentages of 85.8%, 84.5% and 76.1%, respectively, for FRP bars, bonded joints and beams. In contrast, very few tests were performed on specimens using FRP bars with diameters larger than 19 mm [FRP bars (5.0%), bonded joints (4.2%) and beams (1.9%)]. This can be explained by the fact that smaller diameters can accelerate degradation, as the corrosion rates tend to decrease with increasing bar diameter (Benmokrane et al. 2017a), and small-sized FRP bars are also easy for testing. In

addition, for the database of FRP bars, the evaluated mechanical properties include TS (49.0%), ILSS (31.5%), TSS (11.8%) and FS (7.7%), with 80.6% of tests conducted on bare FRP bars and 19.4% on concrete-embedded FRP bars after various environmental conditionings. For the databases of bonded joints and beams, most tests were performed on members with NC (76.8% and 78.5%, respectively), while relatively few tests were carried out on members with SWC/SSC/SWSSC (13.9% and 21.5%, respectively) and HSC (9.3% and 0%, respectively). Since the types of environmental conditioning have a strong relationship with the investigated properties for FRP materials and members, more detailed discussions on the durability of FRP bars, FRP bar-concrete bonded joints and FRP-reinforced concrete beams are given in the following sections.

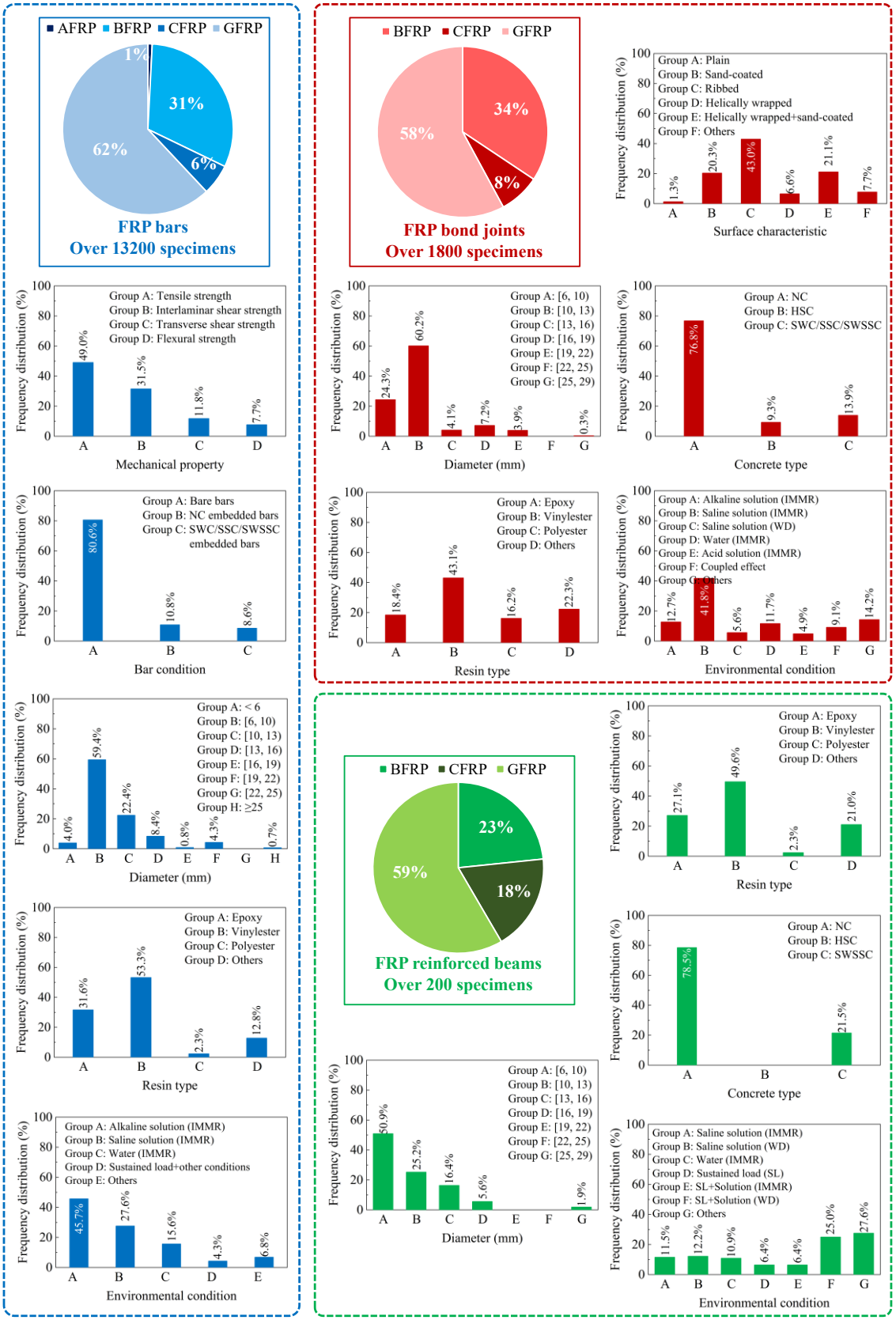


Fig. 2.1 Distribution of test parameters in three assembled databases

2.3 BARE FRP BARS

2.3.1 Single Environmental Effect

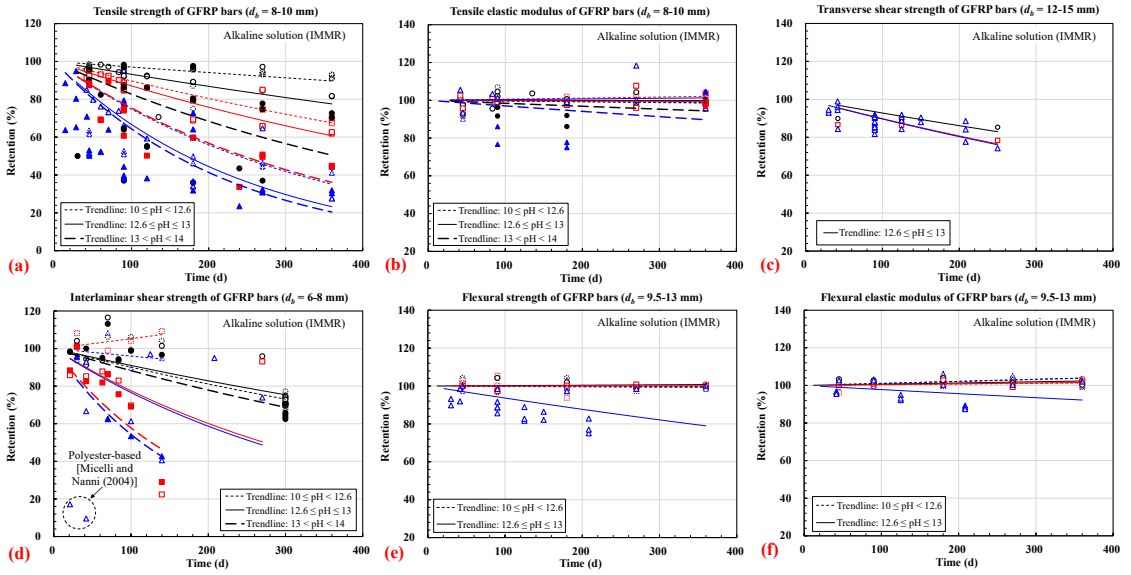
Numerous studies have been conducted on the durability of mechanical properties (i.e., TS, TM, TSS, ILSS, FS and FM) of bare FRP bars subjected to different environmental conditions. To evaluate the single environmental effect on the durability of bare FRP bars, test results from the three most frequently used conditions (i.e., continuous immersion in alkaline, saline and water solutions) and other conditions reported in the existing literature were selected based on the assembled databases (see Tables A1, A2 and A3 in Appendix A). Note that due to the limited test data available for CFRP and AFRP bars as mentioned earlier, the test results presented in the following subsections are mainly limited to those for GFRP and BFRP bars made with vinylester, epoxy and polyester resins (including their modified types), unless otherwise specified. Besides, in order to achieve a more comprehensive assessment of the durability performance of bare FRP bars, most of the comparable cases discussed in this section include AAT data sourced from at least two different studies.

2.3.1.1 Alkaline solution immersion

2.3.1.1.1 Effect of alkaline concentration. Existing studies have indicated that the concentration of alkaline solutions plays a vital role in the durability of FRP bars in alkaline environments (Wang et al. 2022; Wang et al. 2023a). To study the effect of pH on the durability of bare FRP bars, AAT data for GFRP bars with a consistent diameter range and being directly immersed in alkaline solutions with different pH levels at various temperatures (i.e., 20-30℃, 40℃ and 60℃) were collected. As specified by ACI 440.3R (ACI 2012) and ASTM D7957 (ASTM 2022), pH = 12.6-13 is a

representative range of mature concrete pore solution, and thus the pH values herein are classified into three ranges, namely 10 ≤ pH < 12.6, 12.6 ≤ pH ≤ 13 and 13 < pH < 14. Fig. 2.2(a) shows the TS retentions of GFRP bars with respect to the exposure duration. All the selected GFRP bars had the same diameter range (d_b = 8-10 mm) and were subjected to alkaline solutions with different pH levels. A simple exponential regression equation, expressed as $Y = 100\exp(-t/\tau)$ (Phani and Bose 2012), was adopted to generate trendlines based on the selected AAT data, where t represents the aging time and τ denotes the fitting parameter. This equation has been demonstrated to provide reasonably accurate predictions of the durability of FRP bars and exhibits a degradation law consistent with other widely used mathematical equations (Chen et al. 2006; Wu et al. 2015; Feng et al. 2022). The thin dotted, thin solid and thick dashed trendlines in the subfigures correspond to GFRP bars exposed to alkaline solutions with pH ranges of 10 ≤ pH < 12.6, 12.6 ≤ pH ≤ 13 and 13 < pH < 14, respectively. In addition, the number in brackets after each reference in the legend represents the number of test data used in the figure, and such a manner is adopted for the figures in this chapter hereafter. The trendlines in Fig. 2.2(a) demonstrate that the TS retentions of GFRP bars decrease with both exposure time and temperature for all pH levels. This is because the longer the exposure time, the more severe the chemical reactions, while the higher the exposure temperature, the faster the water molecules and hydroxide ions move (Wang et al. 2022). Moreover, higher pH values result in relatively lower strength retentions under the same condition. This phenomenon can be explained by the fact that, in an alkaline solution with a higher pH level, there are more serious chemical reactions between the hydroxide ions and the glass fiber, which may lead to the formation of micro-cracks in GFRP bars (Wang et al. 2022). Compared to the TS of GFRP bars, TM is found to be less affected by the alkaline concentration, exposure duration and exposure temperature

[see Fig 2(b)]. This is reasonable because TM is obtained from the linear-elastic portion of the stress-strain curve of the FRP bars, where the matrix still effectively transfers stress to the fibers, while the TS is calculated at the failure points of FRP bars (Benmokrane et al. 2017b). Since limited test data available for the TSS of bare GFRP bars (d_b = 12-15 mm) in alkaline environments of $10 \leq pH < 12.6$ and $13 < pH < 14$, only those for bars immersed in alkaline solutions with pH values ranging from 12.6 to 13 are shown in Fig. 2.2(c). Similar to TS, the TSS retentions of GFRP bars gradually decrease with time and temperature. For ILSS, as shown in Fig. 2.2(d), the retention trends for GFRP bars with diameters ranging from 6 to 8 mm under different conditions are also similar to those of TS and TSS, with two exceptions of the polyester-based specimens tested by Micelli and Nanni (2004). This is mainly because the polyester resin is much more susceptible to chemical attack by alkalis, while the ILSS is primarily governed by the matrix and the fiber-matrix interface rather than by the fibers. Note that Benmokrane et al. (2017a) reported that the GFRP bars made with polyester resin exhibited a much lower ILSS retention after alkaline conditioning, compared to their vinylester- and epoxy-based counterparts. In Figs. 2.2(e) and 2.2(f), the retentions of FS and FM for GFRP bars with diameters ranging from 9.5 to 13 mm are generally close to each other under the same condition, except for those exposed to alkaline solutions with higher concentrations ($12.6 \leq pH \leq 13$) at 60°C, where both retentions decrease obviously with prolonged exposure. In addition, due to the limited data available with respect to the durability of TSS and flexural properties (FS and FM) of GFRP bars, a significant amount of further research is required to enhance the understanding of these properties.



20-30°C (10 ≤ pH < 12.6)
(a) [Tannous and Saadatmanesh 1998 (2); Wang et al. 2022 (10); Wang et al. 2023 (10)]; (b) [Wang et al. 2022 (7); Wang et al. 2023 (2)]; (d) [Yu et al. 2021 (4); Sun et al. 2023 (16)]; (e) [Wang et al. 2022 (10)]; (f) [Wang et al. 2022 (10)]

40°C (10 ≤ pH < 12.6)
(a) [Wang et al. 2022 (10); Wang et al. 2023 (10)]; (b) [Wang et al. 2022 (10); Wang et al. 2023 (2)]; (d) [Yu et al. 2021 (4)]; (e) [Wang et al. 2022 (10)]; (f) [Wang et al. 2022 (10)]

60°C (10 ≤ pH < 12.6)
(a) [Tannous and Saadatmanesh 1998 (2); Wang et al. 2022 (10); Wang et al. 2023 (10)]; (b) [Wang et al. 2022 (10); Wang et al. 2023 (2)]; (d) [Yu et al. 2021 (4)]; (e) [Wang et al. 2022 (10)]; (f) [Wang et al. 2022 (10)]

20-30°C (12.6 ≤ pH ≤ 13)
(a) [Chen et al. 2006 (4); Chen et al. 2007 (1); Fergani et al. 2018 (3); Lu et al. 2020a (4); Wang et al. 2022 (5); Wang et al. 2023 (5)]; (b) [Fergani et al. 2018 (3); Lu et al. 2020a (4); Wang et al. 2022 (5); Wang et al. 2023 (1)]; (c) [Hosseini et al. 2024 (3)]; (d) [Micelli and Nanni 2004 (1); Wang et al. 2017a (4); Fergani et al. 2018 (1); Yu et al. (4); Sun et al. 2023 (4)]; (e) [Wang et al. 2022 (5)]; (f) [Wang et al. 2022 (5)]

40°C (12.6 ≤ pH ≤ 13)
(a) [Chen et al. 2006 (4); Chen et al. 2007 (1); Fergani et al. 2018 (3); Wang et al. 2022 (5); Wang et al. 2023 (5)]; (b) [Fergani et al. 2018(3); Wang et al. 2022 (5); Wang et al. 2023 (1)]; (c) [Hosseini et al. 2024 (3)]; (d) [Wang et al. 2017a (4); Fergani et al. 2018 (1); Yu et al. (4)]; (e) [Wang et al. 2022 (5)]; (f) [Wang et al. 2022 (5)]

60°C (12.6 ≤ pH ≤ 13)
(a) [Chen et al. 2006 (4); Won and Park 2006 (1); Chen et al. 2007 (1); Benmokrane et al. 2017b (1); Fergani et al. 2018 (3); Wang et al. 2022 (5); Wang et al. 2023 (5)]; (b) [Benmokrane et al. 2017b (1); Fergani et al. 2018 (3); Wang et al. 2022 (5); Wang et al. 2023 (1)]; (c) [Benmokrane et al. 2017a (9); Benmokrane et al. 2020 (12); Arczewska et al. 2021 (12)]; (c) [Benmokrane et al. 2017a (9); Benmokrane et al. 2020 (12); Arczewska et al. 2021 (6); Hosseini et al. 2024 (3)]; (d) [Micelli and Nanni 2004 (2); Benmokrane et al. 2015 (3); Fergani et al. 2018 (1); Yu et al. (4); D'Antino et al. 2023 (1)]; (e) [Benmokrane et al. 2017a (9); Benmokrane 2017b (2); Arczewska et al. 2021 (6); Wang et al. 2022 (5)]; (f) [Benmokrane et al. 2017a (9); Wang et al. 2022 (5)]

20-30°C (13 < pH < 14)
(a) [Al-Zahrani et al. 2002 (4); Sen et al. 2002 (4); Chen et al. 2006 (4); Chen et al. 2007 (3); Wang et al. 2023 (10)]; (b) [Al-Zahrani et al. 2002 (4); Wang et al. 2023 (2)]; (d) [Wang et al. 2017a (4); Pan and Yan 2021 (4); Sun et al. 2023 (4)]

40°C (13 < pH < 14)
(a) [Chen et al. 2006 (4); Chen et al. 2007 (2); Wang et al. 2023 (10)]; (b) [Wang et al. 2023 (2)]; (d) [Wang et al. 2017a (4); Pan and Yan 2021 (4)]

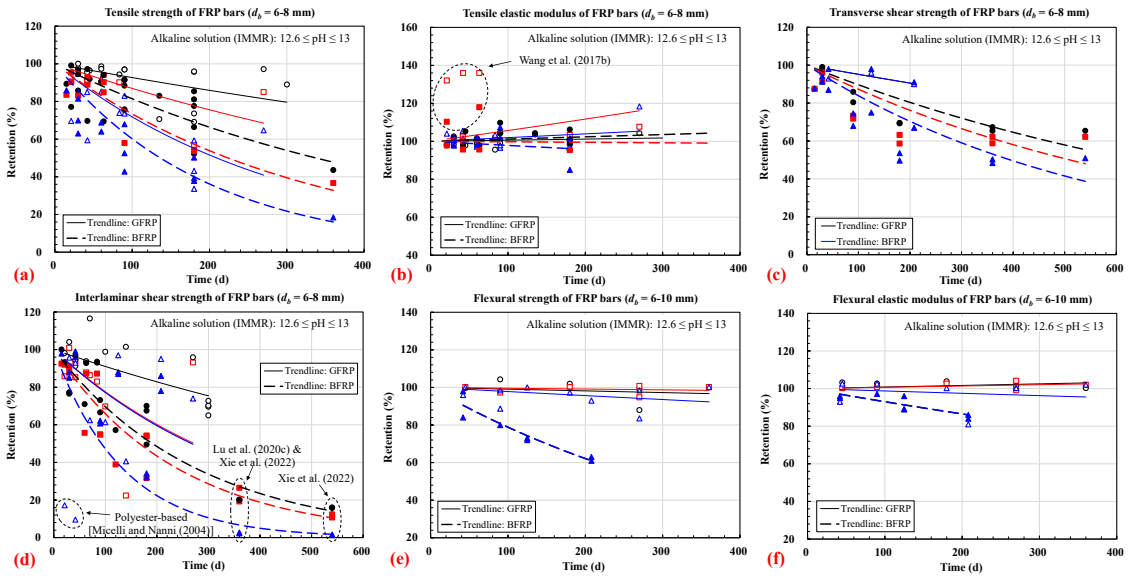
60°C (13 < pH < 14)
(a) [Al-Zahrani et al. 2002 (4); Chen et al. 2006 (4); Chen et al. 2007 (2); Nassar et al. 2022 (6); Wang et al. 2023 (10)]; (b) [Al-Zahrani et al. 2002 (4); Wang et al. 2023 (2)]; (d) [Pan and Yan 2021 (4)]

Fig. 2.2 Effect of alkaline concentration on the durability of bare GFRP bars

2.3.1.1.2 Effect of fiber type. It has been found that the mechanical properties (especially tensile properties) of FRP bars vary depending on the fiber type (Wang et al. 2017a; Wang et al. 2017b; Benmokrane et al. 2020b; Lu et al. 2020a; Lu et al. 2020d). To examine the effect of fiber type on the durability of bare FRP bars immersed in alkaline solutions, GFRP and BFRP bars having the same diameter ranges and under the same exposure conditions (i.e., the alkaline solution with a pH of 12.6-13) are compared in Fig. 2.3. Figs. 2.3(a) and 2.3(b) respectively show the degradation trends of TS and TM for the two types of FRP bars (d_b = 6-8 mm) in alkaline environments.

The thin solid trendlines represent GFRP bars, while the thick dashed ones stand for BFRP bars in these subfigures. It can be seen that the TS retentions of both GFRP and BFRP bars gradually decrease with increasing exposure duration in the 20-30℃, 40℃ and 60℃ alkaline solutions. It is also interesting to find that the trendlines for GFRP bars consistently exhibit higher values than those for BFRP bars, showing that the TS of BFRP bars degrade more severely than that of GFRP bars under the same alkaline conditions [see Fig. 2.3(a)]. This finding has also been confirmed by other researchers (Wang et al. 2017b; Benmokrane et al. 2020b; Wu et al. 2023). In contrast, for TM, there is no clear degradation trend over immersion time for either type of FRP bar, and even significant increases in TM were found for some GFRP and BFRP bars at 40℃, as reported by Wang et al. (2017b) [see Fig. 2.3(b)]. Figs. 2.3(c) to 2.3(f) further illustrate that fiber type has non-negligible impacts on other four mechanical properties (i.e., TSS, ILSS, FS and FM) of FRP bars under the same alkaline conditions, and larger retentions can be found in GFRP bars than those in BFRP bars, although the available data for TSS, FS and FM are quite limited. Nevertheless, as mentioned previously, the TSS, ILSS, FS and FM of FRP bars are primarily governed by the matrix and/or the fiber-matrix interface, which indicates that the observations made in Figs. 2.3(c) to 2.3(f) may result from a combination of several factors (e.g., fiber type, resin type, fiber sizing). For example, Benmokrane et al. (2015) confirmed that the deteriorations of TSS, ILSS and FS in BFRP bars immersed in a 60℃ alkaline solution for up to 5000 hours were caused by the fiber sizing rather than the fiber and resin types, leading to a poor bond between the resin and basalt fibers, as verified by scanning electron microscopy (SEM). Similar conclusions were drawn in their subsequent study on the durability of FRP bars (d_b = 13-15 mm) provided by the same manufacturer but with different fiber types, fiber sizings and resin types (Benmokrane et al. 2020b). Therefore,

the conclusions for this issue need to be further confirmed and improved when more AAT data are available. It is noteworthy that, among the existing literature on BFRP bars reviewed in this study, the majority of referenced BFRP products, excluding literature that does not provide manufacturer information, are sourced from two manufacturers (see Appendix A). The concentrated test data derived from these products may also lead to the above-mentioned underestimations of the material properties of BFRP bars. Thus, more experimental data from a wider range of manufacturers are also urgently needed to achieve a more comprehensive assessment of the durability of BFRP bars.



GFRP_20-30°C
(a) [Fergani et al. 2018 (3); Lu et al. 2020a (4); Lu et al. 2020d (1); Sun et al. 2023 (1); Wang et al. 2023b (8)]; (b) [Fergani et al. 2018 (3); Lu et al. 2020a (4); Lu et al. 2020d (1); Wang et al. 2023b (8)]; (d) [Micelli and Nanni 2004 (1); Wang et al. 2017a (4); Fergani et al. 2018 (1); Yu et al. 2021 (4); Sun et al. 2023 (4)]; (e) [Fergani et al. 2018 (1); Wang et al. 2022 (5)]; (f) [Fergani et al. 2018 (1); Wang et al. 2022 (5)]

GFRP_40°C
(a) [Wang et al. 2017b (3); Fergani et al. 2018 (3); Lu et al. 2020d (1)]; (b) [Wang et al. 2017b (3); Fergani et al. 2018 (3); Lu et al. 2020d (1)]; (d) [Wang et al. 2017a (4); Fergani et al. 2018 (1); Yu et al. 2021 (4)]; (e) [Fergani et al. 2018 (1); Wang et al. 2022 (5)]; (f) [Fergani et al. 2018 (1); Wang et al. 2022 (5)]

GFRP_60°C
(a) [Micelli and Nanni 2004 (2); Fergani et al. 2018 (3); Lu et al. 2020d (1); Wang et al. 2023b (8)]; (b) [Micelli and Nanni 2004 (2); Fergani et al. 2018 (3); Lu et al. 2020d (1); Wang et al. 2023b (8)]; (c) [Benmokrane et al. 2015 (3)]; (d) [Micelli and Nanni 2004 (2); Benmokrane et al. 2015 (3); Fergani et al. 2018 (1); Yu et al. 2021 (4)]; (e) [Benmokrane et al. 2015 (3); Benmokrane et al. 2017b (1); Fergani et al. 2018 (1); Wang et al. 2022 (5)]; (f) [Benmokrane et al. 2015 (3); Fergani et al. 2018 (1); Wang et al. 2022 (5)]

BFRP_20-30°C
(a) [Wu et al. 2014 (3); Wu et al. 2015 (3); Lu et al. 2020a (4); Lu et al. 2020d (1); Lu et al. 2021b (5), Wang et al. 2023b (8)]; (b) [Wu et al. 2014 (3); Wu et al. 2015 (3); Lu et al. 2020a (4); Lu et al. 2020d (1); Wang et al. 2023b (8)]; (c) [Lu et al. 2020c (4); Xie et al. 2022 (6)]; (d) [Wang et al. 2017a (4); Lu et al. 2020c (4); Xie et al. 2022 (7); Feng et al. 2023 (3)]

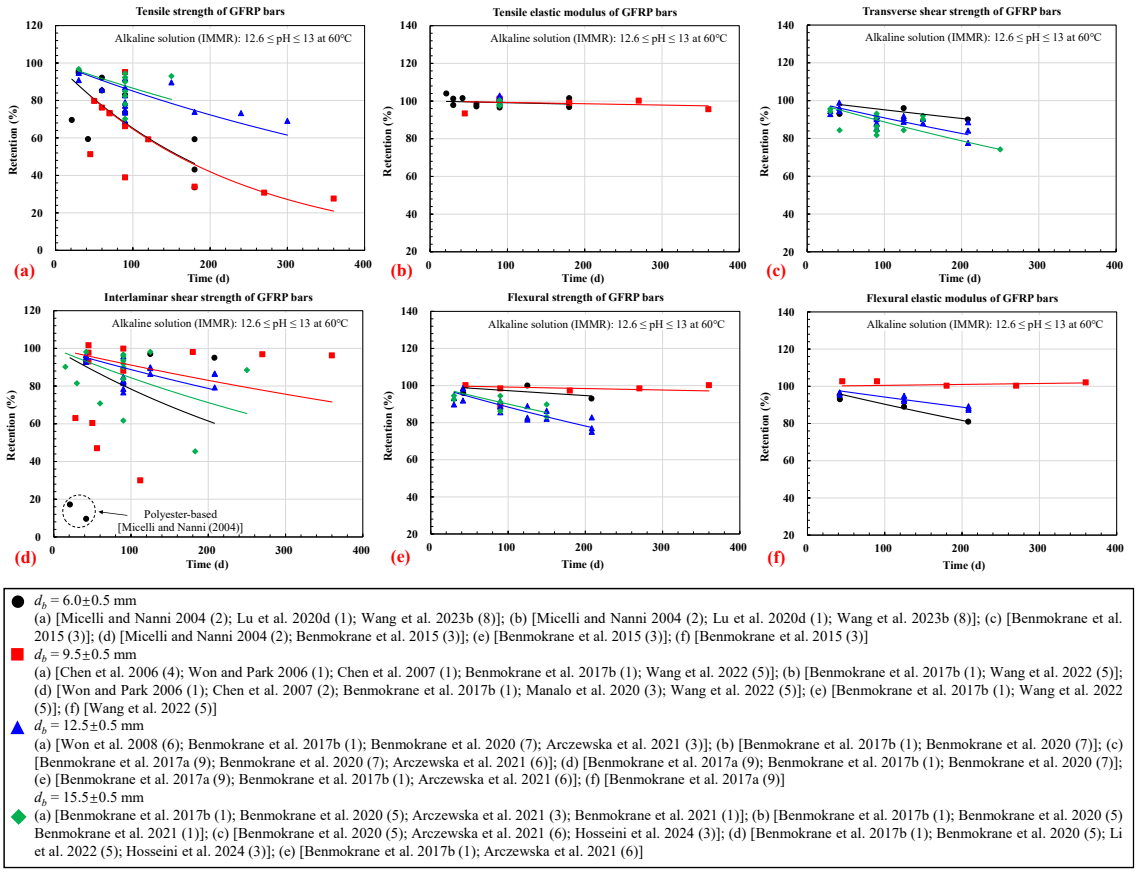
BFRP_40°C
(a) [Wu et al. 2015 (3); Wang et al. 2017b (3); Lu et al. 2020d (1); Lu et al. 2021b (5)]; (b) [Wu et al. 2015 (3); Wang et al. 2017b (3); Lu et al. 2020d (1)]; (c) [Lu et al. 2020c (4); Xie et al. 2022 (6)]; (d) [Wang et al. 2017a (4); Lu et al. 2020c (4); Xie et al. 2022 (7); Feng et al. 2023 (3)]

BFRP_60°C
(a) [Lu et al. 2020d (1); Lu et al. 2021b (5); Wang et al. 2023b (7)]; (b) [Lu et al. 2020d (1); Wang et al. 2023b (7)]; (c) [Benmokrane et al. 2015 (6); Lu et al. 2020c (4); Xie et al. 2022 (6)]; (d) [Benmokrane et al. 2015 (6); Lu et al. 2020c (4); Xie et al. 2022 (7)]; (e) [Benmokrane et al. 2015 (6); Ali et al. 2020 (1)]; (f) [Benmokrane et al. 2015 (6); Ali et al. 2020 (1)]

Fig. 2.3 Effect of fiber type on the durability of bare FRP bars under alkaline conditions

2.3.1.1.3 Effect of bar diameter. Existing research has indicated an appreciable size effect on the long-term performance of FRP bars (Benmokrane et al. 2017b; Ali et al. 2020). To investigate this issue, bare GFRP bars of five different diameter ranges (i.e., 6.0 ± 0.5 mm, 9.5 ± 0.5 mm, 12.5 ± 0.5 mm and 15.5 ± 0.5 mm) immersed in an alkaline solution with a pH of 12.6-13.0 at 60℃ are compared. Figs. 2.4(a) and 2.4(b) respectively show the retentions of TS and TM of GFRP bars of different diameters with respect to exposure time. In general, the TS retentions of all GFRP bars decrease with time, with the smaller GFRP bars exhibiting relatively lower retentions than their larger counterparts under the same conditions [see Fig. 2.4(a)], which is consistent with the findings reported by Tannous and Saadatmanesh (1998), Arczewska et al. (2021) and Lu et al. (2021a). This phenomenon may be caused by the difference in the ratios of ‘‘degraded” to ‘‘undegraded” sectional areas of the bar subjected to harsh conditions (Arczewska et al. 2021). In contrast, Fig. 2.4(b) indicates that, except for the seven circled data points, the diameter has no obvious influence on the TM of GFRP bars. Note that TM is an inherent property of FRP bars, largely depending on the level of fibers contained in the bars (i.e., fiber content), and thus is less affected by the conditioning (Kocaoz et al. 2005). For TSS, as depicted in Fig. 2.4(c), the retentions for different-sized GFRP bars also show a decreasing tendency over time. However, the size effect on the TSS of GFRP bars seems negligible, which is contrary to the findings of Arczewska et al. (2021). Given the limited test results available under this circumstance, further research is needed to verify this observation. Fig. 2.4(d) presents the test results for ILSS, which are highly dispersed, making it difficult to identify any clear effect of diameter on the strength retention of GFRP bars. This discrepancy may be attributed to the following two main reasons: (1) The combinations of different fiber types, resin types and fiber sizings have a great impact on the ILSS durability of FRP

bars, as mentioned previously; (2) Different span-to-diameter ratios used in the short-beam shear tests might yield different ILSS results, as observed by Wang et al. (2017a) and Januš et al. (2022). Specifically, ILSS has been found to slightly decrease with increasing span-to-diameter ratio, despite ASTM D4475 (ASTM 2016a) recommending ratios between 3:1 and 6:1. With respect to FS and FM, Figs. 2.4(e) and 2.4(f) demonstrate that no significant size effect can be observed based on the limited amount of data.



● d_b = 6.0±0.5 mm
(a) [Micelli and Nanni 2004 (2); Lu et al. 2020d (1); Wang et al. 2023b (8)]; (b) [Micelli and Nanni 2004 (2); Lu et al. 2020d (1); Wang et al. 2023b (8)]; (c) [Benmokrane et al. 2015 (3)]; (d) [Micelli and Nanni 2004 (2); Benmokrane et al. 2015 (3)]; (e) [Benmokrane et al. 2015 (3)]; (f) [Benmokrane et al. 2015 (3)]

■ d_b = 9.5±0.5 mm
(a) [Chen et al. 2006 (4); Won and Park 2006 (1); Chen et al. 2007 (1); Benmokrane et al. 2017b (1); Wang et al. 2022 (5)]; (b) [Benmokrane et al. 2017b (1); Wang et al. 2022 (5)]; (d) [Won and Park 2006 (1); Chen et al. 2007 (2); Benmokrane et al. 2017b (1); Manalo et al. 2020 (3); Wang et al. 2022 (5)]; (e) [Benmokrane et al. 2017b (1); Wang et al. 2022 (5)]; (f) [Wang et al. 2022 (5)]

▲ d_b = 12.5±0.5 mm
(a) [Won et al. 2008 (6); Benmokrane et al. 2017b (1); Benmokrane et al. 2020 (7); Arczewska et al. 2021 (3)]; (b) [Benmokrane et al. 2017b (1); Benmokrane et al. 2020 (7)]; (c) [Benmokrane et al. 2017a (9); Benmokrane et al. 2020 (7); Arczewska et al. 2021 (6)]; (d) [Benmokrane et al. 2017a (9); Benmokrane et al. 2017b (1); Benmokrane et al. 2020 (7)]; (e) [Benmokrane et al. 2017a (9); Benmokrane et al. 2017b (1); Arczewska et al. 2021 (6)]; (f) [Benmokrane et al. 2017a (9)]

◆ d_b = 15.5±0.5 mm
(a) [Benmokrane et al. 2017b (1); Benmokrane et al. 2020 (5); Arczewska et al. 2021 (3); Benmokrane et al. 2021 (1)]; (b) [Benmokrane et al. 2017b (1); Benmokrane et al. 2020 (5) Benmokrane et al. 2021 (1)]; (c) [Benmokrane et al. 2020 (5); Arczewska et al. 2021 (6); Hosseini et al. 2024 (3)]; (d) [Benmokrane et al. 2017b (1); Benmokrane et al. 2020 (5); Li et al. 2022 (5); Hosseini et al. 2024 (3)]; (e) [Benmokrane et al. 2017b (1); Arczewska et al. 2021 (6)]

Fig. 2.4 Effect of diameter on the durability of bare GFRP bars under alkaline conditions

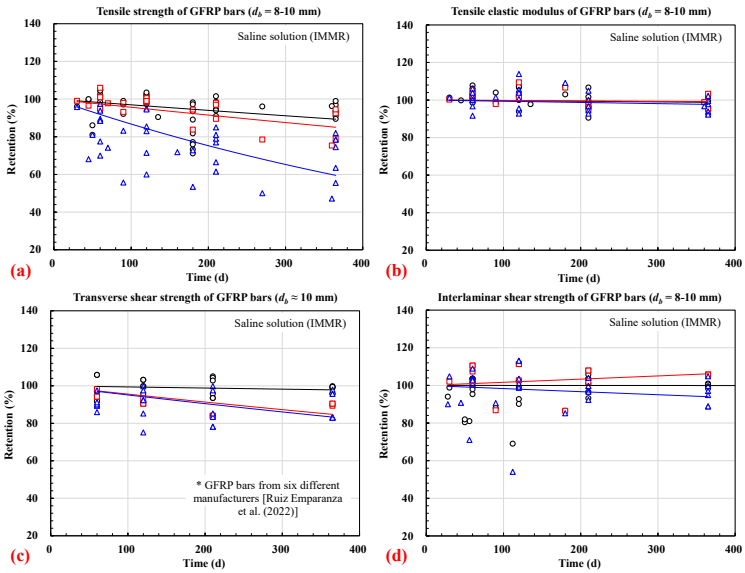
So far, only a limited number of studies have comprehensively addressed the size effect on the durability of FRP bars (Benmokrane et al. 2017b; Ali et al. 2020; Feng et al. 2024b). In contrast to the above findings, Benmokrane et al. (2017b) reported that 9.5 mm GFRP bars exhibited a slightly higher TS retention (95.2%) than their 25.4 mm

counterparts (88.1%) under an alkaline condition due to the presence of shear lag effect (Achillides and Pilakoutas 2004). In contrast, the ILSS and FS of large-sized GFRP bars underwent less deterioration because of the reduced affected thickness in the larger bars. Similar observations on BFRP bars were subsequently noted by Ali et al. (2020). Besides, as shown in Fig. 2.1, existing AAT data for the large-sized FRP bars are notably scarce, especially for those with a diameter of $d_b \geq 20$ mm, irrespective of the conditioning types (Benmokrane et al. 2017b; Benmokrane et al. 2017c; Sawpan 2019; Ali et al. 2020; Sawpan 2021; D'Antino et al. 2023; Feng et al. 2024b). To better understand the degradation behavior of different-sized FRP bars, further research efforts are needed on this issue.

2.3.1.2 Saline solution immersion

2.3.1.2.1 Effect of saline solution. The retentions of different mechanical properties versus exposure time for bare GFRP bars (within a specific range of diameter) immersed in saline solutions at different temperatures are shown in each subfigure of Fig. 2.5. Due to the limited data available for flexural properties in saline environments, only four properties (i.e., TS, TM, TSS and ILSS) are presented. As expected, the TS retention of GFRP bars generally decreases with increasing immersion time and temperature in saline solutions, whereas TM remains stable [see Fig. 2.5(b)]. TSS share a similar retention tendency with TS under saline conditions, as depicted in Fig. 2.5(c), despite the fact that the AAT data for TSS were derived from a single study (Ruiz Emparanza et al. 2022) due to the scarcity of related research. Fig. 2.5(d) reveals considerable scatter in the ILSS data for GFRP bars, which can also be attributed to the various factors affecting the durability of ILSS in FRP bars, as discussed in Section 2.3.1.1.3. Another observation that can be made from Fig. 2.5 is that, compared to alkaline solutions, the TS degradation of GFRP bars is more moderate in saline

solutions. For example, after one year, the trendlines for TS retention of GFRP bars under 60°C saline conditions and 60°C low-pH conditions ($10 \leq pH < 12.6$) terminate at around 60% [Fig. 2.5(a)] and 36% [Fig. 2.2(a)], respectively. This is because glass fibers are particularly sensitive to fluids ingress (e.g., chemical attacks) due to leaching and etching actions, especially in alkaline and water solutions (Chen et al. 2007; Kim et al. 2008; Wang et al. 2017b; Fergani et al. 2018a; Lu et al. 2020a). It is noteworthy that the tensile durability of GFRP bars was found to be insensitive to the saline contents of the exposure solution, as concluded by Wang et al. (2023a).

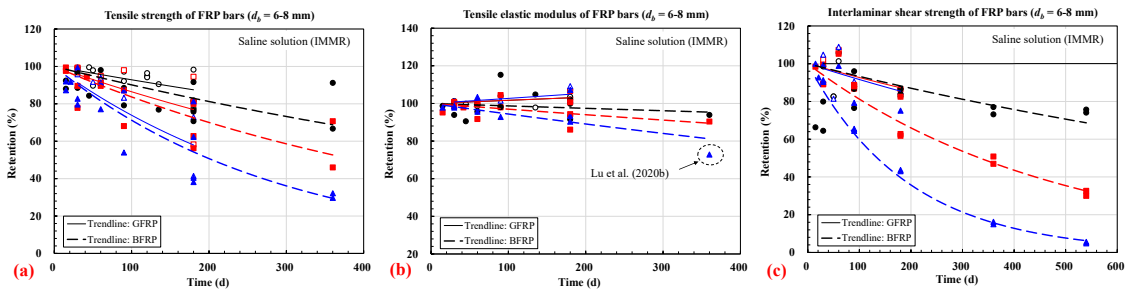


○ 20-30°C
(a) [Tannous and Saadatmanesh 1998 (6); Won and Park 2006 (2); Chen et al. 2007 (1); Lu et al. 2020a (4); Lu et al. 2022a (4); Ruiz Emparanza et al. 2022 (24); Wang et al. 2023 (5)]; (b) [Lu et al. 2020a (4); Lu et al. 2022a (4); Ruiz Emparanza et al. 2022 (24); Wang et al. 2023 (1)]; (c) [Ruiz Emparanza et al. 2022 (24)]; (d) [Won and Park 2006 (2); Manalo et al. 2020 (3); Starkova et al. 2021 (2); Lu et al. 2020a (4); Ruiz Emparanza et al. 2022 (24)]
□ 40°C
(a) [Chen et al. 2007 (1); Lu et al. 2022a (4); Ruiz Emparanza et al. 2022 (12); Wang et al. 2023 (5)]; (b) [Lu et al. 2022a (4); Ruiz Emparanza et al. 2022 (12); Wang et al. 2023 (1)]; (c) [Ruiz Emparanza et al. 2022 (12)]; (d) [Lu et al. 2022a (4); Ruiz Emparanza et al. 2022 (12)]
△ 60°C
(a) [Chen et al. 2007 (1); Aydın and Arslan 2021 (1); Lu et al. 2022a (4); Ruiz Emparanza et al. 2022 (24); Wang et al. 2023 (5)]; (b) [Lu et al. 2022a (4); Ruiz Emparanza et al. 2022 (24); Wang et al. 2023 (1)]; (c) [Ruiz Emparanza et al. 2022 (24)]; (d) [Chen et al. 2007 (1); Manalo et al. 2020 (3); Lu et al. 2022a (4); Ruiz Emparanza et al. 2022 (24)]

Fig. 2.5 Effect of saline solution on the durability of bare GFRP bars

2.3.1.2.2 Effect of fiber type. Fig. 2.6 shows a comparison of mechanical properties between bare GFRP and BFRP bars (d_b = 6-8 mm) exposed to saline conditions at different temperatures. As shown in Figs. 2.6(a) and 2.6(c), the TS and ILSS of both types of FRP bars degrade gradually as the temperature and immersion time increase. Notably, the trendlines for TS retention of GFRP bars are higher than those of BFRP

bars, showing that GFRP bars have better corrosion resistance than the BFRP bars in a saline environment, which is consistent with the findings reported by other researchers (Duo et al. 2021; Wu et al. 2023). However, this conclusion needs to be further verified since most test results were sourced from BFRP bars provided by two manufacturers, as mentioned previously. In addition to TS, more research concerning the durability of shear and flexural properties of FRP bars subjected to saline environments is required to draw a more consolidated conclusion. Conversely, as shown in Fig. 2.6(b), the difference in TM retentions between the two types of FRP bars is not significant, which is similar to that observed in alkaline solutions [see Fig. 2.3(b)].



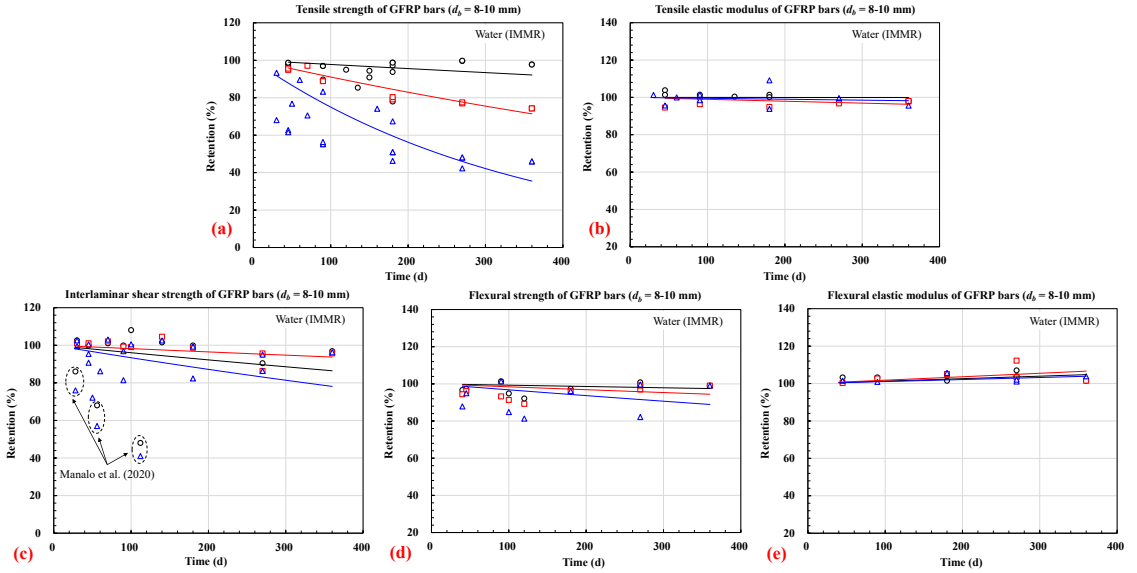
GFRP_20-30°C
(a) [Won et al. 2013 (2); Lu et al. 2020a (4); Lu et al. 2020d (1); Lu et al. 2022a (4); Sun et al. 2022 (3)]; (b) [Lu et al. 2020a (4); Lu et al. 2020d (1); Lu et al. 2022a (4)]; (c) [Won et al. 2013 (2); Starkova et al. 2021 (2); Lu et al. 2022a (4)]
GFRP_40°C
(a) [Lu et al. 2020d (1); Lu et al. 2022a (4)]; (b) [Lu et al. 2020d (1); Lu et al. 2022a (4)]; (c) [Lu et al. 2022a (4)]
GFRP_60°C
(a) [Won 20013 (1); Lu et al. 2020d (1); Lu et al. 2022a (4)]; (b) [Lu et al. 2020d (1); Lu et al. 2022a (4)]; (c) [Won 20013 (1); Lu et al. 2022a (4)]
BFRP_20-30°C
(a) [Lu et al. 2020a (4); Lu et al. 2020b (5); Lu et al. 2020d (1); Lu et al. 2021b (5); Lu et al. 2022a (4)]; (b) [Lu et al. 2020a (4); Lu et al. 2020b (5); Lu et al. 2020d (1); Lu et al. 2022a (4)]; (c) [Lu et al. 2020c (4); Lu et al. 2022a (4); Xie et al. 2022 (7)]
BFRP_40°C
(a) [Wu et al. 2015 (1); Lu et al. 2020b (5); Lu et al. 2020d (1); Lu et al. 2021b (5); Lu et al. 2022a (4)]; (b) [Wu et al. 2015 (1); Lu et al. 2020b (5); Lu et al. 2020d (1); Lu et al. 2022a (4)]; (c) [Lu et al. 2020c (4); Lu et al. 2022a (4); Xie et al. 2022 (7)]
BFRP_60°C
(a) [Quagliarini et al. 2016 (1); Lu et al. 2020b (5); Lu et al. 2020d (1); Lu et al. 2021b (5); Lu et al. 2022a (4)]; (b) [Lu et al. 2020b (5); Lu et al. 2020d (1); Lu et al. 2022a (4)]; (c) [Quagliarini et al. 2016 (1); Lu et al. 2020c (4); Lu et al. 2022a (4); Xie et al. 2022 (7)]

Fig. 2.6 Effect of fiber type on the durability of bare FRP bars under saline conditions

2.3.1.3 Water immersion

2.3.1.3.1 Effect of water. The AAT results of bare GFRP bars having the same diameter range (8-10 mm) immersed in water at different temperatures are shown in each subfigure of Fig. 2.7. Similar to the observations in alkaline environments, the retentions of TS, ILSS and FS of GFRP bars exposed to water show descending trends as both temperature and immersion duration increase, especially for TS [see Figs. 2.7(a),

2.7(c) and 2.7(d)]. The significant differences existing in different studies for ILSS retentions [Fig. 2.7(c)] can also be attributable to the reasons mentioned in Section 2.3.1.1.3. Additionally, it seems that under water conditions, the TS of GFRP bars with diameters of 8-10 mm deteriorates more slowly than under alkaline conditions (especially for the medium and high pH levels, i.e., pH ≥ 12.6) but more rapidly than under saline conditions. For instance, after one year of immersion at 60℃, the TS retentions corresponding to the trendlines for alkaline (12.6 ≤ pH < 13), water and saline solutions are approximately 24%, 36% and 60%, respectively. This indicates that the TS degradation rate of GFRP bars generally obeys the following trend: alkaline > water > saline [see Figs. 2.2(a), 2.5(a) and 2.7(a)]. These observations are consistent with the findings reported by Duo et al. (2021), and similar phenomena regarding ILSS of GFRP bars were also noticed by Manalo et al. (2020). Manalo et al. (2020) concluded that the diffusion rate of water molecules could be slowed down by large salt molecules in saline solutions by blocking the paths, while Almusallam et al. (2013) explained that a very thin layer of salt formed on the surface of FRP bars may decrease the diffusion rate of the solution into the FRP bars, leading to lower water absorption for GFRP bars in saline solutions compared to water, especially at higher temperatures. In contrast, the retentions of TM and FM, however, change insignificantly over time for all exposure temperatures [see Fig. 2.7(b), 2.7(d) and 2.7(e)].



20-30°C
(a) [Tannous and Saadatmanesh 1998 (2); Chen et al. 2007 (1); Davalos et al. 2011 (2); Lu et al. 2020a (4); Wang et al. 2022 (5); Wang et al. 2023 (5)]; (b) [Lu et al. 2020a (4); Wang et al. 2022 (3); Wang et al. 2023 (1)]; (c) [Fergani et al. 2018 (1); Manalo et al. 2020 (3); Yu et al. 2021 (4); Wang et al. 2022 (5)]; (d) [Robert et al. 2010 (3); Fergani et al. 2018 (1); Wang et al. 2022 (5)]; (e) [Fergani et al. 2018 (1); Wang et al. 2022 (5)]

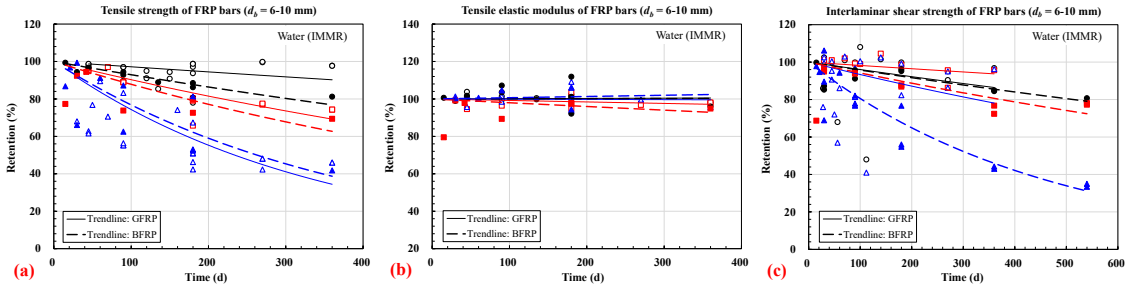
40°C
(a) [Chen et al. 2007 (1); Wang et al. 2022 (5); Wang et al. 2023 (5)]; (b) [Wang et al. 2022 (5); Wang et al. 2023 (1)]; (c) [Fergani et al. 2018 (1); Yu et al. 2021 (4); Wang et al. 2022 (5)]; (d) [Robert et al. 2010 (3); Fergani et al. 2018 (1); Wang et al. 2022 (5)]; (e) [Fergani et al. 2018 (1); Wang et al. 2022 (5)]

60°C
(a) [Mukherjee and Arwikar 2005 (4); Won and Park 2006 (1); Chen et al. 2007 (1); Aydın and Arslan 2021 (1); Wang et al. 2022 (5); Lu et al. 2022a (4); Wang et al. 2023 (5)]; (b) [Wang et al. 2022 (4); Lu et al. 2022a (4); Wang et al. 2023 (1)]; (c) [Won and Park 2006 (1); Chen et al. 2007 (2); Fergani et al. 2018 (1); Manalo et al. 2020 (3); Yu et al. 2021 (4); Lu et al. 2022a (4); Wang et al. 2022 (5)]; (d) [Robert et al. 2010 (3); Fergani et al. 2018 (1); Wang et al. 2022 (5)]; (e) [Fergani et al. 2018 (1); Wang et al. 2022 (5)]

Fig. 2.7 Effect of water on the durability of bare GFRP bars

2.3.1.3.2 Effect of fiber type. Fig. 2.8 shows the effect of fiber type on the durability of bare FRP bars exposed to water at different temperatures. Again, a majority of BFRP bar data were collected from the products provided by two manufacturers, as previously indicated. As shown in Figs. 2.8(a) and 2.8(c), for TS and ILSS, both types of FRP bars show a significant decreasing tendency with the increase of exposure temperature and time, particularly for those exposed to the temperature of 60°C. Besides, both the TS and ILSS of BFRP bars experience larger reductions than those of GFRP bars under the same conditions, except for the TS of GFRP bars at 60°C, where the trendline for GFRP bars is slightly lower than that for BFRP bars. Note that the GFRP bar products used by Lu et al. (2020d) and Wang et al. (2022) were sourced from the same manufacturer, which showed significant degradation after exposure to water at 60°C. Moreover, similar to the observations made in alkaline and saline solutions, the difference in TM retention between the two types of FRP bars is not significant [see Fig. 2.8(b)].

It is evident that, compared to the tensile properties, the durability studies on the shear and flexural properties of FRP bars under water conditions are extremely limited. Hence, more relevant experimental work is needed to draw more comprehensive conclusions about the durability of FRP bars.



GFRP_20-30°C
(a) [Tannous and Saadatmanesh 1998 (2); Chen et al. 2007 (1); Davalos et al. 2011 (2); Lu et al. 2020a (4); Lu et al. 2020d (1); Sun et al. 2022 (1); Wang et al. 2022 (5); Wang et al. 2023 (5)]; (b) [Lu et al. 2020a (4); Lu et al. 2020d (1); Wang et al. 2022 (3); Wang et al. 2023 (1)]; (c) [Fergani et al. 2018 (1); Manalo et al. 2020 (3); Yu et al. 2021 (4); Wang et al. 2022 (5)]

GFRP_40°C
(a) [Chen et al. 2007 (1); Lu et al. 2020d (1); Wang et al. 2022 (5); Wang et al. 2023 (5)]; (b) [Lu et al. 2020d (1); Wang et al. 2022 (5); Wang et al. 2023 (1)]; (c) [Fergani et al. 2018 (1); Yu et al. 2021 (4); Wang et al. 2022 (5)]

GFRP_60°C
(a) [Lu et al. 2020d (1); Lu et al. 2022a (4); Wang et al. 2022 (4); Wang et al. 2023 (5)]; (b) [Lu et al. 2020d (1); Lu et al. 2022a (4); Wang et al. 2022 (4); Wang et al. 2023 (1)]; (c) [Won and Park 2006 (1); Chen et al. 2007 (2); Fergani et al. 2018 (1); Manalo et al. 2020 (3); Yu et al. 2021 (4); Lu et al. 2022a (4); Wang et al. 2022 (5)]

BFRP_20-30°C
(a) [Lu et al. 2020a (4); Lu et al. 2020d (1); Lu et al. 2021b (5)]; (b) [Lu et al. 2020a (4); Lu et al. 2020d (1); Lu et al. 2021b (5)]; (c) [Lu et al. 2020c (4); Xie et al. 2022 (7)]

BFRP_40°C
(a) [Wu et al. 2015 (1); Lu et al. 2020d (1); Lu et al. 2021b (5)]; (b) [Wu et al. 2015 (1); Lu et al. 2020d (1); Lu et al. 2021b (5)]; (c) [Lu et al. 2020c (4); Xie et al. 2022 (7)]

BFRP_60°C
(a) [Quagliarini et al. 2016 (1); Lu et al. 2020d (1); Lu et al. 2021b (5); Lu et al. 2022a (4)]; (b) [Lu et al. 2020d (1); Lu et al. 2022a (4)]; (c) [Quagliarini et al. 2016 (1); Lu et al. 2022a (4); Lu et al. 2022c (4); Xie et al. 2022 (7)]

Fig. 2.8 Effect of fiber type on the durability of bare FRP bars under water conditions

2.3.1.4 Other conditions

In addition to the above-mentioned three commonly simulated conditions, the effects of other conditions such as acid solution immersion, WD cycles, FT cycles, UV radiation and exposure to high and low temperatures on the long-term mechanical properties of bare FRP bars have been experimentally investigated by some researchers. However, since limited test results are available for bare FRP bars under these conditions, only the TS retentions of bare GFRP bars subjected to WD cycles, FT cycles, acid solution immersion and UV radiation are discussed in this section. Note that no standard specifications have been established for most of these conditions, resulting in varying conditioning regimes across different studies with respect to exposure temperature and duration.

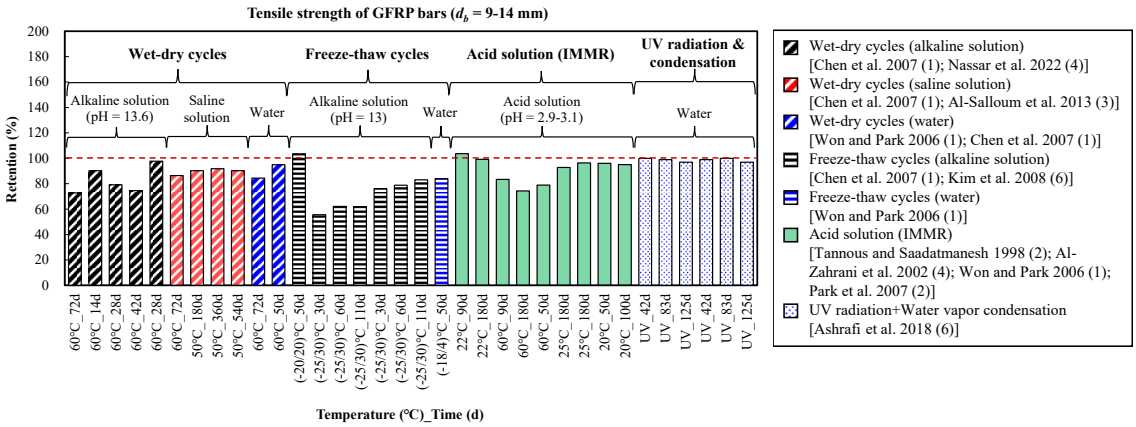


Fig. 2.9 Effects of WD cycles, FT cycles, acid solution immersion and UV radiation on the durability of bare GFRP bars

The TS retentions of GFRP bars (d_b = 9-14 mm) subjected to various conditions, including (1) WD cycles in alkaline, saline and water solutions, (2) FT cycles in alkaline and water solutions, (3) acid solution immersion, and (4) UV radiation with water vapor condensation at different temperatures for different exposure times, are presented in Fig. 2.9. It seems that WD cycles in an alkaline solution (pH = 13.6) result in more severe TS degradation than those in water and saline solutions, which is similar to the degradation law observed under continuous immersion conditions, as mentioned in Section 2.3.1.3.1. For example, the TS retentions of the GFRP bars after 72-day WD cycles in alkaline, saline and water solutions are 72.76%, 86.38% and 84.44%, respectively, as reported in Chen et al. (2007). However, this finding needs to be further confirmed as Chen et al. (2007) is the sole existing study examining the effects of WD cycles in three different solutions on the durability of bare FRP bars. In the cases of FT cycles, significant discrepancies in TS retention of vinylester-based GFRP bars in alkaline solutions have been observed among different studies (Chen et al. 2007; Kim et al. 2008), which can be attributed to the differences in cooling and heating temperatures (-20/20°C and -25/30°C, respectively) as well as inherent differences in the GFRP bars. Compared to the extensive research conducted on GFRP bars immersed in alkaline,

saline and water solutions, significantly fewer studies have investigated the effect of acid solutions on the degradation of GFRP bars. As shown in Fig. 2.9, acid solutions (pH = 2.9~3.1) at temperatures ranging from 20℃ to 25℃ have a negligible effect on the TS of GFRP bars, even after 180 days of exposure. In addition, Al-Zahrani et al. (2002) observed that increasing the exposure temperature from 22℃ to 60℃ resulted in a significant decrease in TS retention under the same acid conditions, which is consistent with the findings from previous discussions on alkaline, saline and water solutions. For the conditioning of UV radiation accompanied with water vapor condensation, the TS of GFRP bars barely changed after exposure for up to 125 days, as reported by Ashrafi et al. (2018). Based on the above discussions, it may be concluded that standard specifications for conditioning regimes under these conditions are needed, and more relevant experimental tests are also required in the future.

2.3.2 Coupled Effects of Environmental and Loading Conditions

As an alternative reinforcement to conventional steel rebar in concrete structures, the coupled effects of environmental conditions and sustained load on the durability of bare FRP bars also represent a critical issue that needs to be evaluated, especially for FRP bars used in prestressed and reinforced concrete structures subjected to high permanent loads. To address this concern, existing AAT results for bare BFRP and GFRP bars under the coupled actions of sustained loading and environmental conditioning (e.g., continuous immersion in alkaline, saline, acid and water solutions) are compared. The mechanical properties considered in this section are limited to TS due to the scarcity of studies focusing on the other properties (Fergani et al. 2018a).

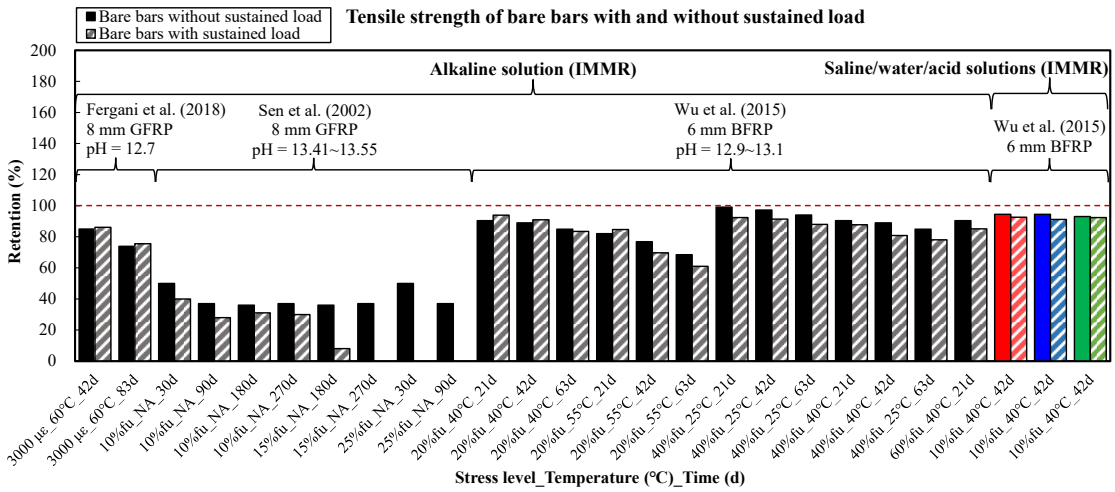


Fig. 2.10 Coupled effects of environmental and loading conditions on the durability of bare FRP bars

Fig. 2.10 compares the TS retentions of bare FRP bars with and without sustained load under the same environmental conditions. Only the AAT data from studies that simultaneously investigated the durability of both stressed and unstressed FRP bars are included in Fig. 2.10, as a result of which the loading condition becomes the sole influencing factor. It is clear that, in alkaline environments, the TS retentions of FRP bars apparently decrease with increasing exposure temperature (Wu et al. 2015) and time (Sen et al. 2002; Wu et al. 2015; Fergani et al. 2018a), regardless of the presence of sustained load. Besides, under the same conditions, the applied sustained load, ranging from 10% to 60% of the short-term tensile strength (f_u) or corresponding to a strain of 3000 microstrains (i.e., 3000 $\mu\varepsilon$), generally has a non-negligible effect on the TS deterioration of bare FRP bars. This phenomenon is primarily because the microcracks in the matrix or those generated by the sustained load would allow the surrounding media to ingress the matrix, thereby accelerating the deterioration of FRP bars (Debaiky Ahmed et al. 2006; Wu et al. 2015; Fergani et al. 2018a). Another interesting observation from Sen et al. (2002) is that, some FRP bars with stress levels of 15% and 25% f_u experienced a complete reduction in TS (100% loss) after exposure

to alkaline solutions, which might be caused by the poor inherent properties of GFRP bars combined with the high alkaline concentration (pH = 13.41-13.55), as reported by the authors.

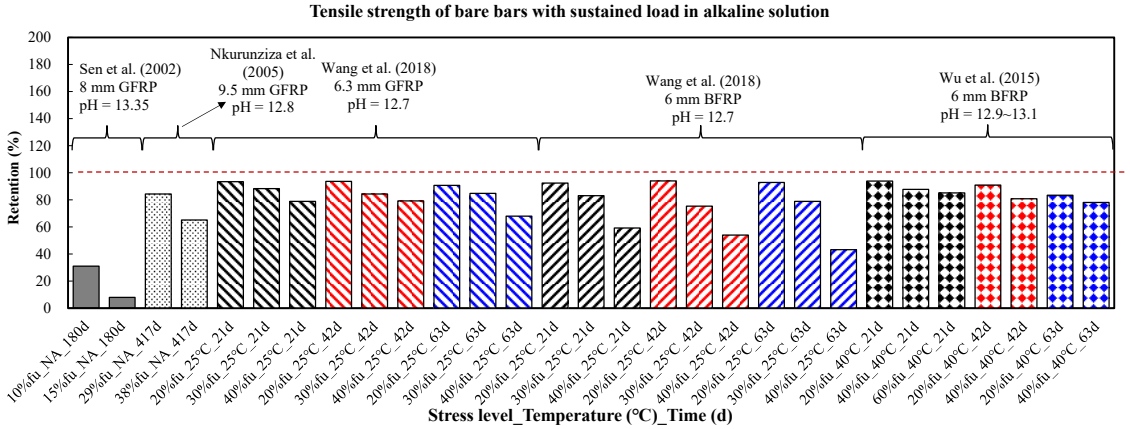


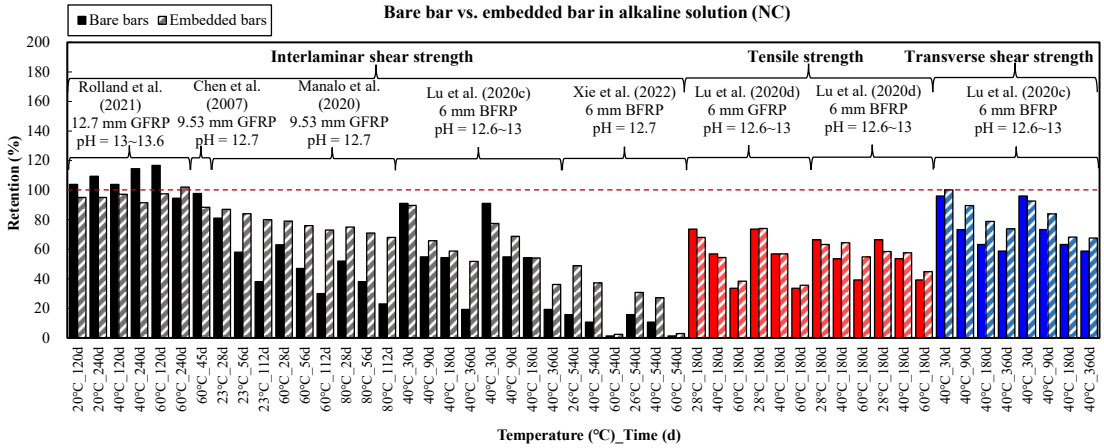
Fig. 2.11 Tensile strength retentions of bare FRP bars with different stress levels under the same alkaline condition

To further study the detrimental effect of sustained load on the durability of bare FRP bars, the TS retentions of FRP bars with different stress levels while exposed to the same alkaline conditions are shown in Fig. 2.11. Note that the data represented by the same pattern in the bar chart corresponds to the same type of FRP bars under the same environmental conditions but with different stress levels. As expected, the TS retentions of bare FRP bars decrease as the stress level increases. However, it should be mentioned that devices for applying sustained stress to FRP bars differed across different studies, indicating a need for standard testing guidelines to ensure more reliable results in this area. In addition to establishing standard testing methods, future research should also focus on the possible size effect on the durability of bare FRP bars with sustained load. Currently, only one study has addressed the durability of stressed bare FPR bars with large diameters ($d_b \geq 20$ mm) (D'Antino et al. 2023), in which the residual TS of 6-, 20- and 32-mm stressed GFRP bars (with sustained load

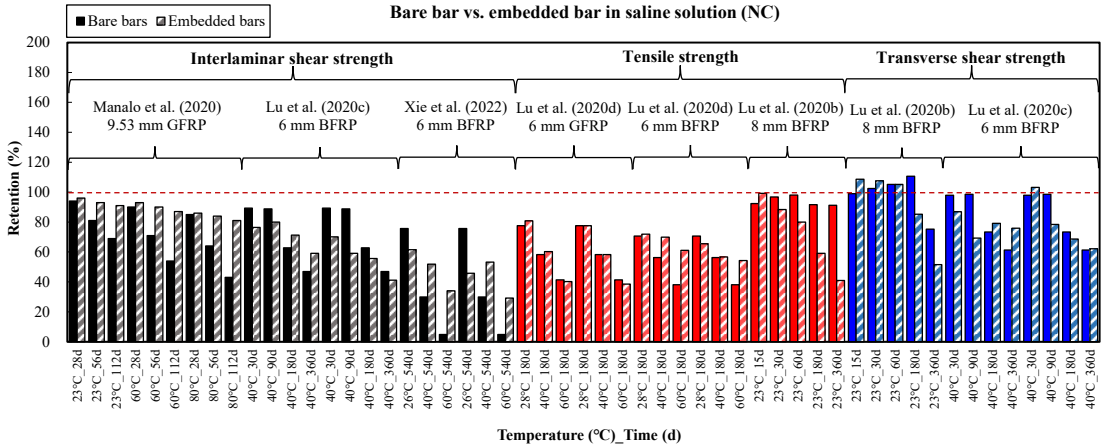
corresponding to 3000 $\mu\varepsilon$) after 42-day immersion in 60℃ alkaline solution (pH = 13) were reported as 92.06%, 87.11% and 86.53%, respectively. The authors suggested an improvement in the manufacturing and testing processes for large-sized GFRP bars.

2.4 FRP BARS EMBEDDED IN CONCRETE

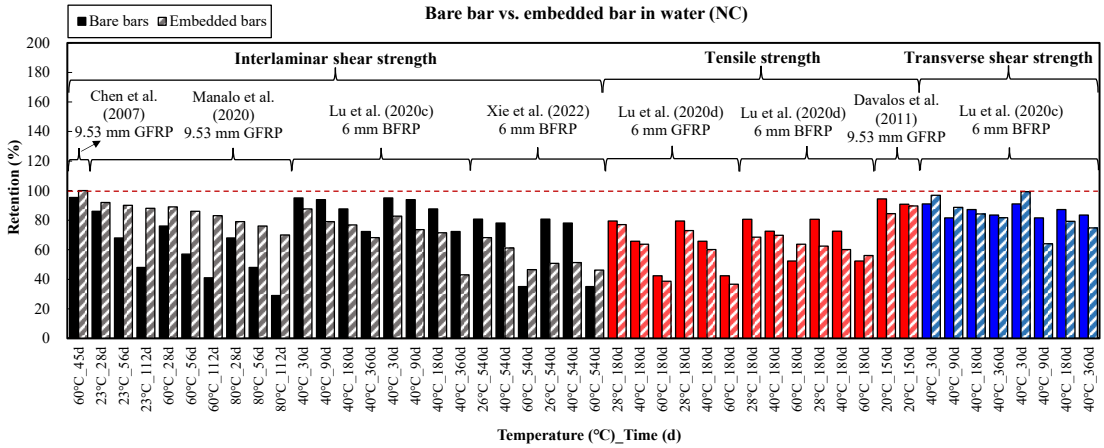
As internal reinforcements, FRP bars are continuously exposed to the concrete environment, which is characterized by high alkalinity, as well as to various external environmental conditions (e.g., high moisture and saline content) during the service life of concrete structures. These factors can simultaneously degrade the FRP bars alone and the bond between FRP bars and concrete. Thus, compared to bare FRP bars that are directly exposed to various environmental conditions, FRP bars embedded in concrete (i.e., concrete-embedded FRP bars) can better represent the real-world conditions encountered in field applications. Currently, the commonly used method for assessing the durability of concrete-embedded FRP bars is to extract the FRP bars from the concrete cover after exposure to simulated conditions for specific exposure time. To evaluate the degradation behavior of FRP bars wrapped in concrete, AAT results related to the TS, ILSS and TSS of concrete-embedded FRP bars subjected to different environmental conditions are compared. In addition, the durability of the BS between FRP bars and concrete is assessed. Note that the concrete type discussed in this section primarily refers to normal concrete unless otherwise specified.



(a) Alkaline solution



(b) Saline solution



(c) Water

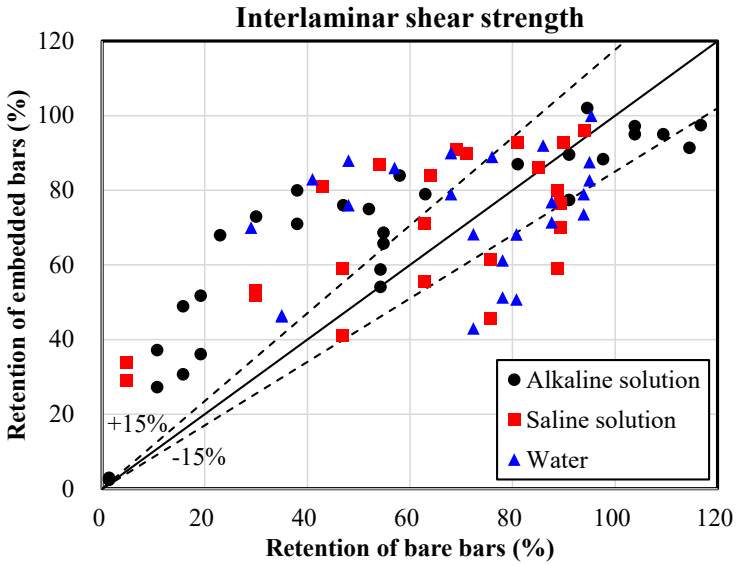
Fig. 2.12 Comparison of mechanical properties between bare FRP bars and concrete-embedded FRP bars under the same condition

2.4.1 Tensile Strength, Interlaminar Shear Strength and Transverse Shear Strength

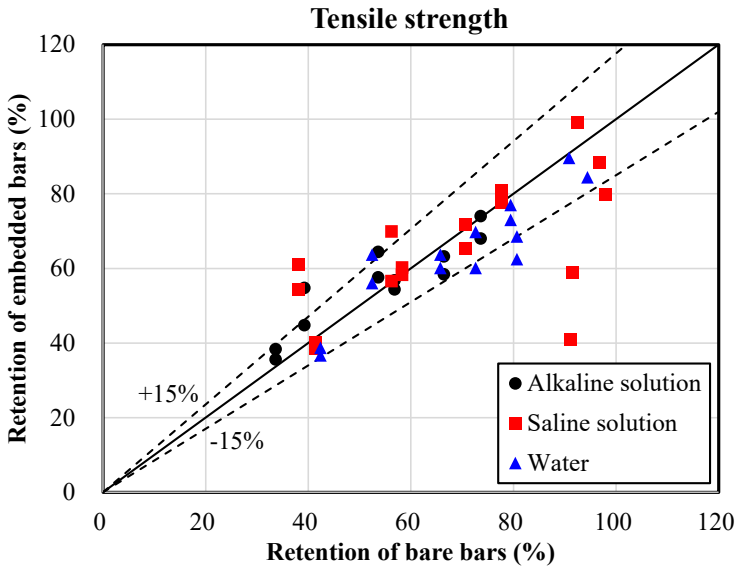
Figs. 2.12(a), 2.12(b) and 2.12(c) show the comparisons of mechanical properties (i.e., ILSS, TS and TSS) between bare and concrete-embedded FRP bars immersed in alkaline, saline and water solutions at different exposure temperatures and durations, respectively. To ensure that the concrete cover becomes the sole influencing parameter, only AAT results from studies that simultaneously focus on the durability of both bare and concrete-embedded FRP bars are included. In Fig. 2.12, it can be found that there exist significant discrepancies in the relationships of mechanical properties between bare and concrete-embedded FRP bars, making it difficult to draw clear conclusions on this issue, regardless of the solution type. For instance, Manalo et al. (2020) observed a noticeably greater reduction in ILSS for bare GFRP bars compared to their concrete-embedded counterparts, regardless of the solution type. In contrast, Rolland et al. (2021) and Lu et al. (2020b) reported opposing trends in alkaline and saline/water environments, respectively. This phenomenon might be attributable to at least the following factors: (1) Concrete covers made with different mix proportions exhibit different alkalinities (i.e., pH levels) and chemical compositions, which has been proven to have a considerable effect on the durability of mechanical properties of concrete-embedded FRP bars (Morales et al. 2021; Xie et al. 2022); (2) Concrete covers with different thicknesses can result in different alkalinities surrounding the FRP bars (Lu et al. 2020b; Lu et al. 2020d; Xie et al. 2022); (3) Inadequate procedures of bar extraction may also influence the reliability of test results for concrete-embedded FRP bars (Gooranorimi and Nanni 2017; Benmokrane et al. 2018).

To have a better insight into the differences between bare and concrete-embedded FRP

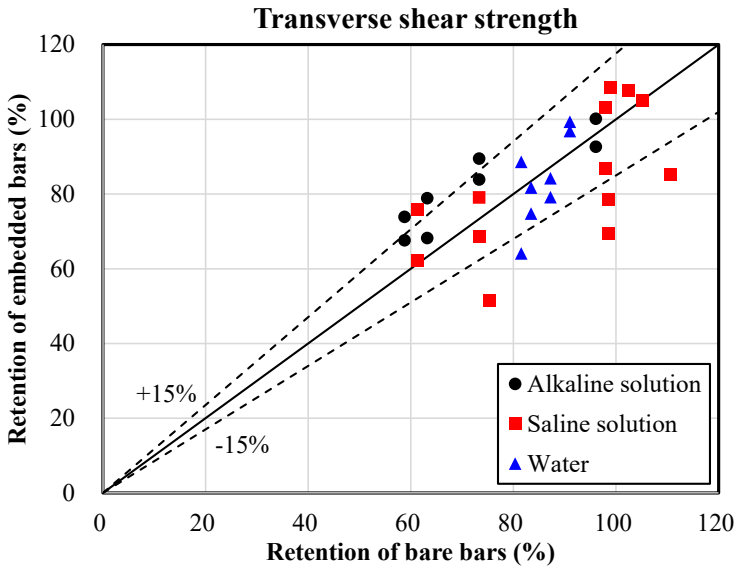
bars, the test data presented in Fig. 2.12 have been regrouped in Fig. 2.13, where the mechanical properties of FRP bars immersed in different solutions are plotted in each subfigure to further compare the effects of solution type on these properties. In Fig. 2.13(a), it is evident that concrete-embedded FRP bars possess relatively higher ILSS retentions than bare FRP bars under the same conditions, especially for the alkaline conditions. This observation can be explained by the reason that the concrete itself might protect the FRP bars from direct exposure to the surrounding solutions (Mufti et al. 2007b; Manalo et al. 2020). However, compared to the ILSS, the differences in TS and TSS between bare and concrete-embedded FRP bars seem to be inconspicuous, as shown in Figs. 2.13(b) and 2.13(c). This phenomenon indicates that the properties of the fiber-resin interface [primarily influence the ILSS (Ali et al. 2020)] of FRP bars are more susceptible to the effects of direct solution immersion compared to the properties of the fibers [predominantly affect TS (Benmokrane et al. 2020b)] and the resin [mainly govern TSS (Montaigu et al. 2013)].



(a) Interlaminar shear strength



(b) Tensile strength



(c) Transverse shear strength

Fig. 2.13 Comparison of mechanical properties between bare and concrete-embedded FRP bars immersed in different solutions

Similar to the research conducted on bare FRP bars, in recent years, considerable efforts have also gone into studying the coupled effects of environmental conditions and sustained load on the durability performance of concrete-embedded FRP bars. Only the TS data from studies that simultaneously investigate the durability of stressed and unstressed concrete-embedded B/GFRP bars are considered herein. Fig. 2.14 presents a

comparison of the TS retentions of concrete-embedded FRP bars subjected to sustained load versus those without sustained load, all under the same environmental condition. It can be found that, at the same stress level, the TS retentions of FRP bars extracted from concrete generally decrease with increasing exposure temperature and time. Additionally, under the same environmental conditions, the strength retentions of concrete-embedded FRP bars with sustained load are generally comparable to that of their unstressed counterparts, with the exception of data for immersion in water and saline solutions from Almusallam and Al-Salloum (2006). These exceptional cases may be mainly caused by the thick layer of high-alkalinity cement paste that coats the GFRP bars at the midpoint of the concrete beam specimens, as reported in Almusallam and Al-Salloum (2006). Fig. 2.15 shows the TS retentions of concrete-embedded FRP bars with different stress levels under the same exposure conditions (including immersion in saline and water solutions). Similar to the behavior observed in bare FRP bars, the deterioration of TS in concrete-embedded FRP bars is generally more pronounced at higher stress levels.

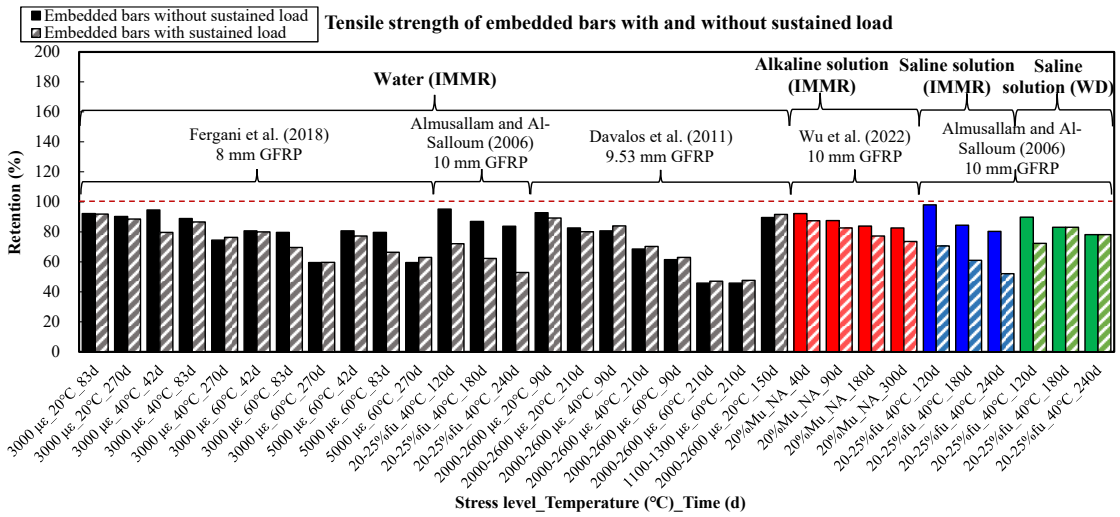


Fig. 2.14 Coupled effects of environmental and loading conditions on the durability of concrete-embedded FRP bars

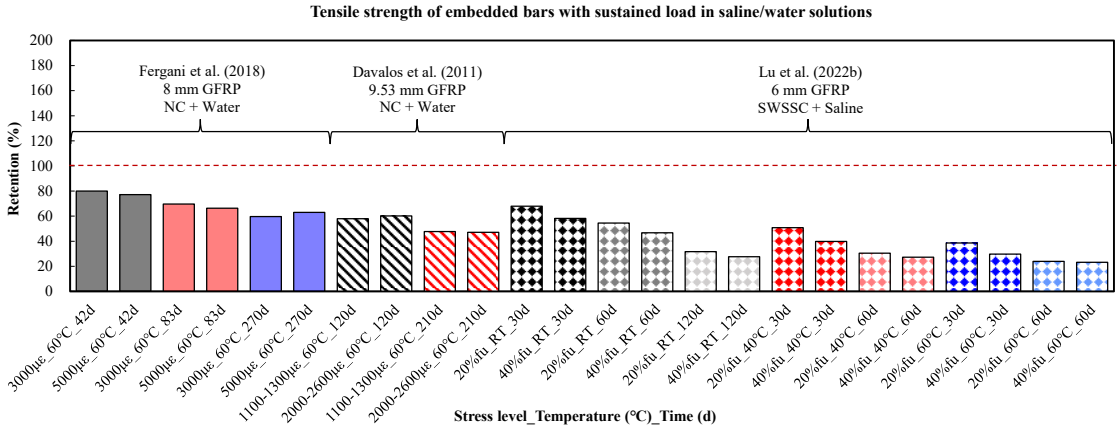


Fig. 2.15 Comparison of tensile strength retentions for concrete-embedded FRP bars with different stress levels

It is worth mentioning that there is no standard specification for the durability of FRP bars wrapped in concrete, and relevant research remains limited. Therefore, considerable efforts are needed in this field.

2.4.2 Bond Strength

Different from the above-mentioned mechanical properties of FRP bars embedded in concrete, the surface configurations (e.g., sand-coated, ribbed, helically-wrapped) of FRP bars have a great impact on the bond behavior as a result of the stress transfer mechanisms between concrete and bars (Solyom and Balázs 2020). Thus, the BS variations in aggressive environments may differ considerably depending on the surface characteristics of FRP bars apart from other factors such as exposure temperature and duration. This section aims to clarify the specific influence of several critical factors on the durability of the bond properties of FRP bars to concrete. Note that the surface treatments of FRP bars discussed in this section are determined based on the extreme external surface conditions. That is to say, sand-coated bars and deformed bars with additional sand-coating are considered to possess the same surface treatment, because the external sand-coated layer mainly influences the post-peak behavior of FRP bars as

demonstrated by Solyom and Balázs (2020). On the other hand, since FRP bars are embedded in the concrete matrix for pullout specimens during exposure, the differences in BS degradation after exposure to various solutions become minor compared to other mechanical properties of FRP bars in the corresponding environments. Given the lack of a clear trend regarding the effect of the bar diameter on BS (Nepomuceno et al. 2021), it is not considered an influencing factor of BS degradation in the following discussions unless otherwise specified.

2.4.2.1 Saline solution immersion

2.4.2.1.1 Effect of surface treatment. As shown in Fig. 2.16, the results show quite a large dispersion for the overall trend. Due to the combined effects of solution immersion and increased temperature, the concrete and FRP bars may undergo post-curing and hygroscopic expansion, respectively, during exposure, resulting in unexpected BS enhancements. Moreover, the BS retentions of ribbed FRP bars generally outperform those of helically-wrapped bars, except those of sand-coated FRP bars under saline solution immersion at 20-30℃ for a certain period. It is interesting to find that a similar trend was also observed in the ultimate BS derived from the well-known modified BPE bond-slip model (Cosenza et al. 1997) for FRP bars. Thus, it can be speculated that the BS degradation extent of FRP bars may have a strong relationship with their ultimate BS. However, when the temperature is increasing, no clear trend could be observed in Fig. 2.16, especially for the 60℃ circumstances. Besides, the long-term test results for helically-wrapped bars seem insufficient in the available literature compared to the other two types of bars, which may need to be further examined in future research. Thus, only ribbed and sand-coated FRP bars are considered in the subsequent discussions.

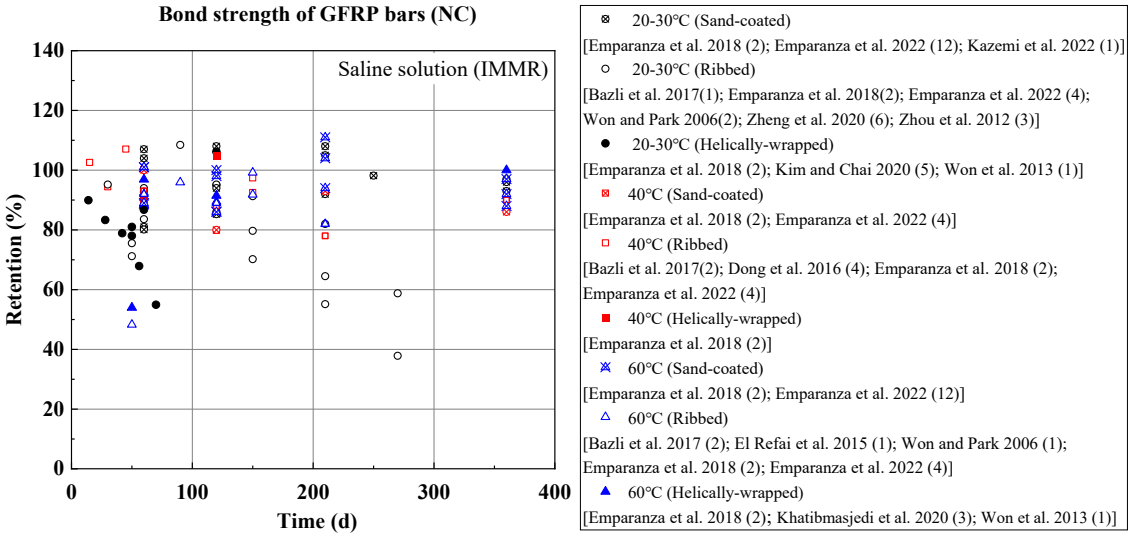


Fig. 2.16 Effect of surface treatment on the durability of bond strength of GFRP bars under saline conditions

2.4.2.1.2 Effects of fiber and resin types. To interpret the effects of fiber and resin types on BS degradation, test results for GFRP, BFRP and CFRP bars from several relevant studies are shown in Fig. 2.17. It can be seen that CFRP bars exhibit the highest BS retentions as a result of the excellent anti-corrosion performance of carbon fibers, while BFRP and GFRP bars possess similar behavior, which is consistent with the observations from Dong et al. (2016a). However, the obtained phenomenon is restricted to exposure durations of less than 100 days due to the unavailable data for BFRP and CFRP bars beyond this range. As mentioned earlier, for any type of FRP bar, there is no observable correlation between temperature variations and BS retention. In addition, the resin type has a great impact on the bar interface, and the alkaline resistance of resin may be directly relevant to the bond durability. In the study conducted by Dong et al. (2016a), they found that the BS retentions of epoxy resin-based BFRP bars were 107.4%, 99.9%, 103.2% and 101.4%, respectively, after 15-, 30-, 45- and 60-day immersion in simulated seawater, while the corresponding values decreased to 97.7%, 98.7%, 94.1% and 91.0% under the same conditions for the vinylester resin-based ones. Conversely, Zheng et al. (2020) reported that better durability of vinylester resin-based

GFRP bars was detected than that of epoxy resin-based ones (see Fig. 2.17). Thus, the long-term performance of resin may also depend on the fiber type and this speculation requires further study and verification based on more available test results.

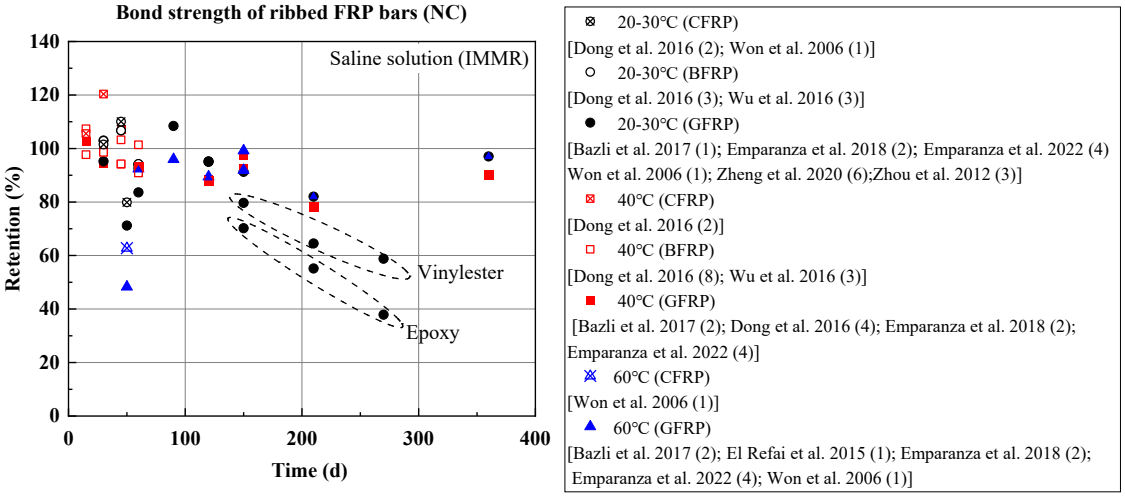


Fig. 2.17 Effects of fiber and resin types on the durability of bond strength of ribbed FRP bars under saline conditions

2.4.2.2 Alkaline solution immersion

2.4.2.2.1 Effect of alkaline concentration. Fig. 2.18 shows the effect of pH on the durability of BS of FRP bars in alkaline environments. It is generally believed that the chemical concentration of alkaline solutions can accelerate both the rate and magnitude of bond degradation due to the increase in hydroxide ions. However, Bazli et al. (2017) revealed that similar BS reduction was observed for the specimens immersed in alkaline solutions with a pH range of 11.0 to 13.6 for 150 days, in which the specimens in the most aggressive environment (pH = 13.6) possessed the highest BS retentions (see Fig. 2.18). Fig. 2.18 also shows that the BS retentions increase with the concentration of alkaline solutions. The reasons for this observation can be attributed to the following two aspects: (1) Concrete matrix provides a barrier to the external environmental conditions and the diffusion of solutions can only be accessed via the voids in concrete.

Consequently, variations in pH may only have a minimal influence on the bar-concrete interface condition; (2) With the increase of pH, a more obvious enhancement in concrete strength is achieved as a result of post-curing, which further improves the compactness of concrete and suppresses the external environmental effects. In addition, regardless of the pH value, sand-coated bars are consistently superior to ribbed bars in terms of durability (see Fig. 2.18).

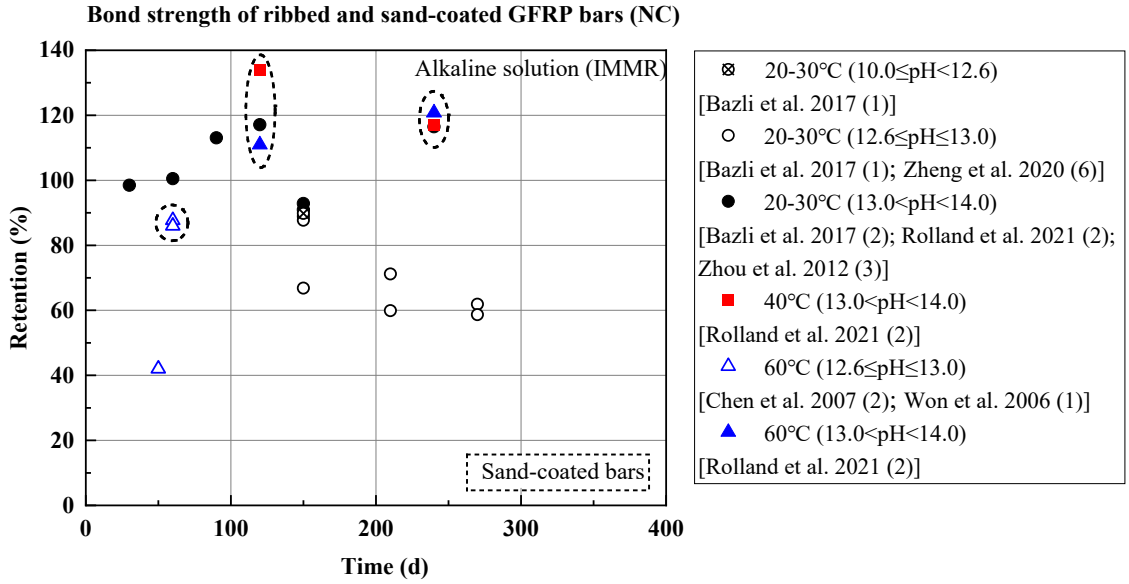


Fig. 2.18 Effect of alkaline concentration on the durability of bond strength of GFRP bars under alkaline conditions

2.4.2.2.2. Effect of fiber type. Fig. 2.19 illustrates the effect of fiber type on the durability of BS of FRP bars under alkaline conditions. Notably, a large dispersion in test results is observed, with most studies focusing on BFRP and GFRP bars rather than CFRP bars. Furthermore, no clear relationship exists between fiber type and BS degradation in alkaline solutions. It should be noted that all sand-coated bars presented in Fig. 2.19 were derived from Lu et al. (2021b), in which the mechanical properties of these BFRP bars were generally found to be inferior to those in other studies, as mentioned previously. As a result, higher retentions of ribbed BFRP bars used by

Hassan et al. (2016) are found under alkaline conditions at 40℃ and 60℃.

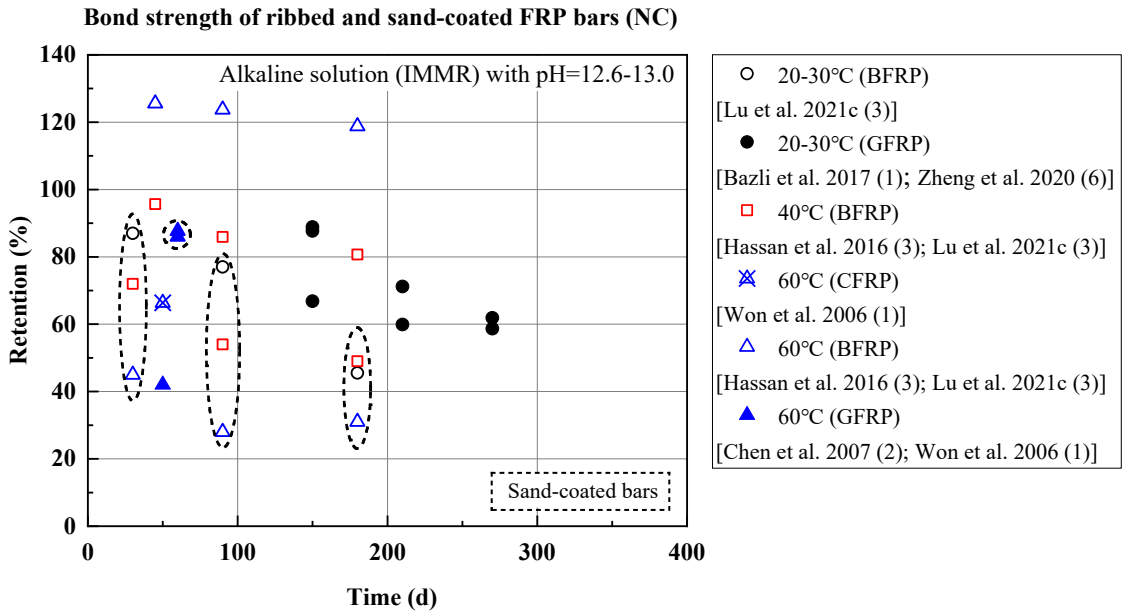


Fig. 2.19 Effect of fiber type on the durability of bond strength of FRP bars under alkaline conditions

2.4.2.3 Water immersion

As shown in Fig. 2.20, similar BS retentions can be observed for the specimens under water immersion compared to those subjected to the aforementioned two types of solutions, with the majority of retentions ranging from 60% to 120%, further indicating that the bond durability is insensitive to the type of solution. After exposure to 20-30℃ water, it can be found that sand-coated bars exhibit stable BS with retentions distributed around 100%, while a conspicuous descending trend is detected for ribbed bars under the same aging conditions. However, the lack of comprehensive test results at higher temperatures makes it difficult to fully quantify the effect of bar surface treatment. Thus, it is suggested that more research is needed in this area.

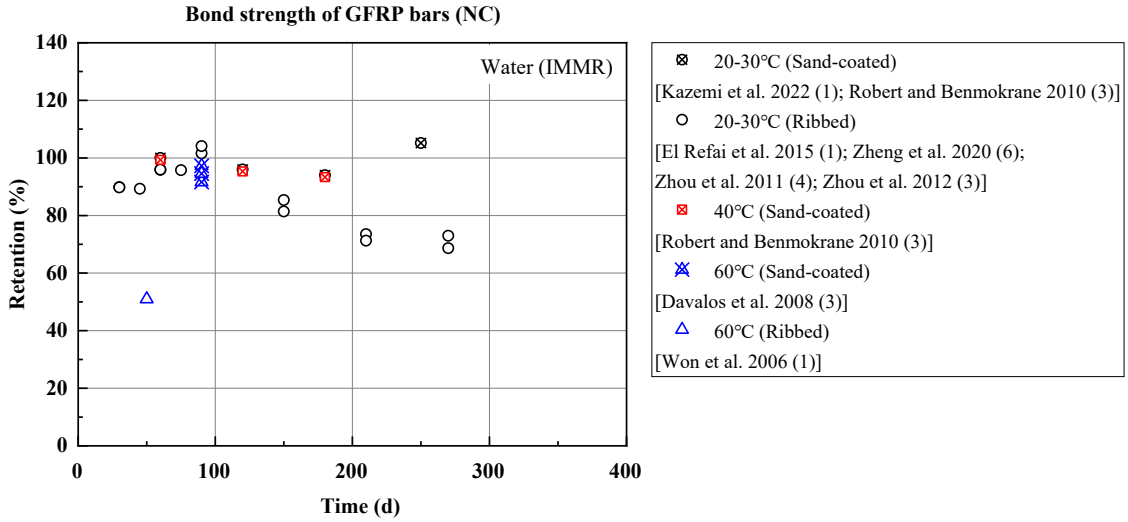
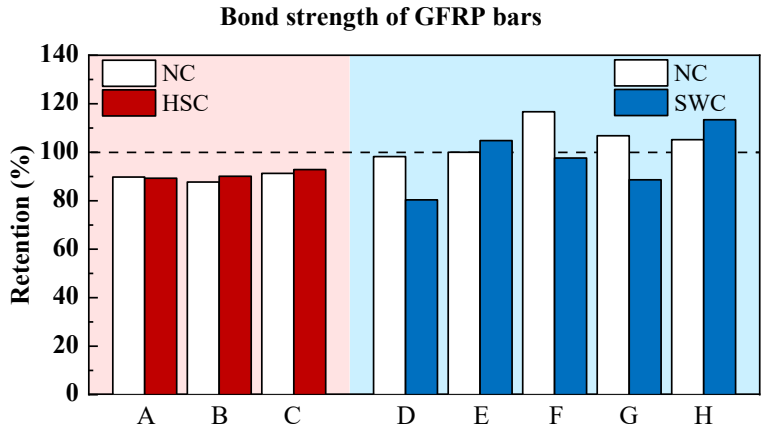


Fig. 2.20 Effect of surface treatment on the durability of bond strength of GFRP bars under water conditions

Apart from the surface characteristics and fiber type of FRP bars, the influence of concrete type on the durability of BS under different environmental conditions is also discussed herein. As shown in Fig. 2.21, NC and HSC possess very similar performance under alkaline and saline solution immersions, which indicates that bond failure may be mainly controlled by the FRP bars rather than the concrete matrix, as noted by Bazli et al. (2017). However, for NC and SWC, no consistent conclusion can be drawn based on the assembled database. Three reasons contribute to this phenomenon. First, due to the presence of chlorides in SWC, the strength development of SWC could be more rapid compared to NC during exposure, leading to improved bond behavior. Second, the coupled effects of alkaline environment and chlorides in SWC may increase the vulnerability of GFRP bars' surface to degradation. Finally, the dissolved chlorides in solutions can also accelerate the rate of portlandite leaching and reduce concrete compactness, and the increased porosity near the bond interface could decrease the BS significantly. Therefore, the interactions resulting from these factors lead to the dispersed observations as in Fig. 2.21.



A: Alkaline solution (IMMR), pH=11.0, 20°C, 150d, ribbed bar (Bazli et al. 2017)
B: Alkaline solution (IMMR), pH=12.7, 20°C, 150d, ribbed bar (Bazli et al. 2017)
C: Saline solution (IMMR), 20°C, 150d, ribbed bar (Bazli et al. 2017)
D: Saline solution (IMMR), 25°C, 250d, sand-coated bar (Kazemi et al. 2022)
E: Saline solution (IMMR), 60°C, 360d, helically-wrapped bar (Khatibmasjedi et al. 2020)
F: Saline solution (IMMR), 60°C, 540d, helically-wrapped bar (Khatibmasjedi et al. 2020)
G: Saline solution (IMMR), 60°C, 720d, helically-wrapped bar (Khatibmasjedi et al. 2020)
H: Water (IMMR), 25°C, 250d, sand-coated bar (Kazemi et al. 2022)

Fig. 2.21 Effect of concrete type on the durability of bond strength of GFRP bars

2.4.3 Relationship Between the Durability of ILSS and BS of FRP Bars

It has been reported that there is a potential relationship between the material degradation of FRP bars (e.g., ILSS) and the corresponding decrease in BS (Bank et al. 1998; Chen et al. 2007). Fig. 2.22 compares the ILSS of bare B/GFRP bars with their corresponding BS under alkaline conditions. As reported by Won and Park (2006) and Lu et al. (2021b), more severe degradation was found in BS than in ILSS under the same conditions. However, an opposite trend was observed by Rolland et al. (2021), where both mechanical properties showed varying degrees of increase. The increased BS may be caused by the coupled effects of the post-curing of concrete and the hygroscopic expansion of FRP bars as mentioned earlier. Similarly, the comparison results for saline conditions are shown in Fig. 2.23. Again, the retention of BS is generally lower than that of ILSS (Won and Park 2006; Won et al. 2013; Lu et al. 2021b; Ruiz Emparanza et al. 2022). The variability in the results reported by Ruiz Emparanza

et al. (2022) could be partially attributed to the significant scatter observed in their tests, as found in the original literature. On the other hand, a comparison between the ILSS of concrete-embedded FRP bars and their corresponding BS is presented in Fig. 2.24, including the results from both alkaline and saline solutions. Conversely, except for the results in Chen et al. (2007), the ILSS of FRP bars embedded in normal concrete exhibits lower retentions than their BS (Khatibmasjedi et al. 2020; Rolland et al. 2021), showing that the ILSS of FRP bars is more sensitive to the concrete environment compared with their BS. However, the possible correlation between the durability of ILSS and BS in FRP bars needs to be further verified due to the limited availability of relevant research.

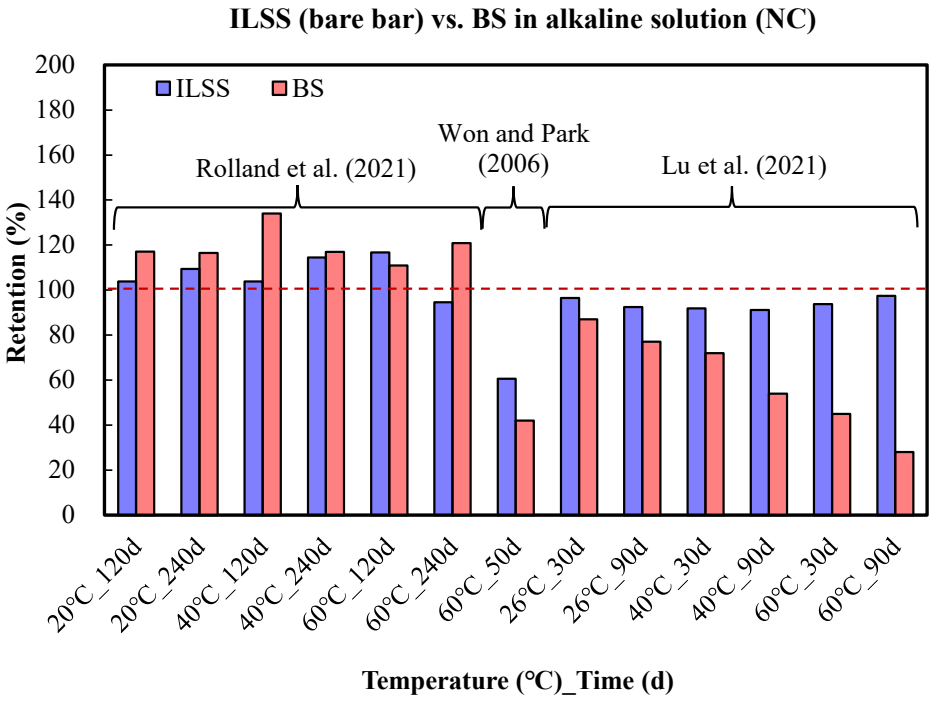


Fig. 2.22 Comparison between interlaminar shear strength of bare FRP bars and their corresponding bond strength under alkaline conditions

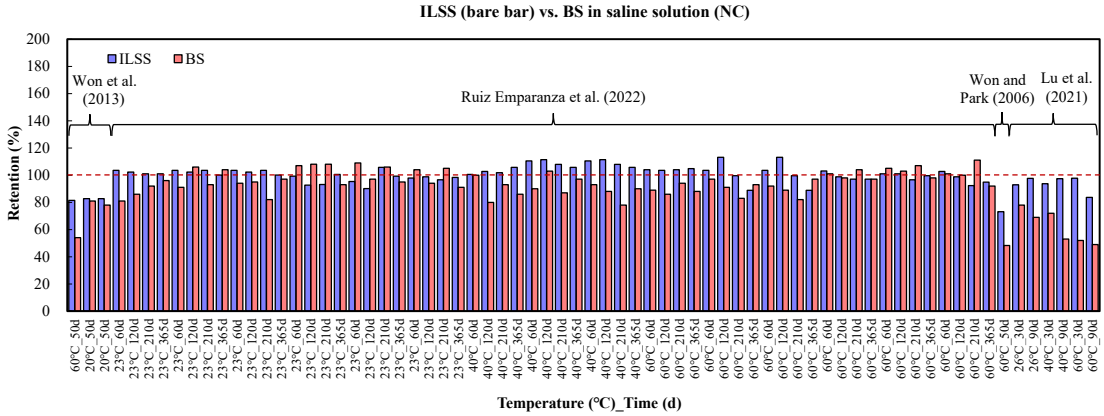


Fig. 2.23 Comparison between interlaminar shear strength of bare FRP bars and their corresponding bond strength under saline conditions

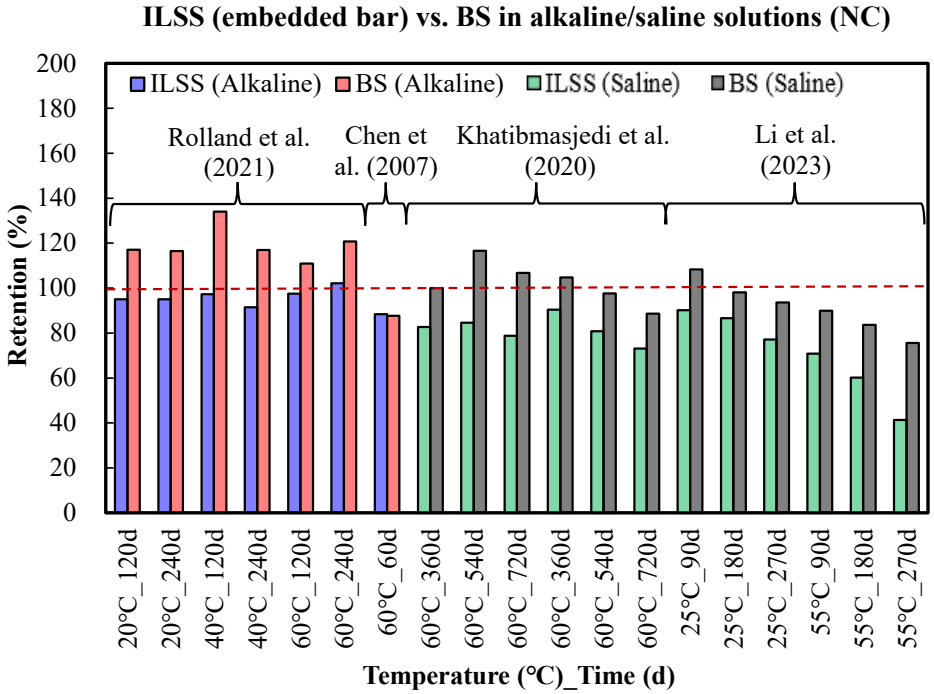


Fig. 2.24 Comparison between interlaminar shear strength of concrete-embedded FRP bars and their corresponding bond strength under alkaline and saline conditions

2.5 FRP-REINFORCED CONCRETE BEAMS

2.5.1 Saline Condition

2.5.1.1 Failure modes and crack patterns

Several studies have investigated the flexural behavior of FRP-reinforced SWSSC

beams under saline solution immersion or wet-dry cycling conditions for different periods (Tannous and Saadatmanesh 1998; Dong et al. 2018c, 2020; Su et al. 2022). As shown in Fig. 2.25, Dong et al. (2018c) found that the failure modes of BFRP-reinforced SWSSC beams tended to shift from flexural failure (concrete crushing) to shear failure (shear compression failure) with the increase in exposure time under seawater immersion conditions. However, no failure mode change was observed for the same batch of beams in seawater WD cycling environments. They concluded that the bond behavior of BFRP stirrups might experience more severe degradation under long-term seawater immersion due to surface damage. Subsequently, the durability of CFRP-reinforced SWSSC beams with the same geometric dimension was assessed under the same environmental condition and exposure duration (Dong et al. 2020). The results showed that although all conditioned beams exhibited similar failure patterns compared with unconditioned specimens, a much sparser cracking spacing was observed in the conditioned beams, which indicated that more conspicuous bond degradation occurred in longitudinal CFRP bars instead of in stirrups. On the other hand, Su et al. (2022) reported that the bond degradation of stirrups was not the sole factor contributing to the change in failure modes after they compared many sets of beams fabricated with different types of stirrups. Thus, it can be speculated that apart from the bond degradation of stirrups, variations in beam size, shear span ratio, concrete strength, reinforcement ratio and aging temperature may also have great impacts on the failure modes and crack patterns of FRP-reinforced concrete beams under saline conditions. Considering that there is limited research on this topic, more research is urgently needed to clarify these issues.

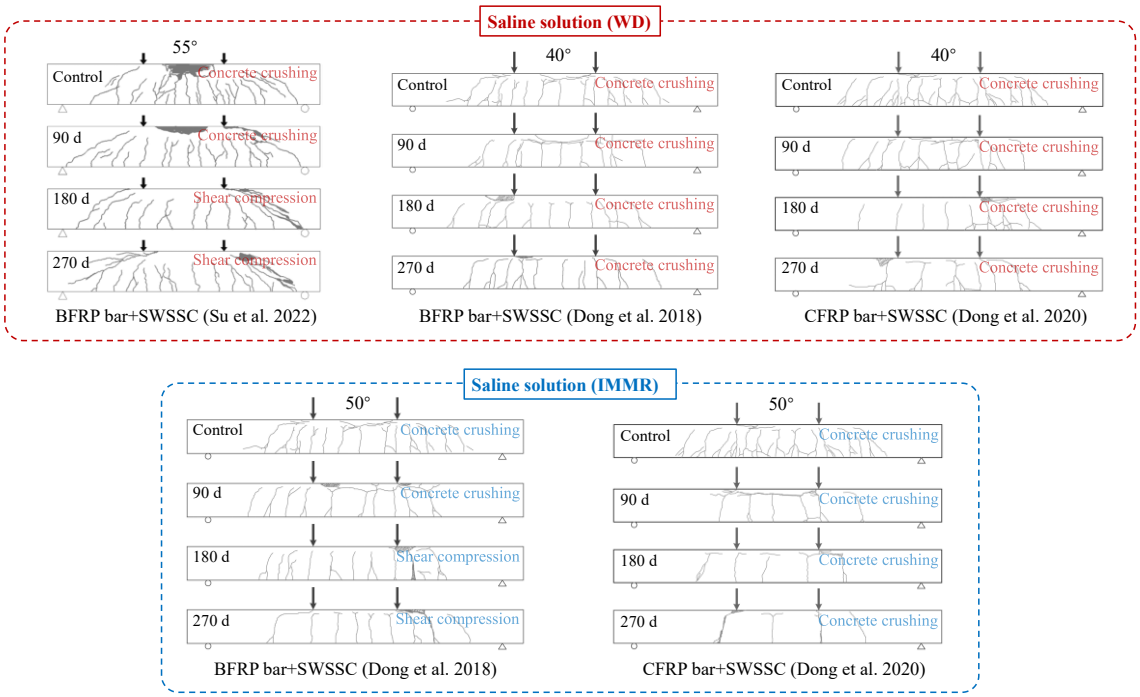


Fig. 2.25 Failure modes of FRP-reinforced SWSSC beams under saline conditions (Dong et al. 2018c, 2020; Su et al. 2022)

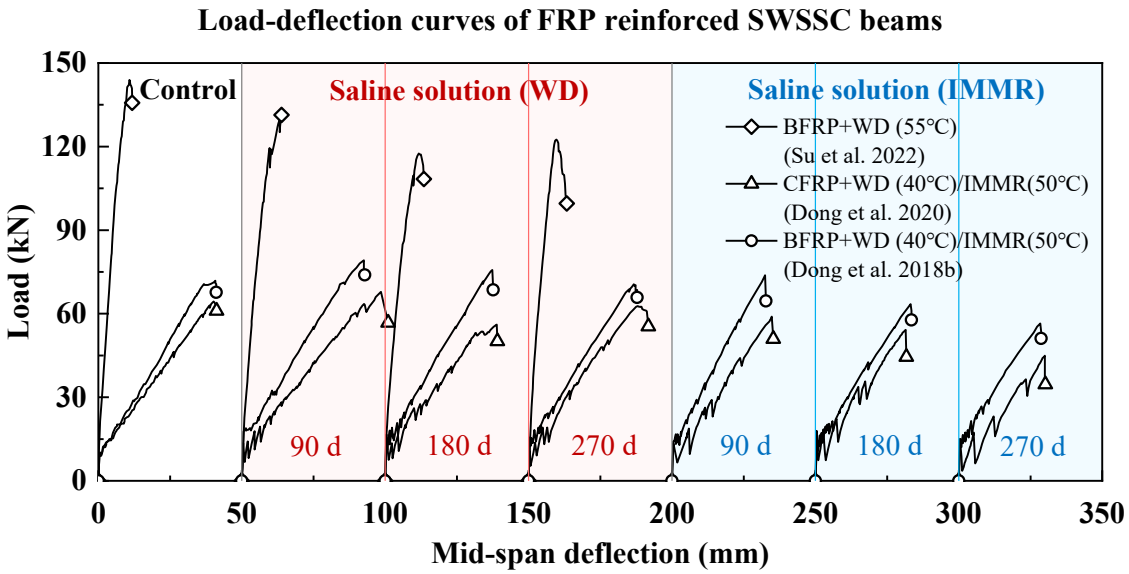


Fig. 2.26 Load-deflection curves of FRP-reinforced concrete beams after saline conditions

2.5.1.2 Load-deflection curves

Fig. 2.26 shows the load-midspan deflection curves for the beams mentioned in Section 2.5.1.1. An obvious phenomenon is that several small load drops occur after concrete

cracking in the conditioned beams studies by Dong et al. (2018c, 2020), especially in the CFRP-reinforced concrete beams. The authors speculated that these changes could be due to the degradation of the bond between FRP bars and concrete. However, such load drops were not detected during the environmental exposure in the study by Su et al. (2022), which indicates that the bond degradation of FRP bars could be ignored in their study. Since the bond durability tests were also conducted by Su et al. (2022) and Dong et al. (2018c) accompanied by the beam durability tests, the bond test results are employed herein to further illustrate this issue. As shown in Fig. 2.27, the BFRP bars in Su et al. (2022) possess more significant bond degradation compared to those in Dong et al. (2018c). That is to say, the bond degradation is not the only reason for the observed load drops. Note that the unconditioned concrete strength of 38.3 MPa and 50.5 MPa was used by Su et al. (2022) and Dong et al. (2018c), respectively, and the shear span ratios of their beams were also different. These differences in the two studies may further influence the post-crack behavior.

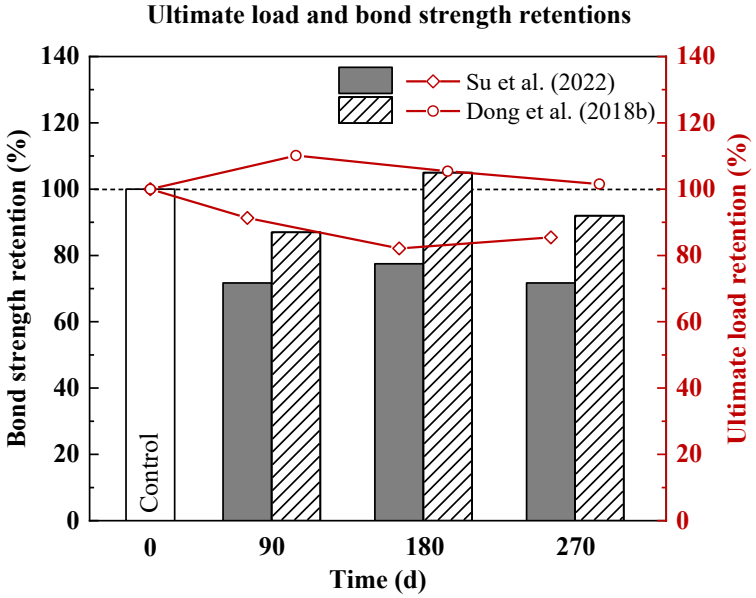
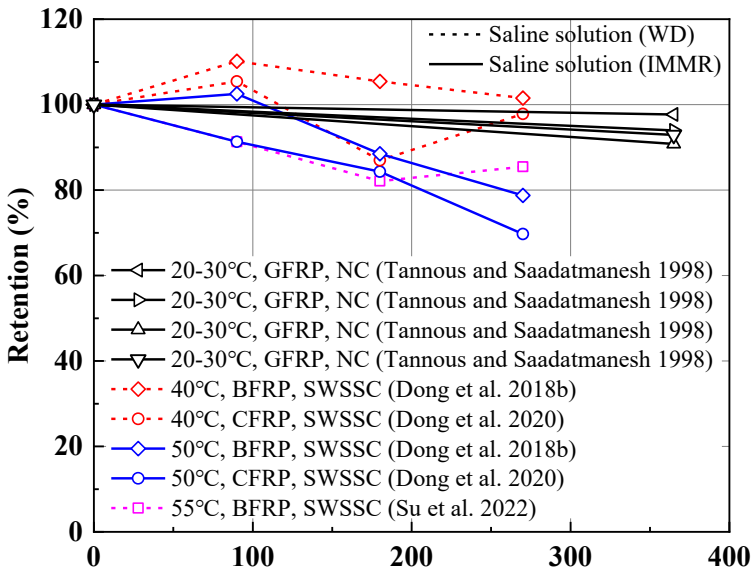


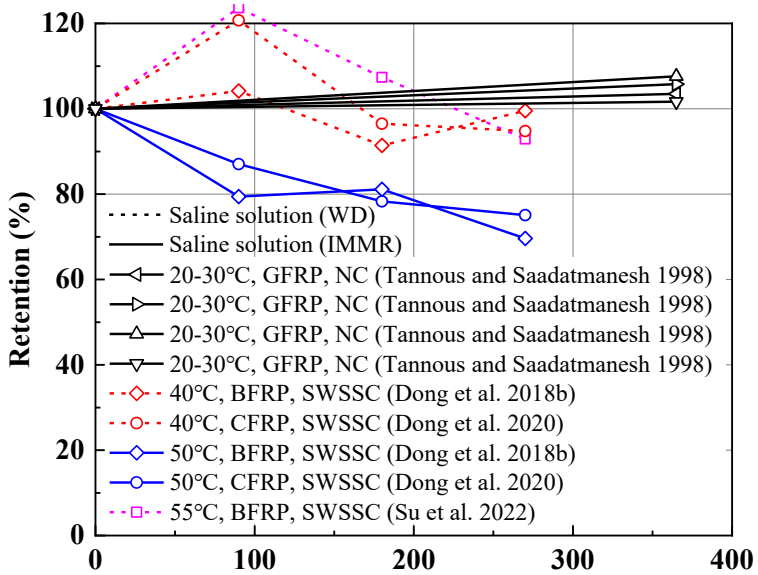
Fig. 2.27 Ultimate load and bond strength retentions

2.5.1.3 Ultimate load and corresponding deflection retentions

Fig. 2.28 shows the ultimate load and corresponding deflection retentions of FRP-reinforced concrete beams under saline conditions. It can be seen from Fig. 2.28(a) that the ultimate load retentions of BFRP-reinforced SWSSC beams outperform those of CFRP-reinforced SWSSC beams under the same environmental condition, regardless of the immersion or WD cycling condition. Moreover, the load degradations are generally proportional to the exposure temperature, which is consistent with the retention variations observed in bare FRP bars. However, it is difficult to distinguish the specific effects of immersion and WD cycling due to the inconsistent temperatures for these two conditions. Conversely, the temperature seems irrelevant to the variations in mid-span deflections, with more detrimental effects observed in the deformations of the beams under immersion [see Fig. 2.28(b)].



(a) Ultimate load



(b) Mid-span deflection

Fig. 2.28 Ultimate load and corresponding deflection retentions of FRP-reinforced concrete beams under saline conditions

To interpret the above phenomena, various factors related to both materials and the interface at different levels (i.e., macro and micro) should be considered as shown in Fig. 2.29 (Chang et al. 2022). For concrete material, external high-temperature and high-humidity environments may promote further hydration of the cement at the early conditioning stage, potentially leading to an increase in the ultimate load of FRP-reinforced concrete beams. However, with the increase of exposure time in saline solutions, concrete cracking may occur due to the formation of expansive products and the concrete strength will decrease. On the other hand, considering the different water absorption capabilities of resin and fiber, the bar-concrete interface could experience uneven expansion after water absorption, which can result in interface cracking and debonding. Subsequently, the internal fibers in FRP bars may become vulnerable in an alkaline environment, making them susceptible to micro-cracks and further degradation of the interface bond. Therefore, the experimental observations are relatively scattered due to the coupled effects of the above-mentioned factors.

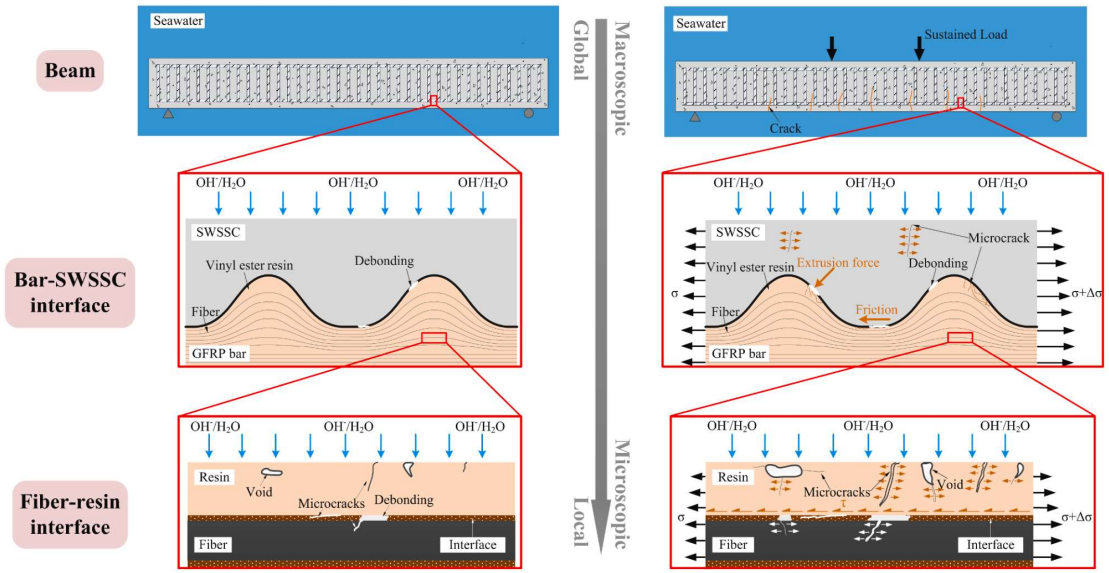


Fig. 2.29 Deterioration mechanism of FRP-reinforced concrete beams under saline conditions (Chang et al. 2022)

2.5.2 Coupled Effects of Environmental and Loading Conditions

Several studies have been conducted to simulate the real loading conditions of FRP-reinforced concrete beams under harsh environments. As depicted in Fig. 2.30, Laoubi et al. (2006) first explored the single effect of sustained load on the flexural performance of FRP-reinforced concrete beams. Lower initial stiffness occurs compared to the reference beams, as a result of the pre-cracking during the application of sustained load, and a more obvious distinction in initial stiffness between the stressed and unstressed beams is detected with the increase of time. However, the stressed and unstressed beams exhibit very similar flexural behavior when the applied load is beyond the sustained load level, which indicates that the sustained load primarily influences the beam behavior at the early loading stage.

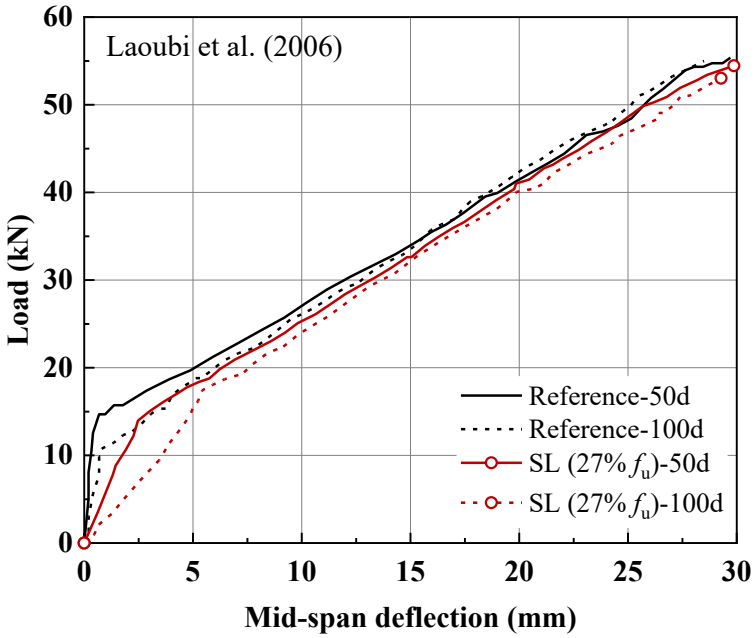
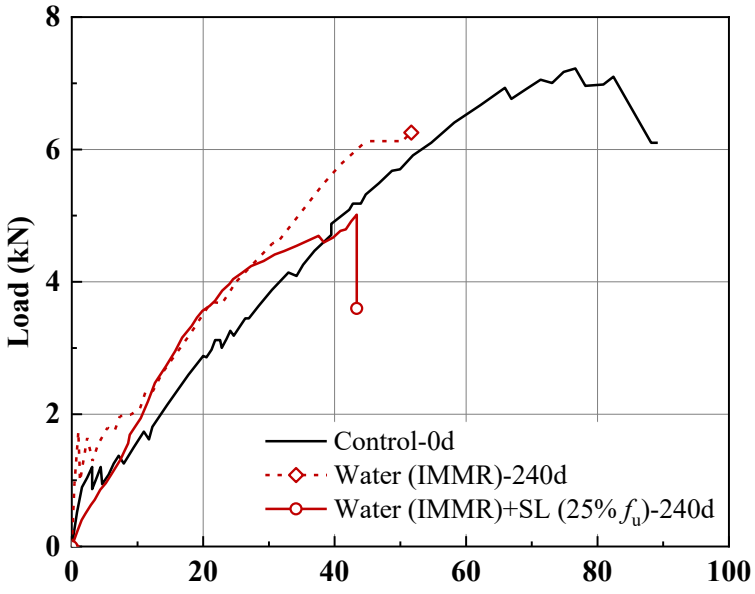


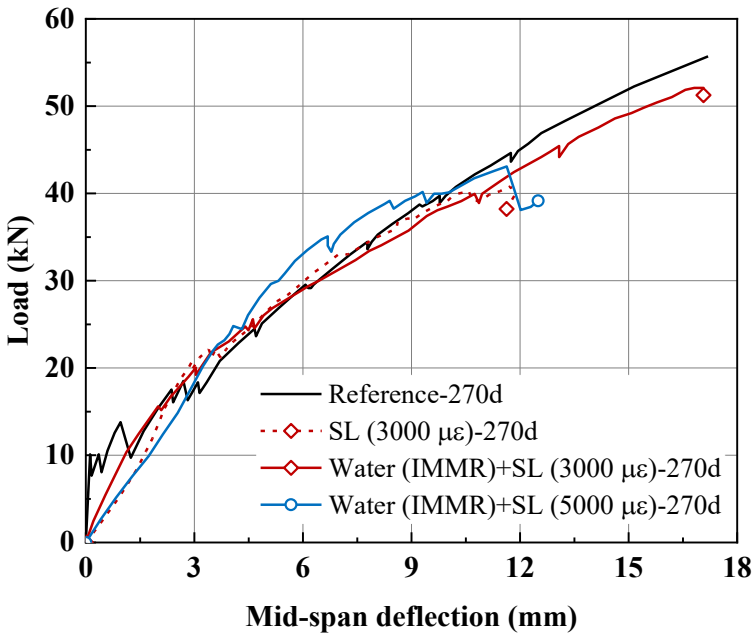
Fig. 2.30 Load-deflection curves of FRP-reinforced concrete beams with sustained load

Under the coupled effects of sustained load and water immersion, similar reduced initial stiffness for the conditioned beams is observed compared to the immersed beams without pre-cracking at the same exposure time (Almusallam and Al-Salloum 2006) [see Fig. 2.31(a)]. In addition, since the slippage between FRP bars and concrete may occur earlier during the sustained loading process, fluctuations at low load levels are effectively eliminated. However, the ultimate load and corresponding deflection both decrease compared with the immersed beams, which contrasts with the observations from Laoubi et al. (2006). That is to say, the coupled effects of sustained load and water immersion may become more severe for the later loading stages. Nevertheless, it is rather difficult to draw a general conclusion herein based on these two studies by Almusallam and Al-Salloum (2006) and Fergani et al. (2018b) since no AAT study relevant to immersed beams was carried out in the latter research. Thus, the degraded stiffness for the stressed beams cannot be verified for the same reason. Another interesting observation in Fig. 2.31(b) is that the initial stiffness and ultimate deflection both increase for the specimens subjected to sustained loading and environmental

conditioning compared with the sustained-loaded beams, which may be attributed to the self-healing capability of concrete in water, as explained by the authors.



(a) Almusallam and Al-Salloum (2005)



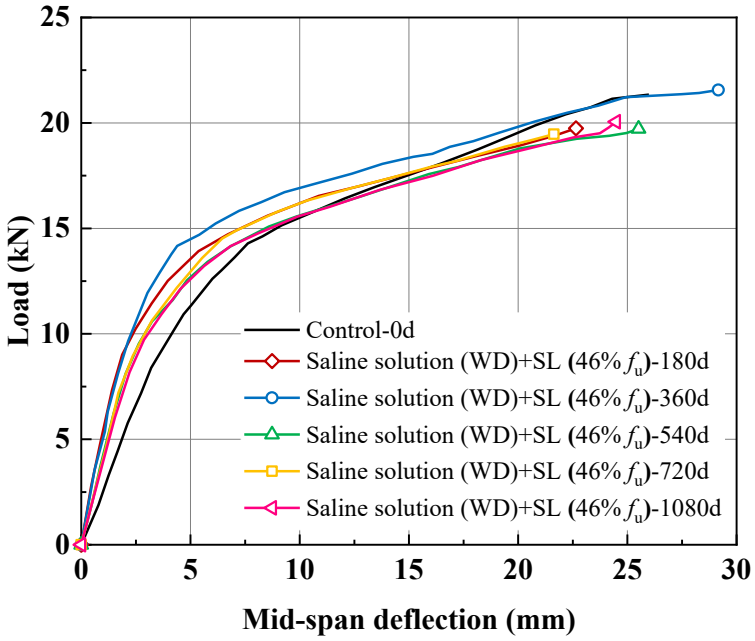
(b) Fergani et al. (2018)

Fig. 2.31 Load-deflection curves of FRP-reinforced concrete beams with sustained load after water solution conditioning

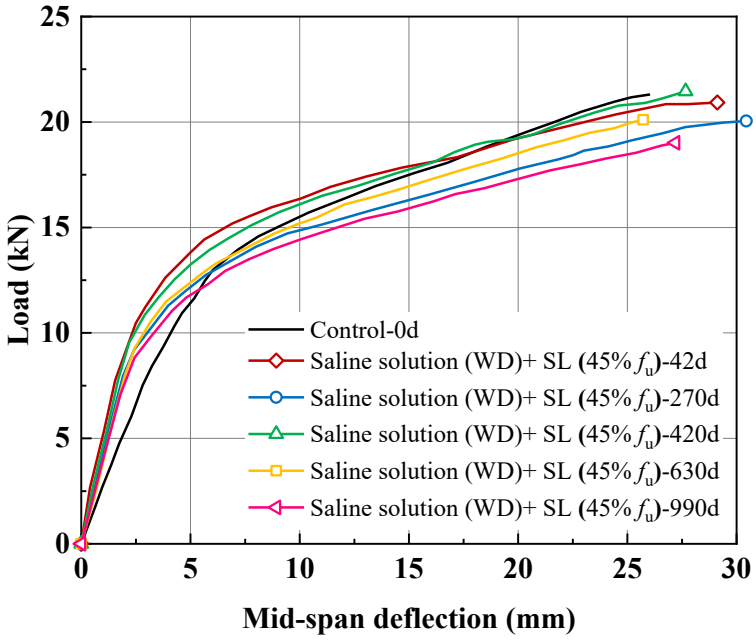
Fig. 2.32 depicts the load-deflection curves of FRP-reinforced concrete beams with sustained load in saline solutions (Sen et al. 1998, 1999; Almusallam and Al-Salloum 2006; Dong et al. 2018a). It is seen that all conditioned beams possess higher initial stiffness compared to the unconditioned beams, which seems controversial to the observations for the sustained-loaded beams in water immersion conditions. Note that all control beams in these studies were unconditioned and tested before the onset of environmental conditioning, rather than concurrently with the conditioned beams. Thus, the unconditioned beams cannot provide a reliable reference for the conditioned beams due to the variations in concrete strength, which has a great impact on the initial stiffness. With the increase of exposure time and sustained load levels, more significant degradation is observed in both ultimate load and mid-span deflection. Additionally, the conditioned beams subjected to the coupled effects of sustained loading and seawater conditioning exhibit a stiffer branch before failure compared with the conditioned beams without sustained load. This may be attributed to the larger residual displacement as a result of sustained loading (Dong et al. 2017a), and this influence could become more conspicuous in saline solutions [see Figs. 2.31(a) and 2.32(c)] due to the detrimental effect of chloride on the concrete compactness and bond performance between FRP bars and concrete.

Fig. 2.33 summarizes the ultimate load of several sustained-loaded beams under different environmental conditions. The results reveal that the sustained load tends to reduce the load capacity of FRP-reinforced concrete beams, regardless of the environmental conditions. This reduction can be interpreted as follows: as depicted in Fig. 2.29, the water molecules can easily access the concrete matrix via the pre-cracks as a result of the sustained load, thereby more pronounced detrimental effects occur at the bar-concrete interface apart from the existing degradations as mentioned in Section

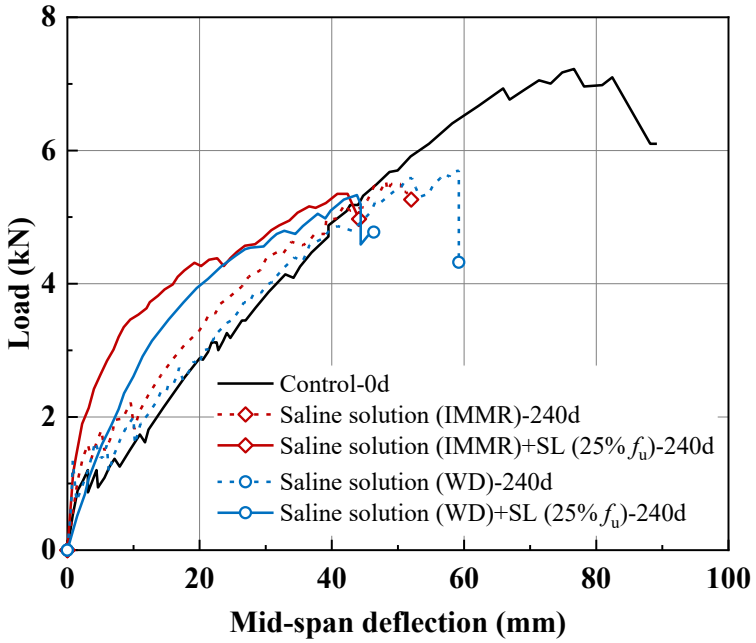
2.5.1, leading to the further propagation of existing micro-cracks and increased damage to the interface.



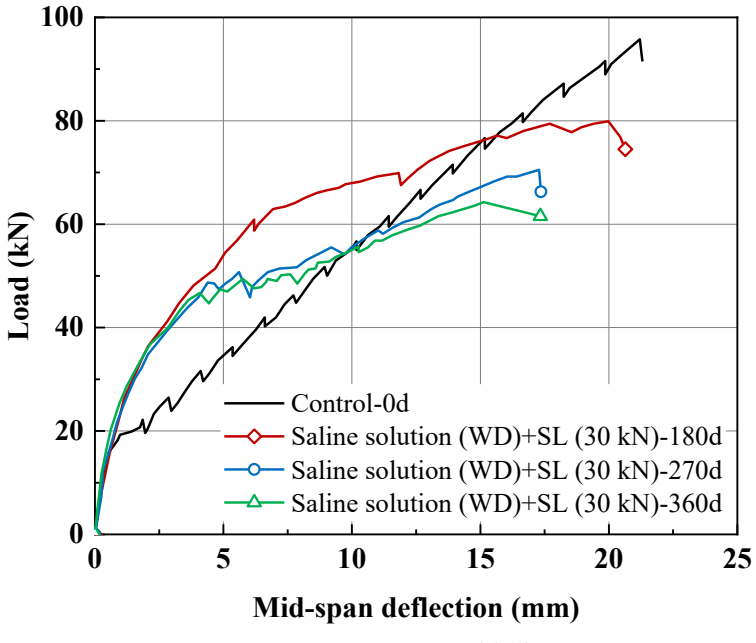
(a) Sen et al. (1998)



(b) Sen et al. (1999)

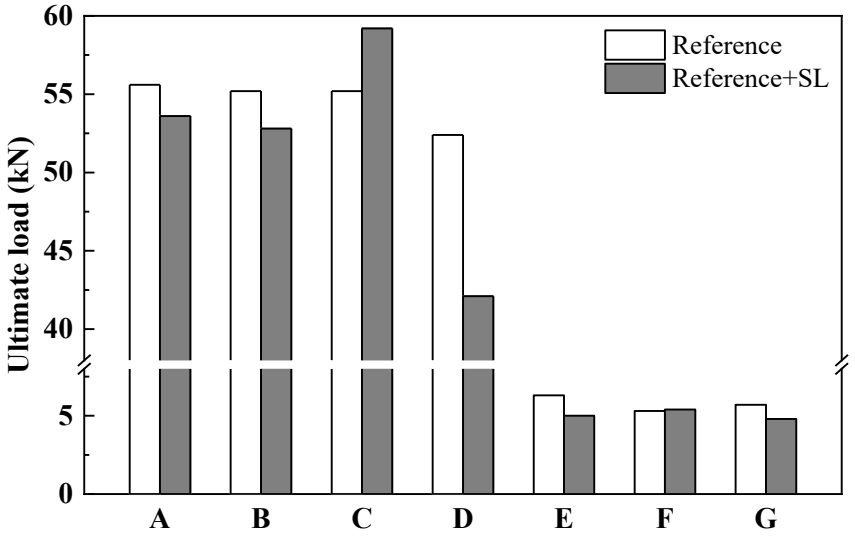


(c) Almusallam and Al-Salloum (2005)



(d) Dong et al. (2018)

Fig. 2.32 Load-deflection curves of FRP-reinforced concrete beams with sustained load in saline solution



A: Ref.=Air, 50d (Laoubi et al. 2006)
B: Ref.=Air, 100d (Laoubi et al. 2006)
C: Ref.=Air, 180d (Laoubi et al. 2006)
D: Ref.=Air, 270d (Fergani et al. 2018)
E: Ref.=Water (IMMR), 240d (Almusallam and Al-Salloum 2005)
F: Ref.=Saline solution (IMMR), 240d (Almusallam and Al-Salloum 2005)
G: Ref.=Saline solution (WD), 240d (Almusallam and Al-Salloum 2005)

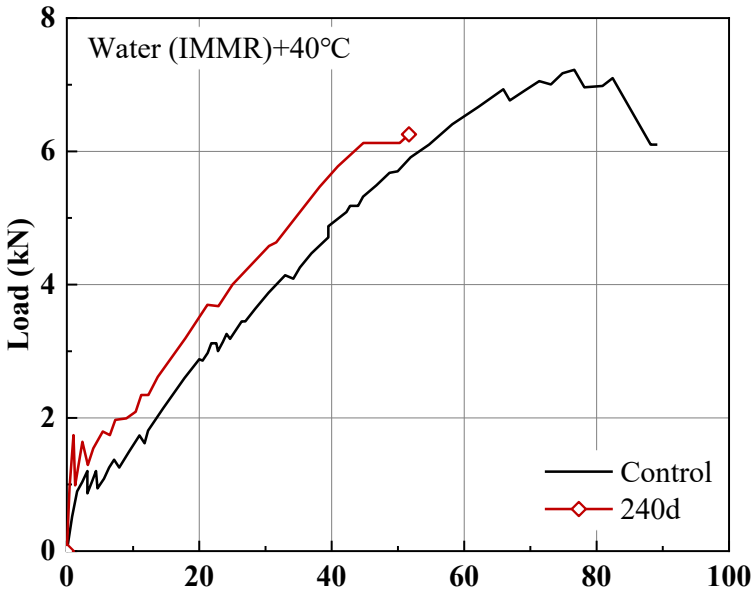
Fig. 2.33 Ultimate load retentions of conditioned FRP-reinforced concrete beams with sustained load

2.5.3 Other Conditions

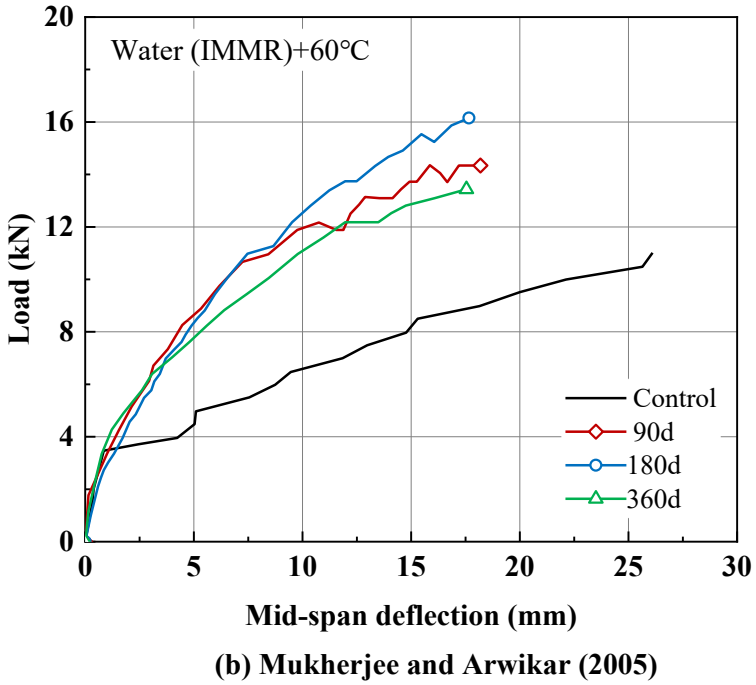
2.5.3.1 Water immersion

Numerous studies have investigated the durability of FRP-reinforced concrete beams under water immersion conditions. It can be seen from Fig. 2.34 that the stiffness of conditioned beams is much larger than that of control beams for Mukherjee and Arwikar (2005), while smaller stiffness of conditioned beams is observed for Lu et al. (2023b), especially for those subjected to long-term exposure (360 days). In addition, the conditioned beams in both Almusallam and Al-Salloum (2006) and Lu et al. (2023b) possess smaller ultimate load and deformation capacities. The reasons for the above phenomena can be attributed to the following aspects. First, the water immersion commenced immediately after 28-day curing in Mukherjee and Arwikar (2005),

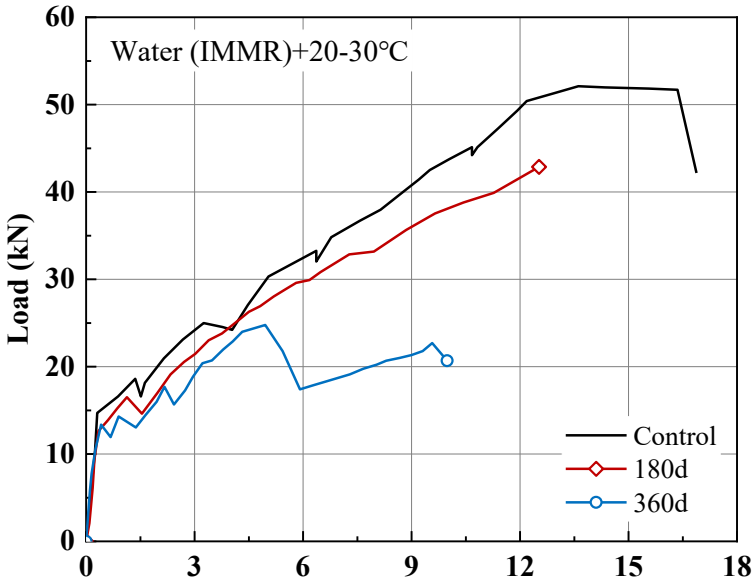
whereas the immersion was postponed to several months later in the other two studies, in which the concrete strength is stable to some extent. Thus, the effect of post-curing of concrete may become more significant during water immersion in Mukherjee and Arwikar (2005), leading to increased stiffness in load-deflection curves. As shown in Fig. 2.35, the variation trends of concrete compressive strength retention are similar to those of ultimate load retention under water immersion conditions. However, the difference between these two retentions indicates that the concrete strength variation is not the only influencing factor. Second, the high temperature and humidity may accelerate the cement hydration and further increase the concrete strength. In addition, as mentioned earlier, the BFRP bars used in Lu et al. (2023b) possessed inferior tensile and bond durability compared with the other BFRP bar products, so it is not surprising that the conditioned beams in their study experienced the highest degradation in terms of strength and stiffness.



(a) Almusallam and Al-Salloum (2005)



(b) Mukherjee and Arwikar (2005)



(c) Lu et al. (2023)

Fig. 2. 34 Load-deflection curves of FRP-reinforced concrete beams under water immersion.

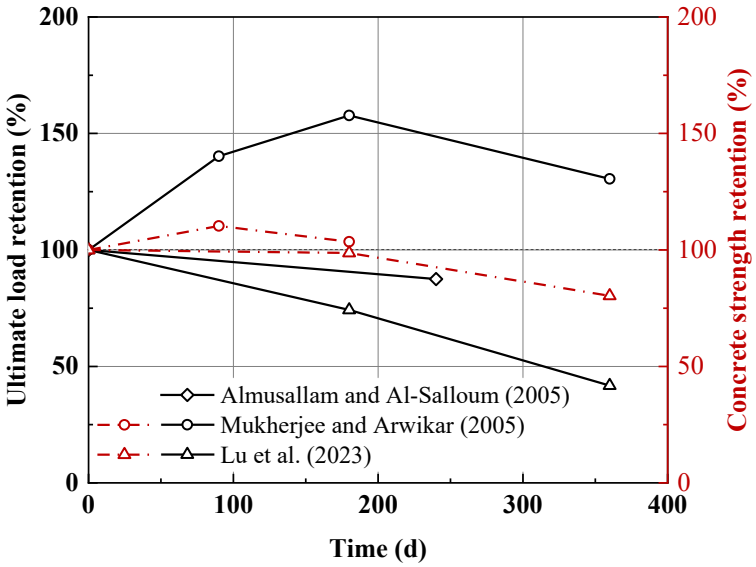
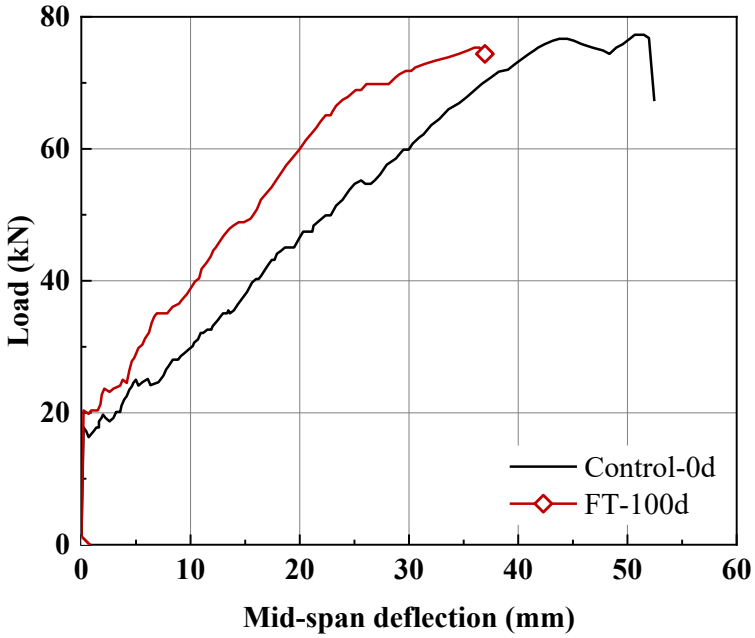


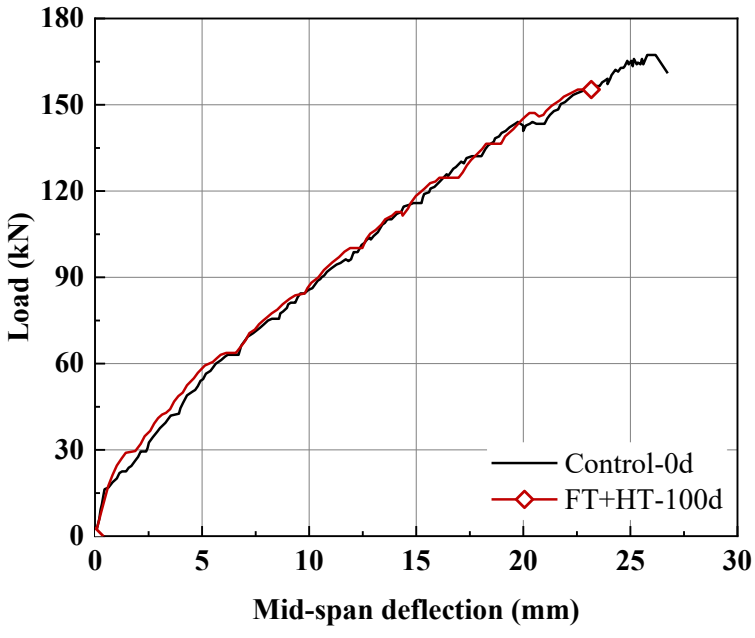
Fig. 2.35 Ultimate load and concrete strength retentions under water immersion

2.5.3.2 Freeze-thaw cycles

It can be detected from Fig. 2.36(a) that the load-deflection curves of conditioned beams exhibit increased stiffness after FT cycles, while the coupled effects of FT and HT cycles make the stiffness increase negligible [see Fig. 2.36(b)]. However, both studies compared the mechanical performance of the conditioned beams with the control beams tested before conditioning (Wang and Belarbi 2013; Khanfour and El Refai 2017). In contrast, Laoubi et al. (2006) tested the conditioned and reference beams simultaneously after conditioning and found an obvious degradation in the stiffness of conditioned beams, which resulted in an increase in midspan deformations. Thus, concrete strength development during FT cycling process should be considered when assessing the performance of conditioned beams. In addition, the degraded initial stiffness caused by sustained load was also detected in their studies under FT cycles.



(a) Khanfour and El Refai (2017)



(b) Wang and Belarbi (2013)

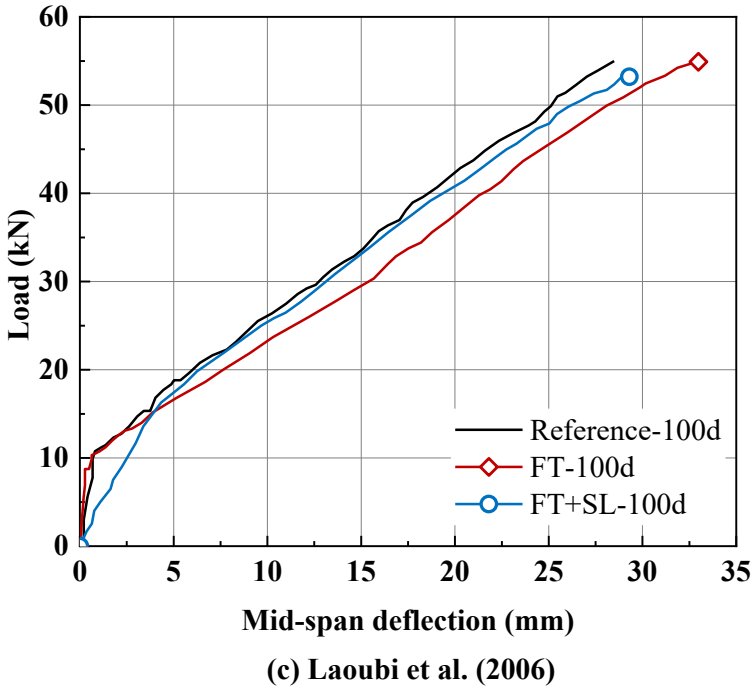


Fig. 2.36 Load-deflection curves of FRP reinforced concrete beams under freeze-thaw cycling conditions

2.6 CONCLUDING REMARKS

This chapter has provided a comprehensive review and systematic assessment of the durability issues associated with FRP bars, covering both material and component levels. Various influencing parameters affecting the long-term mechanical properties of FRP bars and the long-term flexural behavior of FRP-reinforced concrete beams were examined using three newly assembled databases that include over 15,200 specimens. Key findings from the literature review are summarized as follows:

(1) Among various conditioning methods, direct solution immersion has the most pronounced detrimental effects on the long-term mechanical properties of FRP bars. The degradation of tensile strength is most severe in alkaline solutions, followed by water and saline solutions, especially at elevated temperatures. Based on the existing test data, the durability of bare GFRP bars is generally

superior to that of bare BFRP bars after direct solution immersion. Besides, the coupled actions of environmental conditioning and sustained loading can obviously affect the tensile strength of FRP bars. Under the same exposure condition, the deterioration rate increases with the applied stress level for both bare and concrete-embedded FRP bars.

(2) Compared to other mechanical properties of FRP bars, a considerable dispersion has been observed in the test results for bond strength, which may be caused by the coupled effects of the post-curing of concrete and the hygroscopic expansion of FRP bars. Besides, the bond performance of FRP bars in concrete is closely related to their surface treatment.

(3) Based on the available test results for FRP-reinforced concrete beams, the degradation process in FRP-reinforced concrete beams is quite complex because of the interactions among FRP bars, concrete matrix, and bar-concrete interface, resulting in a change of failure modes and some inconsistent experimental observations. In addition, the sustained load tends to reduce the load capacity and overall behavior of FRP-reinforced concrete beams, regardless of the exposure conditions.

On the other hand, based on the review of existing literature, the research gaps to be addressed in this PhD project has also been identified, as summarized below:

(1) Existing studies have demonstrated that no consensus has been reached regarding the size effect on the long-term performance of FRP bars, indicating the need for further experimental investigations to clarify this issue. Moreover, significant discrepancies between the results obtained from AAT and FET have

been observed, highlighting the necessity of establishing a reliable conversion relationship between AAT and FET results for FRP bars.

(2) Given the strong correlation between the bond performance of FRP bars in concrete and their surface treatment, the influence of surface characteristics on the bond durability of FRP bars needs to be investigated. Additionally, emphasis should be placed on establishing long-term bond-slip models that incorporate experimental findings as input parameters.

(3) Compared to FRP bars and FRP bar-to-concrete bonded joints, existing experimental data on FRP-reinforced concrete beams remain inconsistent and limited. Therefore, further investigation into the durability of FRP-reinforced concrete beams under various environmental and loading conditions is needed.

(4) Most durability research has focused on individual tests of FRP bars, FRP bar bonded joints, and FRP-reinforced concrete beams. However, there is an urgent need for more systematic studies that compare the material properties of FRP and concrete with the structural behavior of FRP-concrete members to understand their interactions comprehensively.

CHAPTER 3
LONG-TERM TENSILE PERFORMANCE OF GFRP BARS IN REAL MARINE ENVIRONMENTS

3.1 INTRODUCTION

As reviewed in Chapter 2, GFRP bars have been deemed to be one of potential substitutes for conventional steel rebars due to their exceptional corrosion resistance, especially in chloride-rich scenarios (Lu et al. 2020a; Ruiz Emparanza et al. 2022; Wang et al. 2023a). Compared to AAT, only limited studies have addressed the durability of GFRP bars under actual field conditions, primarily due to the significantly extended durations and increased costs involved. Existing field investigations have mainly focused on GFRP bars extracted from concrete members or structures in service (i.e., concrete-embedded bars), with the aim of assessing their microstructural, physicochemical and mechanical properties. These studies have demonstrated that GFRP bars embedded in concrete structures exhibit no degradation at the microscopic level even after a long period of service (Mufti et al. 2007a; Gooranorimi and Nanni 2017; Benmokrane et al. 2018; Al-Khafaji et al. 2021). However, the extracted GFRP bar samples have shown varying degrees of deterioration in mechanical properties, depending on the specific field conditions and exposure durations (Bakis et al. 2005; Mukherjee and Arwikar 2005; Trejo et al. 2011; Benmokrane et al. 2018; Al-Khafaji et al. 2021; Morales et al. 2021; Ramanathan et al. 2021; Lu et al. 2023a; Al-Zahrani 2024).

In addition to studies on concrete-embedded bars, there is a scarcity of research

concerning bare GFRP bars directly exposed to natural environmental conditions. Al-Salloum et al. (2013) carried out tensile tests on bare GFRP bars exposed at two different sites (i.e., Riyadh and Jubail in Saudi Arabia, respectively representing hot-dry and hot-humid environments of the Middle East) for durations of 6, 12 and 18 months. Their results revealed minimal changes in tensile strength and elastic modulus (less than 1% under both conditions) even after 18-month field exposure, in line with the findings on GFPR bars after direct exposure to the outdoor weather in Saudi Arabia for up to 6 months (Al-Zahrani et al. 2002). Nevertheless, it is important to recognize that natural environmental conditions are much more complex than those simulated in laboratory settings, since multiple influencing factors (e.g., temperature fluctuations, UV radiation, high humidity, WD cycles) can be involved in the former scenario. Moreover, it has been suggested that commonly employed accelerated aging methods, typically involving exposure to aggressive solutions at elevated temperatures, tends to yield highly conservative estimates of the durability performance of GFRP bars (Al-Salloum et al. 2013; Benmokrane et al. 2020a).

Against this background, this chapter reports on FET results for GFRP bars subjected to real marine environments for a long exposure duration of up to four years. Two batches of GFRP bars were respectively exposed in different marine environmental zones (i.e., atmospheric, splash, tidal, and underwater) at two field exposure stations, aiming at clarifying the durability of GFRP bars under varying marine conditions. The residual tensile properties of the GFRP bars with several exposure durations in the field were examined, and the effect of bar diameter on long-term tensile performance was also investigated.

Of note, the FETs were conducted as part of a theme-based research scheme project

entitled “Sustainable Marine Infrastructure Enabled by the Innovative Use of Seawater Sea-Sand Concrete and Fiber-Reinforced Polymer Composites”. This project aims to develop a new type of concrete structures to achieve sustainable marine infrastructure: seawater sea-sand concrete (SSC) structures reinforced with FRP composites (hereafter referred to as FRP-SSC structures). A key objective of the project is to gain an in-depth understanding of the durability and deterioration mechanisms of FRP-SSC materials and structural members after prolonged exposure to real marine environments. Table 3.1 details the FET plan presented in this thesis, including specimen type, concrete casting dates and placement locations across different exposure zones. The casting procedures for each series of specimens are shown in Fig. 3.1. While the majority of the tests summarized in Table 3.1 were conducted by the PhD candidate, he would like to acknowledge the contributions of his colleagues to this large-scale experimental program. In particular, Dr. Cheng Jiang led the preparation and placement of specimens in Series I and conducted tests on both control specimens and those after 8-month exposure. Additionally, Dr. Yiwen Zhang led the preparation and placement of specimens in Series II and performed tests on the 12-month exposed specimens in Series I. Specifically, this chapter only focuses on the durability of GFRP bar, while the investigations of FRP-SSC bonded joints and beams are presented in Chapters 5 and 6, respectively.

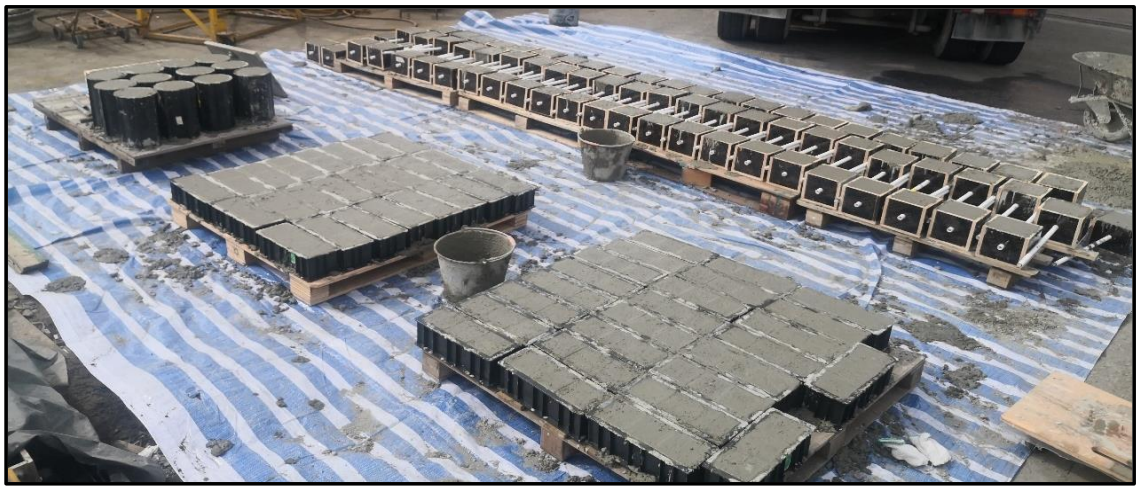
Table 3.1 Plan of field exposure tests

Series	Specimen type	Date of concrete casting	Date of specimen placement	Exposure station	Exposure zone[#]
1st	GFRP bars FRP bar-SSC bonded joints FRP-SSC beams	5 Oct. 2019	14 Jan. 2020	I	A-I, S-I, T-I
2nd	FRP-SSC beams with sustained load	5 Oct. 2019	2 Feb. 2021	I	T-I
3rd	GFRP bars FRP bar-SSC bonded joints	21 Nov. 2021	5 Jan. 2022	II	A-II, U-II

[#]A = atmospheric zone; S = splash zone; T = tidal zone; U = underwater zone.



(a) The 1st and 2nd series of specimens



(b) The 3rd series of specimens

Fig. 3.1 Concrete casting for field exposure tests

3.2 EXPERIMENTAL PROGRAM

3.2.1 Materials

This chapter investigates two batches of helically-wrapped and sand-coated GFRP bar specimens, corresponding to the 1st and 3rd series presented in Table 3.1, both supplied by Dextra Building Products (Guangdong) Co., Ltd. (see Fig. 3.2). Both batches of GFRP bars were manufactured via a pultrusion process using continuous E-glass fibers impregnated with a vinylester-based resin matrix, with a helical yarn wrapping around the bar during production. It is clearly seen from Fig. 3.2 that there is a significant difference between the surface appearances of the two batches of GFPR bars: Batch I specimens exhibit significantly larger rib spacing (i.e., interval spacing of the helical yarn) and a thicker layer of sand coating compared to Batch II. Batch I specimens with diameters of 6 mm and 10 mm [nominal diameters of 6.4 mm and 9.5 mm, respectively, as specified in ACI (2017)] were employed, while only specimens with a diameter of 10 mm were used for Batch II. The physical and mechanical properties of both batches of GFRP bars are summarized in Table 3.2, as provided by the manufacturer.



Fig. 3.2 Close-up view of different batches of GFPR bars

Table 3.2 Physical and mechanical properties of GFRP bars provided by manufacturer

Batch	Nominal diameter (mm)	Diameter (mm)	Tensile strength (MPa)	Elastic modulus (GPa)	Fiber content (%)
I	6.4	6.67	912.3[#]	52.8	83.6
	9.5	9.91	852.9[#]	50.5	81.1
II	9.5	9.89	1037.2[*]	53.0	81.2

[#]Mean value minus 3 times standard deviation.
[*]Minimum value.

3.2.2 Field Exposure Stations

Two field exposure stations were included, with their geographical locations and photographs shown in Fig. 3.3. A large number of 1000-mm-length GFRP bar samples from Batches I and II were prepared prior to exposure. Batch I specimens were transported to the *Hong Kong-Zhuhai-Macau (HZM) Bridge Exposure Station* (denoted as Station I) in January 2020, while Batch II specimens were transported to the *Zhanjiang Port Exposure Station* (denoted as Station II) in January 2022 (see Table 3.1). Fig. 3.4. illustrates the variations in temperature [including minimum and maximum monthly temperatures (Min. and Max.) and mean monthly and annual temperatures (MMT and MAT)] as well as relative humidity (RH) [including mean monthly and annual relative humidities (MMRH and MARH)] in the corresponding regions of the two stations during the exposure period (data sourced from https://www.qweather.com/). Detailed environmental conditions for both stations are provided in Table 3.3 and further described below.

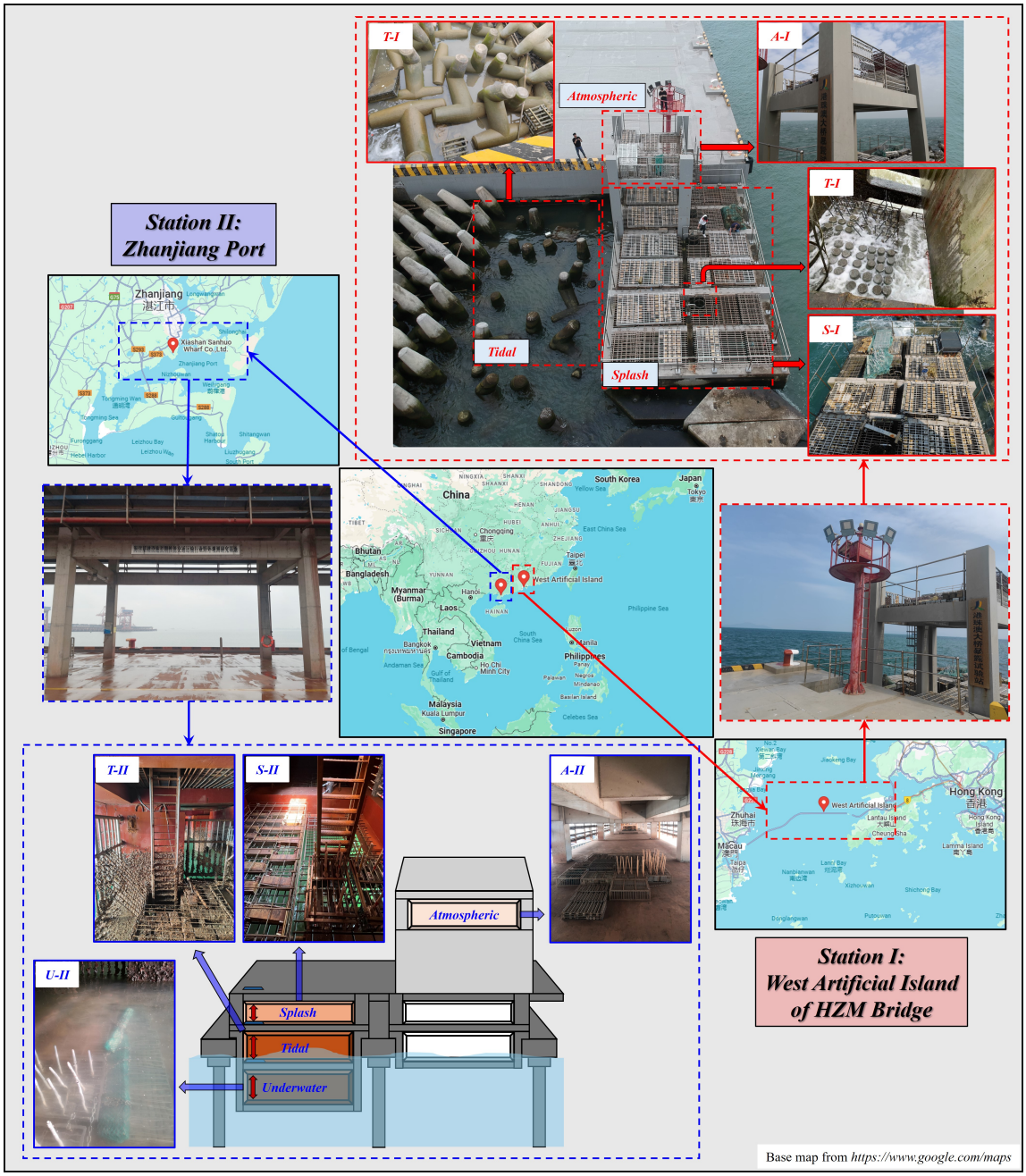
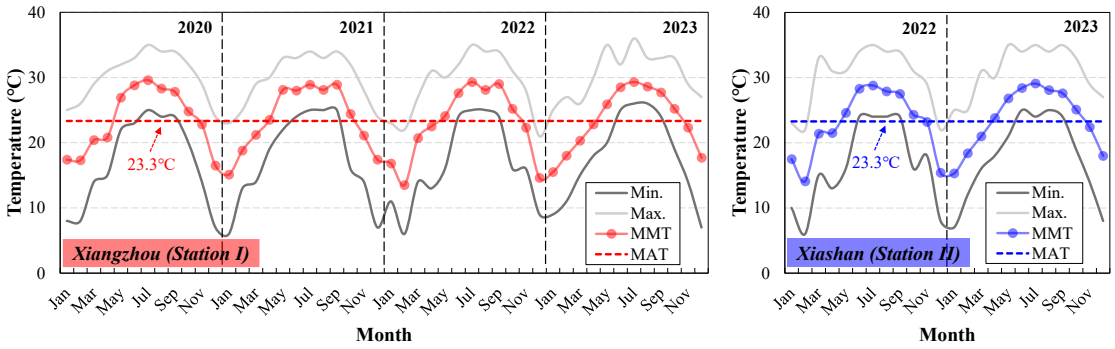
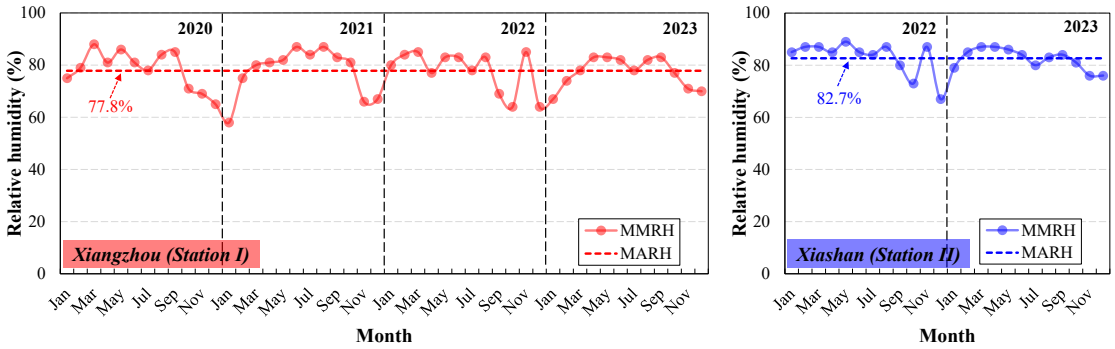


Fig. 3.3 Field exposure stations



(a) Temperature



(b) Relative humidity

Fig. 3.4 Variations of temperature and relative humidity in Xiangzhou (Zhuhai City) and Xiashan (Zhanjiang City) districts during exposure period (obtained from https://www.qweather.com/)

Table 3.3 Environmental characteristics of different exposure zones

Station	Exposure zone	Environmental characteristic[#]
I	A-I	WD (Random); HH; HS; UV; TF
	S-I	WD (Frequent); HH; HS; UV; TF
	T-I	WD (Consecutive); HH; HS; UV; TF; AE; WP; OG
II	A-II	HH; HS; TF
	S-II	WD (Frequent); HH; HS; TF
	T-II	WD (Consecutive); HH; HS; TF; AE; WP; OG
	U-II	HH; HS; TF; OG

[#]AE = abrasion and erosion; OG = organic growth; HH = high humidity; HS = high salinity; TF = temperature fluctuations; UV = ultraviolet radiation; WD = wet-dry cycles; WP = wave pressure.

3.2.2.1 Station I: HZM Bridge Exposure Station

Station I is located on the West Artificial Island of Hong Kong-Zhuhai-Macau (HZM)

Bridge in Xiangzhou District, Zhuhai City, China, characterized by a subtropical monsoon climate. The region experiences annual precipitation ranging from 1700 to 2300 mm, with a concentrated rainy season extending from April to September. As depicted in Fig. 3.4, during the 4-year exposure period (2020 to 2023), the MAT was recorded to be 23.3℃, with minimum and maximum monthly temperatures of 6℃ and 36℃, respectively [Fig. 3.4(a)], and a MARH of 77.8% [Fig. 3.4(b)]. Besides, the region is susceptible to typhoons, particularly between July and September, which can cause extreme weather conditions such as high winds and heavy rainfall.

As illustrated in Fig. 3.3, Station I includes three exposure zones, namely, atmospheric zone (A-I), splash zone (S-I) and tidal zone (T-I), with designed elevations of +6.2 m, +2.5 m, 0.0 m, respectively. The designed average, lowest and highest water levels are +0.54 m, -0.78 m and +1.65 m, respectively. Each exposure zone represents a typical environmental condition, as summarized in Table 3.3. A-I, the zone located above S-I, is characterized by high humidity and salinity (humid marine air with airborne chlorides), UV radiation, temperature fluctuations and random WD cycles caused by rainfall, while for S-I, the zone situated above the high tide level influenced by wave action, experiences frequent WD cycles, high humidity and salinity (severe salt spray), UV radiation as well as temperature fluctuations. T-I, the zone located between low and high tide levels, is subject to consecutive WD cycles, high humidity and salinity, abrasion and erosion from tidal changes, UV radiation, temperature fluctuations, wave pressure and organic growth (e.g., seashells, oysters, algae). Batch I specimens were separately exposed in these three exposure zones for different durations.

3.2.2.2 Station II: Zhanjiang Port Exposure Station

Station II is located at the Xiashan Bulk Cargo Terminal of Zhanjiang Port in Xiashan

District, Zhanjiang City, China, which shares a similar subtropical monsoon climate with Station I, with annual precipitation ranging from 1300 to 1700 mm. During the 2-year exposure period (2022 to 2023), the recorded MAT, minimum and maximum monthly temperatures were 23.3℃, 6℃ and 35℃), respectively, fairly close to those of Station I [Fig. 3.4(a)], while the MARH was slightly higher at 82.7% [Fig. 3.4(b)].

There are four exposure zones at Station II, including atmospheric zone (A-II), splash zone (S-II), tidal zone (T-II) and underwater zone (U-II, also known as submerged zone), with designed elevations of +11.5 m, +4.7 m, +2.0 m and +0.05 m, respectively. The designed lowest and highest water levels are +0.45 m and +4.14 m, respectively. Compared to Station I, Station II exhibits some differences in environmental conditions. As shown in Fig. 3.3, A-II is completely shielded by the overhead structures, while S-II and T-II are situated below the ground level. Therefore, UV radiation is absent in these three zones, and WD cycles do not occur in A-II. Additionally, U-II is constantly submerged, resulting in more stable environmental conditions characterized by 100% humidity, high salinity, minor temperature fluctuations and severe organic growth. It should be noted that Batch II specimens were exposed only in the A-II and U-II zones, with the focus mainly on the durability of GFRP bars subjected to atmospheric and underwater conditions.

3.2.3 Specimen Preparation and Test Method

After reaching the target exposure durations, several GFRP bar specimens from Batches I and II, exposed in different zones, were sampled and subsequently tested in the laboratory to determine their tensile properties. Five replicate specimens were prepared for each test condition (Table 3.4). Before testing, both ends of the 6- and 10-mm GFRP bars were anchored into 200- and 250-mm-length steel tubes (outer diameter = 26 mm;

thickness = 2.5 mm), respectively, with epoxy resin filling the gap between the bars and tubes. To ensure proper centering, each steel tube was equipped with plastic caps at both ends, allowing the GFRP bars to pass through the cap centers. The free length of all specimens was fixed at 400 mm, leading to total lengths of 800 and 900 mm for the 6- and 10-mm GFRP bars specimens, respectively [Fig. 3.5(a)]. To ensure sufficient strength of the epoxy resin, all specimens were cured at ambient temperature for a minimum of seven days.

Tensile tests were performed in accordance with ASTM (2021). An extensometer with a gauge length of 50 mm was instrumented at the mid-length of the specimen to capture strain variation during testing, as shown in Fig. 3.5(b). To prevent damage, the extensometer was removed once the load reached approximately 60% to 70% of the ultimate load obtained from the reference specimens. Testing was conducted using a WAW-1000 testing machine, with applied load and specimen elongation automatically recorded by a computerized data-acquisition system. Loading was displacement-controlled at a constant rate of 4 mm/min.

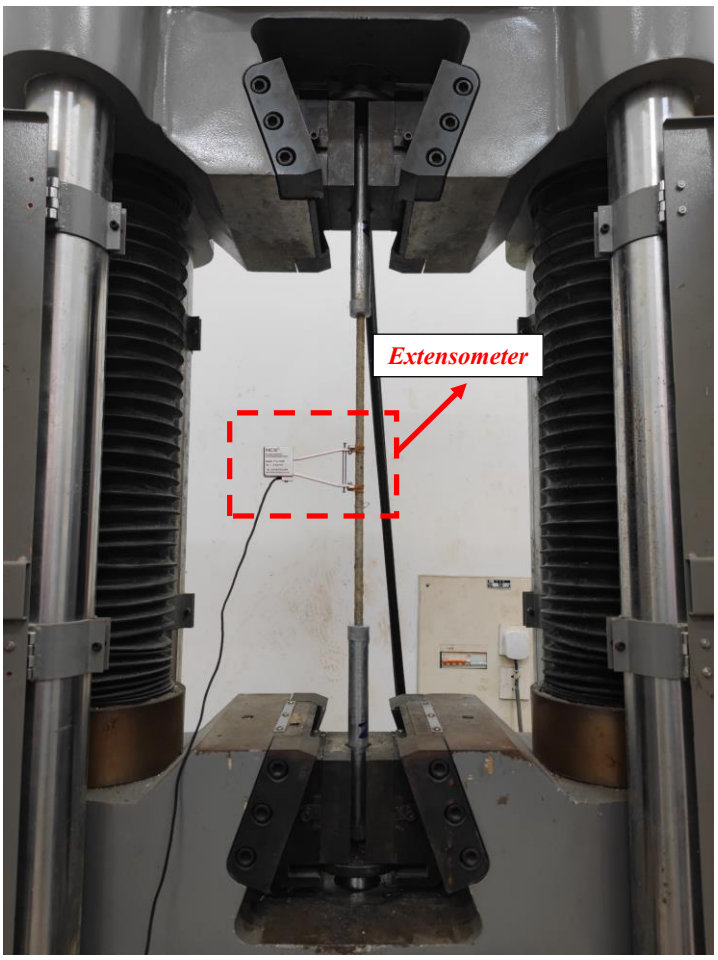
Table 3.4 Test matrix of GFRP bar specimens

Batches of specimen	Station	Environmental condition	Exposure duration[#] (months)	Number of specimens
I (6 and 10 mm)	I	Laboratory (Control)	0	5
		Atmospheric (A-I)	8/12/24/37/48	5/5/5/5/5
		Splash (S-I)	8/12/24/37/48	5/5/5/5/5
		Tidal (T-I)	8/12/24/37/48	5/5/5/5/5
II (10 mm)	II	Laboratory (Control)	0	5
		Atmospheric (A-II)	13/24	5/5
		Underwater (U-II)	13/24	5/5

[#]Due to administrative reasons at the exposure station, the sampling intervals may slightly deviate from exact annual cycles.



(a) Specimen preparation



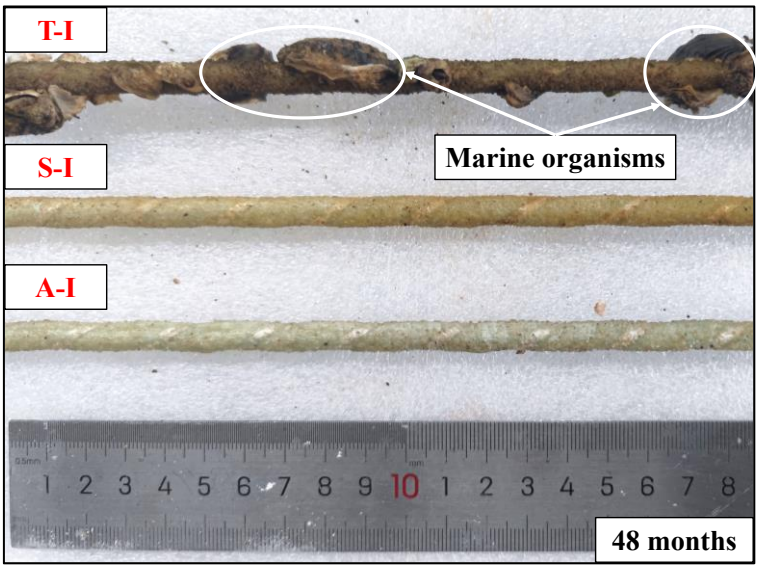
(b) Test set-up

Fig. 3.5 Specimen preparation and test set-up

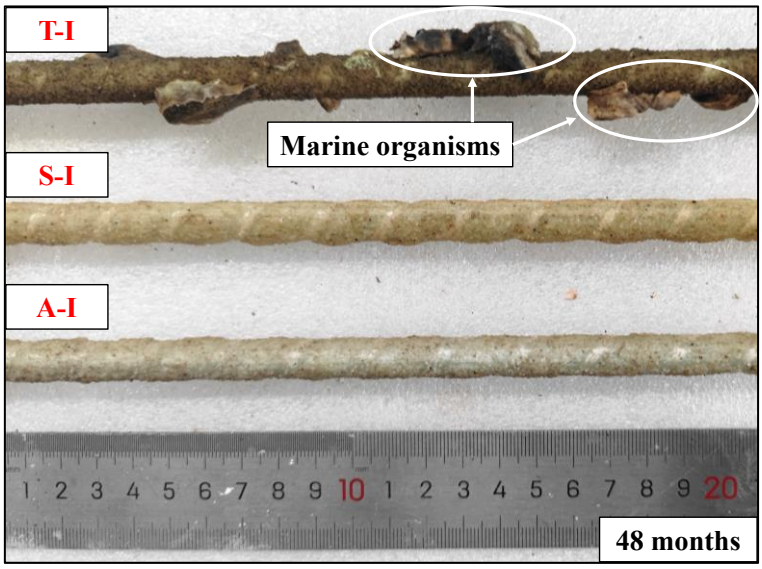
3.3 RESULTS AND DISCUSSION

3.3.1 Surface Characteristic Observations

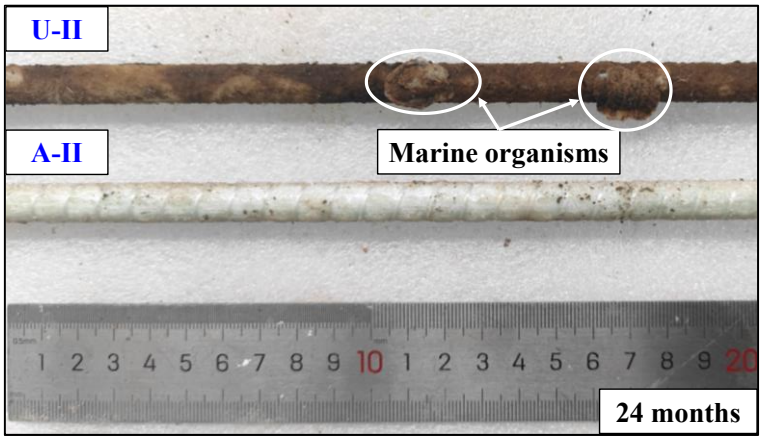
Fig. 3.6 shows the close-up views of the GFRP bars after exposure in different zones of the two stations. It is clearly seen that the specimens taken from T-I and U-II zones had a dark surface color due to algae growth, with additional marine organisms such as barnacles, oysters and seashells attached to the surfaces, particularly pronounced for specimens exposed in the tidal environment (T-I) for 48 months. Specimens exposed in S-I zone displayed a deep shade of yellow, likely resulting from the coupling effects of frequent WD cycles induced by wave action and UV radiation on the resin matrix. In contrast, specimens subjected to atmospheric environments (A-I and A-II) showed minimal surface changes except for a loss of luster when compared to the unexposed reference ones (Fig. 3.2).



(a) 6-mm GFRP bars at Station I



(b) 10-mm GFRP bars at Station I



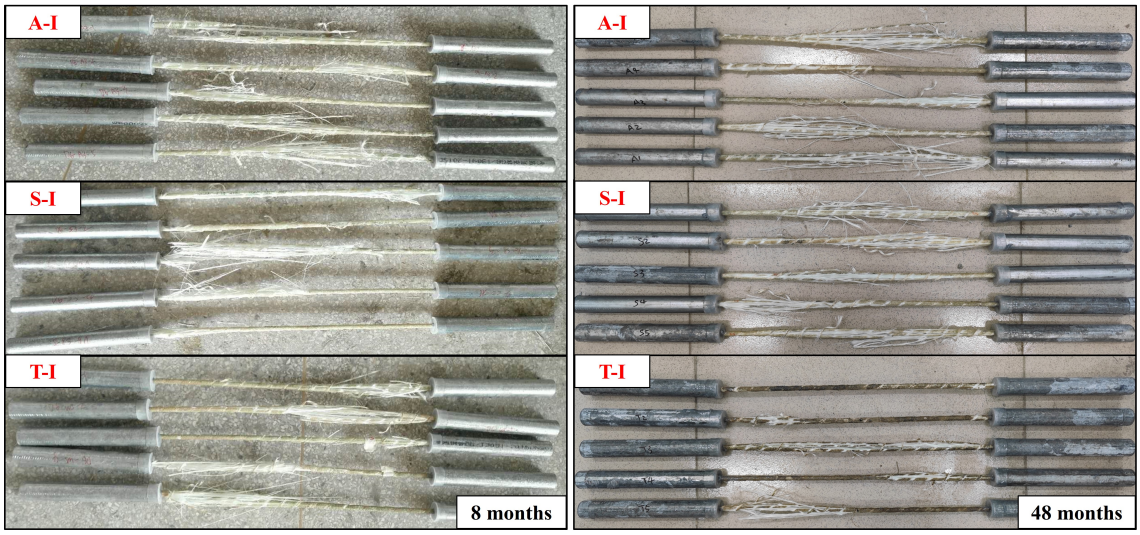
(c) 10-mm GFRP bars at Station II

Fig. 3.6 Surface characteristics of GFRP bars exposed in different exposure zones

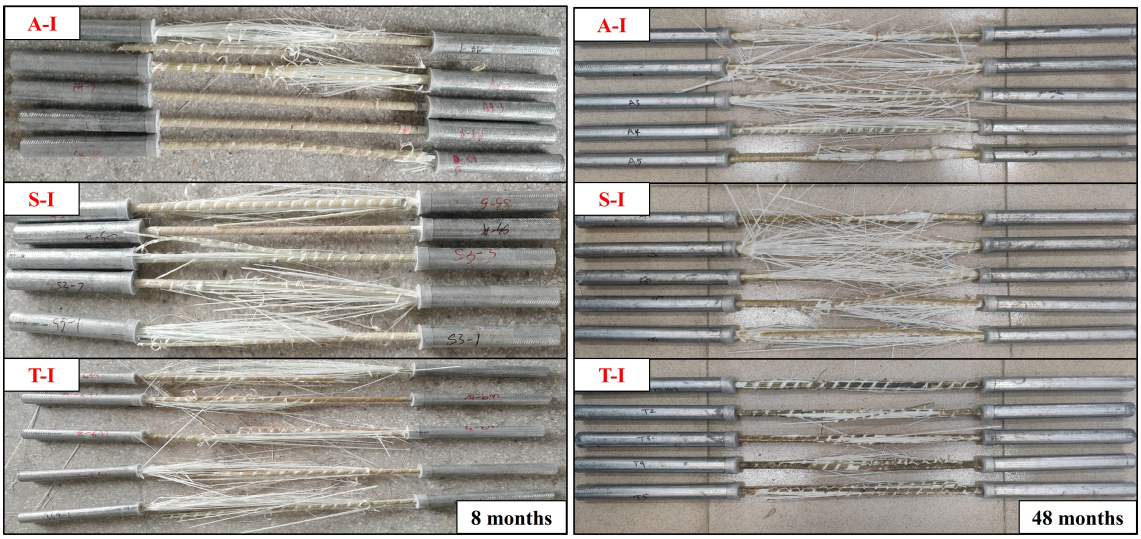
3.3.2 Failure Modes

Fig. 3.7 displays the failure modes of specimens exposed in different exposure zones for varying durations [8 and 48 months for Batch I, as shown in Figs. 3.7(a) and 3.7(b), and 13 and 24 months for Batch II, as shown in Fig. 3.7(c)]. As expected, the failure modes of specimens exposed to the atmospheric (A-I and A-II) and splash (S-I) environments were constant and characterized by the complete damage of resin matrix accompanied by fiber separation and rupture, regardless of exposure duration.

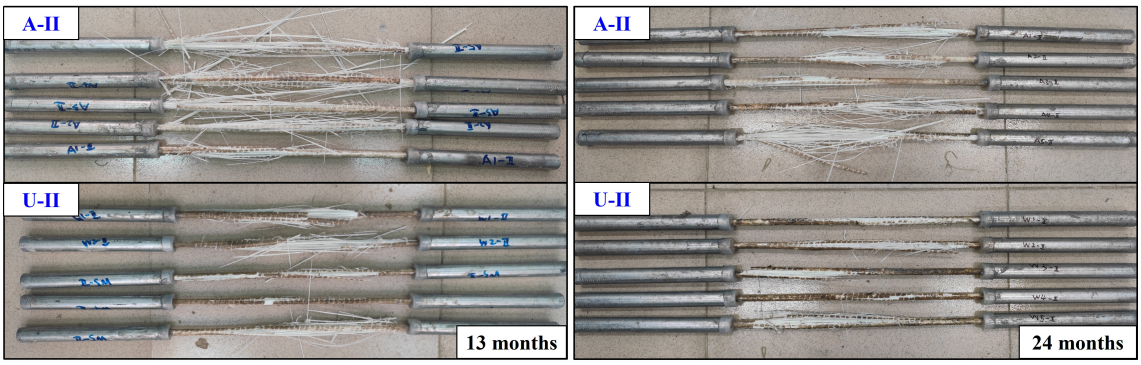
Conversely, for the specimens exposed to the tidal (T-I) and underwater (U-II) environments, localized damage rather than the typical broom-shaped failure was noticed, especially in those with a larger diameter [Figs. 3.7(b) and 3.7(c)]. This indicates that prolonged exposure to consecutive WD cycles (tidal conditions) or continuous immersion (underwater conditions) has a significant impact on the tensile failure modes of GFRP bars. Similar observations have been reported by other researchers (D'Antino et al. 2023; Yue et al. 2024), with the phenomenon potentially attributed to the internal defects induced by resin hydrolysis and cracking.



(a) 6-mm GFRP bars at Station I



(b) 10-mm GFRP bars at Station I



(c) 10-mm GFRP bars at Station II

Fig. 3.7 Failure modes of GFRP bars exposed in different exposure zones

3.3.3 Variations in Tensile Properties of GFRP Bars

The average tensile properties (including tensile strength and elastic modulus) together with standard deviations (SD) and the coefficients of variation (COV) for the two batches of specimens exposed in different zones over various durations are given in Tables 3.5, 3.6 and 3.7. All the test results were calculated based on nominal cross-sectional areas specified by ACI (2017) (i.e., 32 mm^2 and 71 mm^2 for 6- and 10-mm GFRP bars, respectively). The test results of the reference (unexposed) specimens are also included. Note that specimens that failed within or just outside the anchorage were excluded from analysis.

3.3.3.1 Effect of field exposure conditions

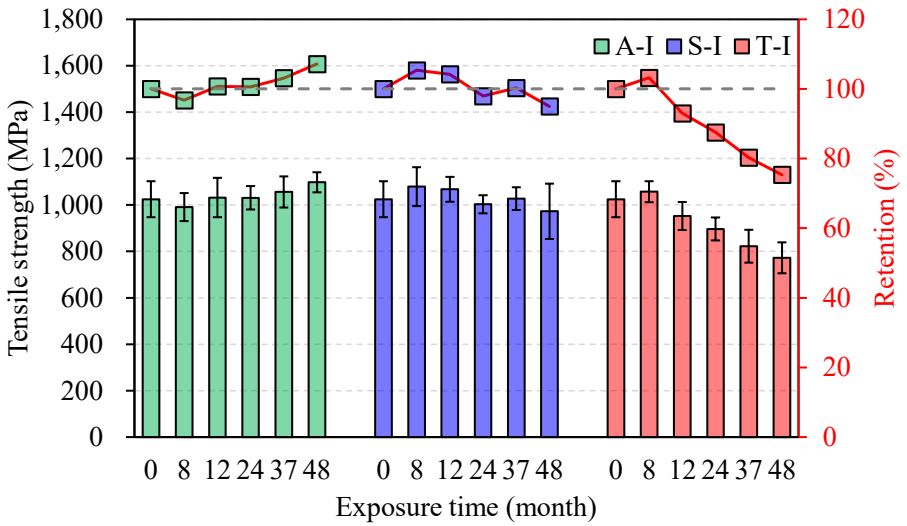
Figs. 3.8(a) and 3.8(b) respectively show the tensile strength variations of 6- and 10-mm GFRP bars (Batch I) exposed in different zones at Station I for up to four years. Under the tidal environment (T-I), a clear decreasing trend in tensile strength was noticed for both bar diameters, with values reducing from 1024.38 MPa and 1224.62 MPa to 771.85 MPa and 993.62 MPa for 6- and 10-mm GFRP bars, respectively, after 48-month field exposure. This suggests that the tidal environment, characterized by cyclic wetting and drying combined with periodic immersion, accelerates the

deterioration of GFRP bars. That is, the repeated exposure to moisture and oxygen appears to promote hydrolysis, plasticization, and swelling on the resin matrix, which in turn leads to weakening of the fiber-matrix interface and the development of microcracks. Besides, glass fibers are particularly sensitive to fluid ingress (e.g., chemical attacks) due to leaching and etching actions, and the prolonged exposure leads to more severe chemical reactions (Chen et al. 2007; Kim et al. 2008; Fergani et al. 2018a; Lu et al. 2020a).

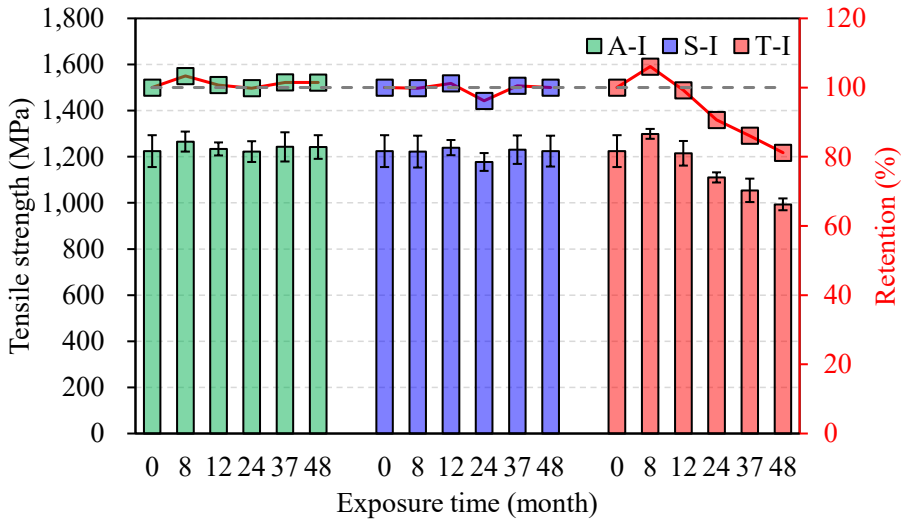
On the contrary, tensile strength of specimens in A-I was almost unchanged throughout the exposure period, with retentions of 96.74~107.15% and 99.82~103.35% for 6- and 10-mm GFRP bars, respectively. These findings align with previous studies on GFRP bars subjected to different atmospheric environments (MAT = 26.0℃ and 27.5℃; RH = 52% and 26%) for up to 18 months, as reported by Al-Salloum et al. (2013). For specimens exposed in S-I, the tensile strength of 10-mm GFRP bars after 48 months remained comparable to unexposed (0-month) specimens (1224.35 MPa versus 1224.62 MPa), while 6-mm GFRP bars exhibited a negligible reduction with a retention of 94.97%. These observations are reasonable because the atmospheric environment, with limited moisture exposure, minimizes hydrolytic degradation, while the splash environment, despite frequent wetting, may not retain sufficient moisture to cause severe deterioration. It is worth highlighting that the tensile strength of FRP bars has been found to be almost unaffected by the conditioning involving UV radiation combined with water-spay or water vapor condensation (Da Silva et al. 2016; Ashrafi et al. 2018).

On the other hand, tensile strength variations of 10-mm GFRP bars (Batch II) exposed at Station II are shown in Fig. 3.8(c). Again, specimens subjected to atmospheric

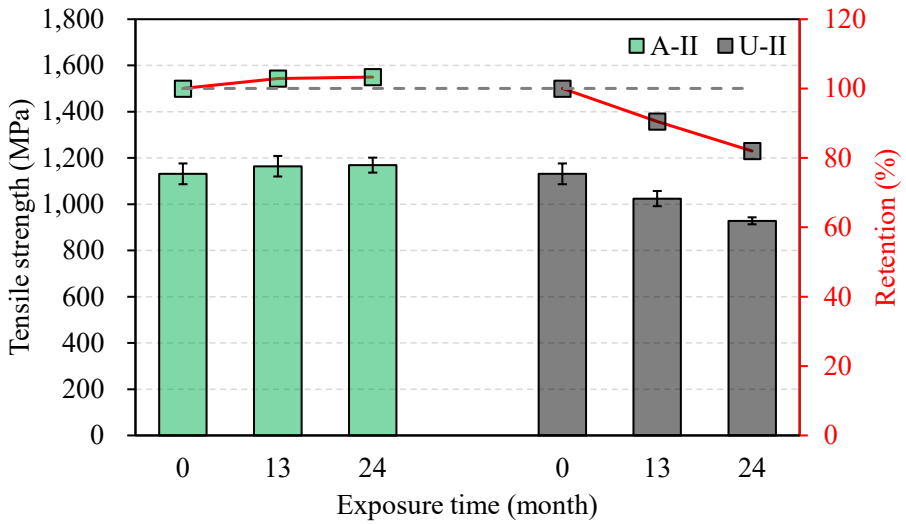
environment (A-II) exhibited insignificant degradation of tensile strength, which is consistent with the observations at Station I (A-I). However, tensile strength of the specimens exposed in U-II remarkably decreased with exposure time, decreasing from 1131.37 MPa to 927.67 MPa after two years. Another important observation is that 10-mm GFRP bars in U-II underwent more severe degradation than those of the same diameter in T-I, with tensile strength retentions of 81.99% and 90.64%, respectively, over 24 months. This difference may be attributed to at least the following two reasons: (1) Continuous seawater immersion in U-II promotes more aggressive chemical reactions than the cyclic exposure in T-I, inducing plasticization of the resin matrix and accelerating hydrolysis, which results in matrix softening and fiber debonding; (2) The much thicker sand-coated layer provides better protection for Batch I specimens (Fig. 3.2), which mitigates the diffusion of harmful ions (Feng et al. 2024a) as well as decelerated the fiber loosening and resin cracking and flaking (Yue et al. 2024).



(a) 6-mm GFRP bars at Station I



(b) 10-mm GFRP bars at Station I

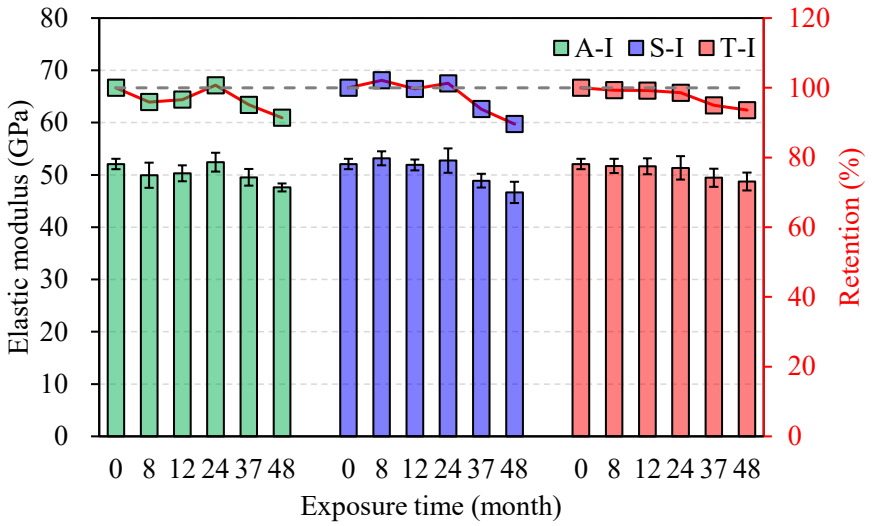


(c) 10-mm GFRP bars at Station II

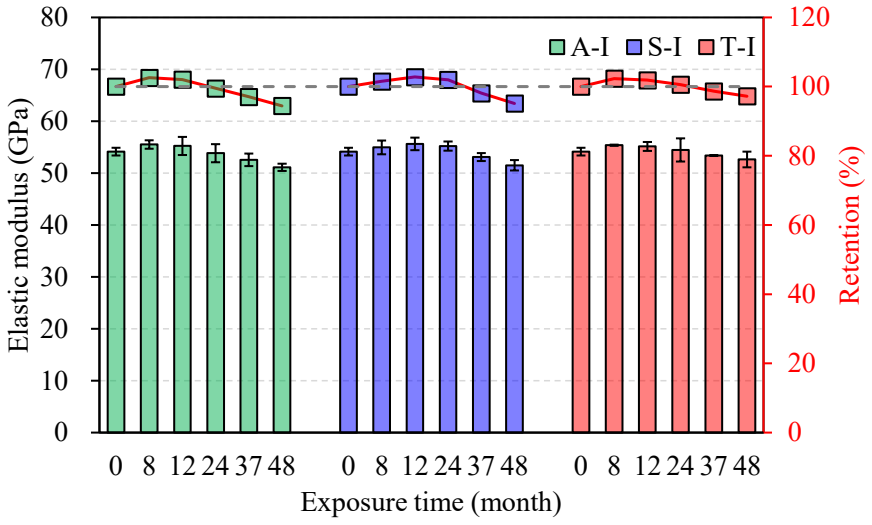
Fig. 3.8 Tensile strength variations of GFRP bars in different field exposure conditions

The variations of tensile elastic modulus for specimens exposed in different zones at both stations are illustrated in Fig. 3.9. Compared to tensile strength, the differences in elastic modulus across environmental conditions were relatively minor for all exposure durations. For example, at Station I, elastic moduli of 6-mm specimens ranged from 46.66 GPa to 53.19 GPa (Table 3.5), while those of 10-mm ones were in the range of 51.10 GPa to 55.62 GPa (Table 3.6), both close to their unexposed counterparts (52.07 GPa and 54.13 GPa for 6- and 10-mm GFRP bars, respectively). Similar phenomena

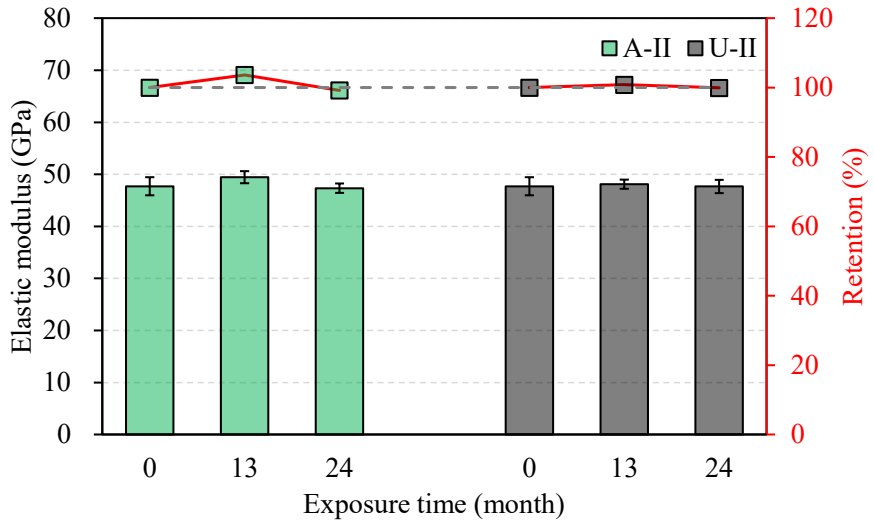
were noticed for specimens at Station II (Table 3.7). This is expected because the elastic modulus of FRP bar is an inherent property of the material, largely governed by fiber content. Thus, it is less affected by the environmental degradation (Kocaoz et al. 2005). Besides, elastic moduli were determined from the linear-elastic portions of stress-strain curves, in which the resin matrix remains effective in transferring stresses to the fibers (Benmokrane et al. 2017b).



(a) 6-mm GFRP bars at Station I



(b) 10-mm GFRP bars at Station I



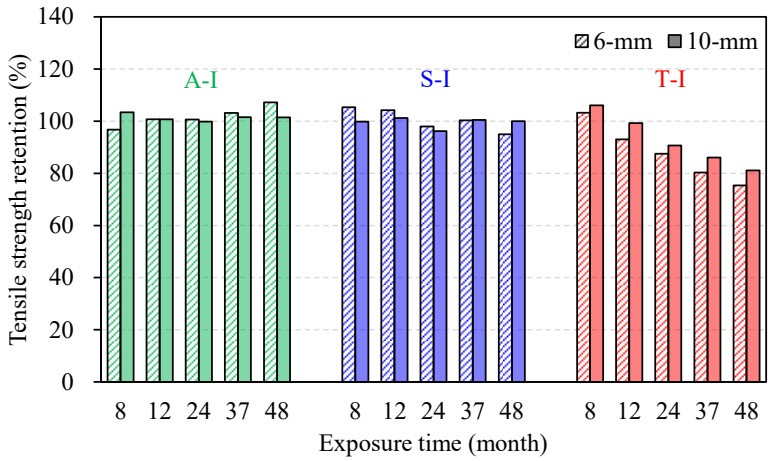
(c) 10-mm GFRP bars at Station II

Fig. 3.9 Elastic modulus variations of GFRP bars in different exposure conditions

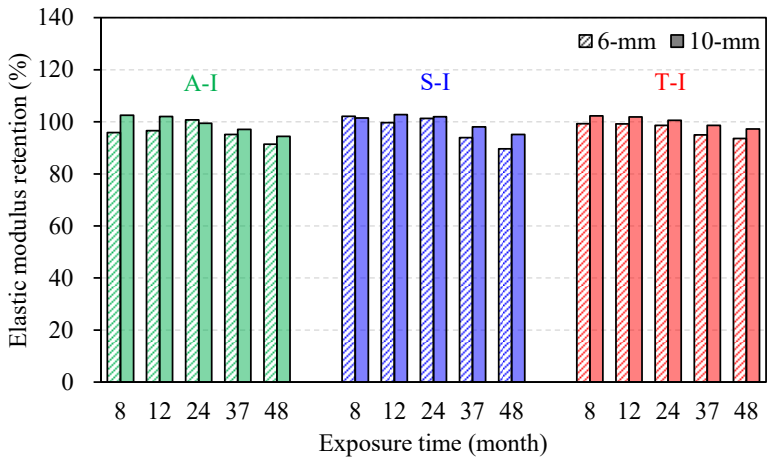
3.3.3.2 Effect of bar diameter

To assess the influence of bar diameter on the durability of GFRP bars in marine environments, Fig. 3.10 compares the retentions of tensile properties for different-sized specimens exposed at Station I. It can be seen from Fig. 3.10(a) that due to the insignificant tensile strength degradation in specimens exposed in A-I and S-I, as discussed previously, no size effect can be observed over the exposure period. For the specimens in T-I, however, the tensile strength deterioration of small-sized specimens (6-mm) was much more pronounced compared to their large-sized counterparts (10-mm), regardless of exposure duration, with retentions of 75.35% and 81.14%, respectively, after four years. Similar findings have been reported in previous studies on GFRP bars immersed in saline solutions (Tannous and Saadatmanesh 1998; Lu et al. 2021a). This size effect may be attributed to the difference between the ratios of "degraded" to "undegraded" areas of the bars subjected to harsh conditions (Arczewska et al. 2021). That is, the larger the bar diameter, the smaller the affected area.

Although elastic moduli of the specimens suffered limited deterioration under the exposure conditions, an interesting observation is that bar diameter seems to have a non-negligible effect on the durability of the tensile elastic modulus, particularly for those subjected to tidal conditions [Fig. 3.10(b)]. Given the fiber contents of the 6- and 10-mm GFRP bars are close to each other (83.6% and 81.1%, respectively, as provided in Table 3.2), this phenomenon may be attributed to the same mechanisms underlying the size effect observed in tensile strength. Although environmental conditions in A-I and S-I are less severe than in T-I, a size effect on elastic modulus retention appears to still exist in most specimens exposed in these two zones.



(a) Tensile strength



(b) Tensile elastic modulus

Fig. 3.10 Comparison of tensile properties of different-sized GFRP bars

Table 3.5 Tensile properties of 6-mm GFRP bars exposed at Station I

Exposure period	Exposure zone	Tensile strength (MPa)				Elastic modulus (GPa)			
		Average	SD	COV (%)	Retention (%)	Average	SD	COV (%)	Retention (%)
0-month	/	1024.38	77.38	7.55	100.00	52.07	1.00	1.92	100.00
8-month	A-I	990.94	60.27	6.08	96.74	49.94	2.41	4.83	95.90
	S-I	1079.06	83.56	7.74	105.34	53.19	1.34	2.52	102.14
	T-I	1057.19	45.22	4.28	103.20	51.72	1.38	2.66	99.32
12-month	A-I	1031.88	85.13	8.25	100.73	50.31	1.53	3.04	96.62
	S-I	1067.50	53.87	5.05	104.21	51.91	1.06	2.04	99.68
	T-I	952.50	60.70	6.37	92.98	51.66	1.51	2.92	99.20
24-month	A-I	1030.54	50.58	4.91	100.60	52.45	1.81	3.45	100.72
	S-I	1003.14	38.98	3.89	97.93	52.74	2.35	4.45	101.29
	T-I	896.44	49.42	5.51	87.51	51.34	2.23	4.35	98.60
37-month	A-I	1056.14	67.14	6.36	103.10	49.53	1.60	3.23	95.11
	S-I	1027.26	49.29	4.80	100.28	48.89	1.34	2.73	93.89
	T-I	822.17	70.60	8.59	80.26	49.46	1.75	3.53	94.97
48-month	A-I	1097.65	43.21	3.94	107.15	47.60	0.74	1.56	91.42
	S-I	972.88	119.27	12.26	94.97	46.66	2.02	4.33	89.61
	T-I	771.85	66.61	8.63	75.35	48.74	1.70	3.49	93.60

Table 3.6 Tensile properties of 10-mm GFRP bars exposed at Station I

Exposure period	Exposure zone	Tensile strength (MPa)				Elastic modulus (GPa)			
		Average	SD	COV (%)	Retention (%)	Average	SD	COV (%)	Retention (%)
0-month	/	1224.62	69.26	5.66	100.00	54.13	0.72	1.34	100.00
8-month	A-I	1265.61	43.10	3.41	103.35	55.50	0.82	1.47	102.54
	S-I	1222.45	68.98	5.64	99.82	54.94	1.33	2.41	101.51
	T-I	1298.87	21.46	1.65	106.06	55.37	0.13	0.23	102.29
12-month	A-I	1233.52	28.34	2.30	100.73	55.23	1.75	3.16	102.03
	S-I	1239.30	32.98	2.66	101.20	55.62	1.23	2.20	102.76
	T-I	1214.96	53.33	4.39	99.21	55.13	0.87	1.58	101.85
24-month	A-I	1222.48	44.90	3.67	99.82	53.84	1.75	3.25	99.46
	S-I	1177.28	38.55	3.27	96.13	55.19	0.90	1.63	101.96
	T-I	1109.94	21.94	1.98	90.64	54.43	2.23	4.11	100.57
37-month	A-I	1242.69	63.55	5.11	101.48	52.53	1.22	2.32	97.05
	S-I	1230.70	61.56	5.00	100.50	53.09	0.75	1.42	98.08
	T-I	1053.92	50.75	4.82	86.06	53.39	0.08	0.15	98.63
48-month	A-I	1242.45	51.19	4.12	101.46	51.10	0.72	1.41	94.41
	S-I	1224.35	66.85	5.46	99.98	51.49	1.00	1.94	95.13
	T-I	993.62	25.79	2.60	81.14	52.62	1.51	2.86	97.22

Table 3.7 Tensile properties of 10-mm GFRP bars exposed at Station II

Exposure period	Exposure zone	Tensile strength (MPa)				Elastic modulus (GPa)			
		Average	SD	COV (%)	Retention (%)	Average	SD	COV (%)	Retention (%)
0-month	/	1131.37	44.73	3.95	100.00	47.70	1.74	3.65	100.00
13-month	A-II	1164.06	44.68	3.84	102.89	49.44	1.17	2.36	103.64
	U-II	1024.00	33.22	3.24	90.51	48.11	0.87	1.80	100.85
24-month	A-II	1168.70	32.17	2.75	103.30	47.33	0.89	1.89	99.22
	U-II	927.67	15.22	1.64	81.99	47.67	1.29	2.71	99.93

3.4 CONCLUSIONS

This chapter presents the results of a field study on two batches of GFRP bars exposed in different marine environmental zones (i.e., atmospheric, splash, tidal and underwater) at two field exposure stations over a period of up to four years, aiming at exploring the durability of GFRP bars subjected to real marine environments. The following conclusions can be drawn based on the results and discussion:

(1) Marine organisms were observed attached to the surfaces of GFPR bars located in the tidal and underwater zones. The appearance of GFRP bars exposed in the splash zone exhibited a color of deep yellow, while minimal surface changes were found for those exposed in both atmospheric zones. Prolonged exposure to tidal and underwater conditions had a significant impact on the failure modes of GFRP bars, with a transition from typical broom-shaped failure to localized damage.

(2) GFRP bars subjected to tidal conditions experienced a noticeable tensile strength reduction after 48-month exposure, compared to those exposed in the atmospheric and splash zones, regardless of bar diameter. Tensile strength deterioration was more severe for GFRP bars exposed underwater than for those of the same diameter subjected to tidal exposure over the same duration. In contrast, the elastic modulus of GFRP bars was comparatively less affected by the different marine environmental conditions.

(3) Large-sized GFRP bars demonstrated better resistance to tensile strength degradation than their small-sized counterparts under tidal exposure, regardless of exposure duration, implying a size effect on the durability of GFRP bars in

terms of tensile strength. Besides, a non-negligible size effect was also observed in the tensile elastic modulus of GFRP bars subjected to marine environments.

CHAPTER 4
PREDICTION MODEL FOR DURABILITY OF FRP BARS

4.1 INTRODUCTION

In Chapter 3, a systematic experimental study has been presented on the long-term performance of GFRP bars subjected to real marine environments for up to four years. In order to estimate the durability of FRP bars in real service environment, currently, several prediction models have been proposed based on the short-term experimental results obtained from AAT studies (Bank et al. 2003; Huang and Aboutaha 2010; Davalos et al. 2011; Serbescu et al. 2015; Dong et al. 2017b; Wang et al. 2024). However, a concern arises from the fact that the severe exposure conditions employed in AAT studies, such as immersion in high pH-level alkaline solutions at elevated temperatures, may not accurately represent the actual conditions experienced by FRP bars during their service life. This discrepancy could result in potential inaccuracies in model predictions. To address this issue, a systematic assessment of these models is essential prior to establishing a reliable conversion relationship between AAT and FET.

In this chapter, existing prediction models concerning the durability of FRP bars were first reviewed. Subsequently, the performance of selected models was assessed against a newly assembled FET database using the AAT results collected from AAT database in Chapter 2. Finally, a refined model was proposed for bare FRP bars in marine environments based on the existing FET results with the aim to develop a consolidated and accurate approach for predicting the long-term performance of FRP bars.

4.2 EXISTING PREDICTION MODELS FOR DURABILITY OF FRP BARS

4.2.1 Empirical Models Based on Arrhenius Theory

Currently, most of the commonly used prediction models for the long-term mechanical properties of FRP bars in real service environment are developed based on Arrhenius theory (Nelson 2009), which assumes that the increasing temperatures and aging time only increase the degradation rate but do not affect the degradation mechanism. Thus, temperature is the sole dominant factor of acceleration in the aging process. The relationship between the degradation rate of FRP bars and the aging temperature can be expressed as follows:

$$k = A \exp\left(-\frac{E_a}{RT}\right) \tag{4.1}$$

where k = degradation rate (1/time); A = constant of material and degradation process; E_a = activation energy of material; R = universal gas constant; and T = temperature in Kelvin.

Eq. (4.1) can be further expressed as:

$$\ln\left(\frac{1}{k}\right) = \frac{E_a}{R} \cdot \frac{1}{T} - \ln A \tag{4.2}$$

In Eq. (4.2), it can be found that the logarithm of $1/k$ (the time for a material property to degrade to a given value) is a linear function of $1/T$ with a slope of E_a/R.

According to the Arrhenius theory, the time shift factor (TSF), a concept proposed by Dejke and Tepfers (2001), for a mechanical property to reach the same retention value

(represented by Y) at different temperatures of T_0 and T_1 can be calculated by the following equation:

$$TSF = \frac{t_0}{t_1} = \frac{\frac{Y}{k_0}}{\frac{Y}{k_1}} = \frac{k_1}{k_0} = \frac{A\exp\left(-\frac{E_a}{RT_1}\right)}{A\exp\left(-\frac{E_a}{RT_0}\right)} = \exp\left[\frac{E_a}{R}\left(\frac{1}{T_0} - \frac{1}{T_1}\right)\right] \quad (4.3)$$

where Y = retention of FRP mechanical property (%); t_0 and t_1 = time required for the mechanical property to reach a given retention value at temperatures of T_0 and T_1, respectively; and k_0 and k_1 = degradation rates at temperatures of T_0 and T_1, respectively.

On the basis of Arrhenius theory, numerous studies have been carried out to predict the long-term performance of FRP bars by using the existing models and the short-term results obtained from AAT studies (Tannous and Saadatmanesh 1998; Bank et al. 2003; Huang and Aboutaha 2010; Davalos et al. 2011; Robert and Benmokrane 2013; Wu et al. 2015; Dong et al. 2017b). At present, there are two main prediction methods for the performance prediction of FRP bars by measuring either "strength retention" or "moisture absorption" (Serbescu et al. 2015). The five widely used prediction models are briefly introduced as follows.

The first model, originally proposed by Litherlan et al. (1981) for predicting the residual strength of glass fiber reinforced concrete (GRC) and later described by Bank et al. (2003) for FRP composites, can be expressed as Eq. (4.4):

$$Y = a\log(t) + b \quad (4.4)$$

where t = aging time; and a and b = fitting parameters of regression equation. However, the following two inherent limitations exist in this model: (1) This model is only a

linear regression of the test results and does not adopt any assumptions related to degradation mechanism; (2) The strength retention at $t = 0$ approaches infinity. Additionally, some researchers have found that, when using this model for FRP bars, the Arrhenius plots fitted using the test results of FRP bars were not parallel to each other (Davalos et al. 2011; Wu et al. 2015), which implied that the degradation mechanism may have changed with exposure time, violating the basic assumption in the Arrhenius theory.

Apart from the single logarithmic model [Eq. (4.4)], the second model, which was proposed by Serbescu et al. (2015) based on the prediction method adopted by *fib* Bulletin 40 (fib 2007), assumes that the strength retention and the aging time have a linear relationship in a double logarithmic scale. The strength retention can be calculated by Eq. (4.5):

$$\log(Y) = a\log(t) + b \tag{4.5}$$

Another two models expressed by Eqs. (4.6) and (4.7) were initially proposed by Phani and Bose (2012) to predict the flexural strength retention of CFRP composite laminates:

$$Y = 100 \exp\left(-\frac{t}{\tau}\right) \tag{4.6}$$

$$Y = (100 - Y_\infty) \exp\left(-\frac{t}{\tau}\right) + Y_\infty \tag{4.7}$$

where τ = fitting parameter; and Y_∞ = retention of mechanical properties of FRP bars (%) at aging time of infinity. These two models assume that the degradation rates of mechanical properties of FRP bars are relatively high at the initial aging, then slow down gradually and finally stabilize. Different from the first two models [i.e., Eqs. (4.4) and (4.5)], the degradation mechanism adopted for these two models is that the

degradation of FRP bars is mainly caused by the fiber-resin interface debonding. The main difference between Eqs. (4.6) and (4.7) is that the residual mechanical properties of FRP bars tend to be zero or a given value Y_∞. It is worth mentioned that Eq. (4.6) is much more conservative than Eq. (4.7) for FRP bar predictions as reported by Wang et al. (2017b) and Feng et al. (2022).

Except for the aforementioned four "strength retention" models, the fifth model, namely "moisture absorption" model, was proposed by Tannous and Saadatmanesh (1998) based on Fick's law, as given in Eq. (4.8):

$$Y = 100\left(1 - \frac{\sqrt{2DCt}}{r_0}\right)^2 \tag{4.8}$$

where D = diffusion coefficient; C = solution ion concentration; and r_0 = radius of FRP bars. The use of this model is limited due to at least the following two reasons: (1) The model assumes that the affected area of FRP bars penetrated by ion erosion completely deteriorates and can no longer bear any load, which may not represent the actual conditions of FRP bars; (2) It is rather complicated to obtain the values of D and C from moisture absorption tests on FRP bars (Dong et al. 2017b).

4.2.2 *fib* Bulletin 40 (2007) Model

To consider the influences such as moisture condition, temperature, desired service-life and diameter on the durability of FRP bars in concrete, *fib* Bullentin 40 (2007) proposed an approach to predict the long-term tensile performance of FRP bars. An environmental strength reduction factor $\eta_{env,t}$, whose inverse (i.e., $1/\eta_{env,t}$) representing the tensile strength retention of FRP bars, was incorporated in this prediction method. When the characteristic value of tensile strength after 1000-hour

exposure $f_{fk1000h}$ is known, $\eta_{env,t}$ can be determined by Eq. (4.9a); otherwise, Eq. (4.9b) is recommended.

$$\eta_{env,t} = \begin{cases} f_{fk1000h}/f_{fk0}/[(100 - R_{10})/100]^n & (a) \\ 1/[(100 - R_{10})/100]^{n+2} & (b) \end{cases} \tag{4.9}$$

where f_{fk0} = characteristic value of tensile strength obtained from the short-term tests; R_{10} = standard reduction of tensile strength in percent per logarithmic decade due to environmental influence, which can be determined by the slope of tensile strength versus time in double logarithmic scale; and n = exponent comprising the sum of moisture (n_{mo}), temperature(n_T), service life (n_{SL}) and diameter (n_d) exponents, as given in Eq. (4.10).

$$n = n_{mo} + n_T + n_{SL} + n_d \tag{4.10}$$

The values of these four influencing parameters adopted in *fib* Bulletin 40 (2007) for different environmental conditions are given in Table 4.1.

Table 4.1 Influencing parameters adopted in *fib* Bulletin 40 (2007)

Parameter	Condition[#]	Value
Moisture (n_{mo})	Dry (RH = 50%)	-1
	Moist (RH = 80%)	0
	Moisture saturated (RH = 100%)	1
Temperature (n_T)	MAT < 5°C	-0.5
	MAT = 5 to 15°C	0
	MAT = 15 to 25°C	0.5
	MAT = 25 to 35°C	1
Service life (n_{SL})	1 year	1
	10 years	2
	50 years	2.7
	100 years	3
Diameter (n_d)	≥ tested	0
	75% of tested	0.5
	50% of tested	1

[#]RH = relative humidity; MAT = mean annual temperature.

4.2.3 Prediction Models Based on Environmental Reduction Factor (ERF)

Based on the single logarithmic prediction model [Eq. (4.4)] and the existing design guidelines/codes for durability specification of FRP bars used as concrete reinforcement, a model that incorporates the effects of temperature, design life (DL) and environmental relative humidity (RH) into the ERF was proposed for tensile durability of FRP bars by Huang and Aboutaha (2010). Eq. (4.11) expresses the ERF (η_E) for FRP bars with specified design service life and service temperature in both saturated and unsaturated concrete conditions:

$$\eta_E = 1 - n_H \cdot [\Delta_1 - \rho \cdot \log(\mathrm{DL} \cdot \mathrm{TSF})] \tag{4.11}$$

where n_H = RH correction factor, which was assumed to be equal to the ratio of mobile water (i.e., capillary and adsorbed water) in concrete under different RHs as shown in Fig. 4.1; Δ_1 = tensile strength reduction after 1-year experimentally exposure or by substituting log (365) into the regression equation; ρ = slope of Arrhenius regression line of the single logarithmic model [Eq. (4.4)]; DL = design life in years; and TSF = time shift factor between the reference temperature and the service temperature, which can be calculated by Eq. (4.3).

Given that the actual service temperature over a year is a fluctuating value rather than a constant value, Huang (2011) further improved the refined model [Eq. (4.11)] by adopting the mean monthly temperature (MMT) instead of the MAT. It was found that the difference between the ERFs by the two methods is limited, with the latter one generating a relatively conservative value (Huang 2011).

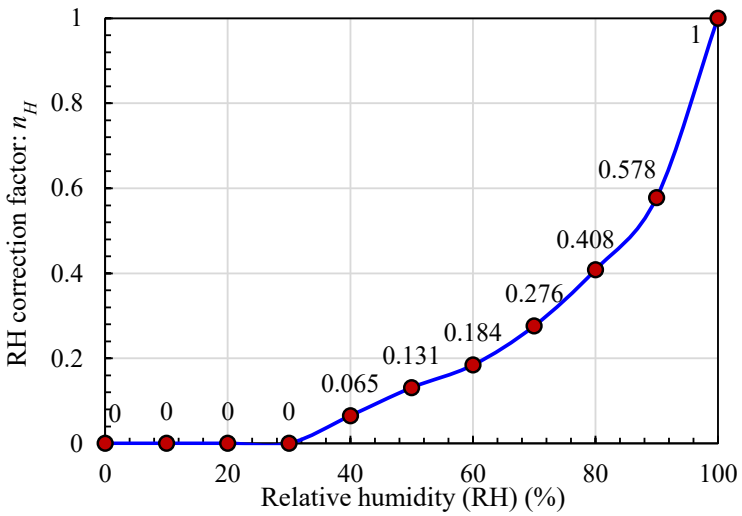


Fig. 4.1 Relationship between RH correction factor and relative humidity (adapted from Huang and Aboutaha 2010)

Based on the approaches taken by Huang and Aboutaha (2010) and Huang (2011), Dong et al. (2017b) proposed a refined model involving the effects of concrete wrapping, temperature fluctuation, DL and RH. In this model, the ERF can be determined by Eq. (4.12):

$$\mathrm{ERF} = 1 - n_H \left[\Delta_1 - \rho \cdot \log\left(\frac{\mathrm{DL} \cdot \mathrm{TSF}}{\alpha \cdot \eta}\right)\right] \tag{4.12}$$

where α = nominal time shift factor for bare FRP bars and concrete-embedded FRP bars immersed in the liquid solution (α = 2.44 and 2.08 were recommended for GFRP and BFRP bars, respectively, before more experimental data is available); and η = correction factor considering the influence of the actual temperature fluctuations, as given in Eq. (4.13).

$$\eta = \frac{12}{\sum_{i=1}^{12} \exp\left[\frac{E_a}{R}\left(\frac{1}{T_{AT}} - \frac{1}{T_{MT}}\right)\right]} \tag{4.13}$$

where T_{AT} = mean annual temperature; and T_{MT} = mean monthly temperature. Table 4.2

summarizes the correction factors required for different types of AAT that classified by Dong et al. (2017b).

Table 4.2 Correction factors (CFs) required for long-term predictions using different types of aging tests [Dong et al. (2017b)]

	AAT with elevated temperatures		
	Type I	Type II	Type III
	Bare bar immersed in solution	Concrete-embedded bar immersed in solution	Concrete-embedded bar exposed to constant humidity environment
Correction factor[#]	α, n_H, η	n_H, η	η

[#] α, n_H, η = CFs for concrete-wrap, RH and temperature fluctuation, respectively.

On the basis of the exponential model [Eq. (4.7)] and the concept introduced by Huang and Aboutaha (2010), Feng et al. (2023) recently developed another refined model that incorporates the effects of RH and temperature fluctuations to predict the deterioration of FRP bars, as expressed in Eq. (4.14).

$$100 - (100 - Y)n_H = (100 - Y_\infty)\exp\left(-\frac{t}{\tau}\right) + Y_\infty \tag{4.14}$$

Different from the previous refined models, daily temperature is used to determine the TSF values in this refined model.

4.3 EXPERIMENTAL DATABASE

To assess the performance of existing prediction models derived from AAT and to establish the conversion relationship between AAT and FET, a filtered FET database was developed, as given in Table 4.3, based on the database (i.e., Table D1) provided in Appendix B. Only GFRP bars [including bare bars, concrete-embedded bars without sustained load (i.e., unstressed) and concrete-embedded bars with sustained load (i.e.,

stressed)] are considered in this chapter due to the limited availability of FET data for other types of FRP bars as mentioned previously. Besides, only the tensile strength of GFRP bars is included in the database for several reasons: (1) It is one of the most critical properties of FRP bars, with various design codes/guidelines [e.g., *fib* Bulletin 40 (2007); (CSA 2019; ACI 2022)] recommending durability-related reduction factors for it; (2) Most prediction models were initially developed to assess the tensile durability of FRP bars; (3) Compared to the tensile properties of GFRP bars, experimental data on other mechanical properties is relatively scarce. The details of the FET datasets included in Table 4.3 are given in the following subsections.

4.3.1 Bare GFRP Bars

Al-Salloum et al. (2013) conducted FET on the 12-mm GFRP bare bars (made with vinylester resin) subjected to two field conditions with exposure times of 6, 12, and 18 months. The exposure sites included Riyadh and Jubail in Saudi Arabia, representing the hot-dry and hot-humid environments of the Middle East, respectively. The MATs of these two locations are similar (27.5℃ and 26℃) with mean annual high and low temperatures of 33℃ and 19℃, respectively, while the mean annual RHs are about 26% and 52%, respectively.

4.3.2 Concrete-Embedded Unstressed GFRP Bars

Morales et al. (2021) carried out FET on the durability of unstressed GFRP bars (9.5-mm and VE-based) embedded in fly ash-based and slag-based seawater concrete (SWC). The SWC elements were exposed to the typical field environment of a subtropical region in South Florida, USA, for varying durations (1, 6, 12 and 24 months). The recorded MAT and RH for the field conditions were 25℃ and 71.2%,

respectively.

4.3.3 Concrete-Embedded Stressed GFRP Bars

A total of three FET studies on stressed GFRP bars embedded in concrete were collected (Bakis et al. 2005; Mukherjee and Arwikar 2005; Trejo et al. 2011). (1) Bakis et al. (2005) presented FET results of the residual tensile properties of 10.2-mm GFRP bars (VE-based) in concrete beams with a sustained load of 20% of ultimate moment M_u (which was roughly 12% of the ultimate tensile strength f_u of the FRP bar, as reported by the authors). Prior to the application of sustained load, the beams were pre-cracked under four-point bending by subjecting them to about 50% M_u. The beams were exposed to the outdoor environment in State College, Pennsylvania, for durations of 12 and 36 months. The MAT in this location is 9°C, with typical daily high and low temperatures of 20~30℃ in the summer and -15~-5℃ in the winter, respectively. (2) The FET carried out by Mukherjee and Arwikar (2005) was similar to that by Bakis et al. (2005). In this study, the pre-cracked concrete beams were exposed to the natural conditions of Mumbai, India. The environment is hot and humid, with the MAT and RH being 27.5℃ and 74.9%, respectively. (3) Trejo et al. (2011) examined the tensile durability of three different types of GFRP bars embedded in concrete slabs. These slabs were subjected to natural weather conditions in Texas, USA, for approximately seven years. Before natural exposure, the slabs were pre-cracked under three-point bending, as a result of which the maximum stress of the inner GFRP bars was less than 30% f_u. The recorded mean daily temperatures of the exposure site were 5~40℃ and the MAT and RH were reported to be 23℃ and 59.3%, respectively.

Table 4.3 FET database for model assessment

Reference	Bar type	Concrete type	Stress level	Exposure site	MAT (°C)	RH (%)	Time (m)	Ret. (%)	Remarks
Al-Salloum et al. (2013)	12 mm (VE)	/	0	Riyadh, Saudi Arabia	27.5	26.0	6	99.66	Bare GFRP bars
							12	99.59	
							18	99.46	
	12 mm (VE)	/	0	Jubail, Saudi Arabia	26.0	52.0	6	99.80	
							12	99.46	
							18	99.46	
Morales et al. (2021)	9.5 mm (VE)	SWC (with fly ash)	0	South Florida, USA	25.0	71.2	1	99.86	Concrete-embedded unstressed GFRP bars
							6	96.69	
							12	100.53	
							24	98.60	
	9.5 mm (VE)	SWC (with slag)	0				1	85.45	
							6	88.87	
							12	88.67	
							24	81.51	
Bakis et al. (2005)	10.2 mm (VE)	NC	20% M_u	Pennsylvania, USA	9.0	57.6*	12	102.85	Concrete-embedded stressed GFRP bars
							36	98.78	
Mukherjee and Arwikar (2005)	9.5 mm (VE)	NC	20% M_u	Mumbai, India	27.5*	74.9*	18	65.43	
							30	61.40	
Trejo et al. (2011)	16 mm (PE)	NC	Preloaded: < 30% f_u	Texas, USA	23.0	59.3*	≈84	87.16	
	16 mm (VE)						≈84	88.32	
	16 mm (VE)						≈84	73.89	
	19 mm (PE)						≈84	92.73	
	19 mm (VE)						≈84	79.34	
	19 mm (VE)						≈84	78.50	

Note: (1) VE = vinylester resin; PE = polyester resin. (2) SWC = seawater concrete; NC = normal concrete. (3) M_u = ultimate moment measured in the beam tests; f_u = ultimate tensile stress of an FRP bar. (4) "*": The data were collected from the online database (https://www.climate.top/).

Upon observing the database given in Table 4.3, in general, it can be found that the GFRP bars for FET studies considered herein were mainly manufactured with vinylester resin and had diameters ranging from 9.5 mm to 19 mm. The majority of these bars were subjected to field exposure for less than three years, while only one study reported test results for specimens exposed in field for seven years (Trejo et al. 2011). In addition, most specimens were placed in exposure sites characterized by hot-humid or hot-dry conditions, with an exception reported in Bakis et al. (2005) being exposed to a cold environment (MAT = 9°C).

4.4 PERFORMANCE OF EXISTING MODELS FOR DURABILITY OF FRP BARS

In this section, three commonly used models [i.e., Arrhenius empirical model, *fib* Bulletin 40 (2007) model and Huang and Aboutaha's (2010) model], as described in Section 4.2, were employed to predict the tensile strength retention of GFRP bars using the AAT database (i.e., Table A1) provided in Chapter 2. These predictions were subsequently compared with the FET results presented in Table 4.3, aiming to evaluate the capability of each model in predicting the deterioration of GFRP bars under actual exposure conditions based on AAT data and provide a comprehensive assessment of model performance.

4.4.1 Arrhenius Empirical Model

As discussed in Section 4.2.1, a potential issue with using logarithmic models to predict the long-term performance of FRP bars is that the Arrhenius plots may not be parallel to each other. Consequently, the less conservative exponential model [i.e., Eq. (4.7)] was applied in this section. To enhance the accuracy of predictions using Arrhenius model,

available AAT results with at least three different temperatures were selected (Bank et al. 2003). Note that Bank et al. (2003) suggested a minimum acceptable coefficient of determination (R^2) of 0.80. As a result, data points that did not meet this criterion (i.e., $R^2 < 0.80$) were first excluded and the remaining ones with at least two different temperatures were then utilized for further calculations.

4.4.1.1 Bare GFRP bars

According to Eq. (4.7), the master curves of selected short-term test data for different conditions are shown in Fig. 4.2, and for reference, the corresponding coefficients of regression equations obtained in the prediction process are listed in Table 4.4. The AAT data used herein is limited to those obtained from bare GFRP bars (with a diameter range of 9.5~12.7 mm) immersed in alkaline, saline and water solutions. The FET data reported by Al-Salloum et al. (2013) (Table 4.3) is also included in each subfigure of Fig. 4.2 to assess the prediction accuracy based on Arrhenius theory. Only the predicted results calculated using a MAT of 26.0℃ are presented herein as a reference since the difference between the predictions for MATs of 26.0℃ and 27.5℃ at the two exposure sites is relatively small, while using the lower MAT with the same dataset yields a more conservative prediction.

Table 4.4 Coefficients of regression equations based on Arrhenius empirical model for bare GFRP bars

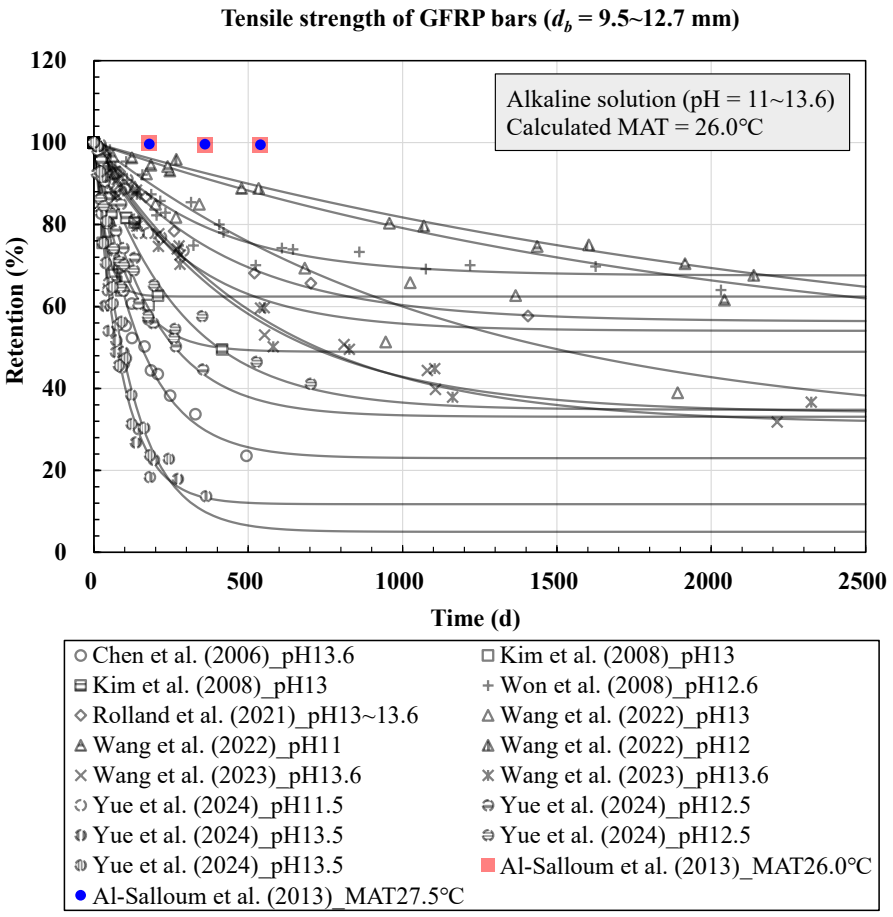
Solution type	Reference	Bar type	pH	T (℃)	Coef. in Eq. (4.7)			Coef. in Eq. (4.2)		TSF	Coef. for master curve		
					τ	Y_∞	R^2	E_a/R	R^2		τ	Y_∞	R^2
Alkaline solution	Chen et al. (2006)	9.53 mm (VE)	13.6	20	165.5	22.31	0.963	2122	0.957	0.86	148.6	22.96	0.985
				40	121.9		0.999			1.37			
				60	68.9		0.996			2.06			
	Kim et al. (2008)	12.7 mm (VE)	13.0	25	35.0	59.90	0.994	2127	0.808	0.98	36.2	62.41	0.972
				40	42.2		0.996			1.37			
				80	13.0		1.000			2.97			
		12.7 mm (Modified VE)	13.0	25	186.7	42.44	0.951	3787	0.949	0.96	277.1	34.77	0.972
				40	159.1		0.929			1.76			
				80	28.6		1.000			6.93			
	Won et al. (2008)	12.7 mm (VE)	12.6	20	429.2	67.59	0.968	3742	0.989	0.77	358.8	67.58	0.953
				40	230.4		0.907			1.75			
				60	90.3		0.949			3.58			
				80	52.5		0.956			6.77			
	Rolland et al. (2021)	12.7 mm (VE)	13.0 ~ 13.6	20	682.1	55.24	1.000	5183	0.992	0.70	418.9	56.36	0.997
				40	187.7		0.999			2.17			
				60	82.2		1.000			5.86			
	Wang et al. (2022)	9.52 mm (VE)	13.0	23	1097.1	30.67	0.961	8926	0.958	0.74	1189.8	29.63	0.967
				40	392.5		0.962			3.80			
				60	38.9		0.995			21.01			
			11.0	23	2426.0	46.78	0.914	11184	0.994	0.68	2044.2	46.13	0.993
				40	416.3		0.995			5.32			
				60	36.8		0.993			45.40			
			12.0	23	2040.0	43.47	(0.717)	11920	1.000	/	2566.1	43.46	0.997
				40	432.2		0.993			5.94			
				60	44.0		0.996			58.36			
	Wang et al. (2023a)	9.52 mm (VE)	13.6	23	641.8	30.90	0.936	7356	0.991	0.78	556.2	31.32	0.991
				40	209.6		0.997			3.00			

				60	40.8		0.999			12.30		
			13.6	23	543.5	33.49	0.944	7499	0.980	0.78	499.0	33.97	0.983
				40	196.0		0.998			3.07		
				60	32.8		0.996			12.91		
	Yue et al. (2024)	12 mm (EP)	11.5	20	363.5	55.37	0.871	2593	0.987	0.84	306.1	54.06	0.934
				40	186.3		0.959			1.47		
				60	126.3		0.915			2.42		
			12.5	20	349.7	19.54	0.940	3175	0.921	0.80	190.9	33.11	0.933
				40	126.7		0.909			1.61		
				60	96.6		0.966			2.95		
			13.5	20	105.8	11.91	0.886	3251	0.983	0.80	89.8	11.75	0.971
				40	60.4		0.991			1.63		
				60	27.7		0.994			3.03		
		12 mm (EP)	12.5	20	138.1	48.18	0.911	5182	0.984	0.70	104.0	48.94	0.948
				40	56.2		0.936			2.17		
				60	16.4		0.933			5.86		
			13.5	20	136.1	8.29	0.919	2074	0.986	0.87	121.4	5.03	0.959
				40	79.6		0.950			1.36		
				60	58.4		0.983			2.03		
Saline solution	Kim et al. (2008)	12.7 mm (VE)	/	25	256.9	45.28	0.895	3994	1.000	0.96	244.3	45.41	0.983
				40	218.3		(0.504)			/		
				80	31.9		0.981			7.70		
	Ruiz Emparanza et al. (2022)	≈10 mm (VE)	/	23	1827.5	57.74	0.943	9713	1.000	0.72	1312.7	57.75	0.994
				40	738.0		(0.706)			/		
				60	47.8		0.987			27.49		
		≈10 mm (VE)	/	23	1986.5	73.34	(0.535)	11935	1.000	/	10823.7	73.21	0.940
				40	1802.1		0.810			5.95		
				60	182.8		0.840			58.65		
	Wang et al. (2023a)	9.52 mm (VE)	/	23	3974.6	49.66	0.915	11959	0.999	0.67	2918.0	49.27	0.996
				40	509.9		0.990			5.97		
				60	44.9		0.993			59.14		
Water	Kim et al. (2008)	12.7 mm (VE)	/	25	73.0	77.53	(0.639)	2723	1.000	/	82.6	78.57	0.947
				40	62.1		0.896			1.50		

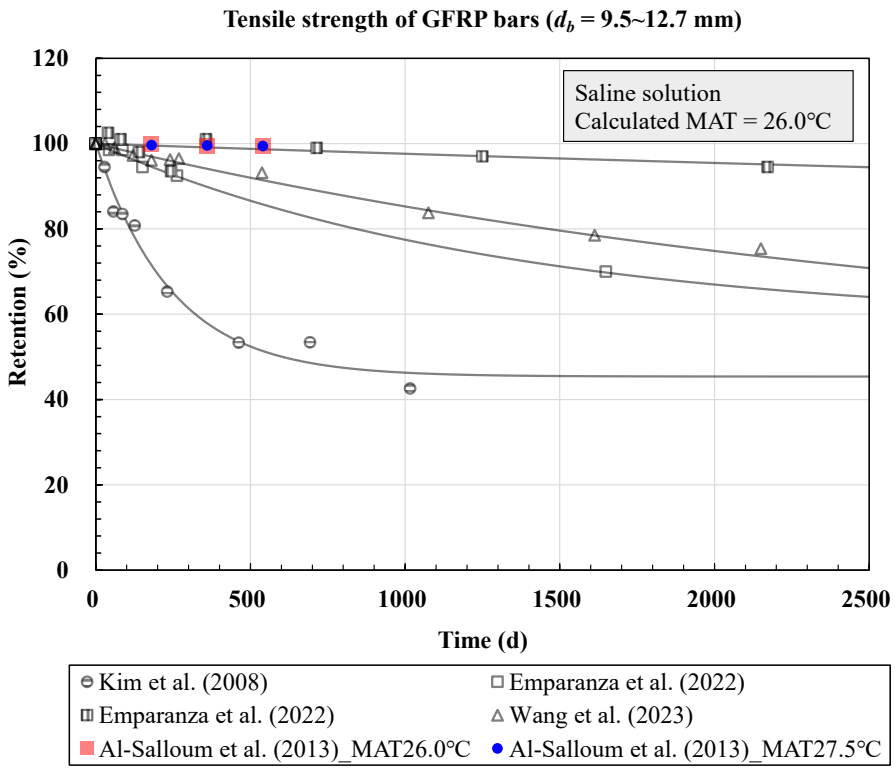
			80	23.2		0.961			4.02			
	12.7 mm	/	25	270.9	43.79	(0.295)	5376	1.000	/	544.1	44.01	0.987
	(Modified VE)		40	245.8		0.857			2.23			
			80	35.2		0.997			15.61			
Wang et al. (2022)	9.52 mm (VE)	/	23	8445.9	48.62	(-0.334)	13279	1.000	/	3288.4	48.73	0.992
			40	454.1		0.966			7.28			
			60	35.6		0.990			92.78			

Note: (1) VE = vinylester resin; EP = epoxy resin. (2) The data in the brackets were excluded from the calculation because the correlation coefficient (R^2) was less than 0.80. (3) All the predicted results were calculated based on the MAT of 26.0℃.

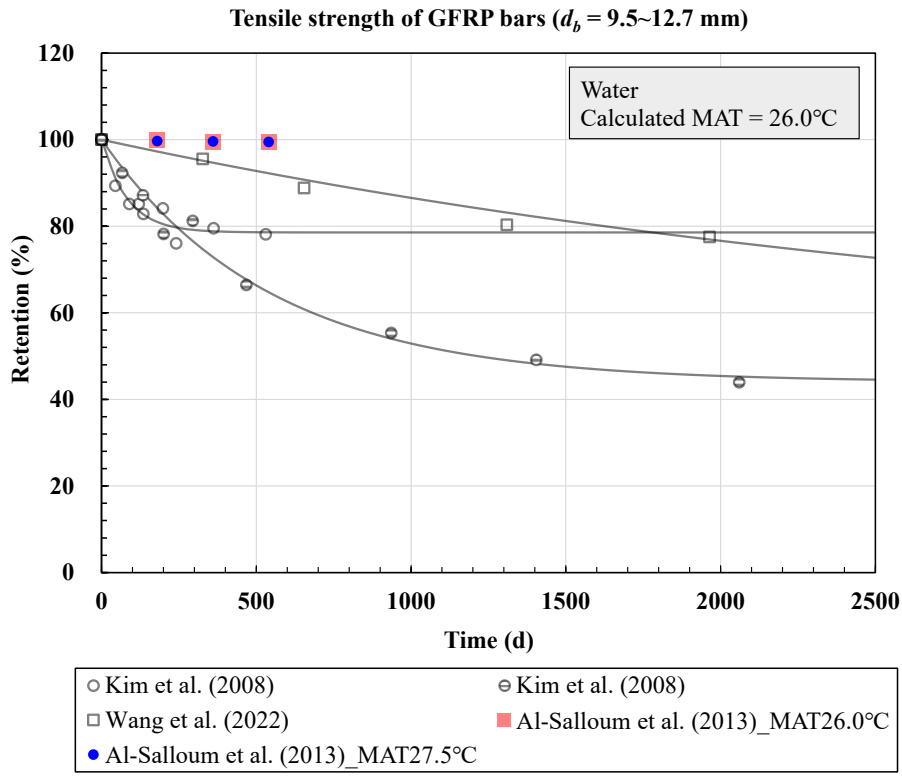
As shown in Figs. 4.2(a)~4.2(c), the prediction curves for different studies vary significantly, regardless of the solution type. This variability can be further evidenced by the distinctly different convergency values Y_∞ observed for the master curves corresponding to different studies. Specifically, the convergence values range from 5.03% to 67.58% for alkaline solutions, 45.41% to 73.21% for saline solutions, and 44.01% to 78.57% for water solutions (see Table 4.4). This is reasonable because the long-term performance of FRP bars is affected by many factors, including fiber, matrix and their interfacial properties (Benmokrane et al. 2020b), bar diameter (Benmokrane et al. 2017b), manufacturing process (Benmokrane et al. 2020b) as well as exposure conditions (e.g., alkaline concentration and saline contents) (Wang et al. 2023a). Another important observation that can be made from Fig. 4.2 is that the FET data points (solid markers) lie above all the master curves of three different solution types, indicating that the selected Arrhenius empirical model provides highly conservative predictions for bare GFRP bars exposed to atmospheric environments [i.e., hot-dry and hot-humid environmental conditions (Al-Salloum et al. 2013)], particularly when AAT data from high pH-level alkaline conditions are used [Fig. 4.2(a)]. The significantly underestimated predictions can be attributed to the fact that direct immersion in a solution is considerably more aggressive than real-world environmental conditions and thus cannot accurately represent the actual field conditions that GFRP bars are subjected to.



(a) Alkaline solution



(b) Saline solution



(c) Water

Fig. 4.2 Comparison between FET result and prediction curves based on Arrhenius empirical model for bare GFRP bars

4.4.1.2 Concrete-embedded unstressed GFRP bars

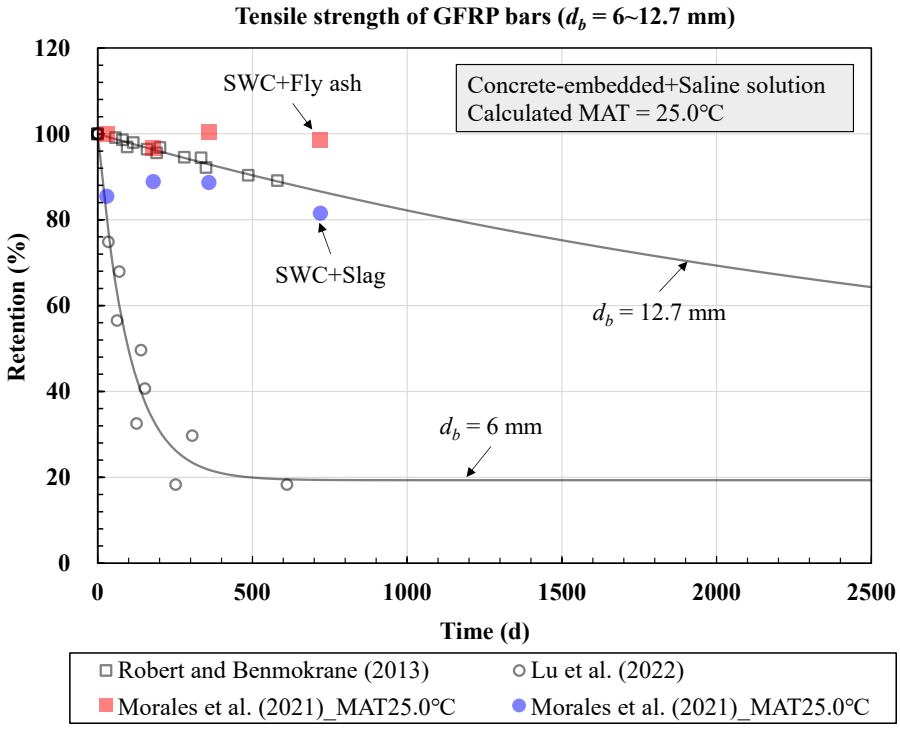
Similar to the bare GFRP bars, the prediction process was also performed on the unstressed GFRP bars wrapped in concrete. The resultant curves were compared with the FET results in Morales et al. (2021) (see Table 4.3) to assess the accuracy of Arrhenius model [Eq. (4.7)]. The master curves for different conditions are displayed in each subfigure of Fig. 4.3 and the corresponding coefficients of regression equations obtained in the prediction process are provided in Table 4.5. Since the AAT data for concrete-embedded unstressed GFRP bars immersed in the alkaline solution is lacking, only those with respect to saline and water solution immersion are presented.

Table 4.5 Coefficients of regression equations based on Arrhenius empirical model for concrete-embedded unstressed GFRP bars

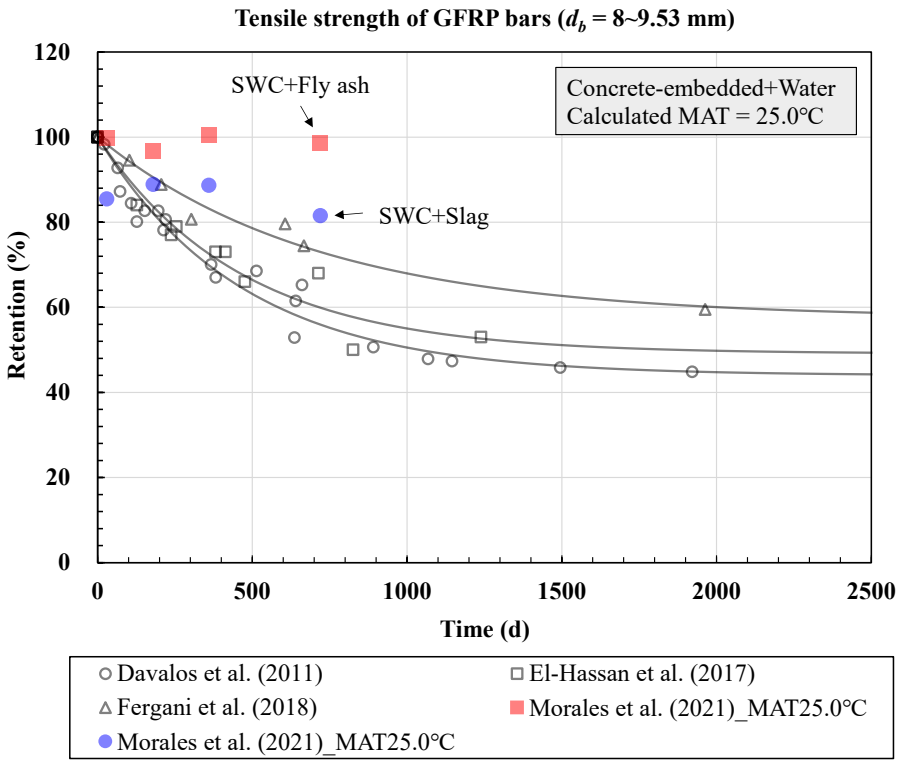
Solution type	Reference	Bar type	Concrete type	T (°C)	Coef. in Eq. (4.7)			Coef. in Eq. (4.2)		TSF	Coef. for master curve		
					τ	Y_∞	R^2	E_a/R	R^2		τ	Y_∞	R^2
Saline solution	Robert and Benmokrane (2013)	12.7 mm (VE)	NC	23	1440.1	68.96	0.940	1792	0.997	0.96	3066.5	35.99	0.972
				40	1015.6		0.994			1.33			
				50	872.6		0.963			1.59			
	Lu et al. (2022)	6 mm (VE)	SWSSC	28	111.8	19.72	0.964	4625	0.851	1.17	102.7	19.34	0.960
				40	35.1		0.993			2.10			
				60	23.8		0.995			5.10			
Water	Davalos et al. (2011)	9.53 mm (VE)	NC	20	618.0	43.21	0.934	5571	0.973	0.73	466.2	43.99	0.972
				40	236.3		0.923			2.45			
				50	92.1		0.987			4.24			
				60	69.2		0.994			7.12			
	El-Hassan et al. (2017)	8 mm (EP)	SWC	20	608.3	44.93	0.952	2874	0.984	0.85	464.9	49.12	0.951
				40	368.9		0.892			1.59			
				60	186.4		0.964			2.75			
	Fergani et al. (2018a)	8 mm (VE)	NC	20	881.8	57.32	(0.656)	5630	1.000	/	715.8	57.43	0.973
				40	291.4		0.999			2.47			
				60	99.0		0.955			7.27			

Note: (1) VE = vinylester resin; EP = epoxy resin. (2) The data in the brackets were excluded from the calculation because the correlation coefficient (R^2) was less than 0.80. (3) All the predicted results were calculated based on the MAT of 25.0°C. (4) NC = normal concrete; SWC = seawater concrete; SWSSC = seawater sea-sand concrete.

In Fig. 4.3, except for the master curve by Robert and Benmokrane (2013), which lies above one of the FET datasets (solid blue square markers) [Fig. 4.3(a)], it is noticed that the prediction model generally underestimates the residual tensile strength of concrete-embedded unstressed GFRP bars after exposure to a hot-humid field environment. This underestimation is particularly pronounced for the GFRP bars wrapped in seawater concrete (SWC) comprised of fly ash, regardless of the solution type. The exceptional case in Fig. 4.3(a) may be caused by the different mix proportions of concrete, which has a non-negligible influence on the degradation mechanism of GFRP bars as demonstrated by Morales et al. (2021), and this issue needs to be further verified due to the limited existing test results. Besides, it is interesting to find that compared to the 12.7-mm GFRP bars in Robert and Benmokrane (2013), the predicted curve for the 6-mm GFRP bars in Lu et al. (2022) exhibits a more pronounced underestimation [Fig. 4.3(a)], which can be attributed to the possible size effect on the long-term tensile strength of GFRP bars as mentioned in Chapter 3.



(a) Saline solution



(b) Water

Fig. 4.3 Comparison between FET results and prediction curves based on Arrhenius empirical model for concrete-embedded unstressed GFRP bars

4.4.1.3 Concrete-embedded stressed GFRP bars

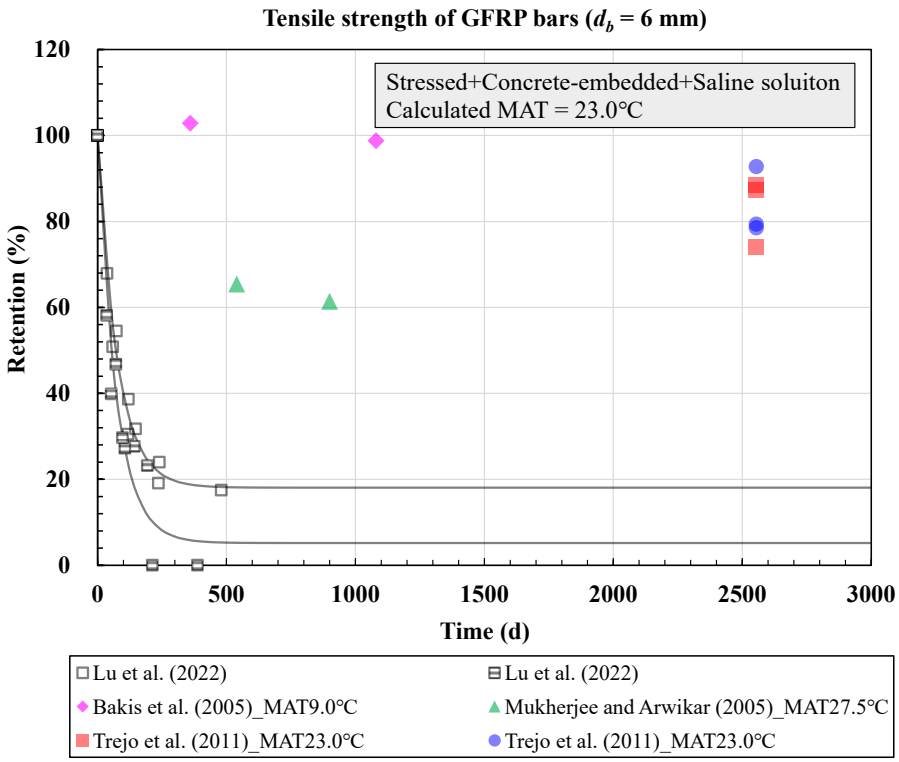
Compared to unstressed GFRP bars embedded in concrete, those covered by concrete and subjected to sustained load can better represent their actual service conditions. On the basis of Arrhenius empirical model, the comparisons between FET results (Bakis et al. 2005; Mukherjee and Arwikar 2005; Trejo et al. 2011) (Table 4.3) and prediction curves for concrete-embedded stressed GFRP bars conditioned in saline and water solutions are depicted in Fig. 4.4, and the corresponding coefficients of regression equations are given in Table 4.6. As a reference, only the predictions based on a MAT of 23.0°C are displayed herein for the same reason as mentioned in Section 4.4.1.1.

Table 4.6 Coefficients of regression equations based on Arrhenius empirical model for concrete-embedded stressed GFRP bars

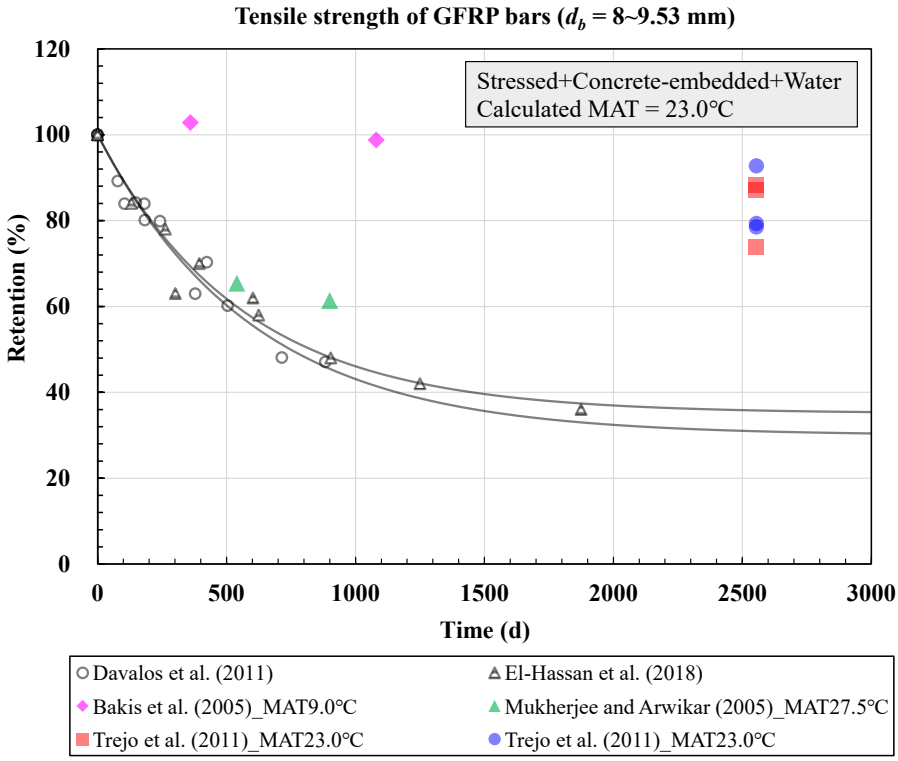
Solution type	Reference	Bar type	Concrete type	Stress level	T (°C)	Coef. in Eq. (4.7)			Coef. in Eq. (4.2)		*TSF*	Coef. for master curve		
						τ	Y_∞	R^2	E_a/R	R^2		τ	Y_∞	R^2
Saline solution	Lu et al. (2022)	6 mm (VE)	SWSSC	20% f_u	28	104.5	17.86	0.965	3697	0.898	1.23	76.2	18.05	0.990
					40	45.2		1.000			1.97			
					60	30.7		1.000			4.00			
				40% f_u	28	106.3	3.99	0.867	3127	0.851	1.19	72.4	5.17	0.964
					40	48.5		0.985			1.77			
					60	37.4		0.977			3.23			
Water	Davalos et al. (2011)	9.53 mm (VE)	NC	2000~2600 $\mu\varepsilon$	20	512.6	37.82	0.940	3831	0.938	0.88	597.4	29.99	0.974
					40	313.6		0.998			2.02			
					60	105.2		0.993			4.21			
	El-Hassan et al. (2018)	8 mm (EP)	SWC	25% f_u	20	732.1	32.28	0.972	3805	0.992	0.88	562.7	35.09	0.974
					40	283.9		0.915			2.00			
					60	154.8		1.000			4.17			

Note: (1) VE = vinylester resin; EP = epoxy resin. (2) f_u = ultimate tensile stress of an FRP bar; $\mu\varepsilon$ = strain of FRP bar. (3) All the predicted results were calculated based on the MAT of 23.0°C. (4) NC = normal concrete; SWC = seawater concrete; SWSSC = seawater sea-sand concrete.

In Fig. 4.4, it is evident that the prediction curves generated by AAT data obviously underestimate the tensile durability of stressed GFRP bars wrapped in concrete, irrespective of the stress level, especially for those conditioned in the environments with relatively low temperatures and/or low RH (Bakis et al. 2005; Trejo et al. 2011). It is worth noting that the diameters of GFRP bars for FET data are in the range of 9.5~19 mm, while those for the selected AAT data are in the range of 6~9.53 mm. The use of AAT data for GFRP bars with relatively small diameters may also result in underestimated predictions when compared to FET results. This discrepancy is likely due to the possible size effect on the tensile strength of GFRP bars, as previously discussed.



(a) Saline solution



(b) Water

Fig. 4.4 Comparison between FET results and prediction curves based on Arrhenius empirical model for concrete-embedded stressed GFRP bars

4.4.2 *fib* Bulletin 40 (2007) Model

Although *fib* Bulletin 40 (2007) model was initially developed for the FRP bars in concrete environments due to the incorporation of a correction term n_{mo} for moisture condition in concrete members, as mentioned in Section 4.2.2, in this section, this section also includes the AAT datasets of bare GFRP bars to assess the applicability of applying this model to bare FRP bars. It should be noted that only the AAT data with a temperature range of 20~30°C were selected for making predictions. This temperature range represents the most moderate scenario for AAT, which might lead to relatively unconservative predictions, and it also corresponds to the common MAT range for FET. Additionally, the data selected were required to have at least three different exposure periods. To achieve a higher prediction accuracy, in this chapter, the correction terms

n_T, n_{mo} and n_{SL} were determined according to the factors recommended by *fib* Bulletin 40 (2007) (Table 4.1) using the interpolation method. When determining the influencing coefficient R_{10}, only datasets from the same literature that meet the requirement of a minimum acceptable R^2 value (i.e., $R^2 \geq 0.80$) were adopted for the calculation (Bank et al. 2003).

4.4.2.1 Bare GFRP bars

In order to obtain the R_{10} values, the tensile strength retention curves of bare GFRP bars (d_b = 9.5~12.7 mm) under alkaline and saline conditions are plotted in Fig. 4.5 on a double logarithmic scale. As per Eqs. (4.9) and (4.10), the coefficients were determined based on the environmental conditions of exposure sites in Al-Salloum et al. (2013) (see Table 4.3) and the predicted retentions $1/\eta_{env,t}$ are summarized in Table 4.7. Fig. 4.5(a) illustrates significant differences in the tensile strength retention curves for alkaline conditions, with the R_{10} values ranging from 2.41% to 45.53% (see Table 4.7). As a result, the retention predictions vary considerably across different studies, which is similar to the observations made in the predictions based on Arrhenius model and can be explained by the reasons mentioned in Section 4.4.1.1. By contrast, the discrepancy between the retention curves for saline conditions is relatively small (R_{10} = 2.05~10.30%), as shown in Fig. 4.5(b). For ease of assessing the model performance, Fig. 4.6 compares the model predictions with the FET results of bare GFRP bars after field exposure to hot-dry and hot-humid environments for up to 18 months (Al-Salloum et al. 2013). It is seen that all the predicted results by *fib* Bulletin 40 (2007) model underestimate the residual tensile strength of bare GFRP bars, regardless of the solution type, particularly for the cases of alkaline solutions with high pH levels (e.g., pH > 13).

Table 4.7 Coefficients and predicted results based on *fib* Bulletin 40 (2007) model for bare GFRP bars

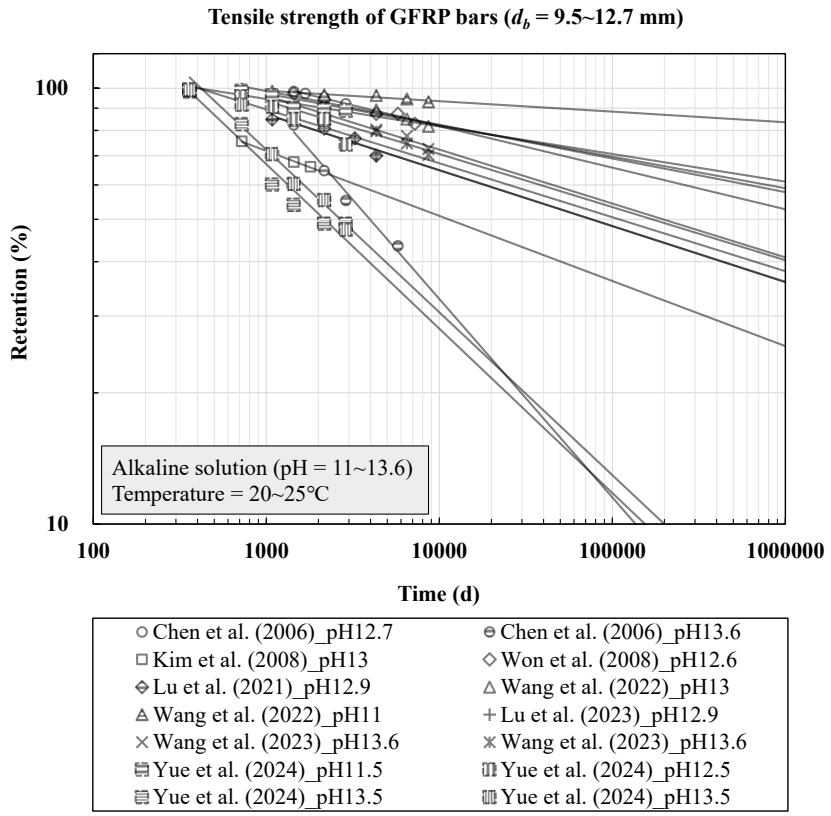
Solution type	Reference	Bar type	PH	T (°C)	Coef. in Eqs. (4.9) and (4.10)										Ret. $1/\eta_{env,t}$ (%)
					R_{10} (%)	R^2	MAT (°C)	n_T	RH (%)	n_{mo}	Time (m)	n_{SL}	n_d	n	$\eta_{env,t}$	
Alkaline solution	Chen et al. (2006)	9.53 mm (VE)	12.7	20	9.54	0.994	27.5	1	26.0	-1	6	0.69	0	0.69	1.31	76.33
											12	1		1.00	1.35	74.02
											18	1.17		1.17	1.37	72.76
							26.0	1	52.0	-0.93	6	0.69		0.76	1.32	75.82
											12	1.00		1.07	1.36	73.52
											18	1.17		1.24	1.38	72.28
			13.6		45.53	0.978	27.5	1	26.0	-1	6	0.69		0.69	5.13	19.48
											12	1		1.00	6.19	16.16
											18	1.17		1.17	6.86	14.58
							26.0	1	52.0	-0.93	6	0.69		0.76	5.35	18.71
											12	1.00		1.07	6.44	15.52
											18	1.17		1.24	7.14	14.00
	Kim et al. (2008)	12.7 mm (VE)	13.0	25	14.93	0.997	27.5	1	26.0	-1	6	0.69		0.69	1.55	64.70
											12	1		1.00	1.62	61.57
											18	1.17		1.17	1.67	59.90
							26.0	1	52.0	-0.93	6	0.69		0.76	1.56	64.01
											12	1.00		1.07	1.64	60.91
											18	1.17		1.24	1.69	59.26
	Won et al. (2008)	12.7 mm (VE)	12.6	20	7.73	0.941	27.5	1	26.0	-1	6	0.69		0.69	1.24	80.52
											12	1		1.00	1.27	78.55
											18	1.17		1.17	1.29	77.49
							26.0	1	52.0	-0.93	6	0.69		0.76	1.25	80.09
											12	1.00		1.07	1.28	78.13
											18	1.17		1.24	1.30	77.07
	Lu et al. (2021a)	11.2 mm (VE)	12.9	20	12.81	0.885	27.5	1	26.0	-1	6	0.69		0.69	1.45	69.14
											12	1		1.00	1.51	66.29
											18	1.17		1.17	1.54	64.76
							26.0	1	52.0	-0.93	6	0.69	0	0.76	1.46	68.51

										12	1.00	0	1.07	1.52	65.69
										18	1.17	0	1.24	1.56	64.17
Wang et al. (2022)	9.52 mm (VE)	13.0	23	7.23	0.948	27.5	1	26.0	-1	6	0.69		0.69	1.22	81.71
										12	1		1.00	1.25	79.85
										18	1.17		1.17	1.27	78.84
						26.0	1	52.0	-0.93	6	0.69	0	0.76	1.23	81.30
										12	1.00	0	1.07	1.26	79.45
										18	1.17	0	1.24	1.27	78.44
		11.0		2.41	0.912	27.5	1	26.0	-1	6	0.69		0.69	1.07	93.63
										12	1		1.00	1.08	92.93
										18	1.17		1.17	1.08	92.55
						26.0	1	52.0	-0.93	6	0.69	0	0.76	1.07	93.48
										12	1.00	0	1.07	1.08	92.78
										18	1.17	0	1.24	1.08	92.40
Lu et al. (2023a)	11.2 mm (VE)	12.9	25	12.83	0.886	27.5	1	26.0	-1	6	0.69		0.69	1.45	69.08
										12	1		1.00	1.51	66.23
										18	1.17		1.17	1.55	64.70
						26.0	1	52.0	-0.93	6	0.69	0	0.76	1.46	68.45
										12	1.00	0	1.07	1.52	65.63
										18	1.17	0	1.24	1.56	64.11
Wang et al. (2023a)	9.52 mm (VE)	13.6	23	12.37	0.986	27.5	1	26.0	-1	6	0.69		0.69	1.43	70.08
										12	1		1.00	1.49	67.29
										18	1.17		1.17	1.52	65.80
						26.0	1	52.0	-0.93	6	0.69	0	0.76	1.44	69.46
										12	1.00	0	1.07	1.50	66.70
										18	1.17	0	1.24	1.53	65.22
		13.6		12.19	0.947	27.5	1	26.0	-1	6	0.69		0.69	1.42	70.47
										12	1		1.00	1.48	67.71
										18	1.17		1.17	1.51	66.23
						26.0	1	52.0	-0.93	6	0.69	0	0.76	1.43	69.86
										12	1.00	0	1.07	1.49	67.12
										18	1.17	0	1.24	1.52	65.66
Yue et al. (2024)	12 mm (EP)	11.5	20	6.31	0.846	27.5	1	26.0	-1	6	0.69		0.69	1.19	83.89

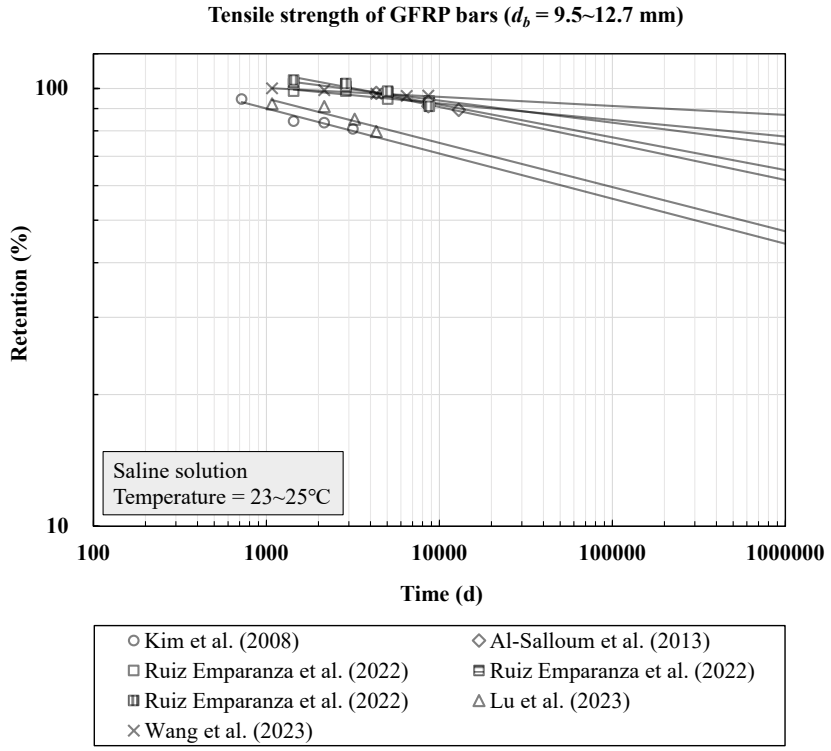
										12	1		1.00	1.22	82.23
										18	1.17		1.17	1.23	81.32
							26.0	1	52.0	-0.93	6	0.69	0	0.76	1.20	83.53
											12	1.00	0	1.07	1.22	81.87
											18	1.17	0	1.24	1.24	80.97
			12.5		12.38	0.858	27.5	1	26.0	-1	6	0.69		0.69	1.43	70.05
											12	1		1.00	1.49	67.26
											18	1.17		1.17	1.52	65.77
							26.0	1	52.0	-0.93	6	0.69	0	0.76	1.44	69.44
											12	1.00	0	1.07	1.50	66.67
											18	1.17	0	1.24	1.53	65.19
			13.5		37.71	0.951	27.5	1	26.0	-1	6	0.69		0.69	3.58	27.95
											12	1		1.00	4.14	24.17
											18	1.17		1.17	4.48	22.30
							26.0	1	52.0	-0.93	6	0.69	0	0.76	3.69	27.08
											12	1.00	0	1.07	4.27	23.42
											18	1.17	0	1.24	4.63	21.61
			13.5		37.35	0.930	27.5	1	26.0	-1	6	0.69		0.69	3.52	28.39
											12	1		1.00	4.07	24.59
											18	1.17		1.17	4.40	22.71
							26.0	1	52.0	-0.93	6	0.69	0	0.76	3.63	27.52
											12	1.00	0	1.07	4.20	23.84
											18	1.17	0	1.24	4.54	22.01
Saline solution	Kim et al. (2008)	12.7 mm (Modified VE)	/	25	10.30	0.913	27.5	1	26.0	-1	6	0.69		0.69	1.34	74.63
											12	1		1.00	1.39	72.18
											18	1.17		1.17	1.41	70.86
							26.0	1	52.0	-0.93	6	0.69	0	0.76	1.35	74.09
											12	1.00	0	1.07	1.40	71.66
											18	1.17	0	1.24	1.42	70.34
	Al-Salloum et al. (2013)	12 mm (VE)	/	23	8.34	0.976	27.5	1	26.0	-1	6	0.69		0.69	1.26	79.10
											12	1		1.00	1.30	77.02
											18	1.17		1.17	1.32	75.88
							26.0	1	52.0	-0.93	6	0.69	0	0.76	1.27	78.64

										12	1.00	0	1.07	1.31	76.57
										18	1.17	0	1.24	1.33	75.44
Ruiz Emparanza et al. (2022)	~10 mm (VE)	/	23	3.77	0.859	27.5	1	26.0	-1	6	0.69		0.69	1.11	90.16
										12	1		1.00	1.12	89.10
										18	1.17		1.17	1.13	88.52
						26.0	1	52.0	-0.93	6	0.69	0	0.76	1.11	89.93
										12	1.00	0	1.07	1.13	88.87
										18	1.17	0	1.24	1.13	88.29
				5.04	0.920	27.5	1	26.0	-1	6	0.69		0.69	1.15	87.00
										12	1		1.00	1.17	85.63
										18	1.17		1.17	1.18	84.88
						26.0	1	52.0	-0.93	6	0.69	0	0.76	1.15	86.70
										12	1.00	0	1.07	1.17	85.34
										18	1.17	0	1.24	1.18	84.59
				7.48	0.887	27.5	1	26.0	-1	6	0.69		0.69	1.23	81.12
										12	1		1.00	1.26	79.21
										18	1.17		1.17	1.28	78.17
						26.0	1	52.0	-0.93	6	0.69	0	0.76	1.24	80.70
										12	1.00	0	1.07	1.27	78.80
										18	1.17	0	1.24	1.29	77.77
Lu et al. (2023a)	11.2 mm (VE)	/	25	10.10	0.813	27.5	1	26.0	-1	6	0.69		0.69	1.33	75.07
										12	1		1.00	1.38	72.66
										18	1.17		1.17	1.40	71.35
						26.0	1	52.0	-0.93	6	0.69	0	0.76	1.34	74.54
										12	1.00	0	1.07	1.39	72.14
										18	1.17	0	1.24	1.41	70.85
Wang et al. (2023a)	9.52 mm (VE)	/	23	2.05	0.966	27.5	1	26.0	-1	6	0.69		0.69	1.06	94.57
										12	1		1.00	1.06	93.97
										18	1.17		1.17	1.07	93.64
						26.0	1	52.0	-0.93	6	0.69	0	0.76	1.06	94.44
										12	1.00	0	1.07	1.07	93.84
										18	1.17	0	1.24	1.07	93.51

Note: (1) VE = vinylester resin; EP = epoxy resin.

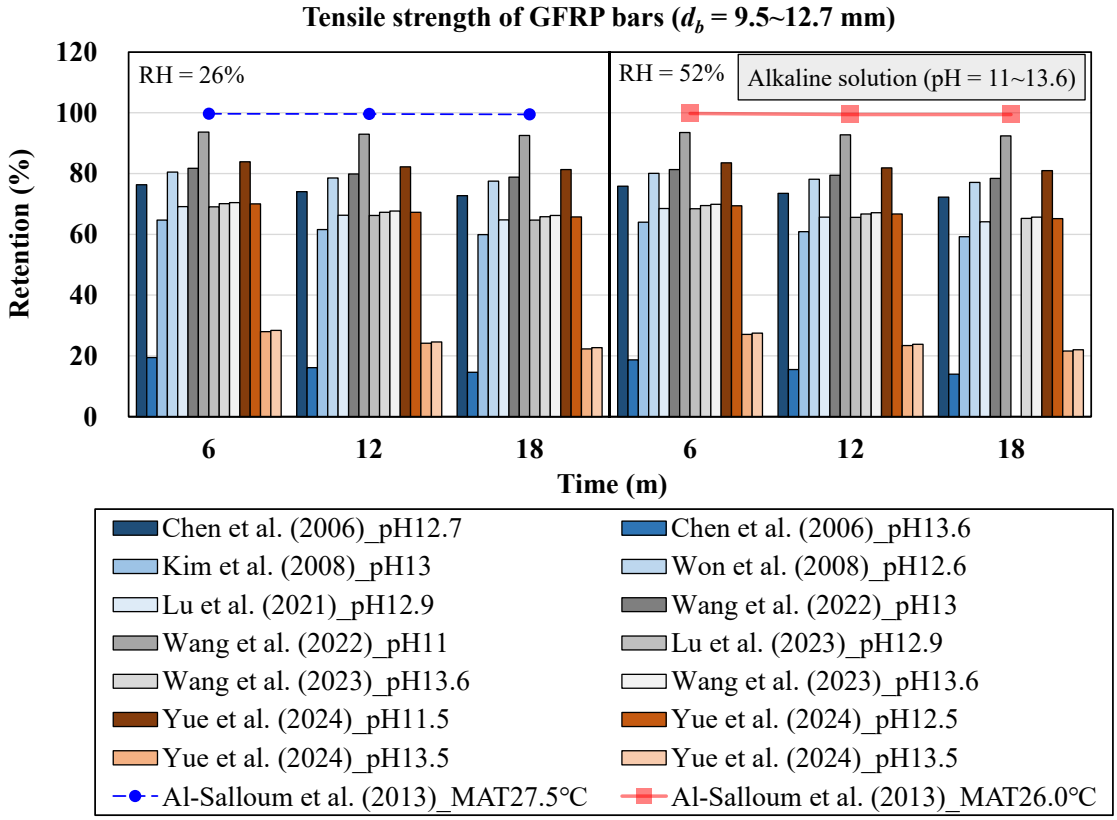


(a) Alkaline solution

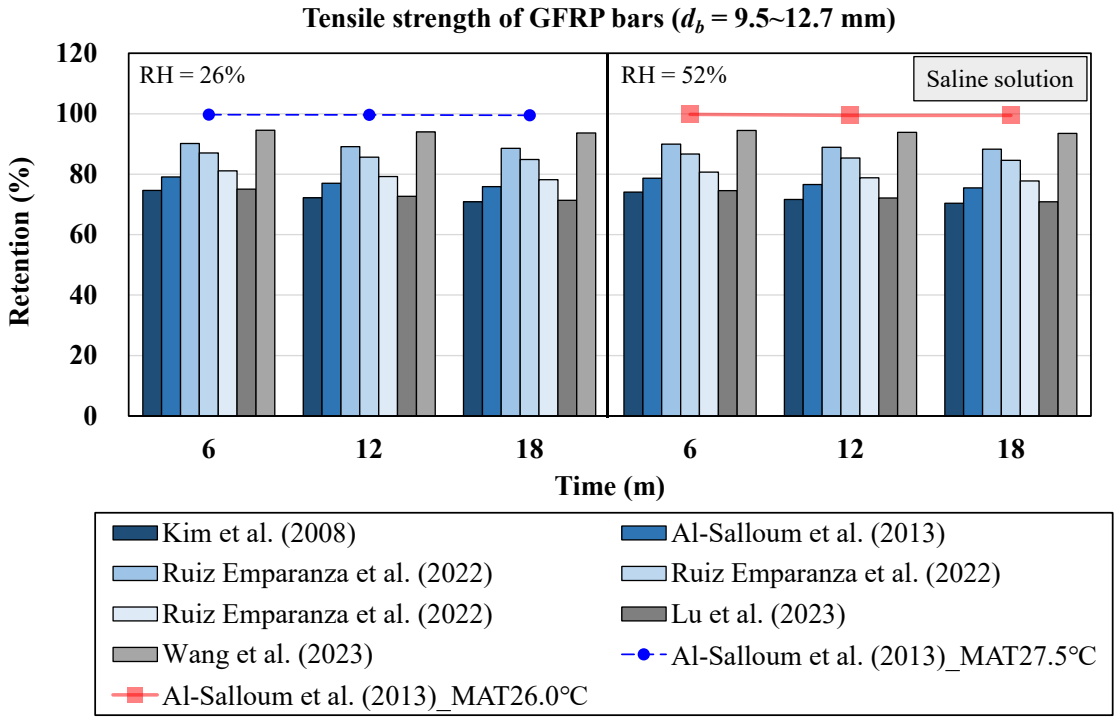


(b) Saline solution

Fig. 4.5 Tensile strength retention curves based on *fib* Bulletin 40 (2007) model for bare GFRP bars



(a) Alkaline solution



(b) Saline solution

Fig. 4.6 Comparison between FET results and predictions based on *fib* Bulletin 40 (2007) model for bare GFRP bars

4.4.2.2 Concrete-embedded unstressed GFRP bars

The tensile strength retention curves based on *fib* Bulletin 40 (2007) model for concrete-embedded unstressed GFRP bars (d_b = 6~12.7 mm) subjected to different solutions are shown in Fig. 4.7, and the coefficients and predictions determined in accordance with the FET details in Morales et al. (2021) are listed in Table 4.8. Similar to the bare GFRP bars, it can be observed from Fig. 4.7 that the R_{10} values for different studies vary significantly. By comparing the FET results with the predicted tensile strength retentions $1/\eta_{env,t}$ for unstressed GFRP bars embedded in concrete and subjected to different solution immersion, as illustrated in Fig. 4.8, it is found that the model predictions generally underestimate the reported FET results to varying degrees. This underestimation is particularly pronounced for the GFRP bars wrapped in SWC incorporating fly ash. For example, after 2-year field exposure in hot-humid environment (MAT = 25℃, RH = 71.2%), the residual tensile strengths of 9.5-mm VE-type GFRP bars wrapped in fly ash- and slag-based SWC are 98.60% and 81.51% (Morales et al. 2021), respectively, while the predicted value determined by 9.53-mm VE-type GFRP bars wrapped in NC and immersed in 20℃ water is only 69.40% (Davalos et al. 2011). Therefore, it might be concluded that *fib* Bulletin 40 (2007) model also gives highly conservative predictions for the concrete-embedded unstressed GFRP bars exposed to natural hot-humid environment.

Table 4.8 Coefficients and predicted results based on *fib* Bulletin 40 (2007) model for concrete-embedded unstressed GFRP bars

Solution type	Reference	Bar type	Concrete type	T (°C)	Coef. in Eqs. (4.9) and (4.10)											Ret. $1/\eta_{env,t}$ (%)
					R_{10} (%)	R^2	MAT (°C)	n_T	RH (%)	n_{mo}	Time (m)	n_{SL}	n_d	n	$\eta_{env,t}$	
Alkaline solution	Wu et al. (2022)	10 mm (VE)	NC	RT	5.61	0.984	25.0	1	71.2	-0.29	1	-0.09	0	0.62	1.16	85.96
											6	0.69		1.40	1.22	82.19
											12	1.00		1.71	1.24	80.74
											24	1.30		2.00	1.26	79.38
Saline solution	Robert and Benmokrane (2013)	12.7 mm (VE)	NC	23	3.79	0.829					1	-0.09	0.5	1.12	1.13	88.64
											6	0.69		1.90	1.16	86.02
											12	1.00		2.21	1.18	85.01
											24	1.30		2.50	1.19	84.04
	Lu et al. (2022)	6 mm (VE)	SWSSC	28	29.64	0.905					1	-0.09	0	0.62	2.51	39.79
											6	0.69		1.40	3.30	30.27
											12	1.00		1.71	3.68	27.17
											24	1.30		2.00	4.08	24.49
Water	Davalos et al. (2011)	9.53 mm (VE)	NC	20	8.72	0.937					1	-0.09	0	0.62	1.27	78.72
											6	0.69		1.40	1.36	73.32
											12	1.00		1.71	1.40	71.29
											24	1.30		2.00	1.44	69.40
	El-Hassan et al. (2017)	8 mm (EP)	SWC	20	12.35	0.952					1	-0.09	0	0.62	1.41	70.78
											6	0.69		1.40	1.57	63.87
											12	1.00		1.71	1.63	61.34
											24	1.30		2.00	1.70	59.00

Note: (1) VE = vinylester resin; EP = epoxy resin. (2) NC = normal concrete; SWC = seawater concrete; SWSSC = seawater sea-sand concrete.

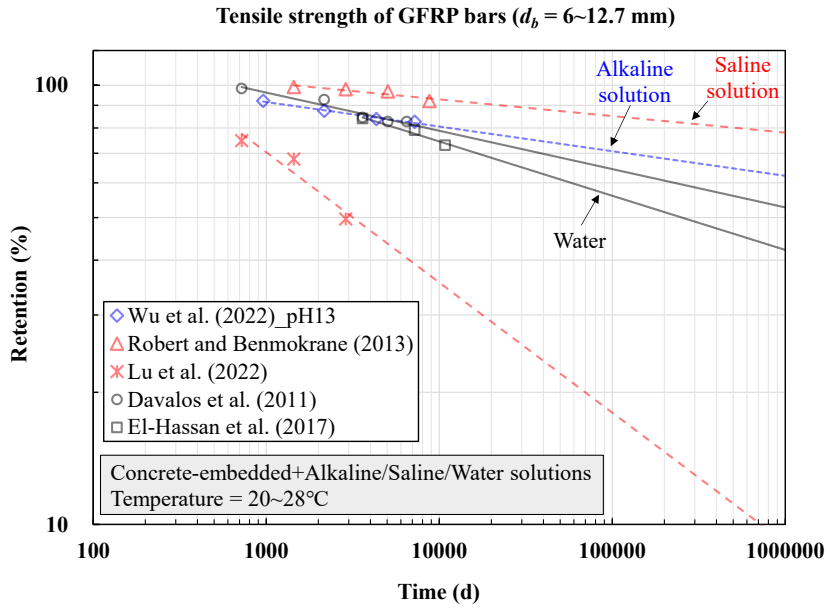


Fig. 4.7 Tensile strength retention curves based on *fib* Bulletin 40 (2007) model for concrete-embedded unstressed GFRP bars

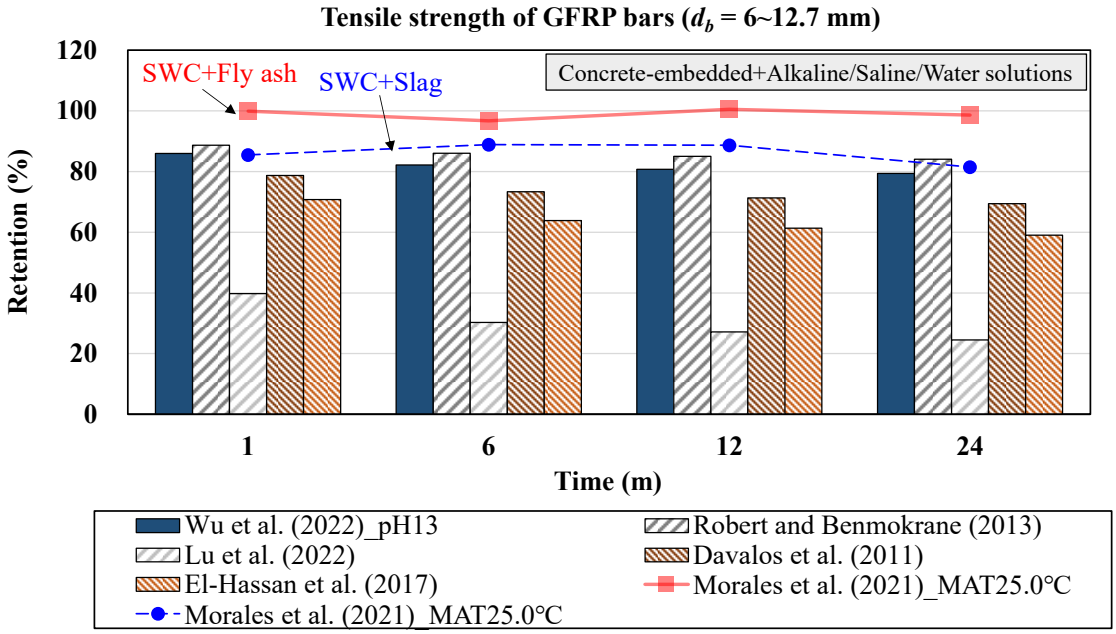


Fig. 4.8 Comparison between FET results and predictions based on *fib* Bulletin 40 (2007) model for concrete-embedded unstressed GFRP bars

4.4.2.3 Concrete-embedded stressed GFRP bars

Fig. 4.9 displays the tensile strength retention curves of concrete-embedded stressed GFRP bars (d_b = 6~10 mm) subjected to different environmental conditions, and the

corresponding coefficients and predicted results obtained on the basis of three FET studies (Bakis et al. 2005; Mukherjee and Arwikar 2005; Trejo et al. 2011) are summarized in Table 4.9. Again, as shown in Fig. 4.9, there exists remarkable differences in the retention curves for different studies, leading to significant variation in the R_{10} values (Table 4.9). This variation is similar to that observed in both bare and concrete-embedded unstressed GFRP bars. Comparing the three FET datasets with the corresponding predictions by *fib* Bulletin 40 (2007) model, as illustrated in Fig. 4.10, the following observations can be made: (1) All the FET results are dramatically underestimated by the predictions using AAT data of Lu et al. (2022), which might be attributable to the use of GFRP bars with a much smaller diameter (d_b = 6 mm) in this study; (2) Although 8-mm GFRP bars were adopted by Fergani et al. (2018a), the corresponding predictions seem to be much greater in magnitude than those of other studies. This can be explained by the fact that the residual tensile strength after 1000h exposure [i.e., $f_{fk1000h}$ in Eq. (4.9a)] has been provided in Fergani et al. (2018a), as a result of which a much larger prediction would be generated using Eq. (4.9a) compared to Eq. (4.9b). Therefore, more developmental work could focus on this aspect to improve the reliability of *fib* Bulletin 40 (2007) model; (3) Probably due to the low MAT (9°C) in the natural environment to which the specimens were exposed, the FET results from Bakis et al. (2005) are significantly underestimated by most of the predictions, irrespective of the solution type, while an opposite trend is observed for the specimens conditioned in hot and humid environments (MAT = 27.5°C and RH = 74.9%) in Mukherjee and Arwikar (2005); (4) For Trejo et al. (2011), although some of the predicted results closely approximate the FET results obtained from the 16- and 19-mm GFRP bars extracted from preloaded concrete beams after 7-year outdoor exposure, the experimental results still exceed the predicted values on average.

Table 4.9 Coefficients and predicted results based on *fib* Bulletin 40 (2007) model for concrete-embedded stressed GFRP bars

Solution type	Reference	Bar type	Concrete type	Stress level	T (℃)	Coef. in Eqs. (4.9) and (4.10)											Ret. $1/\eta_{env,t}$ (%)
						R_{10} (%)	R^2	MAT (℃)	n_T	RH (%)	n_{mo}	Time (m)	n_{SL}	n_d	n	$\eta_{env,t}$	
Alkaline solution	Wu et al. (2022) (pH = 13)	10 mm (VE)	NC	20% M_u	RT	4.96	0.872	9.0	0	57.6	-0.75	12	0.99	0	0.25	1.12	89.19 [a]
												36	1.47	0	0.72	1.15	87.05 [a]
								27.5	1	74.9	-0.17	18	1.17	0	2.00	1.23	81.58 [b]
												30	1.39	0	2.22	1.24	80.67 [b]
								23.0	0.5	59.3	-0.69	84	1.84	0	1.65	1.20	83.05 [c]
				Pre-cracks + 20% M_u		10.30	0.922	9.0	0	57.6	-0.75	12	0.99	0	0.25	1.28	78.32 [a]
												36	1.47	0	0.72	1.34	74.36 [a]
								27.5	1	74.9	-0.17	18	1.17	0	2.00	1.54	64.74 [b]
												30	1.39	0	2.22	1.58	63.19 [b]
								23.0	0.5	59.3	-0.69	84	1.84	0	1.65	1.49	67.25 [c]
Saline solution	Lu et al. (2022)	6 mm (VE)	SWSSC	20% f_u	28	54.92	0.936	9.0	0	57.6	-0.75	12	0.99	0	0.25	5.99	16.69 [a]
												36	1.47	0	0.72	8.76	11.41 [a]
								27.5	1	74.9	-0.17	18	1.17	0	2.00	24.21	4.13 [b]
												30	1.39	0	2.22	28.89	3.46 [b]
								23.0	0.5	59.3	-0.69	84	1.84	0	1.65	18.30	5.46 [c]
				40% f_u		53.62	0.938	9.0	0	57.6	-0.75	12	0.99	0	0.25	5.62	17.79 [a]
												36	1.47	0	0.72	8.11	12.33 [a]
								27.5	1	74.9	-0.17	18	1.17	0	2.00	21.61	4.63 [b]
												30	1.39	0	2.22	25.63	3.90 [b]
								23.0	0.5	59.3	-0.69	84	1.84	0	1.65	16.51	6.06 [c]
Water	Davalos et al. (2011)	9.53 mm (VE)	NC	2000~2600 $\mu\varepsilon$	20	10.74	0.837	9.0	0	57.6	-0.75	12	0.99	0	0.25	1.29	77.47 [a]
												36	1.47	0	0.72	1.36	73.38 [a]
								27.5	1	74.9	-0.17	18	1.17	0	2.00	1.58	63.49 [b]
												30	1.39	0	2.22	1.62	61.91 [b]
								23.0	0.5	59.3	-0.69	84	1.84	0	1.65	1.51	66.07 [c]
	He et al. (2017)	10 mm	NC	20% f_u	23	5.76	0.992	9.0	0	57.6	-0.75	12	0.99	0	0.25	1.14	87.53 [a]
												36	1.47	0	0.72	1.18	85.09 [a]

	(VE)						27.5	1	74.9	-0.17	18	1.17	0	2.00	1.27	78.89 [b]
											30	1.39	0	2.22	1.28	77.86 [b]
							23.0	0.5	59.3	-0.69	84	1.84	0	1.65	1.24	80.55 [c]
			Pre-cracks + 20% f_u		6.06	0.915	9.0	0	57.6	-0.75	12	0.99	0	0.25	1.15	86.89 [a]
											36	1.47	0	0.72	1.19	84.33 [a]
							27.5	1	74.9	-0.17	18	1.17	0	2.00	1.28	77.86 [b]
											30	1.39	0	2.22	1.30	76.79 [b]
							23.0	0.5	59.3	-0.69	84	1.84	0	1.65	1.26	79.59 [c]
			Pre-cracks + 40% f_u		5.18	0.992	9.0	0	57.6	-0.75	12	0.99	0	0.25	1.13	88.73 [a]
											36	1.47	0	0.72	1.16	86.51 [a]
							27.5	1	74.9	-0.17	18	1.17	0	2.00	1.24	80.83 [b]
											30	1.39	0	2.22	1.25	79.88 [b]
							23.0	0.5	59.3	-0.69	84	1.84	0	1.65	1.21	82.35 [c]
El-Hassan et al. (2018)	8 mm (EP)	SWC	25% f_u	20	15.96	0.936	9.0	0	57.6	-0.75	12	0.99	0	0.25	1.48	67.65 [a]
											36	1.47	0	0.72	1.61	62.27 [a]
							27.5	1	74.9	-0.17	18	1.17	0	2.00	2.00	49.88 [b]
											30	1.39	0	2.22	2.08	47.99 [b]
							23.0	0.5	59.3	-0.69	84	1.84	0	1.65	1.89	53.02 [c]
Fergani et al. (2018a)	8 mm (VE)	NC	3000 $\mu\varepsilon$	20	3.97	0.971	9.0	0	57.6	-0.75	12	0.99	0	0.25	1.01	99.00 [a]
											36	1.47	0	0.72	1.03	97.10 [a]
							27.5	1	74.9	-0.17	18	1.17	0	2.00	1.08	92.21 [b]
											30	1.39	0	2.22	1.09	91.38 [b]
							23.0	0.5	59.3	-0.69	84	1.84	0	1.65	1.07	93.53 [c]

Note: (1) VE = vinylester resin; EP = epoxy resin. (2) NC = normal concrete; SWC = seawater concrete; SWSSC = seawater sea-sand concrete. (3) M_u = ultimate moment measured in the beam tests; f_u = ultimate tensile stress of an FRP bar; $\mu\varepsilon$ = tensile strain of FRP bar. (4) [a]Bakis et al. (2005); [b]Mukherjee and Arwikar (2005); [c]Trejo et al. (2011).

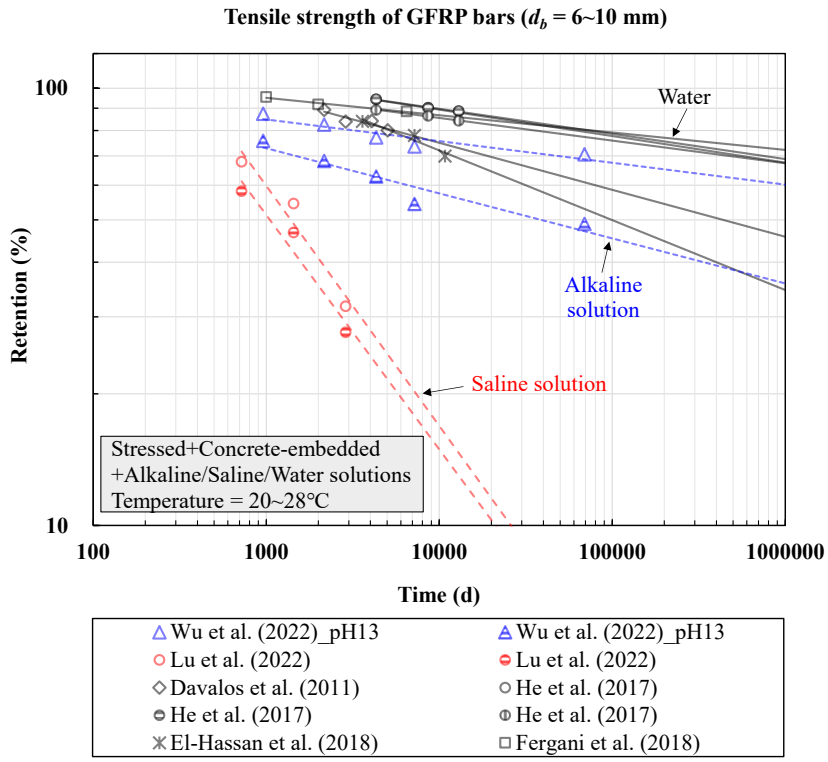


Fig. 4.9 Tensile strength retention curves based on *fib* Bulletin 40 (2007) model for concrete-embedded stressed GFRP bars

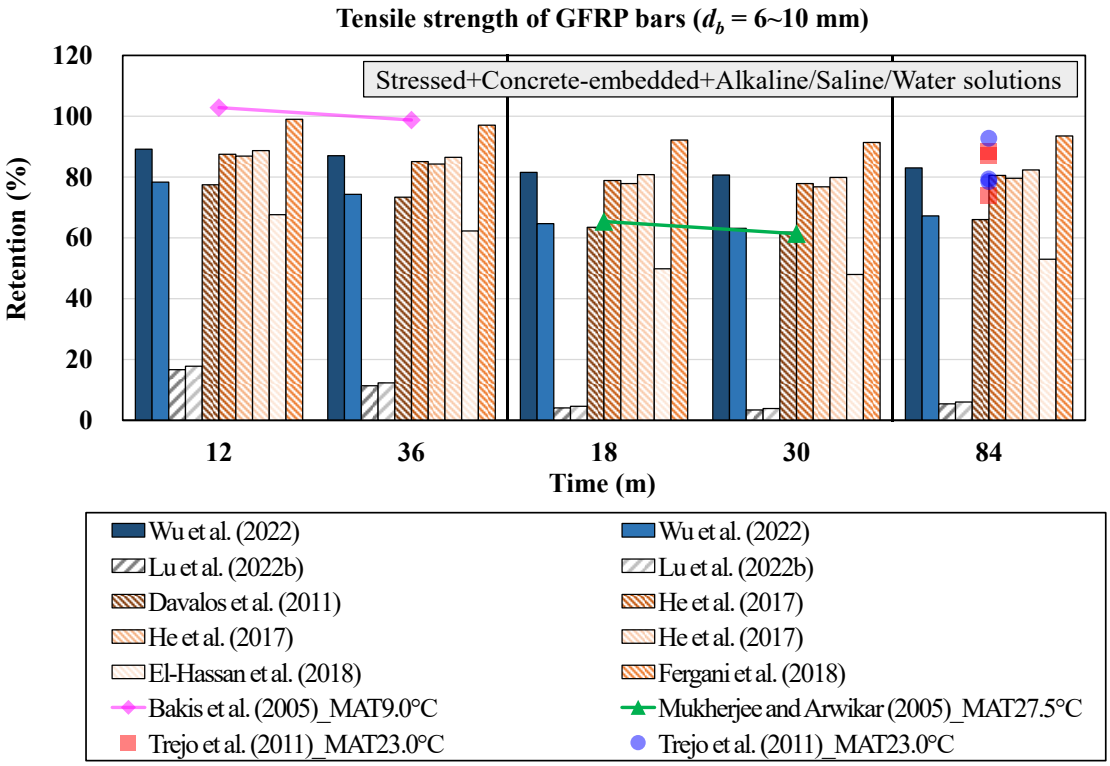


Fig. 4.10 Comparison between FET results and predictions based on *fib* Bulletin 40 (2007) model for concrete-embedded stressed GFRP bars

4.4.3 Huang and Aboutaha's (2010) Model

The ERF-based approach proposed by Huang and Aboutaha (2010) has been adopted by several researchers for predicting the long-term mechanical properites of FRP bars (Dong et al. 2017b; Benmokrane et al. 2020a; Liang et al. 2021). It is worth noting that the ERF value specified in the current ACI code (ACI 2022)] for GFRP bars was determined by Benmokrane et al. (2020a) based on Huang and Aboutaha's (2010) model. Although this model was initially developed for the FRP bars in concrete environment as mentioned in Section 4.2.3, the AAT datasets of bare GFRP bars were also included in this section referring to the method in Benmokrane et al. (2020a). In the prediction process, the RH correction factor n_H was determined according to the curve shown in Fig. 4.1 by the interpolation method. The criteria for selection of AAT data are stated as follows: (1) Datasets with at least two aging temperatures as well as three exposure durations were considered; (2) Only the datasets with R^2 value greater than 0.80 were used (Bank et al. 2003), unless otherwise specified.

4.4.3.1 Bare GFRP bars

Fig. 4.11 shows the comparison of tensile strength retentions of bare GFRP bars between the FET results reported by Al-Salloum et al. (2013) (see Table 4.3) and the predictions derived from different AAT studies based on Huang and Aboutaha's (2010) model. These AAT studies involved GFRP bars with diameters ranging from 9.5 mm to 12.7 mm that were exposed to alkaline and saline solutions. The coefficients determined according to the field conditions of FET study and the predictions η_E are listed in Table 4.10. It should be noted that the value of ρ for each dataset was averaged from the slopes of two regression lines (i.e., the values of a) at two selected temperatures. Table 4.10 reveals that when the RH is less than 30% (i.e., n_H = 0, as

indicated in Table 4.1), the predicted tensile strength retention is consistently 100% (i.e., no GFRP degradation can be observed), closely aligning with those observed after field exposure (i.e., retention = 99.46~99.66%). Consequently, only the results with respect to the field conditions of MAT = 26℃ and RH = 52.0% are presented in Fig. 4.11. Notably, the predicted results generally exhibit good agreement with the FET results, particularly for those produced by AAT data of GFRP bars under relatively moderate conditions, such as the alkaline environments with a pH value not exceeding 13.0 and saline environments. For example, the experimentally determined tensile strength retention for the bare GFRP bars exposed to hot-humid environments for 18 months is 99.46% (Al-Salloum et al. 2013), while the predictions based on AAT data from alkaline (pH = 11.5~13.0) and saline solutions range from 93.05% to 100%.

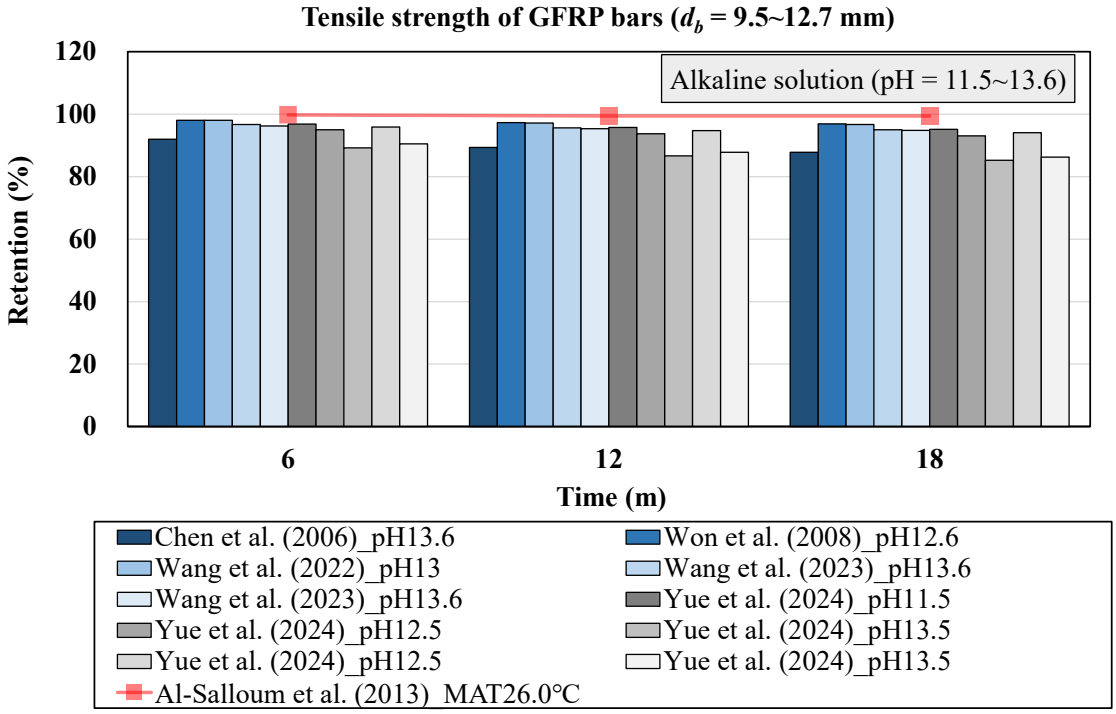
Table 4.10 Coefficients and predicted results based on Huang and Aboutaha's (2010) model for bare GFRP bars

Solution type	Reference	Bar type	PH	T (℃)	Coef. in Eq. (4.4)			Coef. in Eq. (4.11)									Ret. η_E (%)
					a	b	R^2	ρ	Δ_1	E_a/R	MAT (℃)	TSF	RH (%)	n_H	Time (m)	DL (y)	
Alkaline solution	Chen et al. (2006)	9.53 mm (VE)	13.6	20	-0.63	1.90	0.939	0.62	0.709	2251	27.5	1.21	26.0	0.00	6	0.5	100.00
				40	-0.60	1.77	0.994								12	1.0	100.00
															18	1.5	100.00
											26.0	1.17	52.0	0.14	6	0.5	92.01
															12	1.0	89.38
															18	1.5	87.85
	Won et al. (2008)	12.7 mm (VE)	12.6	20	-0.16	1.25	0.950	0.17	0.169	3795	27.5	1.38	26.0	0.00	6	0.5	100.00
				80	-0.17	1.09	0.941								12	1.0	100.00
															18	1.5	100.00
											26.0	1.30	52.0	0.14	6	0.5	98.05
															12	1.0	97.34
															18	1.5	96.92
	Wang et al. (2022)	9.52 mm (VE)	13.0	23	-0.15	1.21	0.956	0.20	0.171	9508	27.5	1.62	26.0	0.00	6	0.5	100.00
				60	-0.25	0.90	0.960								12	1.0	100.00
															18	1.5	100.00
											26.0	1.38	52.0	0.14	6	0.5	98.04
															12	1.0	97.19
															18	1.5	96.70
	Wang et al. (2023a)	9.52 mm (VE)	13.6	23	-0.24	1.34	0.984	0.24	0.268	10786	27.5	1.72	26.0	0.00	6	0.5	100.00
				60	-0.25	0.91	0.905								12	1.0	100.00
															18	1.5	100.00
											26.0	1.44	52.0	0.14	6	0.5	96.69
															12	1.0	95.65
															18	1.5	95.04
			13.6	23	-0.23	1.30	0.961	0.21	0.284	14964	27.5	2.13	26.0	0.00	6	0.5	100.00
				60	-0.19	0.79	0.884								12	1.0	100.00
															18	1.5	100.00

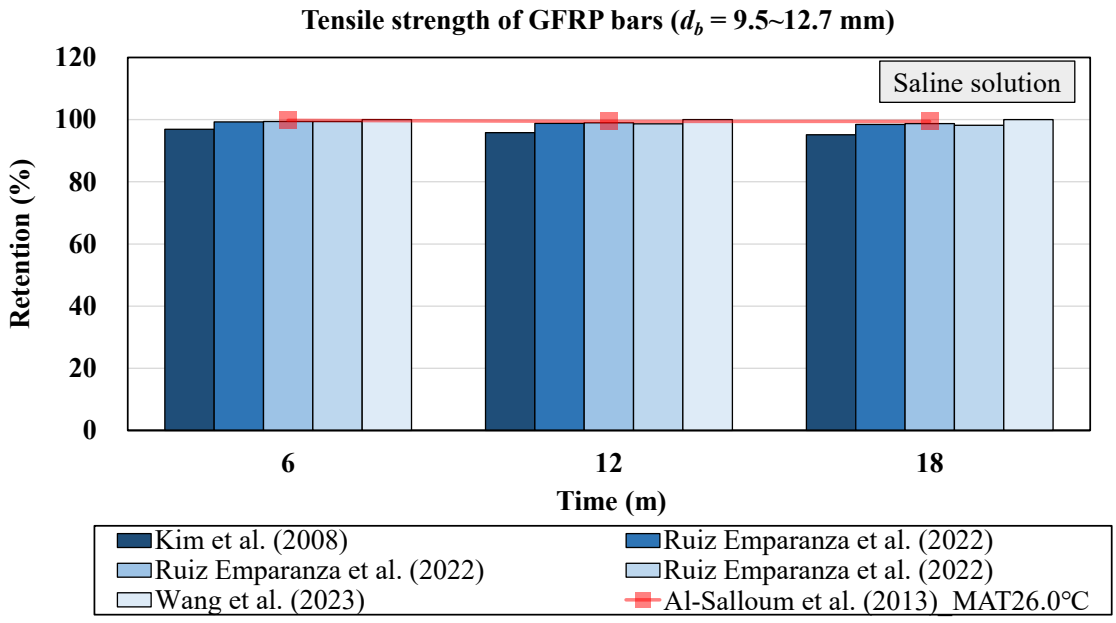
										26.0	1.66	52.0	0.14	6	0.5	96.22
														12	1.0	95.33
														18	1.5	94.81
Yue et al. (2024)	12 mm (EP)	11.5	40	-0.24	1.30	0.950	0.25	0.325	1598	27.5	0.81	26.0	0.00	6	0.5	100.00
			60	-0.25	1.27	0.826								12	1.0	100.00
														18	1.5	100.00
										26.0	0.79	52.0	0.14	6	0.5	96.82
														12	1.0	95.77
														18	1.5	95.15
		12.5	20	-0.25	1.30	0.950	0.29	0.336	11959	27.5	2.77	26.0	0.00	6	0.5	100.00
			40	-0.33	1.27	0.826								12	1.0	100.00
														18	1.5	100.00
										26.0	2.27	52.0	0.14	6	0.5	95.01
														12	1.0	93.77
														18	1.5	93.05
		13.5	20	-0.60	1.67	0.921	0.59	0.873	3755	27.5	1.38	26.0	0.00	6	0.5	100.00
			60	-0.58	1.28	0.927								12	1.0	100.00
														18	1.5	100.00
										26.0	1.29	52.0	0.14	6	0.5	89.22
														12	1.0	86.70
														18	1.5	85.23
		12.5	40	-0.31	1.21	0.911	0.27	0.578	11663	27.5	0.21		0.00	6	0.5	100.00
			60	-0.24	0.94	0.861								12	1.0	100.00
														18	1.5	100.00
										26.0	0.17		0.14	6	0.5	95.93
														12	1.0	94.76
														18	1.5	94.07
		13.5	20	-0.61	1.74	0.952	0.63	0.830	1565	27.5	1.14	26.0	0.00	6	0.5	100.00
			60	-0.65	1.57	0.945								12	1.0	100.00
														18	1.5	100.00
										26.0	1.11	52.0	0.14	6	0.5	90.52
														12	1.0	87.83
														18	1.5	86.25

Saline solution	Kim et al. (2008)	12.7 mm (Modified VE)	/	25 80	-0.21 -0.32	1.24 1.13	0.901 0.918	0.27	0.295	1822	27.5	1.05	26.0	0.00	6 12 18	0.5 1.0 1.5	100.00 100.00 100.00
											26.0	1.02	52.0	0.14	6 12 18	0.5 1.0 1.5	96.93 95.80 95.13
	Ruiz Emparanza et al. (2022)	~10 mm (VE)	/	23 60	-0.08 -0.16	1.14 0.98	0.864 0.831	0.12	0.071	8142	27.5	1.51	26.0	0.00	6 12 18	0.5 1.0 1.5	100.00 100.00 100.00
											26.0	1.32	52.0	0.14	6 12 18	0.5 1.0 1.5	99.31 98.78 98.47
				23 40	-0.11 -0.08	1.24 1.16	0.927 0.989	0.10	0.056	9918	27.5	1.65	26.0	0.00	6 12 18	0.5 1.0 1.5	100.00 100.00 100.00
											26.0	1.40	52.0	0.14	6 12 18	0.5 1.0 1.5	99.43 99.01 98.77
				23 60	-0.17 -0.18	1.36 1.09	0.900 0.990	0.18	0.072	9283	27.5	1.60	26.0	0.00	6 12 18	0.5 1.0 1.5	100.00 100.00 100.00
											26.0	1.37	52.0	0.14	6 12 18	0.5 1.0 1.5	99.39 98.64 98.20
	Wang et al. (2023a)	9.52 mm (VE)	/	40 60	-0.25 -0.21	1.39 1.01	0.972 0.923	0.23	0.242	20023	27.5	0.07	26.0	0.00	6 12 18	0.5 1.0 1.5	100.00 100.00 100.00
											26.0	0.05	52.0	0.14	6 12 18	0.5 1.0 1.5	100.00 100.00 100.00

Note: (1) VE = vinylester resin; EP = epoxy resin.



(a) Alkaline solution



(b) Saline solution

Fig. 4.11 Comparison between FET results and predictions based on Huang and Aboutaha's (2010) model for bare GFRP bars

4.4.3.2 Concrete-embedded unstressed GFRP bars

For the unstressed GFRP bars embedded in concrete, the predicted tensile strength

retentions based on Huang and Aboutaha's (2010) model are compared with the FET results tested by Morales et al. (2021) in Fig. 4.12, and the coefficients obtained in the prediction process are summarized in Table 4.11. Fig. 4.12 clearly shows that for the GFRP bars wrapped in fly ash-based SWC, the model predictions generally agree well with the FET results in the initial two exposure durations (i.e., 1 and 6 months), regardless of the solution type, whereas in the subsequent exposure durations (i.e., 12 and 24 months), the model predictions tend to be slightly smaller in magnitude compared to the FET data. For the slag-based SWC counterparts, however, the FET results for all exposure durations are generally overestimated by the model predictions, and this observation can also be explained by the reasons mentioned in Section 4.4.1.2.

Table 4.11 Coefficients and predicted results based on Huang and Aboutaha's (2010) model for concrete-embedded unstressed GFRP bars

Solution type	Reference	Bar type	Concrete type	T (°C)	Coef. in Eq. (4.4)			Coef. in Eq. (4.11)									Ret. η_E (%)
					a	b	R^2	ρ	Δ_1	E_a/R	MAT (°C)	TSF	RH (%)	n_H	Time (m)	DL (y)	
Saline solution	Robert and Benmokrane (2013)	12.7 mm (VE)	NC	23	-0.08	1.15	0.836	0.09	0.066	267	25.0	1.01	71.2	0.29	1	0.1	100.00
				50	-0.09	1.14	0.835								6	0.5	98.83
															12	1.0	98.06
															24	2.0	97.28
	Lu et al. (2022)	6 mm (VE)	SWSSC	28	-0.42	1.39	0.936	0.40	0.687	7850		0.77			1	0.1	93.70
				60	-0.37	0.96	1.000								6	0.5	84.73
															12	1.0	81.26
															24	2.0	77.78
Water	Davalos et al. (2011)	9.53 mm (VE)	NC	20	-0.18	1.26	0.940	0.21	0.207	1030		1.06			1	0.1	100.00
				40	-0.24	1.24	0.948								6	0.5	95.64
															12	1.0	93.80
															24	2.0	91.96
	El-Hassan et al. (2017)	8 mm (EP)	SWC	20	-0.22	1.33	0.960	0.22	0.242	5989		1.41			1	0.1	98.80
				40	-0.21	1.21	0.731*								6	0.5	93.91
															12	1.0	92.01
															24	2.0	90.12
	Fergani et al. (2018a)	8 mm (VE)	NC	40	-0.25	1.36	0.991	0.26	0.284	3617		0.56			1	0.1	100.00
				60	-0.28	1.28	0.895								6	0.5	95.96
															12	1.0	93.65
															24	2.0	91.34

Note: (1) VE = vinylester resin; EP = epoxy resin. (2) NC = normal concrete; SWC = seawater concrete; SWSSC = seawater sea-sand concrete. (3) *R^2 value at 40°C slightly less than 0.80 was also included.

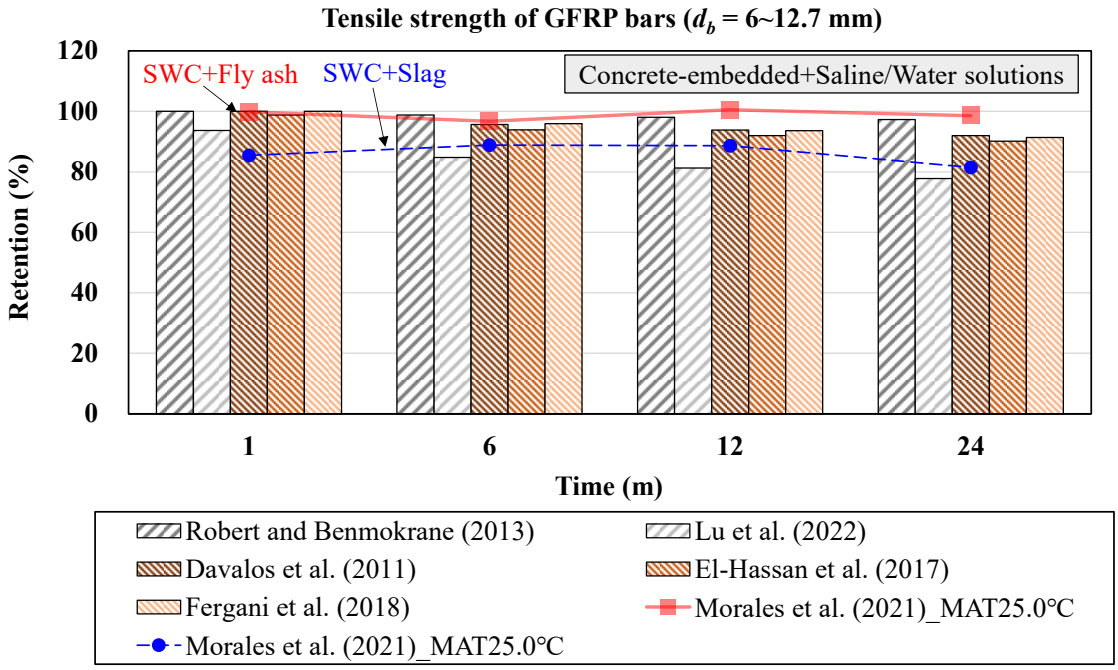


Fig. 4.12 Comparison between FET results and predictions based on Huang and Aboutaha's (2010) model for concrete-embedded unstressed GFRP bars

4.4.3.3 Concrete-embedded stressed GFRP bars

For the concrete-embedded stressed GFRP bars, after filtering the available AAT data according to the selection criteria for Huang and Aboutaha's (2010) model, only two datasets from Lu et al. (2022) were used in the prediction model. Fig. 4.13 shows the predicted tensile strength retentions in comparison with the FET results, with the corresponding coefficients summarized in Table 4.12. Despite the fact that the diameter of GFRP bars used for model prediction [6 mm as in Lu et al. (2022)] is much smaller than those employed in the FET studies (9.5~19 mm), there is an excellent agreement between the FET results from Mukherjee and Arwikar (2005) and the model predictions. For the other two FET studies (Bakis et al. 2005; Trejo et al. 2011), due to the reasons mentioned in preceding sections, the FET results are reasonably underestimated by the predictions as expected.

Table 4.12 Coefficients and predicted results based on Huang and Aboutaha's (2010) model for concrete-embedded stressed GFRP bars

Solution type	Reference	Bar type	Concrete type	Stress level	T (℃)	Coef. in Eq. (4.4)			Coef. in Eq. (4.11)									Ret.
						a	b	R^2	ρ	Δ_1	E_a/R	MAT (℃)	TSF	RH (%)	n_H	Time (m)	DL (y)	η_E (%)
Saline solution	Lu et al. (2022)	6 mm (VE)	SWSSC	20% f_u	28	-0.60	1.58	0.978	0.56	0.958	9979	9.0	0.11	57.6	0.17	12	1.0	92.96 [a]
					40	-0.53	1.27	0.974	0.56				0.11		0.17	36	3.0	88.35 [a]
												27.5	0.95	74.9	0.34	18	1.5	64.45 [b]
													0.95		0.34	30	2.5	60.19 [b]
												23.0	0.57	59.3	0.18	84	7.0	76.61 [c]
				40% f_u	28	-0.51	1.34	0.979	0.50	0.955	4184	9.0	0.39	57.6	0.17	12	1.0	87.12 [a]
					60	-0.49	1.05	0.905	0.50				0.39		0.17	36	3.0	83.03 [a]
												27.5	0.98	74.9	0.34	18	1.5	64.63 [b]
													0.98		0.34	30	2.5	60.85 [b]
												23.0	0.79	59.3	0.18	84	7.0	76.08 [c]

Note: (1) VE = vinylester resin. (2) SWSSC = seawater sea-sand concrete. (3) f_u = ultimate tensile stress of an FRP bar. (4) [a]Bakis et al. (2005); [b]Mukherjee and Arwikar (2005); [c]Trejo et al. (2011).

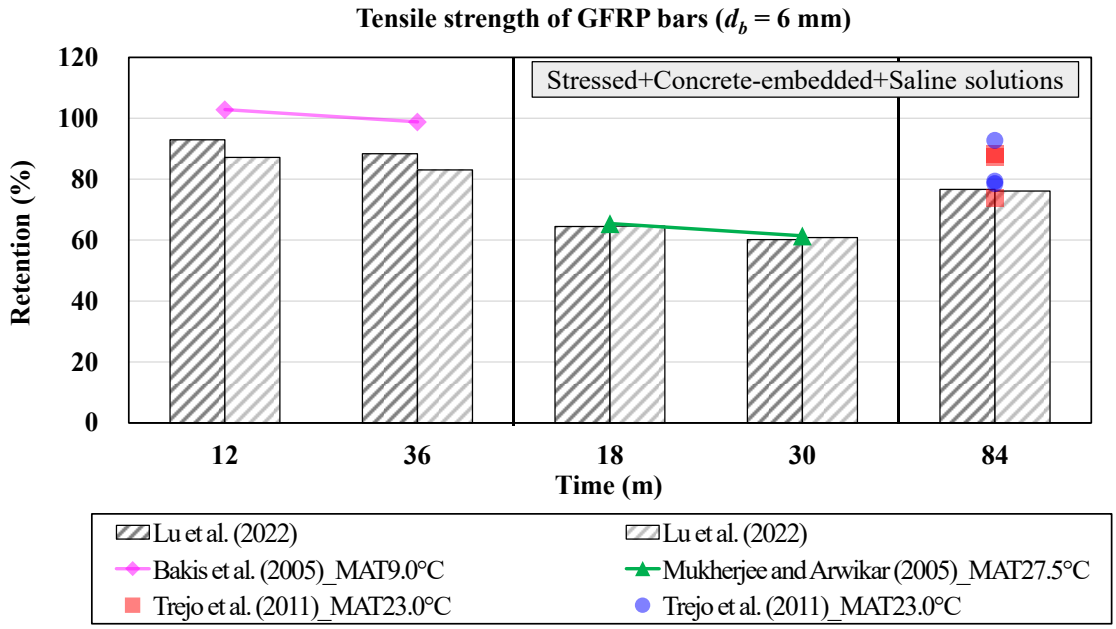


Fig. 4.13 Comparison between FET results and predictions based on Huang and Aboutaha's (2010) model for concrete-embedded stressed GFRP bars

4.4.4 Comparison Between Existing Models

A comparison of performance between the abovementioned three prediction models is presented in this section. To ensure consistency, the AAT data used herein were limited to those that simultaneously meet the selection criteria of the three models. In addition, the statistical indices, including the mean, the standard deviation (SD), the coefficient of variation (COV), and the average absolute error (AAE) [defined as Eq. (4.15)] were used to evaluate the accuracy of the three models.

$$\text{AAE} = \frac{1}{N}\sum_{i=1}^{N}\left|\frac{R_{pre,i} - R_{test,i}}{R_{test,i}}\right| \tag{4.15}$$

where $R_{test,i}$ is the test value for the ith data point; $R_{pre,i}$ is the predicted value for the ith data point; and N is the number of data points.

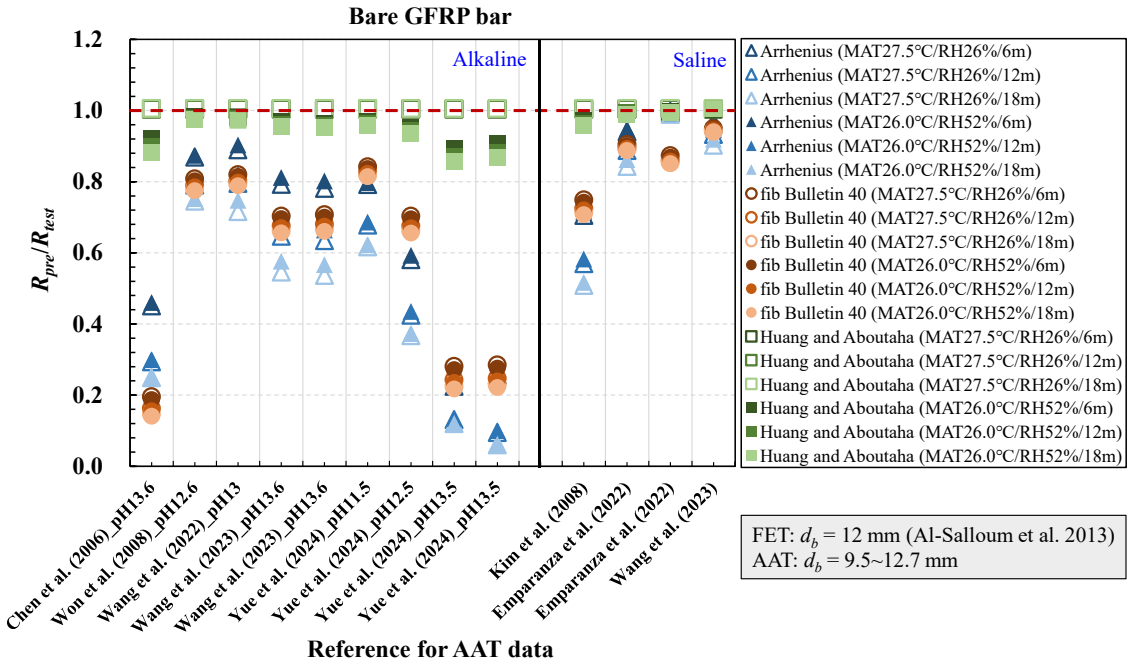
Table 4.13 presents the assessment results for the tensile strength retention ratios

(R_{pre}/R_{test}) calculated by the three models, and the corresponding distributions of retention ratio versus AAT studies are shown in Fig. 4.14. It can be found from Table 4.13 that Huang and Aboutaha's (2010) model provides the most accurate predictions with the average R_{pre}/R_{test} of 0.979, 1.010 and 0.925 for bare, concrete-embedded unstressed and concrete-embedded stressed GFRP bars, respectively. In contrast, the accuracies of Arrhenius empirical model and *fib* Bulletin 40 (2007) model are much poorer, especially for the concrete-embedded stressed GFRP bars (mean = 0.149 and 0.083, respectively), which can also be observed in Fig. 4.14. Besides, the CoV (0.039~0.100) and AAE (0.026~0.082) of Huang and Aboutaha's (2010) model are remarkably lower than those of the other two models, again suggesting that the former performs better in predicting the long-term performance of GFRP bars. It is important to point out that the evaluation of model performance is highly dependent on the size of the database used for model predictions, and therefore additional experimental studies are necessary in the future to enable more robust conclusions.

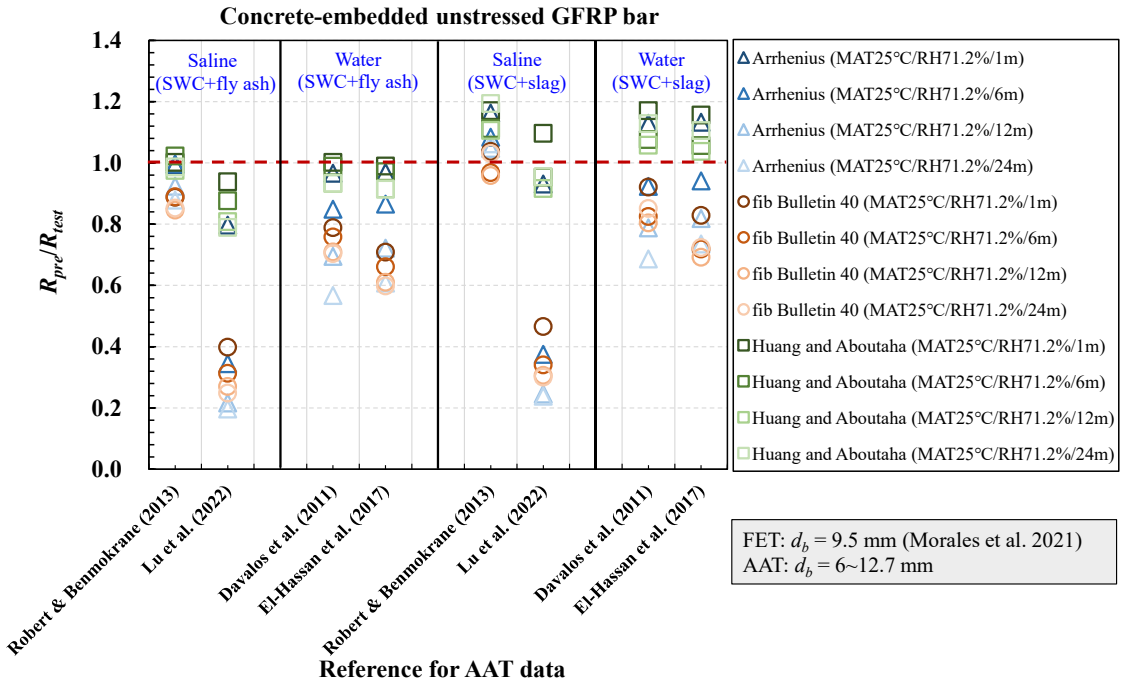
Table 4.13 Assessment of tensile strength retention ratio (R_{pre}/R_{test})

Bar type	Model	Number of data points	Mean	SD	COV	AAE
Bare GFRP bars	Arrhenius	78	0.629	0.280	0.444	0.371
	fib Bulletin 40 (2007)		0.657	0.253	0.386	0.343
	Huang and Aboutaha (2010)		0.979	0.038	0.039	0.026
CE unstressed	Arrhenius	32	0.778	0.285	0.367	0.276
GFRP bars	*fib* Bulletin 40 (2007)		0.688	0.234	0.340	0.360
	Huang and Aboutaha (2010)		1.010	0.101	0.100	0.063
CE stressed	Arrhenius	20	0.149	0.084	0.565	0.851
GFRP bars	*fib* Bulletin 40 (2007)		0.083	0.033	0.394	0.917
	Huang and Aboutaha (2010)		0.925	0.068	0.074	0.082

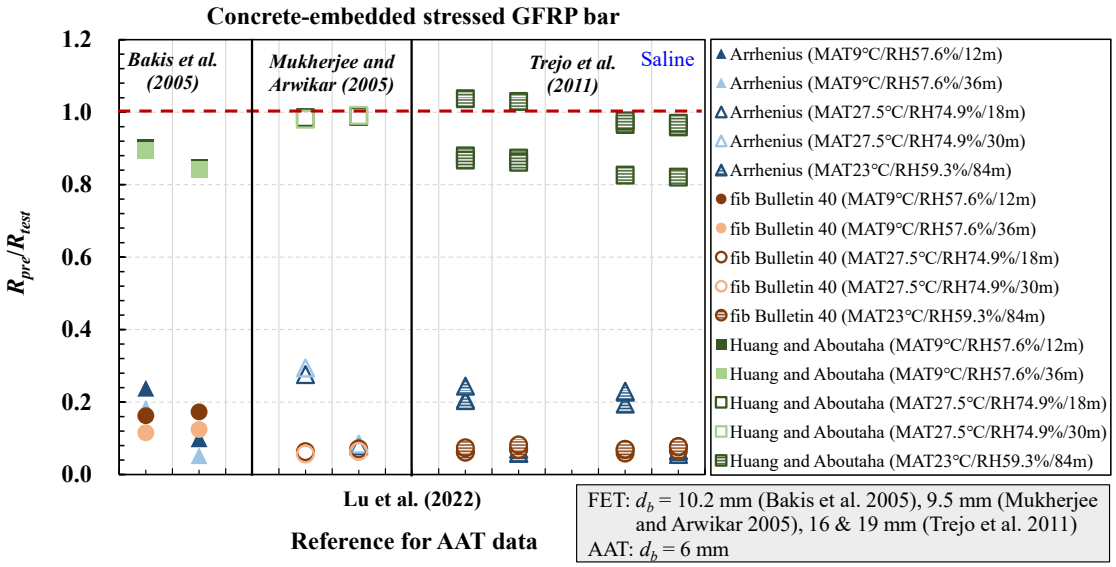
Note: CE = concrete-embedded.



(a) Bare GFRP bars



(b) Concrete-embedded unstressed GFRP bars



(c) Concrete-embedded stressed GFRP bars

Fig. 4.14 Tensile strength retention ratio by different prediction models for GFRP bars

4.5 PROPOSED PREDICTION MODEL

Based on the above assessment results of three existing models for the long-term predictions of GFRP bars, it was found that Huang and Aboutaha's (2010) model offered the highest reliability among the three existing models, and it was deemed applicable to bare GFRP bars subjected to natural weathering. In this section, the accuracy of Huang and Aboutaha's (2010) model was further validated against FET results presented in Chapter 3 for the bare GFRP bars exposed to aggressive marine environments. As provided in Table 4.10, the filtered AAT dataset collected from Ruiz Emparanza et al. (2022) were used to produce predictions due to the following reasons: (1) The GFRP bar products were from different major manufacturers globally, suggesting a more comprehensive analysis; (2) The major constituents (i.e., fiber and resin) and diameters of these GFRP bars were similar to those used in Chapter 3; (3) Natural seawater was employed as conditioning solution, representing a more realistic assessment of durability for GFRP bars in marine environments. The key information of

the GFRP bar specimens used in Ruiz Emparanza et al. (2022) and Chapter 3 is given in Table 4.14. It should be pointed out that the RHs for atmospheric and splash conditions were taken to be recorded values, while those for both the tidal (characterized by consecutive wet-dry cycles) and underwater (characterized by constant submersion) conditions were assumed to be 100%.

Using the prediction coefficients (i.e., ρ, Δ_1 and E_a /R) from Ruiz Emparanza et al. (2022) as provided in Table 4.10 and following the prediction process of Huang and Aboutaha's (2010) model as detailed in Section 4.4.3, the prediction results for bare GFRP bars under various marine environmental conditions (including atmospheric, splash, tidal and underwater environments) are presented in Table 4.15, where the predicted tensile strength retention $\eta_{E,pre}$ was averaged from the predictions produced by the AAT datasets of three different types (i.e., A, C, and D) of GFRP bars. As expected, Huang and Aboutaha's (2010) model provides reasonably accurate predictions for the bare GFRP bars in mild marine environments, such as atmospheric (A-I and A-II) and splash (S-I) conditions, despite a slight underestimation (errors ranging from -5.6 to -0.2), which is similar to that observed in the bare GFRP bars subjected to natural weathering (Al-Salloum et al. 2013). Such an underestimation is believed to be acceptable as it allows slightly conservative predictions to be made in practice. However, this model seems less reliable with regard to the bare GFRP bars subjected to much harsher marine environments with a prolonged period. More specifically, the residual tensile strength of bare GFRP bars exposed to tidal (T-I) and underwater (U-II) conditions for four and two years, respectively, is significantly overestimated by this model.

Table 4.14 Key information of bare GFRP bars used in the selected studies

Reference	Specimen	Diameter (mm)	Fiber content (%)	Resin type	Fiber type	Exposure type	Exposure condition	MAT (°C)	RH (%)	Time (m)
Ruiz Emparanza et al. (2022)	Type-A	10.16	76.3	Vinylester	E-CR Glass	AAT	Seawater immersion at 23/40/60°C	/	/	2/4/7/12
	Type-C	10.09	76.1	Vinylester	E Glass					
	Type-D	10.70	70.1	Vinylester	E-CR Glass					
The present study (Chapter 3)	A-I	9.91	81.1	Vinylester	E Glass	FET	Atmospheric	23.3	77.8	8/12/24/37/48
	S-I						Splash	23.3	77.8	
	T-I						Tidal	23.3	100[#]	
	A-II	9.89	81.2	Vinylester	E Glass	FET	Atmospheric	23.3	82.7	13/24
	U-II						Underwater	23.3	100[#]	

[#]The RHs for both the tidal (characterized by consecutive wet-dry cycles) and underwater (characterized by constant submersion) conditions were assumed to be 100%.

Table 4.15 Comparison between the test and predicted results

FET specimen	Coef. in Eq. (4.11)						$\eta_{E,test}$ (%)	Huang and Aboutaha's (2010) model		Correction factor α_T	Proposed model	
	MAT (℃)	TSF	RH (%)	n_H	Time (m)	DL (y)		$\eta_{E,pre}$[#] (%)	*Error*		$\eta_{E,pre}$ (%)	*Error*
A-I	23.3	1.03	77.8	0.38	8	0.7	(103.35)	98.30	-1.7	1.00	98.30	-1.7
					12	1.0	(100.73)	97.42	-2.6	1.00	97.42	-2.6
					24	2.0	99.82	95.91	-3.9	1.00	95.91	-3.9
					37	3.1	(101.48)	94.96	-5.0	1.00	94.96	-5.0
					48	4.0	(101.46)	94.40	-5.6	1.00	94.40	-5.6
S-I			77.8	0.38	8	0.7	99.82	98.30	-1.5	1.00	98.30	-1.5
					12	1.0	(101.20)	97.42	-2.6	1.00	97.42	-2.6
					24	2.0	96.13	95.91	-0.2	1.00	95.91	-0.2
					37	3.1	(100.50)	94.96	-5.0	1.00	94.96	-5.0
					48	4.0	99.98	94.40	-5.6	1.00	94.40	-5.6
T-I			100	1.00	8	0.7	(106.06)	95.52	-4.5	0.00	100.00	+0.0
					12	1.0	99.21	93.19	-6.1	0.24	98.34	-0.9
					24	2.0	90.64	89.20	-1.6	0.78	91.61	+1.1
					37	3.1	86.06	86.71	+0.8	1.11	85.25	-0.9
					48	4.0	81.14	85.22	+5.0	1.31	80.62	-0.6
A-II	23.3	1.03	82.7	0.45	13	1.1	(102.89)	96.70	-3.3	1.00	96.70	-3.3
					24	2.0	(103.30)	95.10	-4.9	1.00	95.10	-4.9
U-II			100	1.00	13	1.1	90.51	92.73	+2.5	/	/	/
					24	2.0	81.99	89.20	+8.8	/	/	/

Note: (1) The data in the brackets were taken to be 100% in the calculation process. (2) *Error* = $(\eta_{E,pre} - \eta_{E,test})/\eta_{E,test}$. (3) [#]Average value obtained from the predictions produced by the AAT datasets of three different types of GFRP bars.

To address the abovementioned overestimation, the present study refines Huang and Aboutaha's (2010) model [Eq. (4.11)] by introducing a time-dependent correction factor "α_T" ($\alpha_T \geq 0$), to account for the additional effects of tidal exposure on bare GFRP bars:

$$\eta_E = 1 - \alpha_T \cdot n_H \cdot [\Delta_1 - \rho \cdot \log(\mathrm{DL} \cdot \mathrm{TSF})] \tag{4.16}$$

A regression analysis was conducted to obtain the best-fit α_T value, and the α_T values obtained from the AAT results of three types of GFRP bars are shown against exposure time *t* in Fig. 4.15. Based on the regression results, the following equation was proposed for α_T:

$$\alpha_T = 0.77 \cdot \ln(t) - 1.67 \tag{4.17}$$

The average values of α_T and the predictions produced by the proposed model are listed in Table 4.15, while Fig. 4.16 compares the predictions of the proposed model and Huang and Aboutaha's (2010) model against the FET results. It is evident that the proposed model provides highly accurate predictions for GFRP bars in the T-I zone and significantly outperforms Huang and Aboutaha's (2010) model, with error ranges reduced from -6.1~5.0 to -0.9~1.1. Besides, as mentioned previously, Huang and Aboutaha's (2010) model remains applicable to bare GFRP bars exposed to atmospheric and splash environments.

Note that the proposed model, which incorporates the correction factor "α_T", may be applicable solely to bare GFRP bars in tidal environments. Further research is necessary to develop a size-dependent model that can accurately predict the long-term performance of bare GFRP bars in both tidal and underwater environments when more experimental data are available.

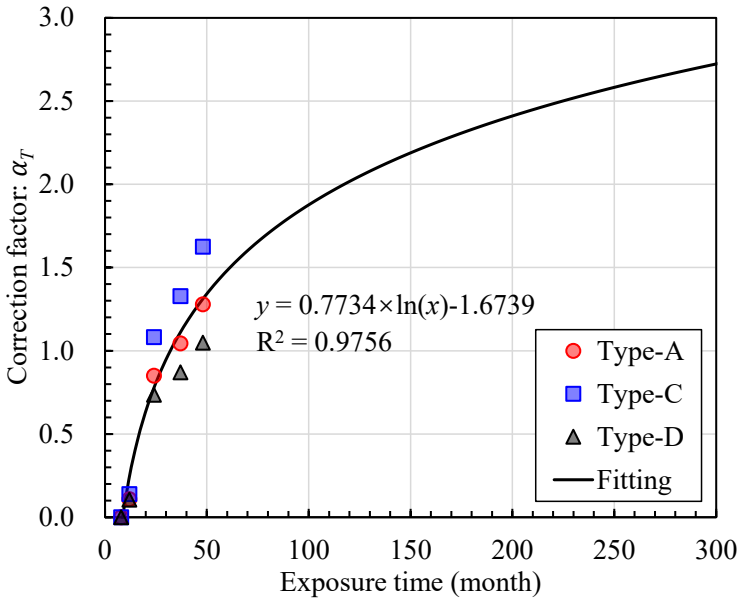


Fig. 4.15 Correction factor α_T value versus exposure time

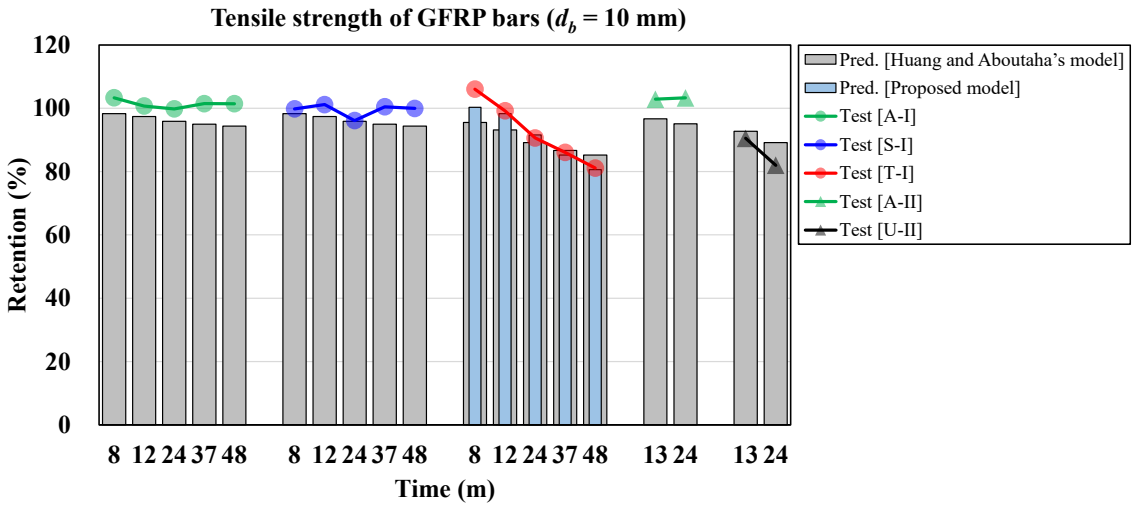


Fig. 4.16 Comparison between FET results and model predictions

4.6 CONCLUSIONS

This chapter presents a comprehensive review of existing models developed for predicting the long-term performance of FRP bars in service. Three widely used prediction models [i.e., Arrhenius empirical model, *fib* Bulletin 40 (2007) model and Huang and Aboutaha's (2010) model] were systematically assessed against FET data sourced from the existing literature. On the basis of the evaluation results of these

models, a refined model that incorporates the additional effects of tidal conditions on bare GFRP bars was proposed, and the accuracy of this newly developed model was also assessed. From the results presented in this chapter, the following conclusions can be drawn:

(1) Compared to the AAT studies, those on or relevant to the durability of FRP bars under real field conditions are quite scarce so far, leading to limited FET data available for model evaluation.

(2) The predictions generated by Arrhenius empirical model and *fib* Bulletin 40 (2007) model using AAT data from different studies might vary significantly, which is caused by the fact that the long-term performance of FRP bars is affected by various factors such as the inherent properties, bar diameter, manufacturing process and types of conditioning.

(3) Huang and Aboutaha's (2010) model was found to perform better than the other two models in predicting the long-term tensile performance of GFRP bars based on the FET database.

(4) The proposed model provides much more accurate predictions for the bare GFRP bars subjected to tidal conditions, while Huang and Aboutaha's (2010) model is applicable to the bare GFRP bars under both atmospheric and splash conditions.

(5) The proposed model may only be applicable to bare GFRP bars with a limited bar diameter range (approximately 10 mm) under tidal conditions. In order to develop a size-dependent prediction model for GFRP bars under both tidal and underwater environmental conditions, more experimental data with wider

ranges of bar sizes are needed.

CHAPTER 5
LONG-TERM BOND PERFORMANCE BETWEEN GFRP BARS AND SEAWATER SEA-SAND CONCRETE IN REAL MARINE ENVIRONMENTS

5.1 INTRODUCTION

As internal reinforcement, the bond between GFRP bars and the surrounding concrete is a critical factor in determining the serviceability of concrete structures reinforced with GFRP bars, and bond durability directly influences the safety and maintenance requirements of such structures (ACI 2022). So far, considerable research has been conducted to assess the long-term bond performance between GFRP bars and normal concrete (NC) under simulated environmental conditions using direct pullout tests (Robert and Benmokrane 2010; Zhou et al. 2011; Bazli et al. 2017; Yan and Lin 2017; Chang et al. 2021; Kazemi et al. 2022; Ruiz Emparanza et al. 2022; Shakiba et al. 2023). However, these studies have reported considerable dispersion in bond strength results, with no clear consensus, as discussed in Chapter 2. For example, Yan and Lin (2017) found that the bond strength of GFRP bars in NC decreased by approximately 10% and 12%, respectively, after exposure to the saline solution at 50℃ and 70℃ for 60 days, whereas Khatibmasjedi et al. (2020) reported an increase of approximate 7% in bond strength after 24 months of seawater immersion at 60℃.

Compared with NC, far fewer studies address the bond durability of GFRP bars in SSC. Chang et al. (2021) experimentally investigated the effect of seawater immersion at 25℃ on bond performance of different-sized GFRP bars in SSC. They found that the bond

strength retention for 12-mm GFRP bars decreased to 92.6% after an exposure period of 270 days, while that for 16-mm GFRP bars increased to 115.7%. Hao (2024) conducted an experimental study on GFRP bar-to-SSC bonded joints subjected to wet-dry cycles in saline solution at 40°C for up to two years. The test results showed that only a slight reduction (7.5%) was detected in bond strength after 24 months. Ke et al. (2024) tested bond durability under hydrothermal aging conditions (saline solution immersion at 23°C, 40°C and 60°C) for up to 360 days and found no degradation in bond strength of the pullout specimens.

Most existing studies on bond durability of GFRP bars in concrete rely on accelerated aging methods, with a notable lack of research on long-term bond performance under actual field and marine conditions (see Table E1 in Appendix B). Given that it is very difficult to infer real-world long-term performance from AAT results, direct FET is necessitated to obtain conclusive data.

Against this background, this chapter presents direct pullout test results for two series of GFRP bar-to-SSC bonded joints after field exposure in four marine environmental zones (i.e., atmospheric, splash, tidal, and underwater) for up to four years. The aim is to assess the long-term bond performance between GFRP bars and SSC in real marine environments, thereby facilitating the broader application of GFRP bars in practice. Additionally, a time-dependent bond stress-slip model for GFRP bars in SSC is proposed, and its accuracy is evaluated.

5.2 EXPERIMENTAL PROGRAM

5.2.1 Materials

5.2.1.1 GFRP bars

As shown in Fig. 5.1, two batches of 10-mm GFRP bars, designated as Batch I and Batch II, were used in this chapter. These GFRP bars are identical in diameter to those employed in Chapter 3. Compared to Batch II, Batch I bars exhibit a larger interval spacing of helical yarn (20 mm versus 8.5 mm) and a thicker sand coating on their surface. The tensile strength and elastic modulus of Batch-I bars were experimentally determined to be 1224.62 MPa and 54.13 GPa, respectively, while the corresponding values for Batch-II bars were measured as 1131.37 MPa and 47.70 GPa, respectively, according to ASTM (2021). Further details regarding the two batches of GFRP bars are provided in Chapter 3.

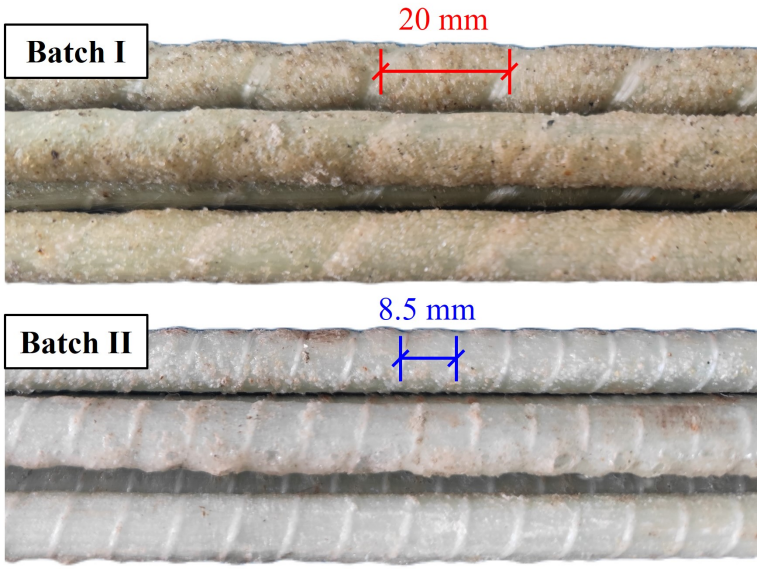


Fig. 5.1 Two batches of GFRP bars used in this chapter

5.2.1.2 Seawater sea-sand concrete

Ready-mixed SSC a designed compressive strength of 55 MPa, provided by Gammon Construction Ltd. in Hong Kong, was used in this chapter. The detailed mix proportions of SSC, including Type I Ordinary Portland cement [as specified in ASTM (2024)], pulverized fuel ash, coarse aggregate (20-mm crushed rock), fine aggregate (10-mm crushed rock), sea-sand, seawater, and superplasticizer (Rheomac 1002, supplied by BASF Hong Kong Limited), are detailed in Table 5.1. The seawater was sourced from local saltwater pumping stations in Hong Kong, and the sea-sand was imported from Malaysia. Sieve analysis was performed on the sea-sand according to GB/T (2022). Based on the grading curve shown in Fig. 5.2, the fineness modulus of the sea-sand was calculated to be 2.68. Additionally, the apparent density (2682 kg/m^3), silt content (4.1%), and shell content (3.4%) of the sea-sand were determined in accordance with JGJ (2006).

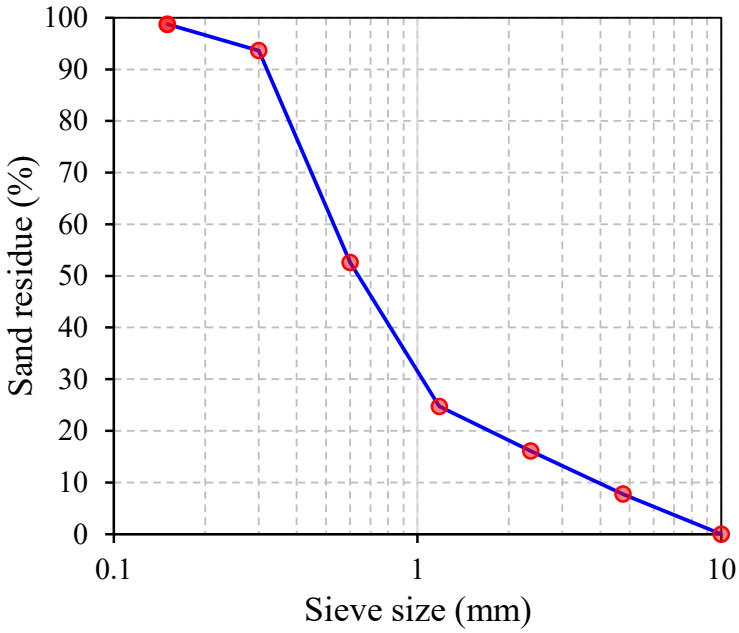


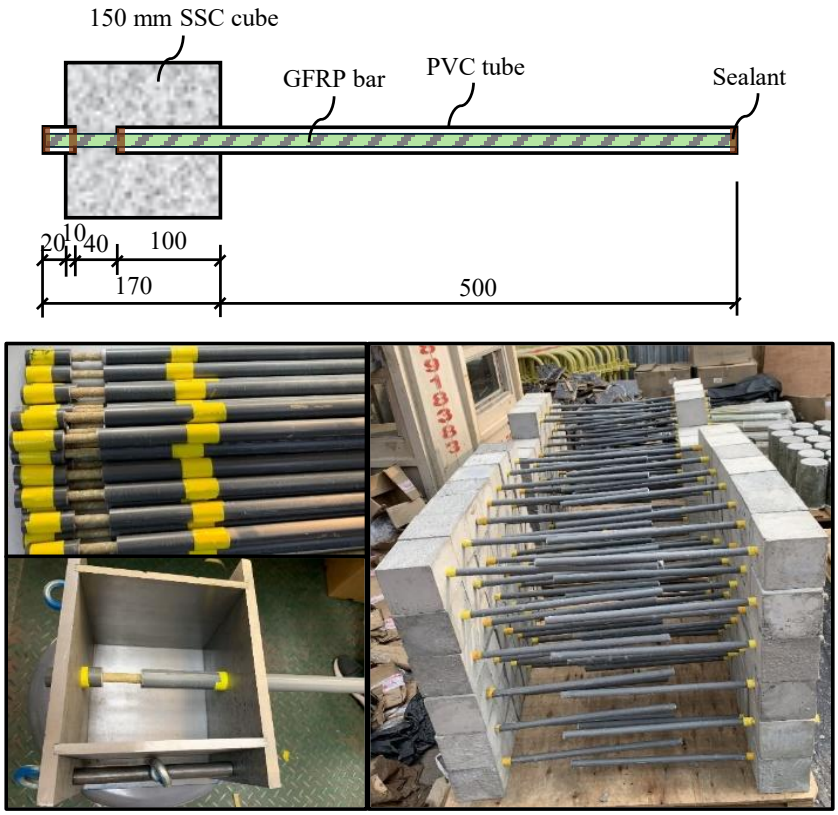
Fig. 5.2 Grading curve of sea-sand

Table 5.1 Mix proportions of SSC

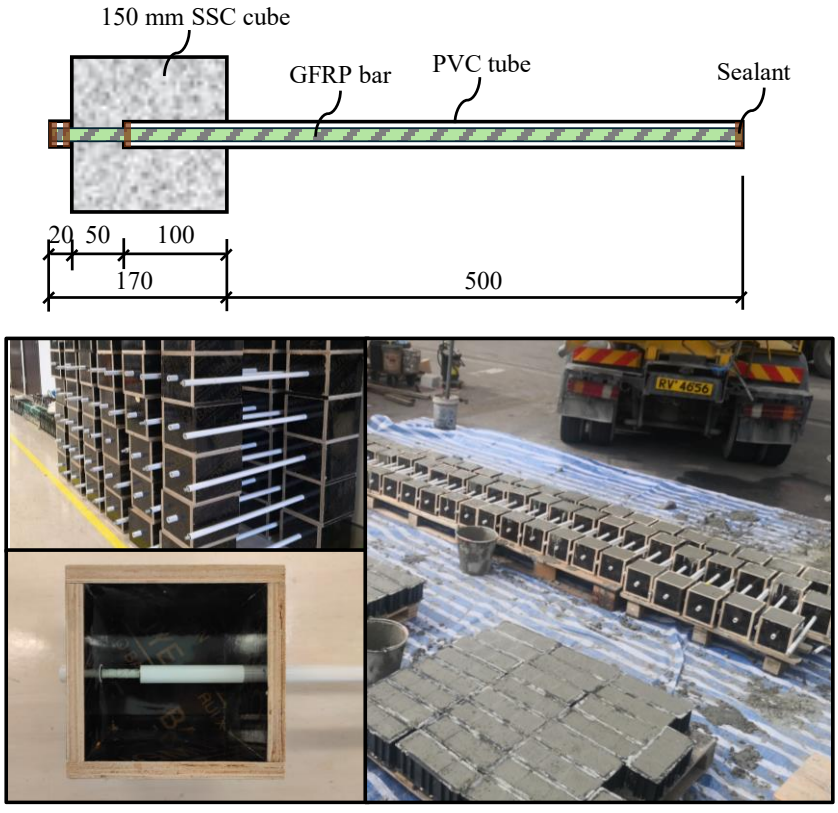
Raw material	Quantity (kg/m^3)	Specific gravity (g/cm^3)	Volume (m^3)
Cement	330	3.15	0.105
Pulverized Fuel Ash	110	2.20	0.050
20-mm Aggregate	565	2.62	0.216
10-mm Aggregate	465	2.62	0.177
Sea-sand	730	2.62	0.279
Seawater	165	1.02	0.162
Superplasticizer	2.65 ± 2.12	1.06	0.003

5.2.2 Design and Preparation of Pullout Specimens

Two series of pullout specimens (referred to as Series I and Series II) were investigated. These respectively correspond to the 1st and 3rd series of FET specimens involved in a theme-based research scheme project (Table 3.1), as detailed in Chapter 3. Series I and II specimens incorporated GFRP bars from Batches I and II, respectively. As illustrated in Fig. 5.3, each pullout specimen consisted of a 670-mm-length GFRP bar embedded concentrically in an SSC cube with a side length of 150 mm. The bonded length of the GFRP bar was set to four times the bar diameter [i.e., $4d_b$ = 40 mm, as shown in Fig. 5.3(a)] for Series I specimens, in accordance with JSCE (1995b), while for Series II specimens, the bonded length was designed as five times the bar diameter [i.e., $5d_b$ = 50 mm, as shown in Fig. 5.3(b)], following ASTM (2020). It is worth mentioning that for FRP bars with bonded lengths shorter than $5d_b$, the bond stress distribution along the bonded length can be assumed uniform, allowing local stress to be equivalent to the average stress (Haskett et al. 2008; Feng et al. 2016). A polyvinyl chloride (PVC) tube was used as a bond breaker for the unbonded section, isolating the GFRP bar from the SSC. Both ends of the PVC tube were sealed with sealant so that the seawater or other chemicals could only penetrate through the concrete cover. To facilitate measurement of free end slip, the GFRP bar protruded 20 mm beyond the SSC cube.



(a) Series I



(b) Series II

Fig. 5.3 Schematic diagram and preparation of pullout specimens (unit: mm)

The two series of specimens were each cast using a single batch of SSC on 5 October 2019 and 21 November 2021, respectively, in Tsing Yi, Hong Kong. The slump values of the two batches of SSC were measured to be 180 mm and 170 mm, respectively. All pullout specimens were cured at ambient temperature and watered for at least seven days. After 28 days of curing, the average compressive strengths of SSC, obtained from three 100-mm concrete cubes according to GB/T (2019), were 60.86 MPa and 64.20 MPa for the two batches, respectively. As per GB/T (2019) and JGJ/T (2016), the corresponding 28-day standard cylindrical strengths of the SSC (diameter =150 mm; height = 300 mm) were approximately 46.25MPa and 48.79 MPa, respectively.

5.2.3 Field Exposure Conditions

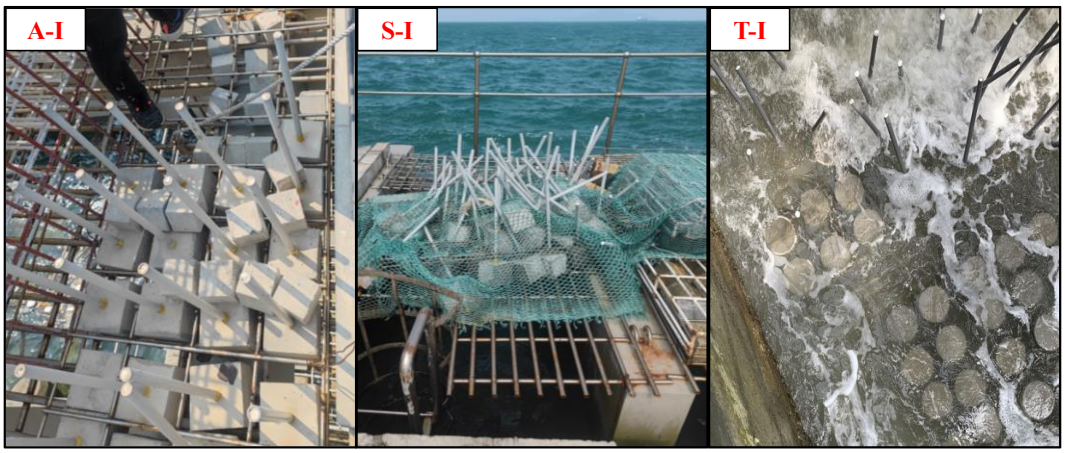
The project included four different marine environmental zone (i.e., atmospheric, splash, tidal and underwater) at two field exposure stations [i.e., the *Hong Kong-Zhuhai-Macau (HZM) Bridge Exposure Station* (Station I) and the *Zhanjiang Port Exposure Station* (Station II)]. Both stations are characterized by typical subtropical marine environments. Temperature and relative humidity changes in the regions of the two stations, as well as the environmental characteristics of the exposure zones, are detailed in Chapter 3.

Fig. 5.4 displays the specimens placed in different exposure zones at the two stations. Field exposure tests for Series I specimens commenced at Station I on 14 January 2020 (approximately three months after casting), while those for Series II specimens started at Station II on 5 January 2022 (approximately 1.5 months after casting). Table 5.2 gives the test matrix of pullout specimens. Series I specimens were exposed in zones A-I, S-I and T-I for five durations (8, 12, 24, 37 and 48 months), while Series II specimens were exposed in zones A-II and U-II for two durations (13 and 24 months). In addition, control (unexposed) specimens were stored in laboratory conditions before testing.

Table 5.2 Test matrix of pullout specimens

Series of specimen	Station	Environmental condition	Exposure duration[#] (months)	Number of specimens
I	I	Laboratory (Control)	0	3
		Atmospheric (A-I)	8/12/24/37/48	5/5/5/5/5
		Splash (S-I)	8/12/24/37/48	5/5/5/5/5
		Tidal (T-I)	8/12/24/37/48	5/5/5/0[*]/3[**]
II	II	Laboratory (Control)	0	3
		Atmospheric (A-II)	13/24	5/5
		Underwater (U-II)	13/24	5/5

[#]Due to administrative reasons at the exposure station, the sampling intervals may slightly deviate from exact annual cycles.
[*]No specimen was collected on the day of sampling due to the elevated water level.
[**]Specimens were composed of a GFRP bar that was not damaged by mechanical actions of waves and tides, as will be discussed subsequently.



(a) Series I specimens at Station I



(b) Series II specimens at Station II

Fig. 5.4 Specimens in different exposure zones

5.2.4 Test Procedure

Once the designated exposure durations were reached, selected pullout specimens were retrieved for laboratory testing. To avoid damage to the GFRP bars from the testing fixture, the loaded ends of the specimens were equipped with steel tubes (length = 200 mm; outer diameter = 26 mm; thickness = 2.5 mm) filled with epoxy resin. All specimens were cured at room temperature for at least seven days before testing to ensure sufficient resin strength.

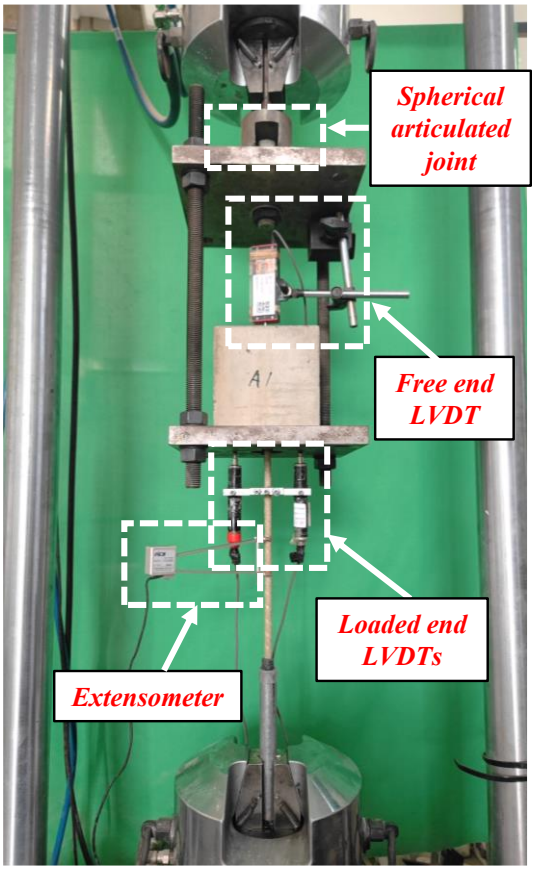


Fig. 5.5 Test set-up

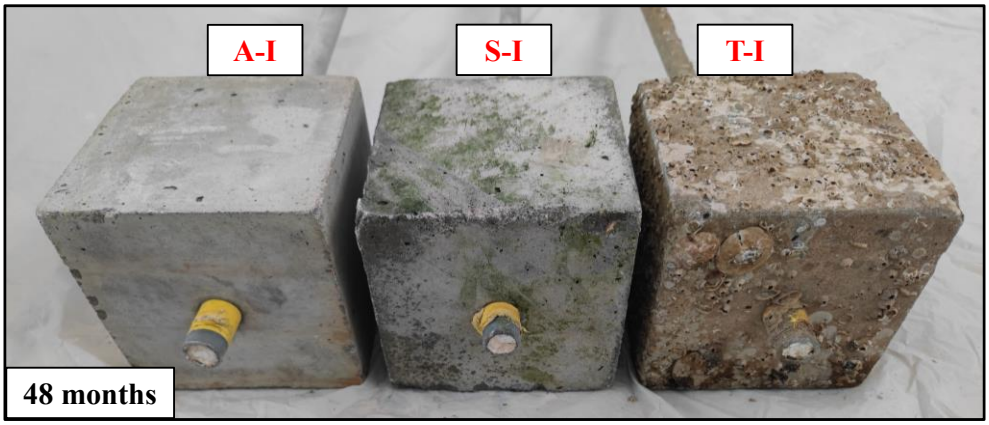
Direct pullout tests were conducted as per ASTM (2020) using an MTS-370 testing machine. As illustrated in Fig. 5.5, a specialized steel frame equipped with a spherical articulated joint was employed, which enabled the specimens to experience a pure tensile loading. To capture relative slip between the concrete and the GFRP bars, two

linear variable differential transformers (LVDTs) were fixed at 180-degree intervals at the loaded end, and an additional LVDT was installed vertically at the free end (i.e., unloaded end) of the GFRP bar. Simultaneously, an extensometer was used to measure strain variations in the GFRP bars during loading. Tests were displacement-controlled at constant rate of 1.2 mm/min. The applied load, displacement and elongation data (obtained by the extensometer) were automatically recorded by a data logger at every second.

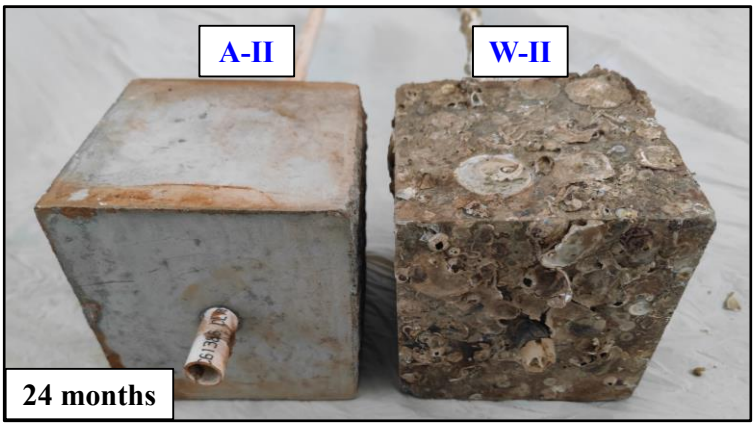
5.3 RESULTS AND DISCUSSION

5.3.1 Visual Observations

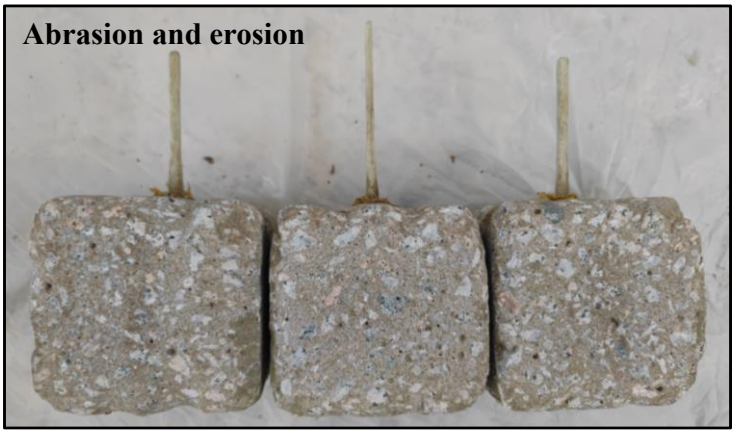
The appearance of pullout specimens after exposure to different zones were photographed, as presented in Fig. 5.6, which includes representative samples from both series after 48 months (Series I) and 24 months (Series II) of exposure. Specimens exposed in the atmospheric zones (A-I and A-II) exhibited no visible changes in appearance feature after prolonged exposure. Probably due to salt deposition, slight color changes were observed in the specimens subjected to splash conditions (S-I), which aligns with the phenomenon reported by Chen et al. (2020). Moreover, mosses and lichen growth were noted on the concrete surfaces in S-I zone. In contrast, specimens from the tidal (T-I) and underwater (U-II) zones had apparent changes in surface color, accompanied by attachment of marine organisms (e.g., barnacles, oysters, seashells). In addition, severe abrasion and erosion induced by the mechanical actions of waves and tides were evident on most T-I specimens after 48-month exposure, as shown in Fig. 5.6(c). Note that specimens exhibiting GFRP bar damage due to the abovementioned mechanical actions were excluded from testing, and the marine organisms on T-I specimens were carefully removed by shovel before testing.



(a) Series I specimens after 48 months of exposure



(b) Series II specimens after 24 months of exposure



(c) Abrasion and erosion occurred in T-I zone (48-month)

Fig. 5.6 Appearance characteristics of specimens exposed in different zones

5.3.2 Failure Modes

All specimens failed by pullout of the GFRP bar from the SSC cube; no instances of

concrete splitting or bar rupture were observed. This demonstrates that the SSC cubes provided sufficient confinement to enable the GFRP bars to achieve maximum bond strength. After testing, all specimens were split to visually investigate the interfacial bond failure. A close visual inspection on the interface between the SSC and the GFRP bar revealed that no significant differences in failure modes were observed within the same series across different exposure conditions and durations. Fig. 5.7 illustrates typical bond failure surfaces for both series of specimens. Clearly, resin residue together with chopped glass fibers attached to the concrete within the bonded length, with broken helical yarns. Severe abrasion was also noticed on the outer layer of the GFRP bars, with the sand-coated layer completely sheared off, particularly in Series I specimens. These phenomena indicate that failure occurred at the fiber-resin interface, with the bond properties primarily governed by the interlaminar shear strength between fibers and resin matrix of the GFRP bars, which is consistent with previous studies (Achillides and Pilakoutas 2004; Xue et al. 2014; Yoo et al. 2015; Zeng et al. 2022).

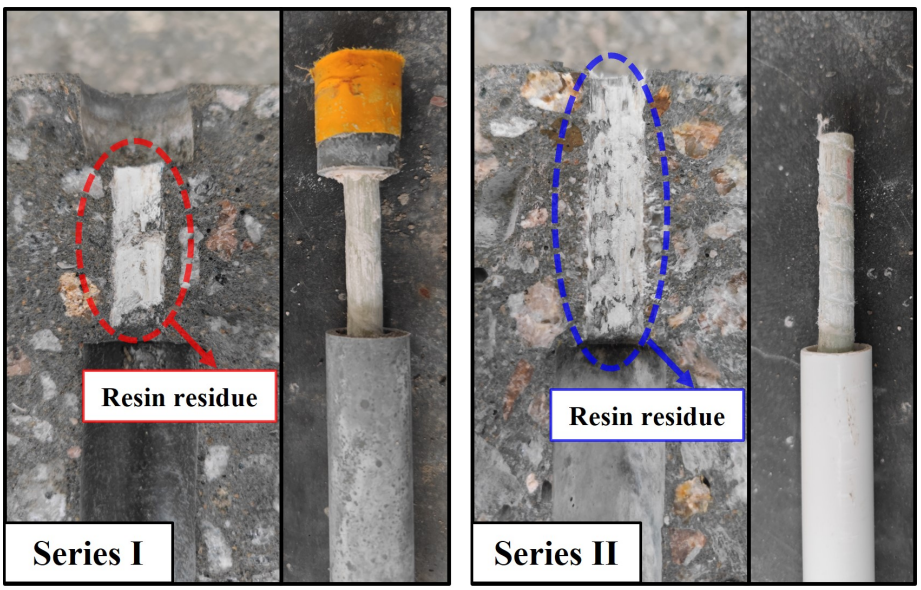


Fig. 5.7 Typical bond failure surface

5.3.3 Bond Stress-Slip Curves

Following ASTM (2020), the average bond stress (τ) was determined by Eq. (5.1):

$$\tau = \frac{P}{\pi d_b l_a} \tag{5.1}$$

where P is the applied pullout force; d_b is the nominal bar diameter (i.e., 9.5 mm); l_a is the actual bonded length of the GFRP bar, measured after splitting each failed specimen to minimize possible errors arising from specimen preparation.

The relative slip at the loaded end (s_l), which accounts for the elastic elongation of the GFRP bar, was calculated using Eq. (5.2):

$$s_l = s_L - s_c \tag{5.2}$$

where s_L is the average displacement obtained by the two LVDTs at the loaded end; s_c is the bar elongation that should be deducted from the total slip at the loaded end. The bar elongation s_c was determined using Eq. (5.3):

$$s_c = \frac{PL_c}{E_f A_f} \tag{5.3}$$

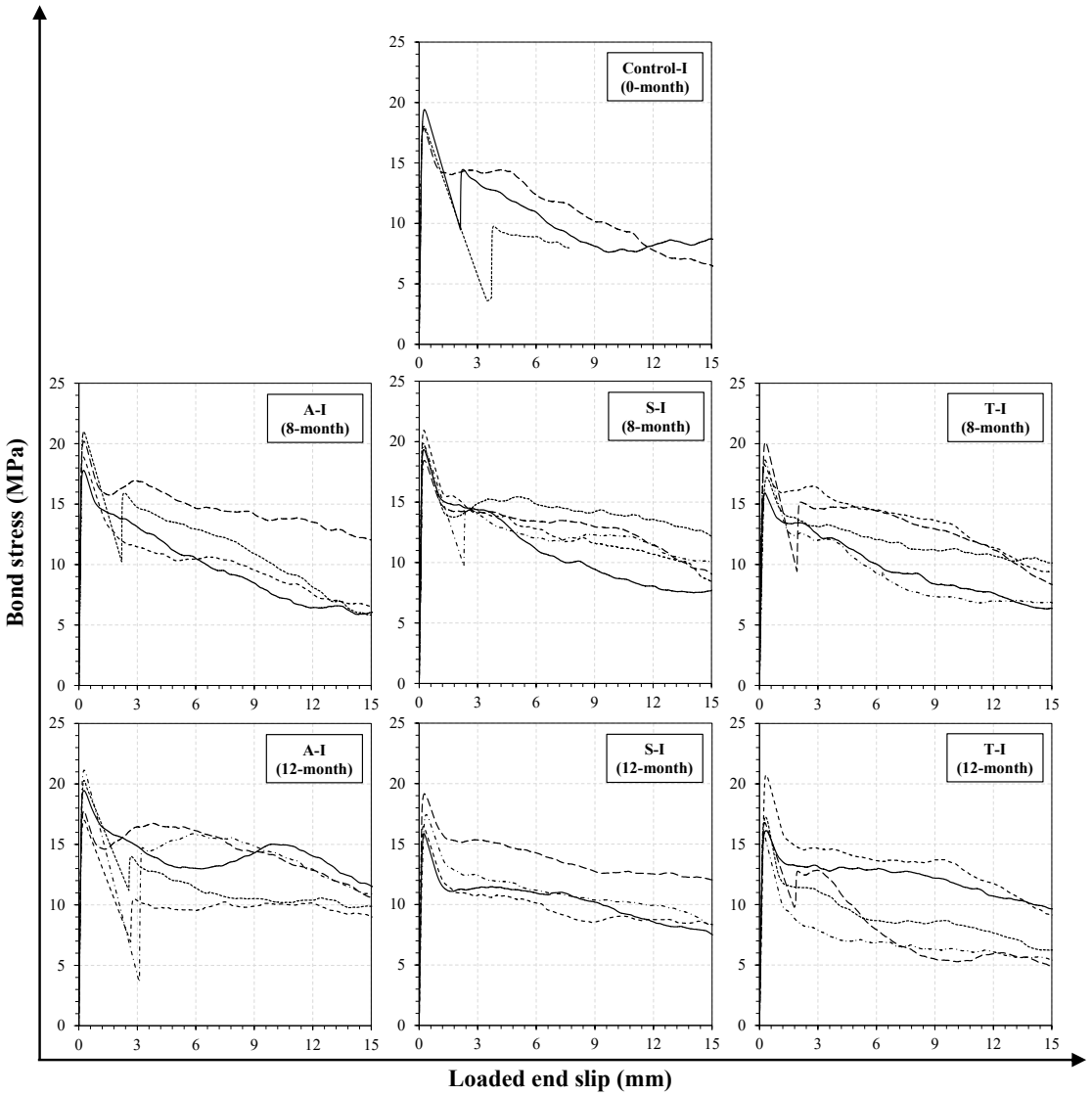
where L_c is the distance between the end of the embedded bar and the point of the attachment of the two loaded-end LVDTs; E_f is the tensile elastic modulus of the GFRP bar, for which the strain variations of the GFRP bar were measured for each specimen by an extensometer as mentioned previously; A_f is the nominal cross-sectional area of the GFRP bar (i.e., 71 mm^2).

Tables 5.3 and 5.4 list the key test results for two series of pullout specimens before and after field exposure, including ultimate bond strength (τ_{max}), loaded end slip at

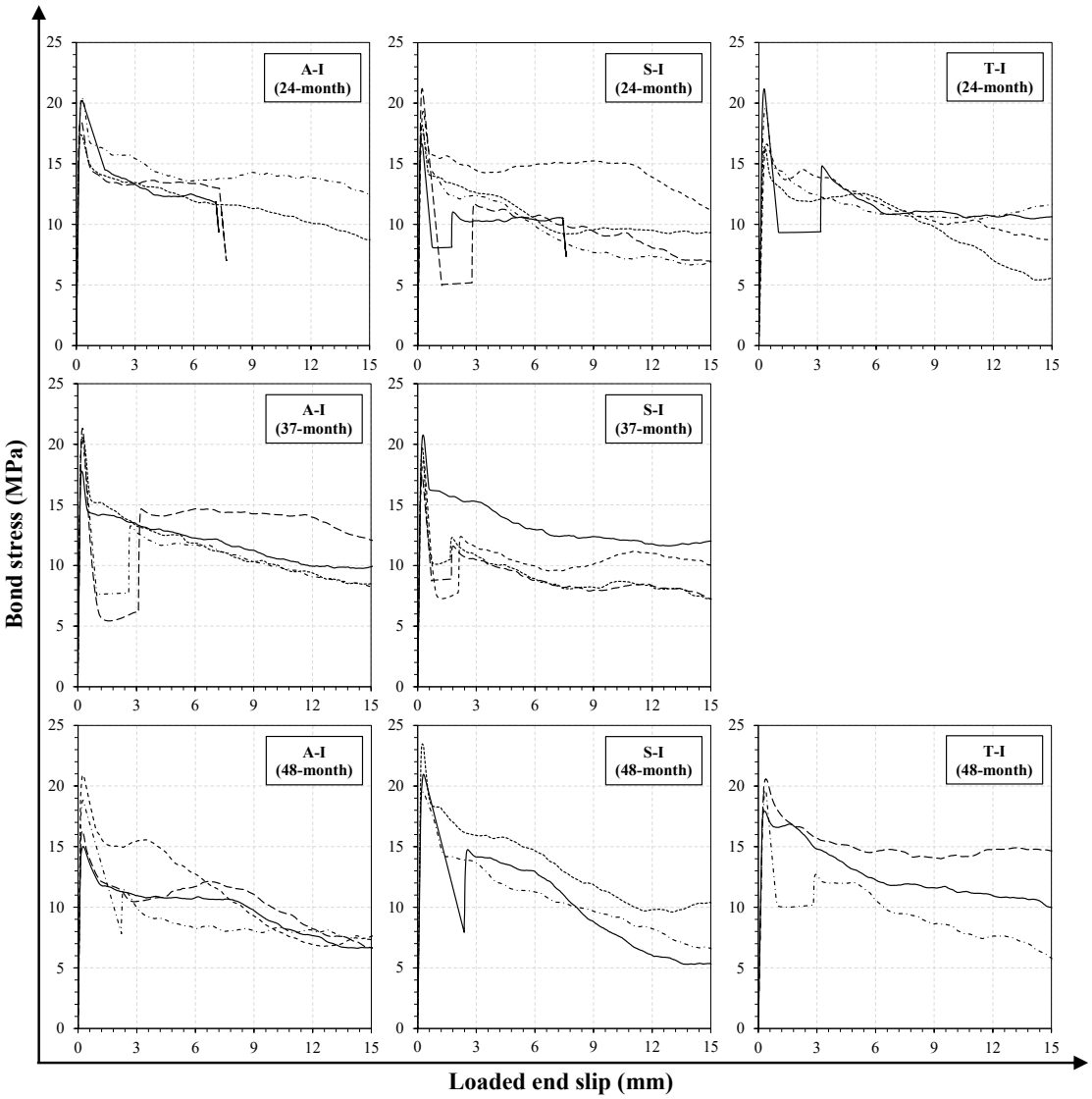
ultimate bond strength (s_m), and bond stiffness (K_b). In addition, the standard deviation (SD) and coefficient of variation (COV) are reported. Currently, there is no standardized method for calculating the bond stiffness of FRP bars, despite its importance as an indicator for serviceability limit state (SLS) design in practical engineering applications. In this chapter, the bond stiffness (K_b) is defined as the secant stiffness at bond stress equal to $0.5\tau_{max}$, as suggested by existing studies (Li et al. 2019; Xiong et al. 2021; Zhou et al. 2024).

Fig. 5.8 shows the bond stress-slip curves for the majority of the test pullout specimens. Missing results correspond to tests suffered from unforeseen problems associated with the test set-up. It is evident that, for the same series of specimens, the overall trends of the bond stress-slip curves were generally unchanged, irrespective of exposure conditions and durations. This indicates that field exposure to marine environments had little influence on the shape of the bond stress-slip curve. However, notable differences in bond-slip behavior were observed between the two batches of GFRP bars due to their distinct surface treatments (see Fig. 5.1). For Series I specimens, the bond stress-slip curves generally exhibited three different stages: (1) The initial stage was up to the maximum bond stress with little slippage, which was mostly attributed to the chemical adhesion and mechanical interlock due to the presence of the sand-coated layer and the helical yarn in the GFRP bars; (2) Due to the debonding of the external sand-coated layer, the second stage appeared with a sudden drop when the peak bond stress was reached, which has been commonly observed in previous studies on sand-coated GFPR bars (Baena et al. 2009; Solyom and Balázs 2020); (3) The third stage (commonly known as the residual stage), in which the friction between the concrete and the GFRP bar became the dominated bond mechanism, was featured as a gradual decrease or a rebound followed by a gradual decrease in bond stress.

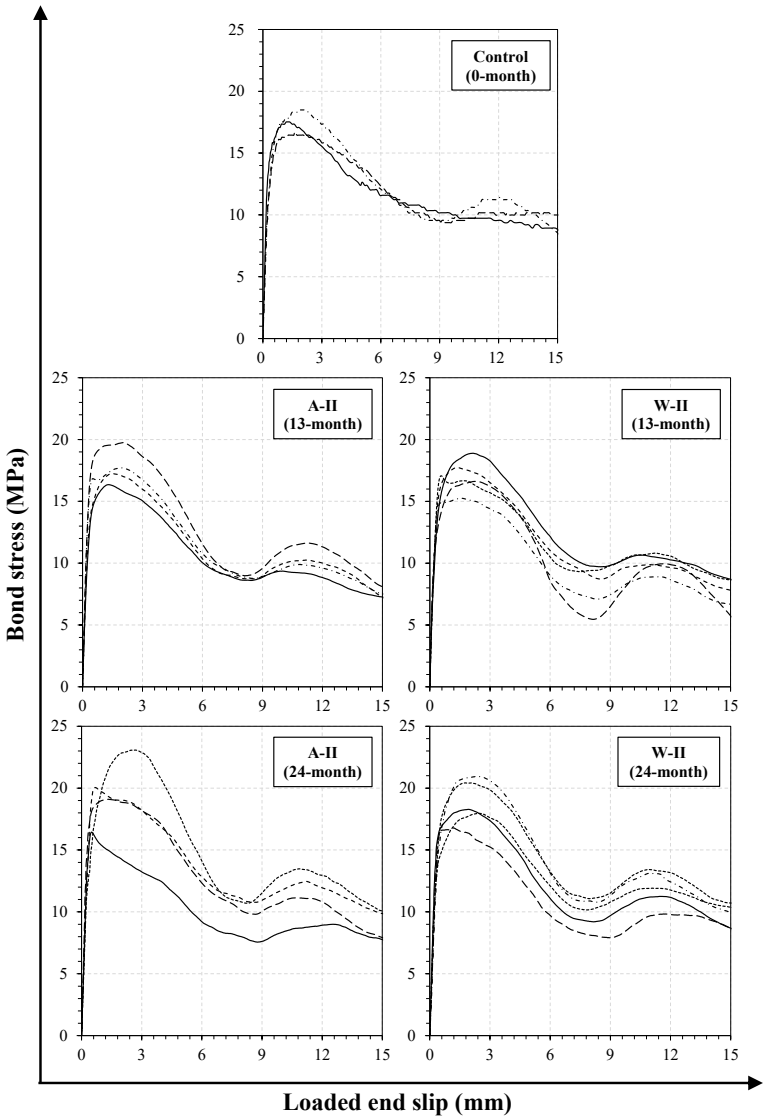
Regarding Series II specimens, the bond mechanism was similar to that of Series I ones, except that the second stage featured a smooth transition segment near the peak stress instead of a sudden drop after the peak. This difference can be explained by t variations in surface profile between the two batches of GFRP bars (Davalos et al. 2008; Baena et al. 2009; Solyom and Balázs 2020; El-Nemr et al. 2023). Besides, an oscillatory behavior, also known as wedging effect (Achillides and Pilakoutas 2004), was observed during the residual stage in Series II specimens, caused by ribs formed by the helical yarn (Hu et al. 2023). Another important observation is that, compared to Series II specimens, the post-peak segments of the bond stress-slip curves for Series I specimens deviated from each other much more obviously and the nonuniform distribution of sand within the GFRP bars is believed to be responsible for this phenomenon.


Control-I
(0-month)
A-I
(8-month)
S-I
(8-month)
T-I
(8-month)
A-I
(12-month)
S-I
(12-month)
T-I
(12-month)
Bond stress (MPa)
Loaded end slip (mm)

(a) Series I



(a) Series I (*continue*)



(b) Series II

Fig. 5.8 Bond stress-slip curves of pullout specimens

Table 5.3 Pullout test results of Series I specimens

Exposure period	Exposure zone	Bond strength τ_{max} (MPa)				Loaded end slip s_m (mm)			Bond stiffness K_b (MPa/mm)			
		Average	SD	COV (%)	Retention (%)	Average	SD	COV (%)	Average	SD	COV (%)	Retention (%)
0-month	/	18.44	0.70	3.78	100.00	0.26	0.02	8.64	129.47	3.50	2.71	100.00
8-month	A-I	19.47	1.22	6.27	105.62	0.25	0.02	8.53	144.46	7.09	4.91	111.57
	S-I	19.66	0.81	4.13	106.65	0.25	0.02	9.89	134.53	9.77	7.26	103.91
	T-I	18.04	1.41	7.83	97.87	0.30	0.04	14.36	108.55	14.73	13.57	83.84
12-month	A-I	19.13	1.54	8.03	103.75	0.27	0.01	4.77	135.74	5.93	4.37	104.84
	S-I	17.24	1.24	7.21	93.49	0.25	0.02	9.32	125.55	10.64	8.48	96.97
	T-I	17.41	1.72	9.85	94.41	0.30	0.06	21.04	98.40	11.04	11.22	76.00
24-month	A-I	19.15	1.26	6.56	103.85	0.27	0.03	10.04	136.25	16.15	11.86	105.23
	S-I	18.59	1.56	8.41	100.86	0.23	0.03	11.68	130.39	8.73	6.70	100.71
	T-I	18.46	2.03	10.97	100.12	0.33	0.05	15.16	88.42	17.61	19.91	68.30
37-month	A-I	20.07	1.35	6.74	108.86	0.23	0.02	6.63	138.08	6.89	4.99	106.65
	S-I	19.12	1.26	6.59	103.71	0.26	0.03	10.82	122.09	9.92	8.12	94.29
	T-I	/	/	/	/	/	/	/	/	/	/	/
48-month	A-I	18.56	2.59	13.95	100.69	0.24	0.01	5.89	132.84	12.95	9.75	102.60
	S-I	19.13	3.03	15.82	103.79	0.26	0.02	8.04	128.88	9.20	7.14	99.54
	T-I	19.39	1.10	5.69	105.18	0.36	0.03	9.07	82.54	3.00	3.64	63.75

Table 5.4 Pullout test results of Series II specimens

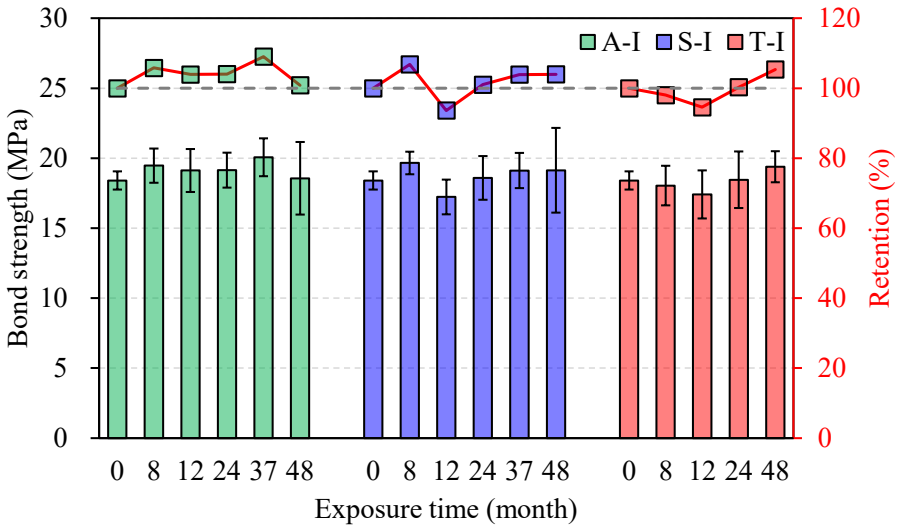
Exposure period	Exposure zone	Bond strength τ_{max} (MPa)				Loaded end slip s_m (mm)			Bond stiffness K_b (MPa/mm)			
		Average	SD	COV (%)	Retention (%)	Average	SD	COV (%)	Average	SD	COV (%)	Retention (%)
0-month	/	17.58	0.72	4.12	100.00	1.65	0.48	29.10	51.32	7.04	13.72	100.00
13-month	A-II	17.85	1.13	6.32	101.57	1.70	0.32	19.12	52.52	6.37	12.13	102.34
	U-II	17.12	1.21	7.05	97.39	1.58	0.60	38.28	51.76	4.99	9.63	100.86
24-month	A-II	19.39	2.19	11.28	110.34	1.29	0.85	66.00	50.86	7.03	13.82	99.11
	U-II	18.88	1.56	8.28	107.42	1.95	0.46	23.48	46.39	5.21	11.23	90.40

5.3.4 Bond Strength

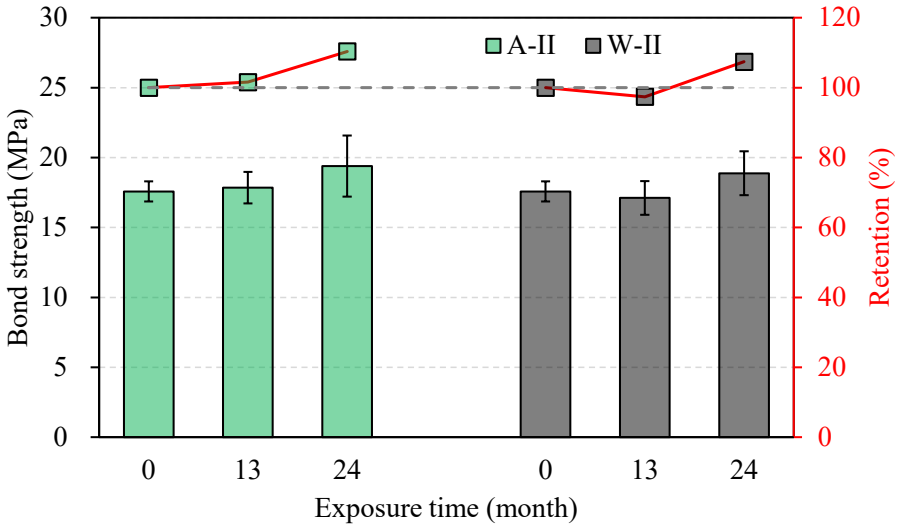
The variations of bond strength as a function of exposure time for both series of specimens under different conditions are shown in Fig. 5.9. It can be generally concluded that both series showed good durability in terms of bond strength throughout the exposure duration. It should be noted that the slightly scattered test results can be attributed to the imperfections in surface treatment during manufacturing (Antonietta Aiello et al. 2007) as well as the difference in interlaminar shear strength existed in the same batch of GFRP bars. Specifically, in Fig. 5.9(a), compared to Series I specimens placed in the laboratory (i.e., exposure time = 0 month), bond strength retentions for those exposed in zones A-I, S-I and T-I fluctuated within the ranges of 100.69~108.86%, 93.49~106.65% and 94.41~105.18%, respectively, implying that these marine environmental conditions had a marginal effect on bond strength. Similarly, as shown in Fig. 5.9(b), no degradation was found in bond strength for Series II specimens, with bond strength retentions of 110.34% and 107.42%, respectively, after exposure in zones A-II and U-II for up to 24 months. These findings aligns with previous AAT studies by Hao (2024) and Ke et al. (2024), which employed GFRP bars from the same manufacturer and SSC mix proportions consistent with the present study.

To be specific, three primary factors may be responsible for the observed durable bond strength of the pullout specimens: (1) The interlaminar shear strength of the GFRP bars provided by the same manufacturer has been shown to be highly durable under harsh exposure conditions (e.g., direct immersion in alkaline solutions with pH values varying from 11 to 13) (Wang et al. 2022). As discussed previously, the bond properties of the two series of specimens were mainly dependent on the interlaminar shear strength of the GFRP bars rather than the concrete strength (Lee et al. 2008); (2) Long-term

exposure to marine environments may lower the pH of SSC due to chloride ingress and/or carbonation (Mufti et al. 2007a; Kwon et al. 2017; Benmokrane et al. 2018; Benzecry et al. 2021), which have beneficial effect on the durability of the GFRP bar-to-SSC interface; (3) Hygroscopic expansion of GFRP bars under high humidity conditions during field exposure may also contribute to bond durability (Davalos et al. 2008; Zhou et al. 2012).



(a) Series I



(b) Series II

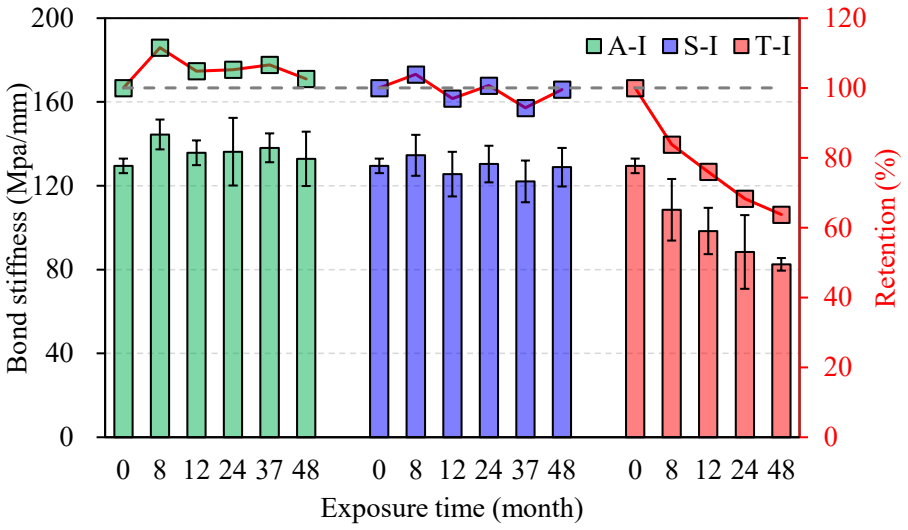
Fig. 5.9 Bond strength variations of pullout specimens in different exposure conditions

5.3.5 Bond Stiffness

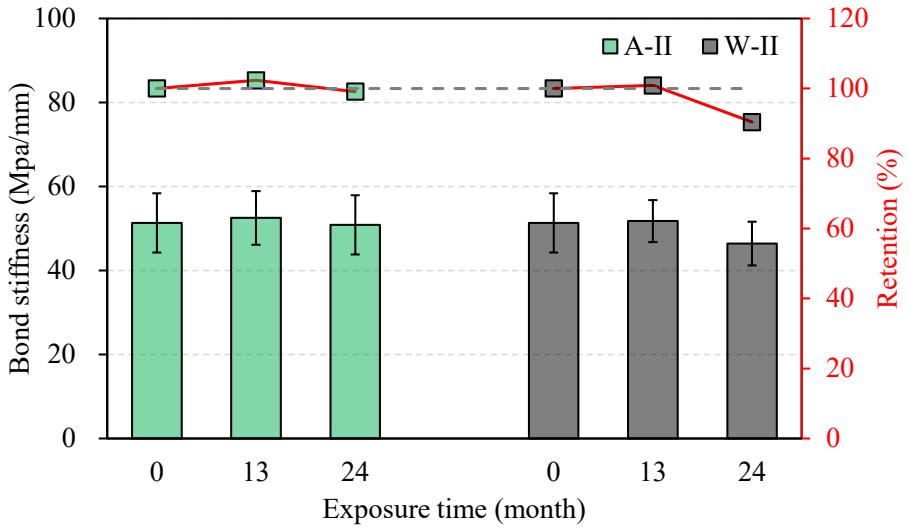
Fig. 5.10 displays the changes in bond stiffness for both series of specimens exposed in different zones over time. As expected, due to the substantially thicker layer of sand coating on Batch I GFRP bars (Solyom and Balázs 2020), the average bond stiffness of the unexposed Series I specimens was considerably larger than that of Series II (129.47 MPa/mm versus 51.32 MPa/mm), which can also be reflected in the much smaller average loaded end slip at bond strength (s_m) for Series I specimens compared to their counterparts (0.26 mm versus 1.65 mm). In Fig. 5.10(a), bond stiffness of Series I specimens remained almost unchanged after long-term exposure to atmospheric (A-I) and splash conditions (S-I), with retentions fluctuating within the ranges of 102.60~111.57% and 94.29~103.91%, respectively. A similar trend was found for Series II specimens exposed to atmospheric conditions (A-II), as depicted in Fig. 5.10(b). As discussed in Section 3.3.3.1, the S-I zone, while subject to frequent wetting, does not retain moisture, which limits hydrolytic degradation. Consequently, bond stiffness degradation in this zone is minimal. Similarly, the A-I and A-II zones, characterized by limited moisture exposure, minimize hydrolytic and chemical attacks, resulting in negligible bond deterioration.

Conversely, compared to control specimens, bond stiffness retentions of Series I specimens under tidal conditions (T-I) significantly decreased with the increase of exposure time, dropping to 83.84%, 76.00%, 68.30% and 63.75%, respectively, after 8-, 12-, 24- and 48-month field exposure [Fig. 5.10(a)]. This decrease in bond stiffness might be attributed to the degradation of the external sand-coated layer as well as the deterioration of the interfacial properties between such layer and the resin matrix of the GFRP bar after prolonged exposure (Bank et al. 1998). As mentioned in Section 3.3.3.1,

in the S-I zone, the cyclic wetting and drying combined with periodic immersion create a highly aggressive environment that accelerates degradation processes. For Series II specimens constantly submerged in seawater (U-II), a slight decline in bond stiffness (approximately 10%) was observed when the exposure duration reached 24 months, which can also be explained by the aggressive chemical reactions induced by that continuous seawater immersion (Section 3.3.3.1), despite the thinner sand-coated layer on Batch II GFRP bars. This observation is in line with findings reported by Yan and Lin (2017) on the long-term bond performance of helically-wrapped and sand-coated GFRP bars in NC (compressive strength = 46.58 MPa) under the conditions of saline solution immersion at 50℃ and 70℃ for up to 60 days, although bond stiffness degradation was not explicitly discussed in their study.



(a) Series I



(b) Series II

Fig. 5.10 Bond stiffness variations of pullout specimens in different exposure conditions

5.4 TIME-DEPENDENT BOND STRESS-SLIP MODEL

The test results highlight the importance of considering bond stiffness degradation in harsh environments and its effect on bond stress-slip behavior. At present, numerous analytical models have been established for bond stress-slip (τ-s) relationship between FRP bars and concrete (Malvar 1994; Rossetti et al. 1995; Cosenza et al. 1997; Rolland et al. 2020). In this chapter, the modified BPE (mBPE) model (Cosenza 1996), which has been proven to be able to provide sufficiently accurate predictions for bond stress-slip curves of FRP bars in concrete (Cosenza et al. 1997; Lin and Zhang 2014), was employed to develop a time-dependent bond stress-slip model for GFRP bars in SSC. Note that only specimens with long-term exposure to tidal conditions (T-I) were considered due to apparent bond stiffness deterioration. Eqs. (5.4) to (5.6) express the nonlinearly ascending, linearly descending and horizontal branches of the mBPE model, respectively:

$$\frac{\tau}{\tau_{max}} = \left(\frac{s}{s_m}\right)^{\alpha} \ (s \leq s_m) \tag{5.4}$$

$$\frac{\tau}{\tau_{max}} = 1 - p\left(\frac{s}{s_m} - 1\right) \ (s_m < s \leq s_r) \tag{5.5}$$

$$\tau = \tau_r \ (s > s_r) \tag{5.6}$$

where τ_r and s_r are the residual bond strength and the corresponding slip, respectively; α and p are curve-fitting parameters.

Given that no significant degradation was found in bond strength of the specimens after 4-year field exposure, the parameter τ_{max} was assumed to be a constant value (denoted τ_0 herein), which can be directly obtained from the test results of the control specimens. As discussed in Section 5.3.3.1, the post-peak segments of the bond stress-slip curves for Series I specimens showed considerably large discrepancies, and thus the analysis in this section mainly focuses on the ascending branches of the curves. To define the parameter α in Eq. (5.4), two time-dependent factors, namely bond stiffness $K_b(t)$ and loaded end slip at bond strength $s_m(t)$, were introduced and calculated by the following equations:

$$K_b(t) = K_0 \cdot Y_K \tag{5.7a}$$

$$Y_K = (100 - a_1)\exp(-b_1 \cdot t) + a_1 \tag{5.7b}$$

$$s_m(t) = s_{m0} \cdot Y_s \tag{5.8a}$$

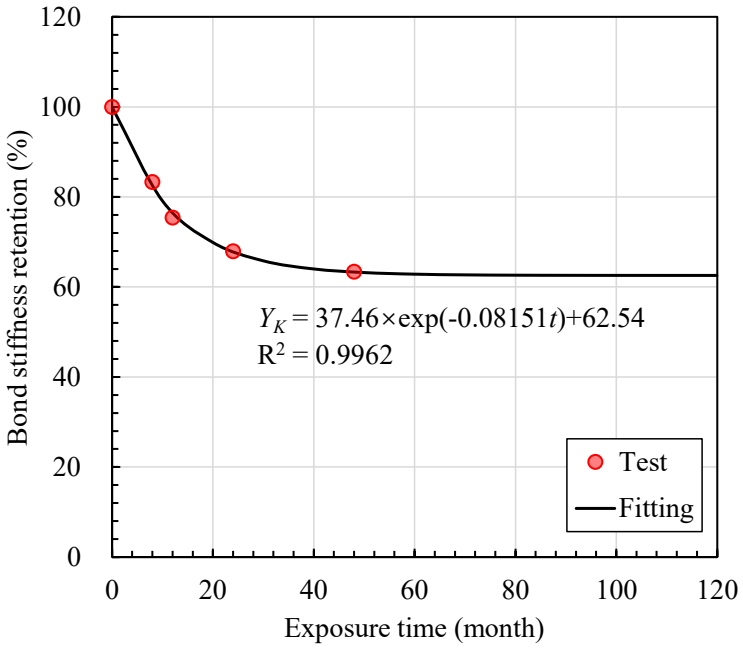
$$Y_s = a_2 \cdot \ln(b_2 \cdot t + c_2) \tag{5.8b}$$

where K_0 and s_{m0} are the initial values of bond stiffness and loaded end slip at bond strength, respectively, which were assumed to be equal to those of the control

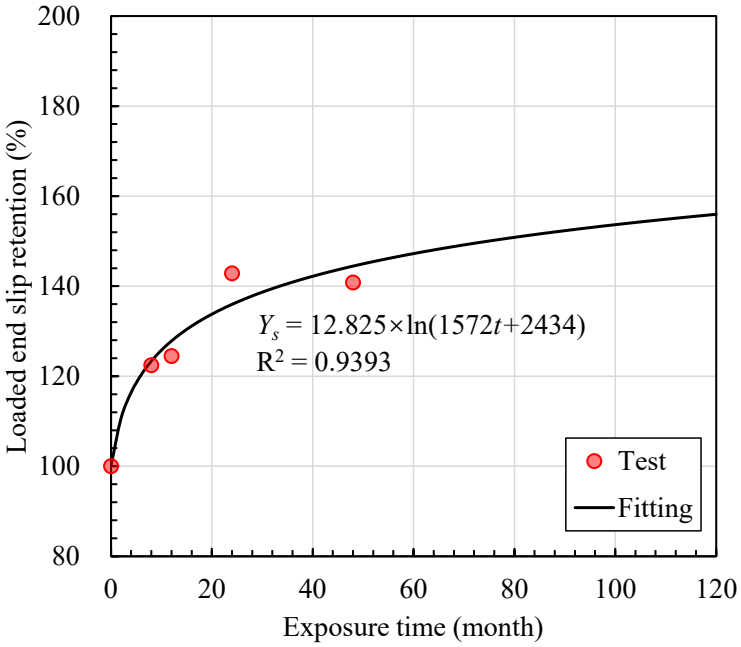
specimens; Y_K and Y_s are the retentions of bond stiffness and loaded end slip at bond strength after field exposure (%), respectively; t is the exposure time in months; a_1, b_1, a_2, $b_2$and c_2 are curve-fitting parameters. As illustrated in Fig. 5.11, the experimental results for bond stiffness (K_b) and loaded end slip at bond strength (s_m) of specimens subjected to tidal conditions for up to 48 months were fitted to Eqs. (5.7b) and (5.8b), respectively.

By substituting $\tau = 0.5\tau_{max} = 0.5\tau_0$ and Eqs. (5.7a) and (5.8a) into Eq. (5.4), the dependence of the parameter α on exposure time was proposed to be described by Eq. (5.9):

$$\alpha = \frac{1}{1 - 1.44 \cdot \ln\left[\frac{\tau_0}{K_b(t) \cdot s_m(t)}\right]} \tag{5.9}$$



(a) Bond stiffness (K_b)



(b) Slip at bond strength (s_m)

Fig. 5.11 Curve fittings of specimens subjected to tidal condition

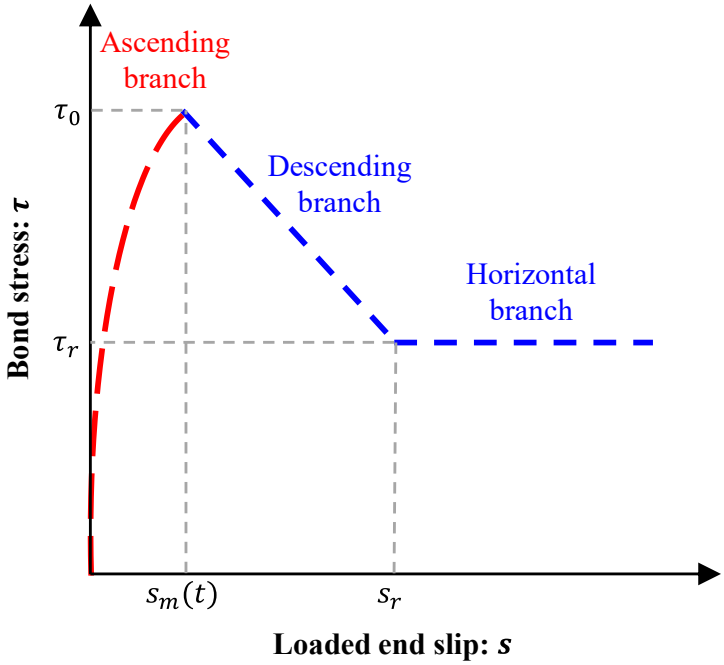


Fig. 5.12 Characteristic curve of the proposed time-dependent bond stress-slip model

To predict the post-peak segments of the bond stress-slip curves, the parameter p derived from the control specimens and the residual bond strength τ_r averaged from all specimens were adopted in this chapter. Fig. 5.12 illustrates the characteristic curve of

the proposed time-dependent bond stress-slip model, with the key parameters (τ_0, τ_r, $s_m(t)$ and s_r) clearly indicated. The predicted bond stress-slip curves generated by the proposed model were compared with the experimental curves obtained from control specimens and those exposed in the T-I zone for up to four years, as shown in Fig. 5.13. The parameters of the prediction model are summarized in Table 5.5. Generally, the prediction curves for the ascending branch by the proposed equation [Eq. (5.9)] agree well with the experimental results. The coefficient of determination (R^2) for the ascending branch before the peak ranges from 0.88 to 0.94, confirming the satisfactory performance of the time-dependent bond stress-slip model and validating the feasibility of incorporating bond stiffness deterioration into the widely used mBPE model.

Table 5.5 Parameters of prediction model for specimens in T-I zone

Exposure time	Ascending branch					Descending branch	Horizontal branch
t (month)	τ_0	$K_b(t)$	$s_m(t)$	α	R^2	p	τ_r
0	18.36	130.21	0.25	0.5563	0.89	0.0495	8.49
8		106.85	0.30	0.5511	0.92		
12		99.78	0.31	0.5658	0.94		
24		88.33	0.33	0.5950	0.93		
48		82.41	0.35	0.5995	0.88		

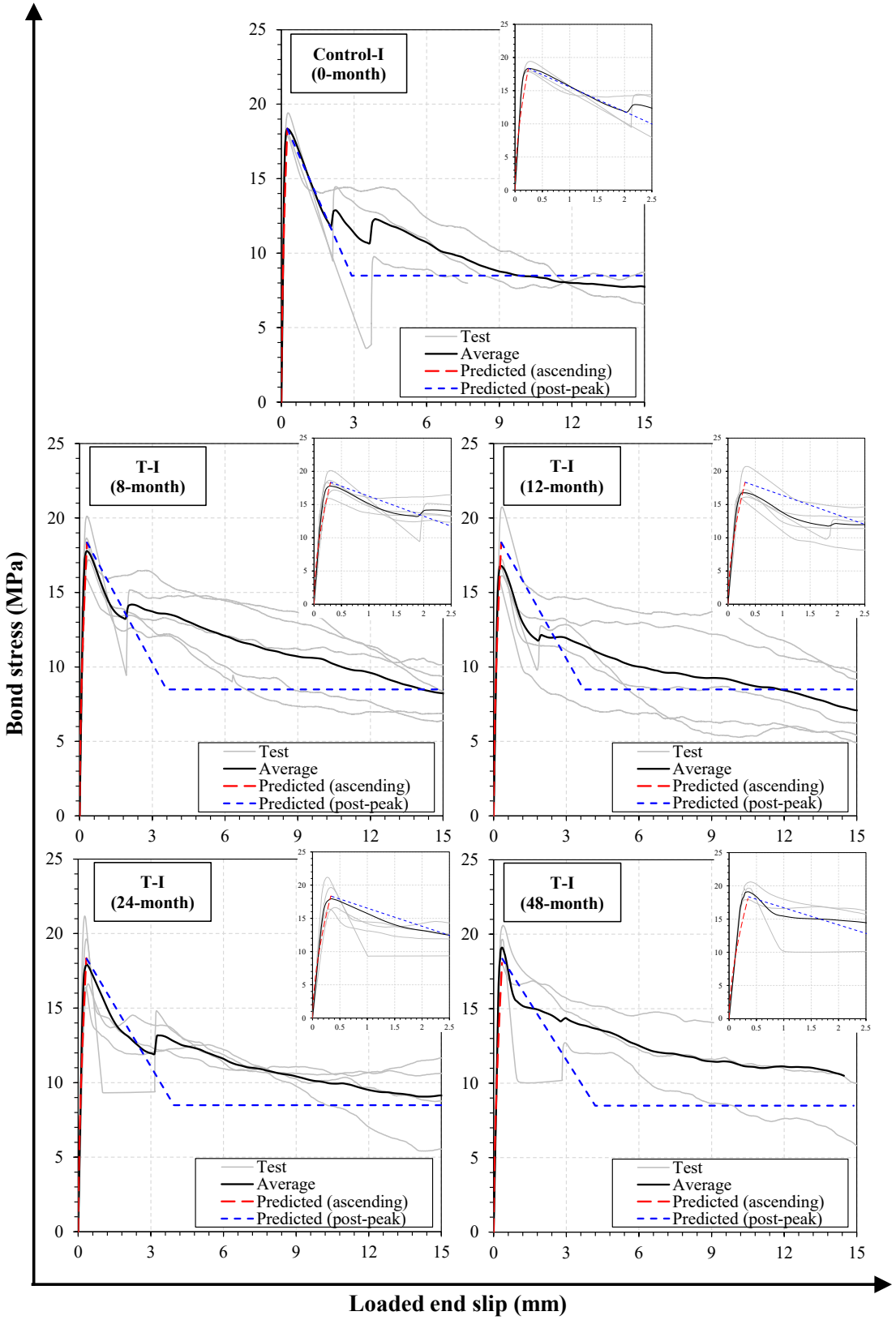


Fig. 5.13 Comparison between predicted and test bond stress-slip curves

5.5 CONCLUSIONS

To evaluate the long-term bond performance of GFRP bars in SSC under real marine environments, this chapter presents the results of direct pullout tests on two series of GFRP bar-to-SSC bonded joints after field exposure in four different marine environmental zones (i.e., atmospheric, splash, tidal and underwater) for up to four years. In addition, a time-dependent bond stress-slip model was proposed. Based on the results and discussion presented in this chapter, the following conclusions can be drawn:

(1) Long-term field exposure led to apparent changes in the surface color of specimens exposed in tidal and underwater zones, accompanied by the attachment of marine organisms to the concrete surface. No visible changes were observed for specimens under atmospheric conditions, while mosses and lichen were found on the concrete surface of those exposed in the splash zone.

(2) The failure modes of all specimens were characterized by shear damage occurring at the fiber-resin interface. No significant differences were found in failure modes of each series of specimens subjected to different conditions throughout the exposure period.

(3) Field exposure to marine environments had minimal impact on the shape of the bond stress-slip curves. However, due to the different surface treatments of the GFRP bars used in the two series of pullout specimens, the corresponding bond-slip behaviors were distinctly different.

(4) The bond strength of the specimens exposed in different zones barely changed after prolonged field exposure, with bond strength retentions of 100.69~105.18%

for Series I specimens after four years and 107.42~110.34% for Series II specimens after two years.

(5) In contrast to specimens exposed in the atmospheric and splash zones, those subjected to tidal conditions exhibited a significant decrease in bond stiffness over time, with bond stiffness retention dropping to 63.75% after 48-month exposure in the field.

(6) Based on the mBPE model, a time-dependent bond stress-slip model for GFRP bars in SSC was proposed. The ascending branches of the prediction curves generally agreed well with the experimental results, with R^2 values for the ascending branch before the peak ranging from 0.88 to 0.94, demonstrating the satisfactory performance of the proposed model.

CHAPTER 6
LONG-TERM FLEXURAL PERFORMANCE OF GFRP-REINFORCED SEAWATER SEA-SAND CONCRETE BEAMS IN REAL MARINE ENVIRONMENTS

6.1 INTRODUCTION

Recent studies have demonstrated the favorable long-term performance of SSC under both laboratory hydrothermal aging conditions (Ke et al. 2024) and natural tidal exposure environments (Jahani et al. 2023). As introduced in Chapter 1, the combination of GFRP bars with SSC provides a potentially sustainable solution for marine infrastructures by capitalizing on the advantages of both materials to improve the durability of FRP-SSC structures subjected to aggressive marine environments. Nevertheless, varying degrees of deterioration may still occur due to multiple factors, including the coupled effects of environmental exposure and mechanical loading, as well as degradation at various material interfaces, as mentioned in Chapter 2.

Currently, only a limited number of studies have focused on the long-term performance of SSC structures reinforced with GFRP bars. Ren et al. (2021) conducted an experimental investigation on FRP-SSC beams exposed to a natural subtropical coastal environment, reporting that the load carrying capacity decreased by approximately 7% after 12 months of exposure compared to 3 months. In a subsequent study, they tested FRP-SSC beams under different sustained-load levels under both natural and simulated

coastal environments (Ren et al. 2024). The test results revealed that, after one year, low sustained loads (e.g., equal to the cracking load) produced negligible changes in flexural behavior, whereas higher sustained loads (e.g., twice the cracking load) tended to reduce load carrying capacity, particularly under outdoor exposure. Chen et al. (2022) carried out field exposure tests on FRP-SSC beams in marine environments for up to 270 days. They observed a 28% increase in load carrying capacity after salt-spray exposure, whereas a 13% decrease was observed for beams exposed to tidal conditions. Chang et al. (2022) investigated the durability of FRP-SSC beams under combined seawater immersion and sustained loading, reporting notable flexural performance degradation after 270 days, with residual load carrying capacities of 77%, 70% and 60% for sustained-load levels of 0%, 25% and 40% of the ultimate load, respectively. By contrast, some researchers have found no degradation in FRP-SSC beams subjected to seawater wet-dry cycles over various exposure durations, irrespective of sustained load presence (Wang et al. 2023b; Hao 2024). Despite these studies, no consensus has yet been reached, and most studies have employed relatively short exposure durations (typically less than one year).

To achieve a more in-depth understanding of the long-term flexural behavior of FRP-SSC beams, particularly under real field conditions, further research (especially involving extended field exposure) is necessary. In this context, this chapter assesses the long-term flexural performance of FRP-SSC beams conditioned in real marine environments. Two series of FRP-SSC beams were prepared and exposed in three different marine environmental zones (i.e., atmospheric, splash, and tidal) for up to four years and subsequently tested under four-point bending, with the examined variables of type of exposure zone, exposure duration and the presence of sustained load.

6.2 EXPERIMENTAL PROGRAM

6.2.1 Materials

6.2.1.1 GFRP bars

GFRP bars used in this chapter were sourced from the same batch (Batch I) as those employed in Chapters 3 and 5. Straight GFRP bars with diameters of 10 mm and 19 mm [nominal diameter = 9.5 mm and 19.1 mm, respectively, as specified by ACI (2017)] were used as longitudinal reinforcement, while bent GFRP bars with a diameter of 6 mm [nominal diameter = 6.4 mm, as per ACI (2017)] were adopted as stirrups. Table 6.1 gives the main properties of these GFRP bars, as provided by the manufacturer.

Table 6.1 Physical and mechanical properties of GFRP bars provided by manufacturer

Bar type	Nominal diameter (mm)	Diameter (mm)	Tensile strength (MPa)	Elastic modulus (GPa)	Fiber content (%)
Straight	9.5	9.91	852.9[#]	50.5	81.1
	19.1	18.64	833.2[#]	46.6	82.5
Stirrup	6.4	6.83	1234.1[*]	56.0	84.1

[#]Mean value minus 3 times standard deviation.
[*]Minimum value.

6.2.1.2 Seawater sea-sand concrete

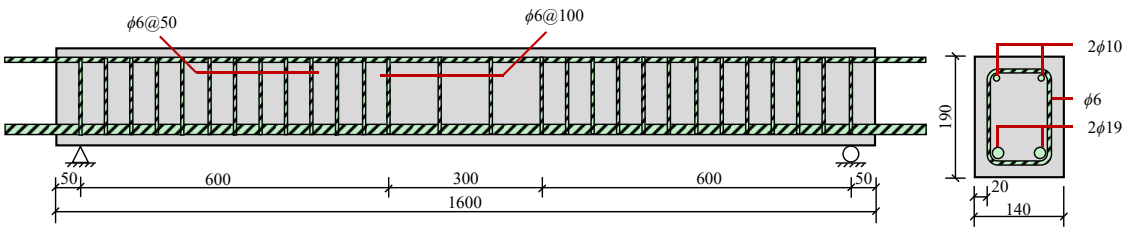
All FRP-SSC beam specimens were cast using SSC with a designed compressive strength of 55 MPa, obtained from the same batch as the Series I specimens described in Chapter 5.

6.2.2 Design and Preparation of FRP-SSC Beam Specimens

Fig. 6.1(a) illustrates the dimensions and reinforcement details of the FRP-SSC beam

specimens. All specimens have a cross-sectional dimension of 140 × 190 mm (width × height) and a total length of 1600 mm, with a designed shear span-to-depth ratio of approximately 3.88. The specimens were designed to be over-reinforced by incorporating two 19-mm GFRP bars as bottom reinforcement, thereby ensuring that failure would be governed by concrete crushing (ACI 2022). Besides, two 10-mm GFRP bars were employed as top reinforcement. To prevent shear failure, 6-mm GFRP stirrups were provided at a spacing of 100 mm in the pure bending section and 50 mm within the shear span. The concrete cover, measured from the specimen surface to the outer surface of the GFRP stirrups, was fixed to be 20 mm on the top, bottom and both sides of the specimens.

All specimens were cast from a single batch of SSC on 5 October 2019 in Tsing Yi, Hong Kong [Fig. 6.1(b)]. After casting, the specimens were cured at ambient temperature and watered for at least seven days. The specimens were divided into two series, namely Series I (FRP-SSC beams without sustained load) and Series II (FRP-SSC beams with sustained load). These two series of beam specimens form part of a theme-based research scheme project detailed in Chapter 3 and correspond to the 1st and 2nd series of specimens for FET, respectively.



(a) Dimension and reinforcement details of test specimens (unit: mm)



(b) Specimen preparation

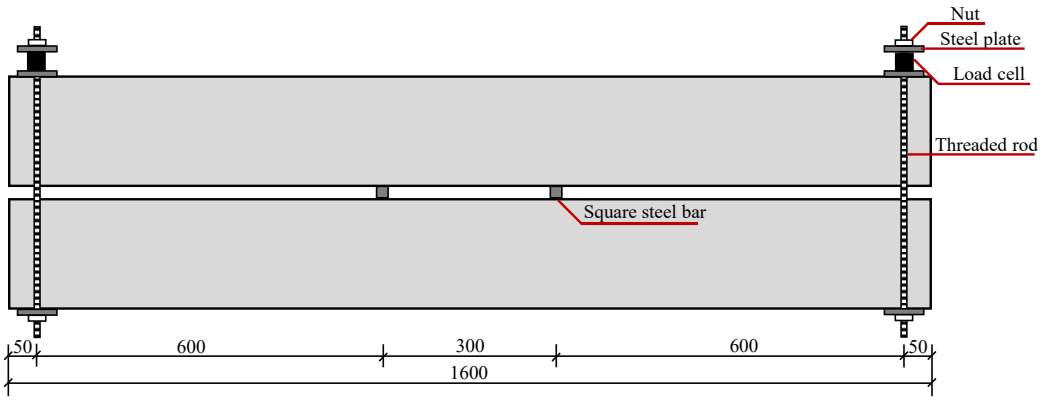
Fig. 6.1 Details and preparation of FRP-SSC beam specimens

6.2.3 Sustained Load

Previous studies have indicated that the service load of FRP-reinforced concrete beams can typically ranges from 30% to 40% of their flexural capacity (Issa et al. 2011; Wang and Belarbi 2011; Carvelli et al. 2013; Elgabbas et al. 2017; El-Nemr et al. 2018). In the present study, the sustained load applied to Series II specimens was set at 30% of the ultimate load averaged from control specimens [approximately 32 kN (see Table 6.3)]. Fig. 6.2(a) shows a schematic diagram of the sustained loading system. Before the application of sustained load, each pair of beams was clamped together using two steel plates, two 20-mm threaded rods, and four nuts on each side. Between the two beams, two square steel bars were placed 300 mm apart to provide support to the specimens. The nuts were tightened using a torque wrench to apply the load. In addition, four load cells, each set at approximately 8 kN, were employed to monitor and control the designed sustained load. As shown in Fig. 6.2(b), several initial cracks appeared in the beam specimens after the application of the sustained load.

It is important to emphasize that throughout the exposure period, the load cells on one pair of beams were not removed in order to monitor load loss in the specimens resulting from relaxation and other uncontrollable factors, such as impacts to the sustained

loading system caused by specimen collapse during typhoon events. The sustained loading system was adjusted annually using a torque wrench to compensate for this load loss. Over each 1-year exposure interval, the total applied load was observed to decrease by approximately 50%.



(a) Schematic diagram (unit: mm)



(b) Specimens under sustained load

Fig. 6.2 Sustained loading system

6.2.4 Field Exposure Conditions

Both series of specimens were exposed at Station I [i.e., the *Hong Kong-Zhuhai-Macau (HZM) Bridge Exposure Station*, as mentioned in Chapter 3], which experiences a subtropical monsoon climate. Further details regarding the changes in temperature and relative humidity during the exposure period, and the environmental characteristics of each exposure zone, can be found in Chapter 3.

Series I specimens were exposed in all three zones (A-I, S-I and T-I) beginning on 14 January 2020 (approximately three months after casting), while Series II specimens were exposed only in the S-I zone starting from 2 February 2021 (approximately 16 months after casting). Fig. 6.3 shows the specimens in situ within the S-I zone. The test matrix for both series is given in Table 6.2. Exposure durations were set at five (8, 12, 24, 37 and 48 months) and three (11, 24 and 35 months) intervals for Series I and II specimens, respectively. Besides, two unloaded specimens were kept in the laboratory before testing to serve as control specimens.



Fig. 6.3 Specimens exposed in splash zone (S-I)

Table 6.2 Test matrix of beam specimens

Series of specimen	Sustained load	Environmental condition	Exposure duration[#] (months)	Number of specimens
/	w/o	Laboratory (Control)	0	2
I	w/o	Atmospheric (A-I)	8/12/24/37/48	2/2/3/2/2
		Splash (S-I)	8/12/24/37/48	2/2/3/3/2
		Tidal (T-I)	8/12/24/37/48	2/2/3/2/2
II	w/	Splash (S-I)	11/24/35	2/2/2

[#]Due to administrative reasons at the exposure station, the sampling intervals may slightly deviate from exact annual cycles.

6.2.5 Instrumentation and Test Set-Up

After field exposure for specified durations, selected specimens were retrieved for testing (Table. 6.2). Prior to testing, the typical measurement locations on all specimens were carefully polished and cleaned to facilitate strain gauge installation. A Type-SDS500 loading machine with a capacity of 500 kN was used to test the specimens. As illustrated in Fig. 6.4, four-point bending tests were performed on the beam specimens with an effective span length of 1500 mm. Load was applied via two load cells fixed on a steel spreader beam at a distance of 300 mm. A displacement-controlled loading rate of 1.2 mm/min was adopted for all tests.

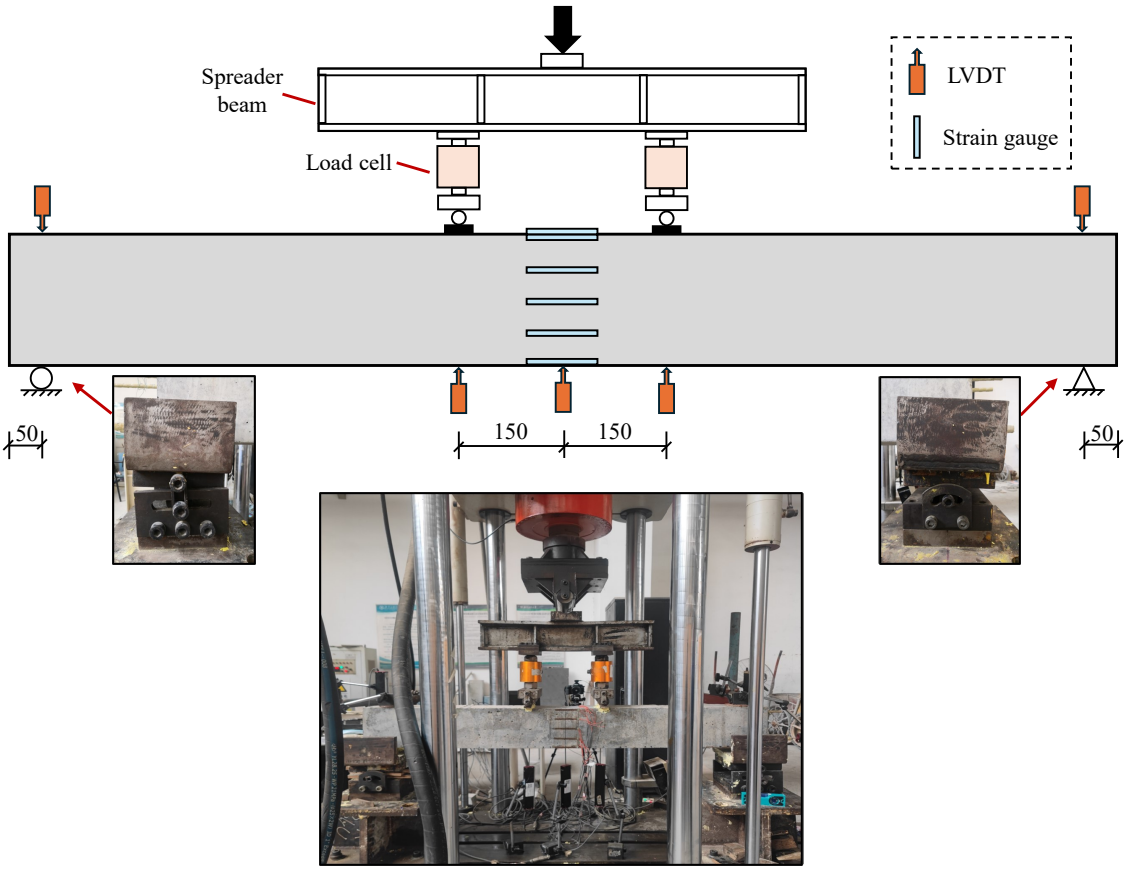


Fig. 6.4 Test set-up (unit: mm)

Three LVDTs were positioned at midspan and at the two loading points to measure deflections, while another two LVDTs were installed at the two supports to compensate

for any settlement. To monitor the concrete strains at midspan, a total of eight 100-mm-length strain gauges were used, of which three were attached to the top surface and another five were evenly distributed along the specimen height. Load, deflection and strain data were automatically recorded at one-second intervals using a data logger. Additionally, to observe crack development and patterns, the digital image correlation (DIC) technique was employed on selected specimens. Before testing, one surface of these specimens was sprayed with white paint, followed by random black speckles. During bending tests, a digital camera was used to implement DIC measurements.

6.3 RESULTS AND DISCUSSION

6.3.1 Appearance Observations

Fig. 6.5 shows the typical appearance characteristics of the beam specimens after 48 months of exposure in different marine environmental zones. Notably, long-term exposure to the atmospheric environment (A-I) had minor influence on the appearance of specimens, while those subjected to randomly alternating moist and dry environment (S-I) experienced slight changes in appearance, including the growth of moss and lichen. For specimens cyclically exposed to seawater or air (T-I), the concrete surface had changed to deep yellow in color, accompanied by attachment of marine organisms such as barnacles and mussels. These observations are similar to those made on pullout specimens exposed at the same field exposure station, as reported in Chapter 4. Before testing, marine organisms on concrete surface of T-I specimens were carefully scraped off.

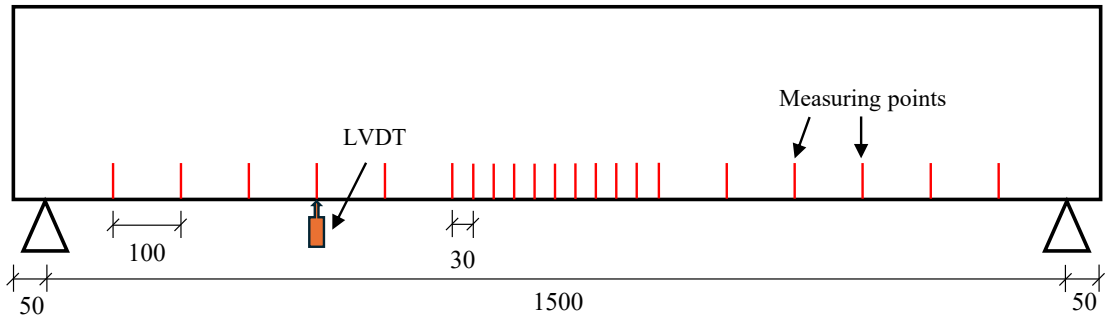


Fig. 6.5 Visual appearance of field-exposed specimens

6.3.2 Long-Term Deflections of FRP-SSC Beams with Sustained Load

The long-term deflections of Series II specimens, resulting from sustained loading and creep, were measured before bending tests. Fig. 6.6 presents the measuring method for residual deflections. A total of 21 measuring points were arranged along the bottom surface of each specimen, with residual deflections recorded using an LVDT. Figs. 6.7(a) 6.7(b) and 6.7(c) depict the residual deflections for a pair of beam specimens after 11, 24 and 35 months of exposure, respectively, which were averaged from two repeated measurements. In addition, the initial deflections recorded prior to the removal of the sustained loading devices in the field are presented in Figs. 6.7(b) and 6.7(c). As expected, the midspan deflections remarkably decreased after the removal of the loading devices (from 5.975 mm to 4.121 mm and from 6.875 mm to 5.244 mm for the cases of 24- and 35-month exposure, respectively), which can be primarily ascribed to the recovery behavior of the SSC. Furthermore, the average residual midspan deflections measured both before and after the removal of the loading devices increased with longer exposure durations. Compared to the specimens exposed for 11 months, those exposed for 24 and 35 months exhibited increases of approximately 14% and

51%, respectively, in average residual midspan deflection.

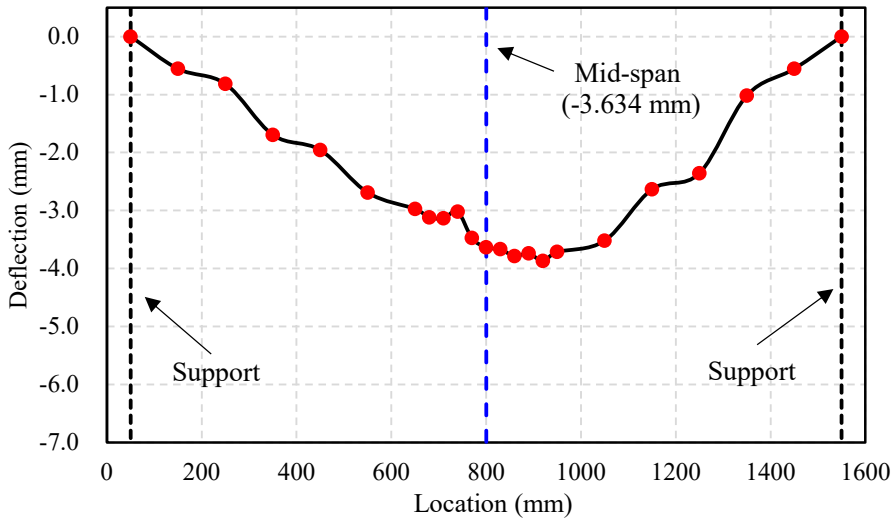


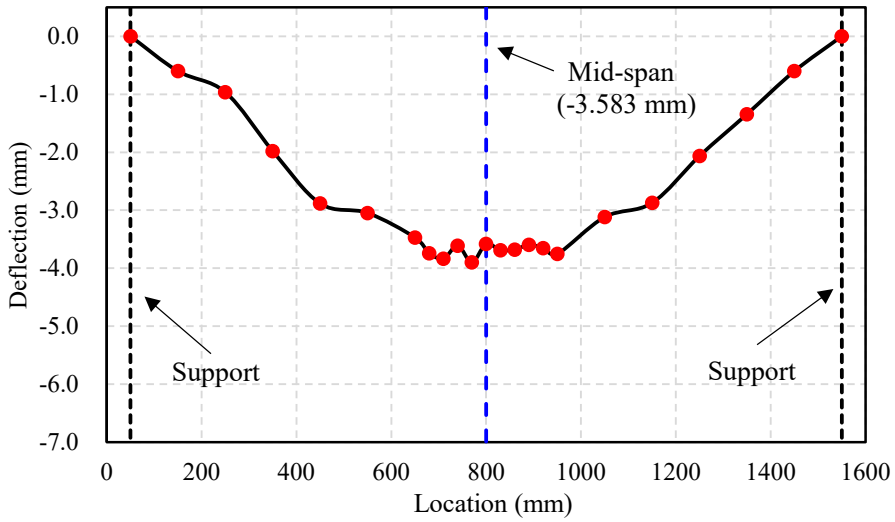
(a) Arrangement of measuring points (unit: mm)



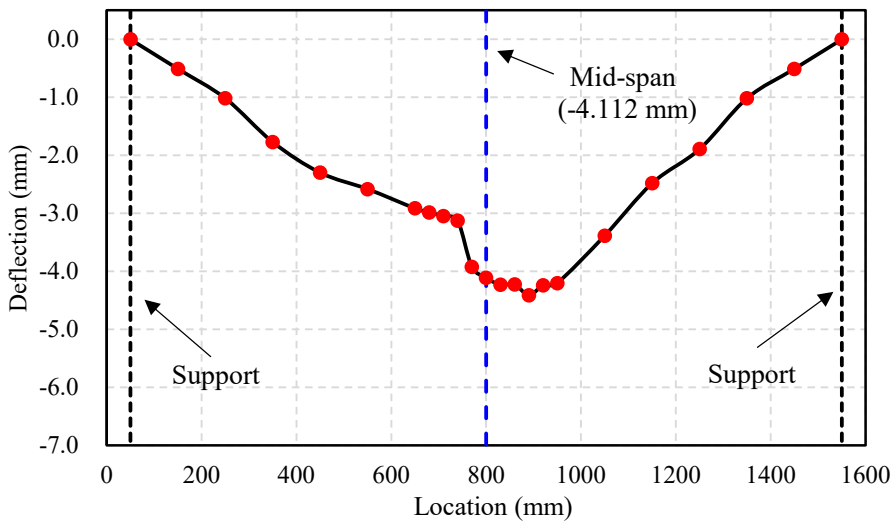
(b) Test set-up

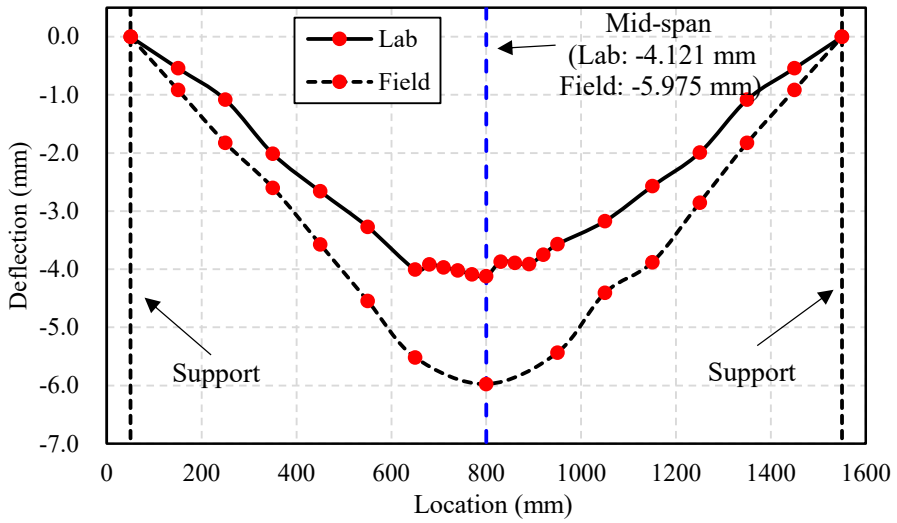
Fig. 6.6 Measuring method for residual deflection



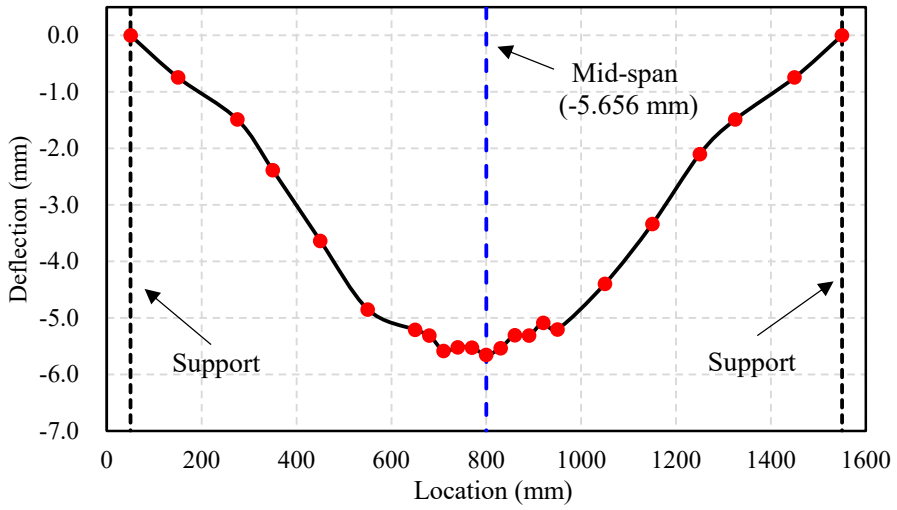


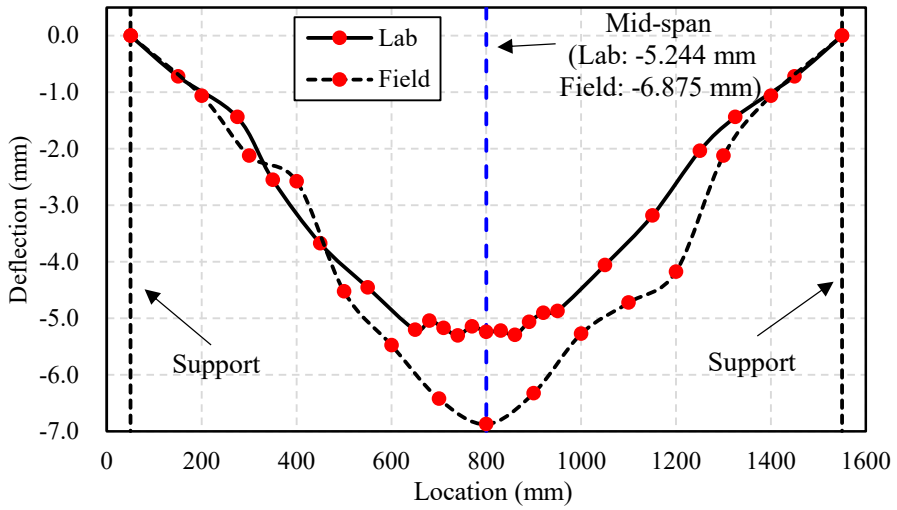
(a) 11-month exposure





(b) 24-month exposure



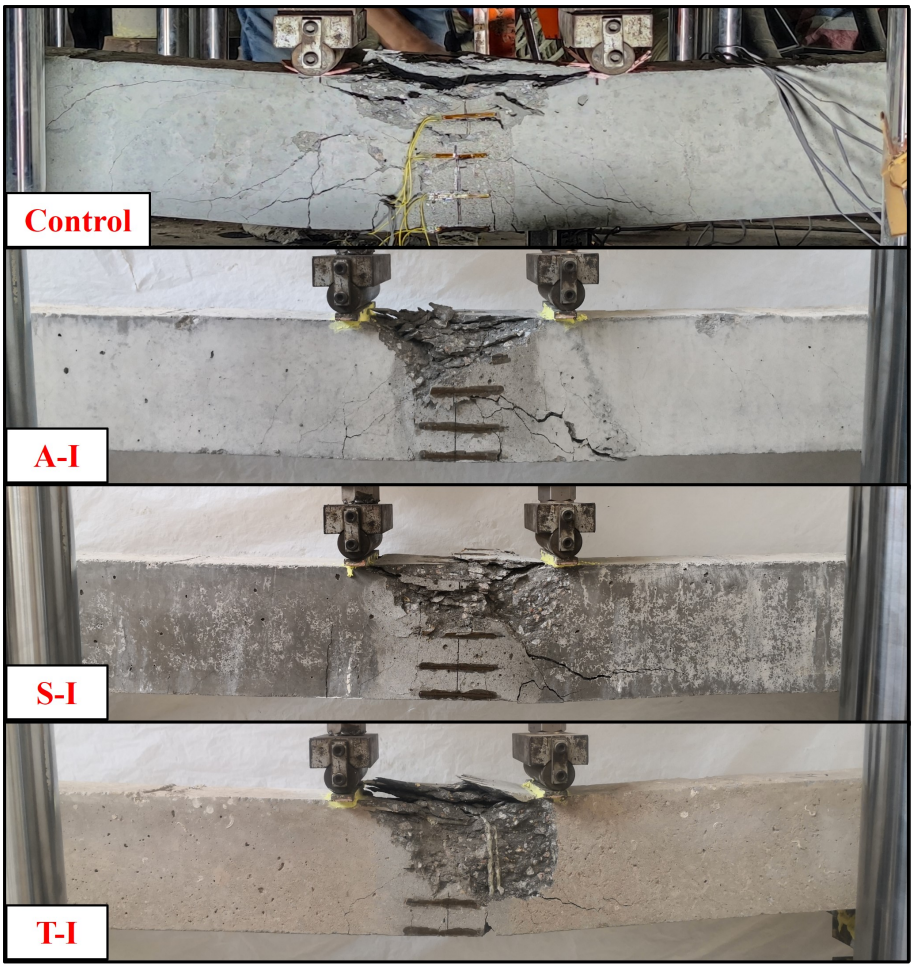


(c) 35-month exposure

Fig. 6.7 Long-term deflections of FRP-SSC beams with sustained load

6.3.3 Failure Modes

Figs. 6.8(a) and 6.8(b) present the typical failure modes observed in the two series of specimens. All specimens exhibited a typical flexural failure mode characterized by SSC crushing, regardless of environmental exposure and sustained loading conditions. This reveals that the specimens were not affected by the long-term field exposure in terms of failure mode due to the relatively high FRP reinforcement ratio employed, even for those with sustained load. These findings align with findings from AAT reported by Wang et al. (2023b) and Hao (2024). Additionally, a crushing failure governed by shear was observed in the 10-mm GFRP bars placed in the compression zone of all specimens, as shown in Fig. 6.8(c).



(a) Typical failure modes of Series I specimens (w/o sustained load)



(b) Typical failure modes of Series II specimens (w/ sustained load)



(c) Crushing failure of GFRP bars in the compression zone

Fig. 6.8 Failure modes

Table 6.3 Key test results of Series I specimens (w/o sustained load)

Exposure period	Exposure zone	Beam specimen ID	P_{cr} (kN)			δ_{cr} (mm)	P_{fp} (kN)			δ_{fp} (mm)	P_{max} (kN)			δ_{max} (mm)
			Meas.	Avg.	Ret. (%)	Meas.	Meas.	Avg.	Ret. (%)	Meas.	Meas.	Avg.	Ret. (%)	Meas.
0-month	/	C1	13.86	13.23	100.00	0.35	109.41	104.58	100.00	17.33	110.67	106.89	100.00	26.79
		C2	12.60			0.31	99.75			15.76	103.11			24.42
8-month	A-I	A1	12.18	13.34	100.79	0.51	109.20	108.26	103.51	19.20	109.20	108.26	101.28	19.20
		A2	14.49			0.87	107.31			18.54	107.31			18.56
	S-I	S1	13.44	13.76	103.97	0.50	111.09	110.36	105.52	19.78	120.75	116.97	109.43	35.69
		S2	14.07			0.64	109.62			19.51	113.19			31.51
	T-I	T1	11.55	13.55	102.38	0.68	99.75	99.44	95.08	16.06	101.64	104.27	97.54	23.94
		T2	15.54			0.76	99.12			16.80	106.89			26.04
12-month	A-I	A1	12.33	12.02	90.89	0.55	99.67	103.62	99.09	19.18	117.54	112.56	105.31	42.13
		A2	11.72			0.47	107.58			20.72	107.58			20.72
	S-I	S1	12.29	12.46	94.14	0.48	101.48	97.76	93.48	20.43	112.62	108.07	101.10	31.75
		S2	12.63			0.73	94.04			18.37	103.52			29.71
	T-I	T1	13.76	12.25	92.60	0.78	105.79	98.24	93.93	19.99	109.19	108.73	101.72	27.79
		T2	10.74			0.44	90.68			18.22	108.26			32.19
24-month	A-I	A1	13.32	12.57	94.98	0.77	107.63	106.81	102.13	20.43	107.63	106.81	99.92	20.43
		A2	12.37			0.74	106.82			19.88	106.82			19.88
		A3	12.01			0.38	105.97			19.68	105.97			19.68
	S-I	S1	14.11	14.08	106.45	0.46	101.59	103.06	98.55	19.22	105.27	110.09	103.00	30.20
		S2	14.57			0.42	102.73			18.38	113.14			36.58
		S3	13.57			0.54	104.86			20.32	111.87			28.22
	T-I	T1	11.65	11.11	83.98	0.70	103.43	97.69	93.41	19.36	103.43	98.03	91.71	19.36
		T2	11.56			0.68	93.24			17.64	94.26			27.72
		T3	10.12			0.50	96.40			18.68	96.40			18.68

Table 6.3. (*Continued*)

Exposure period	Exposure zone	Beam specimen ID	P_{cr} (kN)			δ_{cr} (mm)	P_{fp} (kN)			δ_{fp} (mm)	P_{max} (kN)			δ_{max} (mm)
			Meas.	Avg.	Ret. (%)	Meas.	Meas.	Avg.	Ret. (%)	Meas.	Meas.	Avg.	Ret. (%)	Meas.
37-month	A-I	A1	13.04	13.30	100.51	0.49	116.31	109.31	104.52	21.99	116.31	112.56	105.30	21.99
		A2	13.55			0.77	102.31			20.35	108.80			30.15
	S-I	S1	11.20	11.27	85.19	0.40	98.15	103.07	98.56	18.50	108.74	106.60	99.73	28.92
		S2	11.59			0.42	107.81			21.45	107.81			21.45
		S3	11.02			0.62	103.26			20.69	103.26			20.69
	T-I	T1	13.70	13.01	98.36	0.63	93.89	94.86	90.70	19.22	96.59	96.44	90.23	29.31
		T2	12.32			0.31	95.82			18.20	96.30			19.17
48-month	A-I	A1	11.44	11.39	86.07	0.47	110.94	110.93	106.07	22.94	110.94	110.93	103.78	22.94
		A2	11.33			0.38	110.91			22.09	110.91			22.09
	S-I	S1	12.74	12.20	92.23	0.43	100.63	101.11	96.68	19.97	117.14	113.05	105.76	33.84
		S2	11.67			0.52	101.58			20.04	108.97			32.38
	T-I	T1	11.21	13.39	101.19	0.68	95.06	92.54	88.49	18.12	95.06	98.81	92.44	18.12
		T2	15.57			0.52	90.03			18.44	102.56			29.00

Note: P_{cr} = cracking load; δ_{cr} = midspan deflection at P_{cr}; P_{fp} = first peak load; δ_{fp} = midspan deflection at P_{fp}; P_{max} = maximum load (i.e., load carrying capacity); δ_{max} = midspan deflection at P_{max}.

Table 6.4 Key test results of Series II specimens (w/ sustained load)

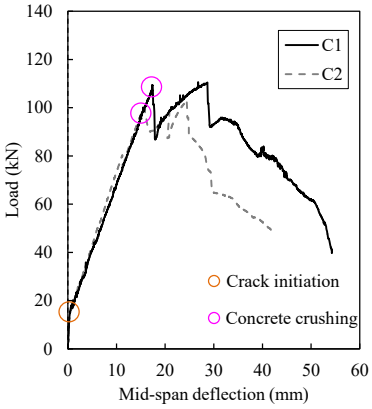
Exposure period	Exposure zone	Beam specimen ID	P_{fp} (kN)			$\delta_{fp}{}^{*}$ (mm)	P_{max} (kN)			δ_{max} (mm)
			Meas.	Avg.	Ret. (%)	Meas.	Meas.	Avg.	Ret. (%)	Meas.
11-month	S-I	S1	101.00	101.73	97.28	18.26	107.50	104.98	98.21	26.18
		S2	102.47			15.96	102.47			15.96
24-month		S1	99.88	98.39	94.08	15.50	108.81	103.45	96.79	27.63
		S2	96.89			16.47	98.10			20.66
35-month		S1	108.14	109.32	104.53	17.60	109.11	109.81	102.73	22.47
		S2	110.50			17.04	110.50			17.04

Note: (1) P_{fp} = first peak load; δ_{fp} = midspan deflection at P_{fp} P_{max} = maximum load (i.e., load carrying capacity); δ_{max} = midspan deflection at P_{max}.
(2) *Actual midspan deflection, i.e., the sum of deflections obtained before and during testing.

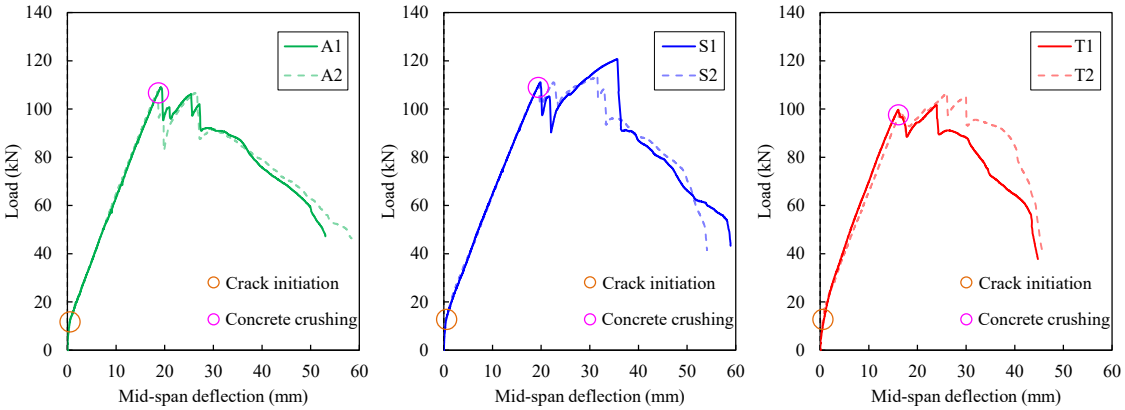
6.3.4 Load-Midspan Deflection Curves

Tables 6.3 and 6.4 tabulate the key test results of Series I and II specimens, respectively, including cracking load (P_{cr}), first peak load (P_{fp}), maximum load (P_{max}) (i.e., load carrying capacity) and their corresponding midspan deflections (δ_{cr}, δ_{fp} and δ_{max}). Since Series II specimens were pre-cracked, the values of P_{cr} and δ_{cr} are not reported.

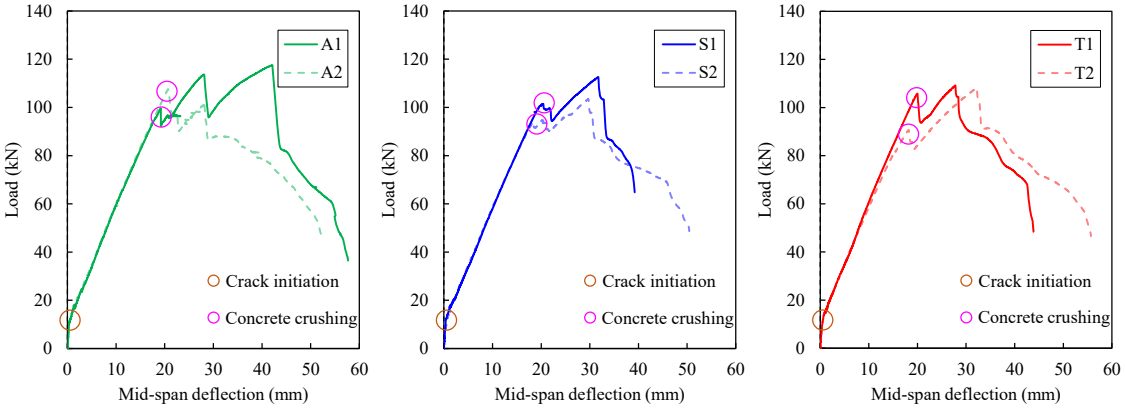
Fig. 6.9 depicts the load-midspan deflection curves of Series I specimens (without sustained load). Each subfigure compares the specimens with the same exposure duration but subjected to different environmental conditions. It is evident that all exposed specimens shared a similar load-deflection behavior with the control ones before concrete crushing, revealing the marginal effect caused by the environmental exposure for up to four years on the load-deflection relationship of the FRP-SSC beams. Prior to the onset of concrete cracking, the load-midspan deflection curves exhibited an initial linear segment with a steep slope (i.e., initial stiffness), followed by a post-cracking linear segment with a markedly reduced slope (i.e., second stiffness). When the first peak load (initiation of concrete crushing) was achieved, a sudden load drop was noticed. However, as concrete crushing progressed, most specimens exhibited a post-peak increase in load accompanied by additional deformability due to the concrete confinement provided by the FRP stirrups (Johnson and Sheikh 2013). Such a confinement effect might allow the core concrete within the stirrups to continue carrying load until failure.



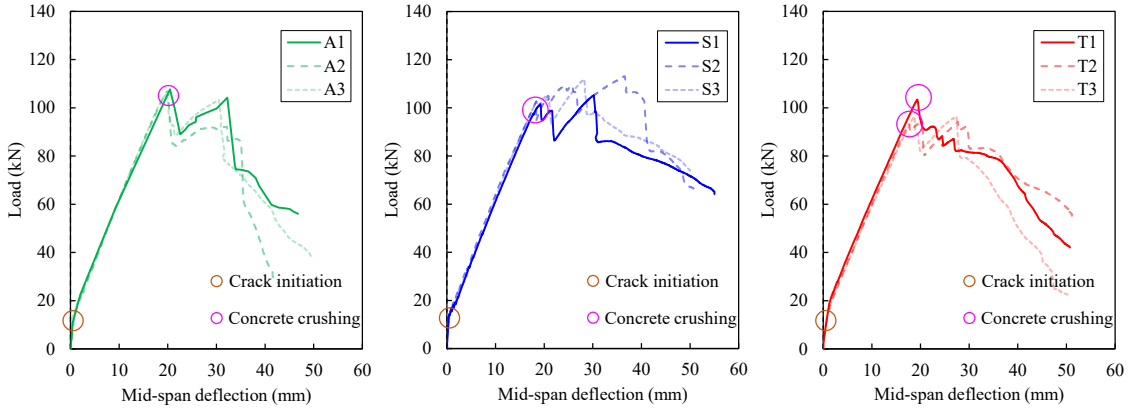
(a) Control



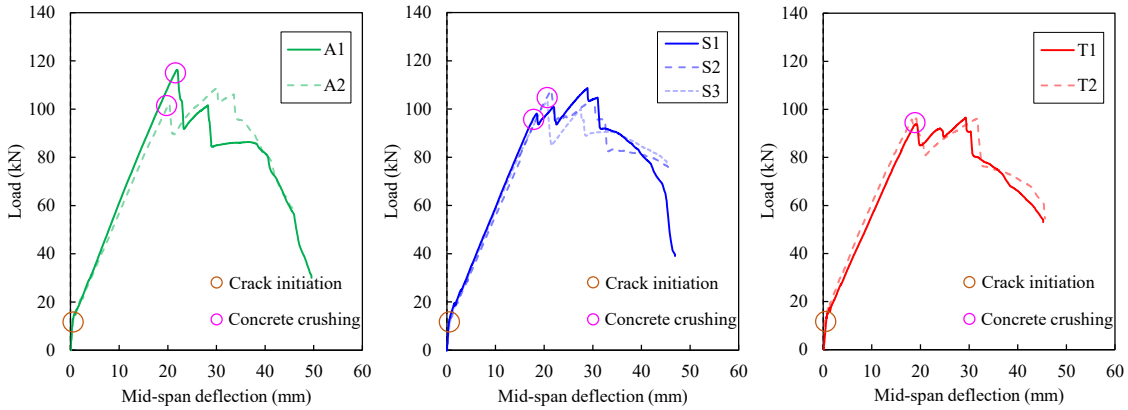
(b) 8-month exposure



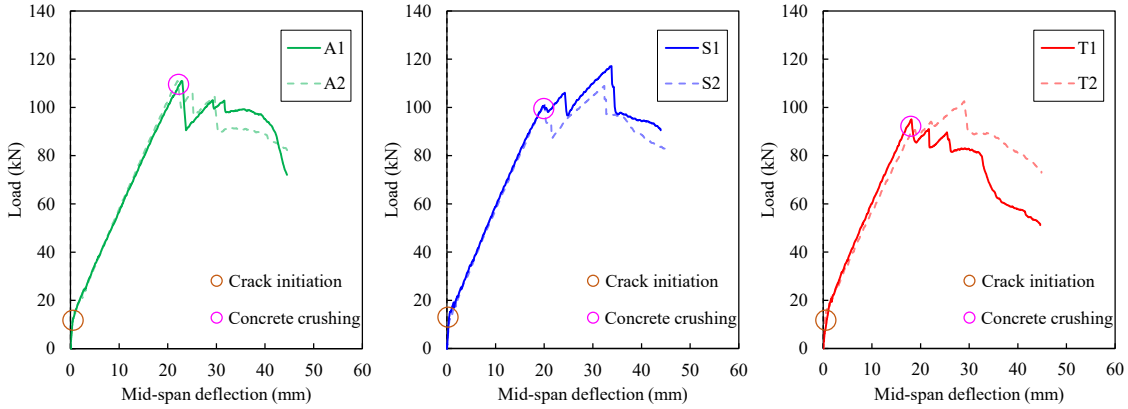
(c) 12-month exposure



(d) 24-month exposure



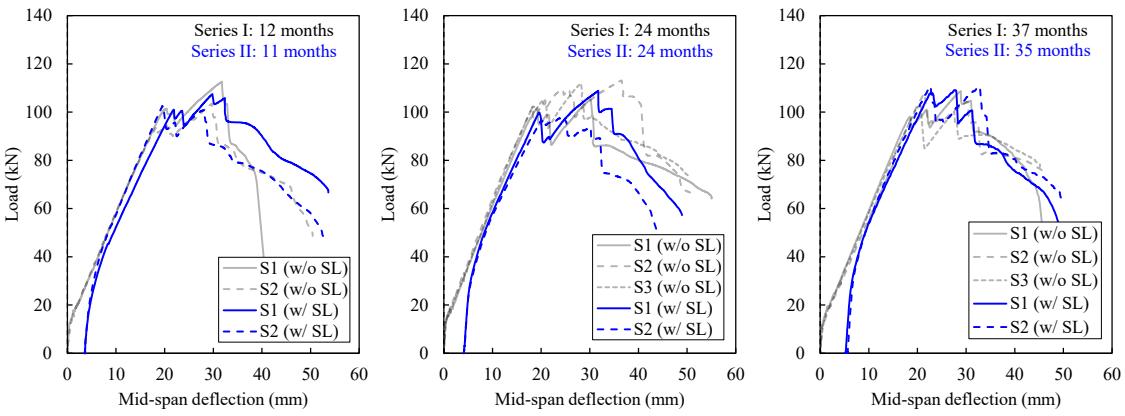
(e) 37-month exposure



(f) 48-month exposure

Fig. 6.9 Load-midspan deflection curves of Series I specimens

The load-midspan deflection curves of Series II specimens (with sustained load) are illustrated in Fig. 6.10. In order to examine the effect of sustained load on the load-deflection relationship of FRP-SSC beams, the curves of Series I specimens subjected to the same environmental conditions (i.e., S-I zone) for 12, 24 and 37 months are also included in the corresponding subfigures for comparison. Considering there existed a residual deflection in the specimens under sustained loading as previously mentioned, the actual midspan deflection, defined as the sum of deflections measured before and during testing, was adopted for Series II specimens, as shown in Fig. 6.10. Compared to Series I specimens, the presence of sustained load significantly influenced the curve shape of Series II specimens in the early loading stage, resulting in a smooth transition between the two segments due to the absence of a distinct concrete cracking stage. An interesting observation is that, when the applied load was in excess of the magnitude of the sustained load, the second stiffness of all specimens tended to be similar. This suggests that, after considering residual deflection, the load-midspan deflection curves of all specimens were comparable before concrete crushing, regardless of the presence of sustained load. For the post-peak load-deflection behavior, no noticeable differences were observed between the two series of specimens.



(a) 11-month exposure (b) 24-month exposure (a) 35-month exposure

Fig. 6.10 Load-midspan deflection curves of Series II specimens

6.3.5 Cracking Load and Flexural Capacity

6.3.5.1 Cracking load

The first cracking load (including the self-weight of the beams) of each Series I specimen is presented in Fig. 6.11. The cracking loads of the two control specimens were 13.86 kN and 12.60 kN, respectively, with an average of 13.23 kN, while those of the specimens exposed in zones A-I, S-I and T-I ranged from 11.33 kN to 14.49 kN, 11.02 kN to 14.57 kN and 10.12 kN to 15.57 kN, respectively, with average values of 12.53 kN, 12.74 kN and 12.52 kN. The insignificant changes in cracking loads between exposed and control specimens demonstrate that marine environmental exposure had negligible impact on cracking load, despite some random variability among exposed specimens.

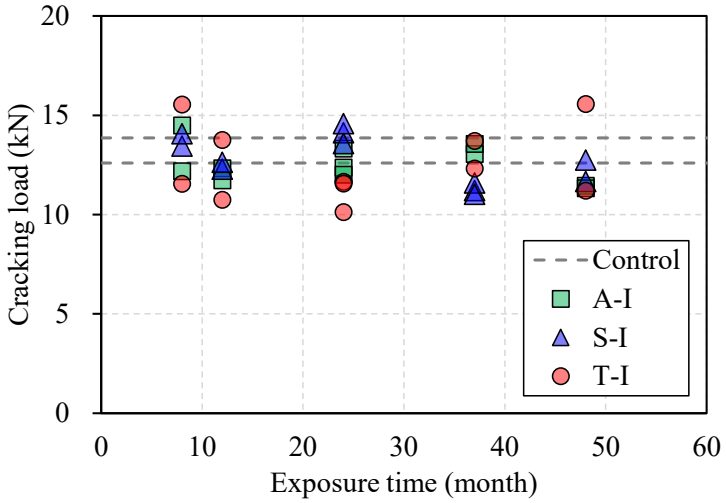


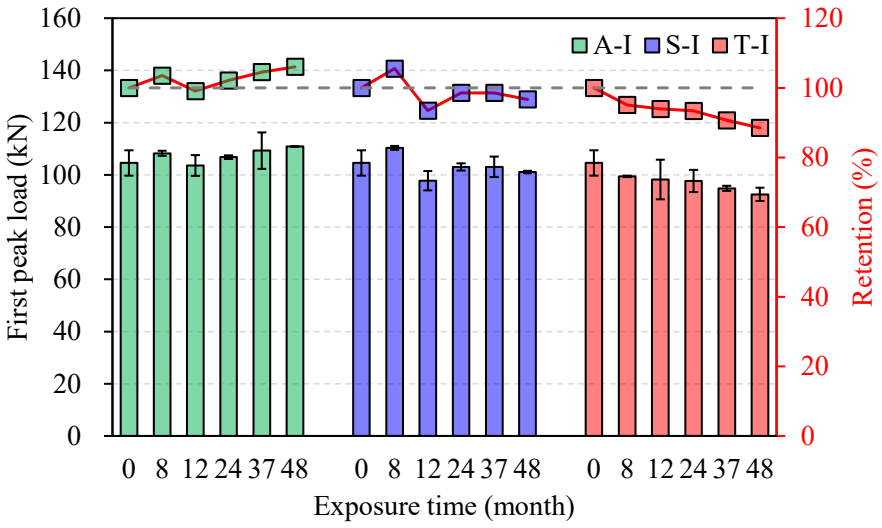
Fig. 6.11 Changes in cracking load of Series I specimens

6.3.5.2 Flexural capacity

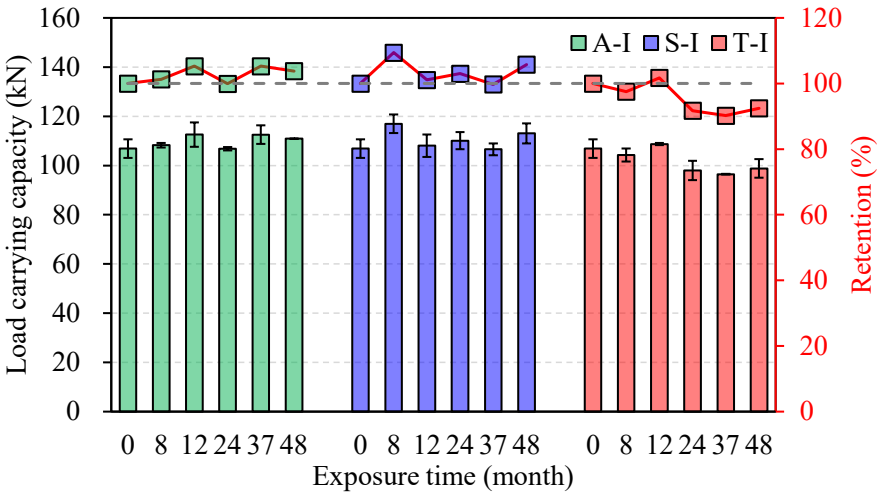
Since most specimens were able to carry additional load beyond the first peak until the crushing failure of the stirrup-confined core concrete (see Figs. 6.9 and 6.10), this section separately discusses two critical parameters: the first peak load and the ultimate load carrying capacity for both series of specimens. Fig. 6.12 presents the variation in

flexural capacity of specimens exposed in different zones. Compared to control specimens, those subjected to atmospheric (A-I) and splash (S-I) environments experienced insignificant changes over up to four years, with retentions of the first peak load fluctuating within 99.09~106.07% and 93.48~105.52%, respectively, while those of the load carrying capacity were in ranges of 99.92~105.31% and 99.73~109.43%, respectively. These results indicate that the flexural capacity of FRP-SSC beams is largely insensitive to these relatively mild environments.

Conversely, for specimens exposed to tidal conditions (T-I), the residual first peak load exhibited a slight decline with time, decreasing from 100% at 0 months to 95.08%, 93.93%, 93.41%, 90.70% and 88.49% at 8, 12, 24, 37 and 48 months, respectively. Similarly, the residual load carrying capacity showed a decreasing trend, with retentions stabilizing at approximately 90% after four years of field exposure. This reduction in flexural capacity can be attributable to two major factors: (1) deterioration of SSC potentially causing premature SSC crushing in the compression zone; and (2) degradation of bond performance (e.g., bond stiffness) between FRP bars and SSC, as presented in Chapter 5.



(a) First peak load



(b) Load carrying capacity

Fig. 6.12 Effect of environmental exposure on flexural capacity

To better understand the causes behind the observable degradation in flexural capacity of FRP-SSC beams in aggressive marine environments (e.g., tidal zone), two concrete cylindrical cores (diameter = 100 mm and height = 100 mm) were drilled from both ends of Series I specimens with 24, 37 and 48 months of field exposure after bending tests. The SSC core samples were tested in accordance with JGJ/T (2016) to study the relationship between the flexural capacity of FRP-SSC beams and the strength of SSC. The preparation procedure for SSC cores is shown in Fig. 6.13. All core samples were capped with high-strength gypsum plaster at both ends to ensure flat loading surfaces for compression testing. Fig. 6.14 compares the load carrying capacities of the beam specimens with the compressive strengths of the corresponding SSC cores (listed in Table 6.5). As shown in Fig. 6.14, the SSC compressive strength seemed to be relatively stable between 24 to 48 months of exposure, indicating good durability of the SSC used in the present study. This finding can be supported by the AAT results on SSC cubes with the same mix proportions reported by Ke et al. (2024) and Hao (2024). Notably, the load carrying capacities of beam specimens showed an unexpectedly weak correlation with their corresponding SSC compressive strengths, especially for

specimens exposed in the T-I zone, indicating that SSC strength was not the primary factor contributing to the degradation of the flexural capacity of FRP-SSC beams.

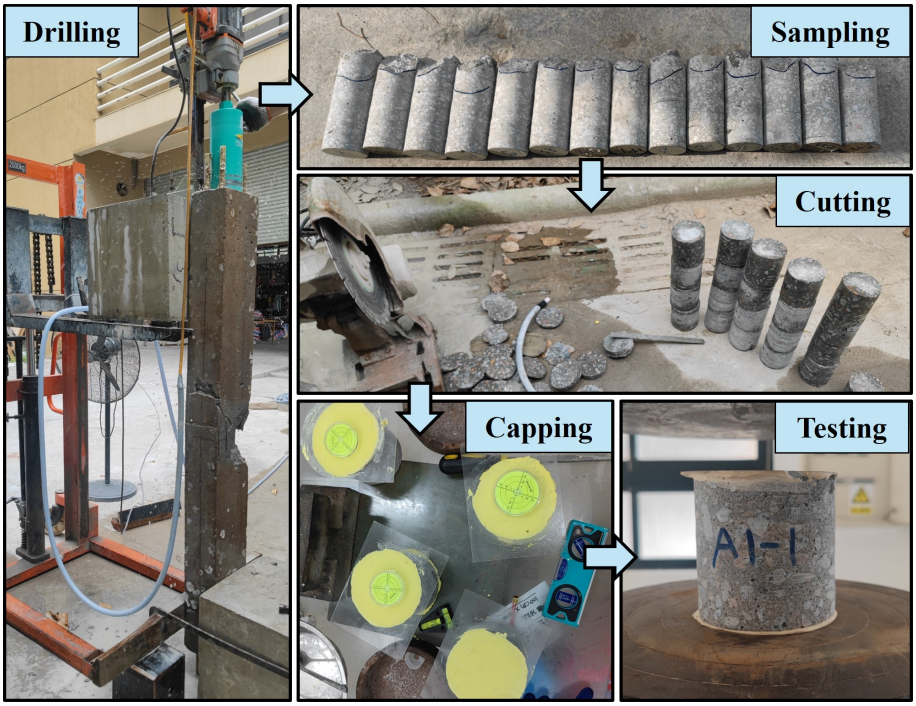


Fig. 6.13 Preparation procedures for SSC cores

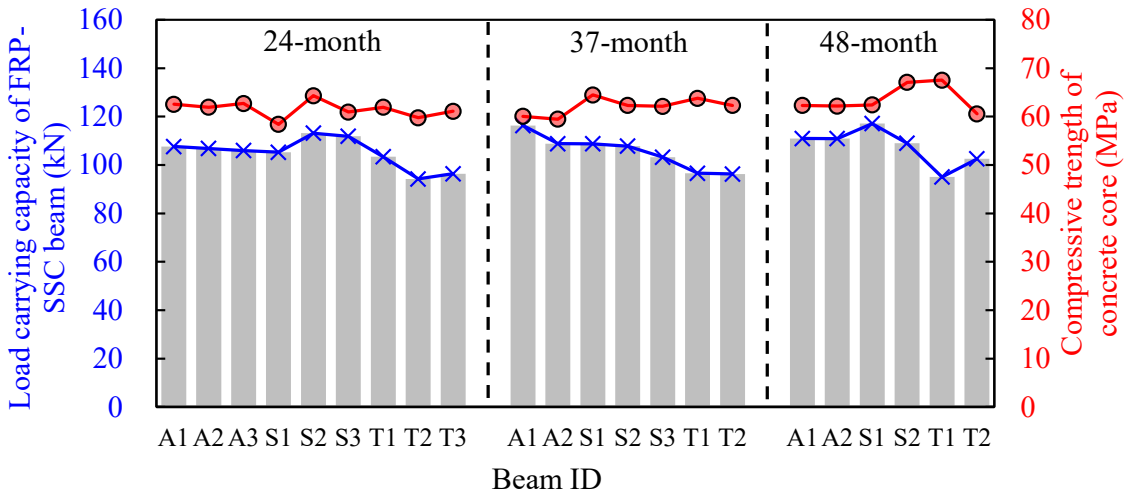


Fig. 6.14 Comparison between the load carrying capacity of Series I specimens and the compressive strength of SSC cores

Table 6.5 Compressive strength of SSC cores drilled from beam specimens

Exposure period	Exposure zone	Specimen ID	Compressive strength (MPa)	
			Meas.	Avg.
24-month	A-I	A1	62.56	62.40
		A2	61.94	
		A3	62.71	
	S-I	S1	58.40	61.23
		S2	64.33	
		S3	60.96	
	T-I	T1	61.95	60.93
		T2	59.76	
		T3	61.10	
37-month	A-I	A1	60.06	59.77
		A2	59.47	
	S-I	S1	64.47	62.96
		S2	62.31	
		S3	62.11	
	T-I	T1	63.78	63.04
		T2	62.30	
48-month	A-I	A1	62.32	62.25
		A2	62.17	
	S-I	S1	62.43	64.76
		S2	67.08	
	T-I	T1	67.53	64.05
		T2	60.58	

To further investigate bond degradation as a potential cause of flexural capacity reduction, the flexural stiffness of Series I specimens was quantitatively analyzed. Fig. 6.15 depicts the changes in flexural stiffness for Series I specimens exposed in different zones. Flexural stiffness was defined as the slope of the load-midspan deflection curve within the range of 30% to 50% of the load carrying capacity (Dong et al. 2017a), with calculated values provided in Table 6.6. It is interesting to find from Fig. 6.15 that no obvious change in flexural stiffness was observed for specimens in the A-I and S-I zones during the 4-year exposure period, whereas the flexural stiffness of those in the T-I zone showed a slight decreasing trend, with around 12% reduction after 48 months. This variation in flexural stiffness degradation might also reflect the distinct chemical

and physical conditions characteristic of each environment, as discussed in Sections 3.3.3.1 and 5.3.5. It should be pointed out that a previous study conducted by Tannous and Saadatmanesh (1999), reported significant flexural stiffness loss and capacity degradation in GFRP-reinforced concrete beams after two years of exposure to simulated deicing salt solutions at ambient temperature. On the other hand, the flexural stiffness of FRP-SSC beam specimens exhibited a similar variation trend with time to the bond stiffness of FRP-SSC pullout specimens exposed in the same zone (Chapter 5), as illustrated in Fig. 6.16. Based on these observations, it is reasonable to speculate that the degradation of flexural capacity in FRP-SSC beams may not be primarily due to the deterioration of SSC compressive strength, but rather more attributable to the deterioration of bond performance between FRP bars and the surrounding SSC under cyclic wet-dry conditions (i.e., tidal zone).

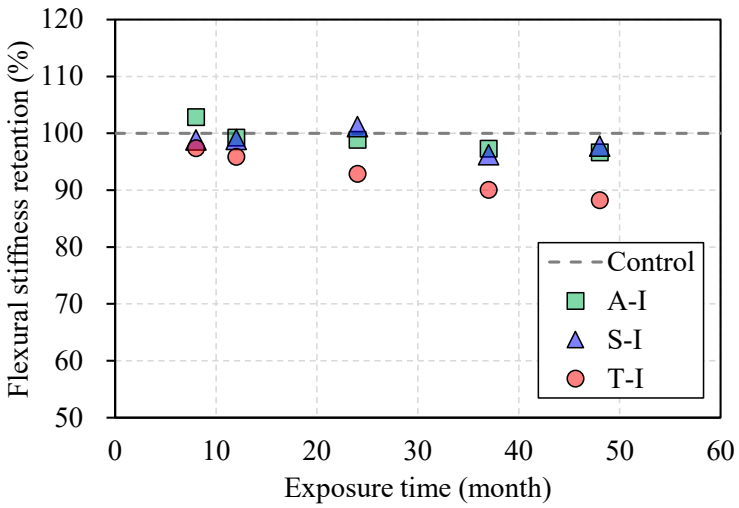


Fig. 6.15 Changes in flexural stiffness of Series I specimens

Table 6.6 Flexural stiffness of Series I specimens (w/o sustained load)

Exposure period	Exposure zone	Specimen ID	Flexural stiffness (kN/mm)		
			Meas.	Avg.	Ret. (%)
0-month	/	C1	4.87	5.18	100.00
		C2	5.49		
8-month	A-I	A1	5.22	5.33	102.89
		A2	5.43		
	S-I	S1	5.29	5.12	98.85
		S2	4.95		
	T-I	T1	5.28	5.04	97.41
		T2	4.81		
12-month	A-I	A1	5.17	5.14	99.25
		A2	5.11		
	S-I	S1	5.19	5.12	98.94
		S2	5.05		
	T-I	T1	5.14	4.96	95.89
		T2	4.79		
24-month	A-I	A1	4.97	5.12	98.89
		A2	5.32		
		A3	5.07		
	S-I	S1	5.08	5.24	101.18
		S2	5.38		
		S3	5.25		
	T-I	T1	4.88	4.81	92.91
		T2	4.88		
		T3	4.67		
37-month	A-I	A1	5.25	5.04	97.34
		A2	4.82		
	S-I	S1	5.05	4.98	96.24
		S2	4.84		
		S3	5.06		
	T-I	T1	4.52	4.66	90.06
		T2	4.81		
48-month	A-I	A1	4.83	5.00	96.66
		A2	5.18		
	S-I	S1	5.10	5.06	97.78
		S2	5.02		
	T-I	T1	4.76	4.57	88.26
		T2	4.38		

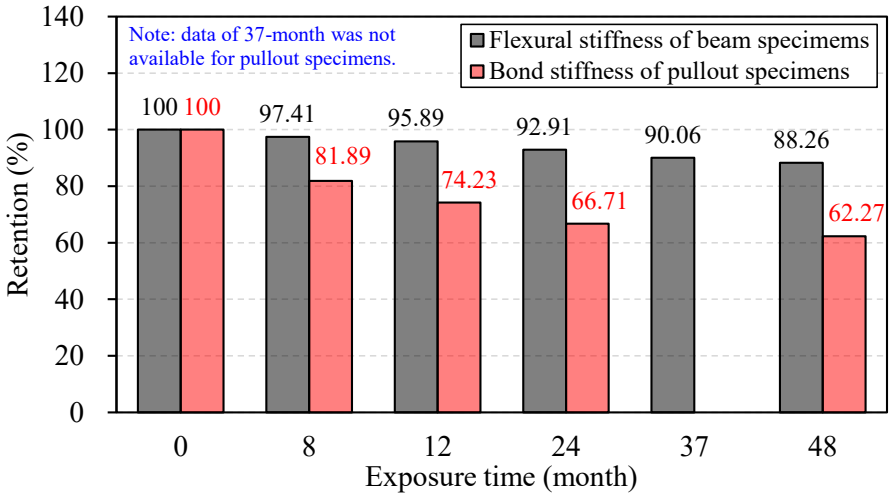


Fig. 6.16 Comparison between retention of flexural stiffness and bond stiffness

Fig. 6.17 compares the flexural capacities of Series I and II specimens after exposure in the S-I zone for up to approximately three years. It is clear that there were no apparent differences in first peak load and load carrying capacity between specimens with and without sustained load, indicating that sustained loading had minimal impact on the long-term flexural capacity of specimens under splash conditions. These findings agree with the observations made by Hao (2024), who reported negligible effect of sustained load on FRP-SSC beams subjected to 40°C saltwater wet-dry cycles for up to 24 months, despite more severe environmental conditions than in the present study. The minimal influence of coupled effects of environmental exposure and sustained load on flexural capacity of FRP-SSC beams can be largely ascribed to the stable properties of SSC (given that failure of the specimens was governed by SSC crushing), the relatively mild environmental conditions of the S-I zone (characterized by alternating moist and dry cycles), as well as the considerable load loss in the sustained loading system, as mentioned previously.

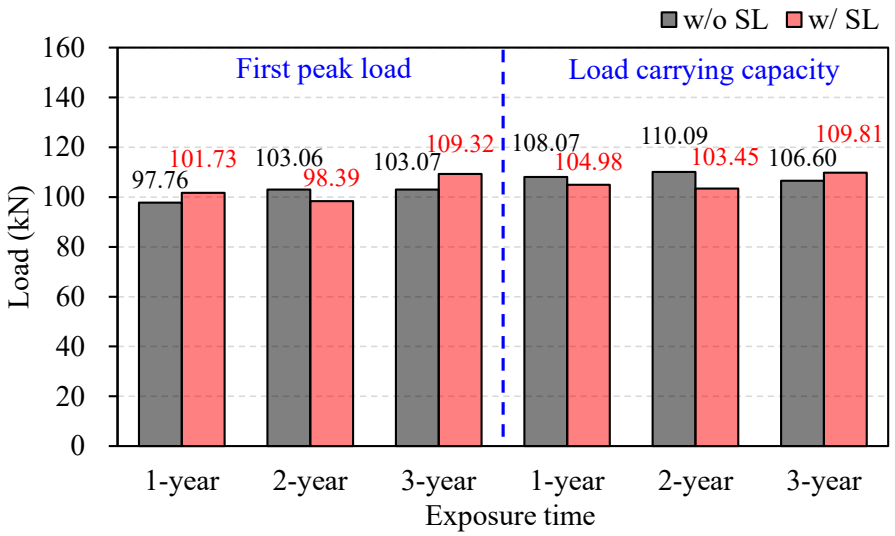


Fig. 6.17 Effect of sustained load on flexural capacity

6.3.6 Crack Width and Distribution

Fig. 6.18 presents the load-maximum crack width curves of representative specimens exposed in each environmental zone for durations of 24 and 48 months. All curves terminate at the first peak load due to the unstable post-peak behavior of the specimens. The crack width was obtained by measuring the elongation of a line segment oriented perpendicular to the crack plane (Huang et al. 2022). It is evident that the load-maximum crack width curves of all specimens were close to each other during the early loading stage (approximately before 30% of P_{fp}). However, with the increase of applied load, specimens exposed to tidal conditions (T-I) possessed significantly greater maximum crack widths compared to those in the A-I and S-I zones at a given load, especially for the 48-month scenario, with measurements of 0.95 mm, 1.00 mm and 1.49 mm for specimens A1, S2, and T1 (48-month exposure), respectively. This indicates that exposure to tidal environments substantially increases the maximum crack width in FRP-SSC beams.

Fig. 6.19 shows the crack distributions, as revealed by DIC strain profile, for the

specimens corresponding to those in Fig. 6.18. It can be seen that the T-I specimens exhibited fewer cracks compared to the A-I and S-I specimens with the same exposure duration. The substantial changes in maximum crack widths and crack distributions observed in specimens conditioned under tidal exposure are believed to be caused by the deterioration of the bond performance between GFRP bars and SSC, which further confirms the bond-induced degradation hypothesis discussed in Section 6.3.5.2.

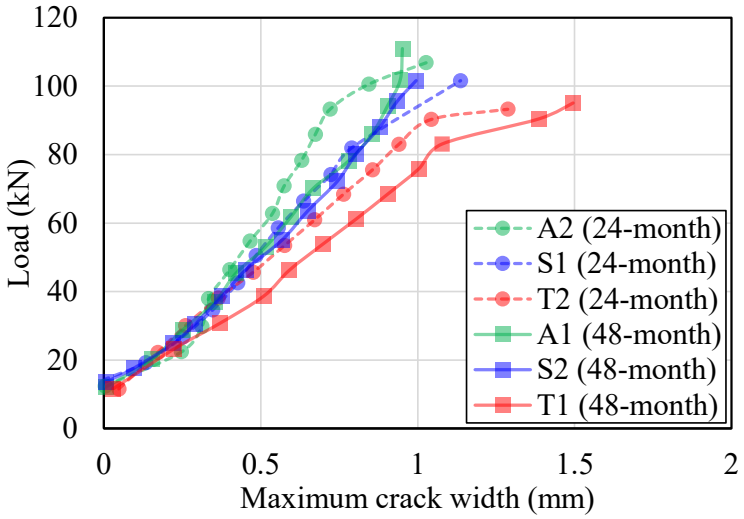


Fig. 6.18 Load-maximum crack width curves

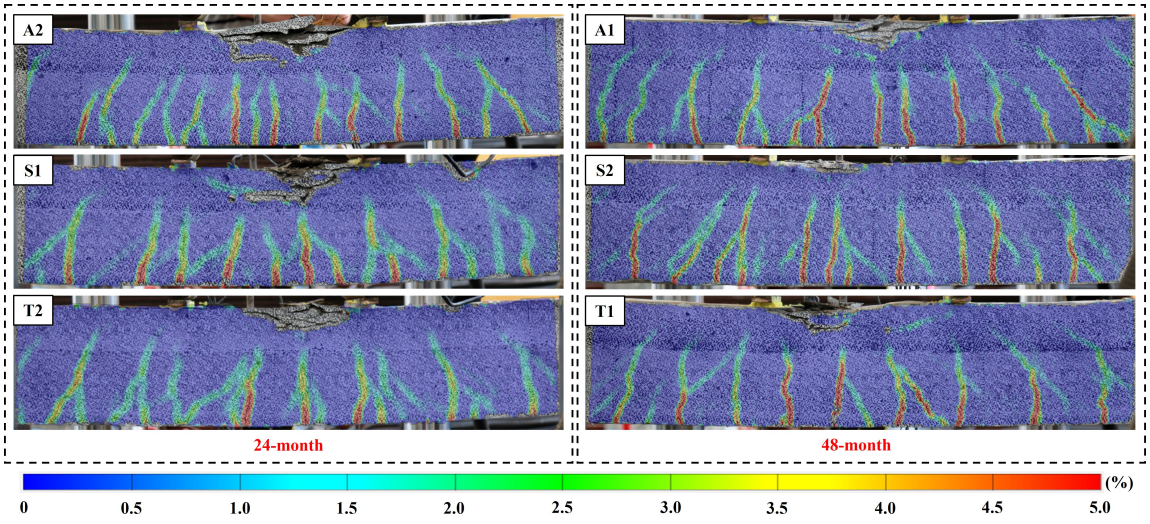


Fig. 6.19 Crack distribution of exposed specimens (left: 24-month; right: 48-month)

6.4 CONCLUSIONS

This chapter assessed the flexural performance of GFRP-reinforced SSC beams after exposure in three different marine environmental zones (i.e., atmospheric, splash and tidal) for up to four years. Additionally, the coupled effects of environmental exposure and sustained loading on these beams were investigated. The main conclusions are summarized as follows:

(1) Compared to specimens exposed to atmospheric and splash conditions, those subjected to tidal conditions demonstrated noticeable changes in appearance, characterized by the attachment of marine organisms to the concrete surface.

(2) Long-term field exposure had no influence on the failure mode of specimens, including those subjected to sustained load. All specimens failed by crushing of the SSC.

(3) The load-deflection relationship of the specimens was not affected by field exposure, regardless of the presence of sustained load. After considering residual deflections in specimens coupled with sustained load, the load-midspan deflection curves of all specimens were comparable before concrete crushing.

(4) No significant changes occurred in flexural capacity of the specimens subjected to atmospheric and splash environments throughout the exposure period, even when coupled with sustained load. In contrast, specimens exposed to a tidal environment underwent an appreciable decrease in the load carrying capacity, stabilizing at approximately 90% retention after four years. This decline is believed to be caused by the deterioration of the bond stiffness between GFPR

bars and the surrounding SSC.

(5) Due to bond degradation between GFRP bars and SSC, the crack widths of specimens exposed to a tidal environment increased significantly, while the crack number decreased. Considering the strong correlation between the long-term bond performance of FRP bars in concrete and their surface treatment, it is expected that these adverse effects could be mitigated if FRP bars with enhanced bond durability are provided.

CHAPTER 7
NUMERICAL SIMULATION OF GFRP-REINFORCED SEAWATER SEA-SAND CONCRETE BEAMS SUBJECTED TO MARINE ENVIRONMENTS

7.1 INTRODUCTION

As reviewed in Chapter 2, numerous experimental studies have been carried out to assess the durability of FRP-reinforced concrete beams using AAT rather than FET, which may not accurately reflect real-world scenarios. However, a notable drawback of FET is that they are often labor-intensive and time-consuming. The finite element (FE) approach emerges as an effective solution, as it allows for the analysis of stress and strain fields within the materials and the interactions between FRP bars and concrete throughout the entire loading process (Achillides and Pilakoutas 2006).

In recent years, a substantial number of numerical studies have focused on the flexural behavior of FRP-reinforced concrete beams (Ng et al. 2020; Veljkovic et al. 2020; Dang and Phan 2021). Different from concrete beams reinforced with conventional steel bars, the flexural design of FRP-reinforced concrete beams is typically governed by the serviceability limit state (SLS) rather than the ultimate limit state (ULS), primarily due to the low elastic modulus of FRP bars (ACI 2015), which demonstrates the importance of accurately predicting deformation properties, such as crack width and deflections. However, many existing studies relied on the assumption of perfect bond to model the interaction between FRP bars and concrete (Buyukkaragoz et al. 2013; Bui et al. 2018;

Mohammed and Said 2022), which may lead to inaccurate results, as the bond-slip relationship is a critical factor in the numerical simulation of reinforced concrete beams (Chen 2010). Additionally, FET results on FRP-SSC beams under tidal conditions have revealed that their flexural durability is largely associated with the degradation of bond stiffness between FRP bars and SSC, rather than the deterioration of SSC compressive strength, as noted in Chapter 6. Although a few recent studies have been conducted on FE modeling of the long-term performance of FRP-SSC beams in coastal environments (Ren et al. 2021) and marine environments (Chen et al. 2022), none have addressed the bond degradation between FRP bars and SSC.

Against this background, this chapter aims to develop a reliable FE model that incorporates a reasonable bond-slip relationship to predict the long-term performance of FRP-SSC beams. The flexural behavior of undegraded FRP-SSC beams is first modeled using the proposed simplified bond stiffness determined from the pullout test results presented in Chapter 5. Subsequently, the accuracy of the FE model, which accounts for the deterioration of bond stiffness, is verified against the test results from Chapter 6, focusing on degraded FRP-SSC beams that have been exposed to tidal conditions for up to four years.

7.2 FINITE ELEMENT MODELING

7.2.1 General

In order to simulate the flexural performance of FRP-SSC beams examined in Chapter 6, a two-dimensional (2D) finite element model was developed using the FE software ABAQUS (2021) within the framework established by Chen (2010). The concrete beam and loading pad of the specimen were modeled using four-node plane stress elements

(CPS4), while the FRP bars were modeled using two-node linear displacement truss elements (T2D2). All element sizes were set to be 5 mm in this chapter based on a mesh convergence study. Taking advantage of geometric symmetry, only one half of the beam was modelled by applying symmetrical boundary conditions. Only the vertical translational degree of freedom was constrained at the support, and the vertical load was applied in a displacement-controlled manner on the loading pad. Additionally, rectangular elastic support and loading pad with steel mechanical properties was employed to mitigate stress concentration near them. In this chapter, the implicit dynamic solution approach was adopted following Chen (2010), as the implicit Hilber-Hughes-Taylor-*a* (HHT-*a*) method (Hilber 1976) is preferred over the explicit approach, provided that a converged solution can be achieved, as stated by Chen et al. (2015).

7.2.2 Material Properties

The SSC was modeled using the concrete damage plasticity (CDP) model, incorporating the crack band model concept (Bažant and Planas 1997) to address the mesh-dependence issue. This approach utilizes crack-opening displacement rather than cracking strain to define the tensile behavior of concrete. The crack band width is determined as the characteristic crack length of an element, which corresponds to the diagonal length of a four-node square element as per Rots (1988). In the FE modeling, the 28-day compressive strength of SSC cylinders (i.e., 46.25 MPa, as presented in Section 6.2.1.2) converted from that of 100-mm SSC cubes was adopted as the cylindrical compressive strength f_c. The Poisson's ratio was taken to be 0.2 and the elastic modulus was calculated by Eq. (7.1) as per ACI (2019):

$$E_c = 4700\sqrt{f_c} \tag{7.1}$$

The plasticity parameters for the CDP model were defined as follows: dilation angle = 35°, flow eccentricity = 0.1, the ratio of initial biaxial compressive strength to initial uniaxial compressive strength = 1.167, the ratio of the second stress invariant on the tensile meridian to that on the compressive meridian = 0.667, and viscosity parameter = 0.

To characterize concrete behavior under uniaxial compression and tension, the equations suggested by Saenz (1964) [Eq. (7.2)] and Jendele and Cervenka (2006) [Eq. (7.3)] were respectively adopted as the foundational model.

$$\sigma = \frac{\alpha\varepsilon}{1 + \left[\left(\alpha\varepsilon_p/\sigma_p\right) - 2\right]\left(\varepsilon/\varepsilon_p\right) + \left(\varepsilon/\varepsilon_p\right)^2} \tag{7.2}$$

$$\frac{\sigma_t}{f_t} = \left[1 + \left(c_1\frac{w_t}{w_{cr}}\right)^3\right]e^{\left(-c_2\frac{w_t}{w_{cr}}\right)} - \frac{w_t}{w_{cr}}(1 + c_1^3)e^{(-c_2)} \tag{7.3a}$$

$$w_{cr} = 5.14\frac{G_F}{f_t} \tag{7.3b}$$

where σ and ε = compressive stress and strain, respectively; σ_p and ε_p = experimentally obtained compressive strength and the corresponding strain (taken to be 0.0025); α = an experimentally obtained coefficient standing for the initial tangent modulus, which was equal to the elastic modulus of the concrete herein; w_t = crack opening displacement; w_{cr} = crack opening displacement corresponding to the status of the complete release of tensile stress or fracture energy; σ_t = tensile stress normal to the crack direction; f_t = tensile strength of concrete under uniaxial tension; G_F = fracture energy; c_1 and c_2 = constants obtained from tensile tests of concrete and set to be 3.0 and 6.93, respectively. Additional details can be found in Chen (2010). Besides, the damage evolution model defined by Chen et al. (2011) was employed, assuming that the equivalent plastic strain

is zero for all post-cracking tensile stress values.

In this chapter, the tensile strength f_t and fracture energy G_F used for the tension-softening curves were estimated by the following two equations (CEB-FIP 1993):

$$f_t = 1.4\left(\frac{f_c - 8}{10}\right)^{\frac{2}{3}} \tag{7.4}$$

$$G_F = (0.0469d_a^2 - 0.5d_a + 26)\left(\frac{f_c}{10}\right)^{0.7} \tag{7.5}$$

where d_a is the maximum aggregate size (assumed to be 20 mm).

The FRP bars were modeled to exhibit linear-elastic-brittle behavior. The material properties provided by the manufacturer, as detailed in Section 6.2.1.1, were used in the FE model.

7.2.3 Bond Behavior Between FRP Bars and SSC

The bond behavior between FRP bars (both longitudinal and transverse) and SSC was modeled using a cohesive interface. The stiffness in the normal direction of the interface was assumed to be infinite, indicating no relative displacement between the FRP bars and the SSC, while that in the shear direction was determined from the measured bond stress-slip curves of pullout specimens, as described in the remainder of this sub-section.

Currently, two approaches can be employed to model the bond behavior between FRP bars and concrete in numerical simulations. One simple approach is to associate the bond effect with concrete material properties (i.e., tension-stiffening model), which integrates the local bar-concrete interface action globally by modifying the stress-strain

relationship of the concrete, while the bond condition between the FRP bars and the surrounding concrete is still assumed to be perfect. However, preliminary numerical studies, not presented here, indicated that the tension-stiffening model failed to provide reasonable predictions for FRP-reinforced concrete beams. The other commonly used approach is to simulate the actual bond-slip relationship between FRP bars and concrete appropriately. As mentioned in Chapter 5, extensive research has focused on developing bond-slip models for FRP bars in concrete (Malvar 1994; Cosenza et al. 1995; Rossetti et al. 1995; Cosenza et al. 1996, 1997; Pecce et al. 2001; Baena et al. 2009; Lee et al. 2012; Rolland et al. 2020). Notably, the CMR model (Cosenza et al. 1995) and the modified BPE (mBPE) model (Cosenza et al. 1996) are the two most widely used models, owing to their predictive accuracy regarding bond properties and their applicability to various surface treatments of FRP bars. However, the undefined slope at the initial point of these two models may significantly increase the possibility of convergence issues and instability in FE modeling (Rolland et al. 2020). To address this challenge and facilitate the modeling process, simplified bond stiffness (K), defined as the secant stiffness at maximum bond stress (i.e., τ_{max}/s_m) was introduced to simulate the bond behavior between FRP bars and SSC. Specifically, the bond-slip relationship was assumed to be characterized by a linear branch with a slope of K up to maximum bond stress, followed by a horizontal branch. For example, in accordance with the parameters provided in Table 5.5, the simplified bond stiffness of the unexposed FRP-SSC beam specimen can be calculated as $K = 18.36/0.25 = 73.44$. It should be highlighted that numerical results not presented here indicate that the post-peak branch (including the descending branch and residual branch) of the bond-slip models has a limited influence on the overall modeling results. Besides, compared to the bond stiffness of FRP bars in concrete, their bond strength has minimal effects on the

deformation properties (e.g., crack width, deflections) of FRP-reinforced concrete beams due to their low elastic modulus, as mentioned previously.

Considering the lack of a definitive trend regarding the influence of bar diameter on bond strength (Nepomuceno et al. 2021) and the insufficient experimental data from pullout tests for FRP bars of varying sizes, this chapter adopts a uniform bond-slip relationship derived from the pullout test results in Chapter 5 for all FRP bars, including tension and compression bars as well as stirrups.

7.2.4 Numerical Results

The experimental results of all undegraded FRP-SSC beams specimens from Series I (Chapter 6) were compared with the numerical results obtained using the developed FE model. The beam specimens included control specimens without environmental exposure, along with those subjected to atmospheric and splash conditions (i.e., A-I and S-I zones) that exhibited no degradation after varying conditioning durations (i.e., 8, 12, 24, 37 and 48 months). Fig. 7.1 presents the experimental load-midspan deflection curves (grey solid lines) alongside the numerical predictions (red solid and dark blue dashed lines with end markers), with all curves terminating after reaching the first peak load (referred to as the ultimate load hereafter). For clarity, only the predicted curves generated by the proposed FE model using the maximum and minimum experimental bond stiffness values are included, according to Table 5.3. It is evident that the load-deflection curves obtained from the FE model generally agree well with the experimental ones. The minimum and maximum predicted ultimate loads are 103.99 and 106.59 kN, respectively, with an average of 105.29 kN, while the tested ones vary from 94.04 to 116.31 kN, averaging 105.23 kN (see Table 6.3), demonstrating satisfactory prediction accuracy. The slightly larger flexural stiffness observed in the

numerical curves compared to the experimental curves during the early loading stage after cracking might be attributed to the fact that as cracks develop, the increasing crack width and stress redistribution within the beam can lead to a reduction in stiffness, which may not be accurately captured by the numerical model, leading to discrepancies with the experimental results.

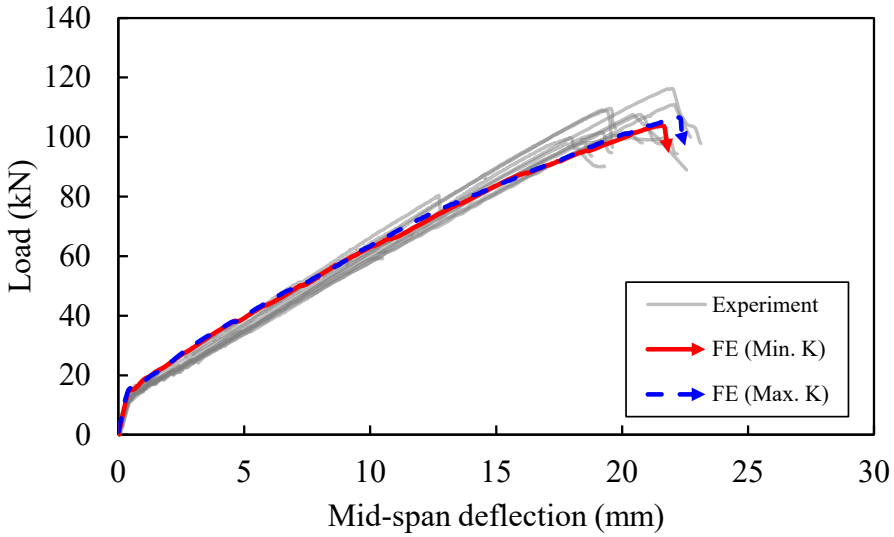


Fig. 7.1 Comparison of experimental and numerical load-midspan deflection curves for representative specimens

Fig. 7.2 compares the experimental crack patterns (obtained by DIC technique) of a selected beam specimen with that predicted by the FE modeling at the ultimate stage. Notably, the predicted failure mode is characterized by concrete crushing, consistent with the experimental observations. Additionally, the crack patterns generated by the FE model is similar to that detected during testing, and the localized crack formation can be accurately captured.

Based on the above discussions, it is reasonable to conclude that the proposed FE model, which incorporates simplified bond stiffness, can provide accurate predictions for the flexural performance of FRP-SSC beams in terms of load-deflection response and crack patterns.

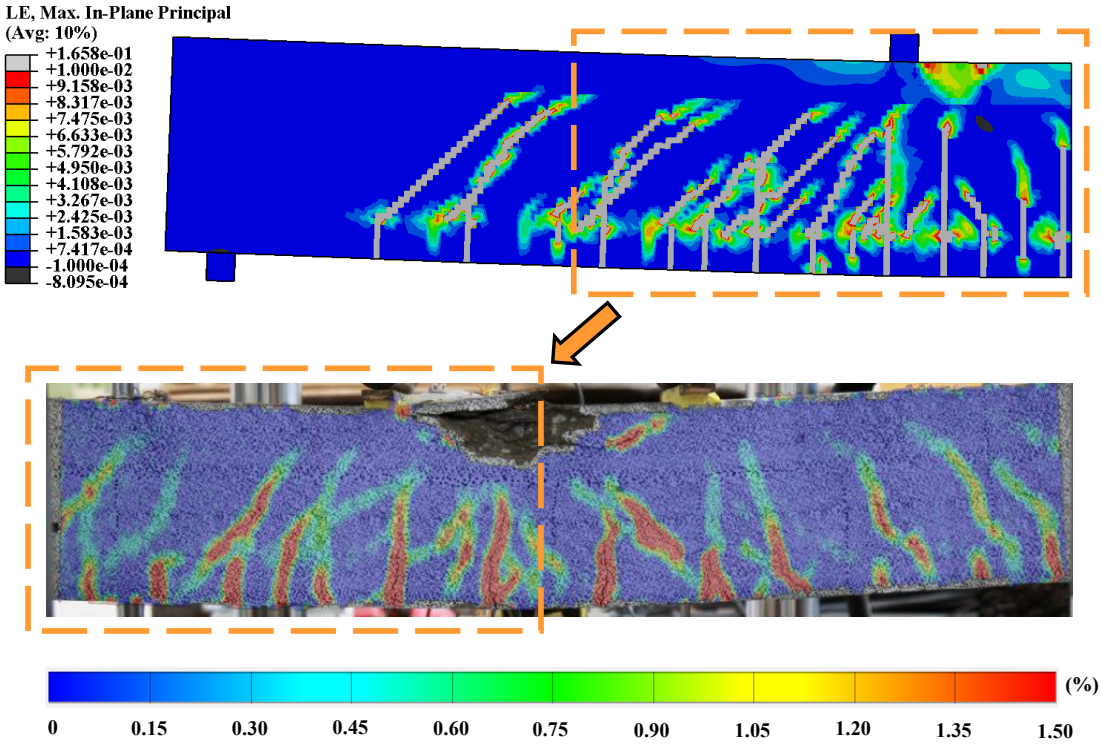


Fig. 7.2 Comparison of experimental and numerical crack patterns for a selected specimen

7.3 VERIFICATION OF FE MODEL FOR LONG-TERM FLEXURAL PERFORMANCE OF FRP-SSC BEAMS

In Chapter 5, a time-dependent bond stress-slip model for FRP bars in SSC was proposed based on the mBPE model using the test results of FRP-SSC bonded joints subjected to prolonged tidal exposure. By using such a time-dependent model, the ultimate bond strength τ_{max} and the corresponding loaded end slip s_m for a specific service life can be obtained. In this section, the test results of FRP-SSC beams exposed to real tidal conditions for up to four years were used to validate the accuracy of the proposed FE model, which incorporates such a time-dependent bond stress-slip model. Similar to the method presented in Section 7.2.3, the K values for beam specimens after 8, 12, 24, 37 and 48 months of field exposure in a tidal environment were determined to

be 60.76, 58.63, 55.12, 53.06 and 51.88, respectively, as per Table 5.5. Note that the 28-day cylindrical compressive strength of SSC was utilized for these specimens for the following three reasons: (1) No significant deterioration in concrete strength was observed over the field exposure period; (2) Preliminary numerical modeling of FRP-SSC beams subjected to marine environments indicated that variations in concrete strength had a limited effect on the numerical results compared to the influence of bond performance between the FRP bars and the surrounding SSC; (3) One of the primary objectives of this study is to develop a reliable FE model incorporating an accurate bond-slip relationship to predict the long-term performance of FRP-SSC beams based on the flexural behavior of unexposed (control) specimens, thereby reducing the need to explicitly account for concrete strength variations.

The experimental and numerical load-midspan deflection curves for FRP-SSC beam specimens with different exposure durations are depicted in Fig. 7.3, where the kinetic energy (an indicator of concrete crushing) obtained during modeling is also given. Clearly, the load-midspan deflection curves predicted by the proposed numerical modeling approach demonstrate satisfactory accuracy. Table 7.1 gives and Fig. 7.4 illustrates the predicted ultimate loads and the corresponding mid-span deflections for the specimens in comparison with the test results. It is obvious that the predicted ultimate loads for all the specimens are found to be close to the test values [Fig. 7.4(a)], with errors within the range of -0.71% to -4.09% (see Table 7.1). Additionally, the mid-span deflections at ultimate load of the specimens are also well predicted [the error ranged from -0.31% to -2.65% (see Table 7.1)], except for those with an exposure duration of eight months [Fig. 7.4(b)].

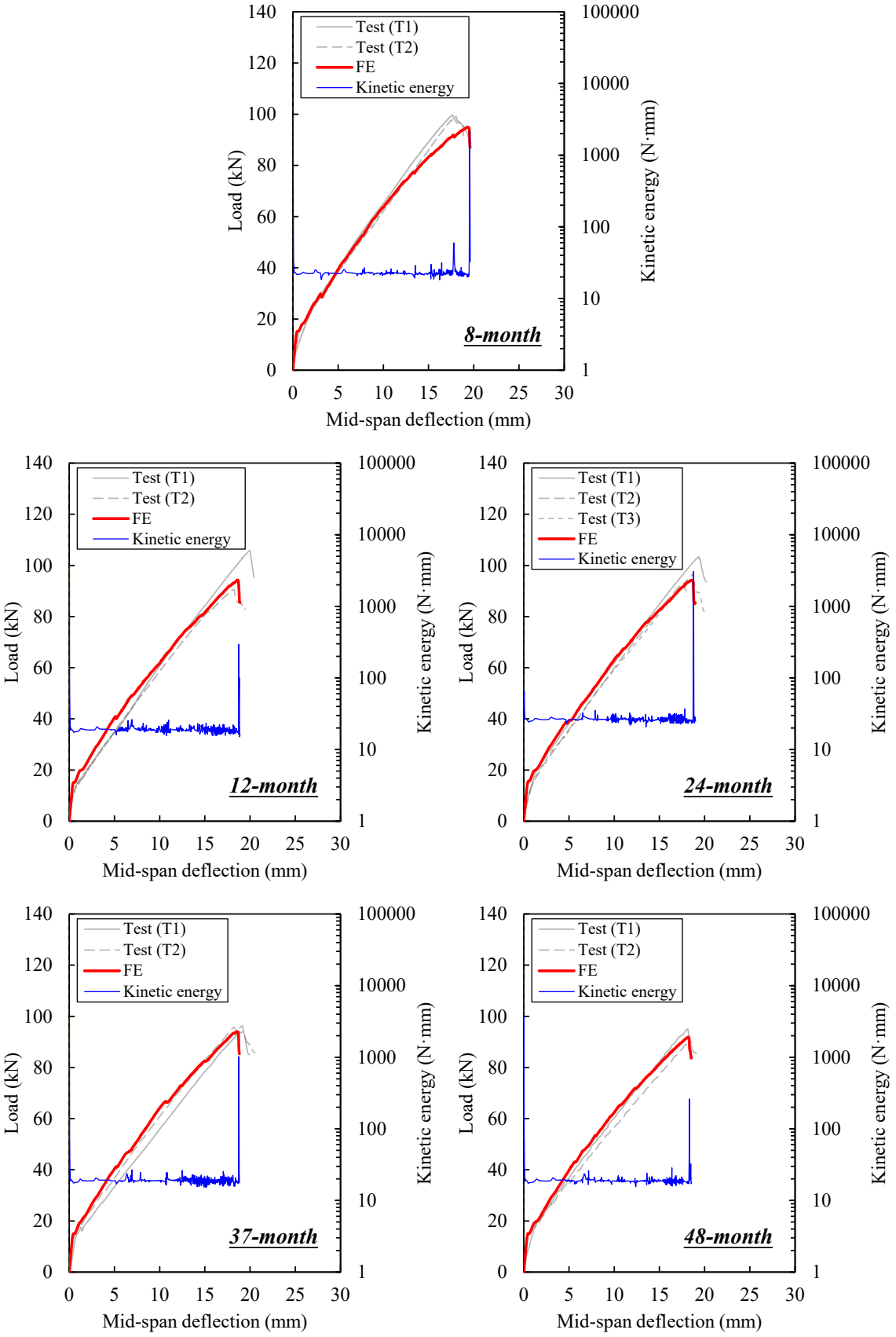
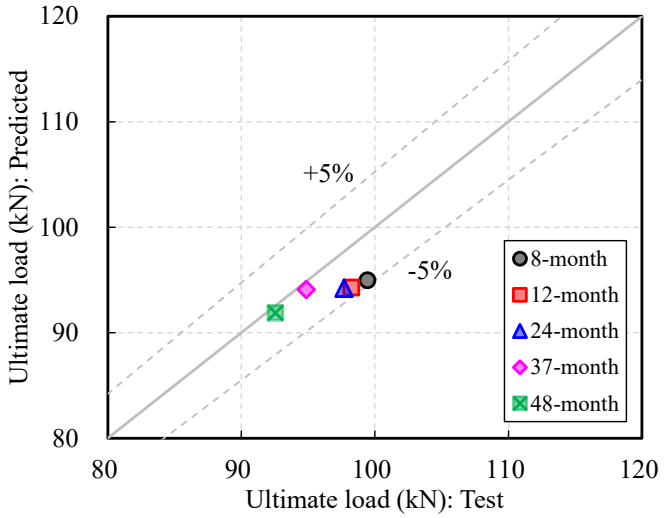


Fig. 7.3 Load-midspan deflection curves for specimens with different exposure durations: test results versus numerical predictions

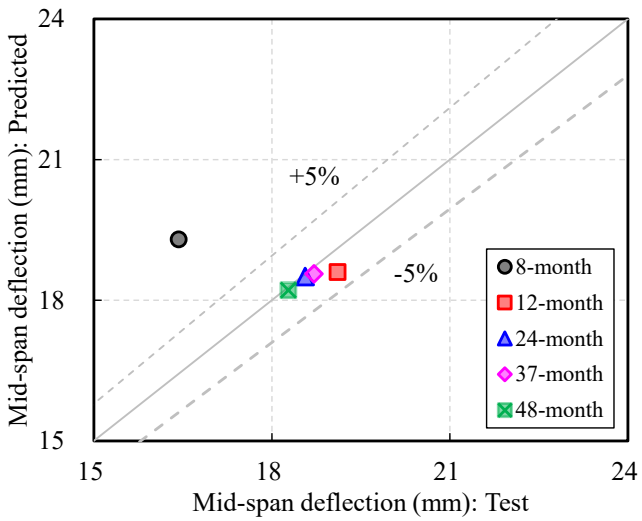
Table 7.1 Comparison between the test and predicted results

Exposure duration (month)	Ultimate load (kN)			Mid-span deflection (mm)		
	P_{test}	P_{pre}	$Error\ (P_{pre} - P_{test})/P_{test}$	δ_{test}	δ_{pre}	$Error\ (\delta_{pre} - \delta_{test})/\delta_{test}$
8	99.44	94.97	-4.49%	16.43	19.30	17.46%
12	98.24	94.29	-4.02%	19.11	18.60	-2.64%
24	97.69	94.23	-3.54%	18.56	18.50	-0.31%
37	94.86	94.09	-0.80%	18.71	18.56	-0.79%
48	92.54	91.89	-0.71%	18.28	18.22	-0.35%

Note: P_{test} = test ultimate load; P_{pre} = predicted ultimate load; δ_{test} = test midspan deflection at P_{test}; δ_{pre} = predicted midspan deflection at P_{pre}.



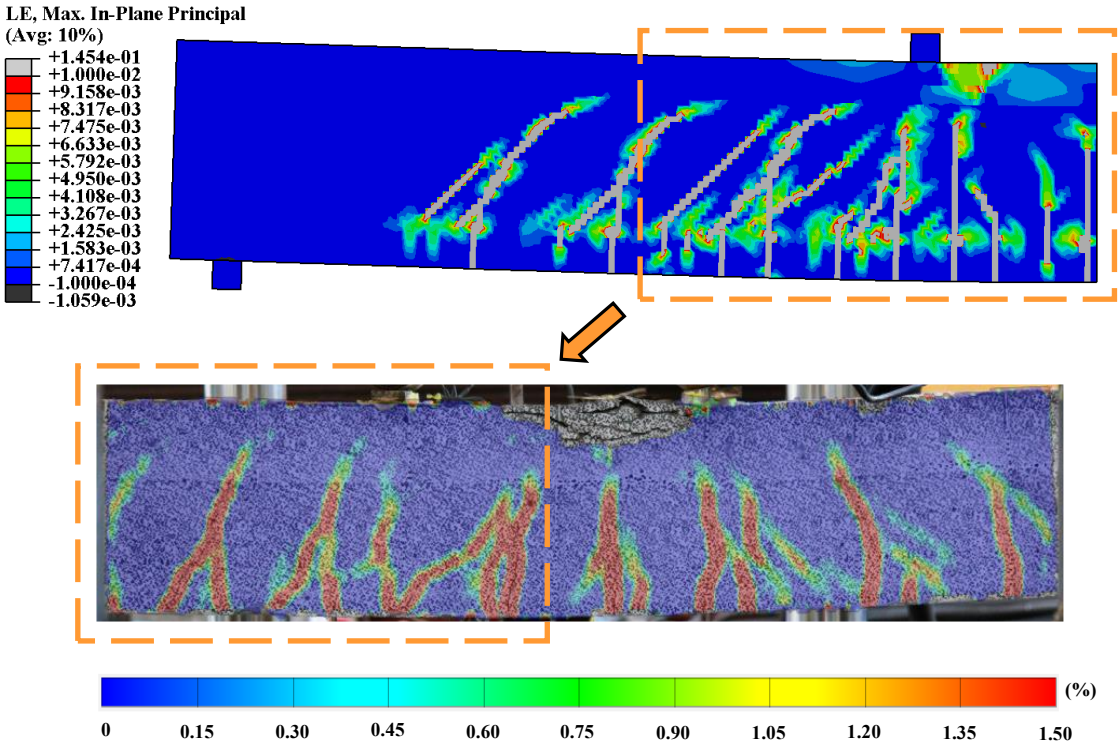
(a) Ultimate load



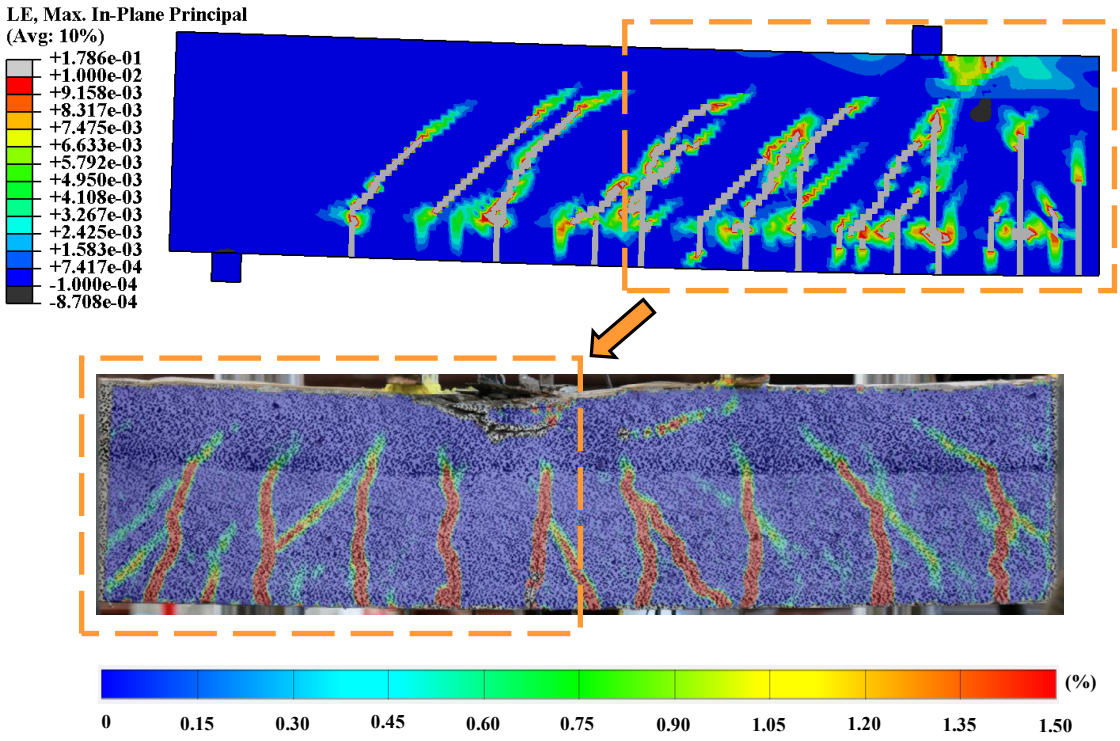
(b) Mid-span deflection

Fig. 7.4 Comparison between predicted and test results: ultimate load and the corresponding mid-span deflection

Fig .7.5 shows the performance of the proposed FE model in predicting the crack patterns of the test beam specimens (with exposure durations of 24 and 48months) at ultimate load, where the test observations detected using DIC technique are the same as those provided in Section 6.3.6. It is seen that the predicted major cracks are in reasonably good agreement with the test observations. However, the numerical results exhibit a greater number of distributed secondary cracks. This discrepancy may be attributed to the bond-slip relationship derived from direct pullout tests, which provides a localized characterization of the bond interface under controlled conditions but neglecting the contribution of the surrounding concrete to load and stress transfer, as well as the stress redistribution occurring under bending (Basaran and Kalkan 2020; Shakiba et al. 2023). Besides, the direct use of the bond stiffness derived from 10-mm GFRP-SSC bonded joints for the different-sized GFRP bars in FRP-SSC beams may also contribute to the above observation. Therefore, further research is needed to determine a more realistic bond stiffness for FE modeling. On the other hand, it is interesting to find that the crack number in specimens with degraded bond stiffness (Fig. 7.5) is relatively smaller than in their undegraded counterparts (Fig. 7.2), which is consistent with the experimental observations reported in Chapter 6.



(a) 24-month



(b) 48-month

Fig. 7.5 Comparisons between predicted and experimental crack patterns for FRP-SSC beam specimens with exposure durations of 24 and 48 months

7.4 CONCLUSIONS

This chapter presents a numerical study on the long-term flexural performance of FRP-SSC beams under tidal conditions. Simplified bond stiffness determined from pullout test results was proposed for FE modeling. The accuracy of the developed FE model considering the deterioration of bond stiffness was also verified. Based on the findings presented in this chapter, the following conclusions can be drawn:

(1) The proposed FE model that considers the bond-slip relationship with simplified bond stiffness for FRP bars in SSC was capable of providing reasonably accurate predictions of the flexural performance of unconditioned FRP-SSC beams in terms of load-deflection response and crack patterns.

(2) By considering the deterioration of bond stiffness between FRP bars and SSC, the proposed numerical approach effectively predicted the long-term flexural performance of FRP-SSC beams under tidal conditions.

(3) Compared to the test observations, the numerical crack patterns at the ultimate stage exhibited more secondary cracks, which is believed to be caused by the slight differences between the bond-slip relationship of GFRP bars in actual beams and in pullout specimens.

CHAPTER 8
CONCLUSIONS

8.1 INTRODUCTION

This thesis has presented an in-depth study spanning from material to component levels to explore the long-term performance of FRP bars and FRP-reinforced SSC beams after prolonged exposure to different marine environmental conditions. The investigation began with a comprehensive review and systematic analysis of AAT data to clarify the effects of various parameters on the durability of FRP bars, FRP bar-to-concrete bonded joints, and FRP-reinforced concrete beams. This foundational understanding was essential for assessing their long-term performance under real-world conditions. A key aspect of this research was the examination of the deterioration mechanisms affecting GFRP-SSC beams after prolonged exposure to marine environments, which was revealed by conducting a series of field exposure tests on GFRP bars, GFRP bar-to-SSC bonded joints, and GFRP-SSC beams. Furthermore, the establishment of a conversion relationship between AAT and FET results is a key to addressing the critical gap regarding the applicability of laboratory findings to real-world scenarios, which was achieved by the proposed refined prediction model for the long-term performance of GFRP bars. Finally, a time-dependent bond stress-slip model for GFRP bars in SSC was developed, and a numerical model for GFRP-SSC beams was established, with due consideration given to the bond stiffness deterioration. The following sections summarize the key findings and recommendations derived from this research.

8.2 LONG-TERM TENSILE PERFORMANCE OF GFRP BARS

The experimental investigation into the long-term tensile performance of GFRP bars aimed at providing critical insights into their durability when subjected to real marine environments. Two batches of GFRP bars with diameters of 6 mm and 10 mm were exposed to various marine environmental conditions (i.e., atmospheric, splash, tidal, and underwater zones) over a period of up to four years. Based on the experimental results presented in Chapter 3, along with a comprehensive review and systematic assessment of existing models, a refined prediction model was developed in Chapter 4. The following conclusions were drawn from these two chapters:

(1) The prolonged exposure to tidal and underwater conditions resulted in notable changes in physical appearance as well as tensile failure modes of the GFRP bars, with the failure modes changing from typical broom-shaped damage to more localized damage, primarily due to the internal defects induced by resin hydrolysis and cracking.

(2) Compared to the GFRP bars exposed in the atmospheric and splash zones, those conditioned in the tidal zone exhibited a significant decrease in tensile strength after 48 months, regardless of their diameter, while underwater conditions appeared to amplify the deterioration of tensile strength. In contrast, the elastic modulus of GFRP bars was less susceptible to marine environments.

(3) Larger GFRP bars demonstrated better resistance to the degradations of both tensile strength and elastic modulus compared to smaller bars under tidal conditions, indicating that the diameter influences the durability of GFRP bars.

(4) Compared to Arrhenius empirical model and *fib* Bulletin 40 (2007) model, Huang and Aboutaha's (2010) model demonstrated better predictive capability for the durability of GFRP bars based on the assembled FET database. The newly developed model, which incorporates a time-dependent correction factor to consider the additional effects of tidal conditions on bare GFRP bars, showed enhanced accuracy in predicting the long-term tensile performance of GFRP bars under tidal exposure. Meanwhile, Huang and Aboutaha's (2010) model remained applicable for bars subjected to atmospheric and splash conditions.

8.3 LONG-TERM BOND PERFORMANCE OF GFRP BARS IN SEAWATER SEA-SAND CONCRETE

Chapter 5 focused on the long-term bond performance of GFRP bars embedded in SSC through direct pullout tests conducted on two series of GFRP bar-to-SSC bonded joints after field exposure in four different marine environmental zones for up to four years. Based on the pullout test results, a bond stress-slip prediction model was proposed for GFRP bars in SSC. From the results and discussions presented in this chapter, the following conclusions were drawn:

(1) All pullout specimens exhibited shear damage at the fiber-resin interface as the failure mode, regardless of the varying exposure scenarios, suggesting that the bond properties were primarily governed by the interlaminar shear strength between the fibers and the resin matrix of the GFRP bars.

(2) The shapes of bond stress-slip curves remained largely unaffected by the field exposure to marine environments. However, the distinct surface treatments for the GFRP bars in the two series of pullout specimens resulted in apparently

different bond-slip behaviors, highlighting the influence of surface characteristics on bond performance.

(3) The bond strength of specimens exposed in different marine environmental zones showed minimal changes after prolonged field exposure, largely attributable to the durable interlaminar shear strength of the GFRP bars. However, specimens subjected to tidal conditions experienced a significant decrease in bond stiffness over time, with retention dropping to 63.75% after 48 months of exposure. This reduction is believed to be caused by the degradation of the external sand-coated layer and the deterioration of the interfacial properties between this layer and the resin matrix of the GFRP bars.

(4) Based on the modified BPE (mBPE) model, a bond stress-slip model incorporating two time-dependent factors was proposed. The ascending branches of the prediction curves closely aligned with the experimental results, demonstrating the effectiveness of the proposed model in predicting the long-term bond behavior of GFRP bars in SSC.

(5) The conclusions presented in this section may be only applicable to pullout specimens whose bond properties are mainly dominated by the fiber-resin interface of the GFRP bars. For specimens involving concrete of relatively low strength, additional experimental data are necessary to verify these conclusions.

8.4 LONG-TERM FLEXURAL PERFORMANCE OF GFRP-REINFORCED SEAWATER SEA-SAND CONCRETE BEAMS

The long-term flexural performance of two series of GFRP-SSC beams (both with and

without sustained load) were experimentally assessed after field exposure to various marine environmental conditions (i.e., atmospheric, splash, and tidal zones), as detailed in Chapter 6. Based on the experimental findings presented in Chapters 5 and 6, an FE model that incorporates the deterioration of bond stiffness between GFRP bars and SSC was introduced in Chapter 7. This model was developed to simulate the flexural performance of GFRP-SSC beams subjected to tidal conditions over specific durations. The key conclusions drawn from Chapters 6 and 7 are summarized as follows:

(1) Long-term field exposure did not affect the failure mode of the beam specimens with and without sustained load, which consistently failed by SSC crushing due to the relatively high FRP reinforcement ratio.

(2) The load-deflection behavior of the specimens remained stable after field exposure, regardless of the presence of sustained load. After accounting for the residual deflection in specimens subjected to sustained load, the load-midspan deflection curves were comparable across all specimens prior to concrete crushing.

(3) Specimens exposed to atmospheric and splash conditions exhibited no significant changes in flexural capacity (including both first peak load and ultimate load carrying capacity) throughout the exposure period, owing to the relatively mild environments, even under sustained loading conditions. In contrast, specimens subjected to tidal conditions experienced a noticeable reduction in load carrying capacity, which stabilized at approximately 90% of the original capacity after four years, resulting from the deterioration of bond stiffness between GFPR bars and the surrounding SSC.

(4) As a result of the degradation of bond performance of GFRP bars in SSC, specimens exposed to tidal conditions showed a significant increase in crack

widths, accompanied by a decrease in crack numbers.

(5) The developed FE model, which accounts for the deterioration of bond stiffness between FRP bars and SSC through the use of proposed time-dependent bond stress-slip model, demonstrated the capacity to provide reasonably accurate predictions of the long-term flexural performance of FRP-SSC beams under tidal conditions, particularly in terms of load-deflection responses and crack patterns.

8.5 FUTURE RESEARCH

This thesis has primarily focused on the long-term performance of FRP bars, FRP bar-to-SSC bonded joints and FRP-SSC beams after prolonged exposure to various marine environmental conditions, utilizing a wide range of experimental and analytical investigations. While the findings of the present research have provided an in-depth understanding of these fields, several important issues remain and require further research, as highlighted below:

(1) The present study examined only the long-term tensile performance of GFRP bars. Additional work is still needed to investigate other mechanical properties, such as interlaminar shear strength, transverse shear strength and flexural properties, to achieve a more comprehensive understanding of their durability. Furthermore, the size effect was identified as a critical factor influencing the durability of GFRP bars under tidal conditions, as discussed in Chapter 3. To clarify this issue, further experimental studies involving a broader range of bar diameters are recommended. Besides, the correction factor incorporated into the proposed prediction model in Chapter 4 was derived solely from the test results of 10-mm GFRP bars under tidal conditions. Therefore, both accelerated

aging tests and field exposure tests are necessary to develop a size-dependent prediction model for GFRP bars in marine environments.

(2) Developing quantitative formulas capable of accurately predicting the degradation behavior of the mechanical properties of FRP bars and the bond properties of FRP bars in concrete under various exposure conditions remain challenging without specifying bar characteristics (e.g., fiber type, fiber volume fraction, resin type, diameter, surface treatment) as well as the environmental exposure conditions. While the review in Chapter 2 and the databases presented in this study form a basis for such development, further research is needed to address this critical issue and to facilitate the effective design and practical application of FRP bars in concrete structures.

(3) Existing research has demonstrated that the long-term bond performance of FRP bar in concrete is closely correlated with their surface characteristics, a finding that was also validated in Chapter 5 of this thesis. Although the framework of the proposed time-dependent bond stress-slip model for GFRP bars (helically wrapped and sand-coated) in SSC can be extended to FRP bars with various surface treatments and concrete matrices, further research is highly worthwhile to develop a prediction model applicable to different scenarios.

(4) As discussed in Chapter 7, the direct use of bond stiffness obtained from the pullout tests of FRP bars in SSC for numerical modeling of FRP-SSC beams may result in discrepancies in crack patterns, indicating the need for further investigations in this field. Additionally, to systematically investigate the influence of critical variables on the performance of the FE model and enhance the understanding of key factors affecting the structural response of FRP-SSC

beams, comprehensive parametric studies are needed. These studies potentially provide deeper insights into parameter sensitivities and guide the optimization of design and modeling approaches.

(5) The development of multi-factor coupling models that integrate environmental, mechanical, and temporal variables is essential to more accurately capture the complex interactions affecting FRP-SSC systems. In addition, establishing a multiscale framework that links material degradation mechanisms to overall structural performance is recommended to achieve a more comprehensive understanding of durability. Furthermore, the exploration of probabilistic prediction tools is suggested to enhance the reliability and broaden the applicability of durability assessments.

REFERENCES

ABAQUS (2021). ABAQUS Analysis User's Manual (Version 2021), Dassault.

Achillides, Z., and Pilakoutas, K. (2004). "Bond behavior of fiber reinforced polymer bars under direct pullout conditions." *Journal of Composites for Construction*. 8(2): 173-181.

Achillides, Z., and Pilakoutas, K. (2006). "FE modelling of bond interaction of FRP bars to concrete." *Structural Concrete*. 7(1): 7-16.

ACI. (2012). *Guide Test Methods for Fiber-Reinforced Polymers (FRPs) for Reinforcing or Strengthening Concrete Structures*. ACI 440.3R-12. MI, USA: Farmington Hills.

ACI. (2015). *Guide for the Design and Construction of Structural Concrete Reinforced with Fiber-Reinforced Polymer (FRP) Bars*. ACI 440.1R-15. MI, USA: Farmington Hills.

ACI. (2017). *Specification for Carbon and Glass Fiber-Reinforced Polymer Bar Materials for Concrete Reinforcement*. ACI 440. 6M-08. MI, USA: Farmington Hills.

ACI. (2019). *Building Code Requirements for Structural Concrete*. ACI 318-19. MI, USA: Farmington Hills.

ACI. (2022). *Building Code Requirements for Structural Concrete Reinforced with Glass Fiber-Reinforced Polymer (GFRP) Bars—Code and Commentary*. ACI 440.11-22. MI, USA: Farmington Hills.

Al-Khafaji, A. F., Haluza, R. T., Benzecry, V., Myers, J. J., Bakis, C. E., and Nanni, A.

(2021). "Durability assessment of 15- to 20-year-old GFRP bars extracted from bridges in the US. II: GFRP bar assessment." *Journal of Composites for Construction*. 25(2): 04021008.

Al-Salloum, Y. A., El-Gamal, S., Almusallam, T. H., Alsayed, S. H., and Aqel, M. (2013). "Effect of harsh environmental conditions on the tensile properties of GFRP bars." *Composites Part B: Engineering*. 45(1): 835-844.

Al-Zahrani, M. M. (2024). "Durability of concrete-embedded GFRP bars after 20 years of tidal zone exposure: Correlation with accelerated aging tests." *Case Studies in Construction Materials*. 21: e03435.

Al-Zahrani, M. M., Al-Dulaijan, S. U., Sharif, A., and Maslehuddin, M. (2002). "Durability performance of glass fiber reinforced plastic reinforcement in harsh environments." *6th Saudi engineering conference*. 3: 307-319.

Ali, A. H., Mohamed, H. M., and Benmokrane, B. (2020). "Bar size effect on long-term durability of sand-coated basalt-FRP composite bars." *Composites Part B: Engineering*. 195: 108059.

Ali, A. H., Mohamed, H. M., Benmokrane, B., ElSafty, A., and Chaallal, O. (2019). "Durability performance and long-term prediction models of sand-coated basalt FRP bars." *Composites Part B: Engineering*. 157: 248-258.

Almusallam, T. H., and Al-Salloum, Y. A. (2006). "Durability of GFRP rebars in concrete beams under sustained loads at severe environments." *Journal of Composite Materials*. 40(7): 623-637.

Almusallam, T. H., Al-Salloum, Y. A., Alsayed, S. H., El-Gamal, S., and Aqel, M. (2013). "Tensile properties degradation of glass fiber-reinforced polymer bars embedded in concrete under severe laboratory and field environmental

conditions." *Journal of Composite Materials*. 47(4): 393-407.

Altalmas, A., El Refai, A., and Abed, F. (2015). "Bond degradation of basalt fiber-reinforced polymer (BFRP) bars exposed to accelerated aging conditions." *Construction and Building Materials*. 81: 162-171.

Antonietta Aiello, M., Leone, M., and Pecce, M. (2007). "Bond performances of FRP rebars-reinforced concrete." *Journal of Materials in Civil Engineering*. 19(3): 205-213.

Arczewska, P., Polak, M. A., and Penlidis, A. (2021). "Degradation of glass fiber reinforced polymer (GFRP) bars in concrete environment." *Construction and Building Materials*. 293: 123451.

Ashrafi, H., Bazli, M., Vatani Oskouei, A., and Bazli, L. (2018). "Effect of sequential exposure to UV radiation and water vapor condensation and extreme temperatures on the mechanical properties of GFRP bars." *Journal of Composites for Construction*. 22(1): 04017047.

ASTM. (2014). *Standard Test Method for Flexural Properties of Fiber Reinforced Pultruded Plastic Rods*. ASTM D4476-14. West Conshohocken, PA.

ASTM. (2016a). *Standard Test Method for Apparent Horizontal Shear Strength of Pultruded Reinforced Plastic Rods By the Short-Beam Method*. ASTM D4475-02. West Conshohocken, PA.

ASTM. (2016b). *Standard Test Method for Tensile Properties of Pultruded Glass-Fiber-Reinforced Plastic Rod*. ASTM D3916-08. West Conshohocken, PA.

ASTM. (2017). *Standard Test Method for Transverse Shear Strength of Fiber-Reinforced Polymer Matrix Composite Bars*. ASTM D7617-11. West

Conshohocken, PA.

ASTM. (2020). *Standard Test Method for Bond Strength of Fiber-Reinforced Polymer Matrix Composite Bars to Concrete by Pullout Testing*. ASTM D7913-14. West Conshohocken, PA.

ASTM. (2021). *Standard Test Method for Tensile Properties of Fiber Reinforced Polymer Matrix Composite Bars*. ASTM D7205-21. West Conshohocken, PA.

ASTM. (2022). *Standard Specification for Solid Round Glass Fiber Reinforced Polymer Bars for Concrete Reinforcement*. ASTM D7957-22. West Conshohocken, PA.

ASTM. (2024). *Standard Specification for Portland Cement*. ASTM C150-22. West Conshohocken, PA.

Baena, M., Torres, L., Turon, A., and Barris, C. (2009). "Experimental study of bond behaviour between concrete and FRP bars using a pull-out test." *Composites Part B: Engineering*. 40(8): 784-797.

Bakis, C. E., Boothby, T. E., and Jia, J. (2007). "Bond durability of glass fiber-reinforced polymer bars embedded in concrete beams." *Journal of Composites for Construction*. 11(3): 269-278.

Bakis, C. E., Boothby, T. E., Schaut, R. A., and Pantano, C. G. (2005). "Tensile strength of GFRP bars under sustained loading in concrete beams." *7th International Symposium of the Fiber-Reinforced Polymer Reinforcement for Reinforced Concrete Structures (FRPRCS-7)*, Kansas City, Missouri. 230: 1429-1446.

Bank, L. C., Gentry, T. R., Thompson, B. P., and Russell, J. S. (2003). "A model specification for FRP composites for civil engineering structures." *Construction*

and Building Materials. 17(6-7): 405-437.

Bank, L. C., Puterman, M., and Katz, A. (1998). "The effect of material degradation on bond properties of fiber reinforced plastic reinforcing bars in concrete." *ACI Materials Journal*. 95(3).

Basaran, B., and Kalkan, I. (2020). "Investigation on variables affecting bond strength between FRP reinforcing bar and concrete by modified hinged beam tests." *Composite Structures*. 242: 112185.

Bažant, Z. P., and Planas, J. (1997). *Fracture and Size Effect in Concrete and Other Quasibrittle Materials*. CRC press.

Bazli, M., Ashrafi, H., and Oskouei, A. V. (2017). "Experiments and probabilistic models of bond strength between GFRP bar and different types of concrete under aggressive environments." *Construction and Building Materials*. 148: 429-443.

Benmokrane, B., Ali, A., and Mohamed, H. (2016). "Microstructural characterization and durability of GFRP reinforcing bars exposed to concrete environment and saline solution." *International Workshop on Seawater Sea-Sand Concrete (SSC) Structures Reinforced with FRP Composites*, The Hong Kong Polytechnic University.

Benmokrane, B., Ali, A. H., Mohamed, H. M., ElSafty, A., and Manalo, A. (2017a). "Laboratory assessment and durability performance of vinyl-ester, polyester, and epoxy glass-FRP bars for concrete structures." *Composites Part B: Engineering*. 114: 163-174.

Benmokrane, B., Brown, V. L., Ali, A. H., Mohamed, K., and Shield, C. (2020a). "Reconsideration of the environmental reduction factor CE for GFRP reinforcing bars in concrete structures." *Journal of Composites for Construction*. 24(4):

06020001.

Benmokrane, B., Elgabbas, F., Ahmed Ehab, A., and Cousin, P. (2015). "Characterization and comparative durability study of glass/vinylester, basalt/vinylester, and basalt/epoxy FRP bars." *Journal of Composites for Construction*. 19(6): 04015008.

Benmokrane, B., Hassan, M., Robert, M., Vijay, P. V., and Manalo, A. (2020b). "Effect of different constituent fiber, resin, and sizing combinations on alkaline resistance of basalt, carbon, and glass FRP bars." *Journal of Composites for Construction*. 24(3): 04020010.

Benmokrane, B., Manalo, A., Bouhet, J.-C., Mohamed, K., and Robert, M. (2017b). "Effects of diameter on the durability of glass fiber–reinforced polymer bars conditioned in alkaline solution." *Journal of Composites for Construction*. 21(5): 04017040.

Benmokrane, B., Nazair, C., Loranger, M.-A., and Manalo, A. (2018). "Field durability study of vinyl-ester–based GFRP rebars in concrete bridge barriers." *Journal of Bridge Engineering*. 23(12): 04018094.

Benmokrane, B., Robert, M., Mohamed, H. M., Ali, A. H., and Cousin, P. (2017c). "Durability assessment of glass FRP solid and hollow bars (rock bolts) for application in ground control of Jurong rock caverns in Singapore." *Journal of Composites for Construction*. 21(3): 06016002.

Benmokrane, B., Wang, P., Ton-That Tan, M., Rahman, H., and Robert, J.-F. (2002). "Durability of glass fiber-reinforced polymer reinforcing bars in concrete environment." *Journal of Composites for Construction*. 6(3): 143-153.

Benzecry, V., Al-Khafaji, A. F., Haluza, R. T., Bakis, C. E., Myers, J. J., and Nanni, A.

(2021). "Durability assessment of 15- to 20-year-old GFRP bars extracted from bridges in the US. I: Selected bridges, bar extraction, and concrete assessment." *Journal of Composites for Construction*. 25(2): 04021007.

Bui, L. V. H., Stitmannaithum, B., and Ueda, T. (2018). "Ductility of concrete beams reinforced with both fiber-reinforced polymer and steel tension bars." *Journal of Advanced Concrete Technology*. 16(11): 531-548.

Buyukkaragoz, A., Kalkan, I., and Lee, J. H. (2013). "A numerical study of the flexural behavior of concrete beams reinforced with AFRP bars." *Strength of Materials*. 45(6): 716-729.

Carvelli, V., Pisani, M. A., and Poggi, C. (2013). "High temperature effects on concrete members reinforced with GFRP rebars." *Composites Part B: Engineering*. 54: 125-132.

CEB-FIP. (1993). *CEB-FIP Model Code 90*. London, UK.

Chang, Y., Wang, Y., Li, B., Wang, M., Zhou, Z., and Ou, J. (2022). "GFRP bar-reinforced seawater sea-sand concrete beam under the combined influence of seawater exposure and sustained load: Durability and degradation mechanism." *Structures*. 43: 1503-1515.

Chang, Y. F., Wang, Y. L., Wang, M. F., Zhou, Z., and Ou, J. P. (2021). "Bond durability and degradation mechanism of GFRP bars in seawater sea-sand concrete under the coupling effect of seawater immersion and sustained load." *Construction and Building Materials*. 307: 124878.

Chen, G. M. (2010). "Behaviour and Strength of RC Beams Shear-Strengthened with Externally Bonded FRP Reinforcement." PhD Thesis, The Hong Kong Polytechnic University, Hong Kong.

Chen, G. M., Liu, P. C., Jiang, T., He, Z. B., Wang, X. M., Lam, L., and Chen, J. F. (2020). "Effects of natural seawater and sea sand on the compressive behaviour of unconfined and carbon fibre-reinforced polymer-confined concrete." *Advances in Structural Engineering*. 23(14): 3102-3116.

Chen, G. M., Teng, J. G., and Chen, J. F. (2011). "Finite-element modeling of intermediate crack debonding in FRP-plated RC beams." *Journal of Composites for Construction*. 15(3): 339-353.

Chen, G. M., Teng, J. G., Chen, J. F., and Xiao, Q. G. (2015). "Finite element modeling of debonding failures in FRP-strengthened RC beams: A dynamic approach." *Computers & Structures*. 158: 167-183.

Chen, Y., Davalos, J. F., and Ray, I. (2006). "Durability prediction for GFRP reinforcing bars using short-term data of accelerated aging tests." *Journal of Composites for Construction*. 10(4): 279-286.

Chen, Y., Davalos, J. F., Ray, I., and Kim, H. Y. (2007). "Accelerated aging tests for evaluations of durability performance of FRP reinforcing bars for concrete structures." *Composite Structures*. 78(1): 101-111.

Chen, Z., Li, S., Zhou, J., Xu, R., and Dai, S. (2022). "Flexural behavior of GFRP bars reinforced seawater sea sand concrete beams exposed to marine environment: Experimental and numerical study." *Construction and Building Materials*. 349: 128784.

Cosenza, E., Manfredi, G., and Realfonzo, R. (1995). "Analytical modelling of bond between FRP reinforcing bars and concrete." *2nd Int. RILEM Symp. (FRPRCS-2)*.

Cosenza, E., Manfredi, G., and Realfonzo, R. (1996). "Bond characteristics and anchorage length of FRP rebars." *2nd International Conference on Advanced*

Composite Materials in Bridges and Structures.

Cosenza, E., Manfredi, G., and Realfonzo, R. (1997). "Behavior and modeling of bond of FRP rebars to concrete." *Journal of Composites for Construction*. 1(2): 40-51.

CSA. (2019). *Specification for Fibre-Reinforced Polymers*. CSA S807-19. Canada.

CSA. (2021). *Design and Construction of Building Components with Fiber-Reinforced Polymers*. CSA S806-12. Canada.

D'Antino, T., Bertolli, V., Pisani, M. A., and Poggi, C. (2023). "Tensile and interlaminar shear behavior of thermoset and thermoplastic GFRP bars exposed to alkaline environment." *Journal of Building Engineering*. 72: 106581.

Da Silva, L. V., Da Silva, F. W., Tarpani, J. R., De Camargo Forte, M. M., and Amico, S. C. (2016). "Ageing effect on the tensile behavior of pultruded CFRP rods." *Materials and Design*. 110: 245-254.

Dang, H. V., and Phan, D. N. (2021). "Experimental investigation and analysis of pure bending plastic hinge zone in hybrid beams reinforced with high reinforcement ratio under static loads." *European Journal of Environmental and Civil Engineering*(6): 1-23.

Davalos, J. F., Chen, Y., and Ray, I. (2008). "Effect of FRP bar degradation on interface bond with high strength concrete." *Cement and Concrete Composites*. 30(8): 722-730.

Davalos, J. F., Chen, Y., and Ray, I. (2011). "Long-term durability prediction models for GFRP bars in concrete environment." *Journal of Composite materials*. 46(16): 1899-1914.

Debaiky Ahmed, S., Nkurunziza, G., Benmokrane, B., and Cousin, P. (2006). "Residual

tensile properties of GFRP reinforcing bars after loading in severe environments." *Journal of Composites for Construction*. 10(5): 370-380.

Dejke, V., and Tepfers, R. (2001). "Durability and service life prediction of GFRP for concrete reinforcement." *Proc., 5th Int. Symp. on Fiber Reinforced Polymers for Reinforced Concrete Structures (FRPRCS-5)*, Thomas Telford, Cambridge, U.K. 2: 505-516.

Dong, Z., and Wu, G. (2019). "Research progress on durability of FRP bars reinforced concrete structures." *China Civil Engineering Journal*. 52: 1-19.

Dong, Z., Wu, G., and Lian, J. (2018a). "Experimental study on the durability of FRP bars reinforced concrete beams in simulated ocean environment." *Science and Engineering of Composite Materials*. 25(6): 1123-1134.

Dong, Z., Wu, G., Xu, B., Wang, X., and Taerwe, L. (2016a). "Bond durability of BFRP bars embedded in concrete under seawater conditions and the long-term bond strength prediction." *Materials and Design*. 92: 552-562.

Dong, Z., Wu, G., and Xu, Y. (2016b). "Experimental study on the bond durability between steel-FRP composite bars (SFCBs) and sea sand concrete in ocean environment." *Construction and Building Materials*. 115: 277-284.

Dong, Z., Wu, G., and Xu, Y. (2017a). "Bond and flexural behavior of sea sand concrete members reinforced with hybrid steel-composite bars presubjected to wet–dry cycles." *Journal of Composites for Construction*. 21(2): 04016095.

Dong, Z., Wu, G., Zhao, X.-L., and Wang, Z.-K. (2017b). "A refined prediction method for the long-term performance of BFRP bars serviced in field environments." *Construction and Building Materials*. 155: 1072-1080.

Dong, Z., Wu, G., Zhao, X. L., Zhu, H., and Lian, J. (2018b). "Bond durability of steel-FRP composite bars embedded in seawater sea-sand concrete under constant bending and shearing stress." *Construction and Building Materials*. 192: 808-817.

Dong, Z., Wu, G., Zhao, X. L., Zhu, H., and Lian, J. L. (2018c). "Durability test on the flexural performance of seawater sea-sand concrete beams completely reinforced with FRP bars." *Construction and Building Materials*. 192: 671-682.

Dong, Z., Wu, G., Zhao, X. L., Zhu, H., and Lian, J. L. (2020). "The durability of seawater sea-sand concrete beams reinforced with metal bars or non-metal bars in the ocean environment." *Advances in Structural Engineering*. 23(2): 334-347.

Duo, Y., Liu, X., Liu, Y., Tafsirojjaman, T., and Sabbrojjaman, M. (2021). "Environmental impact on the durability of FRP reinforcing bars." *Journal of Building Engineering*. 43: 102909.

El-Hassan, H., El-Maaddawy, T., Al-Sallamin, A., and Al-Saidy, A. (2017). "Performance evaluation and microstructural characterization of GFRP bars in seawater-contaminated concrete." *Construction and Building Materials*. 147: 66-78.

El-Hassan, H., El-Maaddawy, T., Al-Sallamin, A., and Al-Saidy, A. (2018). "Durability of glass fiber-reinforced polymer bars conditioned in moist seawater-contaminated concrete under sustained load." *Construction and Building Materials*. 175: 1-13.

El-Nemr, A., Ahmed, E. A., Barris, C., Joyklad, P., Hussain, Q., and Benmokrane, B. (2023). "Bond performance of fiber reinforced polymer bars in normal- and high-strength concrete." *Construction and Building Materials*. 393: 131957.

El-Nemr, A., Ahmed, E. A., El-Safty, A., and Benmokrane, B. (2018). "Evaluation of the flexural strength and serviceability of concrete beams reinforced with different

types of GFRP bars." *Engineering Structures*. 173: 606-619.

El Refai, A., Abed, F., and Altalmas, A. (2015). "Bond durability of basalt fiber-reinforced polymer bars embedded in concrete under direct pullout conditions." *Journal of Composites for Construction*. 19(5).

Elgabbas, F., Ahmed, E. A., and Benmokrane, B. (2017). "Flexural behavior of concrete beams reinforced with ribbed basalt-FRP bars under static loads." *Journal of Composites for Construction*. 21(3): 04016098.

Esmaeili, Y., Eslami, A., Newhook, J., and Benmokrane, B. (2020). "Performance of GFRP-reinforced concrete beams subjected to high-sustained load and natural aging for 10 years." *Journal of Composites for Construction*. 24(5): 04020054.

Feng, G., Guo, S., Zhou, L., Luo, W., Guo, X., Jin, Z., and Zhu, D. (2024a). "Effects of surface characteristics and alkalinity on the deterioration of BFRP bars and BFRP-SSC interface in seawater environment." *Composites Part B: Engineering*. 268: 111072.

Feng, G., Zhu, D., Guo, S., Rahman, M. Z., Jin, Z., and Shi, C. (2022). "A review on mechanical properties and deterioration mechanisms of FRP bars under severe environmental and loading conditions." *Cement and Concrete Composites*. 134: 104758.

Feng, G., Zhu, D., Guo, S., Rahman, M. Z., Ma, W., Yi, Y., Jin, Z., and Shi, C. (2023). "A comparative study of bare and seawater sea sand concrete wrapped basalt fiber-reinforced polymer bars exposed to laboratory and real marine environments." *Construction and Building Materials*. 371: 130764.

Feng, Q., Visintin, P., and Oehlers, D. J. (2016). "Deterioration of bond–slip due to corrosion of steel reinforcement in reinforced concrete." *Magazine of Concrete*

Research. 68(15): 768-781.

Feng, S.-Z., Zeng, J.-J., Zhao, B., Hao, Z.-H., Zhuge, Y., Zhong, Q.-M., and Zhang, Z.-W. (2024b). "Accelerated aging tests of large-diameter GFRP bars in alkaline environment." *Composites Part C: Open Access*. 14: 100486.

Fergani, H., Di Benedetti, M., Miàs Oller, C., Lynsdale, C., and Guadagnini, M. (2018a). "Durability and degradation mechanisms of GFRP reinforcement subjected to severe environments and sustained stress." *Construction and Building Materials*. 170: 637-648.

Fergani, H., Di Benedetti, M., Miàs Oller, C., Lynsdale, C., and Guadagnini, M. (2018b). "Long-term performance of GFRP bars in concrete elements under sustained load and environmental actions." *Composite Structures*. 190: 20-31.

fib. (2007). *FRP Reinforcement in RC Structures*. *fib* Bulletin 40. Lausanne, Switzerland.

GB/T. (2011). *Fiber Reinforced Composite Bars for Civil Engineering*. GB/T 26743-11. Beijing.

GB/T. (2019). *Standard for Test Methods of Concrete Physical and Mechanical Properties*. GB/T 50081. Beijing.

GB/T. (2022). *Sand for Construction*. GB/T 14684. Beijing.

Gooranorimi, O., and Nanni, A. (2017). "GFRP reinforcement in concrete after 15 years of service." *Journal of Composites for Construction*. 21(5): 04017024.

Hao, Z. H. (2024). "Durability of FRP reinforced seawater seasand concrete beams and FRP-strengthened reinforced concrete beams." PhD Thesis, The Hong Kong Polytechnic University, Hong Kong.

Haskett, M., Oehlers, D. J., and Mohamed Ali, M. S. (2008). "Local and global bond characteristics of steel reinforcing bars." *Engineering Structures*. 30(2): 376-383.

Hassan, M., Benmokrane, B., ElSafty, A., and Fam, A. (2016). "Bond durability of basalt-fiber-reinforced-polymer (BFRP) bars embedded in concrete in aggressive environments." *Composites Part B: Engineering*. 106: 262-272.

He, X., Dai, L., and Yang, W. (2017). "Durability and degradation mechanism of GFRP bars embedded in concrete beams with cracks." *Plastics, Rubber and Composites*. 46(1): 17-24.

Hilber, H. (1976). "Analysis and design of numerical integration methods in structural dynamics." *Report no EERC 76-79*, College of Engineering, University of California, Berkeley (California).

Hu, X., Xue, W., Xue, W., and Jiang, J. (2023). "Bond strength of sand-coated deformed GFRP bars in UHPC, HPC, and NC." *Construction and Building Materials*. 403: 133175.

Huang, B., Zhu, J., Weng, K., Li, V. C., and Dai, J. (2022). "Ultra-high-strength engineered/strain-hardening cementitious composites (ECC/SHCC): Material design and effect of fiber hybridization." *Cement and Concrete Composites*. 129.

Huang, J., and Aboutaha, R. (2010). "Environmental reduction factors for GFRP bars used as concrete reinforcement: New scientific approach." *Journal of Composites for Construction*. 14(5): 479-486.

Huang, J. W. (2011). "Durability of glass fiber reinforced polymer (GFRP) bar used as concrete reinforcement: Temperature effect." *Applied Mechanics and Materials*. 94: 1573-1576.

Issa, M. S., Metwally, I. M., and Elzeiny, S. M. (2011). "Influence of fibers on flexural behavior and ductility of concrete beams reinforced with GFRP rebars." *Engineering Structures*. 33(5): 1754-1763.

Jahani, M., Moradi, S., and Shahnoori, S. (2023). "4-year monitoring of degradation mechanisms of seawater sea-sand concrete exposed to tidal conditions: development of chemical composition and micro-performance." *Construction and Building Materials*. 409.

Januš, O., Girgle, F., Rozsypalova, I., Kostiha, V., Prokeš, J., Štěpánek, P., and Čairović, Đ. (2022). "Influence of test parameters on the interlaminar shear strength of FRP bars." *Composite Structures*. 299: 116061.

Jendele, L., and Cervenka, J. (2006). "Finite element modelling of reinforcement with bond." *Computers & Structures*. 84(28): 1780-1791.

JGJ. (2006). *Standard for Technical Requirements and Tests Method of Sand and Crushed Stone (or Gravel) for Ordinary Concrete*. JGJ 52. Beijing.

JGJ/T. (2016). *Technical Specification for Testing Concrete Strength with Drilled Core Method*. JGJ/T 384. Beijing.

Johnson, D. T., and Sheikh, S. A. (2013). "Performance of bent stirrup and headed glass fibre reinforced polymer bars in concrete structures." *Canadian Journal of Civil Engineering*. 40(11): 1082-1090.

JSCE. (1995a). *Recommendations for Design and Construction of Concrete Structures Using Continuous Fiber Reinforced Materials*. JSCE E531-95. Tokyo, Japan.

JSCE. (1995b). *Test Method for Bond Strength of Continuous Fiber Reinforcing Materials by Pull-Out Testing*. JSCE-E539. Tokyo, Japan.

Kamal, A. S. M., and Boulfiza, M. (2011). "Durability of GFRP rebars in simulated concrete solutions under accelerated aging conditions." *Journal of Composites for Construction*. 15: 473-481.

Kazemi, H., Yekrangnia, M., Shakiba, M., Bazli, M., and Vatani Oskouei, A. (2022). "Bond-slip behaviour between GFRP/steel bars and seawater concrete after exposure to environmental conditions." *Engineering Structures*. 268: 114796.

Ke, L. Y. W., Wang, P., and Leung, C. K. Y. (2024). "Early-age microstructure and hydrothermal-aged bond performance at glass fiber reinforced polymer (GFRP) bar - seawater sea-sand concrete (SWSSC) interface." *Construction and Building Materials*. 433: 136709.

Khanfour, M.-A., and El Refai, A. (2017). "Effect of freeze-thaw cycles on concrete reinforced with basalt-fiber reinforced polymers (BFRP) bars." *Construction and Building Materials*. 145: 135-146.

Khatibmasjedi, M., Ramanathan, S., Suraneni, P., and Nanni, A. (2020). "Durability of commercially available GFRP reinforcement in seawater-mixed concrete under accelerated aging conditions." *Journal of Composites for Construction*. 24(4): 04020026.

Kim, H.-Y., Park, Y.-H., You, Y.-J., and Moon, C.-K. (2008). "Short-term durability test for GFRP rods under various environmental conditions." *Composite Structures*. 83(1): 37-47.

Kocaoz, S., Samaranayake, V. A., and Nanni, A. (2005). "Tensile characterization of glass FRP bars." *Composites Part B: Engineering*. 36(2): 127-134.

Kwon, S. J., Lee, H. S., Karthick, S., Saraswathy, V., and Yang, H. M. (2017). "Long-term corrosion performance of blended cement concrete in the marine

environment–A real-time study." *Construction and Building Materials*. 154: 349-360.

Kychkin, A. K., Gavrilieva, A. A., Vasilieva, A. A., Kychkin, A. A., Lebedev, M. P., and Sivtseva, A. V. (2021). "Assessment of extremely cold subarctic climate environment destruction of the basalt fiber reinforced epoxy (BFRE) rebar using its moisture uptake kinetics." *Polymers*. 13(24).

Laoubi, K., El-Salakawy, E., and Benmokrane, B. (2006). "Creep and durability of sand-coated glass FRP bars in concrete elements under freeze/thaw cycling and sustained loads." *Cement and Concrete Composites*. 28(10): 869-878.

Lee, J. Y., Kim, T. Y., Kim, T. J., Yi, C. K., Park, J. S., You, Y. C., and Park, Y. H. (2008). "Interfacial bond strength of glass fiber reinforced polymer bars in high-strength concrete." *Composites Part B: Engineering*. 39(2): 258-270.

Lee, J. Y., Yi, C. K., Cheong, Y. G., and Kim, B. I. (2012). "Bond stress–slip behaviour of two common GFRP rebar types with pullout failure." *Magazine of Concrete Research*. 64(7): 575-591.

Li, L. G., Chen, Z. P., Ouyang, Y., Zhu, J., Chu, S. H., and Kwan, A. K. H. (2019). "Synergistic effects of steel fibres and expansive agent on steel bar-concrete bond." *Cement and Concrete Composites*. 104: 103380.

Li, S., Jin, Z., Chang, H., and Gao, Y. (2024). "Oxygen diffusion into unsaturated seawater and sea sand concrete and its effect on non-uniform corrosion of steel bars." *Journal of Building Engineering*. 84: 108665.

Liang, X., Yin, S., and Hu, C. (2021). "Environmental reduction factors of BFRP bars in coral aggregate concrete in high temperature and high humidity environments." *Structures*. 33: 3017-3024.

Lin, X. S., and Zhang, Y. X. (2014). "Evaluation of bond stress-slip models for FRP reinforcing bars in concrete." *Composite Structures*. 107: 131-141.

Litherlan, K. L., Oakley, D. R., and Proctor, B. A. (1981). "The use of accelerated ageing procedures to predict the long-term strength of GRC composites." *Cement Concrete Research*. 11(3): 455-466.

Lu, C., Ni, M., Chu, T., and He, L. (2020a). "Comparative investigation on tensile performance of FRP bars after exposure to water, seawater, and alkaline solutions." *Journal of Materials in Civil Engineering*. 32(7).

Lu, C., Qi, Z., Zheng, Y., Xuan, G., and Yan, Y. (2023a). "Long-term tensile performance of GFRP bars in loaded concrete and aggressive solutions." *Journal of Bridge Engineering*. 64: 105587.

Lu, C., Yang, Y., and He, L. (2021a). "Mechanical and durability properties of GFRP bars exposed to aggressive solution environments." *Science and Engineering of Composite Materials*. 28(1): 11-23.

Lu, Z., Li, S., Xie, J., Huang, Q., Zhang, B., Huang, P., Li, J., and Li, L. (2022). "Durability of GFRP bars embedded in seawater sea-sand concrete: A coupling effect of prestress and immersion in seawater." *Construction and Building Materials*. 326: 126979.

Lu, Z., Li, W., Zeng, X., and Pan, Y. (2023b). "Durability of BFRP bars and BFRP reinforced seawater sea-sand concrete beams immersed in water and simulated seawater." *Construction and Building Materials*. 363: 129845.

Lu, Z., Su, L., Lai, J., Xie, J., and Yuan, B. (2021b). "Bond durability of BFRP bars embedded in concrete with fly ash in aggressive environments." *Composite Structures*. 271: 114121.

Lu, Z., Su, L., Tan, S., Li, Y., Xie, J., and Liu, F. (2020b). "Long-term shear performance of bare and cement mortar-coated BFRP bars in corrosive environments." *Construction and Building Materials*. 237.

Lu, Z., Su, L., Xian, G., Lu, B., and Xie, J. (2020c). "Durability study of concrete-covered basalt fiber-reinforced polymer (BFRP) bars in marine environment." *Composite Structures*. 234.

Lu, Z., Tan, S., Huang, P., Lei, Z., Liu, F., and Xie, J. (2020d). "Durability of cement mortar-covered BFRP bars in simulated seawater environment." *Construction and Building Materials*. 234.

Malvar, L. J. (1994). "Bond stress-slip characteristics of FRP rebars." *Rep. TR-2013-SHR*, Naval Facilities Engineering Service Center, Port Hueneme, California.

Manalo, A., Maranan, G., Benmokrane, B., Cousin, P., Alajarmeh, O., Ferdous, W., Liang, R., and Hota, G. (2020). "Comparative durability of GFRP composite reinforcing bars in concrete and in simulated concrete environments." *Cement and Concrete Composites*. 109: 103564.

Micelli, F., and Nanni, A. (2004). "Durability of FRP rods for concrete structures." *Construction and Building Materials*. 18(7): 491-503.

Mohammed, S. A., and Said, A. (2022). "Analysis of concrete beams reinforced by GFRP bars with varying parameters." *Journal of the Mechanical Behavior of Materials*. 31(1): 767-774.

Montaigu, M., Robert, M., Ahmed, E. A., and Benmokrane, B. (2013). "Laboratory characterization and evaluation of durability performance of new polyester and vinylester E-glass GFRP dowels for jointed concrete pavement." *Journal of Composites for Construction*. 17(2): 176-187.

Morales, C. N., Claure, G., Emparanza, A. R., and Nanni, A. (2021). "Durability of GFRP reinforcing bars in seawater concrete." *Construction and Building Materials*. 270: 121492.

Mufti, A. A., Banthia, N., Benmokrane, B., Boulfiza, M., and Newhook, J. P. (2007a). "Durability of GFRP composite rods." *Concrete international*. 29(2): 37-42.

Mufti, A. A., Onofrei, M., Benmokrane, B., Banthia, N., Boulfiza, M., Newhook, J. P., Bakht, B., Tadros, G. S., and Brett, P. (2007b). "Field study of glass-fibre-reinforced polymer durability in concrete." *Canadian Journal of Civil Engineering*. 34(3): 355-366.

Mukherjee, A., and Arwikar, S. J. (2005). "Performance of glass fiber-reinforced polymer reinforcing bars in tropical environments-Part I: Structural scale tests." *ACI Structural Journal*. 102(5): 745-753.

Nelson, W. B. (2009). *Accelerated Testing: Statistical Models, Test Plans, and Data Analysis*. John Wiley & Sons.

Nepomuceno, E., Sena-Cruz, J., Correia, L., and D'Antino, T. (2021). "Review on the bond behavior and durability of FRP bars to concrete." *Construction and Building Materials*. 287: 123042.

Ng, P. L., Barros, J. A. O., Kaklauskas, G., and Lam, J. Y. K. (2020). "Deformation analysis of fibre-reinforced polymer reinforced concrete beams by tension-stiffening approach." *Composite Structures*. 234: 111664.

Nishizaki, I., Sasaki, I., and Sakuraba, H. (2016). "Long-term exposure performance of FRP composites in marine environments." *International Workshop on Seawater Sea-Sand Concrete (SSC) Structures Reinforced with FRP Composites*, The Hong Kong Polytechnic University.

Otsuki, N., Hamada, H., and Takeda, N. (2014). "Technical Committee on the Use of Seawater in Concrete, Committee Report: JCI-TC121A." Japan Concrete Institute.

Pecce, M., Manfredi, G., Realfonzo, R., and Cosenza, E. (2001). "Experimental and analytical evaluation of bond properties of GFRP bars." *Journal of Materials in Civil Engineering*. 13(4): 282-290.

Phani, K. K., and Bose, N. R. (2012). "Temperature dependence of hydrothermal ageing of CSM laminate during water immersion." *Composites Science and Technology*. 29(2): 79-87.

Rajput, A. S., and Sharma, U. K. (2017). "Durability and serviceability performance of GFRP rebars as concrete reinforcement." *Indian Concrete Journal*. 91(7): 51-60.

Ramanathan, S., Benzecry, V., Suraneni, P., and Nanni, A. (2021). "Condition assessment of concrete and glass fiber reinforced polymer (GFRP) rebar after 18 years of service life." *Case Studies in Construction Materials*: e00494.

Ren, F., Chen, Z., and Xiong, M. (2024). "Long-term behavior of FRP-bar reinforced seawater sea sand concrete beams under load sustaining and environment weathering." *International Journal of Civil Engineering*. 22(3): 491-504.

Ren, F., Liu, T., Chen, G., Xie, P., Xiong, M. X., Yuan, T., Chen, Y., and Guo, S. (2021). "Flexural behavior and modelling of FRP-bar reinforced seawater sea sand concrete beams exposed to subtropical coastal environment." *Construction and Building Materials*. 309: 125071.

Robert, M., and Benmokrane, B. (2010). "Effect of aging on bond of GFRP bars embedded in concrete." *Cement and Concrete Composites*. 32(6): 461-467.

Robert, M., and Benmokrane, B. (2013). "Combined effects of saline solution and moist

concrete on long-term durability of GFRP reinforcing bars." *Construction and Building Materials*. 38: 274-284.

Rolland, A., Argoul, P., Benzarti, K., Quiertant, M., Chataigner, S., and Khadour, A. (2020). "Analytical and numerical modeling of the bond behavior between FRP reinforcing bars and concrete." *Construction and Building Materials*. 231: 117160.

Rolland, A., Benzarti, K., Quiertant, M., and Chataigner, S. (2021). "Accelerated aging behavior in alkaline environments of GFRP reinforcing bars and their bond with concrete." *Materials*. 14(19).

Rossetti, V. A., Galeota, D., and Giammatteo, M. M. (1995). "Local bond stress-slip relationships of glass fibre reinforced plastic bars embedded in concrete." *Materials and Structures*. 28(6): 340-344.

Rots, J. G. (1988). "Computational Modeling of Concrete Fracture." PhD Thesis, Delft University of Technology, Netherlands.

Ruiz Emparanza, A., Kampmann, R., De Caso, F., Morales, C., and Nanni, A. (2022). "Durability assessment of GFRP rebars in marine environments." *Construction and Building Materials*. 329: 127028.

Saenz, L. P. (1964). "Discussion of 'Equation for the stress-strain curve of concrete' by P. Desayi and S. Krishan." *ACI Journal*. 61(9): 1229-1235.

Sawpan, M. A. (2019). "Shear properties and durability of GFRP reinforcement bar aged in seawater." *Polymer Testing*. 75: 312-320.

Sawpan, M. A. (2021). "Experimental investigation of long term seawater durability and shear properties of pultruded GFRP composite." *Journal of Polymers and the Environment*. 29(11): 3574-3586.

Selicato, F., Moro, M., Bertolini, L., and Nanni, A. (2015). "Towards sustainability of concrete without chloride limits." *ACI Special Publication*. 305: 1-10.

Sen, R., Mullins, G., and Salem, T. (2002). "Durability of E-glass/vinylester reinforcement in alkaline solution." *ACI Structural Journal*. 99(3): 369-375.

Sen, R., Shahawy, M., Sukumar, S., and Rosas, J. (1998). "Durability of carbon pretensioned elements in a marine environment." *ACI Structural Journal*. 95(6): 716-724.

Sen, R., Shahawy, M., Sukumar, S., and Rosas, J. (1999). "Durability of carbon fiber reinforced polymer (CFRP) pretensioned elements under tidal/thermal cycles." *ACI Structural Journal*. 96(3): 450-457.

Serbescu, A., Guadagnini, M., and Pilakoutas, K. (2015). "Mechanical characterization of basalt FRP rebars and long-term strength predictive model." *Journal of Composites for Construction*. 19(2): 04014037.

Shakiba, M., Bazli, M., Karamloo, M., and Doostmohamadi, A. (2023). "Bond between sand-coated GFRP bars and normal-strength, self-compacting, and fiber-reinforced concrete under seawater and alkaline solution." *Journal of Composites for Construction*. 27: 04022098.

Solyom, S., and Balázs, G. L. (2020). "Bond of FRP bars with different surface characteristics." *Construction and Building Materials*. 264: 119839.

Su, C., Wang, X., Ding, L., Wu, Z., and Ma, X. (2022). "Durability of seawater sea sand concrete beams reinforced with carbon nanotube-modified BFRP bars in a marine environment." *Composite Structures*. 292.

Tannous, F. E., and Saadatmanesh, H. (1998). "Environmental effects on the

mechanical properties of E-glass FRP rebars." *ACI Materials Journal*. 95(2): 87-100.

Tannous, F. E., and Saadatmanesh, H. (1999). "Durability of AR glass fiber reinforced plastic bars." *Journal of Composites for Construction*. 3(1): 12-19.

Teng, J. G. (2014). "Performance enhancement of structures through the use of fibre-reinforced polymer (FRP) composites." *23rd Australasian Conference on the Mechanics of Structures and Materials (ACMSM23)*, 9.

Teng, J. G., Yu, T., Dai, J. G., and Chen, G. M. (2011). "FRP composites in new construction: Current status and opportunities." *7th National Conference on FRP Composites in Infrastructure.*

Trejo, D., Gardoni, P., and Kim, J. J. (2011). "Long-term performance of glass fiber-reinforced polymer reinforcement embedded in concrete." *ACI Materials Journal*. 108(6): 605.

Veljkovic, A., Carvelli, V., and Rezazadeh, M. (2020). "Modelling the bond in GFRP bar reinforced concrete thin structural members." *Structures*. 24: 13-26.

Wang, G., Wu, Q., Li, X.-Z., Xu, J., Xu, Y., Shi, W.-H., and Wang, S.-L. (2019). "Microscopic analysis of steel corrosion products in seawater and sea-sand concrete." *Materials*. 12(20): 3330.

Wang, H., and Belarbi, A. (2011). "Ductility characteristics of fiber-reinforced-concrete beams reinforced with FRP rebars." *Construction and Building Materials*. 25(5): 2391-2401.

Wang, H., and Belarbi, A. (2013). "Flexural durability of FRP bars embedded in fiber-reinforced-concrete." *Construction and Building Materials*. 44: 541-550.

Wang, P., Ke, L.-y.-w., Wu, H.-l., and Leung, C. K. Y. (2022). "Lowering exposure pH for durability enhancement of glass fiber reinforcement polymer (GFRP) rebars." *Construction and Building Materials*. 354: 129131.

Wang, P., Ke, L., Wang, Z., Zhao, J., Li, W., and Leung, C. K. Y. (2023a). "Effects of alkaline concentration and saline contents on degradation of tensile properties, microstructure and chemical characterization of glass fiber reinforced polymer (GFRP) rebars." *Journal of Building Engineering*. 69: 106222.

Wang, P., Zhou, Y., Lu, Y., Ke, L., Wu, H., Li, W., and Leung, C. K. (2024). "Predicting long-term tensile degradation of GFRP rebars embedded in concrete with a reconsidered environmental reduction factor CE." *Developments in the Built Environment*. 20: 100583.

Wang, Z., Xie, J., Mai, Z., Liu, P., Lu, Z., and Li, L. (2023b). "Durability of GFRP bar-reinforced seawater–sea sand concrete beams: Coupled effects of sustained loading and exposure to a chloride environment." *Engineering Structures*. 283.

Wang, Z., Zhao, X.-L., Xian, G., Wu, G., Raman, R. S., and Al-Saadi, S. (2017a). "Durability study on interlaminar shear behaviour of basalt-, glass-and carbon-fibre reinforced polymer (B/G/CFRP) bars in seawater sea sand concrete environment." *Construction and Building Materials*. 156: 985-1004.

Wang, Z., Zhao, X.-L., Xian, G., Wu, G., Raman, R. S., and Al-Saadi, S. (2018). "Effect of sustained load and seawater and sea sand concrete environment on durability of basalt-and glass-fibre reinforced polymer (B/GFRP) bars." *Corrosion Science*. 138: 200-218.

Wang, Z., Zhao, X. L., Xian, G., Wu, G., Singh Raman, R. K., Al-Saadi, S., and Haque, A. (2017b). "Long-term durability of basalt- and glass-fibre reinforced polymer

(BFRP/GFRP) bars in seawater and sea sand concrete environment." *Construction and Building Materials*. 139: 467-489.

Won, J.-P., Lee, S.-J., Kim, Y.-J., Jang, C.-I., and Lee, S.-W. (2008). "The effect of exposure to alkaline solution and water on the strength–porosity relationship of GFRP rebar." *Composites Part B: Engineering*. 39(5): 764-772.

Won, J. P., and Park, C. G. (2006). "Effect of environmental exposure on the mechanical and bonding properties of hybrid FRP reinforcing bars for concrete structures." *Journal of Composite Materials*. 40(12): 1063-1076.

Won, J. P., Park, C. G., Lee, S. J., and Hong, B. T. (2013). "Durability of hybrid FRP reinforcing bars in concrete structures exposed to marine environments." *International Journal of Structural Engineering*. 4(1-2): 63-74.

Wu, G., Dong, Z. Q., Wang, X., Zhu, Y., and Wu, Z. S. (2015). "Prediction of long-term performance and durability of BFRP bars under the combined effect of sustained load and corrosive solutions." *Journal of Composites for Construction*. 19(3): 04014058.

Wu, W., He, X., Yang, W., Dai, L., Wang, Y., and He, J. J. C. (2022). "Long-time durability of GFRP bars in the alkaline concrete environment for eight years." *Construction and Building Materials*. 314: 125573.

Wu, W., He, X., Yang, W., Wei, B., and Alam, M. S. (2023). "Durability and microstructure degradation mechanism of FRP-seawater seasand concrete structures: A review." *Construction and Building Materials*. 391: 131825.

Xiao, J., Qiang, C., Nanni, A., and Zhang, K. (2017). "Use of sea-sand and seawater in concrete construction: Current status and future opportunities." *Construction and Building Materials*. 155: 1101-1111.

Xie, J., Li, Y., Lu, Z., Fan, Z., Li, J., and Li, S. (2022). "Effects of immersion in water, alkaline solution, and seawater on the shear performance of basalt FRP bars in seawater–sea sand concrete." *Journal of Composites for Construction*. 26(2): 04021071.

Xiong, Z., Wei, W., Liu, F., Cui, C. Y., Li, L. J., Zou, R., and Zeng, Y. (2021). "Bond behaviour of recycled aggregate concrete with basalt fibre-reinforced polymer bars." *Composite Structures*. 256: 113078.

Xiong, Z., Zhou, K., Ye, Z., He, S., Li, L., Li, Y., Zeng, Y., and Liu, F. (2022). "Bond behavior of basalt fiber reinforced polymer bars in seawater sea-sand concrete exposed to daily temperature variations." *Advances in Structural Engineering*. 25(9): 2021-2039.

Xue, W. C., Zheng, Q. W., Yang, Y., and Fang, Z. Q. (2014). "Bond behavior of sand-coated deformed glass fiber reinforced polymer rebars." *Journal of Reinforced Plastics and Composites*. 33(10): 895-910.

Yan, F., Lin, Z., Zhang, D., Gao, Z., and Li, M. (2017). "Experimental study on bond durability of glass fiber reinforced polymer bars in concrete exposed to harsh environmental agents: Freeze-thaw cycles and alkaline-saline solution." *Composites Part B: Engineering*. 116: 406-421.

Yan, F., and Lin, Z. B. (2017). "Bond durability assessment and long-term degradation prediction for GFRP bars to fiber-reinforced concrete under saline solutions." *Composite Structures*. 161: 393-406.

Yoo, D. Y., Kwon, K. Y., Park, J. J., and Yoon, Y. S. (2015). "Local bond-slip response of GFRP rebar in ultra-high-performance fiber-reinforced concrete." *Composite Structures*. 120: 53-64.

Yue, Y., Wang, W.-w., Zhang, L., Liang, L., and Zhao, Q. (2024). "Effect of sand coating on durability and micro-structural deterioration of GFRP rebar under alkaline environment attack." *Construction and Building Materials*. 413: 134900.

Zeng, J. J., Liao, J. J., Zhuge, Y., Guo, Y. C., Zhou, J. K., Huang, Z. H., and Zhang, L. H. (2022). "Bond behavior between GFRP bars and seawater sea-sand fiber-reinforced ultra-high strength concrete." *Engineering Structures*. 254: 113787.

Zhao, Y., Hu, X., Shi, C., Zhang, Z., and Zhu, D. (2021). "A review on seawater sea-sand concrete: Mixture proportion, hydration, microstructure and properties." *Construction and Building Materials*. 295: 123602.

Zheng, Y., Ni, M., Lu, C., Chu, T., and Wu, X. (2020). "Bond behavior of GFRP-concrete under long-term exposure to aggressive environments." *Journal of Advanced Concrete Technology*. 18: 730-742.

Zhou, C. H., Yang, B., Zhang, Z. H., Yang, Z. J., and Zhang, Z. W. (2024). "Bond-slip behavior of the FRP bar-sea sand concrete interface and its effect on the finite element analysis of RC beam." *Construction and Building Materials*. 436: 136917.

Zhou, J. K., Chen, X. D., and Chen, S. X. (2011). "Durability and service life prediction of GFRP bars embedded in concrete under acid environment." *Nuclear Engineering and Design*. 241(10): 4095-4102.

Zhou, J. K., Chen, X. D., and Chen, S. X. (2012). "Effect of different environments on bond strength of glass fiber-reinforced polymer and steel reinforcing bars." *KSCE Journal of Civil Engineering*. 16(6): 994-1002.

APPENDIX A
DATABASE FOR ACCELERATED AGING TESTS

The results of accelerated aging tests for FRP bars, FRP bar-to-concrete bonded joints, and FRP-reinforced concrete beams, collected from the existing literature, are respectively summarized in Tables A1-A3, B and C, as follows.

Table A1 AAT database for tensile properties of FRP bars

No.	Reference	FRP properties				Environmental condition	Temperature (℃)	Exposure duration (d)	Specimen number (pcs)	Tensile strength retention (%)	Tensile elastic modulus retention (%)
		Manufacturer	Type	Bar diameter (mm)	Resin type						
1	Abbasi and Hogg (2005)	Hughes Brothers Company (Seward, NE, USA)	GFRP	12.7	Polyester	Control	25	0	NA	100.0	100.0
2	Abbasi and Hogg (2005)	Hughes Brothers Company (Seward, NE, USA)	GFRP	12.7	Polyester	Alkaline solution (IMMR)	60	30	NA	94.5	92.3
3	Abbasi and Hogg (2005)	Hughes Brothers Company (Seward, NE, USA)	GFRP	12.7	Polyester	Alkaline solution (IMMR)	60	120	NA	89.1	69.2
4	Abbasi and Hogg (2005)	Hughes Brothers Company (Seward, NE, USA)	GFRP	12.7	Polyester	Alkaline solution (IMMR)	60	240	NA	78.1	56.4
5	Abbasi and Hogg (2005)	Hughes Brothers Company (Seward, NE, USA)	GFRP	12.7	Vinylester	Control	25	0	NA	100.0	100.0
6	Abbasi and Hogg (2005)	Hughes Brothers Company (Seward, NE, USA)	GFRP	12.7	Vinylester	Alkaline solution (IMMR)	60	30	NA	83.9	83.8
7	Abbasi and Hogg (2005)	Hughes Brothers Company (Seward, NE, USA)	GFRP	12.7	Vinylester	Alkaline solution (IMMR)	60	120	NA	80.1	78.4
8	Abbasi and Hogg (2005)	Hughes Brothers Company (Seward, NE, USA)	GFRP	12.7	Modified vinylester	Control	25	0	NA	100.0	100.0
9	Abbasi and Hogg (2005)	Hughes Brothers Company (Seward, NE, USA)	GFRP	12.7	Modified vinylester	Alkaline solution (IMMR)	60	30	NA	94.7	95.1
10	Abbasi and Hogg (2005)	Hughes Brothers Company (Seward, NE, USA)	GFRP	12.7	Modified vinylester	Alkaline solution (IMMR)	60	120	NA	75.5	80.5
11	Ali et al. (2020)	Galen LLC (Russia)	BFRP	9.5	Vinylester	Control	NA	0	4	100.0	100.0
12	Ali et al. (2020)	Galen LLC (Russia)	BFRP	9.5	Vinylester	Alkaline solution (IMMR)	60	90	4	81.5	96.7
13	Ali et al. (2020)	Galen LLC (Russia)	BFRP	12.7	Vinylester	Control	NA	0	4	100.0	100.0
14	Ali et al. (2020)	Galen LLC (Russia)	BFRP	12.7	Vinylester	Alkaline solution (IMMR)	60	90	4	67.1	97.9
15	Ali et al. (2020)	Galen LLC (Russia)	BFRP	15.9	Vinylester	Control	NA	0	4	100.0	100.0
16	Ali et al. (2020)	Galen LLC (Russia)	BFRP	15.9	Vinylester	Alkaline solution (IMMR)	60	90	4	84.9	100.5
17	Ali et al. (2020)	Galen LLC (Russia)	BFRP	19.0	Vinylester	Control	NA	0	4	100.0	100.0
18	Ali et al. (2020)	Galen LLC (Russia)	BFRP	19.0	Vinylester	Alkaline solution (IMMR)	60	90	4	84.2	99.8
19	Ali et al. (2020)	Galen LLC (Russia)	BFRP	25.0	Vinylester	Control	NA	0	4	100.0	100.0
20	Ali et al. (2020)	Galen LLC (Russia)	BFRP	25.0	Vinylester	Alkaline solution (IMMR)	60	90	4	80.3	98.3
21	Almusallam and Al-Salloum (2006)	NA	GFRP	10.0	Vinylester	Control	NA	0	NA	100.0	NA
22	Almusallam and Al-Salloum (2006)	NA	GFRP	10.0	Vinylester	NCE+Water (IMMR)	40	120	4	95.2	NA
23	Almusallam and Al-Salloum (2006)	NA	GFRP	10.0	Vinylester	NCE+Water (IMMR)	40	180	4	86.9	NA

24	Almusallam and Al-Salloum (2006)	NA	GFRP	10.0	Vinylester	NCE+Water (IMMR)	40	240	4	83.7	NA
25	Almusallam and Al-Salloum (2006)	NA	GFRP	10.0	Vinylester	SL (20-25%fu)+NCE+Water (IMMR)	40	120	4	72.1	NA
26	Almusallam and Al-Salloum (2006)	NA	GFRP	10.0	Vinylester	SL (20-25%fu)+NCE+Water (IMMR)	40	180	4	62.3	NA
27	Almusallam and Al-Salloum (2006)	NA	GFRP	10.0	Vinylester	SL (20-25%fu)+NCE+Water (IMMR)	40	240	4	52.9	NA
28	Almusallam and Al-Salloum (2006)	NA	GFRP	10.0	Vinylester	NCE+Seawater (IMMR)	40	120	4	98.0	NA
29	Almusallam and Al-Salloum (2006)	NA	GFRP	10.0	Vinylester	NCE+Seawater (IMMR)	40	180	4	84.4	NA
30	Almusallam and Al-Salloum (2006)	NA	GFRP	10.0	Vinylester	NCE+Seawater (IMMR)	40	240	4	80.3	NA
31	Almusallam and Al-Salloum (2006)	NA	GFRP	10.0	Vinylester	SL (20-25%fu)+NCE+Seawater (IMMR)	40	120	4	70.7	NA
32	Almusallam and Al-Salloum (2006)	NA	GFRP	10.0	Vinylester	SL (20-25%fu)+NCE+Seawater (IMMR)	40	180	4	61.0	NA
33	Almusallam and Al-Salloum (2006)	NA	GFRP	10.0	Vinylester	SL (20-25%fu)+NCE+Seawater (IMMR)	40	240	4	52.1	NA
34	Almusallam and Al-Salloum (2006)	NA	GFRP	10.0	Vinylester	NCE+Seawater (WD)	40	120	4	89.8	NA
35	Almusallam and Al-Salloum (2006)	NA	GFRP	10.0	Vinylester	NCE+Seawater (WD)	40	180	4	83.0	NA
36	Almusallam and Al-Salloum (2006)	NA	GFRP	10.0	Vinylester	NCE+Seawater (WD)	40	240	4	78.2	NA
37	Almusallam and Al-Salloum (2006)	NA	GFRP	10.0	Vinylester	SL (20-25%fu)+NCE+Seawater (WD)	40	120	4	72.3	NA
38	Almusallam and Al-Salloum (2006)	NA	GFRP	10.0	Vinylester	SL (20-25%fu)+NCE+Seawater (WD)	40	180	4	53.0	NA
39	Almusallam and	NA	GFRP	10.0	Vinylester	SL (20-25%fu)+NCE+Seawater	40	240	4	45.0	NA

	Al-Salloum (2006)					(WD)					
40	Al-Salloum et al. (2013)	NA	GFRP	12.0	Vinylester	Reference	23	180	5	100.0	100.0
41	Al-Salloum et al. (2013)	NA	GFRP	12.0	Vinylester	Water (IMMR)	23	180	5	97.3	96.7
42	Al-Salloum et al. (2013)	NA	GFRP	12.0	Vinylester	Water (IMMR)	50	180	5	82.7	95.1
43	Al-Salloum et al. (2013)	NA	GFRP	12.0	Vinylester	Seawater (IMMR)	23	180	5	97.6	100.0
44	Al-Salloum et al. (2013)	NA	GFRP	12.0	Vinylester	Seawater (IMMR)	50	180	5	89.1	96.2
45	Al-Salloum et al. (2013)	NA	GFRP	12.0	Vinylester	Seawater (WD)	50	180	5	90.3	100.5
46	Al-Salloum et al. (2013)	NA	GFRP	12.0	Vinylester	Alkaline solution (IMMR)	50	180	5	85.2	95.6
47	Al-Salloum et al. (2013)	NA	GFRP	12.0	Vinylester	HT	50	180	5	99.7	98.4
48	Al-Salloum et al. (2013)	NA	GFRP	12.0	Vinylester	Reference	23	360	5	100.0	100.0
49	Al-Salloum et al. (2013)	NA	GFRP	12.0	Vinylester	Water (IMMR)	23	360	5	98.2	99.5
50	Al-Salloum et al. (2013)	NA	GFRP	12.0	Vinylester	Water (IMMR)	50	360	5	78.1	100.5
51	Al-Salloum et al. (2013)	NA	GFRP	12.0	Vinylester	Seawater (IMMR)	23	360	5	91.1	96.2
52	Al-Salloum et al. (2013)	NA	GFRP	12.0	Vinylester	Seawater (IMMR)	50	360	5	92.0	97.7
53	Al-Salloum et al. (2013)	NA	GFRP	12.0	Vinylester	Seawater (WD)	50	360	5	91.8	98.7
54	Al-Salloum et al. (2013)	NA	GFRP	12.0	Vinylester	Alkaline solution (IMMR)	50	360	5	80.3	98.0
55	Al-Salloum et al. (2013)	NA	GFRP	12.0	Vinylester	HT	50	360	5	100.7	96.5
56	Al-Salloum et al. (2013)	NA	GFRP	12.0	Vinylester	Reference	23	540	5	100.0	100.0
57	Al-Salloum et al. (2013)	NA	GFRP	12.0	Vinylester	Water (IMMR)	23	540	5	94.7	96.5
58	Al-Salloum et al. (2013)	NA	GFRP	12.0	Vinylester	Water (IMMR)	50	540	5	75.6	97.5
59	Al-Salloum et al. (2013)	NA	GFRP	12.0	Vinylester	Seawater (IMMR)	23	540	5	89.3	97.7
60	Al-Salloum et al. (2013)	NA	GFRP	12.0	Vinylester	Seawater (IMMR)	50	540	5	87.2	97.5
61	Al-Salloum et al. (2013)	NA	GFRP	12.0	Vinylester	Seawater (WD)	50	540	5	90.2	98.0

62	Al-Salloum et al. (2013)	NA	GFRP	12.0	Vinylester	Alkaline solution (IMMR)	50	540	5	76.0	99.2
63	Al-Salloum et al. (2013)	NA	GFRP	12.0	Vinylester	HT	50	540	5	97.0	100.3
64	Al-Zahrani et al. (2002)	NA	GFRP	10.0	Modified vinylester	Control	22	0	NA	100.0	100.0
65	Al-Zahrani et al. (2002)	NA	GFRP	10.0	Modified vinylester	Alkaline solution (IMMR)	22	90	NA	98.2	96.2
66	Al-Zahrani et al. (2002)	NA	GFRP	10.0	Modified vinylester	Alkaline solution (IMMR)	22	180	NA	97.6	86.1
67	Al-Zahrani et al. (2002)	NA	GFRP	10.0	Modified vinylester	Alkaline solution (IMMR)	60	90	NA	78.2	76.7
68	Al-Zahrani et al. (2002)	NA	GFRP	10.0	Modified vinylester	Alkaline solution (IMMR)	60	180	NA	64.1	77.7
69	Al-Zahrani et al. (2002)	NA	GFRP	10.0	Modified vinylester	Alkaline solution with Cl- (IMMR)	22	90	NA	96.9	91.6
70	Al-Zahrani et al. (2002)	NA	GFRP	10.0	Modified vinylester	Alkaline solution with Cl- (IMMR)	22	180	NA	97.1	91.9
71	Al-Zahrani et al. (2002)	NA	GFRP	10.0	Modified vinylester	Alkaline solution with Cl- (IMMR)	60	90	NA	79.4	86.1
72	Al-Zahrani et al. (2002)	NA	GFRP	10.0	Modified vinylester	Alkaline solution with Cl- (IMMR)	60	180	NA	72.7	74.9
73	Al-Zahrani et al. (2002)	NA	GFRP	10.0	Modified vinylester	Acid solution (IMMR)	22	90	NA	103.7	94.9
74	Al-Zahrani et al. (2002)	NA	GFRP	10.0	Modified vinylester	Acid solution (IMMR)	22	180	NA	99.2	87.1
75	Al-Zahrani et al. (2002)	NA	GFRP	10.0	Modified vinylester	Acid solution (IMMR)	60	90	NA	83.4	99.2
76	Al-Zahrani et al. (2002)	NA	GFRP	10.0	Modified vinylester	Acid solution (IMMR)	60	180	NA	74.3	89.6
77	Arczewska et al. (2021)	Schoeck Inc. (Canada)	GFRP	12.0	NA	Control	NA	0	4	100.0	NA
78	Arczewska et al. (2021)	Schoeck Inc. (Canada)	GFRP	12.0	NA	Alkaline solution (IMMR)	50	30	4	96.9	NA
79	Arczewska et al. (2021)	Schoeck Inc. (Canada)	GFRP	12.0	NA	Alkaline solution (IMMR)	50	90	4	95.4	NA
80	Arczewska et al. (2021)	Schoeck Inc. (Canada)	GFRP	12.0	NA	Alkaline solution (IMMR)	50	150	4	94.6	NA
81	Arczewska et al. (2021)	Schoeck Inc. (Canada)	GFRP	12.0	NA	Alkaline solution (IMMR)	60	30	4	94.7	NA
82	Arczewska et al. (2021)	Schoeck Inc. (Canada)	GFRP	12.0	NA	Alkaline solution (IMMR)	60	90	4	91.8	NA
83	Arczewska et al. (2021)	Schoeck Inc. (Canada)	GFRP	12.0	NA	Alkaline solution (IMMR)	60	150	4	89.7	NA
84	Arczewska et al. (2021)	Schoeck Inc. (Canada)	GFRP	12.0	NA	Alkaline solution (IMMR)	70	30	4	93.9	NA

85	Arczewska et al. (2021)	Schoeck Inc. (Canada)	GFRP	12.0	NA	Alkaline solution (IMMR)	70	90	4	86.6	NA
86	Arczewska et al. (2021)	Schoeck Inc. (Canada)	GFRP	12.0	NA	Alkaline solution (IMMR)	70	150	4	82.1	NA
87	Arczewska et al. (2021)	Schoeck Inc. (Canada)	GFRP	16.0	NA	Control	NA	0	4	100.0	NA
88	Arczewska et al. (2021)	Schoeck Inc. (Canada)	GFRP	16.0	NA	Alkaline solution (IMMR)	50	30	4	98.7	NA
89	Arczewska et al. (2021)	Schoeck Inc. (Canada)	GFRP	16.0	NA	Alkaline solution (IMMR)	50	90	4	97.6	NA
90	Arczewska et al. (2021)	Schoeck Inc. (Canada)	GFRP	16.0	NA	Alkaline solution (IMMR)	50	150	4	97.2	NA
91	Arczewska et al. (2021)	Schoeck Inc. (Canada)	GFRP	16.0	NA	Alkaline solution (IMMR)	60	30	4	96.8	NA
92	Arczewska et al. (2021)	Schoeck Inc. (Canada)	GFRP	16.0	NA	Alkaline solution (IMMR)	60	90	4	94.4	NA
93	Arczewska et al. (2021)	Schoeck Inc. (Canada)	GFRP	16.0	NA	Alkaline solution (IMMR)	60	150	4	93.0	NA
94	Arczewska et al. (2021)	Schoeck Inc. (Canada)	GFRP	16.0	NA	Alkaline solution (IMMR)	70	30	4	95.2	NA
95	Arczewska et al. (2021)	Schoeck Inc. (Canada)	GFRP	16.0	NA	Alkaline solution (IMMR)	70	90	4	89.5	NA
96	Arczewska et al. (2021)	Schoeck Inc. (Canada)	GFRP	16.0	NA	Alkaline solution (IMMR)	70	150	4	86.4	NA
97	Ashrafi et al. (2018)	Armastek (Russia)	GFRP	6.0	Epoxy	Control	NA	0	3	100.0	NA
98	Ashrafi et al. (2018)	Armastek (Russia)	GFRP	6.0	Epoxy	UV radiation+Water vapor condensation	/	42	3	102.0	NA
99	Ashrafi et al. (2018)	Armastek (Russia)	GFRP	6.0	Epoxy	UV radiation+Water vapor condensation	/	83	3	97.0	NA
100	Ashrafi et al. (2018)	Armastek (Russia)	GFRP	6.0	Epoxy	UV radiation+Water vapor condensation	/	125	3	95.0	NA
101	Ashrafi et al. (2018)	Armastek (Russia)	GFRP	10.0	Epoxy	Control	NA	0	3	100.0	NA
102	Ashrafi et al. (2018)	Armastek (Russia)	GFRP	10.0	Epoxy	UV radiation+Water vapor condensation	/	42	3	100.0	NA
103	Ashrafi et al. (2018)	Armastek (Russia)	GFRP	10.0	Epoxy	UV radiation+Water vapor condensation	/	83	3	99.0	NA
104	Ashrafi et al. (2018)	Armastek (Russia)	GFRP	10.0	Epoxy	UV radiation+Water vapor condensation	/	125	3	97.0	NA
105	Ashrafi et al. (2018)	Armastek (Russia)	GFRP	14.0	Epoxy	Control	NA	0	3	100.0	NA
106	Ashrafi et al. (2018)	Armastek (Russia)	GFRP	14.0	Epoxy	UV radiation+Water vapor condensation	/	42	3	99.0	NA
107	Ashrafi et al. (2018)	Armastek (Russia)	GFRP	14.0	Epoxy	UV radiation+Water vapor condensation	/	83	3	100.0	NA

108	Ashrafi et al. (2018)	Armastek (Russia)	GFRP	14.0	Epoxy	UV radiation+Water vapor condensation	/	125	3	97.0	NA
109	Aydın and Arslan (2021)	NA	AFRP	10.0	Polyester	Control	NA	0	5	100.0	NA
110	Aydın and Arslan (2021)	NA	AFRP	10.0	Polyester	Water (IMMR)	60	160	5	77.3	NA
111	Aydın and Arslan (2021)	NA	AFRP	10.0	Polyester	Seawater (IMMR)	60	160	5	97.1	NA
112	Aydın and Arslan (2021)	NA	AFRP	10.0	Polyester	Alkaline solution (IMMR)	60	160	5	72.2	NA
113	Aydın and Arslan (2021)	NA	AFRP	10.0	Polyester	HT	60	160	5	84.7	NA
114	Aydın and Arslan (2021)	NA	AFRP	10.0	Polyester	LT	-37	160	5	101.8	NA
115	Aydın and Arslan (2021)	NA	CFRP	10.0	Polyester	Control	NA	0	5	100.0	NA
116	Aydın and Arslan (2021)	NA	CFRP	10.0	Polyester	Water (IMMR)	60	160	5	96.6	NA
117	Aydın and Arslan (2021)	NA	CFRP	10.0	Polyester	Seawater (IMMR)	60	160	5	99.9	NA
118	Aydın and Arslan (2021)	NA	CFRP	10.0	Polyester	Alkaline solution (IMMR)	60	160	5	77.3	NA
119	Aydın and Arslan (2021)	NA	CFRP	10.0	Polyester	HT	60	160	5	92.4	NA
120	Aydın and Arslan (2021)	NA	CFRP	10.0	Polyester	LT	-37	160	5	93.0	NA
121	Aydın and Arslan (2021)	NA	GFRP	10.0	Polyester	Control	NA	0	5	100.0	NA
122	Aydın and Arslan (2021)	NA	GFRP	10.0	Polyester	Water (IMMR)	60	160	5	74.1	NA
123	Aydın and Arslan (2021)	NA	GFRP	10.0	Polyester	Seawater (IMMR)	60	160	5	71.9	NA
124	Aydın and Arslan (2021)	NA	GFRP	10.0	Polyester	Alkaline solution (IMMR)	60	160	5	68.2	NA
125	Aydın and Arslan (2021)	NA	GFRP	10.0	Polyester	HT	60	160	5	95.8	NA
126	Aydın and Arslan (2021)	NA	GFRP	10.0	Polyester	LT	-37	160	5	101.9	NA
127	Bakis et al. (2005)	Hughes Brothers Company (Seward, NE, USA)	GFRP	10.2	Vinylester	Control	23	0	3-6	100.0	100.0
128	Bakis et al. (2005)	Hughes Brothers Company (Seward, NE, USA)	GFRP	10.2	Vinylester	Pre-cracks+SL (20%Mu)+NCE	23	180	3-6	89.8	101.4
129	Bakis et al. (2005)	Hughes Brothers Company (Seward, NE, USA)	GFRP	10.2	Vinylester	Pre-cracks+SL (20%Mu)+NCE	23	480	3-6	92.7	97.7
130	Bakis et al. (2005)	Hughes Brothers Company (Seward, NE, USA)	GFRP	10.2	Vinylester	Pre-cracks+SL (20%Mu)+NCE	23	1090	3-6	94.7	109.3

131	Bakis et al. (2005)	Hughes Brothers Company (Seward, NE, USA)	GFRP	10.2	Vinylester	Pre-cracks+SL (20%Mu)+NCE+Alkaline solution (IMMR)	60	60	3-6	89.0	90.7
132	Bakis et al. (2005)	Hughes Brothers Company (Seward, NE, USA)	GFRP	10.2	Vinylester	Pre-cracks+SL (20%Mu)+NCE+Alkaline solution (IMMR)	60	160	3-6	82.5	88.8
133	Bakis et al. (2005)	Hughes Brothers Company (Seward, NE, USA)	GFRP	10.2	Vinylester	Pre-cracks+SL (20%Mu)+NCE+Alkaline solution (IMMR)	60	390	3-6	75.6	99.5
134	Bakis et al. (2005)	Hughes Brothers Company (Seward, NE, USA)	GFRP	10.2	Vinylester	Pre-cracks+SL (20%Mu)+NCE+Water (FT)	-17/23	90	3-6	99.2	99.1
135	Bakis et al. (2005)	Hughes Brothers Company (Seward, NE, USA)	GFRP	10.2	Vinylester	Pre-cracks+SL (20%Mu)+NCE+Water (FT)	-17/23	150	3-6	85.4	88.8
136	Bakis et al. (2005)	Hughes Brothers Company (Seward, NE, USA)	GFRP	10.2	Vinylester	Pre-cracks+SL (20%Mu)+NCE+Water (FT)	-17/23	405	3-6	84.1	95.8
137	Benmokrane et al. (2002)	NA	GFRP	12.4	Vinylester	Control	22	0	NA	100.0	NA
138	Benmokrane et al. (2002)	NA	GFRP	12.4	Vinylester	SL (30%fu)+Alkaline solution 1 (IMMR)	22	90	3	84.8	NA
139	Benmokrane et al. (2002)	NA	GFRP	12.4	Vinylester	Control	22	0	NA	100.0	NA
140	Benmokrane et al. (2002)	NA	GFRP	12.4	Vinylester	SL (30%fu)+Alkaline solution 1 (IMMR)	22	90	3	85.6	NA
141	Benmokrane et al. (2002)	NA	GFRP	12.4	Vinylester	Control	22	0	NA	100.0	NA
142	Benmokrane et al. (2002)	NA	GFRP	12.4	Vinylester	SL (30%fu)+Alkaline solution 1 (IMMR)	22	90	3	96.0	NA
143	Benmokrane et al. (2002)	NA	GFRP	9.3	Vinylester	Control	22	0	NA	100.0	NA
144	Benmokrane et al. (2002)	NA	GFRP	9.3	Vinylester	SL (30%fu)+Alkaline solution 1 (IMMR)	22	140	5	83.0	NA
145	Benmokrane et al. (2002)	NA	GFRP	9.3	Vinylester	SL (30%fu)+NCE+Alkaline solution 2 (IMMR)	22	140	5	84.0	NA
146	Benmokrane et al. (2002)	NA	GFRP	12.0	Vinylester	Control	22	0	NA	100.0	NA
147	Benmokrane et al. (2002)	NA	GFRP	12.0	Vinylester	SL (30%fu)+Alkaline solution 3 (IMMR)	22	30	10	98.0	NA
148	Benmokrane et al. (2002)	NA	GFRP	12.0	Vinylester	SL (30%fu)+Alkaline solution 3 (IMMR)	22	60	10	100.0	NA
149	Benmokrane et al. (2002)	NA	GFRP	12.0	Vinylester	SL (30%fu)+Alkaline solution 3 (IMMR)	22	30	10	94.0	NA
150	Benmokrane et al. (2002)	NA	GFRP	12.0	Vinylester	SL (30%fu)+Alkaline solution 3 (IMMR)	22	60	10	78.0	NA
151	Benmokrane et al. (2017b)	Pultrall Inc. (Thetford Mines, QC, Canada)	GFRP	9.5	Vinylester	Control	23	0	6	100.0	100.0
152	Benmokrane et al.	Pultrall Inc. (Thetford	GFRP	9.5	Vinylester	Alkaline solution (IMMR)	60	90	6	95.2	100.8

	(2017b)	Mines, QC, Canada)										
153	Benmokrane et al. (2017b)	Pultrall Inc. (Thetford Mines, QC, Canada)	GFRP	12.7	Vinylester	Control	23	0	6	100.0	100.0
154	Benmokrane et al. (2017b)	Pultrall Inc. (Thetford Mines, QC, Canada)	GFRP	12.7	Vinylester	Alkaline solution (IMMR)	60	90	6	86.9	101.0
155	Benmokrane et al. (2017b)	Pultrall Inc. (Thetford Mines, QC, Canada)	GFRP	15.9	Vinylester	Control	23	0	6	100.0	100.0
156	Benmokrane et al. (2017b)	Pultrall Inc. (Thetford Mines, QC, Canada)	GFRP	15.9	Vinylester	Alkaline solution (IMMR)	60	90	6	92.2	100.2
157	Benmokrane et al. (2017b)	Pultrall Inc. (Thetford Mines, QC, Canada)	GFRP	19.1	Vinylester	Control	23	0	6	100.0	100.0
158	Benmokrane et al. (2017b)	Pultrall Inc. (Thetford Mines, QC, Canada)	GFRP	19.1	Vinylester	Alkaline solution (IMMR)	60	90	6	86.3	100.5
159	Benmokrane et al. (2017b)	Pultrall Inc. (Thetford Mines, QC, Canada)	GFRP	25.4	Vinylester	Control	23	0	6	100.0	100.0
160	Benmokrane et al. (2017b)	Pultrall Inc. (Thetford Mines, QC, Canada)	GFRP	25.4	Vinylester	Alkaline solution (IMMR)	60	90	6	88.1	99.8
161	Benmokrane et al. (2017c)	Firep International AG (Switzerland)	GFRP	25.0	Vinylester	Control	23	0	5	100.0	100.0
162	Benmokrane et al. (2017c)	Firep International AG (Switzerland)	GFRP	25.0	Vinylester	Saline solution (IMMR)	23	42	3	99.7	90.6
163	Benmokrane et al. (2017c)	Firep International AG (Switzerland)	GFRP	25.0	Vinylester	Saline solution (IMMR)	23	125	3	98.5	94.4
164	Benmokrane et al. (2017c)	Firep International AG (Switzerland)	GFRP	25.0	Vinylester	Saline solution (IMMR)	23	208	3	101.4	94.6
165	Benmokrane et al. (2017c)	Firep International AG (Switzerland)	GFRP	25.0	Vinylester	Saline solution (IMMR)	40	42	3	97.0	92.3
166	Benmokrane et al. (2017c)	Firep International AG (Switzerland)	GFRP	25.0	Vinylester	Saline solution (IMMR)	40	125	3	95.7	92.3
167	Benmokrane et al. (2017c)	Firep International AG (Switzerland)	GFRP	25.0	Vinylester	Saline solution (IMMR)	40	208	3	94.7	95.1
168	Benmokrane et al. (2017c)	Firep International AG (Switzerland)	GFRP	25.0	Vinylester	Saline solution (IMMR)	50	42	3	97.9	98.0
169	Benmokrane et al. (2017c)	Firep International AG (Switzerland)	GFRP	25.0	Vinylester	Saline solution (IMMR)	50	125	3	96.3	97.5
170	Benmokrane et al. (2017c)	Firep International AG (Switzerland)	GFRP	25.0	Vinylester	Saline solution (IMMR)	50	208	3	95.1	96.5
171	Benmokrane et al. (2020)	Pultrall Inc. (Thetford Mines, QC, Canada)	GFRP	15.0	Vinylester	Control	NA	0	5	100.0	100.0
172	Benmokrane et al. (2020)	Pultrall Inc. (Thetford Mines, QC, Canada)	GFRP	15.0	Vinylester	Alkaline solution (IMMR)	60	90	5	70.2	100.4
173	Benmokrane et al. (2020)	Pultrall Inc. (Thetford Mines, QC, Canada)	GFRP	15.0	Vinylester	Control	NA	0	5	100.0	100.0
174	Benmokrane et al. (2020)	Pultrall Inc. (Thetford Mines, QC, Canada)	GFRP	15.0	Vinylester	Alkaline solution (IMMR)	60	90	5	78.1	98.5
175	Benmokrane et al.	Pultrall Inc. (Thetford	GFRP	15.0	Vinylester	Control	NA	0	5	100.0	100.0

	(2020)	Mines, QC, Canada)									
176	Benmokrane et al. (2020)	Pultrall Inc. (Thetford Mines, QC, Canada)	GFRP	15.0	Vinylester	Alkaline solution (IMMR)	60	90	5	84.9	99.2
177	Benmokrane et al. (2020)	Pultrall Inc. (Thetford Mines, QC, Canada)	GFRP	15.0	Vinylester	Control	NA	0	5	100.0	100.0
178	Benmokrane et al. (2020)	Pultrall Inc. (Thetford Mines, QC, Canada)	GFRP	15.0	Vinylester	Alkaline solution (IMMR)	60	90	5	92.4	97.5
179	Benmokrane et al. (2020)	Pultrall Inc. (Thetford Mines, QC, Canada)	GFRP	15.0	Vinylester	Control	NA	0	5	100.0	100.0
180	Benmokrane et al. (2020)	Pultrall Inc. (Thetford Mines, QC, Canada)	GFRP	15.0	Vinylester	Alkaline solution (IMMR)	60	90	5	82.4	98.0
181	Benmokrane et al. (2020)	Pultrall Inc. (Thetford Mines, QC, Canada)	GFRP	13.0	Vinylester	Control	NA	0	5	100.0	100.0
182	Benmokrane et al. (2020)	Pultrall Inc. (Thetford Mines, QC, Canada)	GFRP	13.0	Vinylester	Alkaline solution (IMMR)	60	90	5	91.4	102.9
183	Benmokrane et al. (2020)	Pultrall Inc. (Thetford Mines, QC, Canada)	GFRP	13.0	Vinylester	Control	NA	0	5	100.0	100.0
184	Benmokrane et al. (2020)	Pultrall Inc. (Thetford Mines, QC, Canada)	GFRP	13.0	Vinylester	Alkaline solution (IMMR)	60	90	5	77.2	101.0
185	Benmokrane et al. (2020)	Pultrall Inc. (Thetford Mines, QC, Canada)	GFRP	13.0	Vinylester	Control	NA	0	5	100.0	100.0
186	Benmokrane et al. (2020)	Pultrall Inc. (Thetford Mines, QC, Canada)	GFRP	13.0	Vinylester	Alkaline solution (IMMR)	60	90	5	82.8	101.1
187	Benmokrane et al. (2020)	Pultrall Inc. (Thetford Mines, QC, Canada)	GFRP	13.0	Vinylester	Control	NA	0	5	100.0	100.0
188	Benmokrane et al. (2020)	Pultrall Inc. (Thetford Mines, QC, Canada)	GFRP	13.0	Vinylester	Alkaline solution (IMMR)	60	90	5	79.0	101.7
189	Benmokrane et al. (2020)	Pultrall Inc. (Thetford Mines, QC, Canada)	GFRP	13.0	Vinylester	Control	NA	0	5	100.0	100.0
190	Benmokrane et al. (2020)	Pultrall Inc. (Thetford Mines, QC, Canada)	GFRP	13.0	Vinylester	Alkaline solution (IMMR)	60	90	5	73.5	102.1
191	Benmokrane et al. (2020)	Pultrall Inc. (Thetford Mines, QC, Canada)	GFRP	13.0	Vinylester	Control	NA	0	5	100.0	100.0
192	Benmokrane et al. (2020)	Pultrall Inc. (Thetford Mines, QC, Canada)	GFRP	13.0	Vinylester	Alkaline solution (IMMR)	60	90	5	69.2	101.1
193	Benmokrane et al. (2020)	Pultrall Inc. (Thetford Mines, QC, Canada)	GFRP	13.0	Vinylester	Control	NA	0	5	100.0	100.0
194	Benmokrane et al. (2020)	Pultrall Inc. (Thetford Mines, QC, Canada)	GFRP	13.0	Vinylester	Alkaline solution (IMMR)	60	90	5	78.9	101.5
195	Benmokrane et al. (2020)	Pultrall Inc. (Thetford Mines, QC, Canada)	BFRP	13.0	Vinylester	Control	NA	0	5	100.0	100.0
196	Benmokrane et al. (2020)	Pultrall Inc. (Thetford Mines, QC, Canada)	BFRP	13.0	Vinylester	Alkaline solution (IMMR)	60	90	5	57.1	104.7
197	Benmokrane et al. (2020)	Pultrall Inc. (Thetford Mines, QC, Canada)	BFRP	13.0	Vinylester	Control	NA	0	5	100.0	100.0
198	Benmokrane et al.	Pultrall Inc. (Thetford	BFRP	13.0	Vinylester	Alkaline solution (IMMR)	60	90	5	60.5	101.2

	(2020)	Mines, QC, Canada)									
199	Benmokrane et al. (2020)	Pultrall Inc. (Thetford Mines, QC, Canada)	BFRP	13.0	Vinylester	Control	NA	0	5	100.0	100.0
200	Benmokrane et al. (2020)	Pultrall Inc. (Thetford Mines, QC, Canada)	BFRP	13.0	Vinylester	Alkaline solution (IMMR)	60	90	5	61.3	100.8
201	Benmokrane et al. (2020)	Pultrall Inc. (Thetford Mines, QC, Canada)	BFRP	13.0	Polyurethane	Control	NA	0	5	100.0	100.0
202	Benmokrane et al. (2020)	Pultrall Inc. (Thetford Mines, QC, Canada)	BFRP	13.0	Polyurethane	Alkaline solution (IMMR)	60	90	5	86.4	100.0
203	Benmokrane et al. (2020)	Pultrall Inc. (Thetford Mines, QC, Canada)	BFRP	13.0	Polyurethane	Control	NA	0	5	100.0	100.0
204	Benmokrane et al. (2020)	Pultrall Inc. (Thetford Mines, QC, Canada)	BFRP	13.0	Polyurethane	Alkaline solution (IMMR)	60	90	5	73.6	101.7
205	Benmokrane et al. (2020)	Pultrall Inc. (Thetford Mines, QC, Canada)	BFRP	13.0	Epoxy	Control	NA	0	5	100.0	100.0
206	Benmokrane et al. (2020)	Pultrall Inc. (Thetford Mines, QC, Canada)	BFRP	13.0	Epoxy	Alkaline solution (IMMR)	60	90	5	85.1	104.7
207	Benmokrane et al. (2020)	Pultrall Inc. (Thetford Mines, QC, Canada)	BFRP	13.0	Epoxy	Control	NA	0	5	100.0	100.0
208	Benmokrane et al. (2020)	Pultrall Inc. (Thetford Mines, QC, Canada)	BFRP	13.0	Epoxy	Alkaline solution (IMMR)	60	90	5	81.8	101.2
209	Benmokrane et al. (2020)	Pultrall Inc. (Thetford Mines, QC, Canada)	CFRP	13.0	Epoxy	Control	NA	0	5	100.0	100.0
210	Benmokrane et al. (2020)	Pultrall Inc. (Thetford Mines, QC, Canada)	CFRP	13.0	Epoxy	Alkaline solution (IMMR)	60	90	5	100.5	101.6
211	Benmokrane et al. (2020)	Pultrall Inc. (Thetford Mines, QC, Canada)	CFRP	13.0	Epoxy	Control	NA	0	5	100.0	100.0
212	Benmokrane et al. (2020)	Pultrall Inc. (Thetford Mines, QC, Canada)	CFRP	13.0	Epoxy	Alkaline solution (IMMR)	60	90	5	100.3	101.0
213	Benmokrane et al. (2020)	Pultrall Inc. (Thetford Mines, QC, Canada)	CFRP	13.0	Vinylester	Control	NA	0	5	100.0	100.0
214	Benmokrane et al. (2020)	Pultrall Inc. (Thetford Mines, QC, Canada)	CFRP	13.0	Vinylester	Alkaline solution (IMMR)	60	90	5	98.8	102.8
215	Benmokrane et al. (2020)	Pultrall Inc. (Thetford Mines, QC, Canada)	CFRP	13.0	Vinylester	Control	NA	0	5	100.0	100.0
216	Benmokrane et al. (2020)	Pultrall Inc. (Thetford Mines, QC, Canada)	CFRP	13.0	Vinylester	Alkaline solution (IMMR)	60	90	5	98.0	99.5
217	Benmokrane et al. (2020)	Pultrall Inc. (Thetford Mines, QC, Canada)	CFRP	13.0	Vinylester	Control	NA	0	5	100.0	100.0
218	Benmokrane et al. (2020)	Pultrall Inc. (Thetford Mines, QC, Canada)	CFRP	13.0	Vinylester	Alkaline solution (IMMR)	60	90	5	95.4	100.4
219	Benmokrane et al. (2021)	B&B FRP Manufacturing Inc. (Toronto, Canada)	GFRP	15.0	Vinylester	Control	NA	0	8	100.0	100.0
220	Benmokrane et al. (2021)	B&B FRP Manufacturing Inc. (Toronto, Canada)	GFRP	15.0	Vinylester	Alkaline solution (IMMR)	60	90	8	90.0	100.0
221	Chen et al. (2006)	Hughes Brothers, Inc.	GFRP	9.5	Vinylester	Control	20	0	3-6	100.0	NA

222	Chen et al. (2006)	Hughes Brothers, Inc.	GFRP	9.5	Vinylester	Alkaline solution 1 (IMMR)	20	60	3-6	82.4	NA
223	Chen et al. (2006)	Hughes Brothers, Inc.	GFRP	9.5	Vinylester	Alkaline solution 1 (IMMR)	20	90	3-6	64.6	NA
224	Chen et al. (2006)	Hughes Brothers, Inc.	GFRP	9.5	Vinylester	Alkaline solution 1 (IMMR)	20	120	3-6	55.3	NA
225	Chen et al. (2006)	Hughes Brothers, Inc.	GFRP	9.5	Vinylester	Alkaline solution 1 (IMMR)	20	240	3-6	43.5	NA
226	Chen et al. (2006)	Hughes Brothers, Inc.	GFRP	9.5	Vinylester	Alkaline solution 1 (IMMR)	40	60	3-6	69.3	NA
227	Chen et al. (2006)	Hughes Brothers, Inc.	GFRP	9.5	Vinylester	Alkaline solution 1 (IMMR)	40	90	3-6	60.7	NA
228	Chen et al. (2006)	Hughes Brothers, Inc.	GFRP	9.5	Vinylester	Alkaline solution 1 (IMMR)	40	120	3-6	50.2	NA
229	Chen et al. (2006)	Hughes Brothers, Inc.	GFRP	9.5	Vinylester	Alkaline solution 1 (IMMR)	40	240	3-6	33.7	NA
230	Chen et al. (2006)	Hughes Brothers, Inc.	GFRP	9.5	Vinylester	Alkaline solution 1 (IMMR)	60	60	3-6	52.3	NA
231	Chen et al. (2006)	Hughes Brothers, Inc.	GFRP	9.5	Vinylester	Alkaline solution 1 (IMMR)	60	90	3-6	44.3	NA
232	Chen et al. (2006)	Hughes Brothers, Inc.	GFRP	9.5	Vinylester	Alkaline solution 1 (IMMR)	60	120	3-6	38.2	NA
233	Chen et al. (2006)	Hughes Brothers, Inc.	GFRP	9.5	Vinylester	Alkaline solution 1 (IMMR)	60	240	3-6	23.5	NA
234	Chen et al. (2006)	Hughes Brothers, Inc.	GFRP	9.5	Vinylester	Control	20	0	3-6	100.0	NA
235	Chen et al. (2006)	Hughes Brothers, Inc.	GFRP	9.5	Vinylester	Alkaline solution 2 (IMMR)	20	60	3-6	98.3	NA
236	Chen et al. (2006)	Hughes Brothers, Inc.	GFRP	9.5	Vinylester	Alkaline solution 2 (IMMR)	20	70	3-6	97.2	NA
237	Chen et al. (2006)	Hughes Brothers, Inc.	GFRP	9.5	Vinylester	Alkaline solution 2 (IMMR)	20	90	3-6	95.0	NA
238	Chen et al. (2006)	Hughes Brothers, Inc.	GFRP	9.5	Vinylester	Alkaline solution 2 (IMMR)	20	120	3-6	92.0	NA
239	Chen et al. (2006)	Hughes Brothers, Inc.	GFRP	9.5	Vinylester	Alkaline solution 2 (IMMR)	40	60	3-6	93.1	NA
240	Chen et al. (2006)	Hughes Brothers, Inc.	GFRP	9.5	Vinylester	Alkaline solution 2 (IMMR)	40	70	3-6	92.4	NA
241	Chen et al. (2006)	Hughes Brothers, Inc.	GFRP	9.5	Vinylester	Alkaline solution 2 (IMMR)	40	90	3-6	86.1	NA
242	Chen et al. (2006)	Hughes Brothers, Inc.	GFRP	9.5	Vinylester	Alkaline solution 2 (IMMR)	40	120	3-6	86.1	NA
243	Chen et al. (2006)	Hughes Brothers, Inc.	GFRP	9.5	Vinylester	Alkaline solution 2 (IMMR)	60	60	3-6	76.2	NA
244	Chen et al. (2006)	Hughes Brothers, Inc.	GFRP	9.5	Vinylester	Alkaline solution 2 (IMMR)	60	70	3-6	73.3	NA
245	Chen et al. (2006)	Hughes Brothers, Inc.	GFRP	9.5	Vinylester	Alkaline solution 2 (IMMR)	60	90	3-6	66.3	NA
246	Chen et al. (2006)	Hughes Brothers, Inc.	GFRP	9.5	Vinylester	Alkaline solution 2 (IMMR)	60	120	3-6	59.3	NA
247	Chen et al. (2007)	Hughes Brothers, Inc.	GFRP	9.5	Vinylester	Control	20	0	6	100.0	NA
248	Chen et al. (2007)	Hughes Brothers, Inc.	GFRP	9.5	Vinylester	Water (IMMR)	20	120	3	94.9	NA
249	Chen et al. (2007)	Hughes Brothers, Inc.	GFRP	9.5	Vinylester	Water (IMMR)	40	70	6	97.0	NA
250	Chen et al. (2007)	Hughes Brothers, Inc.	GFRP	9.5	Vinylester	Water (IMMR)	60	70	6	70.6	NA
251	Chen et al. (2007)	Hughes Brothers, Inc.	GFRP	9.5	Vinylester	Water (WD)	60	72	6	84.4	NA
252	Chen et al. (2007)	Hughes Brothers, Inc.	GFRP	9.5	Vinylester	Alkaline solution 1 (IMMR)	20	120	4	86.1	NA
253	Chen et al. (2007)	Hughes Brothers, Inc.	GFRP	9.5	Vinylester	Alkaline solution 1 (IMMR)	40	70	4	89.2	NA
254	Chen et al. (2007)	Hughes Brothers, Inc.	GFRP	9.5	Vinylester	Alkaline solution 1 (IMMR)	60	70	6	63.9	NA
255	Chen et al. (2007)	Hughes Brothers, Inc.	GFRP	9.5	Vinylester	Alkaline solution 1 (WD)	60	72	6	72.8	NA
256	Chen et al. (2007)	Hughes Brothers, Inc.	GFRP	9.5	Vinylester	Alkaline solution 2 (IMMR)	20	120	4	92.5	NA
257	Chen et al. (2007)	Hughes Brothers, Inc.	GFRP	9.5	Vinylester	Alkaline solution 2 (IMMR)	40	70	4	92.2	NA
258	Chen et al. (2007)	Hughes Brothers, Inc.	GFRP	9.5	Vinylester	Alkaline solution 2 (IMMR)	60	70	5	73.2	NA
259	Chen et al. (2007)	Hughes Brothers, Inc.	GFRP	9.5	Vinylester	Alkaline solution 2 (WD)	60	72	5	80.2	NA
260	Chen et al. (2007)	Hughes Brothers, Inc.	GFRP	9.5	Vinylester	Saline solution (IMMR)	20	120	4	97.4	NA
261	Chen et al. (2007)	Hughes Brothers, Inc.	GFRP	9.5	Vinylester	Saline solution (IMMR)	40	70	6	97.8	NA
262	Chen et al. (2007)	Hughes Brothers, Inc.	GFRP	9.5	Vinylester	Saline solution (IMMR)	60	70	6	74.2	NA
263	Chen et al. (2007)	Hughes Brothers, Inc.	GFRP	9.5	Vinylester	Saline solution (WD)	60	72	5	86.4	NA
264	Chen et al. (2007)	Hughes Brothers, Inc.	GFRP	9.5	Vinylester	Alkaline solution with Cl- (FT)	-20/20	50	4	103.5	NA
265	Chen et al. (2007)	NA	GFRP	9.5	Vinylester	Control	20	0	5	100.0	NA
266	Chen et al. (2007)	NA	GFRP	9.5	Vinylester	Alkaline solution 1 (IMMR)	20	90	4	63.9	NA
267	Chen et al. (2007)	NA	GFRP	9.5	Vinylester	Alkaline solution 1 (IMMR)	20	120	4	54.8	NA

268	Chen et al. (2007)	NA	GFRP	9.5	Vinylester	Alkaline solution 1 (IMMR)	40	60	4	69.0	NA
269	Chen et al. (2007)	NA	GFRP	9.5	Vinylester	Alkaline solution 1 (IMMR)	60	60	3	52.1	NA
270	Chen et al. (2007)	NA	GFRP	9.5	Vinylester	NCE+Water (IMMR)	20	90	3	90.4	NA
271	Chen et al. (2007)	NA	GFRP	9.5	Vinylester	NCE+Alkaline solution 2 (IMMR)	60	90	3	61.2	NA
272	Chen et al. (2007)	Hughes Brothers, Inc.	CFRP	9.0	Epoxy	Control	20	0	5	100.0	NA
273	Chen et al. (2007)	Hughes Brothers, Inc.	CFRP	9.0	Epoxy	Alkaline solution 1 (IMMR)	60	70	4	95.7	NA
274	D'Antino (2023)	Sireg Geotech srl (Italy)	GFRP	6.0	Vinylester	Control	RT	0	5	100.0	100.0
275	D'Antino (2023)	Sireg Geotech srl (Italy)	GFRP	6.0	Vinylester	SL (3000 με)+Alkaline solution (IMMR)	60	42	5	92.1	97.9
276	D'Antino (2023)	Sireg Geotech srl (Italy)	GFRP	20.0	Vinylester	Control	RT	0	5	100.0	100.0
277	D'Antino (2023)	Sireg Geotech srl (Italy)	GFRP	20.0	Vinylester	SL (3000 με)+Alkaline solution (IMMR)	60	42	5	87.1	93.9
278	D'Antino (2023)	Sireg Geotech srl (Italy)	GFRP	32.0	Vinylester	Control	RT	0	5	100.0	100.0
279	D'Antino (2023)	Sireg Geotech srl (Italy)	GFRP	32.0	Vinylester	SL (3000 με)+Alkaline solution (IMMR)	60	42	5	86.5	98.0
280	Davalos et al. (2011)	Hughes Brothers, Inc.	GFRP	9.5	Vinylester	Control	20	0	4	100.0	NA
281	Davalos et al. (2011)	Hughes Brothers, Inc.	GFRP	9.5	Vinylester	NCE+Water (IMMR)	20	30	4	98.3	NA
282	Davalos et al. (2011)	Hughes Brothers, Inc.	GFRP	9.5	Vinylester	NCE+Water (IMMR)	20	90	4	92.7	NA
283	Davalos et al. (2011)	Hughes Brothers, Inc.	GFRP	9.5	Vinylester	NCE+Water (IMMR)	20	150	4	84.4	NA
284	Davalos et al. (2011)	Hughes Brothers, Inc.	GFRP	9.5	Vinylester	NCE+Water (IMMR)	20	210	4	82.6	NA
285	Davalos et al. (2011)	Hughes Brothers, Inc.	GFRP	9.5	Vinylester	NCE+Water (IMMR)	20	270	4	82.6	NA
286	Davalos et al. (2011)	Hughes Brothers, Inc.	GFRP	9.5	Vinylester	NCE+Water (IMMR)	40	30	4	87.2	NA
287	Davalos et al. (2011)	Hughes Brothers, Inc.	GFRP	9.5	Vinylester	NCE+Water (IMMR)	40	90	4	80.6	NA
288	Davalos et al. (2011)	Hughes Brothers, Inc.	GFRP	9.5	Vinylester	NCE+Water (IMMR)	40	150	4	70.0	NA
289	Davalos et al. (2011)	Hughes Brothers, Inc.	GFRP	9.5	Vinylester	NCE+Water (IMMR)	40	210	4	68.5	NA
290	Davalos et al. (2011)	Hughes Brothers, Inc.	GFRP	9.5	Vinylester	NCE+Water (IMMR)	40	270	4	65.2	NA
291	Davalos et al. (2011)	Hughes Brothers, Inc.	GFRP	9.5	Vinylester	NCE+Water (IMMR)	50	30	4	80.1	NA
292	Davalos et al. (2011)	Hughes Brothers, Inc.	GFRP	9.5	Vinylester	NCE+Water (IMMR)	50	90	4	67.0	NA
293	Davalos et al. (2011)	Hughes Brothers, Inc.	GFRP	9.5	Vinylester	NCE+Water (IMMR)	50	150	4	52.9	NA
294	Davalos et al. (2011)	Hughes Brothers, Inc.	GFRP	9.5	Vinylester	NCE+Water (IMMR)	50	210	4	50.6	NA
295	Davalos et al.	Hughes Brothers, Inc.	GFRP	9.5	Vinylester	NCE+Water (IMMR)	50	270	4	47.3	NA

	(2011)											
296	Davalos et al. (2011)	Hughes Brothers, Inc.	GFRP	9.5	Vinylester	NCE+Water (IMMR)	60	30	4	78.1	NA
297	Davalos et al. (2011)	Hughes Brothers, Inc.	GFRP	9.5	Vinylester	NCE+Water (IMMR)	60	90	4	61.5	NA
298	Davalos et al. (2011)	Hughes Brothers, Inc.	GFRP	9.5	Vinylester	NCE+Water (IMMR)	60	150	4	47.8	NA
299	Davalos et al. (2011)	Hughes Brothers, Inc.	GFRP	9.5	Vinylester	NCE+Water (IMMR)	60	210	4	45.8	NA
300	Davalos et al. (2011)	Hughes Brothers, Inc.	GFRP	9.5	Vinylester	NCE+Water (IMMR)	60	270	4	44.8	NA
301	Davalos et al. (2011)	Hughes Brothers, Inc.	GFRP	9.5	Vinylester	SL (2000-2600με)+NCE+Water (IMMR)	20	90	4	89.2	NA
302	Davalos et al. (2011)	Hughes Brothers, Inc.	GFRP	9.5	Vinylester	SL (2000-2600με)+NCE+Water (IMMR)	20	120	4	83.9	NA
303	Davalos et al. (2011)	Hughes Brothers, Inc.	GFRP	9.5	Vinylester	SL (2000-2600με)+NCE+Water (IMMR)	20	170	4	84.2	NA
304	Davalos et al. (2011)	Hughes Brothers, Inc.	GFRP	9.5	Vinylester	SL (2000-2600με)+NCE+Water (IMMR)	20	210	4	80.1	NA
305	Davalos et al. (2011)	Hughes Brothers, Inc.	GFRP	9.5	Vinylester	SL (2000-2600με)+NCE+Water (IMMR)	40	90	4	83.9	NA
306	Davalos et al. (2011)	Hughes Brothers, Inc.	GFRP	9.5	Vinylester	SL (2000-2600με)+NCE+Water (IMMR)	40	120	4	79.9	NA
307	Davalos et al. (2011)	Hughes Brothers, Inc.	GFRP	9.5	Vinylester	SL (2000-2600με)+NCE+Water (IMMR)	40	210	4	70.3	NA
308	Davalos et al. (2011)	Hughes Brothers, Inc.	GFRP	9.5	Vinylester	SL (2000-2600με)+NCE+Water (IMMR)	60	90	4	63.0	NA
309	Davalos et al. (2011)	Hughes Brothers, Inc.	GFRP	9.5	Vinylester	SL (2000-2600με)+NCE+Water (IMMR)	60	120	4	60.2	NA
310	Davalos et al. (2011)	Hughes Brothers, Inc.	GFRP	9.5	Vinylester	SL (2000-2600με)+NCE+Water (IMMR)	60	170	4	48.1	NA
311	Davalos et al. (2011)	Hughes Brothers, Inc.	GFRP	9.5	Vinylester	SL (2000-2600με)+NCE+Water (IMMR)	60	210	4	47.1	NA
312	Davalos et al. (2011)	Hughes Brothers, Inc.	GFRP	9.5	Vinylester	SL (1100-1300με)+NCE+Water (IMMR)	60	120	4	57.9	NA
313	Davalos et al. (2011)	Hughes Brothers, Inc.	GFRP	9.5	Vinylester	SL (1100-1300με)+NCE+Water (IMMR)	60	210	4	47.7	NA
314	Davalos et al. (2011)	Hughes Brothers, Inc.	GFRP	9.5	Vinylester	Water (IMMR)	20	150	4	94.4	NA
315	Davalos et al. (2011)	Hughes Brothers, Inc.	GFRP	9.5	Vinylester	NCE	20	150	4	98.4	NA
316	Davalos et al. (2011)	Hughes Brothers, Inc.	GFRP	9.5	Vinylester	SL (2000-2600με)+NCE	20	150	4	97.6	NA
317	Davalos et al. (2011)	Hughes Brothers, Inc.	GFRP	9.5	Vinylester	Control	20	0	4	100.0	NA
318	Davalos et al.	Hughes Brothers, Inc.	GFRP	9.5	Vinylester	NCE+Water (IMMR)	20	150	4	89.6	NA

	(2011)										
319	Davalos et al. (2011)	Hughes Brothers, Inc.	GFRP	9.5	Vinylester	SL (2000-2600με)+NCE+Water (IMMR)	20	150	4	91.6	NA
320	Davalos et al. (2011)	Hughes Brothers, Inc.	GFRP	9.5	Vinylester	Water (IMMR)	20	150	4	90.8	NA
321	Davalos et al. (2011)	Hughes Brothers, Inc.	GFRP	9.5	Vinylester	NCE	20	150	4	95.2	NA
322	Debaiky et al. (2006)	Pultrall Inc. (Thetford Mines, QC, Canada)	GFRP	15.9	Vinylester	Control	20	0	5	100.0	100.0
323	Debaiky et al. (2006)	Pultrall Inc. (Thetford Mines, QC, Canada)	GFRP	15.9	Vinylester	SL (19-29%fu)+Water (IMMR)	58	30	5	95.9	97.9
324	Debaiky et al. (2006)	Pultrall Inc. (Thetford Mines, QC, Canada)	GFRP	15.9	Vinylester	SL (19-29%fu)+Water (IMMR)	60	60	5	90.0	95.2
325	Debaiky et al. (2006)	Pultrall Inc. (Thetford Mines, QC, Canada)	GFRP	15.9	Vinylester	SL (19-29%fu)+Alkaline solution (IMMR)	55	30	5	97.9	98.8
326	Debaiky et al. (2006)	Pultrall Inc. (Thetford Mines, QC, Canada)	GFRP	15.9	Vinylester	SL (19-29%fu)+Alkaline solution (IMMR)	61	60	5	84.1	94.3
327	Debaiky et al. (2006)	Pultrall Inc. (Thetford Mines, QC, Canada)	GFRP	12.7	Vinylester	Control	20	0	5	100.0	100.0
328	Debaiky et al. (2006)	Pultrall Inc. (Thetford Mines, QC, Canada)	GFRP	12.7	Vinylester	SL (19-29%fu)+Water (IMMR)	60	120	8	84.5	106.2
329	Debaiky et al. (2006)	Pultrall Inc. (Thetford Mines, QC, Canada)	GFRP	12.7	Vinylester	SL (19-29%fu)+Alkaline solution (IMMR)	57	120	7	82.8	110.2
330	Debaiky et al. (2006)	Pultrall Inc. (Thetford Mines, QC, Canada)	GFRP	9.5	Vinylester	Control	20	0	5	100.0	100.0
331	Debaiky et al. (2006)	Pultrall Inc. (Thetford Mines, QC, Canada)	GFRP	9.5	Vinylester	SL (19-29%fu)+Water (IMMR)	72	60	10	98.3	95.3
332	Debaiky et al. (2006)	Pultrall Inc. (Thetford Mines, QC, Canada)	GFRP	9.5	Vinylester	SL (19-29%fu)+Water (IMMR)	20	147	5	92.7	102.3
333	Debaiky et al. (2006)	Pultrall Inc. (Thetford Mines, QC, Canada)	GFRP	9.5	Vinylester	SL (19-29%fu)+Alkaline solution (IMMR)	64	60	7	90.1	92.8
334	Debaiky et al. (2006)	Pultrall Inc. (Thetford Mines, QC, Canada)	GFRP	9.5	Vinylester	SL (19-29%fu)+Alkaline solution (IMMR)	20	147	5	84.3	103.3
335	El-Hassan et al. (2017)	NA	GFRP	7.2	Epoxy	Control	NA	0	NA	100.0	NA
336	El-Hassan et al. (2017)	NA	GFRP	7.2	Epoxy	SWCE+Water (IMMR)	20	150	3	98.0	NA
337	El-Hassan et al. (2017)	NA	GFRP	7.2	Epoxy	SWCE+Water (IMMR)	20	300	3	98.0	NA
338	El-Hassan et al. (2017)	NA	GFRP	7.2	Epoxy	SWCE+Water (IMMR)	20	450	3	98.0	NA
339	El-Hassan et al. (2017)	NA	GFRP	7.2	Epoxy	SWCE+Water (IMMR)	40	150	3	92.0	NA
340	El-Hassan et al. (2017)	NA	GFRP	7.2	Epoxy	SWCE+Water (IMMR)	40	300	3	95.0	NA
341	El-Hassan et al.	NA	GFRP	7.2	Epoxy	SWCE+Water (IMMR)	40	450	3	92.0	NA

	(2017)										
342	El-Hassan et al. (2017)	NA	GFRP	7.2	Epoxy	SWCE+Water (IMMR)	60	150	3	90.0	NA
343	El-Hassan et al. (2017)	NA	GFRP	7.2	Epoxy	SWCE+Water (IMMR)	60	300	3	94.0	NA
344	El-Hassan et al. (2017)	NA	GFRP	7.2	Epoxy	SWCE+Water (IMMR)	60	450	3	85.0	NA
345	El-Hassan et al. (2017)	NA	GFRP	8.0	Epoxy	Control	NA	0	NA	100.0	NA
346	El-Hassan et al. (2017)	NA	GFRP	8.0	Epoxy	SWCE+Water (IMMR)	20	150	3	84.0	NA
347	El-Hassan et al. (2017)	NA	GFRP	8.0	Epoxy	SWCE+Water (IMMR)	20	300	3	79.0	NA
348	El-Hassan et al. (2017)	NA	GFRP	8.0	Epoxy	SWCE+Water (IMMR)	20	450	3	73.0	NA
349	El-Hassan et al. (2017)	NA	GFRP	8.0	Epoxy	SWCE+Water (IMMR)	40	150	3	77.0	NA
350	El-Hassan et al. (2017)	NA	GFRP	8.0	Epoxy	SWCE+Water (IMMR)	40	300	3	66.0	NA
351	El-Hassan et al. (2017)	NA	GFRP	8.0	Epoxy	SWCE+Water (IMMR)	40	450	3	68.0	NA
352	El-Hassan et al. (2017)	NA	GFRP	8.0	Epoxy	SWCE+Water (IMMR)	60	150	3	73.0	NA
353	El-Hassan et al. (2017)	NA	GFRP	8.0	Epoxy	SWCE+Water (IMMR)	60	300	3	50.0	NA
354	El-Hassan et al. (2017)	NA	GFRP	8.0	Epoxy	SWCE+Water (IMMR)	60	450	3	53.0	NA
355	El-Hassan et al. (2018)	NA	GFRP	7.2	Epoxy	Control	NA	0	NA	100.0	NA
356	El-Hassan et al. (2018)	NA	GFRP	7.2	Epoxy	SL (25%fu)+SWCE+Water (IMMR)	20	150	3	90.0	NA
357	El-Hassan et al. (2018)	NA	GFRP	7.2	Epoxy	SL (25%fu)+SWCE+Water (IMMR)	20	300	3	90.0	NA
358	El-Hassan et al. (2018)	NA	GFRP	7.2	Epoxy	SL (25%fu)+SWCE+Water (IMMR)	20	450	3	84.0	NA
359	El-Hassan et al. (2018)	NA	GFRP	7.2	Epoxy	SL (25%fu)+SWCE+Water (IMMR)	40	150	3	84.0	NA
360	El-Hassan et al. (2018)	NA	GFRP	7.2	Epoxy	SL (25%fu)+SWCE+Water (IMMR)	40	300	3	72.0	NA
361	El-Hassan et al. (2018)	NA	GFRP	7.2	Epoxy	SL (25%fu)+SWCE+Water (IMMR)	40	450	3	51.0	NA
362	El-Hassan et al. (2018)	NA	GFRP	7.2	Epoxy	SL (25%fu)+SWCE+Water (IMMR)	60	150	3	72.0	NA
363	El-Hassan et al. (2018)	NA	GFRP	7.2	Epoxy	SL (25%fu)+SWCE+Water (IMMR)	60	300	3	0.0	NA
364	El-Hassan et al.	NA	GFRP	7.2	Epoxy	SL (25%fu)+SWCE+Water	60	450	3	45.0	NA

	(2018)					(IMMR)					
365	El-Hassan et al. (2018)	NA	GFRP	8.0	Epoxy	Control	NA	0	NA	100.0	NA
366	El-Hassan et al. (2018)	NA	GFRP	8.0	Epoxy	SL (25%fu)+SWCE+Water (IMMR)	20	150	3	84.0	NA
367	El-Hassan et al. (2018)	NA	GFRP	8.0	Epoxy	SL (25%fu)+SWCE+Water (IMMR)	20	300	3	78.0	NA
368	El-Hassan et al. (2018)	NA	GFRP	8.0	Epoxy	SL (25%fu)+SWCE+Water (IMMR)	20	450	3	70.0	NA
369	El-Hassan et al. (2018)	NA	GFRP	8.0	Epoxy	SL (25%fu)+SWCE+Water (IMMR)	40	150	3	63.0	NA
370	El-Hassan et al. (2018)	NA	GFRP	8.0	Epoxy	SL (25%fu)+SWCE+Water (IMMR)	40	300	3	62.0	NA
371	El-Hassan et al. (2018)	NA	GFRP	8.0	Epoxy	SL (25%fu)+SWCE+Water (IMMR)	40	450	3	48.0	NA
372	El-Hassan et al. (2018)	NA	GFRP	8.0	Epoxy	SL (25%fu)+SWCE+Water (IMMR)	60	150	3	58.0	NA
373	El-Hassan et al. (2018)	NA	GFRP	8.0	Epoxy	SL (25%fu)+SWCE+Water (IMMR)	60	300	3	42.0	NA
374	El-Hassan et al. (2018)	NA	GFRP	8.0	Epoxy	SL (25%fu)+SWCE+Water (IMMR)	60	450	3	36.0	NA
375	Fergani et al. (2018)	NA	GFRP	8.0	Vinylester	Control	20	0	5	100.0	100.0
376	Fergani et al. (2018)	NA	GFRP	8.0	Vinylester	Alkaline solution (IMMR)	20	42	3	95.5	101.1
377	Fergani et al. (2018)	NA	GFRP	8.0	Vinylester	Alkaline solution (IMMR)	20	83	3	94.3	95.5
378	Fergani et al. (2018)	NA	GFRP	8.0	Vinylester	Alkaline solution (IMMR)	20	270	3	97.1	104.3
379	Fergani et al. (2018)	NA	GFRP	8.0	Vinylester	Alkaline solution (IMMR)	40	42	3	91.2	102.5
380	Fergani et al. (2018)	NA	GFRP	8.0	Vinylester	Alkaline solution (IMMR)	40	83	3	90.1	101.6
381	Fergani et al. (2018)	NA	GFRP	8.0	Vinylester	Alkaline solution (IMMR)	40	270	3	85.0	107.7
382	Fergani et al. (2018)	NA	GFRP	8.0	Vinylester	Alkaline solution (IMMR)	60	42	3	85.0	105.5
383	Fergani et al. (2018)	NA	GFRP	8.0	Vinylester	Alkaline solution (IMMR)	60	83	3	73.9	103.4
384	Fergani et al. (2018)	NA	GFRP	8.0	Vinylester	Alkaline solution (IMMR)	60	270	3	64.7	118.4
385	Fergani et al. (2018)	NA	GFRP	8.0	Vinylester	SL (3000με)+Alkaline solution (IMMR)	60	42	3	86.1	105.0
386	Fergani et al. (2018)	NA	GFRP	8.0	Vinylester	SL (3000με)+Alkaline solution (IMMR)	60	83	3	75.5	100.0
387	Fergani et al.	NA	GFRP	8.0	Vinylester	NCE	20	270	3	99.9	101.1

	(2018)										
388	Fergani et al. (2018)	NA	GFRP	8.0	Vinylester	NCE+Water (IMMR)	20	83	3	92.2	98.6
389	Fergani et al. (2018)	NA	GFRP	8.0	Vinylester	NCE+Water (IMMR)	20	270	3	90.3	98.9
390	Fergani et al. (2018)	NA	GFRP	8.0	Vinylester	NCE+Water (IMMR)	40	42	3	94.6	100.7
391	Fergani et al. (2018)	NA	GFRP	8.0	Vinylester	NCE+Water (IMMR)	40	83	3	88.8	102.5
392	Fergani et al. (2018)	NA	GFRP	8.0	Vinylester	NCE+Water (IMMR)	40	270	3	74.4	104.1
393	Fergani et al. (2018)	NA	GFRP	8.0	Vinylester	NCE+Water (IMMR)	60	42	3	80.7	106.6
394	Fergani et al. (2018)	NA	GFRP	8.0	Vinylester	NCE+Water (IMMR)	60	83	3	79.6	104.8
395	Fergani et al. (2018)	NA	GFRP	8.0	Vinylester	NCE+Water (IMMR)	60	270	3	59.5	98.8
396	Fergani et al. (2018)	NA	GFRP	8.0	Vinylester	SL (3000με)+NCE+Water (IMMR)	20	42	3	95.5	102.7
397	Fergani et al. (2018)	NA	GFRP	8.0	Vinylester	SL (3000με)+NCE+Water (IMMR)	20	83	3	91.8	109.8
398	Fergani et al. (2018)	NA	GFRP	8.0	Vinylester	SL (3000με)+NCE+Water (IMMR)	20	270	3	88.5	98.9
399	Fergani et al. (2018)	NA	GFRP	8.0	Vinylester	SL (3000με)+NCE+Water (IMMR)	40	42	3	79.6	104.3
400	Fergani et al. (2018)	NA	GFRP	8.0	Vinylester	SL (3000με)+NCE+Water (IMMR)	40	83	3	86.6	101.6
401	Fergani et al. (2018)	NA	GFRP	8.0	Vinylester	SL (3000με)+NCE+Water (IMMR)	40	270	3	76.3	102.0
402	Fergani et al. (2018)	NA	GFRP	8.0	Vinylester	SL (3000με)+NCE+Water (IMMR)	60	42	3	80.0	103.9
403	Fergani et al. (2018)	NA	GFRP	8.0	Vinylester	SL (3000με)+NCE+Water (IMMR)	60	83	3	69.6	104.8
404	Fergani et al. (2018)	NA	GFRP	8.0	Vinylester	SL (3000με)+NCE+Water (IMMR)	60	270	3	59.6	108.9
405	Fergani et al. (2018)	NA	GFRP	8.0	Vinylester	SL (5000με)+NCE+Water (IMMR)	60	42	3	77.2	105.9
406	Fergani et al. (2018)	NA	GFRP	8.0	Vinylester	SL (5000με)+NCE+Water (IMMR)	60	83	3	66.3	106.8
407	Fergani et al. (2018)	NA	GFRP	8.0	Vinylester	SL (5000με)+NCE+Water (IMMR)	60	270	3	63.0	103.9
408	Guo et al. (2022a)	NA	BFRP	10.0	Epoxy	Control	21	0	NA	100.0	100.0
409	Guo et al. (2022a)	NA	BFRP	10.0	Epoxy	SWSSC solution (IMMR)	21	30	NA	100.7	100.3
410	Guo et al. (2022a)	NA	BFRP	10.0	Epoxy	SWSSC solution (IMMR)	21	60	NA	97.6	95.0
411	Guo et al. (2022a)	NA	BFRP	10.0	Epoxy	SWSSC solution (IMMR)	21	90	NA	95.7	93.7
412	Guo et al. (2022a)	NA	BFRP	10.0	Epoxy	SWSSC solution (IMMR)	40	30	NA	96.1	101.2

413	Guo et al. (2022a)	NA	BFRP	10.0	Epoxy	SWSSC solution (IMMR)	40	60	NA	88.5	90.7
414	Guo et al. (2022a)	NA	BFRP	10.0	Epoxy	SWSSC solution (IMMR)	40	90	NA	80.6	92.3
415	Guo et al. (2022a)	NA	BFRP	10.0	Epoxy	SWSSC solution (IMMR)	55	30	NA	89.0	84.4
416	Guo et al. (2022a)	NA	BFRP	10.0	Epoxy	SWSSC solution (IMMR)	55	60	NA	49.1	95.0
417	Guo et al. (2022a)	NA	BFRP	10.0	Epoxy	SWSSC solution (IMMR)	55	90	NA	26.2	84.5
418	Guo et al. (2022b)	NA	BFRP	10.0	Epoxy	Control	NA	0	NA	100.0	100.0
419	Guo et al. (2022b)	NA	BFRP	10.0	Epoxy	NCE+Seawater (IMMR)	55	30	NA	92.4	88.6
420	Guo et al. (2022b)	NA	BFRP	10.0	Epoxy	NCE+Seawater (IMMR)	55	60	NA	89.0	89.7
421	Guo et al. (2022b)	NA	BFRP	10.0	Epoxy	NCE+Seawater (IMMR)	55	90	NA	84.2	87.9
422	Guo et al. (2022b)	NA	BFRP	10.0	Epoxy	NCE+Seawater (IMMR)	55	180	NA	77.2	91.8
423	Guo et al. (2022b)	NA	BFRP	10.0	Epoxy	SWSSCE+Seawater (IMMR)	55	30	NA	88.7	87.6
424	Guo et al. (2022b)	NA	BFRP	10.0	Epoxy	SWSSCE+Seawater (IMMR)	55	60	NA	87.6	90.1
425	Guo et al. (2022b)	NA	BFRP	10.0	Epoxy	SWSSCE+Seawater (IMMR)	55	90	NA	79.7	90.9
426	Guo et al. (2022b)	NA	BFRP	10.0	Epoxy	SWSSCE+Seawater (IMMR)	55	180	NA	73.8	88.5
427	Guo et al. (2024)	NA	BFRP	10.0	Epoxy	Control	NA	0	5	100.0	100.0
428	Guo et al. (2024)	NA	BFRP	10.0	Epoxy	NCE+Seawater (IMMR)	55	90	5	84.2	87.9
429	Guo et al. (2024)	NA	BFRP	10.0	Epoxy	NCE+Seawater (IMMR)	55	270	5	73.3	86.2
430	Guo et al. (2024)	NA	BFRP	10.0	Epoxy	NCE+Seawater (IMMR)	55	360	5	73.3	85.9
431	Guo et al. (2024)	NA	BFRP	10.0	Epoxy	SWSSCE+Seawater (IMMR)	55	90	5	79.7	90.9
432	Guo et al. (2024)	NA	BFRP	10.0	Epoxy	SWSSCE+Seawater (IMMR)	55	270	5	65.1	85.1
433	Guo et al. (2024)	NA	BFRP	10.0	Epoxy	SWSSCE+Seawater (IMMR)	55	360	5	66.0	85.4
434	He et al. (2017)	Nanjing Fenghui Composite Material Co. Ltd (China)	GFRP	10.0	Vinylester	Control	23	0	4	100.0	100.0
435	He et al. (2017)	Nanjing Fenghui Composite Material Co. Ltd (China)	GFRP	10.0	Vinylester	Uncondition	23	180	4	98.0	97.5
436	He et al. (2017)	Nanjing Fenghui Composite Material Co. Ltd (China)	GFRP	10.0	Vinylester	Uncondition	23	360	4	97.4	97.4
437	He et al. (2017)	Nanjing Fenghui Composite Material Co. Ltd (China)	GFRP	10.0	Vinylester	Uncondition	23	540	4	96.2	96.3
438	He et al. (2017)	Nanjing Fenghui Composite Material Co. Ltd (China)	GFRP	10.0	Vinylester	SL (20%Mu)+NCE+Tap water (IMMR)	23	180	4	94.3	94.3
439	He et al. (2017)	Nanjing Fenghui Composite Material Co. Ltd (China)	GFRP	10.0	Vinylester	SL (20%Mu)+NCE+Tap water (IMMR)	23	360	4	90.2	96.2
440	He et al. (2017)	Nanjing Fenghui Composite Material Co. Ltd (China)	GFRP	10.0	Vinylester	SL (20%Mu)+NCE+Tap water (IMMR)	23	540	4	88.6	98.6
441	He et al. (2017)	Nanjing Fenghui Composite Material Co. Ltd (China)	GFRP	10.0	Vinylester	Pre-cracks+SL (20%Mu)+NCE+Tap water (IMMR)	23	180	4	93.6	98.6
442	He et al. (2017)	Nanjing Fenghui Composite Material Co. Ltd (China)	GFRP	10.0	Vinylester	Pre-cracks+SL (20%Mu)+NCE+Tap water (IMMR)	23	360	4	91.2	96.2
443	He et al. (2017)	Nanjing Fenghui Composite Material Co. Ltd (China)	GFRP	10.0	Vinylester	Pre-cracks+SL (20%Mu)+NCE+Tap water (IMMR)	23	540	4	87.3	96.6
444	He et al. (2017)	Nanjing Fenghui Composite Material Co. Ltd (China)	GFRP	10.0	Vinylester	Pre-cracks+SL (40%Mu)+NCE+Tap water	23	180	4	89.2	99.2

						(IMMR)					
445	He et al. (2017)	Nanjing Fenghui Composite Material Co. Ltd (China)	GFRP	10.0	Vinylester	Pre-cracks+SL (40%Mu)+NCE+Tap water (IMMR)	23	360	4	86.4	96.4
446	He et al. (2017)	Nanjing Fenghui Composite Material Co. Ltd (China)	GFRP	10.0	Vinylester	Pre-cracks+SL (40%Mu)+NCE+Tap water (IMMR)	23	540	4	84.2	101.2
447	He et al. (2017)	Nanjing Fenghui Composite Material Co. Ltd (China)	GFRP	10.0	Vinylester	SL (20%Mu)+NCE+Alkaline solution (IMMR)	23	180	4	86.3	97.3
448	He et al. (2017)	Nanjing Fenghui Composite Material Co. Ltd (China)	GFRP	10.0	Vinylester	SL (20%Mu)+NCE+Alkaline solution (IMMR)	23	360	4	84.2	96.2
449	He et al. (2017)	Nanjing Fenghui Composite Material Co. Ltd (China)	GFRP	10.0	Vinylester	SL (20%Mu)+NCE+Alkaline solution (IMMR)	23	540	4	79.7	96.7
450	He et al. (2017)	Nanjing Fenghui Composite Material Co. Ltd (China)	GFRP	10.0	Vinylester	Pre-cracks+SL (20%Mu)+NCE+Alkaline solution (IMMR)	23	180	4	84.1	96.2
451	He et al. (2017)	Nanjing Fenghui Composite Material Co. Ltd (China)	GFRP	10.0	Vinylester	Pre-cracks+SL (20%Mu)+NCE+Alkaline solution (IMMR)	23	360	4	80.3	97.7
452	He et al. (2017)	Nanjing Fenghui Composite Material Co. Ltd (China)	GFRP	10.0	Vinylester	Pre-cracks+SL (20%Mu)+NCE+Alkaline solution (IMMR)	23	540	4	77.9	95.4
453	He et al. (2017)	Nanjing Fenghui Composite Material Co. Ltd (China)	GFRP	10.0	Vinylester	Pre-cracks+SL (40%Mu)+NCE+Alkaline solution (IMMR)	23	180	4	83.4	98.3
454	He et al. (2017)	Nanjing Fenghui Composite Material Co. Ltd (China)	GFRP	10.0	Vinylester	Pre-cracks+SL (40%Mu)+NCE+Alkaline solution (IMMR)	23	360	4	78.3	96.4
455	He et al. (2017)	Nanjing Fenghui Composite Material Co. Ltd (China)	GFRP	10.0	Vinylester	Pre-cracks+SL (40%Mu)+NCE+Alkaline solution (IMMR)	23	540	4	75.1	100.6
456	Katsuki and Uomoto (1995)	NA	GFRP	6.0	Vinylester	Control	20	0	20	100.0	NA
457	Katsuki and Uomoto (1995)	NA	GFRP	6.0	Vinylester	Alkaline solution 1 (IMMR)	40	7	20	74.6	NA
458	Katsuki and Uomoto (1995)	NA	GFRP	6.0	Vinylester	Alkaline solution 1 (IMMR)	40	30	20	53.8	NA
459	Katsuki and Uomoto (1995)	NA	GFRP	6.0	Vinylester	Alkaline solution 1 (IMMR)	40	90	20	33.1	NA
460	Katsuki and Uomoto (1995)	NA	GFRP	6.0	Vinylester	Alkaline solution 1 (IMMR)	40	120	20	28.4	NA
461	Katsuki and Uomoto (1995)	NA	AFRP	6.0	Vinylester	Control	20	0	20	100.0	NA
462	Katsuki and Uomoto (1995)	NA	AFRP	6.0	Vinylester	Alkaline solution 2 (IMMR)	40	30	20	101.2	NA
463	Katsuki and	NA	AFRP	6.0	Vinylester	Alkaline solution 2 (IMMR)	40	120	20	95.3	NA

	Uomoto (1995)										
464	Katsuki and Uomoto (1995)	NA	CFRP	6.0	Vinylester	Control	20	0	20	100.0	NA
465	Katsuki and Uomoto (1995)	NA	CFRP	6.0	Vinylester	Alkaline solution 2 (IMMR)	40	30	20	103.0	NA
466	Katsuki and Uomoto (1995)	NA	CFRP	6.0	Vinylester	Alkaline solution 2 (IMMR)	40	120	20	103.7	NA
467	Khatibmasjedi and Nanni (2017)	NA	GFRP	15.8	Vinylester	Control	NA	0	NA	100.0	100.0
468	Khatibmasjedi and Nanni (2017)	NA	GFRP	15.8	Vinylester	NCE+Seawater (IMMR)	60	180	NA	103.5	108.0
469	Khatibmasjedi and Nanni (2017)	NA	GFRP	15.8	Vinylester	SWCE+Seawater (IMMR)	60	180	NA	103.6	106.7
470	Khatibmasjedi et al. (2020)	NA	GFRP	15.8	Vinylester	Control	NA	0	5	100.0	100.0
471	Khatibmasjedi et al. (2020)	NA	GFRP	15.8	Vinylester	NCE+Seawater (IMMR)	60	180	5	103.4	108.7
472	Khatibmasjedi et al. (2020)	NA	GFRP	15.8	Vinylester	NCE+Seawater (IMMR)	60	360	5	98.6	95.7
473	Khatibmasjedi et al. (2020)	NA	GFRP	15.8	Vinylester	NCE+Seawater (IMMR)	60	540	5	88.2	89.2
474	Khatibmasjedi et al. (2020)	NA	GFRP	15.8	Vinylester	NCE+Seawater (IMMR)	60	720	5	74.1	89.2
475	Khatibmasjedi et al. (2020)	NA	GFRP	15.8	Vinylester	SWCE+Seawater (IMMR)	60	180	5	103.7	107.4
476	Khatibmasjedi et al. (2020)	NA	GFRP	15.8	Vinylester	SWCE+Seawater (IMMR)	60	360	5	96.3	97.0
477	Khatibmasjedi et al. (2020)	NA	GFRP	15.8	Vinylester	SWCE+Seawater (IMMR)	60	540	5	79.6	91.8
478	Khatibmasjedi et al. (2020)	NA	GFRP	15.8	Vinylester	SWCE+Seawater (IMMR)	60	720	5	79.0	87.9
479	Kim et al. (2008)	NA	GFRP	12.7	Vinylester	Control	25	0	3	100.0	100.0
480	Kim et al. (2008)	NA	GFRP	12.7	Vinylester	Water (IMMR)	25	30	3	91.6	86.1
481	Kim et al. (2008)	NA	GFRP	12.7	Vinylester	Water (IMMR)	25	60	3	85.8	74.8
482	Kim et al. (2008)	NA	GFRP	12.7	Vinylester	Water (IMMR)	25	90	3	80.0	77.5
483	Kim et al. (2008)	NA	GFRP	12.7	Vinylester	Water (IMMR)	25	132	3	88.9	73.5
484	Kim et al. (2008)	NA	GFRP	12.7	Vinylester	Water (IMMR)	40	30	3	89.3	81.1
485	Kim et al. (2008)	NA	GFRP	12.7	Vinylester	Water (IMMR)	40	60	3	85.1	94.7
486	Kim et al. (2008)	NA	GFRP	12.7	Vinylester	Water (IMMR)	40	90	3	82.8	90.6
487	Kim et al. (2008)	NA	GFRP	12.7	Vinylester	Water (IMMR)	40	132	3	84.1	74.8
488	Kim et al. (2008)	NA	GFRP	12.7	Vinylester	Water (IMMR)	80	30	3	85.1	75.3
489	Kim et al. (2008)	NA	GFRP	12.7	Vinylester	Water (IMMR)	80	60	3	76.0	69.4
490	Kim et al. (2008)	NA	GFRP	12.7	Vinylester	Water (IMMR)	80	90	3	79.5	96.0
491	Kim et al. (2008)	NA	GFRP	12.7	Vinylester	Water (IMMR)	80	132	3	78.1	76.6
492	Kim et al. (2008)	NA	GFRP	12.7	Vinylester	Saline solution (IMMR)	25	30	3	93.0	91.4
493	Kim et al. (2008)	NA	GFRP	12.7	Vinylester	Saline solution (IMMR)	25	60	3	81.6	73.9

494	Kim et al. (2008)	NA	GFRP	12.7	Vinylester	Saline solution (IMMR)	25	90	3	82.5	80.6
495	Kim et al. (2008)	NA	GFRP	12.7	Vinylester	Saline solution (IMMR)	25	132	3	86.4	74.3
496	Kim et al. (2008)	NA	GFRP	12.7	Vinylester	Saline solution (IMMR)	40	30	3	90.6	88.7
497	Kim et al. (2008)	NA	GFRP	12.7	Vinylester	Saline solution (IMMR)	40	60	3	84.3	74.8
498	Kim et al. (2008)	NA	GFRP	12.7	Vinylester	Saline solution (IMMR)	40	90	3	84.4	81.1
499	Kim et al. (2008)	NA	GFRP	12.7	Vinylester	Saline solution (IMMR)	40	132	3	87.4	74.8
500	Kim et al. (2008)	NA	GFRP	12.7	Vinylester	Saline solution (IMMR)	80	30	3	89.7	81.1
501	Kim et al. (2008)	NA	GFRP	12.7	Vinylester	Saline solution (IMMR)	80	60	3	80.6	79.3
502	Kim et al. (2008)	NA	GFRP	12.7	Vinylester	Saline solution (IMMR)	80	90	3	80.0	77.9
503	Kim et al. (2008)	NA	GFRP	12.7	Vinylester	Saline solution (IMMR)	80	132	3	80.7	75.2
504	Kim et al. (2008)	NA	GFRP	12.7	Vinylester	Alkaline solution (IMMR)	25	30	3	75.5	93.2
505	Kim et al. (2008)	NA	GFRP	12.7	Vinylester	Alkaline solution (IMMR)	25	60	3	67.7	89.1
506	Kim et al. (2008)	NA	GFRP	12.7	Vinylester	Alkaline solution (IMMR)	25	75	3	66.0	69.7
507	Kim et al. (2008)	NA	GFRP	12.7	Vinylester	Alkaline solution (IMMR)	40	30	3	78.3	103.4
508	Kim et al. (2008)	NA	GFRP	12.7	Vinylester	Alkaline solution (IMMR)	40	60	3	70.4	74.3
509	Kim et al. (2008)	NA	GFRP	12.7	Vinylester	Alkaline solution (IMMR)	40	75	3	67.3	75.7
510	Kim et al. (2008)	NA	GFRP	12.7	Vinylester	Alkaline solution (IMMR)	80	30	3	63.9	93.2
511	Kim et al. (2008)	NA	GFRP	12.7	Vinylester	Alkaline solution (IMMR)	80	60	3	60.3	111.2
512	Kim et al. (2008)	NA	GFRP	12.7	Vinylester	Alkaline solution (FT)	-25/30	30	3	55.6	73.7
513	Kim et al. (2008)	NA	GFRP	12.7	Vinylester	Alkaline solution (FT)	-25/30	60	3	62.2	82.5
514	Kim et al. (2008)	NA	GFRP	12.7	Vinylester	Alkaline solution (FT)	-25/30	110	3	61.8	78.8
515	Kim et al. (2008)	NA	GFRP	12.7	Modified vinylester	Control	25	0	3	100.0	100.0
516	Kim et al. (2008)	NA	GFRP	12.7	Modified vinylester	Water (IMMR)	25	30	3	94.8	98.3
517	Kim et al. (2008)	NA	GFRP	12.7	Modified vinylester	Water (IMMR)	25	60	3	75.7	105.9
518	Kim et al. (2008)	NA	GFRP	12.7	Modified vinylester	Water (IMMR)	25	90	3	81.7	86.6
519	Kim et al. (2008)	NA	GFRP	12.7	Modified vinylester	Water (IMMR)	25	132	3	87.8	75.3
520	Kim et al. (2008)	NA	GFRP	12.7	Modified vinylester	Water (IMMR)	40	30	3	92.3	94.7
521	Kim et al. (2008)	NA	GFRP	12.7	Modified vinylester	Water (IMMR)	40	60	3	87.1	91.5
522	Kim et al. (2008)	NA	GFRP	12.7	Modified vinylester	Water (IMMR)	40	90	3	78.2	85.2
523	Kim et al. (2008)	NA	GFRP	12.7	Modified vinylester	Water (IMMR)	40	132	3	81.2	76.2
524	Kim et al. (2008)	NA	GFRP	12.7	Modified vinylester	Water (IMMR)	80	30	3	66.4	96.9
525	Kim et al. (2008)	NA	GFRP	12.7	Modified vinylester	Water (IMMR)	80	60	3	55.3	91.1
526	Kim et al. (2008)	NA	GFRP	12.7	Modified vinylester	Water (IMMR)	80	90	3	49.1	93.8
527	Kim et al. (2008)	NA	GFRP	12.7	Modified	Water (IMMR)	80	132	3	43.9	82.0

						vinylester						
528	Kim et al. (2008)	NA		GFRP	12.7	Modified vinylester	Saline solution (IMMR)	25	30	3	94.5	94.1
529	Kim et al. (2008)	NA		GFRP	12.7	Modified vinylester	Saline solution (IMMR)	25	60	3	84.1	86.0
530	Kim et al. (2008)	NA		GFRP	12.7	Modified vinylester	Saline solution (IMMR)	25	90	3	83.5	86.5
531	Kim et al. (2008)	NA		GFRP	12.7	Modified vinylester	Saline solution (IMMR)	25	132	3	80.8	76.1
532	Kim et al. (2008)	NA		GFRP	12.7	Modified vinylester	Saline solution (IMMR)	40	30	3	89.6	93.2
533	Kim et al. (2008)	NA		GFRP	12.7	Modified vinylester	Saline solution (IMMR)	40	60	3	77.2	91.0
534	Kim et al. (2008)	NA		GFRP	12.7	Modified vinylester	Saline solution (IMMR)	40	90	3	81.5	86.0
535	Kim et al. (2008)	NA		GFRP	12.7	Modified vinylester	Saline solution (IMMR)	40	132	3	82.5	78.4
536	Kim et al. (2008)	NA		GFRP	12.7	Modified vinylester	Saline solution (IMMR)	80	30	3	65.3	96.8
537	Kim et al. (2008)	NA		GFRP	12.7	Modified vinylester	Saline solution (IMMR)	80	60	3	53.3	91.0
538	Kim et al. (2008)	NA		GFRP	12.7	Modified vinylester	Saline solution (IMMR)	80	90	3	53.4	89.6
539	Kim et al. (2008)	NA		GFRP	12.7	Modified vinylester	Saline solution (IMMR)	80	132	3	42.6	81.1
540	Kim et al. (2008)	NA		GFRP	12.7	Modified vinylester	Alkaline solution (IMMR)	25	30	3	93.8	96.0
541	Kim et al. (2008)	NA		GFRP	12.7	Modified vinylester	Alkaline solution (IMMR)	25	60	3	82.8	84.5
542	Kim et al. (2008)	NA		GFRP	12.7	Modified vinylester	Alkaline solution (IMMR)	40	30	3	86.6	92.8
543	Kim et al. (2008)	NA		GFRP	12.7	Modified vinylester	Alkaline solution (IMMR)	40	60	3	81.6	89.5
544	Kim et al. (2008)	NA		GFRP	12.7	Modified vinylester	Alkaline solution (IMMR)	40	75	3	80.5	90.9
545	Kim et al. (2008)	NA		GFRP	12.7	Modified vinylester	Alkaline solution (IMMR)	80	30	3	62.6	93.7
546	Kim et al. (2008)	NA		GFRP	12.7	Modified vinylester	Alkaline solution (IMMR)	80	60	3	49.5	91.8
547	Kim et al. (2008)	NA		GFRP	12.7	Modified vinylester	Alkaline solution (FT)	-25/30	30	3	76.1	75.1
548	Kim et al. (2008)	NA		GFRP	12.7	Modified vinylester	Alkaline solution (FT)	-25/30	60	3	78.8	93.6
549	Kim et al. (2008)	NA		GFRP	12.7	Modified vinylester	Alkaline solution (FT)	-25/30	110	3	83.0	76.4
550	Li et al. (2022a)	Jiangsu	Green Materials	BFRP	4.0	Epoxy	Control	25	0	6	100.0	100.0

		Vally New Material T&D Co., Ltd (Nanjing, China)										
551	Li et al. (2022a)	Jiangsu Green Materials Vally New Material T&D Co., Ltd (Nanjing, China)	BFRP	4.0	Epoxy	SWSSCE+Simulated (IMMR)	seawater	25	60	6	97.6	104.0
552	Li et al. (2022a)	Jiangsu Green Materials Vally New Material T&D Co., Ltd (Nanjing, China)	BFRP	4.0	Epoxy	SWSSCE+Simulated (IMMR)	seawater	25	120	6	94.2	105.9
553	Li et al. (2022a)	Jiangsu Green Materials Vally New Material T&D Co., Ltd (Nanjing, China)	BFRP	4.0	Epoxy	SWSSCE+Simulated (IMMR)	seawater	40	60	6	88.2	104.4
554	Li et al. (2022a)	Jiangsu Green Materials Vally New Material T&D Co., Ltd (Nanjing, China)	BFRP	4.0	Epoxy	SWSSCE+Simulated (IMMR)	seawater	40	120	6	81.2	106.5
555	Li et al. (2022a)	Jiangsu Green Materials Vally New Material T&D Co., Ltd (Nanjing, China)	BFRP	4.0	Epoxy	SWSSCE+Simulated (IMMR)	seawater	55	60	6	76.4	102.5
556	Li et al. (2022a)	Jiangsu Green Materials Vally New Material T&D Co., Ltd (Nanjing, China)	BFRP	4.0	Epoxy	SWSSCE+Simulated (IMMR)	seawater	55	90	6	72.0	101.3
557	Li et al. (2022a)	Jiangsu Green Materials Vally New Material T&D Co., Ltd (Nanjing, China)	BFRP	4.0	Epoxy	SWSSCE+Simulated (IMMR)	seawater	55	120	6	69.8	103.4
558	Liu et al. (2019)	Green Material Valley (GMV) New Material Technology Co., Ltd. (Zhenjiang, China)	BFRP	5.8	Vinylester	Control		Na	0	5	100.0	NA
559	Liu et al. (2019)	Green Material Valley (GMV) New Material Technology Co., Ltd. (Zhenjiang, China)	BFRP	5.8	Vinylester	Alkaline solution with Cl- (IMMR)		55	21	5	81.2	NA
560	Liu et al. (2019)	Green Material Valley (GMV) New Material Technology Co., Ltd. (Zhenjiang, China)	BFRP	5.8	Vinylester	Alkaline solution with Cl- (IMMR)		55	42	5	70.8	NA
561	Liu et al. (2019)	Green Material Valley (GMV) New Material Technology Co., Ltd. (Zhenjiang, China)	BFRP	5.8	Vinylester	Alkaline solution with Cl- (IMMR)		55	63	5	61.4	NA
562	Liu et al. (2019)	Green Material Valley (GMV) New Material Technology Co., Ltd. (Zhenjiang, China)	BFRP	5.8	Vinylester	Alkaline solution with Cl- (WD)		55	21	5	98.1	NA
563	Liu et al. (2019)	Green Material Valley (GMV) New Material Technology Co., Ltd.	BFRP	5.8	Vinylester	Alkaline solution with Cl- (WD)		55	42	5	92.2	NA

		(Zhenjiang, China)									
564	Liu et al. (2019)	Green Material Valley (GMV) New Material Technology Co., Ltd. (Zhenjiang, China)	BFRP	5.8	Vinylester	Alkaline solution with Cl- (WD)	55	63	5	83.8	NA
565	Liu et al. (2019)	Green Material Valley (GMV) New Material Technology Co., Ltd. (Zhenjiang, China)	BFRP	5.9	Epoxy	Control	Na	0	5	100.0	NA
566	Liu et al. (2019)	Green Material Valley (GMV) New Material Technology Co., Ltd. (Zhenjiang, China)	BFRP	5.9	Epoxy	Alkaline solution with Cl- (IMMR)	55	21	5	59.7	NA
567	Liu et al. (2019)	Green Material Valley (GMV) New Material Technology Co., Ltd. (Zhenjiang, China)	BFRP	5.9	Epoxy	Alkaline solution with Cl- (IMMR)	55	42	5	26.5	NA
568	Liu et al. (2019)	Green Material Valley (GMV) New Material Technology Co., Ltd. (Zhenjiang, China)	BFRP	5.9	Epoxy	Alkaline solution with Cl- (IMMR)	55	63	5	10.7	NA
569	Liu et al. (2019)	Green Material Valley (GMV) New Material Technology Co., Ltd. (Zhenjiang, China)	BFRP	5.9	Epoxy	Alkaline solution with Cl- (WD)	55	21	5	76.7	NA
570	Liu et al. (2019)	Green Material Valley (GMV) New Material Technology Co., Ltd. (Zhenjiang, China)	BFRP	5.9	Epoxy	Alkaline solution with Cl- (WD)	55	42	5	54.8	NA
571	Liu et al. (2019)	Green Material Valley (GMV) New Material Technology Co., Ltd. (Zhenjiang, China)	BFRP	5.9	Epoxy	Alkaline solution with Cl- (WD)	55	63	5	38.3	NA
572	Liu et al. (2019)	Green Material Valley (GMV) New Material Technology Co., Ltd. (Zhenjiang, China)	BFRP	5.8	Vinylester	Control	Na	0	5	100.0	NA
573	Liu et al. (2019)	Green Material Valley (GMV) New Material Technology Co., Ltd. (Zhenjiang, China)	BFRP	5.8	Vinylester	Alkaline solution with Cl- (IMMR)	55	21	5	73.5	NA
574	Liu et al. (2019)	Green Material Valley (GMV) New Material Technology Co., Ltd. (Zhenjiang, China)	BFRP	5.8	Vinylester	Alkaline solution with Cl- (IMMR)	55	42	5	63.6	NA
575	Liu et al. (2019)	Green Material Valley	BFRP	5.8	Vinylester	Alkaline solution with Cl- (IMMR)	55	63	5	46.3	NA

		(GMV) New Material Technology Co., Ltd. (Zhenjiang, China)								
576	Liu et al. (2019)	Green Material Valley (GMV) New Material Technology Co., Ltd. (Zhenjiang, China)	BFRP	5.8	Vinylester	Alkaline solution with Cl- (WD)	55	21	5	100.0	NA
577	Liu et al. (2019)	Green Material Valley (GMV) New Material Technology Co., Ltd. (Zhenjiang, China)	BFRP	5.8	Vinylester	Alkaline solution with Cl- (WD)	55	42	5	73.5	NA
578	Liu et al. (2019)	Green Material Valley (GMV) New Material Technology Co., Ltd. (Zhenjiang, China)	BFRP	5.8	Vinylester	Alkaline solution with Cl- (WD)	55	63	5	63.6	NA
579	Liu et al. (2024)	JiangSu Tianlong Continuous Basalt Fiber Co., Ltd.	BFRP	8.0	Polyester	Control	25	0	NA	100.0	NA
580	Liu et al. (2024)	JiangSu Tianlong Continuous Basalt Fiber Co., Ltd.	BFRP	8.0	Polyester	Alkaline solution (IMMR)	25	7	NA	96.2	NA
581	Liu et al. (2024)	JiangSu Tianlong Continuous Basalt Fiber Co., Ltd.	BFRP	8.0	Polyester	Alkaline solution (IMMR)	25	14	NA	93.9	NA
582	Liu et al. (2024)	JiangSu Tianlong Continuous Basalt Fiber Co., Ltd.	BFRP	8.0	Polyester	Alkaline solution (IMMR)	25	28	NA	92.5	NA
583	Liu et al. (2024)	JiangSu Tianlong Continuous Basalt Fiber Co., Ltd.	BFRP	8.0	Polyester	Alkaline solution (IMMR)	25	56	NA	92.0	NA
584	Liu et al. (2024)	JiangSu Tianlong Continuous Basalt Fiber Co., Ltd.	BFRP	8.0	Polyester	Alkaline solution (IMMR)	25	112	NA	88.2	NA
585	Liu et al. (2024)	JiangSu Tianlong Continuous Basalt Fiber Co., Ltd.	BFRP	8.0	Polyester	Alkaline solution (IMMR)	40	7	NA	96.5	NA
586	Liu et al. (2024)	JiangSu Tianlong Continuous Basalt Fiber Co., Ltd.	BFRP	8.0	Polyester	Alkaline solution (IMMR)	40	14	NA	95.5	NA
587	Liu et al. (2024)	JiangSu Tianlong Continuous Basalt Fiber Co., Ltd.	BFRP	8.0	Polyester	Alkaline solution (IMMR)	40	28	NA	90.9	NA
588	Liu et al. (2024)	JiangSu Tianlong Continuous Basalt Fiber Co., Ltd.	BFRP	8.0	Polyester	Alkaline solution (IMMR)	40	56	NA	90.3	NA
589	Liu et al. (2024)	JiangSu Tianlong	BFRP	8.0	Polyester	Alkaline solution (IMMR)	40	112	NA	87.6	NA

		Continuous Basalt Fiber Co., Ltd.										
590	Liu et al. (2024)	JiangSu Tianlong Continuous Basalt Fiber Co., Ltd.	BFRP	8.0	Polyester	Alkaline solution (IMMR)	60	7	NA	93.4	NA
591	Liu et al. (2024)	JiangSu Tianlong Continuous Basalt Fiber Co., Ltd.	BFRP	8.0	Polyester	Alkaline solution (IMMR)	60	14	NA	90.7	NA
592	Liu et al. (2024)	JiangSu Tianlong Continuous Basalt Fiber Co., Ltd.	BFRP	8.0	Polyester	Alkaline solution (IMMR)	60	28	NA	85.2	NA
593	Liu et al. (2024)	JiangSu Tianlong Continuous Basalt Fiber Co., Ltd.	BFRP	8.0	Polyester	Alkaline solution (IMMR)	60	56	NA	76.3	NA
594	Liu et al. (2024)	JiangSu Tianlong Continuous Basalt Fiber Co., Ltd.	BFRP	8.0	Polyester	Alkaline solution (IMMR)	60	112	NA	74.4	NA
595	Liu et al. (2024)	JiangSu Tianlong Continuous Basalt Fiber Co., Ltd.	BFRP	8.0	Polyester	Alkaline solution (IMMR)	25	7	NA	98.4	NA
596	Liu et al. (2024)	JiangSu Tianlong Continuous Basalt Fiber Co., Ltd.	BFRP	8.0	Polyester	Alkaline solution (IMMR)	25	14	NA	95.8	NA
597	Liu et al. (2024)	JiangSu Tianlong Continuous Basalt Fiber Co., Ltd.	BFRP	8.0	Polyester	Alkaline solution (IMMR)	25	28	NA	92.4	NA
598	Liu et al. (2024)	JiangSu Tianlong Continuous Basalt Fiber Co., Ltd.	BFRP	8.0	Polyester	Alkaline solution (IMMR)	25	56	NA	90.3	NA
599	Liu et al. (2024)	JiangSu Tianlong Continuous Basalt Fiber Co., Ltd.	BFRP	8.0	Polyester	Alkaline solution (IMMR)	25	112	NA	88.6	NA
600	Liu et al. (2024)	JiangSu Tianlong Continuous Basalt Fiber Co., Ltd.	BFRP	8.0	Polyester	Alkaline solution (IMMR)	40	7	NA	98.4	NA
601	Liu et al. (2024)	JiangSu Tianlong Continuous Basalt Fiber Co., Ltd.	BFRP	8.0	Polyester	Alkaline solution (IMMR)	40	14	NA	93.7	NA
602	Liu et al. (2024)	JiangSu Tianlong Continuous Basalt Fiber Co., Ltd.	BFRP	8.0	Polyester	Alkaline solution (IMMR)	40	28	NA	92.4	NA
603	Liu et al. (2024)	JiangSu Tianlong Continuous Basalt Fiber Co., Ltd.	BFRP	8.0	Polyester	Alkaline solution (IMMR)	40	56	NA	89.3	NA
604	Liu et al. (2024)	JiangSu Tianlong Continuous Basalt Fiber	BFRP	8.0	Polyester	Alkaline solution (IMMR)	40	112	NA	86.5	NA

		Co., Ltd. JiangSu Tianlong										
605	Liu et al. (2024)	Continuous Basalt Fiber Co., Ltd.	BFRP	8.0	Polyester	Alkaline solution (IMMR)	60	7	NA	89.6	NA
		JiangSu Tianlong										
606	Liu et al. (2024)	Continuous Basalt Fiber Co., Ltd.	BFRP	8.0	Polyester	Alkaline solution (IMMR)	60	14	NA	89.8	NA
		JiangSu Tianlong										
607	Liu et al. (2024)	Continuous Basalt Fiber Co., Ltd.	BFRP	8.0	Polyester	Alkaline solution (IMMR)	60	28	NA	89.2	NA
		JiangSu Tianlong										
608	Liu et al. (2024)	Continuous Basalt Fiber Co., Ltd.	BFRP	8.0	Polyester	Alkaline solution (IMMR)	60	56	NA	78.9	NA
		JiangSu Tianlong										
609	Liu et al. (2024)	Continuous Basalt Fiber Co., Ltd.	BFRP	8.0	Polyester	Alkaline solution (IMMR)	60	112	NA	74.0	NA
		JiangSu Tianlong										
610	Liu et al. (2024)	Continuous Basalt Fiber Co., Ltd.	BFRP	8.0	Polyester	Alkaline solution (IMMR)	25	7	NA	98.4	NA
		JiangSu Tianlong										
611	Liu et al. (2024)	Continuous Basalt Fiber Co., Ltd.	BFRP	8.0	Polyester	Alkaline solution (IMMR)	25	14	NA	96.3	NA
		JiangSu Tianlong										
612	Liu et al. (2024)	Continuous Basalt Fiber Co., Ltd.	BFRP	8.0	Polyester	Alkaline solution (IMMR)	25	28	NA	95.1	NA
		JiangSu Tianlong										
613	Liu et al. (2024)	Continuous Basalt Fiber Co., Ltd.	BFRP	8.0	Polyester	Alkaline solution (IMMR)	25	56	NA	94.1	NA
		JiangSu Tianlong										
614	Liu et al. (2024)	Continuous Basalt Fiber Co., Ltd.	BFRP	8.0	Polyester	Alkaline solution (IMMR)	25	112	NA	93.5	NA
		JiangSu Tianlong										
615	Liu et al. (2024)	Continuous Basalt Fiber Co., Ltd.	BFRP	8.0	Polyester	Alkaline solution (IMMR)	40	7	NA	98.0	NA
		JiangSu Tianlong										
616	Liu et al. (2024)	Continuous Basalt Fiber Co., Ltd.	BFRP	8.0	Polyester	Alkaline solution (IMMR)	40	14	NA	94.8	NA
		JiangSu Tianlong										
617	Liu et al. (2024)	Continuous Basalt Fiber Co., Ltd.	BFRP	8.0	Polyester	Alkaline solution (IMMR)	40	28	NA	93.1	NA
		JiangSu Tianlong										
618	Liu et al. (2024)	Continuous Basalt Fiber Co., Ltd.	BFRP	8.0	Polyester	Alkaline solution (IMMR)	40	56	NA	91.2	NA
		JiangSu Tianlong										
619	Liu et al. (2024)	Continuous Basalt Fiber Co., Ltd.	BFRP	8.0	Polyester	Alkaline solution (IMMR)	40	112	NA	89.0	NA

620	Liu et al. (2024)	JiangSu Tianlong Continuous Basalt Fiber Co., Ltd.	BFRP	8.0	Polyester	Alkaline solution (IMMR)	60	7	NA	96.4	NA
621	Liu et al. (2024)	JiangSu Tianlong Continuous Basalt Fiber Co., Ltd.	BFRP	8.0	Polyester	Alkaline solution (IMMR)	60	14	NA	87.8	NA
622	Liu et al. (2024)	JiangSu Tianlong Continuous Basalt Fiber Co., Ltd.	BFRP	8.0	Polyester	Alkaline solution (IMMR)	60	28	NA	80.7	NA
623	Liu et al. (2024)	JiangSu Tianlong Continuous Basalt Fiber Co., Ltd.	BFRP	8.0	Polyester	Alkaline solution (IMMR)	60	56	NA	70.7	NA
624	Liu et al. (2024)	JiangSu Tianlong Continuous Basalt Fiber Co., Ltd.	BFRP	8.0	Polyester	Alkaline solution (IMMR)	60	112	NA	70.1	NA
625	Liu et al. (2024)	JiangSu Tianlong Continuous Basalt Fiber Co., Ltd.	BFRP	8.0	Polyester	Alkaline solution (IMMR)	25	7	NA	97.1	NA
626	Liu et al. (2024)	JiangSu Tianlong Continuous Basalt Fiber Co., Ltd.	BFRP	8.0	Polyester	Alkaline solution (IMMR)	25	14	NA	93.9	NA
627	Liu et al. (2024)	JiangSu Tianlong Continuous Basalt Fiber Co., Ltd.	BFRP	8.0	Polyester	Alkaline solution (IMMR)	25	28	NA	91.8	NA
628	Liu et al. (2024)	JiangSu Tianlong Continuous Basalt Fiber Co., Ltd.	BFRP	8.0	Polyester	Alkaline solution (IMMR)	25	56	NA	89.0	NA
629	Liu et al. (2024)	JiangSu Tianlong Continuous Basalt Fiber Co., Ltd.	BFRP	8.0	Polyester	Alkaline solution (IMMR)	25	112	NA	88.2	NA
630	Liu et al. (2024)	JiangSu Tianlong Continuous Basalt Fiber Co., Ltd.	BFRP	8.0	Polyester	Alkaline solution (IMMR)	40	7	NA	97.5	NA
631	Liu et al. (2024)	JiangSu Tianlong Continuous Basalt Fiber Co., Ltd.	BFRP	8.0	Polyester	Alkaline solution (IMMR)	40	14	NA	93.5	NA
632	Liu et al. (2024)	JiangSu Tianlong Continuous Basalt Fiber Co., Ltd.	BFRP	8.0	Polyester	Alkaline solution (IMMR)	40	28	NA	91.8	NA
633	Liu et al. (2024)	JiangSu Tianlong Continuous Basalt Fiber Co., Ltd.	BFRP	8.0	Polyester	Alkaline solution (IMMR)	40	56	NA	87.1	NA
634	Liu et al. (2024)	JiangSu Tianlong Continuous Basalt Fiber Co., Ltd.	BFRP	8.0	Polyester	Alkaline solution (IMMR)	40	112	NA	84.2	NA
635	Liu et al. (2024)	JiangSu Tianlong	BFRP	8.0	Polyester	Alkaline solution (IMMR)	60	7	NA	95.0	NA

		Continuous Basalt Fiber Co., Ltd.										
636	Liu et al. (2024)	JiangSu Tianlong Continuous Basalt Fiber Co., Ltd.	BFRP	8.0	Polyester	Alkaline solution (IMMR)	60	14	NA	84.6	NA
637	Liu et al. (2024)	JiangSu Tianlong Continuous Basalt Fiber Co., Ltd.	BFRP	8.0	Polyester	Alkaline solution (IMMR)	60	28	NA	79.7	NA
638	Liu et al. (2024)	JiangSu Tianlong Continuous Basalt Fiber Co., Ltd.	BFRP	8.0	Polyester	Alkaline solution (IMMR)	60	56	NA	70.7	NA
639	Liu et al. (2024)	JiangSu Tianlong Continuous Basalt Fiber Co., Ltd.	BFRP	8.0	Polyester	Alkaline solution (IMMR)	60	112	NA	68.4	NA
640	Liu et al. (2024)	JiangSu Tianlong Continuous Basalt Fiber Co., Ltd.	BFRP	8.0	Polyester	Alkaline solution (IMMR)	25	7	NA	88.8	NA
641	Liu et al. (2024)	JiangSu Tianlong Continuous Basalt Fiber Co., Ltd.	BFRP	8.0	Polyester	Alkaline solution (IMMR)	25	14	NA	71.0	NA
642	Liu et al. (2024)	JiangSu Tianlong Continuous Basalt Fiber Co., Ltd.	BFRP	8.0	Polyester	Alkaline solution (IMMR)	25	28	NA	39.2	NA
643	Liu et al. (2024)	JiangSu Tianlong Continuous Basalt Fiber Co., Ltd.	BFRP	8.0	Polyester	Alkaline solution (IMMR)	25	56	NA	26.2	NA
644	Liu et al. (2024)	JiangSu Tianlong Continuous Basalt Fiber Co., Ltd.	BFRP	8.0	Polyester	Alkaline solution (IMMR)	25	112	NA	22.7	NA
645	Liu et al. (2024)	JiangSu Tianlong Continuous Basalt Fiber Co., Ltd.	BFRP	8.0	Polyester	Alkaline solution (IMMR)	40	7	NA	81.1	NA
646	Liu et al. (2024)	JiangSu Tianlong Continuous Basalt Fiber Co., Ltd.	BFRP	8.0	Polyester	Alkaline solution (IMMR)	40	14	NA	57.0	NA
647	Liu et al. (2024)	JiangSu Tianlong Continuous Basalt Fiber Co., Ltd.	BFRP	8.0	Polyester	Alkaline solution (IMMR)	40	28	NA	31.1	NA
648	Liu et al. (2024)	JiangSu Tianlong Continuous Basalt Fiber Co., Ltd.	BFRP	8.0	Polyester	Alkaline solution (IMMR)	40	56	NA	17.1	NA
649	Liu et al. (2024)	JiangSu Tianlong Continuous Basalt Fiber Co., Ltd.	BFRP	8.0	Polyester	Alkaline solution (IMMR)	40	112	NA	13.3	NA
650	Liu et al. (2024)	JiangSu Tianlong Continuous Basalt Fiber	BFRP	8.0	Polyester	Alkaline solution (IMMR)	60	7	NA	63.6	NA

651	Liu et al. (2024)	Co., Ltd. JiangSu Tianlong Continuous Basalt Fiber Co., Ltd.	BFRP	8.0	Polyester	Alkaline solution (IMMR)	60	14	NA	35.0	NA
652	Liu et al. (2024)	JiangSu Tianlong Continuous Basalt Fiber Co., Ltd.	BFRP	8.0	Polyester	Alkaline solution (IMMR)	60	28	NA	12.6	NA
653	Liu et al. (2024)	JiangSu Tianlong Continuous Basalt Fiber Co., Ltd.	BFRP	8.0	Polyester	Alkaline solution (IMMR)	60	56	NA	4.9	NA
654	Lu et al. (2020a)	Nanjing Fenghui Composite Material Co. Ltd (China)	BFRP	8.0	Vinylester	Control	20	0	3	100.0	100.0
655	Lu et al. (2020a)	Nanjing Fenghui Composite Material Co. Ltd (China)	BFRP	8.0	Vinylester	Water (IMMR)	20	45	3	96.7	101.7
656	Lu et al. (2020a)	Nanjing Fenghui Composite Material Co. Ltd (China)	BFRP	8.0	Vinylester	Water (IMMR)	20	90	3	92.9	107.1
657	Lu et al. (2020a)	Nanjing Fenghui Composite Material Co. Ltd (China)	BFRP	8.0	Vinylester	Water (IMMR)	20	135	3	88.9	99.8
658	Lu et al. (2020a)	Nanjing Fenghui Composite Material Co. Ltd (China)	BFRP	8.0	Vinylester	Water (IMMR)	20	180	3	88.5	111.9
659	Lu et al. (2020a)	Nanjing Fenghui Composite Material Co. Ltd (China)	BFRP	8.0	Vinylester	Simulated seawater (IMMR)	20	45	3	84.3	90.5
660	Lu et al. (2020a)	Nanjing Fenghui Composite Material Co. Ltd (China)	BFRP	8.0	Vinylester	Simulated seawater (IMMR)	20	90	3	79.1	115.2
661	Lu et al. (2020a)	Nanjing Fenghui Composite Material Co. Ltd (China)	BFRP	8.0	Vinylester	Simulated seawater (IMMR)	20	135	3	76.8	104.8
662	Lu et al. (2020a)	Nanjing Fenghui Composite Material Co. Ltd (China)	BFRP	8.0	Vinylester	Simulated seawater (IMMR)	20	180	3	75.8	102.1
663	Lu et al. (2020a)	Nanjing Fenghui Composite Material Co. Ltd (China)	BFRP	8.0	Vinylester	Alkaline solution (IMMR)	20	45	3	91.9	105.2
664	Lu et al. (2020a)	Nanjing Fenghui Composite Material Co. Ltd (China)	BFRP	8.0	Vinylester	Alkaline solution (IMMR)	20	90	3	88.4	109.7
665	Lu et al. (2020a)	Nanjing Fenghui Composite Material Co. Ltd (China)	BFRP	8.0	Vinylester	Alkaline solution (IMMR)	20	135	3	83.0	104.3
666	Lu et al. (2020a)	Nanjing Fenghui Composite Material Co. Ltd (China)	BFRP	8.0	Vinylester	Alkaline solution (IMMR)	20	180	3	77.6	106.2
667	Lu et al. (2020a)	Nanjing Fenghui Composite Material Co. Ltd (China)	CFRP	8.0	Vinylester	Control	20	0	3	100.0	100.0
668	Lu et al. (2020a)	Nanjing Fenghui Composite Material Co. Ltd (China)	CFRP	8.0	Vinylester	Water (IMMR)	20	45	3	96.7	102.8
669	Lu et al. (2020a)	Nanjing Fenghui Composite Material Co. Ltd (China)	CFRP	8.0	Vinylester	Water (IMMR)	20	90	3	92.2	95.8
670	Lu et al. (2020a)	Nanjing Fenghui Composite Material Co. Ltd (China)	CFRP	8.0	Vinylester	Water (IMMR)	20	135	3	90.4	97.0
671	Lu et al. (2020a)	Nanjing Fenghui Composite Material Co. Ltd (China)	CFRP	8.0	Vinylester	Water (IMMR)	20	180	3	88.9	104.4

672	Lu et al. (2020a)	Nanjing Fenghui Composite Material Co. Ltd (China)	CFRP	8.0	Vinylester	Simulated seawater (IMMR)	20	45	3	91.1	95.8
673	Lu et al. (2020a)	Nanjing Fenghui Composite Material Co. Ltd (China)	CFRP	8.0	Vinylester	Simulated seawater (IMMR)	20	90	3	84.6	116.5
674	Lu et al. (2020a)	Nanjing Fenghui Composite Material Co. Ltd (China)	CFRP	8.0	Vinylester	Simulated seawater (IMMR)	20	135	3	81.4	105.8
675	Lu et al. (2020a)	Nanjing Fenghui Composite Material Co. Ltd (China)	CFRP	8.0	Vinylester	Simulated seawater (IMMR)	20	180	3	78.8	102.2
676	Lu et al. (2020a)	Nanjing Fenghui Composite Material Co. Ltd (China)	CFRP	8.0	Vinylester	Alkaline solution (IMMR)	20	45	3	99.0	100.4
677	Lu et al. (2020a)	Nanjing Fenghui Composite Material Co. Ltd (China)	CFRP	8.0	Vinylester	Alkaline solution (IMMR)	20	90	3	94.6	107.1
678	Lu et al. (2020a)	Nanjing Fenghui Composite Material Co. Ltd (China)	CFRP	8.0	Vinylester	Alkaline solution (IMMR)	20	135	3	92.8	92.7
679	Lu et al. (2020a)	Nanjing Fenghui Composite Material Co. Ltd (China)	CFRP	8.0	Vinylester	Alkaline solution (IMMR)	20	180	3	82.8	102.6
680	Lu et al. (2020a)	Nanjing Fenghui Composite Material Co. Ltd (China)	GFRP	8.0	Vinylester	Control	20	0	3	100.0	100.0
681	Lu et al. (2020a)	Nanjing Fenghui Composite Material Co. Ltd (China)	GFRP	8.0	Vinylester	Water (IMMR)	20	45	3	97.3	103.8
682	Lu et al. (2020a)	Nanjing Fenghui Composite Material Co. Ltd (China)	GFRP	8.0	Vinylester	Water (IMMR)	20	90	3	89.7	101.4
683	Lu et al. (2020a)	Nanjing Fenghui Composite Material Co. Ltd (China)	GFRP	8.0	Vinylester	Water (IMMR)	20	135	3	85.3	100.4
684	Lu et al. (2020a)	Nanjing Fenghui Composite Material Co. Ltd (China)	GFRP	8.0	Vinylester	Water (IMMR)	20	180	3	78.0	101.4
685	Lu et al. (2020a)	Nanjing Fenghui Composite Material Co. Ltd (China)	GFRP	8.0	Vinylester	Simulated seawater (IMMR)	20	45	3	99.5	99.8
686	Lu et al. (2020a)	Nanjing Fenghui Composite Material Co. Ltd (China)	GFRP	8.0	Vinylester	Simulated seawater (IMMR)	20	90	3	92.1	104.0
687	Lu et al. (2020a)	Nanjing Fenghui Composite Material Co. Ltd (China)	GFRP	8.0	Vinylester	Simulated seawater (IMMR)	20	135	3	90.5	97.8
688	Lu et al. (2020a)	Nanjing Fenghui Composite Material Co. Ltd (China)	GFRP	8.0	Vinylester	Simulated seawater (IMMR)	20	180	3	81.8	103.0
689	Lu et al. (2020a)	Nanjing Fenghui Composite Material Co. Ltd (China)	GFRP	8.0	Vinylester	Alkaline solution (IMMR)	20	45	3	96.5	97.8
690	Lu et al. (2020a)	Nanjing Fenghui Composite Material Co. Ltd (China)	GFRP	8.0	Vinylester	Alkaline solution (IMMR)	20	90	3	75.3	104.6
691	Lu et al. (2020a)	Nanjing Fenghui Composite Material Co. Ltd (China)	GFRP	8.0	Vinylester	Alkaline solution (IMMR)	20	135	3	70.6	103.6
692	Lu et al. (2020a)	Nanjing Fenghui Composite Material Co. Ltd (China)	GFRP	8.0	Vinylester	Alkaline solution (IMMR)	20	180	3	69.2	98.2
693	Lu et al. (2020b)	TuoXin Aerospace Basalt Industrial Co., Ltd. (Sichuan, China)	BFRP	8.0	Epoxy	Control	23	0	5	100.0	100.0
694	Lu et al. (2020b)	TuoXin Aerospace Basalt	BFRP	8.0	Epoxy	Simulated seawater (IMMR)	23	15	5	92.4	98.7

		Industrial Co., Ltd. (Sichuan, China)										
695	Lu et al. (2020b)	TuoXin Aerospace Basalt Industrial Co., Ltd. (Sichuan, China)	BFRP	8.0	Epoxy	Simulated seawater (IMMR)	23	30	5	96.8	93.9
696	Lu et al. (2020b)	TuoXin Aerospace Basalt Industrial Co., Ltd. (Sichuan, China)	BFRP	8.0	Epoxy	Simulated seawater (IMMR)	23	60	5	98.0	95.6
697	Lu et al. (2020b)	TuoXin Aerospace Basalt Industrial Co., Ltd. (Sichuan, China)	BFRP	8.0	Epoxy	Simulated seawater (IMMR)	23	180	5	91.6	93.4
698	Lu et al. (2020b)	TuoXin Aerospace Basalt Industrial Co., Ltd. (Sichuan, China)	BFRP	8.0	Epoxy	Simulated seawater (IMMR)	23	360	5	91.2	93.9
699	Lu et al. (2020b)	TuoXin Aerospace Basalt Industrial Co., Ltd. (Sichuan, China)	BFRP	8.0	Epoxy	Simulated seawater (IMMR)	40	15	5	97.6	95.2
700	Lu et al. (2020b)	TuoXin Aerospace Basalt Industrial Co., Ltd. (Sichuan, China)	BFRP	8.0	Epoxy	Simulated seawater (IMMR)	40	30	5	89.6	98.7
701	Lu et al. (2020b)	TuoXin Aerospace Basalt Industrial Co., Ltd. (Sichuan, China)	BFRP	8.0	Epoxy	Simulated seawater (IMMR)	40	60	5	89.6	91.7
702	Lu et al. (2020b)	TuoXin Aerospace Basalt Industrial Co., Ltd. (Sichuan, China)	BFRP	8.0	Epoxy	Simulated seawater (IMMR)	40	180	5	79.9	94.3
703	Lu et al. (2020b)	TuoXin Aerospace Basalt Industrial Co., Ltd. (Sichuan, China)	BFRP	8.0	Epoxy	Simulated seawater (IMMR)	40	360	5	70.7	90.4
704	Lu et al. (2020b)	TuoXin Aerospace Basalt Industrial Co., Ltd. (Sichuan, China)	BFRP	8.0	Epoxy	Simulated seawater (IMMR)	60	15	5	92.0	97.8
705	Lu et al. (2020b)	TuoXin Aerospace Basalt Industrial Co., Ltd. (Sichuan, China)	BFRP	8.0	Epoxy	Simulated seawater (IMMR)	60	30	5	82.7	97.8
706	Lu et al. (2020b)	TuoXin Aerospace Basalt Industrial Co., Ltd. (Sichuan, China)	BFRP	8.0	Epoxy	Simulated seawater (IMMR)	60	60	5	77.1	95.6
707	Lu et al. (2020b)	TuoXin Aerospace Basalt Industrial Co., Ltd. (Sichuan, China)	BFRP	8.0	Epoxy	Simulated seawater (IMMR)	60	180	5	62.2	93.4
708	Lu et al. (2020b)	TuoXin Aerospace Basalt Industrial Co., Ltd. (Sichuan, China)	BFRP	8.0	Epoxy	Simulated seawater (IMMR)	60	360	5	32.1	72.8
709	Lu et al. (2020b)	TuoXin Aerospace Basalt Industrial Co., Ltd.	BFRP	8.0	Epoxy	NCE+Simulated seawater (IMMR)	23	15	5	99.2	94.3

		(Sichuan, China)									
710	Lu et al. (2020b)	TuoXin Aerospace Basalt Industrial Co., Ltd. (Sichuan, China)	BFRP	8.0	Epoxy	NCE+Simulated seawater (IMMR)	23	30	5	88.4	92.1
711	Lu et al. (2020b)	TuoXin Aerospace Basalt Industrial Co., Ltd. (Sichuan, China)	BFRP	8.0	Epoxy	NCE+Simulated seawater (IMMR)	23	60	5	79.9	92.1
712	Lu et al. (2020b)	TuoXin Aerospace Basalt Industrial Co., Ltd. (Sichuan, China)	BFRP	8.0	Epoxy	NCE+Simulated seawater (IMMR)	23	180	5	59.0	87.7
713	Lu et al. (2020b)	TuoXin Aerospace Basalt Industrial Co., Ltd. (Sichuan, China)	BFRP	8.0	Epoxy	NCE+Simulated seawater (IMMR)	23	360	5	41.0	78.9
714	Lu et al. (2020d)	Dextra Building Products Co., Ltd. (Guangzhou, China)	GFRP	6.0	NA	Control	28	0	5	100.0	100.0
715	Lu et al. (2020d)	Dextra Building Products Co., Ltd. (Guangzhou, China)	GFRP	6.0	NA	Alkaline solution (IMMR)	28	180	5	73.6	101.5
716	Lu et al. (2020d)	Dextra Building Products Co., Ltd. (Guangzhou, China)	GFRP	6.0	NA	Alkaline solution (IMMR)	40	180	5	56.8	103.4
717	Lu et al. (2020d)	Dextra Building Products Co., Ltd. (Guangzhou, China)	GFRP	6.0	NA	Alkaline solution (IMMR)	60	180	5	33.6	101.5
718	Lu et al. (2020d)	Dextra Building Products Co., Ltd. (Guangzhou, China)	GFRP	6.0	NA	Simulated seawater (IMMR)	28	180	5	77.5	103.6
719	Lu et al. (2020d)	Dextra Building Products Co., Ltd. (Guangzhou, China)	GFRP	6.0	NA	Simulated seawater (IMMR)	40	180	5	58.3	101.7
720	Lu et al. (2020d)	Dextra Building Products Co., Ltd. (Guangzhou, China)	GFRP	6.0	NA	Simulated seawater (IMMR)	60	180	5	41.4	101.7
721	Lu et al. (2020d)	Dextra Building Products Co., Ltd. (Guangzhou, China)	GFRP	6.0	NA	Water (IMMR)	28	180	5	79.4	102.3
722	Lu et al. (2020d)	Dextra Building Products Co., Ltd. (Guangzhou, China)	GFRP	6.0	NA	Water (IMMR)	40	180	5	65.7	103.6
723	Lu et al. (2020d)	Dextra Building Products Co., Ltd. (Guangzhou, China)	GFRP	6.0	NA	Water (IMMR)	60	180	5	42.3	106.0
724	Lu et al. (2020d)	Dextra Building Products Co., Ltd. (Guangzhou, China)	GFRP	6.0	NA	NCE 1+Alkaline solution (IMMR)	28	180	5	68.0	106.5

725	Lu et al. (2020d)	Dextra Building Products Co., Ltd. (Guangzhou, China)	GFRP	6.0	NA	NCE 1+Alkaline solution (IMMR)	40	180	5	54.4	100.9
726	Lu et al. (2020d)	Dextra Building Products Co., Ltd. (Guangzhou, China)	GFRP	6.0	NA	NCE 1+Alkaline solution (IMMR)	60	180	5	38.4	105.2
727	Lu et al. (2020d)	Dextra Building Products Co., Ltd. (Guangzhou, China)	GFRP	6.0	NA	NCE 1+Simulated seawater (IMMR)	28	180	5	80.8	103.6
728	Lu et al. (2020d)	Dextra Building Products Co., Ltd. (Guangzhou, China)	GFRP	6.0	NA	NCE 1+Simulated seawater (IMMR)	40	180	5	60.3	106.6
729	Lu et al. (2020d)	Dextra Building Products Co., Ltd. (Guangzhou, China)	GFRP	6.0	NA	NCE 1+Simulated seawater (IMMR)	60	180	5	40.2	101.7
730	Lu et al. (2020d)	Dextra Building Products Co., Ltd. (Guangzhou, China)	GFRP	6.0	NA	NCE 1+Water (IMMR)	28	180	5	77.0	101.7
731	Lu et al. (2020d)	Dextra Building Products Co., Ltd. (Guangzhou, China)	GFRP	6.0	NA	NCE 1+Water (IMMR)	40	180	5	63.7	106.6
732	Lu et al. (2020d)	Dextra Building Products Co., Ltd. (Guangzhou, China)	GFRP	6.0	NA	NCE 1+Water (IMMR)	60	180	5	38.7	102.3
733	Lu et al. (2020d)	Dextra Building Products Co., Ltd. (Guangzhou, China)	GFRP	6.0	NA	NCE 2+Alkaline solution (IMMR)	28	180	5	74.0	105.2
734	Lu et al. (2020d)	Dextra Building Products Co., Ltd. (Guangzhou, China)	GFRP	6.0	NA	NCE 2+Alkaline solution (IMMR)	40	180	5	56.8	105.2
735	Lu et al. (2020d)	Dextra Building Products Co., Ltd. (Guangzhou, China)	GFRP	6.0	NA	NCE 2+Alkaline solution (IMMR)	60	180	5	35.6	102.8
736	Lu et al. (2020d)	Dextra Building Products Co., Ltd. (Guangzhou, China)	GFRP	6.0	NA	NCE 2+Simulated seawater (IMMR)	28	180	5	77.5	106.6
737	Lu et al. (2020d)	Dextra Building Products Co., Ltd. (Guangzhou, China)	GFRP	6.0	NA	NCE 2+Simulated seawater (IMMR)	40	180	5	58.3	104.8
738	Lu et al. (2020d)	Dextra Building Products Co., Ltd. (Guangzhou, China)	GFRP	6.0	NA	NCE 2+Simulated seawater (IMMR)	60	180	5	38.6	104.2
739	Lu et al. (2020d)	Dextra Building Products Co., Ltd. (Guangzhou, China)	GFRP	6.0	NA	NCE 2+Water (IMMR)	28	180	5	73.0	103.6
740	Lu et al. (2020d)	Dextra Building Products	GFRP	6.0	NA	NCE 2+Water (IMMR)	40	180	5	60.1	101.7

		Co., Ltd. (Guangzhou, China)									
741	Lu et al. (2020d)	Dextra Building Products Co., Ltd. (Guangzhou, China)	GFRP	6.0	NA	NCE 2+Water (IMMR)	60	180	5	36.7	101.1
742	Lu et al. (2020d)	TuoXin Aerospace Basalt Industrial Co., Ltd. (Sichuan, China)	BFRP	6.0	NA	Control	28	0	5	100.0	100.0
743	Lu et al. (2020d)	TuoXin Aerospace Basalt Industrial Co., Ltd. (Sichuan, China)	BFRP	6.0	NA	Alkaline solution (IMMR)	28	180	5	66.4	95.4
744	Lu et al. (2020d)	TuoXin Aerospace Basalt Industrial Co., Ltd. (Sichuan, China)	BFRP	6.0	NA	Alkaline solution (IMMR)	40	180	5	53.6	95.4
745	Lu et al. (2020d)	TuoXin Aerospace Basalt Industrial Co., Ltd. (Sichuan, China)	BFRP	6.0	NA	Alkaline solution (IMMR)	60	180	5	39.2	84.9
746	Lu et al. (2020d)	TuoXin Aerospace Basalt Industrial Co., Ltd. (Sichuan, China)	BFRP	6.0	NA	Simulated seawater (IMMR)	28	180	5	70.7	91.5
747	Lu et al. (2020d)	TuoXin Aerospace Basalt Industrial Co., Ltd. (Sichuan, China)	BFRP	6.0	NA	Simulated seawater (IMMR)	40	180	5	56.2	86.1
748	Lu et al. (2020d)	TuoXin Aerospace Basalt Industrial Co., Ltd. (Sichuan, China)	BFRP	6.0	NA	Simulated seawater (IMMR)	60	180	5	38.2	90.3
749	Lu et al. (2020d)	TuoXin Aerospace Basalt Industrial Co., Ltd. (Sichuan, China)	BFRP	6.0	NA	Water (IMMR)	28	180	5	80.6	101.1
750	Lu et al. (2020d)	TuoXin Aerospace Basalt Industrial Co., Ltd. (Sichuan, China)	BFRP	6.0	NA	Water (IMMR)	40	180	5	72.6	97.5
751	Lu et al. (2020d)	TuoXin Aerospace Basalt Industrial Co., Ltd. (Sichuan, China)	BFRP	6.0	NA	Water (IMMR)	60	180	5	52.4	94.4
752	Lu et al. (2020d)	TuoXin Aerospace Basalt Industrial Co., Ltd. (Sichuan, China)	BFRP	6.0	NA	NCE 1+Alkaline solution (IMMR)	28	180	5	63.2	97.2
753	Lu et al. (2020d)	TuoXin Aerospace Basalt Industrial Co., Ltd. (Sichuan, China)	BFRP	6.0	NA	NCE 1+Alkaline solution (IMMR)	40	180	5	64.4	98.5
754	Lu et al. (2020d)	TuoXin Aerospace Basalt Industrial Co., Ltd. (Sichuan, China)	BFRP	6.0	NA	NCE 1+Alkaline solution (IMMR)	60	180	5	54.8	100.9
755	Lu et al. (2020d)	TuoXin Aerospace Basalt Industrial Co., Ltd.	BFRP	6.0	NA	NCE 1+Simulated seawater (IMMR)	28	180	5	71.9	100.6

		(Sichuan, China)									
756	Lu et al. (2020d)	TuoXin Aerospace Basalt Industrial Co., Ltd. (Sichuan, China)	BFRP	6.0	NA	NCE 1+Simulated seawater (IMMR)	40	180	5	69.9	104.2
757	Lu et al. (2020d)	TuoXin Aerospace Basalt Industrial Co., Ltd. (Sichuan, China)	BFRP	6.0	NA	NCE 1+Simulated seawater (IMMR)	60	180	5	61.0	100.0
758	Lu et al. (2020d)	TuoXin Aerospace Basalt Industrial Co., Ltd. (Sichuan, China)	BFRP	6.0	NA	NCE 1+Water (IMMR)	28	180	5	68.5	97.5
759	Lu et al. (2020d)	TuoXin Aerospace Basalt Industrial Co., Ltd. (Sichuan, China)	BFRP	6.0	NA	NCE 1+Water (IMMR)	40	180	5	69.8	98.7
760	Lu et al. (2020d)	TuoXin Aerospace Basalt Industrial Co., Ltd. (Sichuan, China)	BFRP	6.0	NA	NCE 1+Water (IMMR)	60	180	5	63.7	101.1
761	Lu et al. (2020d)	TuoXin Aerospace Basalt Industrial Co., Ltd. (Sichuan, China)	BFRP	6.0	NA	NCE 2+Alkaline solution (IMMR)	28	180	5	58.4	94.8
762	Lu et al. (2020d)	TuoXin Aerospace Basalt Industrial Co., Ltd. (Sichuan, China)	BFRP	6.0	NA	NCE 2+Alkaline solution (IMMR)	40	180	5	57.6	93.5
763	Lu et al. (2020d)	TuoXin Aerospace Basalt Industrial Co., Ltd. (Sichuan, China)	BFRP	6.0	NA	NCE 2+Alkaline solution (IMMR)	60	180	5	44.8	93.5
764	Lu et al. (2020d)	TuoXin Aerospace Basalt Industrial Co., Ltd. (Sichuan, China)	BFRP	6.0	NA	NCE 2+Simulated seawater (IMMR)	28	180	5	65.5	94.5
765	Lu et al. (2020d)	TuoXin Aerospace Basalt Industrial Co., Ltd. (Sichuan, China)	BFRP	6.0	NA	NCE 2+Simulated seawater (IMMR)	40	180	5	56.6	93.9
766	Lu et al. (2020d)	TuoXin Aerospace Basalt Industrial Co., Ltd. (Sichuan, China)	BFRP	6.0	NA	NCE 2+Simulated seawater (IMMR)	60	180	5	54.2	97.6
767	Lu et al. (2020d)	TuoXin Aerospace Basalt Industrial Co., Ltd. (Sichuan, China)	BFRP	6.0	NA	NCE 2+Water (IMMR)	28	180	5	62.5	96.9
768	Lu et al. (2020d)	TuoXin Aerospace Basalt Industrial Co., Ltd. (Sichuan, China)	BFRP	6.0	NA	NCE 2+Water (IMMR)	40	180	5	60.1	95.6
769	Lu et al. (2020d)	TuoXin Aerospace Basalt Industrial Co., Ltd. (Sichuan, China)	BFRP	6.0	NA	NCE 2+Water (IMMR)	60	180	5	56.0	96.2
770	Lu et al. (2021a)	Nanjing Fenghui Composite Material Co. Ltd (China)	GFRP	11.2	Vinylester	Control	20	0	6	100.0	100.0
771	Lu et al. (2021a)	Nanjing Fenghui Composite	GFRP	11.2	Vinylester	Alkaline solution (IMMR)	20	45	6	84.8	98.5

		Material Co. Ltd (China)									
772	Lu et al. (2021a)	Nanjing Fenghui Composite Material Co. Ltd (China)	GFRP	11.2	Vinylester	Alkaline solution (IMMR)	20	90	6	80.8	104.0
773	Lu et al. (2021a)	Nanjing Fenghui Composite Material Co. Ltd (China)	GFRP	11.2	Vinylester	Alkaline solution (IMMR)	20	135	6	76.7	91.0
774	Lu et al. (2021a)	Nanjing Fenghui Composite Material Co. Ltd (China)	GFRP	11.2	Vinylester	Alkaline solution (IMMR)	20	180	6	70.0	95.8
775	Lu et al. (2021a)	Nanjing Fenghui Composite Material Co. Ltd (China)	GFRP	11.2	Vinylester	Saline solution (IMMR)	20	45	6	92.2	93.8
776	Lu et al. (2021a)	Nanjing Fenghui Composite Material Co. Ltd (China)	GFRP	11.2	Vinylester	Saline solution (IMMR)	20	90	6	90.9	110.4
777	Lu et al. (2021a)	Nanjing Fenghui Composite Material Co. Ltd (China)	GFRP	11.2	Vinylester	Saline solution (IMMR)	20	135	6	90.0	110.7
778	Lu et al. (2021a)	Nanjing Fenghui Composite Material Co. Ltd (China)	GFRP	11.2	Vinylester	Saline solution (IMMR)	20	180	6	79.7	102.2
779	Lu et al. (2021a)	Nanjing Fenghui Composite Material Co. Ltd (China)	GFRP	11.2	Vinylester	Water (IMMR)	20	45	6	95.9	110.0
780	Lu et al. (2021a)	Nanjing Fenghui Composite Material Co. Ltd (China)	GFRP	11.2	Vinylester	Water (IMMR)	20	90	6	89.3	105.0
781	Lu et al. (2021a)	Nanjing Fenghui Composite Material Co. Ltd (China)	GFRP	11.2	Vinylester	Water (IMMR)	20	135	6	89.5	104.0
782	Lu et al. (2021a)	Nanjing Fenghui Composite Material Co. Ltd (China)	GFRP	11.2	Vinylester	Water (IMMR)	20	180	6	89.8	102.7
783	Lu et al. (2021a)	Nanjing Fenghui Composite Material Co. Ltd (China)	GFRP	15.6	Vinylester	Control	20	0	6	100.0	100.0
784	Lu et al. (2021a)	Nanjing Fenghui Composite Material Co. Ltd (China)	GFRP	15.6	Vinylester	Alkaline solution (IMMR)	20	45	6	84.2	93.4
785	Lu et al. (2021a)	Nanjing Fenghui Composite Material Co. Ltd (China)	GFRP	15.6	Vinylester	Alkaline solution (IMMR)	20	90	6	82.8	96.7
786	Lu et al. (2021a)	Nanjing Fenghui Composite Material Co. Ltd (China)	GFRP	15.6	Vinylester	Alkaline solution (IMMR)	20	135	6	81.4	102.6
787	Lu et al. (2021a)	Nanjing Fenghui Composite Material Co. Ltd (China)	GFRP	15.6	Vinylester	Alkaline solution (IMMR)	20	180	6	76.7	93.7
788	Lu et al. (2021a)	Nanjing Fenghui Composite Material Co. Ltd (China)	GFRP	15.6	Vinylester	Saline solution (IMMR)	20	45	6	94.6	96.7
789	Lu et al. (2021a)	Nanjing Fenghui Composite Material Co. Ltd (China)	GFRP	15.6	Vinylester	Saline solution (IMMR)	20	90	6	94.3	100.2
790	Lu et al. (2021a)	Nanjing Fenghui Composite Material Co. Ltd (China)	GFRP	15.6	Vinylester	Saline solution (IMMR)	20	135	6	91.2	100.9
791	Lu et al. (2021a)	Nanjing Fenghui Composite Material Co. Ltd (China)	GFRP	15.6	Vinylester	Saline solution (IMMR)	20	180	6	88.4	96.1
792	Lu et al. (2021a)	Nanjing Fenghui Composite Material Co. Ltd (China)	GFRP	15.6	Vinylester	Water (IMMR)	20	45	6	96.6	96.7
793	Lu et al. (2021a)	Nanjing Fenghui Composite Material Co. Ltd (China)	GFRP	15.6	Vinylester	Water (IMMR)	20	90	6	92.9	97.4
794	Lu et al. (2021a)	Nanjing Fenghui Composite	GFRP	15.6	Vinylester	Water (IMMR)	20	135	6	90.0	95.4

		Material Co. Ltd (China)									
795	Lu et al. (2021a)	Nanjing Fenghui Composite Material Co. Ltd (China)	GFRP	15.6	Vinylester	Water (IMMR)	20	180	6	88.1	100.2
796	Lu et al. (2021b)	TuoXin Aerospace Basalt Industrial Co., Ltd. (Sichuan, China)	BFRP	6.0	NA	Control	28	0	5	100.0	100.0
797	Lu et al. (2021b)	TuoXin Aerospace Basalt Industrial Co., Ltd. (Sichuan, China)	BFRP	6.0	NA	Alkaline solution (IMMR)	28	15	5	89.4	NA
798	Lu et al. (2021b)	TuoXin Aerospace Basalt Industrial Co., Ltd. (Sichuan, China)	BFRP	6.0	NA	Alkaline solution (IMMR)	28	30	5	85.7	NA
799	Lu et al. (2021b)	TuoXin Aerospace Basalt Industrial Co., Ltd. (Sichuan, China)	BFRP	6.0	NA	Alkaline solution (IMMR)	28	90	5	75.8	NA
800	Lu et al. (2021b)	TuoXin Aerospace Basalt Industrial Co., Ltd. (Sichuan, China)	BFRP	6.0	NA	Alkaline solution (IMMR)	28	180	5	52.2	NA
801	Lu et al. (2021b)	TuoXin Aerospace Basalt Industrial Co., Ltd. (Sichuan, China)	BFRP	6.0	NA	Alkaline solution (IMMR)	28	360	5	43.6	NA
802	Lu et al. (2021b)	TuoXin Aerospace Basalt Industrial Co., Ltd. (Sichuan, China)	BFRP	6.0	NA	Alkaline solution (IMMR)	40	15	5	83.5	NA
803	Lu et al. (2021b)	TuoXin Aerospace Basalt Industrial Co., Ltd. (Sichuan, China)	BFRP	6.0	NA	Alkaline solution (IMMR)	40	30	5	83.1	NA
804	Lu et al. (2021b)	TuoXin Aerospace Basalt Industrial Co., Ltd. (Sichuan, China)	BFRP	6.0	NA	Alkaline solution (IMMR)	40	90	5	57.9	NA
805	Lu et al. (2021b)	TuoXin Aerospace Basalt Industrial Co., Ltd. (Sichuan, China)	BFRP	6.0	NA	Alkaline solution (IMMR)	40	180	5	54.4	NA
806	Lu et al. (2021b)	TuoXin Aerospace Basalt Industrial Co., Ltd. (Sichuan, China)	BFRP	6.0	NA	Alkaline solution (IMMR)	40	360	5	36.7	NA
807	Lu et al. (2021b)	TuoXin Aerospace Basalt Industrial Co., Ltd. (Sichuan, China)	BFRP	6.0	NA	Alkaline solution (IMMR)	60	15	5	85.9	NA
808	Lu et al. (2021b)	TuoXin Aerospace Basalt Industrial Co., Ltd. (Sichuan, China)	BFRP	6.0	NA	Alkaline solution (IMMR)	60	30	5	63.0	NA
809	Lu et al. (2021b)	TuoXin Aerospace Basalt Industrial Co., Ltd. (Sichuan, China)	BFRP	6.0	NA	Alkaline solution (IMMR)	60	90	5	42.7	NA
810	Lu et al. (2021b)	TuoXin Aerospace Basalt	BFRP	6.0	NA	Alkaline solution (IMMR)	60	180	5	37.8	NA

		Industrial Co., Ltd. (Sichuan, China)									
811	Lu et al. (2021b)	TuoXin Aerospace Basalt Industrial Co., Ltd. (Sichuan, China)	BFRP	6.0	NA	Alkaline solution (IMMR)	60	360	5	18.4	NA
812	Lu et al. (2021b)	TuoXin Aerospace Basalt Industrial Co., Ltd. (Sichuan, China)	BFRP	6.0	NA	Simulated seawater (IMMR)	28	15	5	88.0	NA
813	Lu et al. (2021b)	TuoXin Aerospace Basalt Industrial Co., Ltd. (Sichuan, China)	BFRP	6.0	NA	Simulated seawater (IMMR)	28	30	5	88.5	NA
814	Lu et al. (2021b)	TuoXin Aerospace Basalt Industrial Co., Ltd. (Sichuan, China)	BFRP	6.0	NA	Simulated seawater (IMMR)	28	90	5	88.5	NA
815	Lu et al. (2021b)	TuoXin Aerospace Basalt Industrial Co., Ltd. (Sichuan, China)	BFRP	6.0	NA	Simulated seawater (IMMR)	28	180	5	76.7	NA
816	Lu et al. (2021b)	TuoXin Aerospace Basalt Industrial Co., Ltd. (Sichuan, China)	BFRP	6.0	NA	Simulated seawater (IMMR)	28	360	5	66.7	NA
817	Lu et al. (2021b)	TuoXin Aerospace Basalt Industrial Co., Ltd. (Sichuan, China)	BFRP	6.0	NA	Simulated seawater (IMMR)	40	15	5	99.4	NA
818	Lu et al. (2021b)	TuoXin Aerospace Basalt Industrial Co., Ltd. (Sichuan, China)	BFRP	6.0	NA	Simulated seawater (IMMR)	40	30	5	77.8	NA
819	Lu et al. (2021b)	TuoXin Aerospace Basalt Industrial Co., Ltd. (Sichuan, China)	BFRP	6.0	NA	Simulated seawater (IMMR)	40	90	5	68.0	NA
820	Lu et al. (2021b)	TuoXin Aerospace Basalt Industrial Co., Ltd. (Sichuan, China)	BFRP	6.0	NA	Simulated seawater (IMMR)	40	180	5	62.7	NA
821	Lu et al. (2021b)	TuoXin Aerospace Basalt Industrial Co., Ltd. (Sichuan, China)	BFRP	6.0	NA	Simulated seawater (IMMR)	40	360	5	46.0	NA
822	Lu et al. (2021b)	TuoXin Aerospace Basalt Industrial Co., Ltd. (Sichuan, China)	BFRP	6.0	NA	Simulated seawater (IMMR)	60	15	5	87.2	NA
823	Lu et al. (2021b)	TuoXin Aerospace Basalt Industrial Co., Ltd. (Sichuan, China)	BFRP	6.0	NA	Simulated seawater (IMMR)	60	30	5	79.6	NA
824	Lu et al. (2021b)	TuoXin Aerospace Basalt Industrial Co., Ltd. (Sichuan, China)	BFRP	6.0	NA	Simulated seawater (IMMR)	60	90	5	54.0	NA
825	Lu et al. (2021b)	TuoXin Aerospace Basalt Industrial Co., Ltd.	BFRP	6.0	NA	Simulated seawater (IMMR)	60	180	5	40.5	NA

		(Sichuan, China)									
826	Lu et al. (2021b)	TuoXin Aerospace Basalt Industrial Co., Ltd. (Sichuan, China)	BFRP	6.0	NA	Simulated seawater (IMMR)	60	360	5	29.7	NA
827	Lu et al. (2021b)	TuoXin Aerospace Basalt Industrial Co., Ltd. (Sichuan, China)	BFRP	6.0	NA	Water (IMMR)	28	15	5	99.4	100.6
828	Lu et al. (2021b)	TuoXin Aerospace Basalt Industrial Co., Ltd. (Sichuan, China)	BFRP	6.0	NA	Water (IMMR)	28	30	5	94.4	98.9
829	Lu et al. (2021b)	TuoXin Aerospace Basalt Industrial Co., Ltd. (Sichuan, China)	BFRP	6.0	NA	Water (IMMR)	28	90	5	94.4	103.6
830	Lu et al. (2021b)	TuoXin Aerospace Basalt Industrial Co., Ltd. (Sichuan, China)	BFRP	6.0	NA	Water (IMMR)	28	180	5	86.2	92.1
831	Lu et al. (2021b)	TuoXin Aerospace Basalt Industrial Co., Ltd. (Sichuan, China)	BFRP	6.0	NA	Water (IMMR)	28	360	5	81.2	95.9
832	Lu et al. (2021b)	TuoXin Aerospace Basalt Industrial Co., Ltd. (Sichuan, China)	BFRP	6.0	NA	Water (IMMR)	40	15	5	77.3	79.5
833	Lu et al. (2021b)	TuoXin Aerospace Basalt Industrial Co., Ltd. (Sichuan, China)	BFRP	6.0	NA	Water (IMMR)	40	30	5	92.4	99.1
834	Lu et al. (2021b)	TuoXin Aerospace Basalt Industrial Co., Ltd. (Sichuan, China)	BFRP	6.0	NA	Water (IMMR)	40	90	5	73.8	89.3
835	Lu et al. (2021b)	TuoXin Aerospace Basalt Industrial Co., Ltd. (Sichuan, China)	BFRP	6.0	NA	Water (IMMR)	40	180	5	79.5	97.9
836	Lu et al. (2021b)	TuoXin Aerospace Basalt Industrial Co., Ltd. (Sichuan, China)	BFRP	6.0	NA	Water (IMMR)	40	360	5	69.4	94.9
837	Lu et al. (2021b)	TuoXin Aerospace Basalt Industrial Co., Ltd. (Sichuan, China)	BFRP	6.0	NA	Water (IMMR)	60	15	5	86.8	NA
838	Lu et al. (2021b)	TuoXin Aerospace Basalt Industrial Co., Ltd. (Sichuan, China)	BFRP	6.0	NA	Water (IMMR)	60	30	5	66.1	NA
839	Lu et al. (2021b)	TuoXin Aerospace Basalt Industrial Co., Ltd. (Sichuan, China)	BFRP	6.0	NA	Water (IMMR)	60	90	5	62.5	NA
840	Lu et al. (2021b)	TuoXin Aerospace Basalt Industrial Co., Ltd. (Sichuan, China)	BFRP	6.0	NA	Water (IMMR)	60	180	5	53.1	NA

841	Lu et al. (2021b)	TuoXin Aerospace Basalt Industrial Co., Ltd. (Sichuan, China)	BFRP	6.0	NA	Water (IMMR)			60	360	5	41.8	NA
842	Lu et al. (2021b)	TuoXin Aerospace Basalt Industrial Co., Ltd. (Sichuan, China)	BFRP	6.0	NA	SWSSCE (IMMR)	1+Alkaline	solution	28	15	5	77.2	100.3
843	Lu et al. (2021b)	TuoXin Aerospace Basalt Industrial Co., Ltd. (Sichuan, China)	BFRP	6.0	NA	SWSSCE (IMMR)	1+Alkaline	solution	28	30	5	66.5	96.5
844	Lu et al. (2021b)	TuoXin Aerospace Basalt Industrial Co., Ltd. (Sichuan, China)	BFRP	6.0	NA	SWSSCE (IMMR)	1+Alkaline	solution	28	90	5	52.8	95.6
845	Lu et al. (2021b)	TuoXin Aerospace Basalt Industrial Co., Ltd. (Sichuan, China)	BFRP	6.0	NA	SWSSCE (IMMR)	1+Alkaline	solution	28	180	5	48.9	95.6
846	Lu et al. (2021b)	TuoXin Aerospace Basalt Industrial Co., Ltd. (Sichuan, China)	BFRP	6.0	NA	SWSSCE (IMMR)	1+Alkaline	solution	28	360	5	42.9	86.7
847	Lu et al. (2021b)	TuoXin Aerospace Basalt Industrial Co., Ltd. (Sichuan, China)	BFRP	6.0	NA	SWSSCE (IMMR)	1+Alkaline	solution	40	15	5	69.3	95.1
848	Lu et al. (2021b)	TuoXin Aerospace Basalt Industrial Co., Ltd. (Sichuan, China)	BFRP	6.0	NA	SWSSCE (IMMR)	1+Alkaline	solution	40	30	5	62.4	98.1
849	Lu et al. (2021b)	TuoXin Aerospace Basalt Industrial Co., Ltd. (Sichuan, China)	BFRP	6.0	NA	SWSSCE (IMMR)	1+Alkaline	solution	40	90	5	48.2	94.6
850	Lu et al. (2021b)	TuoXin Aerospace Basalt Industrial Co., Ltd. (Sichuan, China)	BFRP	6.0	NA	SWSSCE (IMMR)	1+Alkaline	solution	40	180	5	42.2	94.6
851	Lu et al. (2021b)	TuoXin Aerospace Basalt Industrial Co., Ltd. (Sichuan, China)	BFRP	6.0	NA	SWSSCE (IMMR)	1+Alkaline	solution	40	360	5	31.4	83.9
852	Lu et al. (2021b)	TuoXin Aerospace Basalt Industrial Co., Ltd. (Sichuan, China)	BFRP	6.0	NA	SWSSCE (IMMR)	1+Alkaline	solution	60	15	5	68.5	98.7
853	Lu et al. (2021b)	TuoXin Aerospace Basalt Industrial Co., Ltd. (Sichuan, China)	BFRP	6.0	NA	SWSSCE (IMMR)	1+Alkaline	solution	60	30	5	61.2	95.7
854	Lu et al. (2021b)	TuoXin Aerospace Basalt Industrial Co., Ltd. (Sichuan, China)	BFRP	6.0	NA	SWSSCE (IMMR)	1+Alkaline	solution	60	90	5	41.1	87.9
855	Lu et al. (2021b)	TuoXin Aerospace Basalt Industrial Co., Ltd. (Sichuan, China)	BFRP	6.0	NA	SWSSCE (IMMR)	1+Alkaline	solution	60	180	5	23.5	95.3
856	Lu et al. (2021b)	TuoXin Aerospace Basalt	BFRP	6.0	NA	SWSSCE	1+Alkaline	solution	60	360	5	0.0	NA

		Industrial Co., Ltd. (Sichuan, China)				(IMMR)								
857	Lu et al. (2021b)	TuoXin Aerospace Basalt Industrial Co., Ltd. (Sichuan, China)	BFRP	6.0	NA	SWSSCE (IMMR)	1+Simulated	seawater	28	15	5	83.6	101.6
858	Lu et al. (2021b)	TuoXin Aerospace Basalt Industrial Co., Ltd. (Sichuan, China)	BFRP	6.0	NA	SWSSCE (IMMR)	1+Simulated	seawater	28	30	5	72.9	104.9
859	Lu et al. (2021b)	TuoXin Aerospace Basalt Industrial Co., Ltd. (Sichuan, China)	BFRP	6.0	NA	SWSSCE (IMMR)	1+Simulated	seawater	28	90	5	66.9	98.2
860	Lu et al. (2021b)	TuoXin Aerospace Basalt Industrial Co., Ltd. (Sichuan, China)	BFRP	6.0	NA	SWSSCE (IMMR)	1+Simulated	seawater	28	180	5	66.9	96.1
861	Lu et al. (2021b)	TuoXin Aerospace Basalt Industrial Co., Ltd. (Sichuan, China)	BFRP	6.0	NA	SWSSCE (IMMR)	1+Simulated	seawater	28	360	5	63.5	92.2
862	Lu et al. (2021b)	TuoXin Aerospace Basalt Industrial Co., Ltd. (Sichuan, China)	BFRP	6.0	NA	SWSSCE (IMMR)	1+Simulated	seawater	40	15	5	69.3	99.8
863	Lu et al. (2021b)	TuoXin Aerospace Basalt Industrial Co., Ltd. (Sichuan, China)	BFRP	6.0	NA	SWSSCE (IMMR)	1+Simulated	seawater	40	30	5	70.6	101.5
864	Lu et al. (2021b)	TuoXin Aerospace Basalt Industrial Co., Ltd. (Sichuan, China)	BFRP	6.0	NA	SWSSCE (IMMR)	1+Simulated	seawater	40	90	5	58.1	105.0
865	Lu et al. (2021b)	TuoXin Aerospace Basalt Industrial Co., Ltd. (Sichuan, China)	BFRP	6.0	NA	SWSSCE (IMMR)	1+Simulated	seawater	40	180	5	56.9	92.5
866	Lu et al. (2021b)	TuoXin Aerospace Basalt Industrial Co., Ltd. (Sichuan, China)	BFRP	6.0	NA	SWSSCE (IMMR)	1+Simulated	seawater	40	360	5	54.7	92.9
867	Lu et al. (2021b)	TuoXin Aerospace Basalt Industrial Co., Ltd. (Sichuan, China)	BFRP	6.0	NA	SWSSCE (IMMR)	1+Simulated	seawater	60	15	5	67.6	98.3
868	Lu et al. (2021b)	TuoXin Aerospace Basalt Industrial Co., Ltd. (Sichuan, China)	BFRP	6.0	NA	SWSSCE (IMMR)	1+Simulated	seawater	60	30	5	63.4	93.1
869	Lu et al. (2021b)	TuoXin Aerospace Basalt Industrial Co., Ltd. (Sichuan, China)	BFRP	6.0	NA	SWSSCE (IMMR)	1+Simulated	seawater	60	90	5	55.2	94.0
870	Lu et al. (2021b)	TuoXin Aerospace Basalt Industrial Co., Ltd. (Sichuan, China)	BFRP	6.0	NA	SWSSCE (IMMR)	1+Simulated	seawater	60	180	5	50.5	92.7
871	Lu et al. (2021b)	TuoXin Aerospace Basalt Industrial Co., Ltd.	BFRP	6.0	NA	SWSSCE (IMMR)	1+Simulated	seawater	60	360	5	37.7	86.2

		(Sichuan, China)									
872	Lu et al. (2021b)	TuoXin Aerospace Basalt Industrial Co., Ltd. (Sichuan, China)	BFRP	6.0	NA	SWSSCE 1+Water (IMMR)	28	15	5	84.1	101.6
873	Lu et al. (2021b)	TuoXin Aerospace Basalt Industrial Co., Ltd. (Sichuan, China)	BFRP	6.0	NA	SWSSCE 1+Water (IMMR)	28	30	5	75.5	104.9
874	Lu et al. (2021b)	TuoXin Aerospace Basalt Industrial Co., Ltd. (Sichuan, China)	BFRP	6.0	NA	SWSSCE 1+Water (IMMR)	28	90	5	63.9	98.2
875	Lu et al. (2021b)	TuoXin Aerospace Basalt Industrial Co., Ltd. (Sichuan, China)	BFRP	6.0	NA	SWSSCE 1+Water (IMMR)	28	180	5	63.9	96.1
876	Lu et al. (2021b)	TuoXin Aerospace Basalt Industrial Co., Ltd. (Sichuan, China)	BFRP	6.0	NA	SWSSCE 1+Water (IMMR)	28	360	5	56.6	92.2
877	Lu et al. (2021b)	TuoXin Aerospace Basalt Industrial Co., Ltd. (Sichuan, China)	BFRP	6.0	NA	SWSSCE 1+Water (IMMR)	40	15	5	69.3	95.9
878	Lu et al. (2021b)	TuoXin Aerospace Basalt Industrial Co., Ltd. (Sichuan, China)	BFRP	6.0	NA	SWSSCE 1+Water (IMMR)	40	30	5	62.0	97.7
879	Lu et al. (2021b)	TuoXin Aerospace Basalt Industrial Co., Ltd. (Sichuan, China)	BFRP	6.0	NA	SWSSCE 1+Water (IMMR)	40	90	5	53.4	98.1
880	Lu et al. (2021b)	TuoXin Aerospace Basalt Industrial Co., Ltd. (Sichuan, China)	BFRP	6.0	NA	SWSSCE 1+Water (IMMR)	40	180	5	52.1	98.5
881	Lu et al. (2021b)	TuoXin Aerospace Basalt Industrial Co., Ltd. (Sichuan, China)	BFRP	6.0	NA	SWSSCE 1+Water (IMMR)	40	360	5	46.5	95.9
882	Lu et al. (2021b)	TuoXin Aerospace Basalt Industrial Co., Ltd. (Sichuan, China)	BFRP	6.0	NA	SWSSCE 1+Water (IMMR)	60	15	5	64.7	95.7
883	Lu et al. (2021b)	TuoXin Aerospace Basalt Industrial Co., Ltd. (Sichuan, China)	BFRP	6.0	NA	SWSSCE 1+Water (IMMR)	60	30	5	57.8	97.0
884	Lu et al. (2021b)	TuoXin Aerospace Basalt Industrial Co., Ltd. (Sichuan, China)	BFRP	6.0	NA	SWSSCE 1+Water (IMMR)	60	90	5	47.5	96.6
885	Lu et al. (2021b)	TuoXin Aerospace Basalt Industrial Co., Ltd. (Sichuan, China)	BFRP	6.0	NA	SWSSCE 1+Water (IMMR)	60	180	5	40.2	93.1
886	Lu et al. (2021b)	TuoXin Aerospace Basalt Industrial Co., Ltd. (Sichuan, China)	BFRP	6.0	NA	SWSSCE 1+Water (IMMR)	60	360	5	35.5	90.1

887	Lu et al. (2021b)	TuoXin Aerospace Basalt Industrial Co., Ltd. (Sichuan, China)	BFRP	6.0	NA	SWSSCE (IMMR)	2+Alkaline	solution	28	15	5	73.9	NA
888	Lu et al. (2021b)	TuoXin Aerospace Basalt Industrial Co., Ltd. (Sichuan, China)	BFRP	6.0	NA	SWSSCE (IMMR)	2+Alkaline	solution	28	30	5	61.7	NA
889	Lu et al. (2021b)	TuoXin Aerospace Basalt Industrial Co., Ltd. (Sichuan, China)	BFRP	6.0	NA	SWSSCE (IMMR)	2+Alkaline	solution	28	90	5	39.5	NA
890	Lu et al. (2021b)	TuoXin Aerospace Basalt Industrial Co., Ltd. (Sichuan, China)	BFRP	6.0	NA	SWSSCE (IMMR)	2+Alkaline	solution	28	180	5	31.9	NA
891	Lu et al. (2021b)	TuoXin Aerospace Basalt Industrial Co., Ltd. (Sichuan, China)	BFRP	6.0	NA	SWSSCE (IMMR)	2+Alkaline	solution	28	360	5	21.4	NA
892	Lu et al. (2021b)	TuoXin Aerospace Basalt Industrial Co., Ltd. (Sichuan, China)	BFRP	6.0	NA	SWSSCE (IMMR)	2+Alkaline	solution	40	15	5	62.3	NA
893	Lu et al. (2021b)	TuoXin Aerospace Basalt Industrial Co., Ltd. (Sichuan, China)	BFRP	6.0	NA	SWSSCE (IMMR)	2+Alkaline	solution	40	30	5	50.6	NA
894	Lu et al. (2021b)	TuoXin Aerospace Basalt Industrial Co., Ltd. (Sichuan, China)	BFRP	6.0	NA	SWSSCE (IMMR)	2+Alkaline	solution	40	90	5	28.5	NA
895	Lu et al. (2021b)	TuoXin Aerospace Basalt Industrial Co., Ltd. (Sichuan, China)	BFRP	6.0	NA	SWSSCE (IMMR)	2+Alkaline	solution	40	180	5	25.1	NA
896	Lu et al. (2021b)	TuoXin Aerospace Basalt Industrial Co., Ltd. (Sichuan, China)	BFRP	6.0	NA	SWSSCE (IMMR)	2+Alkaline	solution	40	360	5	0.0	NA
897	Lu et al. (2021b)	TuoXin Aerospace Basalt Industrial Co., Ltd. (Sichuan, China)	BFRP	6.0	NA	SWSSCE (IMMR)	2+Alkaline	solution	60	15	5	58.8	NA
898	Lu et al. (2021b)	TuoXin Aerospace Basalt Industrial Co., Ltd. (Sichuan, China)	BFRP	6.0	NA	SWSSCE (IMMR)	2+Alkaline	solution	60	30	5	47.2	NA
899	Lu et al. (2021b)	TuoXin Aerospace Basalt Industrial Co., Ltd. (Sichuan, China)	BFRP	6.0	NA	SWSSCE (IMMR)	2+Alkaline	solution	60	90	5	18.4	NA
900	Lu et al. (2021b)	TuoXin Aerospace Basalt Industrial Co., Ltd. (Sichuan, China)	BFRP	6.0	NA	SWSSCE (IMMR)	2+Alkaline	solution	60	180	5	0.0	NA
901	Lu et al. (2021b)	TuoXin Aerospace Basalt Industrial Co., Ltd. (Sichuan, China)	BFRP	6.0	NA	SWSSCE (IMMR)	2+Simulated	seawater	28	15	5	72.2	NA
902	Lu et al. (2021b)	TuoXin Aerospace Basalt	BFRP	6.0	NA	SWSSCE	2+Simulated	seawater	28	30	5	47.5	NA

		Industrial Co., Ltd. (Sichuan, China)				(IMMR)							
903	Lu et al. (2021b)	TuoXin Aerospace Basalt Industrial Co., Ltd. (Sichuan, China)	BFRP	6.0	NA	SWSSCE (IMMR)	2+Simulated seawater	28	90	5	39.9	NA
904	Lu et al. (2021b)	TuoXin Aerospace Basalt Industrial Co., Ltd. (Sichuan, China)	BFRP	6.0	NA	SWSSCE (IMMR)	2+Simulated seawater	28	180	5	38.2	NA
905	Lu et al. (2021b)	TuoXin Aerospace Basalt Industrial Co., Ltd. (Sichuan, China)	BFRP	6.0	NA	SWSSCE (IMMR)	2+Simulated seawater	28	360	5	70.6	NA
906	Lu et al. (2021b)	TuoXin Aerospace Basalt Industrial Co., Ltd. (Sichuan, China)	BFRP	6.0	NA	SWSSCE (IMMR)	2+Simulated seawater	40	15	5	58.8	NA
907	Lu et al. (2021b)	TuoXin Aerospace Basalt Industrial Co., Ltd. (Sichuan, China)	BFRP	6.0	NA	SWSSCE (IMMR)	2+Simulated seawater	40	30	5	51.5	NA
908	Lu et al. (2021b)	TuoXin Aerospace Basalt Industrial Co., Ltd. (Sichuan, China)	BFRP	6.0	NA	SWSSCE (IMMR)	2+Simulated seawater	40	90	5	45.8	NA
909	Lu et al. (2021b)	TuoXin Aerospace Basalt Industrial Co., Ltd. (Sichuan, China)	BFRP	6.0	NA	SWSSCE (IMMR)	2+Simulated seawater	40	180	5	33.3	NA
910	Lu et al. (2021b)	TuoXin Aerospace Basalt Industrial Co., Ltd. (Sichuan, China)	BFRP	6.0	NA	SWSSCE (IMMR)	2+Simulated seawater	40	360	5	27.7	NA
911	Lu et al. (2021b)	TuoXin Aerospace Basalt Industrial Co., Ltd. (Sichuan, China)	BFRP	6.0	NA	SWSSCE (IMMR)	2+Simulated seawater	60	15	5	58.8	NA
912	Lu et al. (2021b)	TuoXin Aerospace Basalt Industrial Co., Ltd. (Sichuan, China)	BFRP	6.0	NA	SWSSCE (IMMR)	2+Simulated seawater	60	30	5	47.2	NA
913	Lu et al. (2021b)	TuoXin Aerospace Basalt Industrial Co., Ltd. (Sichuan, China)	BFRP	6.0	NA	SWSSCE (IMMR)	2+Simulated seawater	60	90	5	18.4	NA
914	Lu et al. (2021b)	TuoXin Aerospace Basalt Industrial Co., Ltd. (Sichuan, China)	BFRP	6.0	NA	SWSSCE (IMMR)	2+Simulated seawater	60	180	5	0.0	NA
915	Lu et al. (2021b)	TuoXin Aerospace Basalt Industrial Co., Ltd. (Sichuan, China)	BFRP	6.0	NA	SWSSCE 2+Water (IMMR)		28	15	5	62.2	93.0
916	Lu et al. (2021b)	TuoXin Aerospace Basalt Industrial Co., Ltd. (Sichuan, China)	BFRP	6.0	NA	SWSSCE 2+Water (IMMR)		28	30	5	60.9	97.6
917	Lu et al. (2021b)	TuoXin Aerospace Basalt Industrial Co., Ltd.	BFRP	6.0	NA	SWSSCE 2+Water (IMMR)		28	90	5	41.6	97.2

		(Sichuan, China)									
918	Lu et al. (2021b)	TuoXin Aerospace Basalt Industrial Co., Ltd. (Sichuan, China)	BFRP	6.0	NA	SWSSCE 2+Water (IMMR)	28	180	5	35.3	102.3
919	Lu et al. (2021b)	TuoXin Aerospace Basalt Industrial Co., Ltd. (Sichuan, China)	BFRP	6.0	NA	SWSSCE 2+Water (IMMR)	28	360	5	34.4	81.5
920	Lu et al. (2021b)	TuoXin Aerospace Basalt Industrial Co., Ltd. (Sichuan, China)	BFRP	6.0	NA	SWSSCE 2+Water (IMMR)	40	15	5	60.1	94.9
921	Lu et al. (2021b)	TuoXin Aerospace Basalt Industrial Co., Ltd. (Sichuan, China)	BFRP	6.0	NA	SWSSCE 2+Water (IMMR)	40	30	5	52.8	89.7
922	Lu et al. (2021b)	TuoXin Aerospace Basalt Industrial Co., Ltd. (Sichuan, China)	BFRP	6.0	NA	SWSSCE 2+Water (IMMR)	40	90	5	34.2	95.7
923	Lu et al. (2021b)	TuoXin Aerospace Basalt Industrial Co., Ltd. (Sichuan, China)	BFRP	6.0	NA	SWSSCE 2+Water (IMMR)	40	180	5	22.9	75.2
924	Lu et al. (2021b)	TuoXin Aerospace Basalt Industrial Co., Ltd. (Sichuan, China)	BFRP	6.0	NA	SWSSCE 2+Water (IMMR)	40	360	5	21.6	57.7
925	Lu et al. (2021b)	TuoXin Aerospace Basalt Industrial Co., Ltd. (Sichuan, China)	BFRP	6.0	NA	SWSSCE 2+Water (IMMR)	60	15	5	54.5	NA
926	Lu et al. (2021b)	TuoXin Aerospace Basalt Industrial Co., Ltd. (Sichuan, China)	BFRP	6.0	NA	SWSSCE 2+Water (IMMR)	60	30	5	44.2	NA
927	Lu et al. (2021b)	TuoXin Aerospace Basalt Industrial Co., Ltd. (Sichuan, China)	BFRP	6.0	NA	SWSSCE 2+Water (IMMR)	60	90	5	25.7	NA
928	Lu et al. (2021b)	TuoXin Aerospace Basalt Industrial Co., Ltd. (Sichuan, China)	BFRP	6.0	NA	SWSSCE 2+Water (IMMR)	60	180	5	22.7	NA
929	Lu et al. (2021b)	TuoXin Aerospace Basalt Industrial Co., Ltd. (Sichuan, China)	BFRP	6.0	NA	SWSSCE 2+Water (IMMR)	60	360	5	0.0	NA
930	Lu et al. (2021c)	Tuo Xin Aerospace Basalt Industrial Co., Ltd. (Chengdu City, China)	BFRP	12.0	Epoxy	Control	26	0	3	100.0	100.0
931	Lu et al. (2021c)	Tuo Xin Aerospace Basalt Industrial Co., Ltd. (Chengdu City, China)	BFRP	12.0	Epoxy	Alkaline solution (IMMR)	26	30	3	91.4	92.7
932	Lu et al. (2021c)	Tuo Xin Aerospace Basalt Industrial Co., Ltd. (Chengdu City, China)	BFRP	12.0	Epoxy	Alkaline solution (IMMR)	26	90	3	83.6	93.8

933	Lu et al. (2021c)	Tuo Xin Aerospace Basalt Industrial Co., Ltd. (Chengdu City, China)	BFRP	12.0	Epoxy	Alkaline solution (IMMR)	26	270	3	72.3	93.8
934	Lu et al. (2021c)	Tuo Xin Aerospace Basalt Industrial Co., Ltd. (Chengdu City, China)	BFRP	12.0	Epoxy	Alkaline solution (IMMR)	40	30	3	83.0	95.4
935	Lu et al. (2021c)	Tuo Xin Aerospace Basalt Industrial Co., Ltd. (Chengdu City, China)	BFRP	12.0	Epoxy	Alkaline solution (IMMR)	40	90	3	76.8	89.9
936	Lu et al. (2021c)	Tuo Xin Aerospace Basalt Industrial Co., Ltd. (Chengdu City, China)	BFRP	12.0	Epoxy	Alkaline solution (IMMR)	40	270	3	52.7	103.8
937	Lu et al. (2021c)	Tuo Xin Aerospace Basalt Industrial Co., Ltd. (Chengdu City, China)	BFRP	12.0	Epoxy	Alkaline solution (IMMR)	60	30	3	78.5	100.5
938	Lu et al. (2021c)	Tuo Xin Aerospace Basalt Industrial Co., Ltd. (Chengdu City, China)	BFRP	12.0	Epoxy	Alkaline solution (IMMR)	60	90	3	75.1	95.4
939	Lu et al. (2021c)	Tuo Xin Aerospace Basalt Industrial Co., Ltd. (Chengdu City, China)	BFRP	12.0	Epoxy	Alkaline solution (IMMR)	60	270	3	33.1	103.3
940	Lu et al. (2021c)	Tuo Xin Aerospace Basalt Industrial Co., Ltd. (Chengdu City, China)	BFRP	12.0	Epoxy	Simulated seawater (IMMR)	26	30	3	94.8	92.7
941	Lu et al. (2021c)	Tuo Xin Aerospace Basalt Industrial Co., Ltd. (Chengdu City, China)	BFRP	12.0	Epoxy	Simulated seawater (IMMR)	26	90	3	91.4	94.9
942	Lu et al. (2021c)	Tuo Xin Aerospace Basalt Industrial Co., Ltd. (Chengdu City, China)	BFRP	12.0	Epoxy	Simulated seawater (IMMR)	26	270	3	85.2	94.9
943	Lu et al. (2021c)	Tuo Xin Aerospace Basalt Industrial Co., Ltd. (Chengdu City, China)	BFRP	12.0	Epoxy	Simulated seawater (IMMR)	40	30	3	94.8	100.5
944	Lu et al. (2021c)	Tuo Xin Aerospace Basalt Industrial Co., Ltd. (Chengdu City, China)	BFRP	12.0	Epoxy	Simulated seawater (IMMR)	40	90	3	84.1	98.8
945	Lu et al. (2021c)	Tuo Xin Aerospace Basalt Industrial Co., Ltd. (Chengdu City, China)	BFRP	12.0	Epoxy	Simulated seawater (IMMR)	40	270	3	68.4	94.9
946	Lu et al. (2021c)	Tuo Xin Aerospace Basalt Industrial Co., Ltd. (Chengdu City, China)	BFRP	12.0	Epoxy	Simulated seawater (IMMR)	60	30	3	79.1	106.1
947	Lu et al. (2021c)	Tuo Xin Aerospace Basalt Industrial Co., Ltd. (Chengdu City, China)	BFRP	12.0	Epoxy	Simulated seawater (IMMR)	60	90	3	67.9	97.7
948	Lu et al. (2021c)	Tuo Xin Aerospace Basalt	BFRP	12.0	Epoxy	Simulated seawater (IMMR)	60	270	3	46.0	97.7

		Industrial Co., Ltd. (Chengdu City, China)									
949	Lu et al. (2022a)	Harbin FRP Institute Co., Ltd. (Harbin, China)	GFRP	8.0	Epoxy	Control	20	0	5	100.0	100.0
950	Lu et al. (2022a)	Harbin FRP Institute Co., Ltd. (Harbin, China)	GFRP	8.0	Epoxy	Simulated seawater (IMMR)	20	30	5	96.1	101.3
951	Lu et al. (2022a)	Harbin FRP Institute Co., Ltd. (Harbin, China)	GFRP	8.0	Epoxy	Simulated seawater (IMMR)	20	60	5	94.2	98.5
952	Lu et al. (2022a)	Harbin FRP Institute Co., Ltd. (Harbin, China)	GFRP	8.0	Epoxy	Simulated seawater (IMMR)	20	90	5	97.2	98.5
953	Lu et al. (2022a)	Harbin FRP Institute Co., Ltd. (Harbin, China)	GFRP	8.0	Epoxy	Simulated seawater (IMMR)	20	180	5	98.3	107.2
954	Lu et al. (2022a)	Harbin FRP Institute Co., Ltd. (Harbin, China)	GFRP	8.0	Epoxy	Simulated seawater (IMMR)	40	30	5	99.1	100.2
955	Lu et al. (2022a)	Harbin FRP Institute Co., Ltd. (Harbin, China)	GFRP	8.0	Epoxy	Simulated seawater (IMMR)	40	60	5	95.0	100.2
956	Lu et al. (2022a)	Harbin FRP Institute Co., Ltd. (Harbin, China)	GFRP	8.0	Epoxy	Simulated seawater (IMMR)	40	90	5	98.0	97.9
957	Lu et al. (2022a)	Harbin FRP Institute Co., Ltd. (Harbin, China)	GFRP	8.0	Epoxy	Simulated seawater (IMMR)	40	180	5	94.4	106.6
958	Lu et al. (2022a)	Harbin FRP Institute Co., Ltd. (Harbin, China)	GFRP	8.0	Epoxy	Simulated seawater (IMMR)	60	30	5	95.8	101.3
959	Lu et al. (2022a)	Harbin FRP Institute Co., Ltd. (Harbin, China)	GFRP	8.0	Epoxy	Simulated seawater (IMMR)	60	60	5	93.9	100.0
960	Lu et al. (2022a)	Harbin FRP Institute Co., Ltd. (Harbin, China)	GFRP	8.0	Epoxy	Simulated seawater (IMMR)	60	90	5	83.2	101.5
961	Lu et al. (2022a)	Harbin FRP Institute Co., Ltd. (Harbin, China)	GFRP	8.0	Epoxy	Simulated seawater (IMMR)	60	180	5	72.8	109.1
962	Lu et al. (2022a)	Harbin FRP Institute Co., Ltd. (Harbin, China)	GFRP	8.0	Epoxy	Water (IMMR)	60	30	5	93.3	101.3
963	Lu et al. (2022a)	Harbin FRP Institute Co., Ltd. (Harbin, China)	GFRP	8.0	Epoxy	Water (IMMR)	60	60	5	89.5	100.0
964	Lu et al. (2022a)	Harbin FRP Institute Co., Ltd. (Harbin, China)	GFRP	8.0	Epoxy	Water (IMMR)	60	90	5	83.2	101.5
965	Lu et al. (2022a)	Harbin FRP Institute Co., Ltd. (Harbin, China)	GFRP	8.0	Epoxy	Water (IMMR)	60	180	5	67.4	109.1
966	Lu et al. (2022a)	TuoXin Aerospace Basalt Industrial Co., Ltd. (Sichuan, China)	BFRP	8.0	Epoxy	Control	20	0	5	100.0	100.0
967	Lu et al. (2022a)	TuoXin Aerospace Basalt Industrial Co., Ltd. (Sichuan, China)	BFRP	8.0	Epoxy	Simulated seawater (IMMR)	20	30	5	99.3	100.0
968	Lu et al. (2022a)	TuoXin Aerospace Basalt Industrial Co., Ltd. (Sichuan, China)	BFRP	8.0	Epoxy	Simulated seawater (IMMR)	20	60	5	91.2	99.4
969	Lu et al. (2022a)	TuoXin Aerospace Basalt	BFRP	8.0	Epoxy	Simulated seawater (IMMR)	20	90	5	87.2	98.0

		Industrial Co., Ltd. (Sichuan, China)									
970	Lu et al. (2022a)	TuoXin Aerospace Basalt Industrial Co., Ltd. (Sichuan, China)	BFRP	8.0	Epoxy	Simulated seawater (IMMR)	20	180	5	81.3	99.8
971	Lu et al. (2022a)	TuoXin Aerospace Basalt Industrial Co., Ltd. (Sichuan, China)	BFRP	8.0	Epoxy	Simulated seawater (IMMR)	40	30	5	99.3	100.8
972	Lu et al. (2022a)	TuoXin Aerospace Basalt Industrial Co., Ltd. (Sichuan, China)	BFRP	8.0	Epoxy	Simulated seawater (IMMR)	40	60	5	91.2	100.6
973	Lu et al. (2022a)	TuoXin Aerospace Basalt Industrial Co., Ltd. (Sichuan, China)	BFRP	8.0	Epoxy	Simulated seawater (IMMR)	40	90	5	87.2	104.4
974	Lu et al. (2022a)	TuoXin Aerospace Basalt Industrial Co., Ltd. (Sichuan, China)	BFRP	8.0	Epoxy	Simulated seawater (IMMR)	40	180	5	81.3	100.6
975	Lu et al. (2022a)	TuoXin Aerospace Basalt Industrial Co., Ltd. (Sichuan, China)	BFRP	8.0	Epoxy	Simulated seawater (IMMR)	60	30	5	99.3	98.6
976	Lu et al. (2022a)	TuoXin Aerospace Basalt Industrial Co., Ltd. (Sichuan, China)	BFRP	8.0	Epoxy	Simulated seawater (IMMR)	60	60	5	91.2	103.4
977	Lu et al. (2022a)	TuoXin Aerospace Basalt Industrial Co., Ltd. (Sichuan, China)	BFRP	8.0	Epoxy	Simulated seawater (IMMR)	60	90	5	87.2	92.8
978	Lu et al. (2022a)	TuoXin Aerospace Basalt Industrial Co., Ltd. (Sichuan, China)	BFRP	8.0	Epoxy	Simulated seawater (IMMR)	60	180	5	81.3	107.2
979	Lu et al. (2022a)	TuoXin Aerospace Basalt Industrial Co., Ltd. (Sichuan, China)	BFRP	8.0	Epoxy	Water (IMMR)	60	30	5	99.3	100.4
980	Lu et al. (2022a)	TuoXin Aerospace Basalt Industrial Co., Ltd. (Sichuan, China)	BFRP	8.0	Epoxy	Water (IMMR)	60	60	5	91.2	100.6
981	Lu et al. (2022a)	TuoXin Aerospace Basalt Industrial Co., Ltd. (Sichuan, China)	BFRP	8.0	Epoxy	Water (IMMR)	60	90	5	87.2	104.6
982	Lu et al. (2022a)	TuoXin Aerospace Basalt Industrial Co., Ltd. (Sichuan, China)	BFRP	8.0	Epoxy	Water (IMMR)	60	180	5	81.3	106.2
983	Lu et al. (2022b)	Shenzhen Haichuan New Material Technology (Shenzhen, China)	GFRP	6.0	Epoxy-vinyl	Control	RT	0	NA	100.0	100.0
984	Lu et al. (2022b)	Shenzhen Haichuan New Material Technology	GFRP	6.0	Epoxy-vinyl	SWSSCE+Simulated seawater (IMMR)	RT	30	NA	74.8	92.8

		(Shenzhen, China)									
985	Lu et al. (2022b)	Shenzhen Haichuan New Material Technology (Shenzhen, China)	GFRP	6.0	Epoxy-vinyl	SWSSCE+Simulated seawater (IMMR)	RT	60	NA	67.9	80.6
986	Lu et al. (2022b)	Shenzhen Haichuan New Material Technology (Shenzhen, China)	GFRP	6.0	Epoxy-vinyl	SWSSCE+Simulated seawater (IMMR)	RT	120	NA	49.6	77.9
987	Lu et al. (2022b)	Shenzhen Haichuan New Material Technology (Shenzhen, China)	GFRP	6.0	Epoxy-vinyl	SWSSCE+Simulated seawater (IMMR)	40	30	NA	56.5	80.6
988	Lu et al. (2022b)	Shenzhen Haichuan New Material Technology (Shenzhen, China)	GFRP	6.0	Epoxy-vinyl	SWSSCE+Simulated seawater (IMMR)	40	60	NA	32.5	64.6
989	Lu et al. (2022b)	Shenzhen Haichuan New Material Technology (Shenzhen, China)	GFRP	6.0	Epoxy-vinyl	SWSSCE+Simulated seawater (IMMR)	40	120	NA	18.3	43.1
990	Lu et al. (2022b)	Shenzhen Haichuan New Material Technology (Shenzhen, China)	GFRP	6.0	Epoxy-vinyl	SWSSCE+Simulated seawater (IMMR)	60	30	NA	40.7	72.9
991	Lu et al. (2022b)	Shenzhen Haichuan New Material Technology (Shenzhen, China)	GFRP	6.0	Epoxy-vinyl	SWSSCE+Simulated seawater (IMMR)	60	60	NA	29.7	56.9
992	Lu et al. (2022b)	Shenzhen Haichuan New Material Technology (Shenzhen, China)	GFRP	6.0	Epoxy-vinyl	SWSSCE+Simulated seawater (IMMR)	60	120	NA	18.3	35.3
993	Lu et al. (2022b)	Shenzhen Haichuan New Material Technology (Shenzhen, China)	GFRP	6.0	Epoxy-vinyl	SL (20%fu)+SWSSCE+Simulated seawater (IMMR)	RT	30	NA	67.9	83.7
994	Lu et al. (2022b)	Shenzhen Haichuan New Material Technology (Shenzhen, China)	GFRP	6.0	Epoxy-vinyl	SL (20%fu)+SWSSCE+Simulated seawater (IMMR)	RT	60	NA	54.5	78.1
995	Lu et al. (2022b)	Shenzhen Haichuan New Material Technology (Shenzhen, China)	GFRP	6.0	Epoxy-vinyl	SL (20%fu)+SWSSCE+Simulated seawater (IMMR)	RT	120	NA	31.7	61.5
996	Lu et al. (2022b)	Shenzhen Haichuan New Material Technology (Shenzhen, China)	GFRP	6.0	Epoxy-vinyl	SL (20%fu)+SWSSCE+Simulated seawater (IMMR)	40	30	NA	50.8	80.9
997	Lu et al. (2022b)	Shenzhen Haichuan New Material Technology (Shenzhen, China)	GFRP	6.0	Epoxy-vinyl	SL (20%fu)+SWSSCE+Simulated seawater (IMMR)	40	60	NA	30.5	58.7
998	Lu et al. (2022b)	Shenzhen Haichuan New Material Technology (Shenzhen, China)	GFRP	6.0	Epoxy-vinyl	SL (20%fu)+SWSSCE+Simulated seawater (IMMR)	40	120	NA	19.1	50.4
999	Lu et al. (2022b)	Shenzhen Haichuan New Material Technology (Shenzhen, China)	GFRP	6.0	Epoxy-vinyl	SL (20%fu)+SWSSCE+Simulated seawater (IMMR)	60	30	NA	38.6	70.9

1000	Lu et al. (2022b)	Shenzhen Haichuan New Material Technology (Shenzhen, China)	GFRP	6.0	Epoxy-vinyl	SL (20%fu)+SWSSCE+Simulated seawater (IMMR)	60	60	NA	24.0	48.8
1001	Lu et al. (2022b)	Shenzhen Haichuan New Material Technology (Shenzhen, China)	GFRP	6.0	Epoxy-vinyl	SL (20%fu)+SWSSCE+Simulated seawater (IMMR)	60	120	NA	17.5	39.9
1002	Lu et al. (2022b)	Shenzhen Haichuan New Material Technology (Shenzhen, China)	GFRP	6.0	Epoxy-vinyl	SL (40%fu)+SWSSCE+Simulated seawater (IMMR)	RT	30	NA	58.2	82.6
1003	Lu et al. (2022b)	Shenzhen Haichuan New Material Technology (Shenzhen, China)	GFRP	6.0	Epoxy-vinyl	SL (40%fu)+SWSSCE+Simulated seawater (IMMR)	RT	60	NA	46.8	73.0
1004	Lu et al. (2022b)	Shenzhen Haichuan New Material Technology (Shenzhen, China)	GFRP	6.0	Epoxy-vinyl	SL (40%fu)+SWSSCE+Simulated seawater (IMMR)	RT	120	NA	27.7	50.1
1005	Lu et al. (2022b)	Shenzhen Haichuan New Material Technology (Shenzhen, China)	GFRP	6.0	Epoxy-vinyl	SL (40%fu)+SWSSCE+Simulated seawater (IMMR)	40	30	NA	39.9	76.2
1006	Lu et al. (2022b)	Shenzhen Haichuan New Material Technology (Shenzhen, China)	GFRP	6.0	Epoxy-vinyl	SL (40%fu)+SWSSCE+Simulated seawater (IMMR)	40	60	NA	27.2	60.7
1007	Lu et al. (2022b)	Shenzhen Haichuan New Material Technology (Shenzhen, China)	GFRP	6.0	Epoxy-vinyl	SL (40%fu)+SWSSCE+Simulated seawater (IMMR)	40	120	NA	0.0	0.0
1008	Lu et al. (2022b)	Shenzhen Haichuan New Material Technology (Shenzhen, China)	GFRP	6.0	Epoxy-vinyl	SL (40%fu)+SWSSCE+Simulated seawater (IMMR)	60	30	NA	29.7	58.6
1009	Lu et al. (2022b)	Shenzhen Haichuan New Material Technology (Shenzhen, China)	GFRP	6.0	Epoxy-vinyl	SL (40%fu)+SWSSCE+Simulated seawater (IMMR)	60	60	NA	23.2	52.7
1010	Lu et al. (2022b)	Shenzhen Haichuan New Material Technology (Shenzhen, China)	GFRP	6.0	Epoxy-vinyl	SL (40%fu)+SWSSCE+Simulated seawater (IMMR)	60	120	NA	0.0	0.0
1011	Lu et al. (2023a)	Tuo Xin Aerospace Basalt Industrial Co., ltd.	BFRP	8.0	Epoxy	Control	28	0	NA	100.0	100.0
1012	Lu et al. (2023a)	Tuo Xin Aerospace Basalt Industrial Co., ltd.	BFRP	8.0	Epoxy	SWSSCE+Water (IMMR)	28	15	NA	83.4	99.1
1013	Lu et al. (2023a)	Tuo Xin Aerospace Basalt Industrial Co., ltd.	BFRP	8.0	Epoxy	SWSSCE+Water (IMMR)	28	30	NA	75.3	98.2
1014	Lu et al. (2023a)	Tuo Xin Aerospace Basalt Industrial Co., ltd.	BFRP	8.0	Epoxy	SWSSCE+Water (IMMR)	28	90	NA	63.3	100.5
1015	Lu et al. (2023a)	Tuo Xin Aerospace Basalt Industrial Co., ltd.	BFRP	8.0	Epoxy	SWSSCE+Water (IMMR)	28	180	NA	63.3	99.1
1016	Lu et al. (2023a)	Tuo Xin Aerospace Basalt Industrial Co., ltd.	BFRP	8.0	Epoxy	SWSSCE+Water (IMMR)	28	360	NA	55.9	92.2
1017	Lu et al. (2023a)	Tuo Xin Aerospace Basalt	BFRP	8.0	Epoxy	SWSSCE+Water (IMMR)	28	540	NA	60.9	96.8

		Industrial Co., ltd.									
1018	Lu et al. (2023a)	Tuo Xin Aerospace Basalt Industrial Co., ltd.	BFRP	8.0	Epoxy	SWSSCE+Water (IMMR)	40	15	NA	68.9	97.2
1019	Lu et al. (2023a)	Tuo Xin Aerospace Basalt Industrial Co., ltd.	BFRP	8.0	Epoxy	SWSSCE+Water (IMMR)	40	30	NA	61.7	98.2
1020	Lu et al. (2023a)	Tuo Xin Aerospace Basalt Industrial Co., ltd.	BFRP	8.0	Epoxy	SWSSCE+Water (IMMR)	40	90	NA	52.7	98.2
1021	Lu et al. (2023a)	Tuo Xin Aerospace Basalt Industrial Co., ltd.	BFRP	8.0	Epoxy	SWSSCE+Water (IMMR)	40	180	NA	51.8	98.2
1022	Lu et al. (2023a)	Tuo Xin Aerospace Basalt Industrial Co., ltd.	BFRP	8.0	Epoxy	SWSSCE+Water (IMMR)	40	360	NA	45.7	95.9
1023	Lu et al. (2023a)	Tuo Xin Aerospace Basalt Industrial Co., ltd.	BFRP	8.0	Epoxy	SWSSCE+Water (IMMR)	40	540	NA	46.8	93.1
1024	Lu et al. (2023a)	Tuo Xin Aerospace Basalt Industrial Co., ltd.	BFRP	8.0	Epoxy	SWSSCE+Water (IMMR)	60	15	NA	63.4	95.4
1025	Lu et al. (2023a)	Tuo Xin Aerospace Basalt Industrial Co., ltd.	BFRP	8.0	Epoxy	SWSSCE+Water (IMMR)	60	30	NA	57.4	97.3
1026	Lu et al. (2023a)	Tuo Xin Aerospace Basalt Industrial Co., ltd.	BFRP	8.0	Epoxy	SWSSCE+Water (IMMR)	60	90	NA	47.6	96.3
1027	Lu et al. (2023a)	Tuo Xin Aerospace Basalt Industrial Co., ltd.	BFRP	8.0	Epoxy	SWSSCE+Water (IMMR)	60	180	NA	39.9	93.1
1028	Lu et al. (2023a)	Tuo Xin Aerospace Basalt Industrial Co., ltd.	BFRP	8.0	Epoxy	SWSSCE+Water (IMMR)	60	360	NA	35.1	89.9
1029	Lu et al. (2023a)	Tuo Xin Aerospace Basalt Industrial Co., ltd.	BFRP	8.0	Epoxy	SWSSCE+Water (IMMR)	60	540	NA	25.6	52.3
1030	Lu et al. (2023a)	Tuo Xin Aerospace Basalt Industrial Co., ltd.	BFRP	8.0	Epoxy	SWSSCE+Simulated seawater (IMMR)	28	15	NA	83.5	101.8
1031	Lu et al. (2023a)	Tuo Xin Aerospace Basalt Industrial Co., ltd.	BFRP	8.0	Epoxy	SWSSCE+Simulated seawater (IMMR)	28	30	NA	72.9	105.0
1032	Lu et al. (2023a)	Tuo Xin Aerospace Basalt Industrial Co., ltd.	BFRP	8.0	Epoxy	SWSSCE+Simulated seawater (IMMR)	28	90	NA	66.5	98.6
1033	Lu et al. (2023a)	Tuo Xin Aerospace Basalt Industrial Co., ltd.	BFRP	8.0	Epoxy	SWSSCE+Simulated seawater (IMMR)	28	180	NA	66.5	96.3
1034	Lu et al. (2023a)	Tuo Xin Aerospace Basalt Industrial Co., ltd.	BFRP	8.0	Epoxy	SWSSCE+Simulated seawater (IMMR)	28	360	NA	63.6	92.7
1035	Lu et al. (2023a)	Tuo Xin Aerospace Basalt Industrial Co., ltd.	BFRP	8.0	Epoxy	SWSSCE+Simulated seawater (IMMR)	28	540	NA	63.1	95.0
1036	Lu et al. (2023a)	Tuo Xin Aerospace Basalt Industrial Co., ltd.	BFRP	8.0	Epoxy	SWSSCE+Simulated seawater (IMMR)	40	15	NA	69.1	100.5
1037	Lu et al. (2023a)	Tuo Xin Aerospace Basalt Industrial Co., ltd.	BFRP	8.0	Epoxy	SWSSCE+Simulated seawater (IMMR)	40	30	NA	70.8	101.8
1038	Lu et al. (2023a)	Tuo Xin Aerospace Basalt Industrial Co., ltd.	BFRP	8.0	Epoxy	SWSSCE+Simulated seawater (IMMR)	40	90	NA	58.5	105.5
1039	Lu et al. (2023a)	Tuo Xin Aerospace Basalt Industrial Co., ltd.	BFRP	8.0	Epoxy	SWSSCE+Simulated seawater (IMMR)	40	180	NA	56.8	92.7
1040	Lu et al. (2023a)	Tuo Xin Aerospace Basalt	BFRP	8.0	Epoxy	SWSSCE+Simulated seawater	40	360	NA	54.7	93.1

		Industrial Co., ltd.				(IMMR)					
1041	Lu et al. (2023a)	Tuo Xin Aerospace Basalt Industrial Co., ltd.	BFRP	8.0	Epoxy	SWSSCE+Simulated seawater (IMMR)	40	540	NA	56.4	101.4
1042	Lu et al. (2023a)	Tuo Xin Aerospace Basalt Industrial Co., ltd.	BFRP	8.0	Epoxy	SWSSCE+Simulated seawater (IMMR)	60	15	NA	66.5	98.6
1043	Lu et al. (2023a)	Tuo Xin Aerospace Basalt Industrial Co., ltd.	BFRP	8.0	Epoxy	SWSSCE+Simulated seawater (IMMR)	60	30	NA	63.1	93.6
1044	Lu et al. (2023a)	Tuo Xin Aerospace Basalt Industrial Co., ltd.	BFRP	8.0	Epoxy	SWSSCE+Simulated seawater (IMMR)	60	90	NA	55.1	94.0
1045	Lu et al. (2023a)	Tuo Xin Aerospace Basalt Industrial Co., ltd.	BFRP	8.0	Epoxy	SWSSCE+Simulated seawater (IMMR)	60	180	NA	50.4	93.1
1046	Lu et al. (2023a)	Tuo Xin Aerospace Basalt Industrial Co., ltd.	BFRP	8.0	Epoxy	SWSSCE+Simulated seawater (IMMR)	60	360	NA	37.7	86.2
1047	Lu et al. (2023a)	Tuo Xin Aerospace Basalt Industrial Co., ltd.	BFRP	8.0	Epoxy	SWSSCE+Simulated seawater (IMMR)	60	540	NA	35.6	77.5
1048	Lu et al. (2023b)	Nanjing Fenghui Composite Material Co. Ltd (China)	GFRP	11.2	Vinylester	Control	25	0	3	100.0	100.0
1049	Lu et al. (2023b)	Nanjing Fenghui Composite Material Co. Ltd (China)	GFRP	11.2	Vinylester	Alkaline solution (IMMR)	25	45	3	84.8	98.6
1050	Lu et al. (2023b)	Nanjing Fenghui Composite Material Co. Ltd (China)	GFRP	11.2	Vinylester	Alkaline solution (IMMR)	25	90	3	80.8	103.9
1051	Lu et al. (2023b)	Nanjing Fenghui Composite Material Co. Ltd (China)	GFRP	11.2	Vinylester	Alkaline solution (IMMR)	25	135	3	76.7	100.1
1052	Lu et al. (2023b)	Nanjing Fenghui Composite Material Co. Ltd (China)	GFRP	11.2	Vinylester	Alkaline solution (IMMR)	25	180	3	70.0	95.8
1053	Lu et al. (2023b)	Nanjing Fenghui Composite Material Co. Ltd (China)	GFRP	11.2	Vinylester	Saline solution (IMMR)	25	45	3	92.2	98.9
1054	Lu et al. (2023b)	Nanjing Fenghui Composite Material Co. Ltd (China)	GFRP	11.2	Vinylester	Saline solution (IMMR)	25	90	3	90.9	100.0
1055	Lu et al. (2023b)	Nanjing Fenghui Composite Material Co. Ltd (China)	GFRP	11.2	Vinylester	Saline solution (IMMR)	25	135	3	85.0	100.6
1056	Lu et al. (2023b)	Nanjing Fenghui Composite Material Co. Ltd (China)	GFRP	11.2	Vinylester	Saline solution (IMMR)	25	180	3	79.7	102.3
1057	Lu et al. (2023b)	Nanjing Fenghui Composite Material Co. Ltd (China)	GFRP	11.2	Vinylester	NCE	15.6	366	3	97.8	NA
1058	Lu et al. (2023b)	Nanjing Fenghui Composite Material Co. Ltd (China)	GFRP	11.2	Vinylester	SL (15-20%fu)+NCE	15.6	366	6	92.8	NA
1059	Lu et al. (2023b)	Nanjing Fenghui Composite Material Co. Ltd (China)	GFRP	11.2	Vinylester	SL (15-20%fu)+NCE+Saline solution (WD)	15.6	366	9	90.7	NA
1060	Micelli and Nanni (2004)	NA	GFRP	6.4	Polyester	Control	22	0	5	100.0	100.0
1061	Micelli and Nanni (2004)	NA	GFRP	6.4	Polyester	Alkaline solution (IMMR)	60	21	3	69.6	104.0
1062	Micelli and Nanni (2004)	NA	GFRP	6.4	Polyester	Alkaline solution (IMMR)	60	42	3	59.4	101.6
1063	Micelli and Nanni	NA	GFRP	6.4	Polyester	FT+HT+RH+UV	-18-4/16-49	NA	4	93.4	91.6

	(2004)										
1064	Micelli and Nanni (2004)	NA	CFRP	8.3	Modified epoxy	Control	22	0	4	100.0	100.0
1065	Micelli and Nanni (2004)	NA	CFRP	8.3	Modified epoxy	Alkaline solution (IMMR)	60	21	3	99.3	97.9
1066	Micelli and Nanni (2004)	NA	CFRP	8.3	Modified epoxy	Alkaline solution (IMMR)	60	42	3	92.0	98.8
1067	Micelli and Nanni (2004)	NA	CFRP	8.3	Modified epoxy	FT+HT+RH+UV	-18-4/16-49	NA	4	101.2	97.7
1068	Micelli and Nanni (2004)	NA	CFRP	8.0	Modified epoxy	Control	22	0	4	100.0	100.0
1069	Micelli and Nanni (2004)	NA	CFRP	8.0	Modified epoxy	FT+HT+RH+UV	-18-4/16-49	NA	4	95.3	103.8
1070	Micelli and Nanni (2004)	NA	CFRP	7.9	Modified epoxy	Control	22	0	4	100.0	100.0
1071	Micelli and Nanni (2004)	NA	CFRP	7.9	Modified epoxy	Alkaline solution (IMMR)	60	21	3	100.3	103.7
1072	Micelli and Nanni (2004)	NA	CFRP	7.9	Modified epoxy	Alkaline solution (IMMR)	60	42	3	100.2	107.5
1073	Micelli and Nanni (2004)	NA	CFRP	7.9	Modified epoxy	FT+HT+RH+UV	-18-4/16-49	NA	4	99.7	95.7
1074	Morales et al. (2021)	NA	GFRP	9.5	Vinylester	Control	25	0	5	100.0	100.0
1075	Morales et al. (2021)	NA	GFRP	9.5	Vinylester	SWCE 1+Seawater (IMMR)	60	30	3	93.0	102.5
1076	Morales et al. (2021)	NA	GFRP	9.5	Vinylester	SWCE 1+Seawater (IMMR)	60	180	3	82.6	98.3
1077	Morales et al. (2021)	NA	GFRP	9.5	Vinylester	SWCE 1+Seawater (IMMR)	60	360	3	74.9	95.9
1078	Morales et al. (2021)	NA	GFRP	9.5	Vinylester	SWCE 1+Seawater (IMMR)	60	720	3	73.8	95.0
1079	Morales et al. (2021)	NA	GFRP	9.5	Vinylester	SWCE 2+Seawater (IMMR)	60	30	3	79.4	98.8
1080	Morales et al. (2021)	NA	GFRP	9.5	Vinylester	SWCE 2+Seawater (IMMR)	60	180	3	75.4	99.0
1081	Morales et al. (2021)	NA	GFRP	9.5	Vinylester	SWCE 2+Seawater (IMMR)	60	360	3	65.6	93.2
1082	Morales et al. (2021)	NA	GFRP	9.5	Vinylester	SWCE 2+Seawater (IMMR)	60	720	3	69.1	101.4
1083	Mukherjee and Arwikar (2005)	NA	GFRP	9.5	Vinylester	Control	NA	0	NA	100.0	NA
1084	Mukherjee and Arwikar (2005)	NA	GFRP	9.5	Vinylester	Reference	RT	720	NA	91.4	NA
1085	Mukherjee and Arwikar (2005)	NA	GFRP	9.5	Vinylester	Water (IMMR)	60	30	NA	68.0	NA
1086	Mukherjee and	NA	GFRP	9.5	Vinylester	Water (IMMR)	60	90	NA	56.4	NA

	Arwikar (2005)										
1087	Mukherjee and Arwikar (2005)	NA	GFRP	9.5	Vinylester	Water (IMMR)	60	180	NA	46.3	NA
1088	Mukherjee and Arwikar (2005)	NA	GFRP	9.5	Vinylester	Water (IMMR)	60	270	NA	42.3	NA
1089	Mukherjee and Arwikar (2005)	NA	GFRP	9.5	Vinylester	Pre-cracks+SL (20%Mu)+NCE+Water (IMMR)	60	90	NA	58.0	NA
1090	Mukherjee and Arwikar (2005)	NA	GFRP	9.5	Vinylester	Pre-cracks+SL (20%Mu)+NCE+Water (IMMR)	60	180	NA	44.3	NA
1091	Mukherjee and Arwikar (2005)	NA	GFRP	9.5	Vinylester	Pre-cracks+SL (20%Mu)+NCE+Water (IMMR)	60	360	NA	35.0	NA
1092	Nassar et al. (2022)	NA	GFRP	6.4, 9.4	Vinylester	Control	NA	0	6	100.0	NA
1093	Nassar et al. (2022)	NA	GFRP	6.4, 9.4	Vinylester	Alkaline solution (IMMR)	60	14	6	70.8	NA
1094	Nassar et al. (2022)	NA	GFRP	6.4, 9.4	Vinylester	Alkaline solution (IMMR)	60	28	6	65.8	NA
1095	Nassar et al. (2022)	NA	GFRP	6.4, 9.4	Vinylester	Alkaline solution (IMMR)	60	42	6	61.8	NA
1096	Nassar et al. (2022)	NA	GFRP	6.4, 9.4	Vinylester	Alkaline solution (WD)	60	14	6	75.1	NA
1097	Nassar et al. (2022)	NA	GFRP	6.4, 9.4	Vinylester	Alkaline solution (WD)	60	28	6	66.1	NA
1098	Nassar et al. (2022)	NA	GFRP	6.4, 9.4	Vinylester	Alkaline solution (WD)	60	42	6	62.8	NA
1099	Nassar et al. (2022)	NA	GFRP	9.4	Vinylester	Control	NA	0	6	100.0	NA
1100	Nassar et al. (2022)	NA	GFRP	9.4	Vinylester	Alkaline solution (IMMR)	60	14	6	88.5	NA
1101	Nassar et al. (2022)	NA	GFRP	9.4	Vinylester	Alkaline solution (IMMR)	60	28	6	80.3	NA
1102	Nassar et al. (2022)	NA	GFRP	9.4	Vinylester	Alkaline solution (IMMR)	60	42	6	70.8	NA
1103	Nassar et al. (2022)	NA	GFRP	9.4	Vinylester	Alkaline solution (WD)	60	14	6	90.2	NA
1104	Nassar et al. (2022)	NA	GFRP	9.4	Vinylester	Alkaline solution (WD)	60	28	6	79.1	NA
1105	Nassar et al. (2022)	NA	GFRP	9.4	Vinylester	Alkaline solution (WD)	60	42	6	74.5	NA
1106	Nassar et al. (2022)	NA	GFRP	8.0	Polyester	Control	NA	0	6	100.0	NA
1107	Nassar et al. (2022)	NA	GFRP	8.0	Polyester	Alkaline solution (IMMR)	60	14	6	63.7	NA
1108	Nassar et al. (2022)	NA	GFRP	8.0	Polyester	Alkaline solution (IMMR)	60	28	6	65.2	NA
1109	Nassar et al.	NA	GFRP	8.0	Polyester	Alkaline solution (WD)	60	14	6	76.8	NA

	(2022)										
1110	Nassar et al. (2022)	NA	GFRP	8.0	Polyester	Alkaline solution (WD)	60	28	6	59.8	NA
1111	Nassar et al. (2022)	NA	GFRP	9.4	Polyester	Control	NA	0	6	100.0	NA
1112	Nassar et al. (2022)	NA	GFRP	9.4	Polyester	Alkaline solution (IMMR)	60	28	6	94.9	NA
1113	Nassar et al. (2022)	NA	GFRP	9.4	Polyester	Alkaline solution (WD)	60	28	6	97.7	NA
1114	Nkurunziza et al. (2005)	NA	GFRP	9.5	Vinylester	Control	NA	0	5	100.0	100.0
1115	Nkurunziza et al. (2005)	NA	GFRP	9.5	Vinylester	SL (25%fu)+Water (IMMR)	NA	417	5	92.7	102.3
1116	Nkurunziza et al. (2005)	NA	GFRP	9.5	Vinylester	SL (38%fu)+Water (IMMR)	NA	417	5	96.2	100.5
1117	Nkurunziza et al. (2005)	NA	GFRP	9.5	Vinylester	SL (29%fu)+Alkaline solution (IMMR)	NA	417	5	84.3	103.3
1118	Nkurunziza et al. (2005)	NA	GFRP	9.5	Vinylester	SL (38%fu)+Alkaline solution (IMMR)	NA	417	5	65.2	101.3
1119	Park et al. (2007)	Hughes Brothers Company (Seward, NE, USA)	GFRP	12.7	Vinylester	Control	23	0	NA	100.0	NA
1120	Park et al. (2007)	Hughes Brothers Company (Seward, NE, USA)	GFRP	12.7	Vinylester	Acid solution (IMMR)	20	50	NA	96.0	NA
1121	Park et al. (2007)	Hughes Brothers Company (Seward, NE, USA)	GFRP	12.7	Vinylester	Acid solution (IMMR)	20	100	NA	95.0	NA
1122	Park et al. (2007)	Hughes Brothers Company (Seward, NE, USA)	GFRP	12.7	Vinylester	Saline solution 1 (IMMR)	20	50	NA	99.0	NA
1123	Park et al. (2007)	Hughes Brothers Company (Seward, NE, USA)	GFRP	12.7	Vinylester	Saline solution 2 (IMMR)	20	50	NA	98.0	NA
1124	Quagliarini et al. (2016)	NA	BFRP	8.0	Vinylester	Control	NA	0	3	100.0	NA
1125	Quagliarini et al. (2016)	NA	BFRP	8.0	Vinylester	Water (IMMR)	60	21	3	96.8	NA
1126	Quagliarini et al. (2016)	NA	BFRP	8.0	Vinylester	Saline solution (IMMR)	60	21	3	91.8	NA
1127	Rifai et al. (2020)	NA	BFRP	11.0	Epoxy	Control	NA	0	3	100.0	NA
1128	Rifai et al. (2020)	NA	BFRP	11.0	Epoxy	Alkaline solution (IMMR)	20	90	3	95.7	NA
1129	Rifai et al. (2020)	NA	BFRP	11.0	Epoxy	Alkaline solution (IMMR)	20	180	3	97.4	NA
1130	Rifai et al. (2020)	NA	BFRP	11.0	Epoxy	Alkaline solution (IMMR)	20	270	3	91.5	NA
1131	Rifai et al. (2020)	NA	BFRP	11.0	Epoxy	Alkaline solution (IMMR)	40	90	3	98.2	NA
1132	Rifai et al. (2020)	NA	BFRP	11.0	Epoxy	Alkaline solution (IMMR)	40	180	3	95.0	NA
1133	Rifai et al. (2020)	NA	BFRP	11.0	Epoxy	Alkaline solution (IMMR)	40	270	3	83.0	NA
1134	Rifai et al. (2020)	NA	BFRP	11.0	Epoxy	Alkaline solution (IMMR)	60	90	3	95.8	NA
1135	Rifai et al. (2020)	NA	BFRP	11.0	Epoxy	Alkaline solution (IMMR)	60	180	3	87.2	NA
1136	Rifai et al. (2020)	NA	BFRP	11.0	Epoxy	Alkaline solution (IMMR)	60	270	3	71.5	NA
1137	Rifai et al. (2020)	NA	BFRP	11.0	Epoxy	NCE+Water (IMMR)	20	90	3	94.4	NA

1138	Rifai et al. (2020)	NA	BFRP	11.0	Epoxy	NCE+Water (IMMR)	20	180	3	93.6	NA
1139	Rifai et al. (2020)	NA	BFRP	11.0	Epoxy	NCE+Water (IMMR)	20	270	3	88.0	NA
1140	Rifai et al. (2020)	NA	BFRP	11.0	Epoxy	NCE+Water (IMMR)	40	90	3	93.8	NA
1141	Rifai et al. (2020)	NA	BFRP	11.0	Epoxy	NCE+Water (IMMR)	40	180	3	90.2	NA
1142	Rifai et al. (2020)	NA	BFRP	11.0	Epoxy	NCE+Water (IMMR)	40	270	3	88.4	NA
1143	Rifai et al. (2020)	NA	BFRP	11.0	Epoxy	NCE+Water (IMMR)	60	90	3	90.7	NA
1144	Rifai et al. (2020)	NA	BFRP	11.0	Epoxy	NCE+Water (IMMR)	60	180	3	90.4	NA
1145	Rifai et al. (2020)	NA	BFRP	11.0	Epoxy	NCE+Water (IMMR)	60	270	3	85.1	NA
1146	Robert et al. (2009)	Pultrall Inc. (Thetford Mines, QC, Canada)	GFRP	12.7	Vinylester	Control	23	0	5	100.0	100.0
1147	Robert et al. (2009)	Pultrall Inc. (Thetford Mines, QC, Canada)	GFRP	12.7	Vinylester	NCE+Water (IMMR)	23	60	5	95.6	98.1
1148	Robert et al. (2009)	Pultrall Inc. (Thetford Mines, QC, Canada)	GFRP	12.7	Vinylester	NCE+Water (IMMR)	23	120	5	89.1	102.2
1149	Robert et al. (2009)	Pultrall Inc. (Thetford Mines, QC, Canada)	GFRP	12.7	Vinylester	NCE+Water (IMMR)	23	180	5	91.0	104.6
1150	Robert et al. (2009)	Pultrall Inc. (Thetford Mines, QC, Canada)	GFRP	12.7	Vinylester	NCE+Water (IMMR)	23	240	5	90.6	99.5
1151	Robert et al. (2009)	Pultrall Inc. (Thetford Mines, QC, Canada)	GFRP	12.7	Vinylester	NCE+Water (IMMR)	40	60	5	95.8	106.0
1152	Robert et al. (2009)	Pultrall Inc. (Thetford Mines, QC, Canada)	GFRP	12.7	Vinylester	NCE+Water (IMMR)	40	120	5	84.5	99.5
1153	Robert et al. (2009)	Pultrall Inc. (Thetford Mines, QC, Canada)	GFRP	12.7	Vinylester	NCE+Water (IMMR)	40	180	5	89.8	101.1
1154	Robert et al. (2009)	Pultrall Inc. (Thetford Mines, QC, Canada)	GFRP	12.7	Vinylester	NCE+Water (IMMR)	40	240	5	89.8	102.2
1155	Robert et al. (2009)	Pultrall Inc. (Thetford Mines, QC, Canada)	GFRP	12.7	Vinylester	NCE+Water (IMMR)	50	60	5	97.3	103.0
1156	Robert et al. (2009)	Pultrall Inc. (Thetford Mines, QC, Canada)	GFRP	12.7	Vinylester	NCE+Water (IMMR)	50	120	5	91.4	99.5
1157	Robert et al. (2009)	Pultrall Inc. (Thetford Mines, QC, Canada)	GFRP	12.7	Vinylester	NCE+Water (IMMR)	50	180	5	90.2	103.0
1158	Robert et al. (2009)	Pultrall Inc. (Thetford Mines, QC, Canada)	GFRP	12.7	Vinylester	NCE+Water (IMMR)	50	240	5	84.4	102.2
1159	Robert and Benmokrane (2013)	NA	GFRP	12.7	Vinylester	Control	23	0	6	100.0	100.0
1160	Robert and Benmokrane (2013)	NA	GFRP	12.7	Vinylester	NCE+Saline solution (IMMR)	23	60	6	99.1	106.7
1161	Robert and Benmokrane (2013)	NA	GFRP	12.7	Vinylester	NCE+Saline solution (IMMR)	23	120	6	98.0	97.8
1162	Robert and Benmokrane (2013)	NA	GFRP	12.7	Vinylester	NCE+Saline solution (IMMR)	23	210	6	96.8	106.7

1163	Robert and Benmokrane (2013)	NA	GFRP	12.7	Vinylester	NCE+Saline solution (IMMR)	23	365	6	92.1	104.4
1164	Robert and Benmokrane (2013)	NA	GFRP	12.7	Vinylester	NCE+Saline solution (IMMR)	40	60	6	98.6	104.4
1165	Robert and Benmokrane (2013)	NA	GFRP	12.7	Vinylester	NCE+Saline solution (IMMR)	40	120	6	96.4	97.8
1166	Robert and Benmokrane (2013)	NA	GFRP	12.7	Vinylester	NCE+Saline solution (IMMR)	40	210	6	94.5	104.4
1167	Robert and Benmokrane (2013)	NA	GFRP	12.7	Vinylester	NCE+Saline solution (IMMR)	40	365	6	90.4	108.9
1168	Robert and Benmokrane (2013)	NA	GFRP	12.7	Vinylester	NCE+Saline solution (IMMR)	50	60	6	97.0	106.7
1169	Robert and Benmokrane (2013)	NA	GFRP	12.7	Vinylester	NCE+Saline solution (IMMR)	50	120	6	95.6	100.0
1170	Robert and Benmokrane (2013)	NA	GFRP	12.7	Vinylester	NCE+Saline solution (IMMR)	50	210	6	94.4	106.7
1171	Robert and Benmokrane (2013)	NA	GFRP	12.7	Vinylester	NCE+Saline solution (IMMR)	50	365	6	89.1	111.1
1172	Robert and Benmokrane (2013)	NA	GFRP	12.7	Vinylester	NCE+Saline solution (IMMR)	70	120	6	94.4	102.2
1173	Rolland et al. (2021)	Pultrall Inc. (Thetford Mines, QC, Canada)	GFRP	12.7	Vinylester	Control	20	0	5	100.0	100.0
1174	Rolland et al. (2021)	Pultrall Inc. (Thetford Mines, QC, Canada)	GFRP	12.7	Vinylester	Alkaline solution (IMMR)	20	120	5	92.8	100.8
1175	Rolland et al. (2021)	Pultrall Inc. (Thetford Mines, QC, Canada)	GFRP	12.7	Vinylester	Alkaline solution (IMMR)	20	240	5	86.7	101.3
1176	Rolland et al. (2021)	Pultrall Inc. (Thetford Mines, QC, Canada)	GFRP	12.7	Vinylester	Alkaline solution (IMMR)	40	120	5	78.4	98.9
1177	Rolland et al. (2021)	Pultrall Inc. (Thetford Mines, QC, Canada)	GFRP	12.7	Vinylester	Alkaline solution (IMMR)	40	240	5	68.1	97.0
1178	Rolland et al. (2021)	Pultrall Inc. (Thetford Mines, QC, Canada)	GFRP	12.7	Vinylester	Alkaline solution (IMMR)	60	120	5	65.6	100.9
1179	Rolland et al. (2021)	Pultrall Inc. (Thetford Mines, QC, Canada)	GFRP	12.7	Vinylester	Alkaline solution (IMMR)	60	240	5	57.7	92.8
1180	Ruiz Emparanza et al. (2022)	NA	GFRP	10.0	Vinylester	Control	23	0	5	100.0	100.0

1181	Ruiz Emparanza et al. (2022)	NA	GFRP	10.0	Vinylester	Seawater (IMMR)	23	60	3	98.5	102.2
1182	Ruiz Emparanza et al. (2022)	NA	GFRP	10.0	Vinylester	Seawater (IMMR)	23	120	3	98.5	93.9
1183	Ruiz Emparanza et al. (2022)	NA	GFRP	10.0	Vinylester	Seawater (IMMR)	23	210	3	94.5	101.7
1184	Ruiz Emparanza et al. (2022)	NA	GFRP	10.0	Vinylester	Seawater (IMMR)	23	365	3	92.5	99.4
1185	Ruiz Emparanza et al. (2022)	NA	GFRP	10.0	Vinylester	Seawater (IMMR)	40	60	3	106.0	105.0
1186	Ruiz Emparanza et al. (2022)	NA	GFRP	10.0	Vinylester	Seawater (IMMR)	40	120	3	98.5	102.8
1187	Ruiz Emparanza et al. (2022)	NA	GFRP	10.0	Vinylester	Seawater (IMMR)	40	210	3	89.5	96.1
1188	Ruiz Emparanza et al. (2022)	NA	GFRP	10.0	Vinylester	Seawater (IMMR)	40	365	3	79.0	103.3
1189	Ruiz Emparanza et al. (2022)	NA	GFRP	10.0	Vinylester	Seawater (IMMR)	60	60	3	70.0	106.1
1190	Ruiz Emparanza et al. (2022)	NA	GFRP	10.0	Vinylester	Seawater (IMMR)	60	120	3	60.0	105.6
1191	Ruiz Emparanza et al. (2022)	NA	GFRP	10.0	Vinylester	Seawater (IMMR)	60	210	3	61.5	100.0
1192	Ruiz Emparanza et al. (2022)	NA	GFRP	10.0	Vinylester	Seawater (IMMR)	60	365	3	55.5	97.8
1193	Ruiz Emparanza et al. (2022)	NA	GFRP	10.0	Vinylester	Control	23	0	5	100.0	100.0
1194	Ruiz Emparanza et al. (2022)	NA	GFRP	10.0	Vinylester	Seawater (IMMR)	23	60	3	105.0	101.1
1195	Ruiz Emparanza et al. (2022)	NA	GFRP	10.0	Vinylester	Seawater (IMMR)	23	120	3	102.0	100.0
1196	Ruiz Emparanza et al. (2022)	NA	GFRP	10.0	Vinylester	Seawater (IMMR)	23	210	3	94.0	90.6
1197	Ruiz Emparanza et al. (2022)	NA	GFRP	10.0	Vinylester	Seawater (IMMR)	23	365	3	97.0	95.6
1198	Ruiz Emparanza et al. (2022)	NA	GFRP	10.0	Vinylester	Seawater (IMMR)	40	60	3	101.0	103.3
1199	Ruiz Emparanza et al. (2022)	NA	GFRP	10.0	Vinylester	Seawater (IMMR)	40	120	3	100.5	101.7
1200	Ruiz Emparanza et al. (2022)	NA	GFRP	10.0	Vinylester	Seawater (IMMR)	40	210	3	98.0	98.9
1201	Ruiz Emparanza et al. (2022)	NA	GFRP	10.0	Vinylester	Seawater (IMMR)	40	365	3	92.5	95.0
1202	Ruiz Emparanza et al. (2022)	NA	GFRP	10.0	Vinylester	Seawater (IMMR)	60	60	3	89.5	101.7
1203	Ruiz Emparanza et al. (2022)	NA	GFRP	10.0	Vinylester	Seawater (IMMR)	60	120	3	95.0	100.6

1204	Ruiz Emparanza et al. (2022)	NA	GFRP	10.0	Vinylester	Seawater (IMMR)	60	210	3	77.0	100.0
1205	Ruiz Emparanza et al. (2022)	NA	GFRP	10.0	Vinylester	Seawater (IMMR)	60	365	3	74.5	93.3
1206	Ruiz Emparanza et al. (2022)	NA	GFRP	10.0	Vinylester	Control	23	0	5	100.0	100.0
1207	Ruiz Emparanza et al. (2022)	NA	GFRP	10.0	Vinylester	Seawater (IMMR)	23	60	3	102.5	101.1
1208	Ruiz Emparanza et al. (2022)	NA	GFRP	10.0	Vinylester	Seawater (IMMR)	23	120	3	101.0	102.2
1209	Ruiz Emparanza et al. (2022)	NA	GFRP	10.0	Vinylester	Seawater (IMMR)	23	210	3	98.0	96.7
1210	Ruiz Emparanza et al. (2022)	NA	GFRP	10.0	Vinylester	Seawater (IMMR)	23	365	3	93.5	96.1
1211	Ruiz Emparanza et al. (2022)	NA	GFRP	10.0	Vinylester	Seawater (IMMR)	40	60	3	101.0	102.2
1212	Ruiz Emparanza et al. (2022)	NA	GFRP	10.0	Vinylester	Seawater (IMMR)	40	120	3	99.0	109.4
1213	Ruiz Emparanza et al. (2022)	NA	GFRP	10.0	Vinylester	Seawater (IMMR)	40	210	3	97.0	95.0
1214	Ruiz Emparanza et al. (2022)	NA	GFRP	10.0	Vinylester	Seawater (IMMR)	40	365	3	94.5	95.6
1215	Ruiz Emparanza et al. (2022)	NA	GFRP	10.0	Vinylester	Seawater (IMMR)	60	60	3	97.5	103.9
1216	Ruiz Emparanza et al. (2022)	NA	GFRP	10.0	Vinylester	Seawater (IMMR)	60	120	3	85.5	113.9
1217	Ruiz Emparanza et al. (2022)	NA	GFRP	10.0	Vinylester	Seawater (IMMR)	60	210	3	79.0	96.7
1218	Ruiz Emparanza et al. (2022)	NA	GFRP	10.0	Vinylester	Seawater (IMMR)	60	365	3	78.5	99.4
1219	Ruiz Emparanza et al. (2022)	NA	GFRP	10.0	Vinylester	Control	23	0	5	100.0	100.0
1220	Ruiz Emparanza et al. (2022)	NA	GFRP	10.0	Vinylester	Seawater (IMMR)	23	60	3	104.5	103.3
1221	Ruiz Emparanza et al. (2022)	NA	GFRP	10.0	Vinylester	Seawater (IMMR)	23	120	3	102.5	101.7
1222	Ruiz Emparanza et al. (2022)	NA	GFRP	10.0	Vinylester	Seawater (IMMR)	23	210	3	98.5	96.1
1223	Ruiz Emparanza et al. (2022)	NA	GFRP	10.0	Vinylester	Seawater (IMMR)	23	365	3	91.0	96.1
1224	Ruiz Emparanza et al. (2022)	NA	GFRP	10.0	Vinylester	Seawater (IMMR)	60	60	3	77.5	96.7
1225	Ruiz Emparanza et al. (2022)	NA	GFRP	10.0	Vinylester	Seawater (IMMR)	60	120	3	71.5	95.6
1226	Ruiz Emparanza et al. (2022)	NA	GFRP	10.0	Vinylester	Seawater (IMMR)	60	210	3	66.5	94.4

1227	Ruiz Emparanza et al. (2022)	NA	GFRP	10.0	Vinylester	Seawater (IMMR)	60	365	3	63.5	93.9
1228	Ruiz Emparanza et al. (2022)	NA	GFRP	10.0	Epoxy	Control	23	0	5	100.0	100.0
1229	Ruiz Emparanza et al. (2022)	NA	GFRP	10.0	Epoxy	Seawater (IMMR)	23	60	3	105.0	107.8
1230	Ruiz Emparanza et al. (2022)	NA	GFRP	10.0	Epoxy	Seawater (IMMR)	23	120	3	103.5	106.7
1231	Ruiz Emparanza et al. (2022)	NA	GFRP	10.0	Epoxy	Seawater (IMMR)	23	210	3	101.5	98.3
1232	Ruiz Emparanza et al. (2022)	NA	GFRP	10.0	Epoxy	Seawater (IMMR)	23	365	3	89.5	94.4
1233	Ruiz Emparanza et al. (2022)	NA	GFRP	10.0	Epoxy	Seawater (IMMR)	60	60	3	88.5	91.7
1234	Ruiz Emparanza et al. (2022)	NA	GFRP	10.0	Epoxy	Seawater (IMMR)	60	120	3	83.0	92.8
1235	Ruiz Emparanza et al. (2022)	NA	GFRP	10.0	Epoxy	Seawater (IMMR)	60	210	3	81.0	92.8
1236	Ruiz Emparanza et al. (2022)	NA	GFRP	10.0	Epoxy	Seawater (IMMR)	60	365	3	78.5	92.2
1237	Ruiz Emparanza et al. (2022)	NA	GFRP	10.0	Vinylester	Control	23	0	5	100.0	100.0
1238	Ruiz Emparanza et al. (2022)	NA	GFRP	10.0	Vinylester	Seawater (IMMR)	23	60	3	104.5	106.1
1239	Ruiz Emparanza et al. (2022)	NA	GFRP	10.0	Vinylester	Seawater (IMMR)	23	120	3	100.0	107.2
1240	Ruiz Emparanza et al. (2022)	NA	GFRP	10.0	Vinylester	Seawater (IMMR)	23	210	3	91.0	106.7
1241	Ruiz Emparanza et al. (2022)	NA	GFRP	10.0	Vinylester	Seawater (IMMR)	23	365	3	99.0	101.7
1242	Ruiz Emparanza et al. (2022)	NA	GFRP	10.0	Vinylester	Seawater (IMMR)	60	60	3	88.5	100.0
1243	Ruiz Emparanza et al. (2022)	NA	GFRP	10.0	Vinylester	Seawater (IMMR)	60	120	3	94.5	103.9
1244	Ruiz Emparanza et al. (2022)	NA	GFRP	10.0	Vinylester	Seawater (IMMR)	60	210	3	85.0	105.0
1245	Ruiz Emparanza et al. (2022)	NA	GFRP	10.0	Vinylester	Seawater (IMMR)	60	365	3	82.0	102.2
1246	Sen et al. (2002)	NA	GFRP	8.0	Vinylester	Control	NA	0	3	100.0	NA
1247	Sen et al. (2002)	NA	GFRP	8.0	Vinylester	Alkaline solution (IMMR)	NA	30	3	50.0	NA
1248	Sen et al. (2002)	NA	GFRP	8.0	Vinylester	Alkaline solution (IMMR)	NA	90	3	37.0	NA
1249	Sen et al. (2002)	NA	GFRP	8.0	Vinylester	Alkaline solution (IMMR)	NA	180	3	36.0	NA
1250	Sen et al. (2002)	NA	GFRP	8.0	Vinylester	Alkaline solution (IMMR)	NA	270	3	37.0	NA
1251	Sen et al. (2002)	NA	GFRP	8.0	Vinylester	SL (10%fu)+Alkaline solution (IMMR)	NA	30	3	40.0	NA
1252	Sen et al. (2002)	NA	GFRP	8.0	Vinylester	SL (10%fu)+Alkaline solution	NA	90	3	28.0	NA

1253	Sen et al. (2002)	NA	GFRP	8.0	Vinylester	SL (10%fu)+Alkaline solution (IMMR)	NA	180	3	31.0	NA
1254	Sen et al. (2002)	NA	GFRP	8.0	Vinylester	SL (10%fu)+Alkaline solution (IMMR)	NA	270	3	30.0	NA
1255	Sen et al. (2002)	NA	GFRP	8.0	Vinylester	SL (15%fu)+Alkaline solution (IMMR)	NA	180	3	8.0	NA
1256	Sen et al. (2002)	NA	GFRP	8.0	Vinylester	SL (15%fu)+Alkaline solution (IMMR)	NA	270	3	0.0	NA
1257	Sen et al. (2002)	NA	GFRP	8.0	Vinylester	SL (25%fu)+Alkaline solution (IMMR)	NA	30	3	0.0	NA
1258	Sen et al. (2002)	NA	GFRP	8.0	Vinylester	SL (25%fu)+Alkaline solution (IMMR)	NA	90	3	0.0	NA
1259	Serbescu et al. (2015)	MagmaTech Ltd. (U.K.)	BFRP	3.0	Epoxy	Control	20	0	5	100.0	NA
1260	Serbescu et al. (2015)	MagmaTech Ltd. (U.K.)	BFRP	3.0	Epoxy	Water (IMMR)	20	42	5	100.0	NA
1261	Serbescu et al. (2015)	MagmaTech Ltd. (U.K.)	BFRP	3.0	Epoxy	Water (IMMR)	60	8	3	84.6	NA
1262	Serbescu et al. (2015)	MagmaTech Ltd. (U.K.)	BFRP	3.0	Epoxy	Water (IMMR)	60	42	5	64.0	NA
1263	Serbescu et al. (2015)	MagmaTech Ltd. (U.K.)	BFRP	3.0	Epoxy	Alkaline solution 1 (IMMR)	20	42	5	92.0	NA
1264	Serbescu et al. (2015)	MagmaTech Ltd. (U.K.)	BFRP	3.0	Epoxy	Alkaline solution 1 (IMMR)	60	42	5	56.2	NA
1265	Serbescu et al. (2015)	MagmaTech Ltd. (U.K.)	BFRP	4.0	Vinylester	Control	20	0	5	100.0	100.0
1266	Serbescu et al. (2015)	MagmaTech Ltd. (U.K.)	BFRP	4.0	Vinylester	Alkaline solution 2 (IMMR)	60	4	5	99.0	111.8
1267	Serbescu et al. (2015)	MagmaTech Ltd. (U.K.)	BFRP	5.0	Vinylester	Control	20	0	5	100.0	100.0
1268	Serbescu et al. (2015)	MagmaTech Ltd. (U.K.)	BFRP	5.0	Vinylester	Alkaline solution 2 (IMMR)	60	4	5	87.3	107.9
1269	Serbescu et al. (2015)	MagmaTech Ltd. (U.K.)	BFRP	6.0	Vinylester	Control	20	0	9	100.0	100.0
1270	Serbescu et al. (2015)	MagmaTech Ltd. (U.K.)	BFRP	6.0	Vinylester	Alkaline solution 2 (IMMR)	20	4	5	93.3	NA
1271	Serbescu et al. (2015)	MagmaTech Ltd. (U.K.)	BFRP	6.0	Vinylester	Alkaline solution 2 (IMMR)	20	42	5	89.1	NA
1272	Serbescu et al. (2015)	MagmaTech Ltd. (U.K.)	BFRP	6.0	Vinylester	Alkaline solution 2 (IMMR)	20	208	5	92.8	NA
1273	Serbescu et al. (2015)	MagmaTech Ltd. (U.K.)	BFRP	6.0	Vinylester	Alkaline solution 2 (IMMR)	40	4	5	96.7	NA
1274	Serbescu et al. (2015)	MagmaTech Ltd. (U.K.)	BFRP	6.0	Vinylester	Alkaline solution 2 (IMMR)	40	42	5	87.0	NA
1275	Serbescu et al.	MagmaTech Ltd. (U.K.)	BFRP	6.0	Vinylester	Alkaline solution 2 (IMMR)	40	208	5	83.6	NA

	(2015)										
1276	Serbescu et al. (2015)	MagmaTech Ltd. (U.K.)	BFRP	6.0	Vinylester	Alkaline solution 2 (IMMR)	60	4	9	93.4	104.8
1277	Serbescu et al. (2015)	MagmaTech Ltd. (U.K.)	BFRP	6.0	Vinylester	Alkaline solution 2 (IMMR)	60	42	5	80.0	NA
1278	Serbescu et al. (2015)	MagmaTech Ltd. (U.K.)	BFRP	6.0	Vinylester	Alkaline solution 2 (IMMR)	60	208	5	68.8	NA
1279	Serbescu et al. (2015)	MagmaTech Ltd. (U.K.)	BFRP	7.0	Vinylester	Control	20	0	5	100.0	100.0
1280	Serbescu et al. (2015)	MagmaTech Ltd. (U.K.)	BFRP	7.0	Vinylester	Alkaline solution 2 (IMMR)	60	4	5	105.4	102.4
1281	Silva et al. (2016）	NA	CFRP	3.0	Epoxy	Control	23	0	5	100.0	100.0
1282	Silva et al. (2016）	NA	CFRP	3.0	Epoxy	Water (IMMR)	60	31	5	84.0	98.3
1283	Silva et al. (2016）	NA	CFRP	3.0	Epoxy	Water (IMMR)	60	125	5	81.8	93.4
1284	Silva et al. (2016）	NA	CFRP	3.0	Epoxy	Simulated seawater (IMMR)	60	31	5	88.4	99.4
1285	Silva et al. (2016）	NA	CFRP	3.0	Epoxy	Simulated seawater (IMMR)	60	125	5	80.1	93.4
1286	Silva et al. (2016）	NA	CFRP	3.0	Epoxy	UV+Water-spray	23/63	63	5	99.4	92.0
1287	Silva et al. (2016）	NA	CFRP	3.0	Epoxy	UV+Water-spray	23/63	125	5	93.4	95.1
1288	Silva et al. (2016）	NA	CFRP	3.0	Vinylester	Control	23	0	5	100.0	100.0
1289	Silva et al. (2016）	NA	CFRP	3.0	Vinylester	Water (IMMR)	60	31	5	95.2	101.7
1290	Silva et al. (2016）	NA	CFRP	3.0	Vinylester	Water (IMMR)	60	125	5	94.6	91.4
1291	Silva et al. (2016）	NA	CFRP	3.0	Vinylester	Simulated seawater (IMMR)	60	31	5	98.6	95.7
1292	Silva et al. (2016）	NA	CFRP	3.0	Vinylester	Simulated seawater (IMMR)	60	125	5	90.5	94.8
1293	Silva et al. (2016）	NA	CFRP	3.0	Vinylester	UV+Water-spray	23/63	63	5	98.0	91.4
1294	Silva et al. (2016）	NA	CFRP	3.0	Vinylester	UV+Water-spray	23/63	125	5	95.9	91.7
1295	Su et al. (2022)	Jiangsu Green Materials Vally New Material T&D Co., Ltd (Nanjing, China)	BFRP	12.0	Epoxy	Control	NA	0	3	100.0	NA
1296	Su et al. (2022)	Jiangsu Green Materials Vally New Material T&D	BFRP	12.0	Epoxy	Simulated seawater (IMMR)	55	21	3	74.3	NA

		Co., Ltd (Nanjing, China)								
1297	Su et al. (2022)	Jiangsu Green Materials Vally New Material T&D Co., Ltd (Nanjing, China)	BFRP	12.0	Epoxy	Simulated seawater (IMMR)	55	42	3	59.1	NA
1298	Su et al. (2022)	Jiangsu Green Materials Vally New Material T&D Co., Ltd (Nanjing, China)	BFRP	12.0	Epoxy	Simulated seawater (IMMR)	55	63	3	58.4	NA
1299	Sun et al. (2022)	Fei Boer New Material Technology Co. (Jiangsu, China)	GFRP	6.0	Epoxy	Control	NA	0	NA	100.0	NA
1300	Sun et al. (2022)	Fei Boer New Material Technology Co. (Jiangsu, China)	GFRP	6.0	Epoxy	Water (IMMR)	NA	120	NA	91.0	NA
1301	Sun et al. (2022)	Fei Boer New Material Technology Co. (Jiangsu, China)	GFRP	6.0	Epoxy	Saline solution 1 (IMMR)	NA	120	NA	94.7	NA
1302	Sun et al. (2022)	Fei Boer New Material Technology Co. (Jiangsu, China)	GFRP	6.0	Epoxy	Saline solution 2 (IMMR)	NA	120	NA	94.2	NA
1303	Sun et al. (2022)	Fei Boer New Material Technology Co. (Jiangsu, China)	GFRP	6.0	Epoxy	Saline solution 3 (IMMR)	NA	120	NA	96.4	NA
1304	Sun et al. (2023)	NA	GFRP	6.0	Epoxy	Control	NA	0	5	100.0	NA
1305	Sun et al. (2023)	NA	GFRP	6.0	Epoxy	Alkaline solution (IMMR)	NA	300	5	98.8	NA
1306	Sun et al. (2023)	NA	GFRP	6.0	Epoxy	Alkaline solution (IMMR)	NA	300	5	98.1	NA
1307	Sun et al. (2023)	NA	GFRP	6.0	Epoxy	Alkaline solution (IMMR)	NA	300	5	97.2	NA
1308	Sun et al. (2023)	NA	GFRP	6.0	Epoxy	Alkaline solution (IMMR)	NA	300	5	90.1	NA
1309	Sun et al. (2023)	NA	GFRP	6.0	Epoxy	Alkaline solution (IMMR)	NA	300	5	89.0	NA
1310	Sun et al. (2023)	NA	GFRP	6.0	Epoxy	Alkaline solution (IMMR)	NA	300	5	86.5	NA
1311	Tannous and Saadatmanesh (1998)	NA	GFRP	10.0	Polyester	Control	25	0	3	100.0	NA
1312	Tannous and Saadatmanesh (1998)	NA	GFRP	10.0	Polyester	Water (IMMR)	25	180	3	93.7	NA
1313	Tannous and Saadatmanesh (1998)	NA	GFRP	10.0	Polyester	Alkaline solution (IMMR)	25	180	3	75.0	NA
1314	Tannous and Saadatmanesh (1998)	NA	GFRP	10.0	Polyester	Alkaline solution (IMMR)	60	180	3	71.4	NA
1315	Tannous and Saadatmanesh (1998)	NA	GFRP	10.0	Polyester	Acid solution (IMMR)	25	180	3	92.9	NA
1316	Tannous and Saadatmanesh	NA	GFRP	10.0	Polyester	Saline solution 1 (IMMR)	25	180	3	89.1	NA

	(1998)										
1317	Tannous and Saadatmanesh (1998)	NA	GFRP	10.0	Polyester	Saline solution 2 (IMMR)	25	180	3	73.3	NA
1318	Tannous and Saadatmanesh (1998)	NA	GFRP	10.0	Polyester	Saline solution 3 (IMMR)	25	180	3	71.2	NA
1319	Tannous and Saadatmanesh (1998)	NA	GFRP	10.0	Polyester	UV	25	180	3	99.4	NA
1320	Tannous and Saadatmanesh (1998)	NA	GFRP	10.0	Vinylester	Control	25	0	3	100.0	NA
1321	Tannous and Saadatmanesh (1998)	NA	GFRP	10.0	Vinylester	Water (IMMR)	25	180	3	97.1	NA
1322	Tannous and Saadatmanesh (1998)	NA	GFRP	10.0	Vinylester	Alkaline solution (IMMR)	25	180	3	87.0	NA
1323	Tannous and Saadatmanesh (1998)	NA	GFRP	10.0	Vinylester	Alkaline solution (IMMR)	60	180	3	79.7	NA
1324	Tannous and Saadatmanesh (1998)	NA	GFRP	10.0	Vinylester	Acid solution (IMMR)	25	180	3	96.3	NA
1325	Tannous and Saadatmanesh (1998)	NA	GFRP	10.0	Vinylester	Saline solution 1 (IMMR)	25	180	3	93.5	NA
1326	Tannous and Saadatmanesh (1998)	NA	GFRP	10.0	Vinylester	Saline solution 2 (IMMR)	25	180	3	77.1	NA
1327	Tannous and Saadatmanesh (1998)	NA	GFRP	10.0	Vinylester	Saline solution 3 (IMMR)	25	180	3	76.0	NA
1328	Tannous and Saadatmanesh (1998)	NA	GFRP	19.5	Polyester	Control	25	0	3	100.0	NA
1329	Tannous and Saadatmanesh (1998)	NA	GFRP	19.5	Polyester	Water (IMMR)	25	180	3	95.2	NA
1330	Tannous and Saadatmanesh (1998)	NA	GFRP	19.5	Polyester	Alkaline solution (IMMR)	25	180	3	81.3	NA
1331	Tannous and Saadatmanesh (1998)	NA	GFRP	19.5	Polyester	Alkaline solution (IMMR)	60	180	3	80.0	NA

1332	Tannous and Saadatmanesh (1998)	NA	GFRP	19.5	Polyester	Acid solution (IMMR)	25	180	3	93.6	NA
1333	Tannous and Saadatmanesh (1998)	NA	GFRP	19.5	Polyester	Saline solution 1 (IMMR)	25	180	3	92.3	NA
1334	Tannous and Saadatmanesh (1998)	NA	GFRP	19.5	Polyester	Saline solution 2 (IMMR)	25	180	3	87.9	NA
1335	Tannous and Saadatmanesh (1998)	NA	GFRP	19.5	Polyester	Saline solution 3 (IMMR)	25	180	3	89.1	NA
1336	Tannous and Saadatmanesh (1998)	NA	GFRP	19.5	Vinylester	Control	25	0	3	100.0	NA
1337	Tannous and Saadatmanesh (1998)	NA	GFRP	19.5	Vinylester	Water (IMMR)	25	180	3	96.7	NA
1338	Tannous and Saadatmanesh (1998)	NA	GFRP	19.5	Vinylester	Alkaline solution (IMMR)	25	180	3	89.1	NA
1339	Tannous and Saadatmanesh (1998)	NA	GFRP	19.5	Vinylester	Alkaline solution (IMMR)	60	180	3	87.8	NA
1340	Tannous and Saadatmanesh (1998)	NA	GFRP	19.5	Vinylester	Acid solution (IMMR)	25	180	3	95.7	NA
1341	Tannous and Saadatmanesh (1998)	NA	GFRP	19.5	Vinylester	Saline solution 1 (IMMR)	25	180	3	94.8	NA
1342	Tannous and Saadatmanesh (1998)	NA	GFRP	19.5	Vinylester	Saline solution 2 (IMMR)	25	180	3	94.0	NA
1343	Tannous and Saadatmanesh (1998)	NA	GFRP	19.5	Vinylester	Saline solution 3 (IMMR)	25	180	3	91.6	NA
1344	Wang et al. (2017b)	Jiangsu Green Materials Vally New Material T&D Co., Ltd (Nanjing, China)	BFRP	6.0	Epoxy	Control	32	0	3	100.0	100.0
1345	Wang et al. (2017b)	Jiangsu Green Materials Vally New Material T&D Co., Ltd (Nanjing, China)	BFRP	6.0	Epoxy	SWSSC solution 1 (IMMR)	32	21	2	97.5	112.8
1346	Wang et al. (2017b)	Jiangsu Green Materials Vally New Material T&D Co., Ltd (Nanjing, China)	BFRP	6.0	Epoxy	SWSSC solution 1 (IMMR)	32	42	2	92.5	102.6
1347	Wang et al.	Jiangsu Green Materials	BFRP	6.0	Epoxy	SWSSC solution 1 (IMMR)	32	63	2	92.7	NA

	(2017b)		Vally New Material T&D Co., Ltd (Nanjing, China)										
1348	Wang et al. (2017b)		Jiangsu Green Materials Vally New Material T&D Co., Ltd (Nanjing, China)	BFRP	6.0	Epoxy	SWSSC solution 1 (IMMR)	40	21	2	94.2	110.3
1349	Wang et al. (2017b)		Jiangsu Green Materials Vally New Material T&D Co., Ltd (Nanjing, China)	BFRP	6.0	Epoxy	SWSSC solution 1 (IMMR)	40	42	2	88.7	NA
1350	Wang et al. (2017b)		Jiangsu Green Materials Vally New Material T&D Co., Ltd (Nanjing, China)	BFRP	6.0	Epoxy	SWSSC solution 1 (IMMR)	40	63	2	81.6	NA
1351	Wang et al. (2017b)		Jiangsu Green Materials Vally New Material T&D Co., Ltd (Nanjing, China)	BFRP	6.0	Epoxy	SWSSC solution 1 (IMMR)	48	21	2	93.0	107.7
1352	Wang et al. (2017b)		Jiangsu Green Materials Vally New Material T&D Co., Ltd (Nanjing, China)	BFRP	6.0	Epoxy	SWSSC solution 1 (IMMR)	48	42	2	82.4	107.7
1353	Wang et al. (2017b)		Jiangsu Green Materials Vally New Material T&D Co., Ltd (Nanjing, China)	BFRP	6.0	Epoxy	SWSSC solution 1 (IMMR)	48	63	2	59.1	117.9
1354	Wang et al. (2017b)		Jiangsu Green Materials Vally New Material T&D Co., Ltd (Nanjing, China)	BFRP	6.0	Epoxy	SWSSC solution 1 (IMMR)	55	21	2	67.2	102.6
1355	Wang et al. (2017b)		Jiangsu Green Materials Vally New Material T&D Co., Ltd (Nanjing, China)	BFRP	6.0	Epoxy	SWSSC solution 1 (IMMR)	55	42	2	37.5	92.3
1356	Wang et al. (2017b)		Jiangsu Green Materials Vally New Material T&D Co., Ltd (Nanjing, China)	BFRP	6.0	Epoxy	SWSSC solution 1 (IMMR)	55	63	2	26.1	100.0
1357	Wang et al. (2017b)		Jiangsu Green Materials Vally New Material T&D Co., Ltd (Nanjing, China)	BFRP	6.0	Epoxy	SWSSC solution 2 (IMMR)	32	21	2	99.3	117.9
1358	Wang et al. (2017b)		Jiangsu Green Materials Vally New Material T&D Co., Ltd (Nanjing, China)	BFRP	6.0	Epoxy	SWSSC solution 2 (IMMR)	32	42	2	93.8	100.0
1359	Wang et al. (2017b)		Jiangsu Green Materials Vally New Material T&D Co., Ltd (Nanjing, China)	BFRP	6.0	Epoxy	SWSSC solution 2 (IMMR)	32	63	2	97.9	115.4
1360	Wang et al. (2017b)		Jiangsu Green Materials Vally New Material T&D Co., Ltd (Nanjing, China)	BFRP	6.0	Epoxy	SWSSC solution 2 (IMMR)	40	21	2	95.3	110.3
1361	Wang et al. (2017b)		Jiangsu Green Materials Vally New Material T&D Co., Ltd (Nanjing, China)	BFRP	6.0	Epoxy	SWSSC solution 2 (IMMR)	40	42	2	93.0	100.0
1362	Wang et al. (2017b)		Jiangsu Green Materials Vally New Material T&D	BFRP	6.0	Epoxy	SWSSC solution 2 (IMMR)	40	63	2	90.2	117.9

			Co., Ltd (Nanjing, China)									
1363	Wang et al. (2017b)		Jiangsu Green Materials Vally New Material T&D Co., Ltd (Nanjing, China)	BFRP	6.0	Epoxy	SWSSC solution 2 (IMMR)	55	21	2	89.7	112.8
1364	Wang et al. (2017b)		Jiangsu Green Materials Vally New Material T&D Co., Ltd (Nanjing, China)	BFRP	6.0	Epoxy	SWSSC solution 2 (IMMR)	55	42	2	81.1	110.3
1365	Wang et al. (2017b)		Jiangsu Green Materials Vally New Material T&D Co., Ltd (Nanjing, China)	BFRP	6.0	Epoxy	SWSSC solution 2 (IMMR)	55	63	2	77.4	120.5
1366	Wang et al. (2017b)		Harbin FRP Institute (Harbin, China)	GFRP	6.3	Epoxy	Control	32	0	3	100.0	100.0
1367	Wang et al. (2017b)		Harbin FRP Institute (Harbin, China)	GFRP	6.3	Epoxy	SWSSC solution 1 (IMMR)	32	21	2	89.9	NA
1368	Wang et al. (2017b)		Harbin FRP Institute (Harbin, China)	GFRP	6.3	Epoxy	SWSSC solution 1 (IMMR)	32	42	2	91.2	NA
1369	Wang et al. (2017b)		Harbin FRP Institute (Harbin, China)	GFRP	6.3	Epoxy	SWSSC solution 1 (IMMR)	32	63	2	87.3	NA
1370	Wang et al. (2017b)		Harbin FRP Institute (Harbin, China)	GFRP	6.3	Epoxy	SWSSC solution 1 (IMMR)	40	21	2	85.3	136.0
1371	Wang et al. (2017b)		Harbin FRP Institute (Harbin, China)	GFRP	6.3	Epoxy	SWSSC solution 1 (IMMR)	40	42	2	89.8	NA
1372	Wang et al. (2017b)		Harbin FRP Institute (Harbin, China)	GFRP	6.3	Epoxy	SWSSC solution 1 (IMMR)	40	63	2	90.7	NA
1373	Wang et al. (2017b)		Harbin FRP Institute (Harbin, China)	GFRP	6.3	Epoxy	SWSSC solution 1 (IMMR)	55	21	2	80.7	124.0
1374	Wang et al. (2017b)		Harbin FRP Institute (Harbin, China)	GFRP	6.3	Epoxy	SWSSC solution 1 (IMMR)	55	42	2	68.7	NA
1375	Wang et al. (2017b)		Harbin FRP Institute (Harbin, China)	GFRP	6.3	Epoxy	SWSSC solution 1 (IMMR)	55	63	2	80.1	NA
1376	Wang et al. (2017b)		Harbin FRP Institute (Harbin, China)	GFRP	6.3	Epoxy	SWSSC solution 2 (IMMR)	32	21	2	97.5	132.0
1377	Wang et al. (2017b)		Harbin FRP Institute (Harbin, China)	GFRP	6.3	Epoxy	SWSSC solution 2 (IMMR)	32	42	2	95.1	136.0
1378	Wang et al. (2017b)		Harbin FRP Institute (Harbin, China)	GFRP	6.3	Epoxy	SWSSC solution 2 (IMMR)	32	63	2	97.8	136.0
1379	Wang et al. (2017b)		Harbin FRP Institute (Harbin, China)	GFRP	6.3	Epoxy	SWSSC solution 2 (IMMR)	40	21	2	90.6	132.0
1380	Wang et al. (2017b)		Harbin FRP Institute (Harbin, China)	GFRP	6.3	Epoxy	SWSSC solution 2 (IMMR)	40	42	2	90.8	136.0
1381	Wang et al. (2017b)		Harbin FRP Institute (Harbin, China)	GFRP	6.3	Epoxy	SWSSC solution 2 (IMMR)	40	63	2	94.1	136.0
1382	Wang et al. (2017b)		Harbin FRP Institute (Harbin, China)	GFRP	6.3	Epoxy	SWSSC solution 2 (IMMR)	55	21	2	91.2	132.0
1383	Wang et al. (2017b)		Harbin FRP Institute (Harbin, China)	GFRP	6.3	Epoxy	SWSSC solution 2 (IMMR)	55	42	2	92.5	132.0

1384	Wang et al. (2017b)	Harbin FRP Institute (Harbin, China)	GFRP	6.3	Epoxy	SWSSC solution 2 (IMMR)	55	63	2	89.5	132.0
1385	Wang et al. (2018)	Jiangsu Green Materials Vally New Material T&D Co., Ltd (Nanjing, China)	BFRP	6.0	Epoxy	Control	25	0	5	100.0	100.0
1386	Wang et al. (2018)	Jiangsu Green Materials Vally New Material T&D Co., Ltd (Nanjing, China)	BFRP	6.0	Epoxy	SL (20%fu)+SWSSC solution (IMMR)	25	21	2	92.4	97.6
1387	Wang et al. (2018)	Jiangsu Green Materials Vally New Material T&D Co., Ltd (Nanjing, China)	BFRP	6.0	Epoxy	SL (20%fu)+SWSSC solution (IMMR)	25	42	2	94.0	104.8
1388	Wang et al. (2018)	Jiangsu Green Materials Vally New Material T&D Co., Ltd (Nanjing, China)	BFRP	6.0	Epoxy	SL (20%fu)+SWSSC solution (IMMR)	25	63	2	92.9	104.8
1389	Wang et al. (2018)	Jiangsu Green Materials Vally New Material T&D Co., Ltd (Nanjing, China)	BFRP	6.0	Epoxy	SL (20%fu)+SWSSC solution (IMMR)	40	21	2	88.4	97.6
1390	Wang et al. (2018)	Jiangsu Green Materials Vally New Material T&D Co., Ltd (Nanjing, China)	BFRP	6.0	Epoxy	SL (20%fu)+SWSSC solution (IMMR)	40	42	2	89.8	109.5
1391	Wang et al. (2018)	Jiangsu Green Materials Vally New Material T&D Co., Ltd (Nanjing, China)	BFRP	6.0	Epoxy	SL (20%fu)+SWSSC solution (IMMR)	40	63	2	81.7	102.4
1392	Wang et al. (2018)	Jiangsu Green Materials Vally New Material T&D Co., Ltd (Nanjing, China)	BFRP	6.0	Epoxy	SL (20%fu)+SWSSC solution (IMMR)	55	21	2	69.6	109.5
1393	Wang et al. (2018)	Jiangsu Green Materials Vally New Material T&D Co., Ltd (Nanjing, China)	BFRP	6.0	Epoxy	SL (20%fu)+SWSSC solution (IMMR)	55	42	2	59.8	111.9
1394	Wang et al. (2018)	Jiangsu Green Materials Vally New Material T&D Co., Ltd (Nanjing, China)	BFRP	6.0	Epoxy	SL (20%fu)+SWSSC solution (IMMR)	55	63	2	55.1	104.8
1395	Wang et al. (2018)	Jiangsu Green Materials Vally New Material T&D Co., Ltd (Nanjing, China)	BFRP	6.0	Epoxy	SL (30%fu)+SWSSC solution (IMMR)	25	21	2	83.1	107.1
1396	Wang et al. (2018)	Jiangsu Green Materials Vally New Material T&D Co., Ltd (Nanjing, China)	BFRP	6.0	Epoxy	SL (30%fu)+SWSSC solution (IMMR)	25	42	2	75.4	107.1
1397	Wang et al. (2018)	Jiangsu Green Materials Vally New Material T&D Co., Ltd (Nanjing, China)	BFRP	6.0	Epoxy	SL (30%fu)+SWSSC solution (IMMR)	25	63	2	78.9	109.5
1398	Wang et al. (2018)	Jiangsu Green Materials Vally New Material T&D Co., Ltd (Nanjing, China)	BFRP	6.0	Epoxy	SL (40%fu)+SWSSC solution (IMMR)	25	21	2	59.2	90.5
1399	Wang et al. (2018)	Jiangsu Green Materials Vally New Material T&D	BFRP	6.0	Epoxy	SL (40%fu)+SWSSC solution (IMMR)	25	42	2	54.0	95.2

				Co., Ltd (Nanjing, China)										
1400	Wang et al. (2018)			Jiangsu Green Materials Vally New Material T&D Co., Ltd (Nanjing, China)	BFRP	6.0	Epoxy	SL (40%fu)+SWSSC (IMMR)	solution	25	63	2	43.2	NA
1401	Wang et al. (2018)			Jiangsu Green Materials Vally New Material T&D Co., Ltd (Nanjing, China)	BFRP	6.0	Epoxy	SL (40%fu)+SWSSC (IMMR)	solution	40	21	2	0.0	NA
1402	Wang et al. (2018)			Harbin FRP Institute (Harbin, China)	GFRP	6.3	Epoxy	Control		25	0	5	100.0	100.0
1403	Wang et al. (2018)			Harbin FRP Institute (Harbin, China)	GFRP	6.3	Epoxy	SL (20%fu)+SWSSC (IMMR)	solution	25	21	2	93.4	97.2
1404	Wang et al. (2018)			Harbin FRP Institute (Harbin, China)	GFRP	6.3	Epoxy	SL (20%fu)+SWSSC (IMMR)	solution	25	42	2	93.7	97.2
1405	Wang et al. (2018)			Harbin FRP Institute (Harbin, China)	GFRP	6.3	Epoxy	SL (20%fu)+SWSSC (IMMR)	solution	25	63	2	90.7	102.8
1406	Wang et al. (2018)			Harbin FRP Institute (Harbin, China)	GFRP	6.3	Epoxy	SL (20%fu)+SWSSC (IMMR)	solution	40	21	2	86.8	100.0
1407	Wang et al. (2018)			Harbin FRP Institute (Harbin, China)	GFRP	6.3	Epoxy	SL (20%fu)+SWSSC (IMMR)	solution	40	42	2	82.0	100.0
1408	Wang et al. (2018)			Harbin FRP Institute (Harbin, China)	GFRP	6.3	Epoxy	SL (20%fu)+SWSSC (IMMR)	solution	40	63	2	74.1	97.2
1409	Wang et al. (2018)			Harbin FRP Institute (Harbin, China)	GFRP	6.3	Epoxy	SL (20%fu)+SWSSC (IMMR)	solution	55	21	2	68.7	105.6
1410	Wang et al. (2018)			Harbin FRP Institute (Harbin, China)	GFRP	6.3	Epoxy	SL (20%fu)+SWSSC (IMMR)	solution	55	42	2	73.4	100.0
1411	Wang et al. (2018)			Harbin FRP Institute (Harbin, China)	GFRP	6.3	Epoxy	SL (20%fu)+SWSSC (IMMR)	solution	55	63	2	58.6	97.2
1412	Wang et al. (2018)			Harbin FRP Institute (Harbin, China)	GFRP	6.3	Epoxy	SL (30%fu)+SWSSC (IMMR)	solution	25	21	2	88.3	97.2
1413	Wang et al. (2018)			Harbin FRP Institute (Harbin, China)	GFRP	6.3	Epoxy	SL (30%fu)+SWSSC (IMMR)	solution	25	42	2	84.3	97.2
1414	Wang et al. (2018)			Harbin FRP Institute (Harbin, China)	GFRP	6.3	Epoxy	SL (30%fu)+SWSSC (IMMR)	solution	25	63	2	84.8	97.2
1415	Wang et al. (2018)			Harbin FRP Institute (Harbin, China)	GFRP	6.3	Epoxy	SL (40%fu)+SWSSC (IMMR)	solution	25	21	2	78.9	100.0
1416	Wang et al. (2018)			Harbin FRP Institute (Harbin, China)	GFRP	6.3	Epoxy	SL (40%fu)+SWSSC (IMMR)	solution	25	42	2	79.2	94.4
1417	Wang et al. (2018)			Harbin FRP Institute (Harbin, China)	GFRP	6.3	Epoxy	SL (40%fu)+SWSSC (IMMR)	solution	25	63	2	68.0	88.9
1418	Wang et al. (2018)			Harbin FRP Institute (Harbin, China)	GFRP	6.3	Epoxy	SL (40%fu)+SWSSC (IMMR)	solution	40	21	2	0.0	NA
1419	Wang et al. (2022)			Dextra Co., ltd (Dongguan, China)	GFRP	9.5	Vinylester	Control		23	0	5	100.0	100.0
1420	Wang et al. (2022)			Dextra Co., ltd (Dongguan, China)	GFRP	9.5	Vinylester	Water (IMMR)		23	45	5	98.7	101.3
1421	Wang et al.			Dextra Co., ltd (Dongguan,	GFRP	9.5	Vinylester	Water (IMMR)		23	90	5	97.0	99.5

	(2022)			China)									
1422	Wang (2022)	et	al.	Dextra Co., ltd (Dongguan, China)	GFRP	9.5	Vinylester	Water (IMMR)	23	180	5	98.7	100.1
1423	Wang (2022)	et	al.	Dextra Co., ltd (Dongguan, China)	GFRP	9.5	Vinylester	Water (IMMR)	23	270	5	99.8	NA
1424	Wang (2022)	et	al.	Dextra Co., ltd (Dongguan, China)	GFRP	9.5	Vinylester	Water (IMMR)	23	360	5	97.7	NA
1425	Wang (2022)	et	al.	Dextra Co., ltd (Dongguan, China)	GFRP	9.5	Vinylester	Water (IMMR)	40	45	5	95.5	94.6
1426	Wang (2022)	et	al.	Dextra Co., ltd (Dongguan, China)	GFRP	9.5	Vinylester	Water (IMMR)	40	90	5	88.8	96.4
1427	Wang (2022)	et	al.	Dextra Co., ltd (Dongguan, China)	GFRP	9.5	Vinylester	Water (IMMR)	40	180	5	80.3	94.9
1428	Wang (2022)	et	al.	Dextra Co., ltd (Dongguan, China)	GFRP	9.5	Vinylester	Water (IMMR)	40	270	5	77.5	96.8
1429	Wang (2022)	et	al.	Dextra Co., ltd (Dongguan, China)	GFRP	9.5	Vinylester	Water (IMMR)	40	360	5	74.3	98.1
1430	Wang (2022)	et	al.	Dextra Co., ltd (Dongguan, China)	GFRP	9.5	Vinylester	Water (IMMR)	60	45	5	61.6	95.7
1431	Wang (2022)	et	al.	Dextra Co., ltd (Dongguan, China)	GFRP	9.5	Vinylester	Water (IMMR)	60	90	5	55.2	98.5
1432	Wang (2022)	et	al.	Dextra Co., ltd (Dongguan, China)	GFRP	9.5	Vinylester	Water (IMMR)	60	180	5	51.0	93.9
1433	Wang (2022)	et	al.	Dextra Co., ltd (Dongguan, China)	GFRP	9.5	Vinylester	Water (IMMR)	60	270	5	48.1	99.6
1434	Wang (2022)	et	al.	Dextra Co., ltd (Dongguan, China)	GFRP	9.5	Vinylester	Water (IMMR)	60	360	5	46.0	NA
1435	Wang (2022)	et	al.	Dextra Co., ltd (Dongguan, China)	GFRP	9.5	Vinylester	Alkaline solution 1 (IMMR)	23	45	5	98.4	97.5
1436	Wang (2022)	et	al.	Dextra Co., ltd (Dongguan, China)	GFRP	9.5	Vinylester	Alkaline solution 1 (IMMR)	23	90	5	96.6	106.9
1437	Wang (2022)	et	al.	Dextra Co., ltd (Dongguan, China)	GFRP	9.5	Vinylester	Alkaline solution 1 (IMMR)	23	180	5	96.2	NA
1438	Wang (2022)	et	al.	Dextra Co., ltd (Dongguan, China)	GFRP	9.5	Vinylester	Alkaline solution 1 (IMMR)	23	270	5	94.5	98.8
1439	Wang (2022)	et	al.	Dextra Co., ltd (Dongguan, China)	GFRP	9.5	Vinylester	Alkaline solution 1 (IMMR)	23	360	5	93.1	NA
1440	Wang (2022)	et	al.	Dextra Co., ltd (Dongguan, China)	GFRP	9.5	Vinylester	Alkaline solution 1 (IMMR)	40	45	5	94.1	93.5
1441	Wang (2022)	et	al.	Dextra Co., ltd (Dongguan, China)	GFRP	9.5	Vinylester	Alkaline solution 1 (IMMR)	40	90	5	88.8	99.4
1442	Wang (2022)	et	al.	Dextra Co., ltd (Dongguan, China)	GFRP	9.5	Vinylester	Alkaline solution 1 (IMMR)	40	180	5	80.3	100.4
1443	Wang (2022)	et	al.	Dextra Co., ltd (Dongguan, China)	GFRP	9.5	Vinylester	Alkaline solution 1 (IMMR)	40	270	5	74.7	100.1
1444	Wang	et	al.	Dextra Co., ltd (Dongguan,	GFRP	9.5	Vinylester	Alkaline solution 1 (IMMR)	40	360	5	70.4	104.1

	(2022)			China)									
1445	Wang (2022)	et	al.	Dextra Co., ltd (Dongguan, China)	GFRP	9.5	Vinylester	Alkaline solution 1 (IMMR)	60	45	5	61.6	90.1
1446	Wang (2022)	et	al.	Dextra Co., ltd (Dongguan, China)	GFRP	9.5	Vinylester	Alkaline solution 1 (IMMR)	60	90	5	52.4	99.3
1447	Wang (2022)	et	al.	Dextra Co., ltd (Dongguan, China)	GFRP	9.5	Vinylester	Alkaline solution 1 (IMMR)	60	180	5	49.9	100.6
1448	Wang (2022)	et	al.	Dextra Co., ltd (Dongguan, China)	GFRP	9.5	Vinylester	Alkaline solution 1 (IMMR)	60	270	5	46.4	97.3
1449	Wang (2022)	et	al.	Dextra Co., ltd (Dongguan, China)	GFRP	9.5	Vinylester	Alkaline solution 1 (IMMR)	60	360	5	44.2	100.3
1450	Wang (2022)	et	al.	Dextra Co., ltd (Dongguan, China)	GFRP	9.5	Vinylester	Alkaline solution 2 (IMMR)	23	45	5	97.7	95.5
1451	Wang (2022)	et	al.	Dextra Co., ltd (Dongguan, China)	GFRP	9.5	Vinylester	Alkaline solution 2 (IMMR)	23	90	5	94.1	NA
1452	Wang (2022)	et	al.	Dextra Co., ltd (Dongguan, China)	GFRP	9.5	Vinylester	Alkaline solution 2 (IMMR)	23	180	5	95.9	98.0
1453	Wang (2022)	et	al.	Dextra Co., ltd (Dongguan, China)	GFRP	9.5	Vinylester	Alkaline solution 2 (IMMR)	23	270	5	93.4	98.1
1454	Wang (2022)	et	al.	Dextra Co., ltd (Dongguan, China)	GFRP	9.5	Vinylester	Alkaline solution 2 (IMMR)	23	360	5	91.3	98.8
1455	Wang (2022)	et	al.	Dextra Co., ltd (Dongguan, China)	GFRP	9.5	Vinylester	Alkaline solution 2 (IMMR)	40	45	5	95.9	97.1
1456	Wang (2022)	et	al.	Dextra Co., ltd (Dongguan, China)	GFRP	9.5	Vinylester	Alkaline solution 2 (IMMR)	40	90	5	88.8	97.8
1457	Wang (2022)	et	al.	Dextra Co., ltd (Dongguan, China)	GFRP	9.5	Vinylester	Alkaline solution 2 (IMMR)	40	180	5	79.6	101.9
1458	Wang (2022)	et	al.	Dextra Co., ltd (Dongguan, China)	GFRP	9.5	Vinylester	Alkaline solution 2 (IMMR)	40	270	5	75.0	102.9
1459	Wang (2022)	et	al.	Dextra Co., ltd (Dongguan, China)	GFRP	9.5	Vinylester	Alkaline solution 2 (IMMR)	40	360	5	67.6	101.6
1460	Wang (2022)	et	al.	Dextra Co., ltd (Dongguan, China)	GFRP	9.5	Vinylester	Alkaline solution 2 (IMMR)	60	45	5	63.3	91.6
1461	Wang (2022)	et	al.	Dextra Co., ltd (Dongguan, China)	GFRP	9.5	Vinylester	Alkaline solution 2 (IMMR)	60	90	5	51.0	97.0
1462	Wang (2022)	et	al.	Dextra Co., ltd (Dongguan, China)	GFRP	9.5	Vinylester	Alkaline solution 2 (IMMR)	60	180	5	46.0	99.7
1463	Wang (2022)	et	al.	Dextra Co., ltd (Dongguan, China)	GFRP	9.5	Vinylester	Alkaline solution 2 (IMMR)	60	270	5	44.6	97.6
1464	Wang (2022)	et	al.	Dextra Co., ltd (Dongguan, China)	GFRP	9.5	Vinylester	Alkaline solution 2 (IMMR)	60	360	5	41.0	98.9
1465	Wang (2022)	et	al.	Dextra Co., ltd (Dongguan, China)	GFRP	9.5	Vinylester	Alkaline solution 3 (IMMR)	23	45	5	95.5	92.4
1466	Wang (2022)	et	al.	Dextra Co., ltd (Dongguan, China)	GFRP	9.5	Vinylester	Alkaline solution 3 (IMMR)	23	90	5	92.4	102.1
1467	Wang	et	al.	Dextra Co., ltd (Dongguan,	GFRP	9.5	Vinylester	Alkaline solution 3 (IMMR)	23	180	5	89.2	100.6

	(2022)			China)									
1468	Wang (2022)	et	al.	Dextra Co., ltd (Dongguan, China)	GFRP	9.5	Vinylester	Alkaline solution 3 (IMMR)	23	270	5	84.9	96.8
1469	Wang (2022)	et	al.	Dextra Co., ltd (Dongguan, China)	GFRP	9.5	Vinylester	Alkaline solution 3 (IMMR)	23	360	5	81.7	99.4
1470	Wang (2022)	et	al.	Dextra Co., ltd (Dongguan, China)	GFRP	9.5	Vinylester	Alkaline solution 3 (IMMR)	40	45	5	92.4	95.6
1471	Wang (2022)	et	al.	Dextra Co., ltd (Dongguan, China)	GFRP	9.5	Vinylester	Alkaline solution 3 (IMMR)	40	90	5	84.9	99.1
1472	Wang (2022)	et	al.	Dextra Co., ltd (Dongguan, China)	GFRP	9.5	Vinylester	Alkaline solution 3 (IMMR)	40	180	5	69.4	97.5
1473	Wang (2022)	et	al.	Dextra Co., ltd (Dongguan, China)	GFRP	9.5	Vinylester	Alkaline solution 3 (IMMR)	40	270	5	65.8	95.9
1474	Wang (2022)	et	al.	Dextra Co., ltd (Dongguan, China)	GFRP	9.5	Vinylester	Alkaline solution 3 (IMMR)	40	360	5	62.6	98.5
1475	Wang (2022)	et	al.	Dextra Co., ltd (Dongguan, China)	GFRP	9.5	Vinylester	Alkaline solution 3 (IMMR)	60	45	5	51.3	93.4
1476	Wang (2022)	et	al.	Dextra Co., ltd (Dongguan, China)	GFRP	9.5	Vinylester	Alkaline solution 3 (IMMR)	60	90	5	38.9	101.3
1477	Wang (2022)	et	al.	Dextra Co., ltd (Dongguan, China)	GFRP	9.5	Vinylester	Alkaline solution 3 (IMMR)	60	180	5	34.0	99.1
1478	Wang (2022)	et	al.	Dextra Co., ltd (Dongguan, China)	GFRP	9.5	Vinylester	Alkaline solution 3 (IMMR)	60	270	5	30.8	100.2
1479	Wang (2022)	et	al.	Dextra Co., ltd (Dongguan, China)	GFRP	9.5	Vinylester	Alkaline solution 3 (IMMR)	60	360	5	27.6	95.7
1480	Wang (2023a)	et	al.	Dextra Co., Ltd (Dongguan, China)	GFRP	9.5	Vinylester	Control	23	0	5	100.0	100.0
1481	Wang (2023a)	et	al.	Dextra Co., Ltd (Dongguan, China)	GFRP	9.5	Vinylester	Water (IMMR)	23	45	5	98.4	NA
1482	Wang (2023a)	et	al.	Dextra Co., Ltd (Dongguan, China)	GFRP	9.5	Vinylester	Water (IMMR)	23	90	5	97.0	NA
1483	Wang (2023a)	et	al.	Dextra Co., Ltd (Dongguan, China)	GFRP	9.5	Vinylester	Water (IMMR)	23	180	5	98.7	NA
1484	Wang (2023a)	et	al.	Dextra Co., Ltd (Dongguan, China)	GFRP	9.5	Vinylester	Water (IMMR)	23	270	5	99.6	NA
1485	Wang (2023a)	et	al.	Dextra Co., Ltd (Dongguan, China)	GFRP	9.5	Vinylester	Water (IMMR)	23	360	5	97.8	98.1
1486	Wang (2023a)	et	al.	Dextra Co., Ltd (Dongguan, China)	GFRP	9.5	Vinylester	Water (IMMR)	40	45	5	94.8	NA
1487	Wang (2023a)	et	al.	Dextra Co., Ltd (Dongguan, China)	GFRP	9.5	Vinylester	Water (IMMR)	40	90	5	89.0	NA
1488	Wang (2023a)	et	al.	Dextra Co., Ltd (Dongguan, China)	GFRP	9.5	Vinylester	Water (IMMR)	40	180	5	79.1	NA
1489	Wang (2023a)	et	al.	Dextra Co., Ltd (Dongguan, China)	GFRP	9.5	Vinylester	Water (IMMR)	40	270	5	76.9	NA
1490	Wang	et	al.	Dextra Co., Ltd (Dongguan,	GFRP	9.5	Vinylester	Water (IMMR)	40	360	5	74.2	97.8

	(2023a)			China)									
1491	Wang (2023a)	et	al.	Dextra Co., Ltd (Dongguan, China)	GFRP	9.5	Vinylester	Water (IMMR)	60	45	5	62.7	NA
1492	Wang (2023a)	et	al.	Dextra Co., Ltd (Dongguan, China)	GFRP	9.5	Vinylester	Water (IMMR)	60	90	5	55.2	NA
1493	Wang (2023a)	et	al.	Dextra Co., Ltd (Dongguan, China)	GFRP	9.5	Vinylester	Water (IMMR)	60	180	5	50.9	NA
1494	Wang (2023a)	et	al.	Dextra Co., Ltd (Dongguan, China)	GFRP	9.5	Vinylester	Water (IMMR)	60	270	5	48.0	NA
1495	Wang (2023a)	et	al.	Dextra Co., Ltd (Dongguan, China)	GFRP	9.5	Vinylester	Water (IMMR)	60	360	5	45.9	95.6
1496	Wang (2023a)	et	al.	Dextra Co., Ltd (Dongguan, China)	GFRP	9.5	Vinylester	Alkaline solution 1 (IMMR)	23	45	5	98.4	NA
1497	Wang (2023a)	et	al.	Dextra Co., Ltd (Dongguan, China)	GFRP	9.5	Vinylester	Alkaline solution 1 (IMMR)	23	90	5	96.4	NA
1498	Wang (2023a)	et	al.	Dextra Co., Ltd (Dongguan, China)	GFRP	9.5	Vinylester	Alkaline solution 1 (IMMR)	23	180	5	96.1	NA
1499	Wang (2023a)	et	al.	Dextra Co., Ltd (Dongguan, China)	GFRP	9.5	Vinylester	Alkaline solution 1 (IMMR)	23	270	5	94.4	NA
1500	Wang (2023a)	et	al.	Dextra Co., Ltd (Dongguan, China)	GFRP	9.5	Vinylester	Alkaline solution 1 (IMMR)	23	360	5	92.8	99.2
1501	Wang (2023a)	et	al.	Dextra Co., Ltd (Dongguan, China)	GFRP	9.5	Vinylester	Alkaline solution 1 (IMMR)	40	45	5	94.0	NA
1502	Wang (2023a)	et	al.	Dextra Co., Ltd (Dongguan, China)	GFRP	9.5	Vinylester	Alkaline solution 1 (IMMR)	40	90	5	88.3	NA
1503	Wang (2023a)	et	al.	Dextra Co., Ltd (Dongguan, China)	GFRP	9.5	Vinylester	Alkaline solution 1 (IMMR)	40	180	5	80.1	NA
1504	Wang (2023a)	et	al.	Dextra Co., Ltd (Dongguan, China)	GFRP	9.5	Vinylester	Alkaline solution 1 (IMMR)	40	270	5	74.6	NA
1505	Wang (2023a)	et	al.	Dextra Co., Ltd (Dongguan, China)	GFRP	9.5	Vinylester	Alkaline solution 1 (IMMR)	40	360	5	70.1	103.6
1506	Wang (2023a)	et	al.	Dextra Co., Ltd (Dongguan, China)	GFRP	9.5	Vinylester	Alkaline solution 1 (IMMR)	60	45	5	61.7	NA
1507	Wang (2023a)	et	al.	Dextra Co., Ltd (Dongguan, China)	GFRP	9.5	Vinylester	Alkaline solution 1 (IMMR)	60	90	5	52.6	NA
1508	Wang (2023a)	et	al.	Dextra Co., Ltd (Dongguan, China)	GFRP	9.5	Vinylester	Alkaline solution 1 (IMMR)	60	180	5	49.4	NA
1509	Wang (2023a)	et	al.	Dextra Co., Ltd (Dongguan, China)	GFRP	9.5	Vinylester	Alkaline solution 1 (IMMR)	60	270	5	46.4	NA
1510	Wang (2023a)	et	al.	Dextra Co., Ltd (Dongguan, China)	GFRP	9.5	Vinylester	Alkaline solution 1 (IMMR)	60	360	5	44.2	100.5
1511	Wang (2023a)	et	al.	Dextra Co., Ltd (Dongguan, China)	GFRP	9.5	Vinylester	Alkaline solution 2 (IMMR)	23	45	5	97.1	NA
1512	Wang (2023a)	et	al.	Dextra Co., Ltd (Dongguan, China)	GFRP	9.5	Vinylester	Alkaline solution 2 (IMMR)	23	90	5	94.2	NA
1513	Wang	et	al.	Dextra Co., Ltd (Dongguan,	GFRP	9.5	Vinylester	Alkaline solution 2 (IMMR)	23	180	5	95.5	NA

	(2023a)			China)									
1514	Wang (2023a)	et	al.	Dextra Co., Ltd (Dongguan, China)	GFRP	9.5	Vinylester	Alkaline solution 2 (IMMR)	23	270	5	93.2	NA
1515	Wang (2023a)	et	al.	Dextra Co., Ltd (Dongguan, China)	GFRP	9.5	Vinylester	Alkaline solution 2 (IMMR)	23	360	5	90.9	98.9
1516	Wang (2023a)	et	al.	Dextra Co., Ltd (Dongguan, China)	GFRP	9.5	Vinylester	Alkaline solution 2 (IMMR)	40	45	5	96.1	NA
1517	Wang (2023a)	et	al.	Dextra Co., Ltd (Dongguan, China)	GFRP	9.5	Vinylester	Alkaline solution 2 (IMMR)	40	90	5	88.9	NA
1518	Wang (2023a)	et	al.	Dextra Co., Ltd (Dongguan, China)	GFRP	9.5	Vinylester	Alkaline solution 2 (IMMR)	40	180	5	79.1	NA
1519	Wang (2023a)	et	al.	Dextra Co., Ltd (Dongguan, China)	GFRP	9.5	Vinylester	Alkaline solution 2 (IMMR)	40	270	5	74.6	NA
1520	Wang (2023a)	et	al.	Dextra Co., Ltd (Dongguan, China)	GFRP	9.5	Vinylester	Alkaline solution 2 (IMMR)	40	360	5	67.2	101.4
1521	Wang (2023a)	et	al.	Dextra Co., Ltd (Dongguan, China)	GFRP	9.5	Vinylester	Alkaline solution 2 (IMMR)	60	45	5	63.5	NA
1522	Wang (2023a)	et	al.	Dextra Co., Ltd (Dongguan, China)	GFRP	9.5	Vinylester	Alkaline solution 2 (IMMR)	60	90	5	51.0	NA
1523	Wang (2023a)	et	al.	Dextra Co., Ltd (Dongguan, China)	GFRP	9.5	Vinylester	Alkaline solution 2 (IMMR)	60	180	5	46.3	NA
1524	Wang (2023a)	et	al.	Dextra Co., Ltd (Dongguan, China)	GFRP	9.5	Vinylester	Alkaline solution 2 (IMMR)	60	270	5	44.4	NA
1525	Wang (2023a)	et	al.	Dextra Co., Ltd (Dongguan, China)	GFRP	9.5	Vinylester	Alkaline solution 2 (IMMR)	60	360	5	41.1	98.9
1526	Wang (2023a)	et	al.	Dextra Co., Ltd (Dongguan, China)	GFRP	9.5	Vinylester	Alkaline solution 3 (IMMR)	23	45	5	95.6	NA
1527	Wang (2023a)	et	al.	Dextra Co., Ltd (Dongguan, China)	GFRP	9.5	Vinylester	Alkaline solution 3 (IMMR)	23	90	5	92.0	NA
1528	Wang (2023a)	et	al.	Dextra Co., Ltd (Dongguan, China)	GFRP	9.5	Vinylester	Alkaline solution 3 (IMMR)	23	180	5	89.0	NA
1529	Wang (2023a)	et	al.	Dextra Co., Ltd (Dongguan, China)	GFRP	9.5	Vinylester	Alkaline solution 3 (IMMR)	23	270	5	84.5	NA
1530	Wang (2023a)	et	al.	Dextra Co., Ltd (Dongguan, China)	GFRP	9.5	Vinylester	Alkaline solution 3 (IMMR)	23	360	5	81.5	99.2
1531	Wang (2023a)	et	al.	Dextra Co., Ltd (Dongguan, China)	GFRP	9.5	Vinylester	Alkaline solution 3 (IMMR)	40	45	5	92.3	NA
1532	Wang (2023a)	et	al.	Dextra Co., Ltd (Dongguan, China)	GFRP	9.5	Vinylester	Alkaline solution 3 (IMMR)	40	90	5	84.6	NA
1533	Wang (2023a)	et	al.	Dextra Co., Ltd (Dongguan, China)	GFRP	9.5	Vinylester	Alkaline solution 3 (IMMR)	40	180	5	68.8	NA
1534	Wang (2023a)	et	al.	Dextra Co., Ltd (Dongguan, China)	GFRP	9.5	Vinylester	Alkaline solution 3 (IMMR)	40	270	5	65.7	NA
1535	Wang (2023a)	et	al.	Dextra Co., Ltd (Dongguan, China)	GFRP	9.5	Vinylester	Alkaline solution 3 (IMMR)	40	360	5	61.8	98.1
1536	Wang	et	al.	Dextra Co., Ltd (Dongguan,	GFRP	9.5	Vinylester	Alkaline solution 3 (IMMR)	60	45	5	51.4	NA

	(2023a)			China)									
1537	Wang (2023a)	et	al.	Dextra Co., Ltd (Dongguan, China)	GFRP	9.5	Vinylester	Alkaline solution 3 (IMMR)	60	90	5	39.0	NA
1538	Wang (2023a)	et	al.	Dextra Co., Ltd (Dongguan, China)	GFRP	9.5	Vinylester	Alkaline solution 3 (IMMR)	60	180	5	34.1	NA
1539	Wang (2023a)	et	al.	Dextra Co., Ltd (Dongguan, China)	GFRP	9.5	Vinylester	Alkaline solution 3 (IMMR)	60	270	5	31.0	NA
1540	Wang (2023a)	et	al.	Dextra Co., Ltd (Dongguan, China)	GFRP	9.5	Vinylester	Alkaline solution 3 (IMMR)	60	360	5	27.7	95.6
1541	Wang (2023a)	et	al.	Dextra Co., Ltd (Dongguan, China)	GFRP	9.5	Vinylester	Simulated seawater (IMMR)	23	45	5	100.0	NA
1542	Wang (2023a)	et	al.	Dextra Co., Ltd (Dongguan, China)	GFRP	9.5	Vinylester	Simulated seawater (IMMR)	23	90	5	99.0	NA
1543	Wang (2023a)	et	al.	Dextra Co., Ltd (Dongguan, China)	GFRP	9.5	Vinylester	Simulated seawater (IMMR)	23	180	5	97.2	NA
1544	Wang (2023a)	et	al.	Dextra Co., Ltd (Dongguan, China)	GFRP	9.5	Vinylester	Simulated seawater (IMMR)	23	270	5	96.1	NA
1545	Wang (2023a)	et	al.	Dextra Co., Ltd (Dongguan, China)	GFRP	9.5	Vinylester	Simulated seawater (IMMR)	23	360	5	96.3	98.9
1546	Wang (2023a)	et	al.	Dextra Co., Ltd (Dongguan, China)	GFRP	9.5	Vinylester	Simulated seawater (IMMR)	40	45	5	96.5	NA
1547	Wang (2023a)	et	al.	Dextra Co., Ltd (Dongguan, China)	GFRP	9.5	Vinylester	Simulated seawater (IMMR)	40	90	5	93.2	NA
1548	Wang (2023a)	et	al.	Dextra Co., Ltd (Dongguan, China)	GFRP	9.5	Vinylester	Simulated seawater (IMMR)	40	180	5	83.8	NA
1549	Wang (2023a)	et	al.	Dextra Co., Ltd (Dongguan, China)	GFRP	9.5	Vinylester	Simulated seawater (IMMR)	40	270	5	78.5	NA
1550	Wang (2023a)	et	al.	Dextra Co., Ltd (Dongguan, China)	GFRP	9.5	Vinylester	Simulated seawater (IMMR)	40	360	5	75.4	98.9
1551	Wang (2023a)	et	al.	Dextra Co., Ltd (Dongguan, China)	GFRP	9.5	Vinylester	Simulated seawater (IMMR)	60	45	5	68.1	NA
1552	Wang (2023a)	et	al.	Dextra Co., Ltd (Dongguan, China)	GFRP	9.5	Vinylester	Simulated seawater (IMMR)	60	90	5	55.7	NA
1553	Wang (2023a)	et	al.	Dextra Co., Ltd (Dongguan, China)	GFRP	9.5	Vinylester	Simulated seawater (IMMR)	60	180	5	53.4	NA
1554	Wang (2023a)	et	al.	Dextra Co., Ltd (Dongguan, China)	GFRP	9.5	Vinylester	Simulated seawater (IMMR)	60	270	5	50.1	NA
1555	Wang (2023a)	et	al.	Dextra Co., Ltd (Dongguan, China)	GFRP	9.5	Vinylester	Simulated seawater (IMMR)	60	360	5	47.2	96.7
1556	Wang (2023a)	et	al.	Dextra Co., Ltd (Dongguan, China)	GFRP	9.5	Vinylester	NC solution (IMMR)	23	45	5	95.6	NA
1557	Wang (2023a)	et	al.	Dextra Co., Ltd (Dongguan, China)	GFRP	9.5	Vinylester	NC solution (IMMR)	23	90	5	86.3	NA
1558	Wang (2023a)	et	al.	Dextra Co., Ltd (Dongguan, China)	GFRP	9.5	Vinylester	NC solution (IMMR)	23	180	5	80.4	NA
1559	Wang	et	al.	Dextra Co., Ltd (Dongguan,	GFRP	9.5	Vinylester	NC solution (IMMR)	23	270	5	77.7	NA

	(2023a)			China)									
1560	Wang (2023a)	et	al.	Dextra Co., Ltd (Dongguan, China)	GFRP	9.5	Vinylester	NC solution (IMMR)	23	360	5	72.6	100.3
1561	Wang (2023a)	et	al.	Dextra Co., Ltd (Dongguan, China)	GFRP	9.5	Vinylester	NC solution (IMMR)	40	45	5	87.4	NA
1562	Wang (2023a)	et	al.	Dextra Co., Ltd (Dongguan, China)	GFRP	9.5	Vinylester	NC solution (IMMR)	40	90	5	74.0	NA
1563	Wang (2023a)	et	al.	Dextra Co., Ltd (Dongguan, China)	GFRP	9.5	Vinylester	NC solution (IMMR)	40	180	5	59.6	NA
1564	Wang (2023a)	et	al.	Dextra Co., Ltd (Dongguan, China)	GFRP	9.5	Vinylester	NC solution (IMMR)	40	270	5	50.7	NA
1565	Wang (2023a)	et	al.	Dextra Co., Ltd (Dongguan, China)	GFRP	9.5	Vinylester	NC solution (IMMR)	40	360	5	44.4	96.7
1566	Wang (2023a)	et	al.	Dextra Co., Ltd (Dongguan, China)	GFRP	9.5	Vinylester	NC solution (IMMR)	60	45	5	53.0	NA
1567	Wang (2023a)	et	al.	Dextra Co., Ltd (Dongguan, China)	GFRP	9.5	Vinylester	NC solution (IMMR)	60	90	5	39.7	NA
1568	Wang (2023a)	et	al.	Dextra Co., Ltd (Dongguan, China)	GFRP	9.5	Vinylester	NC solution (IMMR)	60	180	5	31.8	NA
1569	Wang (2023a)	et	al.	Dextra Co., Ltd (Dongguan, China)	GFRP	9.5	Vinylester	NC solution (IMMR)	60	270	5	30.9	NA
1570	Wang (2023a)	et	al.	Dextra Co., Ltd (Dongguan, China)	GFRP	9.5	Vinylester	NC solution (IMMR)	60	360	5	30.4	104.7
1571	Wang (2023a)	et	al.	Dextra Co., Ltd (Dongguan, China)	GFRP	9.5	Vinylester	SWSSC solution (IMMR)	23	45	5	90.4	NA
1572	Wang (2023a)	et	al.	Dextra Co., Ltd (Dongguan, China)	GFRP	9.5	Vinylester	SWSSC solution (IMMR)	23	90	5	87.5	NA
1573	Wang (2023a)	et	al.	Dextra Co., Ltd (Dongguan, China)	GFRP	9.5	Vinylester	SWSSC solution (IMMR)	23	180	5	79.6	NA
1574	Wang (2023a)	et	al.	Dextra Co., Ltd (Dongguan, China)	GFRP	9.5	Vinylester	SWSSC solution (IMMR)	23	270	5	74.6	NA
1575	Wang (2023a)	et	al.	Dextra Co., Ltd (Dongguan, China)	GFRP	9.5	Vinylester	SWSSC solution (IMMR)	23	360	5	70.3	99.5
1576	Wang (2023a)	et	al.	Dextra Co., Ltd (Dongguan, China)	GFRP	9.5	Vinylester	SWSSC solution (IMMR)	40	45	5	88.4	NA
1577	Wang (2023a)	et	al.	Dextra Co., Ltd (Dongguan, China)	GFRP	9.5	Vinylester	SWSSC solution (IMMR)	40	90	5	74.8	NA
1578	Wang (2023a)	et	al.	Dextra Co., Ltd (Dongguan, China)	GFRP	9.5	Vinylester	SWSSC solution (IMMR)	40	180	5	59.7	NA
1579	Wang (2023a)	et	al.	Dextra Co., Ltd (Dongguan, China)	GFRP	9.5	Vinylester	SWSSC solution (IMMR)	40	270	5	49.5	NA
1580	Wang (2023a)	et	al.	Dextra Co., Ltd (Dongguan, China)	GFRP	9.5	Vinylester	SWSSC solution (IMMR)	40	360	5	44.8	99.2
1581	Wang (2023a)	et	al.	Dextra Co., Ltd (Dongguan, China)	GFRP	9.5	Vinylester	SWSSC solution (IMMR)	60	45	5	50.2	NA
1582	Wang	et	al.	Dextra Co., Ltd (Dongguan,	GFRP	9.5	Vinylester	SWSSC solution (IMMR)	60	90	5	37.8	NA

	(2023a)			China)									
1583	Wang (2023a)	et	al.	Dextra Co., Ltd (Dongguan, China)	GFRP	9.5	Vinylester	SWSSC solution (IMMR)	60	180	5	36.6	NA
1584	Wang (2023a)	et	al.	Dextra Co., Ltd (Dongguan, China)	GFRP	9.5	Vinylester	SWSSC solution (IMMR)	60	270	5	32.4	NA
1585	Wang (2023a)	et	al.	Dextra Co., Ltd (Dongguan, China)	GFRP	9.5	Vinylester	SWSSC solution (IMMR)	60	360	5	31.9	104.4
1586	Wang (2023b)	et	al.	NA	GFRP	6.0	Epoxy	Control	RT	0	6	100.0	100.0
1587	Wang (2023b)	et	al.	NA	GFRP	6.0	Epoxy	Alkaline solution (IMMR)	30	30	6	97.7	102.6
1588	Wang (2023b)	et	al.	NA	GFRP	6.0	Epoxy	Alkaline solution (IMMR)	30	60	6	98.6	99.2
1589	Wang (2023b)	et	al.	NA	GFRP	6.0	Epoxy	Alkaline solution (IMMR)	30	90	6	97.0	100.9
1590	Wang (2023b)	et	al.	NA	GFRP	6.0	Epoxy	Alkaline solution (IMMR)	30	180	6	95.7	100.5
1591	Wang (2023b)	et	al.	NA	GFRP	6.0	Epoxy	Alkaline solution (IMMR)	45	30	6	98.1	100.2
1592	Wang (2023b)	et	al.	NA	GFRP	6.0	Epoxy	Alkaline solution (IMMR)	45	60	6	98.1	97.5
1593	Wang (2023b)	et	al.	NA	GFRP	6.0	Epoxy	Alkaline solution (IMMR)	45	90	6	97.5	99.4
1594	Wang (2023b)	et	al.	NA	GFRP	6.0	Epoxy	Alkaline solution (IMMR)	45	180	6	90.7	102.0
1595	Wang (2023b)	et	al.	NA	GFRP	6.0	Epoxy	Alkaline solution (IMMR)	60	30	6	95.6	101.3
1596	Wang (2023b)	et	al.	NA	GFRP	6.0	Epoxy	Alkaline solution (IMMR)	60	60	6	92.2	97.2
1597	Wang (2023b)	et	al.	NA	GFRP	6.0	Epoxy	Alkaline solution (IMMR)	60	90	6	83.0	96.6
1598	Wang (2023b)	et	al.	NA	GFRP	6.0	Epoxy	Alkaline solution (IMMR)	60	180	6	59.3	99.2
1599	Wang (2023b)	et	al.	NA	GFRP	6.0	Epoxy	Alkaline solution (IMMR)	30	30	6	100.0	98.1
1600	Wang (2023b)	et	al.	NA	GFRP	6.0	Epoxy	Alkaline solution (IMMR)	30	60	6	97.3	98.7
1601	Wang (2023b)	et	al.	NA	GFRP	6.0	Epoxy	Alkaline solution (IMMR)	30	90	6	96.9	99.0
1602	Wang (2023b)	et	al.	NA	GFRP	6.0	Epoxy	Alkaline solution (IMMR)	30	180	6	95.9	100.2
1603	Wang (2023b)	et	al.	NA	GFRP	6.0	Epoxy	Alkaline solution (IMMR)	45	30	6	99.1	98.1
1604	Wang (2023b)	et	al.	NA	GFRP	6.0	Epoxy	Alkaline solution (IMMR)	45	60	6	96.8	99.4
1605	Wang	et	al.	NA	GFRP	6.0	Epoxy	Alkaline solution (IMMR)	45	90	6	95.4	97.7

	(2023b)												
1606	Wang et al. (2023b)			NA	GFRP	6.0	Epoxy	Alkaline solution (IMMR)	45	180	6	78.9	100.0
1607	Wang et al. (2023b)			NA	GFRP	6.0	Epoxy	Alkaline solution (IMMR)	60	30	6	94.7	97.9
1608	Wang et al. (2023b)			NA	GFRP	6.0	Epoxy	Alkaline solution (IMMR)	60	60	6	85.3	98.5
1609	Wang et al. (2023b)			NA	GFRP	6.0	Epoxy	Alkaline solution (IMMR)	60	90	6	73.6	97.9
1610	Wang et al. (2023b)			NA	GFRP	6.0	Epoxy	Alkaline solution (IMMR)	60	180	6	43.1	96.8
1611	Wang et al. (2023b)			NA	BFRP	6.0	Epoxy	Control	RT	0	6	100.0	100.0
1612	Wang et al. (2023b)			NA	BFRP	6.0	Epoxy	Alkaline solution (IMMR)	30	30	6	96.6	102.0
1613	Wang et al. (2023b)			NA	BFRP	6.0	Epoxy	Alkaline solution (IMMR)	30	60	6	90.5	101.6
1614	Wang et al. (2023b)			NA	BFRP	6.0	Epoxy	Alkaline solution (IMMR)	30	90	6	91.4	104.4
1615	Wang et al. (2023b)			NA	BFRP	6.0	Epoxy	Alkaline solution (IMMR)	30	180	6	81.1	99.0
1616	Wang et al. (2023b)			NA	BFRP	6.0	Epoxy	Alkaline solution (IMMR)	45	30	6	92.4	101.8
1617	Wang et al. (2023b)			NA	BFRP	6.0	Epoxy	Alkaline solution (IMMR)	45	60	6	89.3	104.2
1618	Wang et al. (2023b)			NA	BFRP	6.0	Epoxy	Alkaline solution (IMMR)	45	90	6	83.6	101.2
1619	Wang et al. (2023b)			NA	BFRP	6.0	Epoxy	Alkaline solution (IMMR)	45	180	6	60.3	101.0
1620	Wang et al. (2023b)			NA	BFRP	6.0	Epoxy	Alkaline solution (IMMR)	60	30	6	69.9	97.8
1621	Wang et al. (2023b)			NA	BFRP	6.0	Epoxy	Alkaline solution (IMMR)	60	60	6	64.0	98.2
1622	Wang et al. (2023b)			NA	BFRP	6.0	Epoxy	Alkaline solution (IMMR)	60	90	6	52.5	107.3
1623	Wang et al. (2023b)			NA	BFRP	6.0	Epoxy	Alkaline solution (IMMR)	30	30	6	94.5	101.8
1624	Wang et al. (2023b)			NA	BFRP	6.0	Epoxy	Alkaline solution (IMMR)	30	60	6	90.2	101.0
1625	Wang et al. (2023b)			NA	BFRP	6.0	Epoxy	Alkaline solution (IMMR)	30	90	6	91.5	104.2
1626	Wang et al. (2023b)			NA	BFRP	6.0	Epoxy	Alkaline solution (IMMR)	30	180	6	85.4	100.8
1627	Wang et al. (2023b)			NA	BFRP	6.0	Epoxy	Alkaline solution (IMMR)	45	30	6	93.5	100.8
1628	Wang	et	al.	NA	BFRP	6.0	Epoxy	Alkaline solution (IMMR)	45	60	6	88.0	101.8

	(2023b)										
1629	Wang et al. (2023b)	NA	BFRP	6.0	Epoxy	Alkaline solution (IMMR)	45	90	6	79.2	100.4
1630	Wang et al. (2023b)	NA	BFRP	6.0	Epoxy	Alkaline solution (IMMR)	45	180	6	71.3	102.7
1631	Wang et al. (2023b)	NA	BFRP	6.0	Epoxy	Alkaline solution (IMMR)	60	30	6	81.5	101.7
1632	Wang et al. (2023b)	NA	BFRP	6.0	Epoxy	Alkaline solution (IMMR)	60	60	6	68.8	101.9
1633	Wang et al. (2023b)	NA	BFRP	6.0	Epoxy	Alkaline solution (IMMR)	60	90	6	67.9	101.7
1634	Wang et al. (2023b)	NA	BFRP	6.0	Epoxy	Alkaline solution (IMMR)	60	180	6	50.2	101.1
1635	Won and Park (2006)	NA	CFRP	9.0	Vinylester	Control	NA	0	6	100.0	NA
1636	Won and Park (2006)	NA	CFRP	9.0	Vinylester	Alkaline solution (IMMR)	60	50	6	84.0	NA
1637	Won and Park (2006)	NA	CFRP	9.0	Vinylester	Acid solution (IMMR)	60	50	6	92.0	NA
1638	Won and Park (2006)	NA	CFRP	9.0	Vinylester	Saline solution 1 (IMMR)	60	50	6	89.0	NA
1639	Won and Park (2006)	NA	CFRP	9.0	Vinylester	Water (IMMR)	60	50	6	87.8	NA
1640	Won and Park (2006)	NA	CFRP	9.0	Vinylester	Water (WD)	23/60	50	6	92.8	NA
1641	Won and Park (2006)	NA	CFRP	9.0	Vinylester	HT	60	50	6	89.0	NA
1642	Won and Park (2006)	NA	CFRP	9.0	Vinylester	Water (FT)	-18/4	50	6	92.8	NA
1643	Won and Park (2006)	NA	CFRP	9.0	Vinylester	Saline solution 2 (IMMR)	23	50	6	92.8	NA
1644	Won and Park (2006)	NA	CFRP	9.0	Vinylester	Saline solution 3 (IMMR)	23	50	6	91.1	NA
1645	Won and Park (2006)	NA	GFRP	9.0	Vinylester	Control	NA	0	6	100.0	NA
1646	Won and Park (2006)	NA	GFRP	9.0	Vinylester	Alkaline solution (IMMR)	60	50	6	79.7	NA
1647	Won and Park (2006)	NA	GFRP	9.0	Vinylester	Saline solution 1 (IMMR)	60	50	6	81.0	NA
1648	Won and Park (2006)	NA	GFRP	9.0	Vinylester	Acid solution (IMMR)	60	50	6	78.9	NA
1649	Won and Park (2006)	NA	GFRP	9.0	Vinylester	Water (IMMR)	60	50	6	76.8	NA
1650	Won and Park (2006)	NA	GFRP	9.0	Vinylester	Water (WD)	23/60	50	6	94.9	NA
1651	Won and Park	NA	GFRP	9.0	Vinylester	HT	60	50	6	91.1	NA

	(2006)										
1652	Won and Park (2006)	NA	GFRP	9.0	Vinylester	Water (FT)	-18/4	50	6	84.0	NA
1653	Won and Park (2006)	NA	GFRP	9.0	Vinylester	Saline solution 2 (IMMR)	23	50	6	86.1	NA
1654	Won and Park (2006)	NA	GFRP	9.0	Vinylester	Saline solution 3 (IMMR)	23	50	6	81.0	NA
1655	Won et al. (2008)	Hughes Brothers Company (Seward, NE, USA)	GFRP	12.7	Vinylester	Control	22	0	NA	100.0	NA
1656	Won et al. (2008)	Hughes Brothers Company (Seward, NE, USA)	GFRP	12.7	Vinylester	Water (IMMR)	20	50	NA	99.0	NA
1657	Won et al. (2008)	Hughes Brothers Company (Seward, NE, USA)	GFRP	12.7	Vinylester	Water (IMMR)	20	100	NA	97.0	NA
1658	Won et al. (2008)	Hughes Brothers Company (Seward, NE, USA)	GFRP	12.7	Vinylester	Alkaline solution (IMMR)	20	30	NA	99.2	NA
1659	Won et al. (2008)	Hughes Brothers Company (Seward, NE, USA)	GFRP	12.7	Vinylester	Alkaline solution (IMMR)	20	60	NA	97.3	NA
1660	Won et al. (2008)	Hughes Brothers Company (Seward, NE, USA)	GFRP	12.7	Vinylester	Alkaline solution (IMMR)	20	90	NA	94.1	NA
1661	Won et al. (2008)	Hughes Brothers Company (Seward, NE, USA)	GFRP	12.7	Vinylester	Alkaline solution (IMMR)	20	180	NA	87.4	NA
1662	Won et al. (2008)	Hughes Brothers Company (Seward, NE, USA)	GFRP	12.7	Vinylester	Alkaline solution (IMMR)	20	240	NA	87.4	NA
1663	Won et al. (2008)	Hughes Brothers Company (Seward, NE, USA)	GFRP	12.7	Vinylester	Alkaline solution (IMMR)	20	300	NA	82.9	NA
1664	Won et al. (2008)	Hughes Brothers Company (Seward, NE, USA)	GFRP	12.7	Vinylester	Alkaline solution (IMMR)	40	30	NA	98.2	NA
1665	Won et al. (2008)	Hughes Brothers Company (Seward, NE, USA)	GFRP	12.7	Vinylester	Alkaline solution (IMMR)	40	60	NA	95.4	NA
1666	Won et al. (2008)	Hughes Brothers Company (Seward, NE, USA)	GFRP	12.7	Vinylester	Alkaline solution (IMMR)	40	90	NA	92.2	NA
1667	Won et al. (2008)	Hughes Brothers Company (Seward, NE, USA)	GFRP	12.7	Vinylester	Alkaline solution (IMMR)	40	180	NA	85.4	NA
1668	Won et al. (2008)	Hughes Brothers Company (Seward, NE, USA)	GFRP	12.7	Vinylester	Alkaline solution (IMMR)	40	240	NA	78.1	NA
1669	Won et al. (2008)	Hughes Brothers Company (Seward, NE, USA)	GFRP	12.7	Vinylester	Alkaline solution (IMMR)	40	300	NA	70.1	NA
1670	Won et al. (2008)	Hughes Brothers Company (Seward, NE, USA)	GFRP	12.7	Vinylester	Alkaline solution (IMMR)	60	30	NA	90.9	NA
1671	Won et al. (2008)	Hughes Brothers Company (Seward, NE, USA)	GFRP	12.7	Vinylester	Alkaline solution (IMMR)	60	60	NA	85.8	NA
1672	Won et al. (2008)	Hughes Brothers Company (Seward, NE, USA)	GFRP	12.7	Vinylester	Alkaline solution (IMMR)	60	90	NA	74.9	NA
1673	Won et al. (2008)	Hughes Brothers Company (Seward, NE, USA)	GFRP	12.7	Vinylester	Alkaline solution (IMMR)	60	180	NA	73.9	NA
1674	Won et al. (2008)	Hughes Brothers Company	GFRP	12.7	Vinylester	Alkaline solution (IMMR)	60	240	NA	73.3	NA

		(Seward, NE, USA)									
1675	Won et al. (2008)	Hughes Brothers Company (Seward, NE, USA)	GFRP	12.7	Vinylester	Alkaline solution (IMMR)	60	300	NA	69.1	NA
1676	Won et al. (2008)	Hughes Brothers Company (Seward, NE, USA)	GFRP	12.7	Vinylester	Alkaline solution (IMMR)	80	30	NA	82.2	NA
1677	Won et al. (2008)	Hughes Brothers Company (Seward, NE, USA)	GFRP	12.7	Vinylester	Alkaline solution (IMMR)	80	60	NA	80.0	NA
1678	Won et al. (2008)	Hughes Brothers Company (Seward, NE, USA)	GFRP	12.7	Vinylester	Alkaline solution (IMMR)	80	90	NA	74.2	NA
1679	Won et al. (2008)	Hughes Brothers Company (Seward, NE, USA)	GFRP	12.7	Vinylester	Alkaline solution (IMMR)	80	180	NA	70.1	NA
1680	Won et al. (2008)	Hughes Brothers Company (Seward, NE, USA)	GFRP	12.7	Vinylester	Alkaline solution (IMMR)	80	240	NA	69.8	NA
1681	Won et al. (2008)	Hughes Brothers Company (Seward, NE, USA)	GFRP	12.7	Vinylester	Alkaline solution (IMMR)	80	300	NA	64.0	NA
1682	Won et al. (2013)	Hughes Brothers Company (Seward, NE, USA)	GFRP	6.0	Vinylester	Control	NA	0	NA	100.0	NA
1683	Won et al. (2013)	Hughes Brothers Company (Seward, NE, USA)	GFRP	6.0	Vinylester	Saline solution 1 (IMMR)	60	50	NA	91.7	NA
1684	Won et al. (2013)	Hughes Brothers Company (Seward, NE, USA)	GFRP	6.0	Vinylester	Saline solution 2 (IMMR)	20	50	NA	97.9	NA
1685	Won et al. (2013)	Hughes Brothers Company (Seward, NE, USA)	GFRP	6.0	Vinylester	Saline solution 3 (IMMR)	20	50	NA	89.6	NA
1686	Won et al. (2013)	Hughes Brothers Company (Seward, NE, USA)	GFRP	6.0	Vinylester	Saline solution 1 (WD)	20/60	50	NA	79.1	NA
1687	Won et al. (2013)	Hughes Brothers Company (Seward, NE, USA)	GFRP	6.0	Vinylester	Saline solution 4 (FT)	-10/20	50	NA	79.1	NA
1688	Wu et al. (2014)	NA	BFRP	6.0	Vinylester	Control	NA	0	5	100.0	100.0
1689	Wu et al. (2014)	NA	BFRP	6.0	Vinylester	Alkaline solution (IMMR)	25	21	5	77.1	98.4
1690	Wu et al. (2014)	NA	BFRP	6.0	Vinylester	Alkaline solution (IMMR)	25	42	5	69.6	97.4
1691	Wu et al. (2014)	NA	BFRP	6.0	Vinylester	Alkaline solution (IMMR)	25	63	5	69.4	97.8
1692	Wu et al. (2014)	NA	BFRP	6.0	Vinylester	Alkaline solution (IMMR)	55	21	5	66.8	98.6
1693	Wu et al. (2014)	NA	BFRP	6.0	Vinylester	Alkaline solution (IMMR)	55	42	5	61.7	96.4
1694	Wu et al. (2014)	NA	BFRP	6.0	Vinylester	Alkaline solution (IMMR)	55	63	5	60.6	97.7
1695	Wu et al. (2014)	NA	BFRP	12.0	Vinylester	Control	NA	0	5	100.0	100.0
1696	Wu et al. (2014)	NA	BFRP	12.0	Vinylester	Alkaline solution (IMMR)	25	21	5	95.2	103.7
1697	Wu et al. (2014)	NA	BFRP	12.0	Vinylester	Alkaline solution (IMMR)	25	42	5	83.6	104.5
1698	Wu et al. (2014)	NA	BFRP	12.0	Vinylester	Alkaline solution (IMMR)	25	63	5	82.0	103.1
1699	Wu et al. (2014)	NA	BFRP	12.0	Vinylester	Alkaline solution (IMMR)	55	21	5	74.1	101.7
1700	Wu et al. (2014)	NA	BFRP	12.0	Vinylester	Alkaline solution (IMMR)	55	42	5	62.6	103.1
1701	Wu et al. (2014)	NA	BFRP	12.0	Vinylester	Alkaline solution (IMMR)	55	63	5	61.4	98.4
1702	Wu et al. (2015)	NA	BFRP	6.0	Epoxy	Control	25	0	5	100.0	100.0
1703	Wu et al. (2015)	NA	BFRP	6.0	Epoxy	Alkaline solution (IMMR)	25	21	5	99.1	97.8
1704	Wu et al. (2015)	NA	BFRP	6.0	Epoxy	Alkaline solution (IMMR)	25	42	5	97.2	97.8
1705	Wu et al. (2015)	NA	BFRP	6.0	Epoxy	Alkaline solution (IMMR)	25	63	5	94.1	97.8
1706	Wu et al. (2015)	NA	BFRP	6.0	Epoxy	Alkaline solution (IMMR)	40	21	5	90.3	97.8

1707	Wu et al. (2015)	NA	BFRP	6.0	Epoxy	Alkaline solution (IMMR)	40	42	5	88.9	95.7
1708	Wu et al. (2015)	NA	BFRP	6.0	Epoxy	Alkaline solution (IMMR)	40	63	5	84.8	95.7
1709	Wu et al. (2015)	NA	BFRP	6.0	Epoxy	Alkaline solution (IMMR)	55	21	5	82.0	100.0
1710	Wu et al. (2015)	NA	BFRP	6.0	Epoxy	Alkaline solution (IMMR)	55	42	5	76.8	97.8
1711	Wu et al. (2015)	NA	BFRP	6.0	Epoxy	Alkaline solution (IMMR)	55	63	5	68.5	97.8
1712	Wu et al. (2015)	NA	BFRP	6.0	Epoxy	SL (20%fu)+Alkaline solution (IMMR)	40	21	5	93.9	97.8
1713	Wu et al. (2015)	NA	BFRP	6.0	Epoxy	SL (20%fu)+Alkaline solution (IMMR)	40	42	5	90.9	97.8
1714	Wu et al. (2015)	NA	BFRP	6.0	Epoxy	SL (20%fu)+Alkaline solution (IMMR)	40	63	5	83.4	97.8
1715	Wu et al. (2015)	NA	BFRP	6.0	Epoxy	SL (20%fu)+Alkaline solution (IMMR)	55	21	5	84.6	97.8
1716	Wu et al. (2015)	NA	BFRP	6.0	Epoxy	SL (20%fu)+Alkaline solution (IMMR)	55	42	5	69.7	97.8
1717	Wu et al. (2015)	NA	BFRP	6.0	Epoxy	SL (20%fu)+Alkaline solution (IMMR)	55	63	5	60.9	97.8
1718	Wu et al. (2015)	NA	BFRP	6.0	Epoxy	SL (40%%fu)+Alkaline solution (IMMR)	25	21	5	92.3	97.8
1719	Wu et al. (2015)	NA	BFRP	6.0	Epoxy	SL (40%%fu)+Alkaline solution (IMMR)	25	42	5	91.3	97.8
1720	Wu et al. (2015)	NA	BFRP	6.0	Epoxy	SL (40%%fu)+Alkaline solution (IMMR)	25	63	5	87.9	97.8
1721	Wu et al. (2015)	NA	BFRP	6.0	Epoxy	SL (40%%fu)+Alkaline solution (IMMR)	40	21	5	87.8	97.8
1722	Wu et al. (2015)	NA	BFRP	6.0	Epoxy	SL (40%%fu)+Alkaline solution (IMMR)	40	42	5	80.8	95.7
1723	Wu et al. (2015)	NA	BFRP	6.0	Epoxy	SL (40%%fu)+Alkaline solution (IMMR)	40	63	5	78.1	95.7
1724	Wu et al. (2015)	NA	BFRP	6.0	Epoxy	SL (60%fu)+Alkaline solution (IMMR)	40	21	5	85.1	93.5
1725	Wu et al. (2015)	NA	BFRP	6.0	Epoxy	Water (IMMR)	40	42	5	94.4	97.8
1726	Wu et al. (2015)	NA	BFRP	6.0	Epoxy	SL (10%fu)+Water (IMMR)	40	42	5	91.2	100.0
1727	Wu et al. (2015)	NA	BFRP	6.0	Epoxy	Simulated seawater (IMMR)	40	42	5	94.4	97.8
1728	Wu et al. (2015)	NA	BFRP	6.0	Epoxy	SL (10%fu)+Simulated seawater (IMMR)	40	42	5	92.6	97.8
1729	Wu et al. (2015)	NA	BFRP	6.0	Epoxy	Acid solution (IMMR)	40	42	5	93.1	97.8
1730	Wu et al. (2015)	NA	BFRP	6.0	Epoxy	SL (10%fu)+Acid solution (IMMR)	40	42	5	92.3	97.8
1731	Wu et al. (2022)	NA	GFRP	10.0	Vinylester	Control	NA	0	4	100.0	100.0
1732	Wu et al. (2022)	NA	GFRP	10.0	Vinylester	NCE+Alkaline solution (IMMR)	NA	40	4	92.2	101.4
1733	Wu et al. (2022)	NA	GFRP	10.0	Vinylester	NCE+Alkaline solution (IMMR)	NA	90	4	87.5	101.8
1734	Wu et al. (2022)	NA	GFRP	10.0	Vinylester	NCE+Alkaline solution (IMMR)	NA	180	4	83.8	98.6
1735	Wu et al. (2022)	NA	GFRP	10.0	Vinylester	NCE+Alkaline solution (IMMR)	NA	300	4	82.6	101.6
1736	Wu et al. (2022)	NA	GFRP	10.0	Vinylester	SL (20%Mu)+NCE+Alkaline solution (IMMR)	NA	40	4	87.4	100.8
1737	Wu et al. (2022)	NA	GFRP	10.0	Vinylester	SL (20%Mu)+NCE+Alkaline	NA	90	4	82.6	98.4

						solution (IMMR)					
1738	Wu et al. (2022)	NA	GFRP	10.0	Vinylester	SL (20%Mu)+NCE+Alkaline solution (IMMR)	NA	180	4	77.2	97.5
1739	Wu et al. (2022)	NA	GFRP	10.0	Vinylester	SL (20%Mu)+NCE+Alkaline solution (IMMR)	NA	300	4	73.6	97.3
1740	Wu et al. (2022)	NA	GFRP	10.0	Vinylester	SL (20%Mu)+NCE+Alkaline solution (IMMR)	NA	2880	4	70.6	100.6
1741	Wu et al. (2022)	NA	GFRP	10.0	Vinylester	Pre-cracks+NCE+Alkaline solution (IMMR)	NA	40	4	81.4	NA
1742	Wu et al. (2022)	NA	GFRP	10.0	Vinylester	Pre-cracks+NCE+Alkaline solution (IMMR)	NA	90	4	73.7	NA
1743	Wu et al. (2022)	NA	GFRP	10.0	Vinylester	Pre-cracks+NCE+Alkaline solution (IMMR)	NA	180	4	68.6	NA
1744	Wu et al. (2022)	NA	GFRP	10.0	Vinylester	Pre-cracks+NCE+Alkaline solution (IMMR)	NA	300	4	63.1	NA
1745	Wu et al. (2022)	NA	GFRP	10.0	Vinylester	Pre-cracks+SL (20%Mu)+NCE+Alkaline solution (IMMR)	NA	40	4	75.8	NA
1746	Wu et al. (2022)	NA	GFRP	10.0	Vinylester	Pre-cracks+SL (20%Mu)+NCE+Alkaline solution (IMMR)	NA	90	4	68.2	NA
1747	Wu et al. (2022)	NA	GFRP	10.0	Vinylester	Pre-cracks+SL (20%Mu)+NCE+Alkaline solution (IMMR)	NA	180	4	62.8	NA
1748	Wu et al. (2022)	NA	GFRP	10.0	Vinylester	Pre-cracks+SL (20%Mu)+NCE+Alkaline solution (IMMR)	NA	300	4	54.4	NA
1749	Wu et al. (2022)	NA	GFRP	10.0	Vinylester	Pre-cracks+SL (20%Mu)+NCE+Alkaline solution (IMMR)	NA	2880	4	49.0	NA
1750	Yi et al. (2022)	Jiangsu Green Materials Vally New Material T&D Co., Ltd (Nanjing, China)	BFRP	8.0	Epoxy	Control	25	0	4	100.0	100.0
1751	Yi et al. (2022)	Jiangsu Green Materials Vally New Material T&D Co., Ltd (Nanjing, China)	BFRP	8.0	Epoxy	SWSSC solution 1 (IMMR)	25	180	4	84.6	93.6
1752	Yi et al. (2022)	Jiangsu Green Materials Vally New Material T&D Co., Ltd (Nanjing, China)	BFRP	8.0	Epoxy	SWSSC solution 1 (IMMR)	25	360	4	70.0	92.2
1753	Yi et al. (2022)	Jiangsu Green Materials Vally New Material T&D Co., Ltd (Nanjing, China)	BFRP	8.0	Epoxy	SWSSC solution 1 (IMMR)	25	540	4	62.8	91.0
1754	Yi et al. (2022)	Jiangsu Green Materials Vally New Material T&D Co., Ltd (Nanjing, China)	BFRP	8.0	Epoxy	SWSSC solution 1 (IMMR)	40	60	4	77.5	93.6
1755	Yi et al. (2022)	Jiangsu Green Materials	BFRP	8.0	Epoxy	SWSSC solution 1 (IMMR)	40	180	4	54.7	89.4

		Vally New Material T&D Co., Ltd (Nanjing, China)									
1756	Yi et al. (2022)	Jiangsu Green Materials Vally New Material T&D Co., Ltd (Nanjing, China)	BFRP	8.0	Epoxy	SWSSC solution 1 (IMMR)	40	270	4	43.5	89.4
1757	Yi et al. (2022)	Jiangsu Green Materials Vally New Material T&D Co., Ltd (Nanjing, China)	BFRP	8.0	Epoxy	SWSSC solution 1 (IMMR)	55	30	4	79.1	93.4
1758	Yi et al. (2022)	Jiangsu Green Materials Vally New Material T&D Co., Ltd (Nanjing, China)	BFRP	8.0	Epoxy	SWSSC solution 1 (IMMR)	55	90	4	39.9	83.5
1759	Yi et al. (2022)	Jiangsu Green Materials Vally New Material T&D Co., Ltd (Nanjing, China)	BFRP	8.0	Epoxy	SWSSC solution 1 (IMMR)	55	180	4	25.2	81.6
1760	Yi et al. (2022)	Jiangsu Green Materials Vally New Material T&D Co., Ltd (Nanjing, China)	BFRP	8.0	Epoxy	SWSSC solution 2 (IMMR)	25	180	4	88.5	94.3
1761	Yi et al. (2022)	Jiangsu Green Materials Vally New Material T&D Co., Ltd (Nanjing, China)	BFRP	8.0	Epoxy	SWSSC solution 2 (IMMR)	25	360	4	87.0	94.5
1762	Yi et al. (2022)	Jiangsu Green Materials Vally New Material T&D Co., Ltd (Nanjing, China)	BFRP	8.0	Epoxy	SWSSC solution 2 (IMMR)	25	540	4	83.4	93.6
1763	Yi et al. (2022)	Jiangsu Green Materials Vally New Material T&D Co., Ltd (Nanjing, China)	BFRP	8.0	Epoxy	SWSSC solution 2 (IMMR)	40	60	4	85.7	94.8
1764	Yi et al. (2022)	Jiangsu Green Materials Vally New Material T&D Co., Ltd (Nanjing, China)	BFRP	8.0	Epoxy	SWSSC solution 2 (IMMR)	40	180	4	76.4	95.2
1765	Yi et al. (2022)	Jiangsu Green Materials Vally New Material T&D Co., Ltd (Nanjing, China)	BFRP	8.0	Epoxy	SWSSC solution 2 (IMMR)	40	270	4	73.0	93.1
1766	Yi et al. (2022)	Jiangsu Green Materials Vally New Material T&D Co., Ltd (Nanjing, China)	BFRP	8.0	Epoxy	SWSSC solution 2 (IMMR)	55	30	4	84.0	94.2
1767	Yi et al. (2022)	Jiangsu Green Materials Vally New Material T&D Co., Ltd (Nanjing, China)	BFRP	8.0	Epoxy	SWSSC solution 2 (IMMR)	55	90	4	70.1	94.8
1768	Yi et al. (2022)	Jiangsu Green Materials Vally New Material T&D Co., Ltd (Nanjing, China)	BFRP	8.0	Epoxy	SWSSC solution 2 (IMMR)	55	180	4	68.1	92.1
1769	Yi et al. (2022)	Jiangsu Green Materials Vally New Material T&D Co., Ltd (Nanjing, China)	BFRP	8.0	Epoxy	SWSSC solution 3 (IMMR)	25	180	4	88.6	94.9
1770	Yi et al. (2022)	Jiangsu Green Materials Vally New Material T&D	BFRP	8.0	Epoxy	SWSSC solution 3 (IMMR)	25	360	4	86.2	94.4

		Co., Ltd (Nanjing, China)									
1771	Yi et al. (2022)	Jiangsu Green Materials Vally New Material T&D Co., Ltd (Nanjing, China)	BFRP	8.0	Epoxy	SWSSC solution 3 (IMMR)	25	540	4	84.8	94.7
1772	Yi et al. (2022)	Jiangsu Green Materials Vally New Material T&D Co., Ltd (Nanjing, China)	BFRP	8.0	Epoxy	SWSSC solution 3 (IMMR)	40	60	4	86.3	95.2
1773	Yi et al. (2022)	Jiangsu Green Materials Vally New Material T&D Co., Ltd (Nanjing, China)	BFRP	8.0	Epoxy	SWSSC solution 3 (IMMR)	40	180	4	78.2	94.5
1774	Yi et al. (2022)	Jiangsu Green Materials Vally New Material T&D Co., Ltd (Nanjing, China)	BFRP	8.0	Epoxy	SWSSC solution 3 (IMMR)	40	270	4	74.7	94.4
1775	Yi et al. (2022)	Jiangsu Green Materials Vally New Material T&D Co., Ltd (Nanjing, China)	BFRP	8.0	Epoxy	SWSSC solution 3 (IMMR)	55	30	4	85.7	95.1
1776	Yi et al. (2022)	Jiangsu Green Materials Vally New Material T&D Co., Ltd (Nanjing, China)	BFRP	8.0	Epoxy	SWSSC solution 3 (IMMR)	55	90	4	71.2	95.5
1777	Yi et al. (2022)	Jiangsu Green Materials Vally New Material T&D Co., Ltd (Nanjing, China)	BFRP	8.0	Epoxy	SWSSC solution 3 (IMMR)	55	180	4	68.7	94.6
1778	Yi et al. (2022)	Jiangsu Green Materials Vally New Material T&D Co., Ltd (Nanjing, China)	BFRP	8.0	Epoxy	SWSSCE 1+Simulated seawater (IMMR)	25	180	4	86.9	92.5
1779	Yi et al. (2022)	Jiangsu Green Materials Vally New Material T&D Co., Ltd (Nanjing, China)	BFRP	8.0	Epoxy	SWSSCE 1+Simulated seawater (IMMR)	25	360	4	78.8	94.3
1780	Yi et al. (2022)	Jiangsu Green Materials Vally New Material T&D Co., Ltd (Nanjing, China)	BFRP	8.0	Epoxy	SWSSCE 1+Simulated seawater (IMMR)	25	540	4	77.9	92.7
1781	Yi et al. (2022)	Jiangsu Green Materials Vally New Material T&D Co., Ltd (Nanjing, China)	BFRP	8.0	Epoxy	SWSSCE 1+Simulated seawater (IMMR)	40	90	4	75.4	99.9
1782	Yi et al. (2022)	Jiangsu Green Materials Vally New Material T&D Co., Ltd (Nanjing, China)	BFRP	8.0	Epoxy	SWSSCE 1+Simulated seawater (IMMR)	40	180	4	61.5	98.4
1783	Yi et al. (2022)	Jiangsu Green Materials Vally New Material T&D Co., Ltd (Nanjing, China)	BFRP	8.0	Epoxy	SWSSCE 1+Simulated seawater (IMMR)	40	270	4	55.3	93.6
1784	Yi et al. (2022)	Jiangsu Green Materials Vally New Material T&D Co., Ltd (Nanjing, China)	BFRP	8.0	Epoxy	SWSSCE 1+Simulated seawater (IMMR)	55	90	4	60.8	94.8
1785	Yi et al. (2022)	Jiangsu Green Materials Vally New Material T&D Co., Ltd (Nanjing, China)	BFRP	8.0	Epoxy	SWSSCE 1+Simulated seawater (IMMR)	55	180	4	47.0	90.2

1786	Yi et al. (2022)	Jiangsu Green Materials Vally New Material T&D Co., Ltd (Nanjing, China)	BFRP	8.0	Epoxy	SWSSCE (IMMR)	1+Simulated	seawater	55	270	4	46.1	89.5
1787	Yi et al. (2022)	Jiangsu Green Materials Vally New Material T&D Co., Ltd (Nanjing, China)	BFRP	8.0	Epoxy	SWSSCE (IMMR)	2+Simulated	seawater	25	180	4	88.5	93.5
1788	Yi et al. (2022)	Jiangsu Green Materials Vally New Material T&D Co., Ltd (Nanjing, China)	BFRP	8.0	Epoxy	SWSSCE (IMMR)	2+Simulated	seawater	25	360	4	87.5	94.5
1789	Yi et al. (2022)	Jiangsu Green Materials Vally New Material T&D Co., Ltd (Nanjing, China)	BFRP	8.0	Epoxy	SWSSCE (IMMR)	2+Simulated	seawater	25	540	4	86.4	93.5
1790	Yi et al. (2022)	Jiangsu Green Materials Vally New Material T&D Co., Ltd (Nanjing, China)	BFRP	8.0	Epoxy	SWSSCE (IMMR)	2+Simulated	seawater	40	90	4	95.0	101.2
1791	Yi et al. (2022)	Jiangsu Green Materials Vally New Material T&D Co., Ltd (Nanjing, China)	BFRP	8.0	Epoxy	SWSSCE (IMMR)	2+Simulated	seawater	40	180	4	92.8	101.2
1792	Yi et al. (2022)	Jiangsu Green Materials Vally New Material T&D Co., Ltd (Nanjing, China)	BFRP	8.0	Epoxy	SWSSCE (IMMR)	2+Simulated	seawater	40	270	4	89.7	102.0
1793	Yi et al. (2022)	Jiangsu Green Materials Vally New Material T&D Co., Ltd (Nanjing, China)	BFRP	8.0	Epoxy	SWSSCE (IMMR)	2+Simulated	seawater	55	90	4	89.0	101.3
1794	Yi et al. (2022)	Jiangsu Green Materials Vally New Material T&D Co., Ltd (Nanjing, China)	BFRP	8.0	Epoxy	SWSSCE (IMMR)	2+Simulated	seawater	55	180	4	86.5	101.5
1795	Yi et al. (2022)	Jiangsu Green Materials Vally New Material T&D Co., Ltd (Nanjing, China)	BFRP	8.0	Epoxy	SWSSCE (IMMR)	2+Simulated	seawater	55	270	4	85.1	101.9
1796	Yi et al. (2022)	Jiangsu Green Materials Vally New Material T&D Co., Ltd (Nanjing, China)	BFRP	8.0	Epoxy	SWSSCE (IMMR)	3+Simulated	seawater	25	180	4	92.2	94.3
1797	Yi et al. (2022)	Jiangsu Green Materials Vally New Material T&D Co., Ltd (Nanjing, China)	BFRP	8.0	Epoxy	SWSSCE (IMMR)	3+Simulated	seawater	25	360	4	86.4	93.3
1798	Yi et al. (2022)	Jiangsu Green Materials Vally New Material T&D Co., Ltd (Nanjing, China)	BFRP	8.0	Epoxy	SWSSCE (IMMR)	3+Simulated	seawater	25	540	4	87.4	93.5
1799	Yi et al. (2022)	Jiangsu Green Materials Vally New Material T&D Co., Ltd (Nanjing, China)	BFRP	8.0	Epoxy	SWSSCE (IMMR)	3+Simulated	seawater	40	90	4	93.9	101.2
1800	Yi et al. (2022)	Jiangsu Green Materials Vally New Material T&D Co., Ltd (Nanjing, China)	BFRP	8.0	Epoxy	SWSSCE (IMMR)	3+Simulated	seawater	40	180	4	91.0	102.2
1801	Yi et al. (2022)	Jiangsu Green Materials	BFRP	8.0	Epoxy	SWSSCE	3+Simulated	seawater	40	270	4	90.4	101.5

		Vally New Material T&D Co., Ltd (Nanjing, China)				(IMMR)							
1802	Yi et al. (2022)	Jiangsu Green Materials Vally New Material T&D Co., Ltd (Nanjing, China)	BFRP	8.0	Epoxy	SWSSCE (IMMR)	3+Simulated	seawater	55	90	4	90.7	102.1
1803	Yi et al. (2022)	Jiangsu Green Materials Vally New Material T&D Co., Ltd (Nanjing, China)	BFRP	8.0	Epoxy	SWSSCE (IMMR)	3+Simulated	seawater	55	180	4	87.0	101.2
1804	Yi et al. (2022)	Jiangsu Green Materials Vally New Material T&D Co., Ltd (Nanjing, China)	BFRP	8.0	Epoxy	SWSSCE (IMMR)	3+Simulated	seawater	55	270	4	86.4	101.8
1805	Yin et al. (2022)	NA	BFRP	8.0	Epoxy	Control			NA	0	3	100.0	100.0
1806	Yin et al. (2022)	NA	BFRP	8.0	Epoxy	SWSSCE (WD)	1+Simulated	seawater	NA	0	3	95.7	98.0
1807	Yin et al. (2022)	NA	BFRP	8.0	Epoxy	SWSSCE (WD)	1+Simulated	seawater	30	60	3	88.3	117.6
1808	Yin et al. (2022)	NA	BFRP	8.0	Epoxy	SWSSCE (WD)	1+Simulated	seawater	30	120	3	79.8	95.2
1809	Yin et al. (2022)	NA	BFRP	8.0	Epoxy	SWSSCE (WD)	1+Simulated	seawater	30	180	3	76.6	96.6
1810	Yin et al. (2022)	NA	BFRP	8.0	Epoxy	SWSSCE (WD)	1+Simulated	seawater	45	60	3	88.0	96.3
1811	Yin et al. (2022)	NA	BFRP	8.0	Epoxy	SWSSCE (WD)	1+Simulated	seawater	45	120	3	75.9	101.4
1812	Yin et al. (2022)	NA	BFRP	8.0	Epoxy	SWSSCE (WD)	1+Simulated	seawater	45	180	3	70.5	96.6
1813	Yin et al. (2022)	NA	BFRP	8.0	Epoxy	SWSSCE (WD)	1+Simulated	seawater	60	60	3	84.2	97.3
1814	Yin et al. (2022)	NA	BFRP	8.0	Epoxy	SWSSCE (WD)	1+Simulated	seawater	60	120	3	68.0	86.8
1815	Yin et al. (2022)	NA	BFRP	8.0	Epoxy	SWSSCE (WD)	1+Simulated	seawater	60	180	3	58.1	95.6
1816	Yin et al. (2022)	NA	BFRP	8.0	Epoxy	SWSSCE (WD)	1+Simulated	seawater	45	180	3	76.7	99.3
1817	Yin et al. (2022)	NA	BFRP	8.0	Epoxy	SWSSCE (WD)	1+Simulated	seawater	45	180	3	60.6	88.2
1818	Yin et al. (2022)	NA	BFRP	8.0	Epoxy	SWSSCE (WD)	2+Simulated	seawater	45	60	3	88.5	99.8
1819	Yin et al. (2022)	NA	BFRP	8.0	Epoxy	SWSSCE (WD)	2+Simulated	seawater	45	120	3	76.9	92.5
1820	Yin et al. (2022)	NA	BFRP	8.0	Epoxy	SWSSCE (WD)	2+Simulated	seawater	45	180	3	68.7	96.9
1821	Yin et al. (2022)	NA	BFRP	8.0	Epoxy	SWSSCE (WD)	3+Simulated	seawater	45	60	3	81.4	103.3
1822	Yin et al. (2022)	NA	BFRP	8.0	Epoxy	SWSSCE (WD)	3+Simulated	seawater	45	120	3	73.9	94.0

1823	Yin et al. (2022)	NA	BFRP	8.0	Epoxy	SWSSCE 3+Simulated seawater (WD)	45	180	3	63.7	93.8
1824	Yue et al. (2024)	Jiangsu Hengde New Materials Co., Ltd. (Jiangsu, China)	GFRP	12.0	Epoxy	Control	20	0	3	100.0	NA
1825	Yue et al. (2024)	Jiangsu Hengde New Materials Co., Ltd. (Jiangsu, China)	GFRP	12.0	Epoxy	Alkaline solution (IMMR)	20	15	3	100.0	NA
1826	Yue et al. (2024)	Jiangsu Hengde New Materials Co., Ltd. (Jiangsu, China)	GFRP	12.0	Epoxy	Alkaline solution (IMMR)	20	30	3	99.5	NA
1827	Yue et al. (2024)	Jiangsu Hengde New Materials Co., Ltd. (Jiangsu, China)	GFRP	12.0	Epoxy	Alkaline solution (IMMR)	20	45	3	98.6	NA
1828	Yue et al. (2024)	Jiangsu Hengde New Materials Co., Ltd. (Jiangsu, China)	GFRP	12.0	Epoxy	Alkaline solution (IMMR)	20	60	3	95.8	NA
1829	Yue et al. (2024)	Jiangsu Hengde New Materials Co., Ltd. (Jiangsu, China)	GFRP	12.0	Epoxy	Alkaline solution (IMMR)	20	90	3	94.3	NA
1830	Yue et al. (2024)	Jiangsu Hengde New Materials Co., Ltd. (Jiangsu, China)	GFRP	12.0	Epoxy	Alkaline solution (IMMR)	20	120	3	92.9	NA
1831	Yue et al. (2024)	Jiangsu Hengde New Materials Co., Ltd. (Jiangsu, China)	GFRP	12.0	Epoxy	Alkaline solution (IMMR)	40	15	3	100.0	NA
1832	Yue et al. (2024)	Jiangsu Hengde New Materials Co., Ltd. (Jiangsu, China)	GFRP	12.0	Epoxy	Alkaline solution (IMMR)	40	30	3	99.1	NA
1833	Yue et al. (2024)	Jiangsu Hengde New Materials Co., Ltd. (Jiangsu, China)	GFRP	12.0	Epoxy	Alkaline solution (IMMR)	40	45	3	96.7	NA
1834	Yue et al. (2024)	Jiangsu Hengde New Materials Co., Ltd. (Jiangsu, China)	GFRP	12.0	Epoxy	Alkaline solution (IMMR)	40	60	3	95.3	NA
1835	Yue et al. (2024)	Jiangsu Hengde New Materials Co., Ltd. (Jiangsu, China)	GFRP	12.0	Epoxy	Alkaline solution (IMMR)	40	90	3	91.5	NA
1836	Yue et al. (2024)	Jiangsu Hengde New Materials Co., Ltd. (Jiangsu, China)	GFRP	12.0	Epoxy	Alkaline solution (IMMR)	40	120	3	89.2	NA
1837	Yue et al. (2024)	Jiangsu Hengde New Materials Co., Ltd. (Jiangsu, China)	GFRP	12.0	Epoxy	Alkaline solution (IMMR)	60	15	3	97.2	NA
1838	Yue et al. (2024)	Jiangsu Hengde New Materials Co., Ltd.	GFRP	12.0	Epoxy	Alkaline solution (IMMR)	60	30	3	96.7	NA

		(Jiangsu, China)										
1839	Yue et al. (2024)	Jiangsu Hengde New Materials Co., Ltd. (Jiangsu, China)	GFRP	12.0	Epoxy	Alkaline solution (IMMR)	60	45	3	92.9	NA
1840	Yue et al. (2024)	Jiangsu Hengde New Materials Co., Ltd. (Jiangsu, China)	GFRP	12.0	Epoxy	Alkaline solution (IMMR)	60	60	3	91.0	NA
1841	Yue et al. (2024)	Jiangsu Hengde New Materials Co., Ltd. (Jiangsu, China)	GFRP	12.0	Epoxy	Alkaline solution (IMMR)	60	90	3	86.3	NA
1842	Yue et al. (2024)	Jiangsu Hengde New Materials Co., Ltd. (Jiangsu, China)	GFRP	12.0	Epoxy	Alkaline solution (IMMR)	60	120	3	85.9	NA
1843	Yue et al. (2024)	Jiangsu Hengde New Materials Co., Ltd. (Jiangsu, China)	GFRP	12.0	Epoxy	Alkaline solution (IMMR)	20	15	3	99.1	NA
1844	Yue et al. (2024)	Jiangsu Hengde New Materials Co., Ltd. (Jiangsu, China)	GFRP	12.0	Epoxy	Alkaline solution (IMMR)	20	30	3	98.6	NA
1845	Yue et al. (2024)	Jiangsu Hengde New Materials Co., Ltd. (Jiangsu, China)	GFRP	12.0	Epoxy	Alkaline solution (IMMR)	20	45	3	96.2	NA
1846	Yue et al. (2024)	Jiangsu Hengde New Materials Co., Ltd. (Jiangsu, China)	GFRP	12.0	Epoxy	Alkaline solution (IMMR)	20	60	3	90.1	NA
1847	Yue et al. (2024)	Jiangsu Hengde New Materials Co., Ltd. (Jiangsu, China)	GFRP	12.0	Epoxy	Alkaline solution (IMMR)	20	90	3	89.2	NA
1848	Yue et al. (2024)	Jiangsu Hengde New Materials Co., Ltd. (Jiangsu, China)	GFRP	12.0	Epoxy	Alkaline solution (IMMR)	20	120	3	88.7	NA
1849	Yue et al. (2024)	Jiangsu Hengde New Materials Co., Ltd. (Jiangsu, China)	GFRP	12.0	Epoxy	Alkaline solution (IMMR)	40	15	3	99.5	NA
1850	Yue et al. (2024)	Jiangsu Hengde New Materials Co., Ltd. (Jiangsu, China)	GFRP	12.0	Epoxy	Alkaline solution (IMMR)	40	30	3	94.3	NA
1851	Yue et al. (2024)	Jiangsu Hengde New Materials Co., Ltd. (Jiangsu, China)	GFRP	12.0	Epoxy	Alkaline solution (IMMR)	40	45	3	92.5	NA
1852	Yue et al. (2024)	Jiangsu Hengde New Materials Co., Ltd. (Jiangsu, China)	GFRP	12.0	Epoxy	Alkaline solution (IMMR)	40	60	3	88.2	NA
1853	Yue et al. (2024)	Jiangsu Hengde New Materials Co., Ltd. (Jiangsu, China)	GFRP	12.0	Epoxy	Alkaline solution (IMMR)	40	90	3	81.1	NA

1854	Yue et al. (2024)	Jiangsu Hengde New Materials Co., Ltd. (Jiangsu, China)	GFRP	12.0	Epoxy	Alkaline solution (IMMR)	40	120	3	77.8	NA
1855	Yue et al. (2024)	Jiangsu Hengde New Materials Co., Ltd. (Jiangsu, China)	GFRP	12.0	Epoxy	Alkaline solution (IMMR)	60	15	3	93.9	NA
1856	Yue et al. (2024)	Jiangsu Hengde New Materials Co., Ltd. (Jiangsu, China)	GFRP	12.0	Epoxy	Alkaline solution (IMMR)	60	30	3	92.5	NA
1857	Yue et al. (2024)	Jiangsu Hengde New Materials Co., Ltd. (Jiangsu, China)	GFRP	12.0	Epoxy	Alkaline solution (IMMR)	60	45	3	91.0	NA
1858	Yue et al. (2024)	Jiangsu Hengde New Materials Co., Ltd. (Jiangsu, China)	GFRP	12.0	Epoxy	Alkaline solution (IMMR)	60	60	3	77.8	NA
1859	Yue et al. (2024)	Jiangsu Hengde New Materials Co., Ltd. (Jiangsu, China)	GFRP	12.0	Epoxy	Alkaline solution (IMMR)	60	90	3	76.9	NA
1860	Yue et al. (2024)	Jiangsu Hengde New Materials Co., Ltd. (Jiangsu, China)	GFRP	12.0	Epoxy	Alkaline solution (IMMR)	60	120	3	73.6	NA
1861	Yue et al. (2024)	Jiangsu Hengde New Materials Co., Ltd. (Jiangsu, China)	GFRP	12.0	Epoxy	Alkaline solution (IMMR)	20	15	3	98.1	NA
1862	Yue et al. (2024)	Jiangsu Hengde New Materials Co., Ltd. (Jiangsu, China)	GFRP	12.0	Epoxy	Alkaline solution (IMMR)	20	30	3	95.8	NA
1863	Yue et al. (2024)	Jiangsu Hengde New Materials Co., Ltd. (Jiangsu, China)	GFRP	12.0	Epoxy	Alkaline solution (IMMR)	20	45	3	90.6	NA
1864	Yue et al. (2024)	Jiangsu Hengde New Materials Co., Ltd. (Jiangsu, China)	GFRP	12.0	Epoxy	Alkaline solution (IMMR)	20	60	3	85.0	NA
1865	Yue et al. (2024)	Jiangsu Hengde New Materials Co., Ltd. (Jiangsu, China)	GFRP	12.0	Epoxy	Alkaline solution (IMMR)	20	90	3	85.0	NA
1866	Yue et al. (2024)	Jiangsu Hengde New Materials Co., Ltd. (Jiangsu, China)	GFRP	12.0	Epoxy	Alkaline solution (IMMR)	20	120	3	74.2	NA
1867	Yue et al. (2024)	Jiangsu Hengde New Materials Co., Ltd. (Jiangsu, China)	GFRP	12.0	Epoxy	Alkaline solution (IMMR)	40	15	3	83.6	NA
1868	Yue et al. (2024)	Jiangsu Hengde New Materials Co., Ltd. (Jiangsu, China)	GFRP	12.0	Epoxy	Alkaline solution (IMMR)	40	30	3	80.3	NA
1869	Yue et al. (2024)	Jiangsu Hengde New	GFRP	12.0	Epoxy	Alkaline solution (IMMR)	40	45	3	78.4	NA

		Materials Co., Ltd. (Jiangsu, China)										
1870	Yue et al. (2024)	Jiangsu Hengde New Materials Co., Ltd. (Jiangsu, China)	GFRP	12.0	Epoxy	Alkaline solution (IMMR)	40	60	3	63.9	NA
1871	Yue et al. (2024)	Jiangsu Hengde New Materials Co., Ltd. (Jiangsu, China)	GFRP	12.0	Epoxy	Alkaline solution (IMMR)	40	90	3	60.6	NA
1872	Yue et al. (2024)	Jiangsu Hengde New Materials Co., Ltd. (Jiangsu, China)	GFRP	12.0	Epoxy	Alkaline solution (IMMR)	40	120	3	55.9	NA
1873	Yue et al. (2024)	Jiangsu Hengde New Materials Co., Ltd. (Jiangsu, China)	GFRP	12.0	Epoxy	Alkaline solution (IMMR)	60	15	3	86.4	NA
1874	Yue et al. (2024)	Jiangsu Hengde New Materials Co., Ltd. (Jiangsu, China)	GFRP	12.0	Epoxy	Alkaline solution (IMMR)	60	30	3	85.0	NA
1875	Yue et al. (2024)	Jiangsu Hengde New Materials Co., Ltd. (Jiangsu, China)	GFRP	12.0	Epoxy	Alkaline solution (IMMR)	60	45	3	71.8	NA
1876	Yue et al. (2024)	Jiangsu Hengde New Materials Co., Ltd. (Jiangsu, China)	GFRP	12.0	Epoxy	Alkaline solution (IMMR)	60	60	3	56.8	NA
1877	Yue et al. (2024)	Jiangsu Hengde New Materials Co., Ltd. (Jiangsu, China)	GFRP	12.0	Epoxy	Alkaline solution (IMMR)	60	90	3	50.2	NA
1878	Yue et al. (2024)	Jiangsu Hengde New Materials Co., Ltd. (Jiangsu, China)	GFRP	12.0	Epoxy	Alkaline solution (IMMR)	60	120	3	44.6	NA
1879	Yue et al. (2024)	Jiangsu Hengde New Materials Co., Ltd. (Jiangsu, China)	GFRP	12.0	Epoxy	Alkaline solution (IMMR)	20	15	3	99.1	NA
1880	Yue et al. (2024)	Jiangsu Hengde New Materials Co., Ltd. (Jiangsu, China)	GFRP	12.0	Epoxy	Alkaline solution (IMMR)	20	30	3	82.6	NA
1881	Yue et al. (2024)	Jiangsu Hengde New Materials Co., Ltd. (Jiangsu, China)	GFRP	12.0	Epoxy	Alkaline solution (IMMR)	20	45	3	60.1	NA
1882	Yue et al. (2024)	Jiangsu Hengde New Materials Co., Ltd. (Jiangsu, China)	GFRP	12.0	Epoxy	Alkaline solution (IMMR)	20	60	3	54.0	NA
1883	Yue et al. (2024)	Jiangsu Hengde New Materials Co., Ltd. (Jiangsu, China)	GFRP	12.0	Epoxy	Alkaline solution (IMMR)	20	90	3	48.8	NA
1884	Yue et al. (2024)	Jiangsu Hengde New Materials Co.,	GFRP	12.0	Epoxy	Alkaline solution (IMMR)	20	120	3	48.8	NA

		(Jiangsu, China)										
1885	Yue et al. (2024)	Jiangsu Hengde New Materials Co., Ltd. (Jiangsu, China)	GFRP	12.0	Epoxy	Alkaline solution (IMMR)	40	15	3	86.4	NA
1886	Yue et al. (2024)	Jiangsu Hengde New Materials Co., Ltd. (Jiangsu, China)	GFRP	12.0	Epoxy	Alkaline solution (IMMR)	40	30	3	65.7	NA
1887	Yue et al. (2024)	Jiangsu Hengde New Materials Co., Ltd. (Jiangsu, China)	GFRP	12.0	Epoxy	Alkaline solution (IMMR)	40	45	3	51.6	NA
1888	Yue et al. (2024)	Jiangsu Hengde New Materials Co., Ltd. (Jiangsu, China)	GFRP	12.0	Epoxy	Alkaline solution (IMMR)	40	60	3	46.0	NA
1889	Yue et al. (2024)	Jiangsu Hengde New Materials Co., Ltd. (Jiangsu, China)	GFRP	12.0	Epoxy	Alkaline solution (IMMR)	40	90	3	30.1	NA
1890	Yue et al. (2024)	Jiangsu Hengde New Materials Co., Ltd. (Jiangsu, China)	GFRP	12.0	Epoxy	Alkaline solution (IMMR)	40	120	3	22.5	NA
1891	Yue et al. (2024)	Jiangsu Hengde New Materials Co., Ltd. (Jiangsu, China)	GFRP	12.0	Epoxy	Alkaline solution (IMMR)	60	15	3	63.9	NA
1892	Yue et al. (2024)	Jiangsu Hengde New Materials Co., Ltd. (Jiangsu, China)	GFRP	12.0	Epoxy	Alkaline solution (IMMR)	60	30	3	45.1	NA
1893	Yue et al. (2024)	Jiangsu Hengde New Materials Co., Ltd. (Jiangsu, China)	GFRP	12.0	Epoxy	Alkaline solution (IMMR)	60	45	3	26.8	NA
1894	Yue et al. (2024)	Jiangsu Hengde New Materials Co., Ltd. (Jiangsu, China)	GFRP	12.0	Epoxy	Alkaline solution (IMMR)	60	60	3	18.3	NA
1895	Yue et al. (2024)	Jiangsu Hengde New Materials Co., Ltd. (Jiangsu, China)	GFRP	12.0	Epoxy	Alkaline solution (IMMR)	60	90	3	17.8	NA
1896	Yue et al. (2024)	Jiangsu Hengde New Materials Co., Ltd. (Jiangsu, China)	GFRP	12.0	Epoxy	Alkaline solution (IMMR)	60	120	3	13.6	NA
1897	Yue et al. (2024)	Jiangsu Hengde New Materials Co., Ltd. (Jiangsu, China)	GFRP	12.0	Epoxy	Control	20	0	3	100.0	NA
1898	Yue et al. (2024)	Jiangsu Hengde New Materials Co., Ltd. (Jiangsu, China)	GFRP	12.0	Epoxy	Alkaline solution (IMMR)	20	15	3	98.2	NA
1899	Yue et al. (2024)	Jiangsu Hengde New Materials Co., Ltd. (Jiangsu, China)	GFRP	12.0	Epoxy	Alkaline solution (IMMR)	20	30	3	98.7	NA

1900	Yue et al. (2024)	Jiangsu Hengde New Materials Co., Ltd. (Jiangsu, China)	GFRP	12.0	Epoxy	Alkaline solution (IMMR)	20	45	3	96.0	NA
1901	Yue et al. (2024)	Jiangsu Hengde New Materials Co., Ltd. (Jiangsu, China)	GFRP	12.0	Epoxy	Alkaline solution (IMMR)	20	60	3	94.2	NA
1902	Yue et al. (2024)	Jiangsu Hengde New Materials Co., Ltd. (Jiangsu, China)	GFRP	12.0	Epoxy	Alkaline solution (IMMR)	20	90	3	90.1	NA
1903	Yue et al. (2024)	Jiangsu Hengde New Materials Co., Ltd. (Jiangsu, China)	GFRP	12.0	Epoxy	Alkaline solution (IMMR)	20	120	3	84.3	NA
1904	Yue et al. (2024)	Jiangsu Hengde New Materials Co., Ltd. (Jiangsu, China)	GFRP	12.0	Epoxy	Alkaline solution (IMMR)	40	15	3	97.8	NA
1905	Yue et al. (2024)	Jiangsu Hengde New Materials Co., Ltd. (Jiangsu, China)	GFRP	12.0	Epoxy	Alkaline solution (IMMR)	40	30	3	96.0	NA
1906	Yue et al. (2024)	Jiangsu Hengde New Materials Co., Ltd. (Jiangsu, China)	GFRP	12.0	Epoxy	Alkaline solution (IMMR)	40	45	3	91.5	NA
1907	Yue et al. (2024)	Jiangsu Hengde New Materials Co., Ltd. (Jiangsu, China)	GFRP	12.0	Epoxy	Alkaline solution (IMMR)	40	60	3	84.3	NA
1908	Yue et al. (2024)	Jiangsu Hengde New Materials Co., Ltd. (Jiangsu, China)	GFRP	12.0	Epoxy	Alkaline solution (IMMR)	40	90	3	78.9	NA
1909	Yue et al. (2024)	Jiangsu Hengde New Materials Co., Ltd. (Jiangsu, China)	GFRP	12.0	Epoxy	Alkaline solution (IMMR)	40	120	3	71.3	NA
1910	Yue et al. (2024)	Jiangsu Hengde New Materials Co., Ltd. (Jiangsu, China)	GFRP	12.0	Epoxy	Alkaline solution (IMMR)	60	15	3	97.8	NA
1911	Yue et al. (2024)	Jiangsu Hengde New Materials Co., Ltd. (Jiangsu, China)	GFRP	12.0	Epoxy	Alkaline solution (IMMR)	60	30	3	89.7	NA
1912	Yue et al. (2024)	Jiangsu Hengde New Materials Co., Ltd. (Jiangsu, China)	GFRP	12.0	Epoxy	Alkaline solution (IMMR)	60	45	3	83.4	NA
1913	Yue et al. (2024)	Jiangsu Hengde New Materials Co., Ltd. (Jiangsu, China)	GFRP	12.0	Epoxy	Alkaline solution (IMMR)	60	60	3	79.8	NA
1914	Yue et al. (2024)	Jiangsu Hengde New Materials Co., Ltd. (Jiangsu, China)	GFRP	12.0	Epoxy	Alkaline solution (IMMR)	60	90	3	73.1	NA
1915	Yue et al. (2024)	Jiangsu Hengde New	GFRP	12.0	Epoxy	Alkaline solution (IMMR)	60	120	3	60.1	NA

		Materials Co., Ltd. (Jiangsu, China)										
1916	Yue et al. (2024)	Jiangsu Hengde New Materials Co., Ltd. (Jiangsu, China)	GFRP	12.0	Epoxy	Alkaline solution (IMMR)	20	15	3	97.8	NA
1917	Yue et al. (2024)	Jiangsu Hengde New Materials Co., Ltd. (Jiangsu, China)	GFRP	12.0	Epoxy	Alkaline solution (IMMR)	20	30	3	98.7	NA
1918	Yue et al. (2024)	Jiangsu Hengde New Materials Co., Ltd. (Jiangsu, China)	GFRP	12.0	Epoxy	Alkaline solution (IMMR)	20	45	3	96.0	NA
1919	Yue et al. (2024)	Jiangsu Hengde New Materials Co., Ltd. (Jiangsu, China)	GFRP	12.0	Epoxy	Alkaline solution (IMMR)	20	60	3	93.7	NA
1920	Yue et al. (2024)	Jiangsu Hengde New Materials Co., Ltd. (Jiangsu, China)	GFRP	12.0	Epoxy	Alkaline solution (IMMR)	20	90	3	89.7	NA
1921	Yue et al. (2024)	Jiangsu Hengde New Materials Co., Ltd. (Jiangsu, China)	GFRP	12.0	Epoxy	Alkaline solution (IMMR)	20	120	3	84.3	NA
1922	Yue et al. (2024)	Jiangsu Hengde New Materials Co., Ltd. (Jiangsu, China)	GFRP	12.0	Epoxy	Alkaline solution (IMMR)	40	15	3	97.8	NA
1923	Yue et al. (2024)	Jiangsu Hengde New Materials Co., Ltd. (Jiangsu, China)	GFRP	12.0	Epoxy	Alkaline solution (IMMR)	40	30	3	95.5	NA
1924	Yue et al. (2024)	Jiangsu Hengde New Materials Co., Ltd. (Jiangsu, China)	GFRP	12.0	Epoxy	Alkaline solution (IMMR)	40	45	3	91.5	NA
1925	Yue et al. (2024)	Jiangsu Hengde New Materials Co., Ltd. (Jiangsu, China)	GFRP	12.0	Epoxy	Alkaline solution (IMMR)	40	60	3	84.3	NA
1926	Yue et al. (2024)	Jiangsu Hengde New Materials Co., Ltd. (Jiangsu, China)	GFRP	12.0	Epoxy	Alkaline solution (IMMR)	40	90	3	78.9	NA
1927	Yue et al. (2024)	Jiangsu Hengde New Materials Co., Ltd. (Jiangsu, China)	GFRP	12.0	Epoxy	Alkaline solution (IMMR)	40	120	3	71.8	NA
1928	Yue et al. (2024)	Jiangsu Hengde New Materials Co., Ltd. (Jiangsu, China)	GFRP	12.0	Epoxy	Alkaline solution (IMMR)	60	15	3	97.8	NA
1929	Yue et al. (2024)	Jiangsu Hengde New Materials Co., Ltd. (Jiangsu, China)	GFRP	12.0	Epoxy	Alkaline solution (IMMR)	60	30	3	89.7	NA
1930	Yue et al. (2024)	Jiangsu Hengde New Materials Co., Ltd.	GFRP	12.0	Epoxy	Alkaline solution (IMMR)	60	45	3	83.4	NA

		(Jiangsu, China)										
1931	Yue et al. (2024)	Jiangsu Hengde New Materials Co., Ltd. (Jiangsu, China)	GFRP	12.0	Epoxy	Alkaline solution (IMMR)	60	60	3	79.8	NA
1932	Yue et al. (2024)	Jiangsu Hengde New Materials Co., Ltd. (Jiangsu, China)	GFRP	12.0	Epoxy	Alkaline solution (IMMR)	60	90	3	73.1	NA
1933	Yue et al. (2024)	Jiangsu Hengde New Materials Co., Ltd. (Jiangsu, China)	GFRP	12.0	Epoxy	Alkaline solution (IMMR)	60	120	3	60.1	NA
1934	Yue et al. (2024)	Jiangsu Hengde New Materials Co., Ltd. (Jiangsu, China)	GFRP	12.0	Epoxy	Alkaline solution (IMMR)	20	15	3	92.4	NA
1935	Yue et al. (2024)	Jiangsu Hengde New Materials Co., Ltd. (Jiangsu, China)	GFRP	12.0	Epoxy	Alkaline solution (IMMR)	20	30	3	86.2	NA
1936	Yue et al. (2024)	Jiangsu Hengde New Materials Co., Ltd. (Jiangsu, China)	GFRP	12.0	Epoxy	Alkaline solution (IMMR)	20	45	3	91.5	NA
1937	Yue et al. (2024)	Jiangsu Hengde New Materials Co., Ltd. (Jiangsu, China)	GFRP	12.0	Epoxy	Alkaline solution (IMMR)	20	60	3	80.4	NA
1938	Yue et al. (2024)	Jiangsu Hengde New Materials Co., Ltd. (Jiangsu, China)	GFRP	12.0	Epoxy	Alkaline solution (IMMR)	20	90	3	73.7	NA
1939	Yue et al. (2024)	Jiangsu Hengde New Materials Co., Ltd. (Jiangsu, China)	GFRP	12.0	Epoxy	Alkaline solution (IMMR)	20	120	3	71.0	NA
1940	Yue et al. (2024)	Jiangsu Hengde New Materials Co., Ltd. (Jiangsu, China)	GFRP	12.0	Epoxy	Alkaline solution (IMMR)	40	15	3	84.4	NA
1941	Yue et al. (2024)	Jiangsu Hengde New Materials Co., Ltd. (Jiangsu, China)	GFRP	12.0	Epoxy	Alkaline solution (IMMR)	40	30	3	74.1	NA
1942	Yue et al. (2024)	Jiangsu Hengde New Materials Co., Ltd. (Jiangsu, China)	GFRP	12.0	Epoxy	Alkaline solution (IMMR)	40	45	3	70.1	NA
1943	Yue et al. (2024)	Jiangsu Hengde New Materials Co., Ltd. (Jiangsu, China)	GFRP	12.0	Epoxy	Alkaline solution (IMMR)	40	60	3	68.8	NA
1944	Yue et al. (2024)	Jiangsu Hengde New Materials Co., Ltd. (Jiangsu, China)	GFRP	12.0	Epoxy	Alkaline solution (IMMR)	40	90	3	65.2	NA
1945	Yue et al. (2024)	Jiangsu Hengde New Materials Co., Ltd. (Jiangsu, China)	GFRP	12.0	Epoxy	Alkaline solution (IMMR)	40	120	3	52.2	NA

1946	Yue et al. (2024)	Jiangsu Hengde New Materials Co., Ltd. (Jiangsu, China)	GFRP	12.0	Epoxy	Alkaline solution (IMMR)	60	15	3	64.7	NA
1947	Yue et al. (2024)	Jiangsu Hengde New Materials Co., Ltd. (Jiangsu, China)	GFRP	12.0	Epoxy	Alkaline solution (IMMR)	60	30	3	57.6	NA
1948	Yue et al. (2024)	Jiangsu Hengde New Materials Co., Ltd. (Jiangsu, China)	GFRP	12.0	Epoxy	Alkaline solution (IMMR)	60	45	3	54.5	NA
1949	Yue et al. (2024)	Jiangsu Hengde New Materials Co., Ltd. (Jiangsu, China)	GFRP	12.0	Epoxy	Alkaline solution (IMMR)	60	60	3	57.6	NA
1950	Yue et al. (2024)	Jiangsu Hengde New Materials Co., Ltd. (Jiangsu, China)	GFRP	12.0	Epoxy	Alkaline solution (IMMR)	60	90	3	46.4	NA
1951	Yue et al. (2024)	Jiangsu Hengde New Materials Co., Ltd. (Jiangsu, China)	GFRP	12.0	Epoxy	Alkaline solution (IMMR)	60	120	3	41.1	NA
1952	Yue et al. (2024)	Jiangsu Hengde New Materials Co., Ltd. (Jiangsu, China)	GFRP	12.0	Epoxy	Alkaline solution (IMMR)	20	15	3	99.1	NA
1953	Yue et al. (2024)	Jiangsu Hengde New Materials Co., Ltd. (Jiangsu, China)	GFRP	12.0	Epoxy	Alkaline solution (IMMR)	20	30	3	91.5	NA
1954	Yue et al. (2024)	Jiangsu Hengde New Materials Co., Ltd. (Jiangsu, China)	GFRP	12.0	Epoxy	Alkaline solution (IMMR)	20	45	3	70.5	NA
1955	Yue et al. (2024)	Jiangsu Hengde New Materials Co., Ltd. (Jiangsu, China)	GFRP	12.0	Epoxy	Alkaline solution (IMMR)	20	60	3	60.3	NA
1956	Yue et al. (2024)	Jiangsu Hengde New Materials Co., Ltd. (Jiangsu, China)	GFRP	12.0	Epoxy	Alkaline solution (IMMR)	20	90	3	55.4	NA
1957	Yue et al. (2024)	Jiangsu Hengde New Materials Co., Ltd. (Jiangsu, China)	GFRP	12.0	Epoxy	Alkaline solution (IMMR)	20	120	3	47.3	NA
1958	Yue et al. (2024)	Jiangsu Hengde New Materials Co., Ltd. (Jiangsu, China)	GFRP	12.0	Epoxy	Alkaline solution (IMMR)	40	15	3	92.9	NA
1959	Yue et al. (2024)	Jiangsu Hengde New Materials Co., Ltd. (Jiangsu, China)	GFRP	12.0	Epoxy	Alkaline solution (IMMR)	40	30	3	80.8	NA
1960	Yue et al. (2024)	Jiangsu Hengde New Materials Co., Ltd. (Jiangsu, China)	GFRP	12.0	Epoxy	Alkaline solution (IMMR)	40	45	3	60.7	NA
1961	Yue et al. (2024)	Jiangsu Hengde New Materials Co., Ltd. (Jiangsu, China)	GFRP	12.0	Epoxy	Alkaline solution (IMMR)	40	60	3	45.5	NA

		Materials Co., Ltd. (Jiangsu, China)										
1962	Yue et al. (2024)	Jiangsu Hengde New Materials Co., Ltd. (Jiangsu, China)	GFRP	12.0	Epoxy	Alkaline solution (IMMR)	40	90	3	31.3	NA
1963	Yue et al. (2024)	Jiangsu Hengde New Materials Co., Ltd. (Jiangsu, China)	GFRP	12.0	Epoxy	Alkaline solution (IMMR)	40	120	3	30.4	NA
1964	Yue et al. (2024)	Jiangsu Hengde New Materials Co., Ltd. (Jiangsu, China)	GFRP	12.0	Epoxy	Alkaline solution (IMMR)	60	15	3	75.5	NA
1965	Yue et al. (2024)	Jiangsu Hengde New Materials Co., Ltd. (Jiangsu, China)	GFRP	12.0	Epoxy	Alkaline solution (IMMR)	60	30	3	64.7	NA
1966	Yue et al. (2024)	Jiangsu Hengde New Materials Co., Ltd. (Jiangsu, China)	GFRP	12.0	Epoxy	Alkaline solution (IMMR)	60	45	3	56.3	NA
1967	Yue et al. (2024)	Jiangsu Hengde New Materials Co., Ltd. (Jiangsu, China)	GFRP	12.0	Epoxy	Alkaline solution (IMMR)	60	60	3	38.4	NA
1968	Yue et al. (2024)	Jiangsu Hengde New Materials Co., Ltd. (Jiangsu, China)	GFRP	12.0	Epoxy	Alkaline solution (IMMR)	60	90	3	23.7	NA
1969	Yue et al. (2024)	Jiangsu Hengde New Materials Co., Ltd. (Jiangsu, China)	GFRP	12.0	Epoxy	Alkaline solution (IMMR)	60	120	3	22.8	NA
1970	Zhang and Ou (2007)	NA	CFRP	NA	Epoxy	Control	NA	0	5	100.0	100.0
1971	Zhang and Ou (2007)	NA	CFRP	NA	Epoxy	Acid solution (IMMR)	60	28	5	98.5	85.6
1972	Zhang and Ou (2007)	NA	CFRP	NA	Epoxy	Acid solution (IMMR)	60	56	5	97.1	85.5
1973	Zhang and Ou (2007)	NA	CFRP	NA	Epoxy	Alkaline solution (IMMR)	60	28	5	98.4	86.6
1974	Zhang and Ou (2007)	NA	CFRP	NA	Epoxy	Alkaline solution (IMMR)	60	56	5	98.4	83.5
1975	Zhang and Ou (2007)	NA	CFRP	NA	Epoxy	Saline solution (IMMR)	60	28	5	98.2	85.9
1976	Zhang and Ou (2007)	NA	CFRP	NA	Epoxy	Saline solution (IMMR)	60	56	5	96.3	85.5
1977	Zhang and Ou (2007)	NA	CFRP	NA	Epoxy	Control	NA	0	5	100.0	100.0
1978	Zhang and Ou (2007)	NA	CFRP	NA	Epoxy	Water (FT)	-17.8/7	6	5	100.6	100.6
1979	Zhang and Ou (2007)	NA	CFRP	NA	Epoxy	Water (FT)	-17.8/7	13	5	103.5	103.1

1980	Zhang and Ou (2007)	NA	CFRP	NA	Epoxy	Water (FT)	-17.8/7	19	5	106.8	103.5
1981	Zhang and Ou (2007)	NA	CFRP	NA	Epoxy	Water (FT)	-17.8/7	25	5	111.5	103.9
1982	Zhang and Ou (2007)	NA	CFRP	NA	Epoxy	Water (FT)	-17.8/7	31	5	106.0	104.0
1983	Zhang and Ou (2007)	NA	CFRP	NA	Epoxy	Water (FT)	-17.8/7	38	5	102.2	105.4
1984	Zhang and Ou (2007)	NA	GFRP	NA	Epoxy	Control	NA	0	5	100.0	100.0
1985	Zhang and Ou (2007)	NA	GFRP	NA	Epoxy	Acid solution (IMMR)	60	28	5	97.0	99.4
1986	Zhang and Ou (2007)	NA	GFRP	NA	Epoxy	Acid solution (IMMR)	60	56	5	87.5	97.3
1987	Zhang and Ou (2007)	NA	GFRP	NA	Epoxy	Alkaline solution (IMMR)	60	28	5	91.2	96.3
1988	Zhang and Ou (2007)	NA	GFRP	NA	Epoxy	Alkaline solution (IMMR)	60	56	5	75.2	95.3
1989	Zhang and Ou (2007)	NA	GFRP	NA	Epoxy	Saline solution (IMMR)	60	28	5	95.6	99.0
1990	Zhang and Ou (2007)	NA	GFRP	NA	Epoxy	Saline solution (IMMR)	60	56	5	93.2	98.0
1991	Zhang and Ou (2007)	NA	GFRP	NA	Epoxy	Control	NA	0	5	100.0	100.0
1992	Zhang and Ou (2007)	NA	GFRP	NA	Epoxy	Water (FT)	-17.8/7	6	5	97.1	102.0
1993	Zhang and Ou (2007)	NA	GFRP	NA	Epoxy	Water (FT)	-17.8/7	13	5	90.1	102.7
1994	Zhang and Ou (2007)	NA	GFRP	NA	Epoxy	Water (FT)	-17.8/7	19	5	95.0	103.2
1995	Zhang and Ou (2007)	NA	GFRP	NA	Epoxy	Water (FT)	-17.8/7	25	5	98.0	103.9
1996	Zhang and Ou (2007)	NA	GFRP	NA	Epoxy	Water (FT)	-17.8/7	31	5	94.7	104.9
1997	Zhang and Ou (2007)	NA	GFRP	NA	Epoxy	Water (FT)	-17.8/7	38	5	90.6	105.8
1998	Zhao et al. (2024)	NA	GFRP	6.0	Epoxy	Control	25	0	5	100.0	100.0
1999	Zhao et al. (2024)	NA	GFRP	6.0	Epoxy	Alkaline solution (IMMR)	25	21	3	98.0	101.1
2000	Zhao et al. (2024)	NA	GFRP	6.0	Epoxy	Alkaline solution (IMMR)	25	42	3	95.6	101.7
2001	Zhao et al. (2024)	NA	GFRP	6.0	Epoxy	Alkaline solution (IMMR)	25	63	3	91.7	102.3
2002	Zhao et al. (2024)	NA	GFRP	6.0	Epoxy	Alkaline solution (IMMR)	25	84	3	88.4	NA
2003	Zhao et al. (2024)	NA	GFRP	6.0	Epoxy	Alkaline solution (IMMR)	40	21	3	89.1	101.7
2004	Zhao et al. (2024)	NA	GFRP	6.0	Epoxy	Alkaline solution (IMMR)	40	42	3	81.5	102.3
2005	Zhao et al. (2024)	NA	GFRP	6.0	Epoxy	Alkaline solution (IMMR)	40	63	3	69.2	99.4
2006	Zhao et al. (2024)	NA	GFRP	6.0	Epoxy	Alkaline solution (IMMR)	40	84	3	48.4	88.6
2007	Zhao et al. (2024)	NA	GFRP	6.0	Epoxy	Alkaline solution (IMMR)	55	21	3	49.2	81.7

2008	Zhao et al. (2024)	NA	GFRP	6.0	Epoxy	Alkaline solution (IMMR)	55	42	3	19.0	56.6
2009	Zhao et al. (2024)	NA	GFRP	6.0	Epoxy	Alkaline solution (IMMR)	55	63	3	4.9	0.0
2010	Zhao et al. (2024)	NA	GFRP	6.0	Epoxy	Alkaline solution (IMMR)	55	84	3	0.0	0.0
2011	Zhao et al. (2024)	NA	GFRP	6.0	Vinylester	Control	25	0	5	100.0	100.0
2012	Zhao et al. (2024)	NA	GFRP	6.0	Vinylester	Alkaline solution (IMMR)	25	21	3	100.5	100.6
2013	Zhao et al. (2024)	NA	GFRP	6.0	Vinylester	Alkaline solution (IMMR)	25	42	3	94.8	105.3
2014	Zhao et al. (2024)	NA	GFRP	6.0	Vinylester	Alkaline solution (IMMR)	25	63	3	97.1	106.4
2015	Zhao et al. (2024)	NA	GFRP	6.0	Vinylester	Alkaline solution (IMMR)	25	84	3	93.3	97.7
2016	Zhao et al. (2024)	NA	GFRP	6.0	Vinylester	Alkaline solution (IMMR)	40	21	3	100.5	105.3
2017	Zhao et al. (2024)	NA	GFRP	6.0	Vinylester	Alkaline solution (IMMR)	40	42	3	86.7	102.9
2018	Zhao et al. (2024)	NA	GFRP	6.0	Vinylester	Alkaline solution (IMMR)	40	63	3	82.8	100.6
2019	Zhao et al. (2024)	NA	GFRP	6.0	Vinylester	Alkaline solution (IMMR)	40	84	3	73.4	101.2
2020	Zhao et al. (2024)	NA	GFRP	6.0	Vinylester	Alkaline solution (IMMR)	55	21	3	76.9	104.1
2021	Zhao et al. (2024)	NA	GFRP	6.0	Vinylester	Alkaline solution (IMMR)	55	42	3	66.2	98.8
2022	Zhao et al. (2024)	NA	GFRP	6.0	Vinylester	Alkaline solution (IMMR)	55	63	3	61.7	101.8
2023	Zhao et al. (2024)	NA	GFRP	6.0	Vinylester	Alkaline solution (IMMR)	55	84	3	54.8	87.1

Notes:

(1) IMMR = Immersion; WD = Wet-dry cycle; FT = Freeze-thaw cycle; HT = High temperature; LT = Low temperature; RT = Room temperature; RH = Relative humidity; UV = Ultraviolet radiation; SL = Sustained load;

(2) NC = Normal concrete; SWC = Seawater concrete; SWSSC = Seawater sea-sand concrete; NCE = Normal concrete-embedded; SWCE= Seawater concrete-embedded; SWSSCE = Sea water sea-sand concrete-embedded;

(3) f_u is the ultimate tensile strength of FRP bars; M_u is the ultimate moment measured in the beam tests;

(4) Control = Unconditioned specimens without environmental exposure and time aging effect; Reference = Unconditioned specimens without environmental exposure but with time aging effect;

(5) NA = Not applicable.

Table A2 AAT database for shear properties of FRP bars

No.	Reference	FRP properties				Environmental condition	Temperature (℃)	Exposure duration (d)	Specimen number (pcs)	Transverse shear strength retention (%)	Specimen number (pcs)	Interlaminar shear strength retention (%)
		Manufacturer	Type	Bar diameter (mm)	Resin type							
1	Ali et al. (2019)	Pultrall Inc. (Thetford Mines, QC, Canada)	BFRP	19.0	Vinylester	Control	22	0	6	100.0	6	100.0
2	Ali et al. (2019)	Pultrall Inc. (Thetford Mines, QC, Canada)	BFRP	19.0	Vinylester	Alkaline solution (IMMR)	22	42	6	99.6	6	98.3
3	Ali et al. (2019)	Pultrall Inc. (Thetford Mines, QC, Canada)	BFRP	19.0	Vinylester	Alkaline solution (IMMR)	22	125	6	99.2	6	93.0
4	Ali et al. (2019)	Pultrall Inc. (Thetford Mines, QC, Canada)	BFRP	19.0	Vinylester	Alkaline solution (IMMR)	22	208	6	94.2	6	86.0
5	Ali et al. (2019)	Pultrall Inc. (Thetford Mines, QC, Canada)	BFRP	19.0	Vinylester	Alkaline solution (IMMR)	40	42	6	98.3	6	94.0
6	Ali et al. (2019)	Pultrall Inc. (Thetford Mines, QC, Canada)	BFRP	19.0	Vinylester	Alkaline solution (IMMR)	40	125	6	96.7	6	91.0
7	Ali et al. (2019)	Pultrall Inc. (Thetford Mines, QC, Canada)	BFRP	19.0	Vinylester	Alkaline solution (IMMR)	40	208	6	92.1	6	84.3
8	Ali et al. (2019)	Pultrall Inc. (Thetford Mines, QC, Canada)	BFRP	19.0	Vinylester	Alkaline solution (IMMR)	60	42	6	96.7	6	93.3
9	Ali et al. (2019)	Pultrall Inc. (Thetford Mines, QC, Canada)	BFRP	19.0	Vinylester	Alkaline solution (IMMR)	60	125	6	95.4	6	90.0
10	Ali et al. (2019)	Pultrall Inc. (Thetford Mines, QC, Canada)	BFRP	19.0	Vinylester	Alkaline solution (IMMR)	60	208	6	88.8	6	80.3
11	Ali et al. (2020)	Galen LLC (Russia)	BFRP	9.5	Vinylester	Control	NA	0	4	100.0	4	100.0
12	Ali et al. (2020)	Galen LLC (Russia)	BFRP	9.5	Vinylester	Alkaline solution (IMMR)	60	90	4	90.5	4	84.5
13	Ali et al. (2020)	Galen LLC (Russia)	BFRP	12.7	Vinylester	Control	NA	0	4	100.0	4	100.0
14	Ali et al. (2020)	Galen LLC (Russia)	BFRP	12.7	Vinylester	Alkaline solution (IMMR)	60	90	4	81.8	4	76.9
15	Ali et al. (2020)	Galen LLC (Russia)	BFRP	15.9	Vinylester	Control	NA	0	4	100.0	4	100.0
16	Ali et al. (2020)	Galen LLC (Russia)	BFRP	15.9	Vinylester	Alkaline solution (IMMR)	60	90	4	94.5	4	86.8
17	Ali et al. (2020)	Galen LLC (Russia)	BFRP	19.0	Vinylester	Control	NA	0	4	100.0	4	100.0
18	Ali et al. (2020)	Galen LLC (Russia)	BFRP	19.0	Vinylester	Alkaline solution (IMMR)	60	90	4	94.8	4	90.5
19	Ali et al. (2020)	Galen LLC (Russia)	BFRP	25.0	Vinylester	Control	NA	0	4	100.0	4	100.0

20	Ali et al. (2020)	Galen LLC (Russia)	BFRP	25.0	Vinylester	Alkaline solution (IMMR)	60	90	4	92.6	4	91.8
21	Arczewska et al. (2021)	Pultrall Inc. (Thetford Mines, QC, Canada)	GFRP	12.7	NA	Control	NA	0	3	100.0	NA	NA
22	Arczewska et al. (2021)	Pultrall Inc. (Thetford Mines, QC, Canada)	GFRP	12.7	NA	Alkaline solution (IMMR)	50	30	3	96.1	NA	NA
23	Arczewska et al. (2021)	Pultrall Inc. (Thetford Mines, QC, Canada)	GFRP	12.7	NA	Alkaline solution (IMMR)	50	90	3	94.2	NA	NA
24	Arczewska et al. (2021)	Pultrall Inc. (Thetford Mines, QC, Canada)	GFRP	12.7	NA	Alkaline solution (IMMR)	50	150	3	93.3	NA	NA
25	Arczewska et al. (2021)	Pultrall Inc. (Thetford Mines, QC, Canada)	GFRP	12.7	NA	Alkaline solution (IMMR)	60	30	3	92.9	NA	NA
26	Arczewska et al. (2021)	Pultrall Inc. (Thetford Mines, QC, Canada)	GFRP	12.7	NA	Alkaline solution (IMMR)	60	90	3	90.2	NA	NA
27	Arczewska et al. (2021)	Pultrall Inc. (Thetford Mines, QC, Canada)	GFRP	12.7	NA	Alkaline solution (IMMR)	60	150	3	88.0	NA	NA
28	Arczewska et al. (2021)	Pultrall Inc. (Thetford Mines, QC, Canada)	GFRP	12.7	NA	Alkaline solution (IMMR)	70	30	3	90.6	NA	NA
29	Arczewska et al. (2021)	Pultrall Inc. (Thetford Mines, QC, Canada)	GFRP	12.7	NA	Alkaline solution (IMMR)	70	90	3	86.6	NA	NA
30	Arczewska et al. (2021)	Pultrall Inc. (Thetford Mines, QC, Canada)	GFRP	12.7	NA	Alkaline solution (IMMR)	70	150	3	83.9	NA	NA
31	Arczewska et al. (2021)	Pultrall Inc. (Thetford Mines, QC, Canada)	GFRP	15.9	NA	Control	NA	0	3	100.0	NA	NA
32	Arczewska et al. (2021)	Pultrall Inc. (Thetford Mines, QC, Canada)	GFRP	15.9	NA	Alkaline solution (IMMR)	50	30	3	97.2	NA	NA
33	Arczewska et al. (2021)	Pultrall Inc. (Thetford Mines, QC, Canada)	GFRP	15.9	NA	Alkaline solution (IMMR)	50	90	3	95.6	NA	NA
34	Arczewska et al. (2021)	Pultrall Inc. (Thetford Mines, QC, Canada)	GFRP	15.9	NA	Alkaline solution (IMMR)	50	150	3	94.3	NA	NA
35	Arczewska et al. (2021)	Pultrall Inc. (Thetford Mines, QC, Canada)	GFRP	15.9	NA	Alkaline solution (IMMR)	60	30	3	94.3	NA	NA
36	Arczewska et al. (2021)	Pultrall Inc. (Thetford Mines, QC, Canada)	GFRP	15.9	NA	Alkaline solution (IMMR)	60	90	3	91.7	NA	NA
37	Arczewska et al. (2021)	Pultrall Inc. (Thetford Mines, QC, Canada)	GFRP	15.9	NA	Alkaline solution (IMMR)	60	150	3	90.2	NA	NA
38	Arczewska et al. (2021)	Pultrall Inc. (Thetford Mines, QC, Canada)	GFRP	15.9	NA	Alkaline solution (IMMR)	70	30	3	92.5	NA	NA
39	Arczewska et al. (2021)	Pultrall Inc. (Thetford Mines, QC, Canada)	GFRP	15.9	NA	Alkaline solution (IMMR)	70	90	3	89.4	NA	NA
40	Arczewska et al. (2021)	Pultrall Inc. (Thetford Mines, QC, Canada)	GFRP	15.9	NA	Alkaline solution (IMMR)	70	150	3	87.0	NA	NA
41	Arczewska et al. (2021)	Schoeck Inc. (Canada)	GFRP	12.0	NA	Control	NA	0	3	100.0	NA	NA
42	Arczewska et al. (2021)	Schoeck Inc. (Canada)	GFRP	12.0	NA	Alkaline solution (IMMR)	50	30	3	97.1	NA	NA

43	Arczewska et al. (2021)	Schoeck Inc. (Canada)	GFRP	12.0	NA	Alkaline solution (IMMR)	50	90	3	95.2	NA	NA
44	Arczewska et al. (2021)	Schoeck Inc. (Canada)	GFRP	12.0	NA	Alkaline solution (IMMR)	50	150	3	94.5	NA	NA
45	Arczewska et al. (2021)	Schoeck Inc. (Canada)	GFRP	12.0	NA	Alkaline solution (IMMR)	60	30	3	94.5	NA	NA
46	Arczewska et al. (2021)	Schoeck Inc. (Canada)	GFRP	12.0	NA	Alkaline solution (IMMR)	60	90	3	91.7	NA	NA
47	Arczewska et al. (2021)	Schoeck Inc. (Canada)	GFRP	12.0	NA	Alkaline solution (IMMR)	60	150	3	90.4	NA	NA
48	Arczewska et al. (2021)	Schoeck Inc. (Canada)	GFRP	12.0	NA	Alkaline solution (IMMR)	70	30	3	91.9	NA	NA
49	Arczewska et al. (2021)	Schoeck Inc. (Canada)	GFRP	12.0	NA	Alkaline solution (IMMR)	70	90	3	85.4	NA	NA
50	Arczewska et al. (2021)	Schoeck Inc. (Canada)	GFRP	12.0	NA	Alkaline solution (IMMR)	70	150	3	83.1	NA	NA
51	Arczewska et al. (2021)	Schoeck Inc. (Canada)	GFRP	16.0	NA	Control	NA	0	3	100.0	NA	NA
52	Arczewska et al. (2021)	Schoeck Inc. (Canada)	GFRP	16.0	NA	Alkaline solution (IMMR)	50	30	3	97.9	NA	NA
53	Arczewska et al. (2021)	Schoeck Inc. (Canada)	GFRP	16.0	NA	Alkaline solution (IMMR)	50	90	3	96.4	NA	NA
54	Arczewska et al. (2021)	Schoeck Inc. (Canada)	GFRP	16.0	NA	Alkaline solution (IMMR)	50	150	3	95.5	NA	NA
55	Arczewska et al. (2021)	Schoeck Inc. (Canada)	GFRP	16.0	NA	Alkaline solution (IMMR)	60	30	3	95.6	NA	NA
56	Arczewska et al. (2021)	Schoeck Inc. (Canada)	GFRP	16.0	NA	Alkaline solution (IMMR)	60	90	3	93.1	NA	NA
57	Arczewska et al. (2021)	Schoeck Inc. (Canada)	GFRP	16.0	NA	Alkaline solution (IMMR)	60	150	3	92.0	NA	NA
58	Arczewska et al. (2021)	Schoeck Inc. (Canada)	GFRP	16.0	NA	Alkaline solution (IMMR)	70	30	3	93.7	NA	NA
59	Arczewska et al. (2021)	Schoeck Inc. (Canada)	GFRP	16.0	NA	Alkaline solution (IMMR)	70	90	3	89.8	NA	NA
60	Arczewska et al. (2021)	Schoeck Inc. (Canada)	GFRP	16.0	NA	Alkaline solution (IMMR)	70	150	3	87.5	NA	NA
61	Ashrafi et al. (2018)	Armastek (Russia)	GFRP	10.0	Epoxy	Control	NA	0	NA	NA	3	100.0
62	Ashrafi et al. (2018)	Armastek (Russia)	GFRP	10.0	Epoxy	UV radiation+Water vapor condensation	/	42	NA	NA	3	94.0
63	Ashrafi et al. (2018)	Armastek (Russia)	GFRP	10.0	Epoxy	UV radiation+Water vapor condensation	/	83	NA	NA	3	90.0
64	Ashrafi et al. (2018)	Armastek (Russia)	GFRP	10.0	Epoxy	UV radiation+Water vapor condensation	/	125	NA	NA	3	85.0
65	Ashrafi et al. (2018)	Armastek (Russia)	GFRP	14.0	Epoxy	Control	NA	0	NA	NA	3	100.0

66	Ashrafi et al. (2018)	Armastek (Russia)	GFRP	14.0	Epoxy	UV radiation+Water vapor condensation	/	42	NA	NA	3	103.0
67	Ashrafi et al. (2018)	Armastek (Russia)	GFRP	14.0	Epoxy	UV radiation+Water vapor condensation	/	83	NA	NA	3	99.0
68	Ashrafi et al. (2018)	Armastek (Russia)	GFRP	14.0	Epoxy	UV radiation+Water vapor condensation	/	125	NA	NA	3	95.0
69	Benmokrane et al. (2015)	NA	BFRP	6.0	Epoxy	Control	NA	0	6	100.0	6	100.0
70	Benmokrane et al. (2015)	NA	BFRP	6.0	Epoxy	Alkaline solution (IMMR)	60	42	6	98.0	6	99.0
71	Benmokrane et al. (2015)	NA	BFRP	6.0	Epoxy	Alkaline solution (IMMR)	60	125	6	98.0	6	88.0
72	Benmokrane et al. (2015)	NA	BFRP	6.0	Epoxy	Alkaline solution (IMMR)	60	208	6	91.0	6	86.0
73	Benmokrane et al. (2015)	NA	BFRP	6.0	Vinylester	Control	NA	0	6	100.0	6	100.0
74	Benmokrane et al. (2015)	NA	BFRP	6.0	Vinylester	Alkaline solution (IMMR)	60	42	6	87.0	6	96.0
75	Benmokrane et al. (2015)	NA	BFRP	6.0	Vinylester	Alkaline solution (IMMR)	60	125	6	75.0	6	87.0
76	Benmokrane et al. (2015)	NA	BFRP	6.0	Vinylester	Alkaline solution (IMMR)	60	208	6	67.0	6	78.0
77	Benmokrane et al. (2015)	NA	GFRP	6.0	Vinylester	Control	NA	0	6	100.0	6	100.0
78	Benmokrane et al. (2015)	NA	GFRP	6.0	Vinylester	Alkaline solution (IMMR)	60	42	6	93.0	6	93.0
79	Benmokrane et al. (2015)	NA	GFRP	6.0	Vinylester	Alkaline solution (IMMR)	60	125	6	96.0	6	97.0
80	Benmokrane et al. (2015)	NA	GFRP	6.0	Vinylester	Alkaline solution (IMMR)	60	208	6	90.0	6	95.0
81	Benmokrane et al. (2017a)	Firep International AG (Switzerland)	GFRP	12.0	Polyester	Control	NA	0	6	100.0	6	100.0
82	Benmokrane et al. (2017a)	Firep International AG (Switzerland)	GFRP	12.0	Polyester	Alkaline solution (IMMR)	60	42	6	94.4	6	92.8
83	Benmokrane et al. (2017a)	Firep International AG (Switzerland)	GFRP	12.0	Polyester	Alkaline solution (IMMR)	60	125	6	88.8	6	86.4
84	Benmokrane et al. (2017a)	Firep International AG (Switzerland)	GFRP	12.0	Polyester	Alkaline solution (IMMR)	60	208	6	77.6	6	79.2
85	Benmokrane et al. (2017a)	Firep International AG (Switzerland)	GFRP	12.0	Vinylester	Control	NA	0	6	100.0	6	100.0
86	Benmokrane et al. (2017a)	Firep International AG (Switzerland)	GFRP	12.0	Vinylester	Alkaline solution (IMMR)	60	42	6	96.1	6	96.5
87	Benmokrane et al. (2017a)	Firep International AG (Switzerland)	GFRP	12.0	Vinylester	Alkaline solution (IMMR)	60	125	6	90.7	6	89.5
88	Benmokrane et al. (2017a)	Firep International AG (Switzerland)	GFRP	12.0	Vinylester	Alkaline solution (IMMR)	60	208	6	84.1	6	86.4

89	Benmokrane et al. (2017a)	Firep International AG (Switzerland)	GFRP	12.0	Epoxy	Control	NA	0	6	100.0	6	100.0
90	Benmokrane et al. (2017a)	Firep International AG (Switzerland)	GFRP	12.0	Epoxy	Alkaline solution (IMMR)	60	42	6	98.9	6	95.2
91	Benmokrane et al. (2017a)	Firep International AG (Switzerland)	GFRP	12.0	Epoxy	Alkaline solution (IMMR)	60	125	6	91.9	6	89.9
92	Benmokrane et al. (2017a)	Firep International AG (Switzerland)	GFRP	12.0	Epoxy	Alkaline solution (IMMR)	60	208	6	88.5	6	86.6
93	Benmokrane et al. (2017b)	Pultrall Inc. (Thetford Mines, QC, Canada)	GFRP	9.5	Vinylester	Control	23	0	NA	NA	6	100.0
94	Benmokrane et al. (2017b)	Pultrall Inc. (Thetford Mines, QC, Canada)	GFRP	9.5	Vinylester	Alkaline solution (IMMR)	60	90	NA	NA	6	88.1
95	Benmokrane et al. (2017b)	Pultrall Inc. (Thetford Mines, QC, Canada)	GFRP	12.7	Vinylester	Control	23	0	NA	NA	6	100.0
96	Benmokrane et al. (2017b)	Pultrall Inc. (Thetford Mines, QC, Canada)	GFRP	12.7	Vinylester	Alkaline solution (IMMR)	60	90	NA	NA	6	95.7
97	Benmokrane et al. (2017b)	Pultrall Inc. (Thetford Mines, QC, Canada)	GFRP	15.9	Vinylester	Control	23	0	NA	NA	6	100.0
98	Benmokrane et al. (2017b)	Pultrall Inc. (Thetford Mines, QC, Canada)	GFRP	15.9	Vinylester	Alkaline solution (IMMR)	60	90	NA	NA	6	90.0
99	Benmokrane et al. (2017b)	Pultrall Inc. (Thetford Mines, QC, Canada)	GFRP	19.1	Vinylester	Control	23	0	NA	NA	6	100.0
100	Benmokrane et al. (2017b)	Pultrall Inc. (Thetford Mines, QC, Canada)	GFRP	19.1	Vinylester	Alkaline solution (IMMR)	60	90	NA	NA	6	93.0
101	Benmokrane et al. (2017b)	Pultrall Inc. (Thetford Mines, QC, Canada)	GFRP	25.4	Vinylester	Control	23	0	NA	NA	6	100.0
102	Benmokrane et al. (2017b)	Pultrall Inc. (Thetford Mines, QC, Canada)	GFRP	25.4	Vinylester	Alkaline solution (IMMR)	60	90	NA	NA	6	100.8
103	Benmokrane et al. (2020)	Pultrall Inc. (Thetford Mines, QC, Canada)	GFRP	15.0	Vinylester	Control	NA	0	4	100.0	4-6	100.0
104	Benmokrane et al. (2020)	Pultrall Inc. (Thetford Mines, QC, Canada)	GFRP	15.0	Vinylester	Alkaline solution (IMMR)	60	90	4	84.2	4-6	96.7
105	Benmokrane et al. (2020)	Pultrall Inc. (Thetford Mines, QC, Canada)	GFRP	15.0	Vinylester	Control	NA	0	4	100.0	4-6	100.0
106	Benmokrane et al. (2020)	Pultrall Inc. (Thetford Mines, QC, Canada)	GFRP	15.0	Vinylester	Alkaline solution (IMMR)	60	90	4	81.7	4-6	93.5
107	Benmokrane et al. (2020)	Pultrall Inc. (Thetford Mines, QC, Canada)	GFRP	15.0	Vinylester	Control	NA	0	4	100.0	4-6	100.0
108	Benmokrane et al. (2020)	Pultrall Inc. (Thetford Mines, QC, Canada)	GFRP	15.0	Vinylester	Alkaline solution (IMMR)	60	90	4	83.9	4-6	96.0
109	Benmokrane et al. (2020)	Pultrall Inc. (Thetford Mines, QC, Canada)	GFRP	15.0	Vinylester	Control	NA	0	4	100.0	4-6	100.0
110	Benmokrane et al. (2020)	Pultrall Inc. (Thetford Mines, QC, Canada)	GFRP	15.0	Vinylester	Alkaline solution (IMMR)	60	90	4	86.3	4-6	91.8
111	Benmokrane et al. (2020)	Pultrall Inc. (Thetford Mines, QC, Canada)	GFRP	15.0	Vinylester	Control	NA	0	4	100.0	4-6	100.0

112	Benmokrane et al. (2020)	Pultrall Inc. (Thetford Mines, QC, Canada)	GFRP	15.0	Vinylester	Alkaline solution (IMMR)	60	90	4	91.4	4-6	83.8
113	Benmokrane et al. (2020)	Pultrall Inc. (Thetford Mines, QC, Canada)	GFRP	13.0	Vinylester	Control	NA	0	4	100.0	4-6	100.0
114	Benmokrane et al. (2020)	Pultrall Inc. (Thetford Mines, QC, Canada)	GFRP	13.0	Vinylester	Alkaline solution (IMMR)	60	90	4	91.6	4-6	81.7
115	Benmokrane et al. (2020)	Pultrall Inc. (Thetford Mines, QC, Canada)	GFRP	13.0	Vinylester	Control	NA	0	4	100.0	4-6	100.0
116	Benmokrane et al. (2020)	Pultrall Inc. (Thetford Mines, QC, Canada)	GFRP	13.0	Vinylester	Alkaline solution (IMMR)	60	90	4	87.5	4-6	82.3
117	Benmokrane et al. (2020)	Pultrall Inc. (Thetford Mines, QC, Canada)	GFRP	13.0	Vinylester	Control	NA	0	4	100.0	4-6	100.0
118	Benmokrane et al. (2020)	Pultrall Inc. (Thetford Mines, QC, Canada)	GFRP	13.0	Vinylester	Alkaline solution (IMMR)	60	90	4	91.8	4-6	76.7
119	Benmokrane et al. (2020)	Pultrall Inc. (Thetford Mines, QC, Canada)	GFRP	13.0	Vinylester	Control	NA	0	4	100.0	4-6	100.0
120	Benmokrane et al. (2020)	Pultrall Inc. (Thetford Mines, QC, Canada)	GFRP	13.0	Vinylester	Alkaline solution (IMMR)	60	90	4	88.1	4-6	82.7
121	Benmokrane et al. (2020)	Pultrall Inc. (Thetford Mines, QC, Canada)	GFRP	13.0	Vinylester	Control	NA	0	4	100.0	4-6	100.0
122	Benmokrane et al. (2020)	Pultrall Inc. (Thetford Mines, QC, Canada)	GFRP	13.0	Vinylester	Alkaline solution (IMMR)	60	90	4	90.6	4-6	82.8
123	Benmokrane et al. (2020)	Pultrall Inc. (Thetford Mines, QC, Canada)	GFRP	13.0	Vinylester	Control	NA	0	4	100.0	4-6	100.0
124	Benmokrane et al. (2020)	Pultrall Inc. (Thetford Mines, QC, Canada)	GFRP	13.0	Vinylester	Alkaline solution (IMMR)	60	90	4	85.1	4-6	78.5
125	Benmokrane et al. (2020)	Pultrall Inc. (Thetford Mines, QC, Canada)	GFRP	13.0	Vinylester	Control	NA	0	4	100.0	4-6	100.0
126	Benmokrane et al. (2020)	Pultrall Inc. (Thetford Mines, QC, Canada)	GFRP	13.0	Vinylester	Alkaline solution (IMMR)	60	90	4	85.4	4-6	84.9
127	Benmokrane et al. (2020)	Pultrall Inc. (Thetford Mines, QC, Canada)	BFRP	13.0	Vinylester	Control	NA	0	4	100.0	4-6	100.0
128	Benmokrane et al. (2020)	Pultrall Inc. (Thetford Mines, QC, Canada)	BFRP	13.0	Vinylester	Alkaline solution (IMMR)	60	90	4	75.2	4-6	79.7
129	Benmokrane et al. (2020)	Pultrall Inc. (Thetford Mines, QC, Canada)	BFRP	13.0	Vinylester	Control	NA	0	4	100.0	4-6	100.0
130	Benmokrane et al. (2020)	Pultrall Inc. (Thetford Mines, QC, Canada)	BFRP	13.0	Vinylester	Alkaline solution (IMMR)	60	90	4	83.2	4-6	63.1
131	Benmokrane et al. (2020)	Pultrall Inc. (Thetford Mines, QC, Canada)	BFRP	13.0	Vinylester	Control	NA	0	4	100.0	4-6	100.0
132	Benmokrane et al. (2020)	Pultrall Inc. (Thetford Mines, QC, Canada)	BFRP	13.0	Vinylester	Alkaline solution (IMMR)	60	90	4	100.8	4-6	71.2
133	Benmokrane et al. (2020)	Pultrall Inc. (Thetford Mines, QC, Canada)	BFRP	13.0	Polyurethane	Control	NA	0	4	100.0	4-6	100.0
134	Benmokrane et al. (2020)	Pultrall Inc. (Thetford Mines, QC, Canada)	BFRP	13.0	Polyurethane	Alkaline solution (IMMR)	60	90	4	90.2	4-6	70.9

135	Benmokrane et al. (2020)	Pultrall Inc. (Thetford Mines, QC, Canada)	BFRP	13.0	Polyurethane	Control	NA	0	4	100.0	4-6	100.0
136	Benmokrane et al. (2020)	Pultrall Inc. (Thetford Mines, QC, Canada)	BFRP	13.0	Polyurethane	Alkaline solution (IMMR)	60	90	4	84.6	4-6	75.8
137	Benmokrane et al. (2020)	Pultrall Inc. (Thetford Mines, QC, Canada)	BFRP	13.0	Epoxy	Control	NA	0	4	100.0	4-6	100.0
138	Benmokrane et al. (2020)	Pultrall Inc. (Thetford Mines, QC, Canada)	BFRP	13.0	Epoxy	Alkaline solution (IMMR)	60	90	4	89.3	4-6	72.5
139	Benmokrane et al. (2020)	Pultrall Inc. (Thetford Mines, QC, Canada)	BFRP	13.0	Epoxy	Control	NA	0	4	100.0	4-6	100.0
140	Benmokrane et al. (2020)	Pultrall Inc. (Thetford Mines, QC, Canada)	BFRP	13.0	Epoxy	Alkaline solution (IMMR)	60	90	4	93.1	4-6	74.7
141	Benmokrane et al. (2020)	Pultrall Inc. (Thetford Mines, QC, Canada)	CFRP	13.0	Epoxy	Control	NA	0	4	100.0	4-6	100.0
142	Benmokrane et al. (2020)	Pultrall Inc. (Thetford Mines, QC, Canada)	CFRP	13.0	Epoxy	Alkaline solution (IMMR)	60	90	4	91.7	4-6	77.4
143	Benmokrane et al. (2020)	Pultrall Inc. (Thetford Mines, QC, Canada)	CFRP	13.0	Epoxy	Control	NA	0	4	100.0	4-6	100.0
144	Benmokrane et al. (2020)	Pultrall Inc. (Thetford Mines, QC, Canada)	CFRP	13.0	Epoxy	Alkaline solution (IMMR)	60	90	4	85.1	4-6	73.7
145	Benmokrane et al. (2020)	Pultrall Inc. (Thetford Mines, QC, Canada)	CFRP	13.0	Vinylester	Control	NA	0	4	100.0	4-6	100.0
146	Benmokrane et al. (2020)	Pultrall Inc. (Thetford Mines, QC, Canada)	CFRP	13.0	Vinylester	Alkaline solution (IMMR)	60	90	4	90.9	4-6	70.8
147	Benmokrane et al. (2020)	Pultrall Inc. (Thetford Mines, QC, Canada)	CFRP	13.0	Vinylester	Control	NA	0	4	100.0	4-6	100.0
148	Benmokrane et al. (2020)	Pultrall Inc. (Thetford Mines, QC, Canada)	CFRP	13.0	Vinylester	Alkaline solution (IMMR)	60	90	4	84.2	4-6	61.0
149	Benmokrane et al. (2020)	Pultrall Inc. (Thetford Mines, QC, Canada)	CFRP	13.0	Vinylester	Control	NA	0	4	100.0	4-6	100.0
150	Benmokrane et al. (2020)	Pultrall Inc. (Thetford Mines, QC, Canada)	CFRP	13.0	Vinylester	Alkaline solution (IMMR)	60	90	4	97.6	4-6	65.8
151	Chen et al. (2007)	Hughes Brothers, Inc.	GFRP	9.5	Vinylester	Control	20	0	NA	NA	6	100.0
152	Chen et al. (2007)	Hughes Brothers, Inc.	GFRP	9.5	Vinylester	Water (IMMR)	60	45	NA	NA	5	95.3
153	Chen et al. (2007)	Hughes Brothers, Inc.	GFRP	9.5	Vinylester	Water (FT)	-20/20	50	NA	NA	5	102.3
154	Chen et al. (2007)	Hughes Brothers, Inc.	GFRP	9.5	Vinylester	Water (FT)	-20/20	100	NA	NA	5	93.0
155	Chen et al. (2007)	Hughes Brothers, Inc.	GFRP	9.5	Vinylester	Alkaline solution 1 (IMMR)	60	45	NA	NA	6	90.7
156	Chen et al. (2007)	Hughes Brothers, Inc.	GFRP	9.5	Vinylester	Alkaline solution 2 (IMMR)	60	45	NA	NA	6	97.7
157	Chen et al. (2007)	Hughes Brothers, Inc.	GFRP	9.5	Vinylester	Alkaline solution with Cl- (FT)	-20/20	50	NA	NA	5	102.3

158	Chen et al. (2007)	Hughes Brothers, Inc.	GFRP	9.5	Vinylester	Alkaline solution with Cl- (FT)	-20/20	100	NA	NA	5	97.7
159	Chen et al. (2007)	Hughes Brothers, Inc.	GFRP	9.5	Vinylester	NCE+Water (IMMR)	20	60	NA	NA	5	100.0
160	Chen et al. (2007)	Hughes Brothers, Inc.	GFRP	9.5	Vinylester	NCE+Alkaline solution 2 (IMMR)	60	60	NA	NA	5	88.4
161	Chen et al. (2007)	NA	GFRP	9.5	Vinylester	Control	20	0	NA	NA	6	100.0
162	Chen et al. (2007)	NA	GFRP	9.5	Vinylester	Water (IMMR)	60	45	NA	NA	6	90.7
163	Chen et al. (2007)	NA	GFRP	9.5	Vinylester	Water (FT)	-20/20	50	NA	NA	5	86.0
164	Chen et al. (2007)	NA	GFRP	9.5	Vinylester	Alkaline solution 1 (IMMR)	60	45	NA	NA	6	79.1
165	Chen et al. (2007)	NA	GFRP	9.5	Vinylester	Alkaline solution 2 (IMMR)	60	45	NA	NA	6	93.0
166	Chen et al. (2007)	NA	GFRP	9.5	Vinylester	Saline solution (IMMR)	60	45	NA	NA	5	90.7
167	Chen et al. (2007)	NA	GFRP	9.5	Vinylester	Alkaline solution with Cl- (FT)	-20/20	50	NA	NA	5	97.7
168	Chen et al. (2007)	NA	GFRP	9.5	Vinylester	Alkaline solution with Cl- (FT)	-20/20	100	NA	NA	5	90.7
169	Chen et al. (2007)	Hughes Brothers, Inc.	CFRP	9.0	Epoxy	Control	20	0	NA	NA	9	116.3
170	Chen et al. (2007)	Hughes Brothers, Inc.	CFRP	9.0	Epoxy	Alkaline solution 1 (FT)	-20/20	100	NA	NA	5	111.6
171	D'Antino (2023)	Sireg Geotech srl (Italy)	GFRP	6.0	Vinylester	Control	RT	0	NA	NA	5	100.0
172	D'Antino (2023)	Sireg Geotech srl (Italy)	GFRP	6.0	Vinylester	Alkaline solution (IMMR)	60	42	NA	NA	5	66.7
173	D'Antino (2023)	Sireg Geotech srl (Italy)	GFRP	20.0	Vinylester	Control	RT	0	NA	NA	5	100.0
174	D'Antino (2023)	Sireg Geotech srl (Italy)	GFRP	20.0	Vinylester	Alkaline solution (IMMR)	60	42	NA	NA	5	113.1
175	D'Antino (2023)	Sireg Geotech srl (Italy)	GFRP	32.0	Vinylester	Control	RT	0	NA	NA	5	100.0
176	D'Antino (2023)	Sireg Geotech srl (Italy)	GFRP	32.0	Vinylester	Alkaline solution (IMMR)	60	42	NA	NA	5	123.2
177	Feng et al. (2023)	Green Material Valley (GMV) New Material Technology Co., Ltd. (Zhenjiang, China)	BFRP	8.0	Epoxy	Control	25	0	NA	NA	5	100.0
178	Feng et al. (2023)	Green Material Valley (GMV) New Material Technology Co., Ltd. (Zhenjiang, China)	BFRP	8.0	Epoxy	Alkaline solution 1 (IMMR)	25	60	NA	NA	5	93.1

179	Feng et al. (2023)	Green Material Valley (GMV) New Material Technology Co., Ltd. (Zhenjiang, China)	BFRP	8.0	Epoxy	Alkaline solution 1 (IMMR)	25	120	NA	NA	5	87.1
180	Feng et al. (2023)	Green Material Valley (GMV) New Material Technology Co., Ltd. (Zhenjiang, China)	BFRP	8.0	Epoxy	Alkaline solution 1 (IMMR)	25	180	NA	NA	5	73.5
181	Feng et al. (2023)	Green Material Valley (GMV) New Material Technology Co., Ltd. (Zhenjiang, China)	BFRP	8.0	Epoxy	Alkaline solution 1 (IMMR)	40	60	NA	NA	5	82.6
182	Feng et al. (2023)	Green Material Valley (GMV) New Material Technology Co., Ltd. (Zhenjiang, China)	BFRP	8.0	Epoxy	Alkaline solution 1 (IMMR)	40	120	NA	NA	5	69.5
183	Feng et al. (2023)	Green Material Valley (GMV) New Material Technology Co., Ltd. (Zhenjiang, China)	BFRP	8.0	Epoxy	Alkaline solution 1 (IMMR)	40	180	NA	NA	5	58.3
184	Feng et al. (2023)	Green Material Valley (GMV) New Material Technology Co., Ltd. (Zhenjiang, China)	BFRP	8.0	Epoxy	Alkaline solution 1 (IMMR)	55	60	NA	NA	5	79.4
185	Feng et al. (2023)	Green Material Valley (GMV) New Material Technology Co., Ltd. (Zhenjiang, China)	BFRP	8.0	Epoxy	Alkaline solution 1 (IMMR)	55	120	NA	NA	5	51.2
186	Feng et al. (2023)	Green Material Valley (GMV) New Material Technology Co., Ltd. (Zhenjiang, China)	BFRP	8.0	Epoxy	Alkaline solution 1 (IMMR)	55	180	NA	NA	5	46.5
187	Feng et al. (2023)	Green Material Valley (GMV) New Material Technology Co., Ltd. (Zhenjiang, China)	BFRP	8.0	Epoxy	Alkaline solution 2 (IMMR)	25	60	NA	NA	5	71.0
188	Feng et al. (2023)	Green Material Valley (GMV) New Material Technology Co., Ltd. (Zhenjiang, China)	BFRP	8.0	Epoxy	Alkaline solution 2 (IMMR)	25	120	NA	NA	5	57.2
189	Feng et al. (2023)	Green Material Valley (GMV) New Material Technology Co., Ltd. (Zhenjiang, China)	BFRP	8.0	Epoxy	Alkaline solution 2 (IMMR)	25	180	NA	NA	5	49.5
190	Feng et al. (2023)	Green Material Valley (GMV) New Material	BFRP	8.0	Epoxy	Alkaline solution 2 (IMMR)	40	60	NA	NA	5	55.7

		Technology Co., Ltd. (Zhenjiang, China)										
191	Feng et al. (2023)	Green Material Valley (GMV) New Material Technology Co., Ltd. (Zhenjiang, China)	BFRP	8.0	Epoxy	Alkaline solution 2 (IMMR)	40	120	NA	NA	5	38.9
192	Feng et al. (2023)	Green Material Valley (GMV) New Material Technology Co., Ltd. (Zhenjiang, China)	BFRP	8.0	Epoxy	Alkaline solution 2 (IMMR)	40	180	NA	NA	5	31.6
193	Feng et al. (2023)	Green Material Valley (GMV) New Material Technology Co., Ltd. (Zhenjiang, China)	BFRP	8.0	Epoxy	Alkaline solution 2 (IMMR)	55	60	NA	NA	5	37.6
194	Feng et al. (2023)	Green Material Valley (GMV) New Material Technology Co., Ltd. (Zhenjiang, China)	BFRP	8.0	Epoxy	Alkaline solution 2 (IMMR)	55	120	NA	NA	5	21.5
195	Feng et al. (2023)	Green Material Valley (GMV) New Material Technology Co., Ltd. (Zhenjiang, China)	BFRP	8.0	Epoxy	Alkaline solution 2 (IMMR)	55	180	NA	NA	5	7.7
196	Feng et al. (2023)	Green Material Valley (GMV) New Material Technology Co., Ltd. (Zhenjiang, China)	BFRP	8.0	Epoxy	SWSSCE 1+Simulated seawater (IMMR)	25	60	NA	NA	5	94.4
197	Feng et al. (2023)	Green Material Valley (GMV) New Material Technology Co., Ltd. (Zhenjiang, China)	BFRP	8.0	Epoxy	SWSSCE 1+Simulated seawater (IMMR)	25	120	NA	NA	5	90.1
198	Feng et al. (2023)	Green Material Valley (GMV) New Material Technology Co., Ltd. (Zhenjiang, China)	BFRP	8.0	Epoxy	SWSSCE 1+Simulated seawater (IMMR)	25	180	NA	NA	5	87.1
199	Feng et al. (2023)	Green Material Valley (GMV) New Material Technology Co., Ltd. (Zhenjiang, China)	BFRP	8.0	Epoxy	SWSSCE 1+Simulated seawater (IMMR)	40	60	NA	NA	5	91.6
200	Feng et al. (2023)	Green Material Valley (GMV) New Material Technology Co., Ltd. (Zhenjiang, China)	BFRP	8.0	Epoxy	SWSSCE 1+Simulated seawater (IMMR)	40	120	NA	NA	5	86.5
201	Feng et al. (2023)	Green Material Valley (GMV) New Material Technology Co., Ltd. (Zhenjiang, China)	BFRP	8.0	Epoxy	SWSSCE 1+Simulated seawater (IMMR)	40	180	NA	NA	5	85.6

202	Feng et al. (2023)	Green Material Valley (GMV) New Material Technology Co., Ltd. (Zhenjiang, China)	BFRP	8.0	Epoxy	SWSSCE seawater (IMMR)	1+Simulated	55	60	NA	NA	5	88.2
203	Feng et al. (2023)	Green Material Valley (GMV) New Material Technology Co., Ltd. (Zhenjiang, China)	BFRP	8.0	Epoxy	SWSSCE seawater (IMMR)	1+Simulated	55	120	NA	NA	5	84.1
204	Feng et al. (2023)	Green Material Valley (GMV) New Material Technology Co., Ltd. (Zhenjiang, China)	BFRP	8.0	Epoxy	SWSSCE seawater (IMMR)	1+Simulated	55	180	NA	NA	5	81.3
205	Feng et al. (2023)	Green Material Valley (GMV) New Material Technology Co., Ltd. (Zhenjiang, China)	BFRP	8.0	Epoxy	SWSSCE seawater (IMMR)	2+Simulated	25	60	NA	NA	5	89.2
206	Feng et al. (2023)	Green Material Valley (GMV) New Material Technology Co., Ltd. (Zhenjiang, China)	BFRP	8.0	Epoxy	SWSSCE seawater (IMMR)	2+Simulated	25	120	NA	NA	5	79.1
207	Feng et al. (2023)	Green Material Valley (GMV) New Material Technology Co., Ltd. (Zhenjiang, China)	BFRP	8.0	Epoxy	SWSSCE seawater (IMMR)	2+Simulated	25	180	NA	NA	5	72.5
208	Feng et al. (2023)	Green Material Valley (GMV) New Material Technology Co., Ltd. (Zhenjiang, China)	BFRP	8.0	Epoxy	SWSSCE seawater (IMMR)	2+Simulated	40	60	NA	NA	5	82.2
209	Feng et al. (2023)	Green Material Valley (GMV) New Material Technology Co., Ltd. (Zhenjiang, China)	BFRP	8.0	Epoxy	SWSSCE seawater (IMMR)	2+Simulated	40	120	NA	NA	5	71.0
210	Feng et al. (2023)	Green Material Valley (GMV) New Material Technology Co., Ltd. (Zhenjiang, China)	BFRP	8.0	Epoxy	SWSSCE seawater (IMMR)	2+Simulated	40	180	NA	NA	5	59.4
211	Feng et al. (2023)	Green Material Valley (GMV) New Material Technology Co., Ltd. (Zhenjiang, China)	BFRP	8.0	Epoxy	SWSSCE seawater (IMMR)	2+Simulated	55	60	NA	NA	5	66.5
212	Feng et al. (2023)	Green Material Valley (GMV) New Material Technology Co., Ltd. (Zhenjiang, China)	BFRP	8.0	Epoxy	SWSSCE seawater (IMMR)	2+Simulated	55	120	NA	NA	5	63.0
213	Feng et al. (2023)	Green Material Valley (GMV) New Material	BFRP	8.0	Epoxy	SWSSCE seawater (IMMR)	2+Simulated	55	180	NA	NA	5	53.8

		Technology Co., Ltd. (Zhenjiang, China)										
214	Fergani et al. (2018)	NA	GFRP	8.0	Vinylester	Control	20	0	NA	NA	5	100.0
215	Fergani et al. (2018)	NA	GFRP	8.0	Vinylester	Alkaline solution (IMMR)	20	270	NA	NA	3	95.9
216	Fergani et al. (2018)	NA	GFRP	8.0	Vinylester	Alkaline solution (IMMR)	40	270	NA	NA	3	93.2
217	Fergani et al. (2018)	NA	GFRP	8.0	Vinylester	Alkaline solution (IMMR)	60	270	NA	NA	3	74.0
218	Fergani et al. (2018)	NA	GFRP	8.0	Vinylester	SL (3000με)+Alkaline solution (IMMR)	20	270	NA	NA	3	90.4
219	Fergani et al. (2018)	NA	GFRP	8.0	Vinylester	SL (3000με)+Alkaline solution (IMMR)	40	270	NA	NA	3	87.7
220	Fergani et al. (2018)	NA	GFRP	8.0	Vinylester	SL (3000με)+Alkaline solution (IMMR)	60	270	NA	NA	3	83.6
221	Fergani et al. (2018)	NA	GFRP	8.0	Vinylester	Water (IMMR)	20	270	NA	NA	3	90.4
222	Fergani et al. (2018)	NA	GFRP	8.0	Vinylester	Water (IMMR)	40	270	NA	NA	3	86.3
223	Fergani et al. (2018)	NA	GFRP	8.0	Vinylester	Water (IMMR)	60	270	NA	NA	3	86.3
224	Fergani et al. (2018)	NA	GFRP	8.0	Vinylester	SL (3000με)+Water (IMMR)	20	270	NA	NA	3	89.0
225	Fergani et al. (2018)	NA	GFRP	8.0	Vinylester	SL (3000με)+Water (IMMR)	40	270	NA	NA	3	87.7
226	Fergani et al. (2018)	NA	GFRP	8.0	Vinylester	SL (3000με)+Water (IMMR)	60	270	NA	NA	3	86.3
227	Guo et al. (2024)	NA	BFRP	10.0	Epoxy	Control	NA	0	NA	NA	3	100.0
228	Guo et al. (2024)	NA	BFRP	10.0	Epoxy	NCE+Seawater (IMMR)	55	30	NA	NA	0	88.4
229	Guo et al. (2024)	NA	BFRP	10.0	Epoxy	NCE+Seawater (IMMR)	55	60	NA	NA	0	85.1
230	Guo et al. (2024)	NA	BFRP	10.0	Epoxy	NCE+Seawater (IMMR)	55	90	NA	NA	0	80.3
231	Guo et al. (2024)	NA	BFRP	10.0	Epoxy	NCE+Seawater (IMMR)	55	180	NA	NA	1	68.9
232	Guo et al. (2024)	NA	BFRP	10.0	Epoxy	NCE+Seawater (IMMR)	55	270	NA	NA	1	68.2
233	Guo et al. (2024)	NA	BFRP	10.0	Epoxy	NCE+Seawater (IMMR)	55	360	NA	NA	3	67.9
234	Guo et al. (2024)	NA	BFRP	10.0	Epoxy	SWSSCE+Seawater (IMMR)	21	30	NA	NA	3	101.1
235	Guo et al. (2024)	NA	BFRP	10.0	Epoxy	SWSSCE+Seawater (IMMR)	21	60	NA	NA	3	96.0

236	Guo et al. (2024)	NA	BFRP	10.0	Epoxy	SWSSCE+Seawater (IMMR)	21	90	NA	NA	3	94.6
237	Guo et al. (2024)	NA	BFRP	10.0	Epoxy	SWSSCE+Seawater (IMMR)	21	180	NA	NA	3	88.6
238	Guo et al. (2024)	NA	BFRP	10.0	Epoxy	SWSSCE+Seawater (IMMR)	21	270	NA	NA	3	86.0
239	Guo et al. (2024)	NA	BFRP	10.0	Epoxy	SWSSCE+Seawater (IMMR)	21	360	NA	NA	3	86.9
240	Guo et al. (2024)	NA	BFRP	10.0	Epoxy	SWSSCE+Seawater (IMMR)	40	30	NA	NA	3	91.5
241	Guo et al. (2024)	NA	BFRP	10.0	Epoxy	SWSSCE+Seawater (IMMR)	40	60	NA	NA	3	90.1
242	Guo et al. (2024)	NA	BFRP	10.0	Epoxy	SWSSCE+Seawater (IMMR)	40	90	NA	NA	3	86.2
243	Guo et al. (2024)	NA	BFRP	10.0	Epoxy	SWSSCE+Seawater (IMMR)	40	180	NA	NA	3	80.1
244	Guo et al. (2024)	NA	BFRP	10.0	Epoxy	SWSSCE+Seawater (IMMR)	40	270	NA	NA	3	82.0
245	Guo et al. (2024)	NA	BFRP	10.0	Epoxy	SWSSCE+Seawater (IMMR)	40	360	NA	NA	3	81.2
246	Guo et al. (2024)	NA	BFRP	10.0	Epoxy	SWSSCE+Seawater (IMMR)	55	30	NA	NA	3	86.2
247	Guo et al. (2024)	NA	BFRP	10.0	Epoxy	SWSSCE+Seawater (IMMR)	55	60	NA	NA	3	80.6
248	Guo et al. (2024)	NA	BFRP	10.0	Epoxy	SWSSCE+Seawater (IMMR)	55	90	NA	NA	3	76.6
249	Guo et al. (2024)	NA	BFRP	10.0	Epoxy	SWSSCE+Seawater (IMMR)	55	180	NA	NA	3	65.2
250	Guo et al. (2024)	NA	BFRP	10.0	Epoxy	SWSSCE+Seawater (IMMR)	55	270	NA	NA	3	62.3
251	Guo et al. (2024)	NA	BFRP	10.0	Epoxy	SWSSCE+Seawater (IMMR)	55	360	NA	NA	3	62.5
252	Hosseini et al. (2024)	Pultrall Inc. (Thetford Mines, QC, Canada)	GFRP	15.0	Vinylester	Control	24	0	5	100.0	5	100.0
253	Hosseini et al. (2024)	Pultrall Inc. (Thetford Mines, QC, Canada)	GFRP	15.0	Vinylester	Alkaline solution (IMMR)	24	42	5	89.9	5	101.9
254	Hosseini et al. (2024)	Pultrall Inc. (Thetford Mines, QC, Canada)	GFRP	15.0	Vinylester	Alkaline solution (IMMR)	24	125	5	88.5	5	100.0
255	Hosseini et al. (2024)	Pultrall Inc. (Thetford Mines, QC, Canada)	GFRP	15.0	Vinylester	Alkaline solution (IMMR)	24	250	5	85.3	5	98.1
256	Hosseini et al. (2024)	Pultrall Inc. (Thetford Mines, QC, Canada)	GFRP	15.0	Vinylester	Alkaline solution (IMMR)	40	42	5	86.6	5	101.9
257	Hosseini et al. (2024)	Pultrall Inc. (Thetford Mines, QC, Canada)	GFRP	15.0	Vinylester	Alkaline solution (IMMR)	40	125	5	86.2	5	100.0
258	Hosseini et al. (2024)	Pultrall Inc. (Thetford Mines, QC, Canada)	GFRP	15.0	Vinylester	Alkaline solution (IMMR)	40	250	5	78.3	5	96.2

259	Hosseini et al. (2024)	Pultrall Inc. (Thetford Mines, QC, Canada)	GFRP	15.0	Vinylester	Alkaline solution (IMMR)	50	42	5	84.3	5	100.0
260	Hosseini et al. (2024)	Pultrall Inc. (Thetford Mines, QC, Canada)	GFRP	15.0	Vinylester	Alkaline solution (IMMR)	50	125	5	84.8	5	98.1
261	Hosseini et al. (2024)	Pultrall Inc. (Thetford Mines, QC, Canada)	GFRP	15.0	Vinylester	Alkaline solution (IMMR)	50	250	5	77.4	5	92.3
262	Hosseini et al. (2024)	Pultrall Inc. (Thetford Mines, QC, Canada)	GFRP	15.0	Vinylester	Alkaline solution (IMMR)	60	42	5	84.3	5	98.1
263	Hosseini et al. (2024)	Pultrall Inc. (Thetford Mines, QC, Canada)	GFRP	15.0	Vinylester	Alkaline solution (IMMR)	60	125	5	84.3	5	98.1
264	Hosseini et al. (2024)	Pultrall Inc. (Thetford Mines, QC, Canada)	GFRP	15.0	Vinylester	Alkaline solution (IMMR)	60	250	5	74.2	5	88.5
265	Khatibmasjedi and Nanni (2017)	NA	GFRP	15.8	Vinylester	Control	NA	0	NA	100.0	NA	100.0
266	Khatibmasjedi and Nanni (2017)	NA	GFRP	15.8	Vinylester	NCE+Seawater (IMMR)	60	180	NA	95.2	NA	93.8
267	Khatibmasjedi and Nanni (2017)	NA	GFRP	15.8	Vinylester	SWCE+Seawater (IMMR)	60	180	NA	87.6	NA	103.4
268	Khatibmasjedi et al. (2020)	NA	GFRP	15.8	Vinylester	Control	NA	0	5	100.0	5	100.0
269	Khatibmasjedi et al. (2020)	NA	GFRP	15.8	Vinylester	NCE+Seawater (IMMR)	60	180	5	94.9	5	94.2
270	Khatibmasjedi et al. (2020)	NA	GFRP	15.8	Vinylester	NCE+Seawater (IMMR)	60	360	5	76.6	5	82.7
271	Khatibmasjedi et al. (2020)	NA	GFRP	15.8	Vinylester	NCE+Seawater (IMMR)	60	540	5	72.8	5	84.6
272	Khatibmasjedi et al. (2020)	NA	GFRP	15.8	Vinylester	NCE+Seawater (IMMR)	60	720	5	70.6	5	78.8
273	Khatibmasjedi et al. (2020)	NA	GFRP	15.8	Vinylester	SWCE+Seawater (IMMR)	60	180	5	87.2	5	103.8
274	Khatibmasjedi et al. (2020)	NA	GFRP	15.8	Vinylester	SWCE+Seawater (IMMR)	60	360	5	85.1	5	90.4
275	Khatibmasjedi et al. (2020)	NA	GFRP	15.8	Vinylester	SWCE+Seawater (IMMR)	60	540	5	83.0	5	80.8
276	Khatibmasjedi et al. (2020)	NA	GFRP	15.8	Vinylester	SWCE+Seawater (IMMR)	60	720	5	74.9	5	73.1
277	Kim et al. (2008)	NA	GFRP	12.7	Vinylester	Control	25	0	NA	NA	8	100.0
278	Kim et al. (2008)	NA	GFRP	12.7	Vinylester	Water (IMMR)	80	90	NA	NA	8	89.4
279	Kim et al. (2008)	NA	GFRP	12.7	Vinylester	Saline solution (IMMR)	80	90	NA	NA	8	87.5
280	Kim et al.	NA	GFRP	12.7	Vinylester	Alkaline solution (IMMR)	40	60	NA	NA	8	83.2

	(2008)												
281	Kim et al. (2008)	NA	GFRP	12.7	Vinylester	Alkaline solution (FT)	-25/30	60	NA	NA	8	70.7
282	Kim et al. (2008)	NA	GFRP	12.7	Modified vinylester	Control	25	0	NA	NA	8	100.0
283	Kim et al. (2008)	NA	GFRP	12.7	Modified vinylester	Water (IMMR)	80	90	NA	NA	8	76.6
284	Kim et al. (2008)	NA	GFRP	12.7	Modified vinylester	Saline solution (IMMR)	80	90	NA	NA	8	79.9
285	Kim et al. (2008)	NA	GFRP	12.7	Modified vinylester	Alkaline solution (IMMR)	40	60	NA	NA	8	76.1
286	Kim et al. (2008)	NA	GFRP	12.7	Modified vinylester	Alkaline solution (FT)	-25/30	60	NA	NA	8	94.1
287	Li et al. (2022b)	Shandong Safety Industrial Co., Ltd. (China)	GFRP	16.0	NA	Control	NA	0	NA	NA	NA	100.0
288	Li et al. (2022b)	Shandong Safety Industrial Co., Ltd. (China)	GFRP	16.0	NA	Seawater (IMMR)	25	15	NA	NA	NA	98.5
289	Li et al. (2022b)	Shandong Safety Industrial Co., Ltd. (China)	GFRP	16.0	NA	Seawater (IMMR)	25	30	NA	NA	NA	98.2
290	Li et al. (2022b)	Shandong Safety Industrial Co., Ltd. (China)	GFRP	16.0	NA	Seawater (IMMR)	25	60	NA	NA	NA	95.9
291	Li et al. (2022b)	Shandong Safety Industrial Co., Ltd. (China)	GFRP	16.0	NA	Seawater (IMMR)	25	90	NA	NA	NA	94.8
292	Li et al. (2022b)	Shandong Safety Industrial Co., Ltd. (China)	GFRP	16.0	NA	Seawater (IMMR)	25	183	NA	NA	NA	91.8
293	Li et al. (2022b)	Shandong Safety Industrial Co., Ltd. (China)	GFRP	16.0	NA	Seawater (IMMR)	40	15	NA	NA	NA	97.1
294	Li et al. (2022b)	Shandong Safety Industrial Co., Ltd. (China)	GFRP	16.0	NA	Seawater (IMMR)	40	30	NA	NA	NA	96.0
295	Li et al. (2022b)	Shandong Safety Industrial Co., Ltd. (China)	GFRP	16.0	NA	Seawater (IMMR)	40	60	NA	NA	NA	93.9
296	Li et al. (2022b)	Shandong Safety Industrial Co., Ltd. (China)	GFRP	16.0	NA	Seawater (IMMR)	40	90	NA	NA	NA	92.3
297	Li et al. (2022b)	Shandong Safety Industrial Co., Ltd. (China)	GFRP	16.0	NA	Seawater (IMMR)	40	183	NA	NA	NA	86.6

298	Li et al. (2022b)	Shandong Safety Industrial Co., Ltd. (China)	GFRP	16.0	NA	Seawater (IMMR)	60	15	NA	NA	NA	94.4
299	Li et al. (2022b)	Shandong Safety Industrial Co., Ltd. (China)	GFRP	16.0	NA	Seawater (IMMR)	60	30	NA	NA	NA	89.9
300	Li et al. (2022b)	Shandong Safety Industrial Co., Ltd. (China)	GFRP	16.0	NA	Seawater (IMMR)	60	60	NA	NA	NA	83.3
301	Li et al. (2022b)	Shandong Safety Industrial Co., Ltd. (China)	GFRP	16.0	NA	Seawater (IMMR)	60	90	NA	NA	NA	75.5
302	Li et al. (2022b)	Shandong Safety Industrial Co., Ltd. (China)	GFRP	16.0	NA	Seawater (IMMR)	60	183	NA	NA	NA	66.4
303	Li et al. (2022b)	Shandong Safety Industrial Co., Ltd. (China)	GFRP	16.0	NA	Alkaline solution with Cl- (IMMR)	25	15	NA	NA	NA	95.9
304	Li et al. (2022b)	Shandong Safety Industrial Co., Ltd. (China)	GFRP	16.0	NA	Alkaline solution with Cl- (IMMR)	25	30	NA	NA	NA	93.2
305	Li et al. (2022b)	Shandong Safety Industrial Co., Ltd. (China)	GFRP	16.0	NA	Alkaline solution with Cl- (IMMR)	25	60	NA	NA	NA	87.2
306	Li et al. (2022b)	Shandong Safety Industrial Co., Ltd. (China)	GFRP	16.0	NA	Alkaline solution with Cl- (IMMR)	25	90	NA	NA	NA	81.8
307	Li et al. (2022b)	Shandong Safety Industrial Co., Ltd. (China)	GFRP	16.0	NA	Alkaline solution with Cl- (IMMR)	25	183	NA	NA	NA	78.3
308	Li et al. (2022b)	Shandong Safety Industrial Co., Ltd. (China)	GFRP	16.0	NA	Alkaline solution with Cl- (IMMR)	40	15	NA	NA	NA	95.5
309	Li et al. (2022b)	Shandong Safety Industrial Co., Ltd. (China)	GFRP	16.0	NA	Alkaline solution with Cl- (IMMR)	40	30	NA	NA	NA	92.5
310	Li et al. (2022b)	Shandong Safety Industrial Co., Ltd. (China)	GFRP	16.0	NA	Alkaline solution with Cl- (IMMR)	40	60	NA	NA	NA	85.5
311	Li et al. (2022b)	Shandong Safety Industrial Co., Ltd. (China)	GFRP	16.0	NA	Alkaline solution with Cl- (IMMR)	40	90	NA	NA	NA	77.9
312	Li et al. (2022b)	Shandong Safety Industrial Co., Ltd. (China)	GFRP	16.0	NA	Alkaline solution with Cl- (IMMR)	40	183	NA	NA	NA	68.7
313	Li et al.	Shandong Safety	GFRP	16.0	NA	Alkaline solution with Cl-	60	15	NA	NA	NA	90.2

	(2022b)		Industrial Co., Ltd. (China)					(IMMR)								
314	Li et al. (2022b)		Shandong Safety Industrial Co., Ltd. (China)	GFRP	16.0	NA		Alkaline solution with Cl- (IMMR)		60	30	NA	NA	NA	81.5	
315	Li et al. (2022b)		Shandong Safety Industrial Co., Ltd. (China)	GFRP	16.0	NA		Alkaline solution with Cl- (IMMR)		60	60	NA	NA	NA	70.8	
316	Li et al. (2022b)		Shandong Safety Industrial Co., Ltd. (China)	GFRP	16.0	NA		Alkaline solution with Cl- (IMMR)		60	90	NA	NA	NA	61.7	
317	Li et al. (2022b)		Shandong Safety Industrial Co., Ltd. (China)	GFRP	16.0	NA		Alkaline solution with Cl- (IMMR)		60	183	NA	NA	NA	45.4	
318	Li et al. (2022b)		Shandong Safety Industrial Co., Ltd. (China)	GFRP	16.0	NA		SWCE+Seawater (IMMR)		25	15	NA	NA	NA	97.8	
319	Li et al. (2022b)		Shandong Safety Industrial Co., Ltd. (China)	GFRP	16.0	NA		SWCE+Seawater (IMMR)		25	30	NA	NA	NA	96.6	
320	Li et al. (2022b)		Shandong Safety Industrial Co., Ltd. (China)	GFRP	16.0	NA		SWCE+Seawater (IMMR)		25	60	NA	NA	NA	94.4	
321	Li et al. (2022b)		Shandong Safety Industrial Co., Ltd. (China)	GFRP	16.0	NA		SWCE+Seawater (IMMR)		25	90	NA	NA	NA	92.4	
322	Li et al. (2022b)		Shandong Safety Industrial Co., Ltd. (China)	GFRP	16.0	NA		SWCE+Seawater (IMMR)		25	183	NA	NA	NA	89.2	
323	Li et al. (2022b)		Shandong Safety Industrial Co., Ltd. (China)	GFRP	16.0	NA		SWCE+Seawater (IMMR)		40	15	NA	NA	NA	96.7	
324	Li et al. (2022b)		Shandong Safety Industrial Co., Ltd. (China)	GFRP	16.0	NA		SWCE+Seawater (IMMR)		40	30	NA	NA	NA	94.9	
325	Li et al. (2022b)		Shandong Safety Industrial Co., Ltd. (China)	GFRP	16.0	NA		SWCE+Seawater (IMMR)		40	60	NA	NA	NA	91.2	
326	Li et al. (2022b)		Shandong Safety Industrial Co., Ltd. (China)	GFRP	16.0	NA		SWCE+Seawater (IMMR)		40	90	NA	NA	NA	88.1	
327	Li et al. (2022b)		Shandong Safety Industrial Co., Ltd. (China)	GFRP	16.0	NA		SWCE+Seawater (IMMR)		40	183	NA	NA	NA	80.2	
328	Li et al. (2022b)		Shandong Safety Industrial Co., Ltd.	GFRP	16.0	NA		SWCE+Seawater (IMMR)		60	15	NA	NA	NA	92.9	

		(China)										
329	Li et al. (2022b)	Shandong Safety Industrial Co., Ltd. (China)	GFRP	16.0	NA	SWCE+Seawater (IMMR)	60	30	NA	NA	NA	87.0
330	Li et al. (2022b)	Shandong Safety Industrial Co., Ltd. (China)	GFRP	16.0	NA	SWCE+Seawater (IMMR)	60	60	NA	NA	NA	76.6
331	Li et al. (2022b)	Shandong Safety Industrial Co., Ltd. (China)	GFRP	16.0	NA	SWCE+Seawater (IMMR)	60	90	NA	NA	NA	68.3
332	Li et al. (2022b)	Shandong Safety Industrial Co., Ltd. (China)	GFRP	16.0	NA	SWCE+Seawater (IMMR)	60	183	NA	NA	NA	53.1
333	Li et al. (2023)	NA	BFRP	8.0	Epoxy	Control	NA	0	NA	NA	4	100.0
334	Li et al. (2023)	NA	BFRP	8.0	Epoxy	SWSSCE+Simulated seawater (IMMR)	25	90	NA	NA	4	90.2
335	Li et al. (2023)	NA	BFRP	8.0	Epoxy	SWSSCE+Simulated seawater (IMMR)	25	180	NA	NA	4	86.6
336	Li et al. (2023)	NA	BFRP	8.0	Epoxy	SWSSCE+Simulated seawater (IMMR)	25	270	NA	NA	4	77.2
337	Li et al. (2023)	NA	BFRP	8.0	Epoxy	SWSSCE+Simulated seawater (IMMR)	55	90	NA	NA	4	70.9
338	Li et al. (2023)	NA	BFRP	8.0	Epoxy	SWSSCE+Simulated seawater (IMMR)	55	180	NA	NA	4	60.2
339	Li et al. (2023)	NA	BFRP	8.0	Epoxy	SWSSCE+Simulated seawater (IMMR)	55	270	NA	NA	4	41.3
340	Liu et al. (2019)	Green Material Valley (GMV) New Material Technology Co., Ltd. (Zhenjiang, China)	BFRP	5.8	Vinylester	Control	Na	0	5	100.0	NA	NA
341	Liu et al. (2019)	Green Material Valley (GMV) New Material Technology Co., Ltd. (Zhenjiang, China)	BFRP	5.8	Vinylester	Alkaline solution with Cl- (WD)	55	21	5	94.6	NA	NA
342	Liu et al. (2019)	Green Material Valley (GMV) New Material Technology Co., Ltd. (Zhenjiang, China)	BFRP	5.8	Vinylester	Alkaline solution with Cl- (WD)	55	42	5	87.8	NA	NA
343	Liu et al. (2019)	Green Material Valley (GMV) New Material Technology Co., Ltd. (Zhenjiang, China)	BFRP	5.8	Vinylester	Alkaline solution with Cl- (WD)	55	63	5	77.8	NA	NA
344	Liu et al. (2019)	Green Material Valley (GMV) New Material Technology Co., Ltd. (Zhenjiang, China)	BFRP	5.9	Epoxy	Control	Na	0	5	100.0	NA	NA

345	Liu et al. (2019)	Green Material Valley (GMV) New Material Technology Co., Ltd. (Zhenjiang, China)	BFRP	5.9	Epoxy	Alkaline solution with Cl- (WD)	55	21	5	90.2	NA	NA
346	Liu et al. (2019)	Green Material Valley (GMV) New Material Technology Co., Ltd. (Zhenjiang, China)	BFRP	5.9	Epoxy	Alkaline solution with Cl- (WD)	55	42	5	73.6	NA	NA
347	Liu et al. (2019)	Green Material Valley (GMV) New Material Technology Co., Ltd. (Zhenjiang, China)	BFRP	5.9	Epoxy	Alkaline solution with Cl- (WD)	55	63	5	63.6	NA	NA
348	Liu et al. (2019)	Green Material Valley (GMV) New Material Technology Co., Ltd. (Zhenjiang, China)	BFRP	5.8	Vinylester	Control	Na	0	5	100.0	NA	NA
349	Liu et al. (2019)	Green Material Valley (GMV) New Material Technology Co., Ltd. (Zhenjiang, China)	BFRP	5.8	Vinylester	Alkaline solution with Cl- (WD)	55	21	5	95.5	NA	NA
350	Liu et al. (2019)	Green Material Valley (GMV) New Material Technology Co., Ltd. (Zhenjiang, China)	BFRP	5.8	Vinylester	Alkaline solution with Cl- (WD)	55	42	5	84.7	NA	NA
351	Liu et al. (2019)	Green Material Valley (GMV) New Material Technology Co., Ltd. (Zhenjiang, China)	BFRP	5.8	Vinylester	Alkaline solution with Cl- (WD)	55	63	5	73.0	NA	NA
352	Lu et al. (2020b)	TuoXin Aerospace Basalt Industrial Co., Ltd. (Sichuan, China)	BFRP	8.0	Epoxy	Control	23	0	5	100.0	NA	NA
353	Lu et al. (2020b)	TuoXin Aerospace Basalt Industrial Co., Ltd. (Sichuan, China)	BFRP	8.0	Epoxy	Simulated seawater (IMMR)	23	15	5	99.0	NA	NA
354	Lu et al. (2020b)	TuoXin Aerospace Basalt Industrial Co., Ltd. (Sichuan, China)	BFRP	8.0	Epoxy	Simulated seawater (IMMR)	23	30	5	102.4	NA	NA
355	Lu et al. (2020b)	TuoXin Aerospace Basalt Industrial Co., Ltd. (Sichuan, China)	BFRP	8.0	Epoxy	Simulated seawater (IMMR)	23	60	5	105.2	NA	NA
356	Lu et al. (2020b)	TuoXin Aerospace Basalt Industrial Co., Ltd. (Sichuan, China)	BFRP	8.0	Epoxy	Simulated seawater (IMMR)	23	180	5	110.7	NA	NA
357	Lu et al. (2020b)	TuoXin Aerospace Basalt Industrial Co., Ltd. (Sichuan, China)	BFRP	8.0	Epoxy	Simulated seawater (IMMR)	23	360	5	75.3	NA	NA

358	Lu et al. (2020b)	TuoXin Aerospace Basalt Industrial Co., Ltd. (Sichuan, China)	BFRP	8.0	Epoxy	Simulated seawater (IMMR)	40	15	5	91.8	NA	NA
359	Lu et al. (2020b)	TuoXin Aerospace Basalt Industrial Co., Ltd. (Sichuan, China)	BFRP	8.0	Epoxy	Simulated seawater (IMMR)	40	30	5	94.2	NA	NA
360	Lu et al. (2020b)	TuoXin Aerospace Basalt Industrial Co., Ltd. (Sichuan, China)	BFRP	8.0	Epoxy	Simulated seawater (IMMR)	40	60	5	103.4	NA	NA
361	Lu et al. (2020b)	TuoXin Aerospace Basalt Industrial Co., Ltd. (Sichuan, China)	BFRP	8.0	Epoxy	Simulated seawater (IMMR)	40	180	5	103.8	NA	NA
362	Lu et al. (2020b)	TuoXin Aerospace Basalt Industrial Co., Ltd. (Sichuan, China)	BFRP	8.0	Epoxy	Simulated seawater (IMMR)	40	360	5	58.8	NA	NA
363	Lu et al. (2020b)	TuoXin Aerospace Basalt Industrial Co., Ltd. (Sichuan, China)	BFRP	8.0	Epoxy	Simulated seawater (IMMR)	60	15	5	87.6	NA	NA
364	Lu et al. (2020b)	TuoXin Aerospace Basalt Industrial Co., Ltd. (Sichuan, China)	BFRP	8.0	Epoxy	Simulated seawater (IMMR)	60	30	5	84.9	NA	NA
365	Lu et al. (2020b)	TuoXin Aerospace Basalt Industrial Co., Ltd. (Sichuan, China)	BFRP	8.0	Epoxy	Simulated seawater (IMMR)	60	60	5	94.5	NA	NA
366	Lu et al. (2020b)	TuoXin Aerospace Basalt Industrial Co., Ltd. (Sichuan, China)	BFRP	8.0	Epoxy	Simulated seawater (IMMR)	60	180	5	84.2	NA	NA
367	Lu et al. (2020b)	TuoXin Aerospace Basalt Industrial Co., Ltd. (Sichuan, China)	BFRP	8.0	Epoxy	Simulated seawater (IMMR)	60	360	5	18.6	NA	NA
368	Lu et al. (2020b)	TuoXin Aerospace Basalt Industrial Co., Ltd. (Sichuan, China)	BFRP	8.0	Epoxy	NCE+Simulated seawater (IMMR)	23	15	5	108.6	NA	NA
369	Lu et al. (2020b)	TuoXin Aerospace Basalt Industrial Co., Ltd. (Sichuan, China)	BFRP	8.0	Epoxy	NCE+Simulated seawater (IMMR)	23	30	5	107.6	NA	NA
370	Lu et al. (2020b)	TuoXin Aerospace Basalt Industrial Co., Ltd. (Sichuan, China)	BFRP	8.0	Epoxy	NCE+Simulated seawater (IMMR)	23	60	5	105.2	NA	NA
371	Lu et al. (2020b)	TuoXin Aerospace Basalt Industrial Co., Ltd. (Sichuan, China)	BFRP	8.0	Epoxy	NCE+Simulated seawater (IMMR)	23	180	5	85.2	NA	NA
372	Lu et al. (2020b)	TuoXin Aerospace Basalt Industrial Co., Ltd. (Sichuan, China)	BFRP	8.0	Epoxy	NCE+Simulated seawater (IMMR)	23	360	5	51.5	NA	NA
373	Lu et al.	TuoXin	BFRP	6.0	Epoxy	Control	28	0	5	100.0	5	100.0

	(2020c)	Aerospace Basalt Industrial Co., Ltd. (Sichuan, China) TuoXin											
374	Lu et al. (2020c)	Aerospace Basalt Industrial Co., Ltd. (Sichuan, China) TuoXin	BFRP	6.0	Epoxy	Water (IMMR)	28	30	5	99.4	5	87.2	
375	Lu et al. (2020c)	Aerospace Basalt Industrial Co., Ltd. (Sichuan, China) TuoXin	BFRP	6.0	Epoxy	Water (IMMR)	28	90	5	87.2	5	95.7	
376	Lu et al. (2020c)	Aerospace Basalt Industrial Co., Ltd. (Sichuan, China) TuoXin	BFRP	6.0	Epoxy	Water (IMMR)	28	180	5	77.6	5	96.2	
377	Lu et al. (2020c)	Aerospace Basalt Industrial Co., Ltd. (Sichuan, China) TuoXin	BFRP	6.0	Epoxy	Water (IMMR)	28	360	5	77.6	5	85.0	
378	Lu et al. (2020c)	Aerospace Basalt Industrial Co., Ltd. (Sichuan, China) TuoXin	BFRP	6.0	Epoxy	Water (IMMR)	40	30	5	91.0	5	95.0	
379	Lu et al. (2020c)	Aerospace Basalt Industrial Co., Ltd. (Sichuan, China) TuoXin	BFRP	6.0	Epoxy	Water (IMMR)	40	90	5	81.5	5	93.9	
380	Lu et al. (2020c)	Aerospace Basalt Industrial Co., Ltd. (Sichuan, China) TuoXin	BFRP	6.0	Epoxy	Water (IMMR)	40	180	5	87.2	5	87.6	
381	Lu et al. (2020c)	Aerospace Basalt Industrial Co., Ltd. (Sichuan, China) TuoXin	BFRP	6.0	Epoxy	Water (IMMR)	40	360	5	83.4	5	72.4	
382	Lu et al. (2020c)	Aerospace Basalt Industrial Co., Ltd. (Sichuan, China) TuoXin	BFRP	6.0	Epoxy	Water (IMMR)	60	30	5	99.4	5	89.6	
383	Lu et al. (2020c)	Aerospace Basalt Industrial Co., Ltd. (Sichuan, China) TuoXin	BFRP	6.0	Epoxy	Water (IMMR)	60	90	5	84.4	5	77.8	
384	Lu et al. (2020c)	Aerospace Basalt Industrial Co., Ltd.	BFRP	6.0	Epoxy	Water (IMMR)	60	180	5	83.1	5	56.0	

			(Sichuan, China)										
385	Lu et al. (2020c)		TuoXin Aerospace Basalt Industrial Co., Ltd. (Sichuan, China)	BFRP	6.0	Epoxy	Water (IMMR)	60	360	5	79.1	5	44.2
386	Lu et al. (2020c)		TuoXin Aerospace Basalt Industrial Co., Ltd. (Sichuan, China)	BFRP	6.0	Epoxy	Simulated seawater (IMMR)	28	30	5	98.1	5	79.9
387	Lu et al. (2020c)		TuoXin Aerospace Basalt Industrial Co., Ltd. (Sichuan, China)	BFRP	6.0	Epoxy	Simulated seawater (IMMR)	28	90	5	84.6	5	76.5
388	Lu et al. (2020c)		TuoXin Aerospace Basalt Industrial Co., Ltd. (Sichuan, China)	BFRP	6.0	Epoxy	Simulated seawater (IMMR)	28	180	5	75.0	5	82.7
389	Lu et al. (2020c)		TuoXin Aerospace Basalt Industrial Co., Ltd. (Sichuan, China)	BFRP	6.0	Epoxy	Simulated seawater (IMMR)	28	360	5	71.2	5	73.2
390	Lu et al. (2020c)		TuoXin Aerospace Basalt Industrial Co., Ltd. (Sichuan, China)	BFRP	6.0	Epoxy	Simulated seawater (IMMR)	40	30	5	98.0	5	89.3
391	Lu et al. (2020c)		TuoXin Aerospace Basalt Industrial Co., Ltd. (Sichuan, China)	BFRP	6.0	Epoxy	Simulated seawater (IMMR)	40	90	5	98.6	5	88.8
392	Lu et al. (2020c)		TuoXin Aerospace Basalt Industrial Co., Ltd. (Sichuan, China)	BFRP	6.0	Epoxy	Simulated seawater (IMMR)	40	180	5	73.3	5	62.8
393	Lu et al. (2020c)		TuoXin Aerospace Basalt Industrial Co., Ltd. (Sichuan, China)	BFRP	6.0	Epoxy	Simulated seawater (IMMR)	40	360	5	61.3	5	46.9
394	Lu et al. (2020c)		TuoXin Aerospace Basalt Industrial Co., Ltd. (Sichuan, China)	BFRP	6.0	Epoxy	Simulated seawater (IMMR)	60	30	5	98.1	5	91.3
395	Lu et al. (2020c)		TuoXin Aerospace Basalt Industrial Co., Ltd. (Sichuan, China)	BFRP	6.0	Epoxy	Simulated seawater (IMMR)	60	90	5	79.1	5	65.5
396	Lu et	al.	TuoXin	BFRP	6.0	Epoxy	Simulated seawater (IMMR)	60	180	5	66.1	5	43.7

	(2020c)	Aerospace Basalt Industrial Co., Ltd. (Sichuan, China) TuoXin											
397	Lu et al. (2020c)	Aerospace Basalt Industrial Co., Ltd. (Sichuan, China) TuoXin	BFRP	6.0	Epoxy	Simulated seawater (IMMR)	60	360	5	56.9	5	16.2	
398	Lu et al. (2020c)	Aerospace Basalt Industrial Co., Ltd. (Sichuan, China) TuoXin	BFRP	6.0	Epoxy	Alkaline solution (IMMR)	28	30	5	98.1	5	76.5	
399	Lu et al. (2020c)	Aerospace Basalt Industrial Co., Ltd. (Sichuan, China) TuoXin	BFRP	6.0	Epoxy	Alkaline solution (IMMR)	28	90	5	85.9	5	73.2	
400	Lu et al. (2020c)	Aerospace Basalt Industrial Co., Ltd. (Sichuan, China) TuoXin	BFRP	6.0	Epoxy	Alkaline solution (IMMR)	28	180	5	69.3	5	67.5	
401	Lu et al. (2020c)	Aerospace Basalt Industrial Co., Ltd. (Sichuan, China) TuoXin	BFRP	6.0	Epoxy	Alkaline solution (IMMR)	28	360	5	65.4	5	20.3	
402	Lu et al. (2020c)	Aerospace Basalt Industrial Co., Ltd. (Sichuan, China) TuoXin	BFRP	6.0	Epoxy	Alkaline solution (IMMR)	40	30	5	96.1	5	91.0	
403	Lu et al. (2020c)	Aerospace Basalt Industrial Co., Ltd. (Sichuan, China) TuoXin	BFRP	6.0	Epoxy	Alkaline solution (IMMR)	40	90	5	73.3	5	54.8	
404	Lu et al. (2020c)	Aerospace Basalt Industrial Co., Ltd. (Sichuan, China) TuoXin	BFRP	6.0	Epoxy	Alkaline solution (IMMR)	40	180	5	63.2	5	54.3	
405	Lu et al. (2020c)	Aerospace Basalt Industrial Co., Ltd. (Sichuan, China) TuoXin	BFRP	6.0	Epoxy	Alkaline solution (IMMR)	40	360	5	58.8	5	19.2	
406	Lu et al. (2020c)	Aerospace Basalt Industrial Co., Ltd. (Sichuan, China) TuoXin	BFRP	6.0	Epoxy	Alkaline solution (IMMR)	60	30	5	94.2	5	87.9	
407	Lu et al. (2020c)	Aerospace Basalt Industrial Co., Ltd.	BFRP	6.0	Epoxy	Alkaline solution (IMMR)	60	90	5	74.6	5	62.2	

			(Sichuan, China)										
408	Lu et al. (2020c)		TuoXin Aerospace Basalt Industrial Co., Ltd. (Sichuan, China)	BFRP	6.0	Epoxy	Alkaline solution (IMMR)	60	180	5	53.6	5	34.2
409	Lu et al. (2020c)		TuoXin Aerospace Basalt Industrial Co., Ltd. (Sichuan, China)	BFRP	6.0	Epoxy	Alkaline solution (IMMR)	60	360	5	48.4	5	2.2
410	Lu et al. (2020c)		TuoXin Aerospace Basalt Industrial Co., Ltd. (Sichuan, China)	BFRP	6.0	Epoxy	NCE 1+Water (IMMR)	40	30	5	96.8	5	87.6
411	Lu et al. (2020c)		TuoXin Aerospace Basalt Industrial Co., Ltd. (Sichuan, China)	BFRP	6.0	Epoxy	NCE 1+Water (IMMR)	40	90	5	88.6	5	79.0
412	Lu et al. (2020c)		TuoXin Aerospace Basalt Industrial Co., Ltd. (Sichuan, China)	BFRP	6.0	Epoxy	NCE 1+Water (IMMR)	40	180	5	84.2	5	76.8
413	Lu et al. (2020c)		TuoXin Aerospace Basalt Industrial Co., Ltd. (Sichuan, China)	BFRP	6.0	Epoxy	NCE 1+Water (IMMR)	40	360	5	81.7	5	68.2
414	Lu et al. (2020c)		TuoXin Aerospace Basalt Industrial Co., Ltd. (Sichuan, China)	BFRP	6.0	Epoxy	NCE 1+Simulated seawater (IMMR)	40	30	5	86.9	5	76.5
415	Lu et al. (2020c)		TuoXin Aerospace Basalt Industrial Co., Ltd. (Sichuan, China)	BFRP	6.0	Epoxy	NCE 1+Simulated seawater (IMMR)	40	90	5	69.3	5	79.9
416	Lu et al. (2020c)		TuoXin Aerospace Basalt Industrial Co., Ltd. (Sichuan, China)	BFRP	6.0	Epoxy	NCE 1+Simulated seawater (IMMR)	40	180	5	79.1	5	71.2
417	Lu et al. (2020c)		TuoXin Aerospace Basalt Industrial Co., Ltd. (Sichuan, China)	BFRP	6.0	Epoxy	NCE 1+Simulated seawater (IMMR)	40	360	5	75.8	5	59.1
418	Lu et al. (2020c)		TuoXin Aerospace Basalt Industrial Co., Ltd. (Sichuan, China)	BFRP	6.0	Epoxy	NCE 1+Alkaline solution (IMMR)	40	30	5	100.2	5	89.6
419	Lu et al.		TuoXin	BFRP	6.0	Epoxy	NCE 1+Alkaline solution	40	90	5	89.5	5	65.8

	(2020c)	Aerospace Basalt Industrial Co., Ltd. (Sichuan, China) TuoXin				(IMMR)							
420	Lu et al. (2020c)	Aerospace Basalt Industrial Co., Ltd. (Sichuan, China) TuoXin	BFRP	6.0	Epoxy	NCE 1+Alkaline solution (IMMR)	40	180	5	78.9	5	58.8	
421	Lu et al. (2020c)	Aerospace Basalt Industrial Co., Ltd. (Sichuan, China) TuoXin	BFRP	6.0	Epoxy	NCE 1+Alkaline solution (IMMR)	40	360	5	73.9	5	51.8	
422	Lu et al. (2020c)	Aerospace Basalt Industrial Co., Ltd. (Sichuan, China) TuoXin	BFRP	6.0	Epoxy	NCE 2+Water (IMMR)	40	30	5	99.3	5	82.7	
423	Lu et al. (2020c)	Aerospace Basalt Industrial Co., Ltd. (Sichuan, China) TuoXin	BFRP	6.0	Epoxy	NCE 2+Water (IMMR)	40	90	5	64.1	5	73.6	
424	Lu et al. (2020c)	Aerospace Basalt Industrial Co., Ltd. (Sichuan, China) TuoXin	BFRP	6.0	Epoxy	NCE 2+Water (IMMR)	40	180	5	79.2	5	71.5	
425	Lu et al. (2020c)	Aerospace Basalt Industrial Co., Ltd. (Sichuan, China) TuoXin	BFRP	6.0	Epoxy	NCE 2+Water (IMMR)	40	360	5	74.8	5	43.0	
426	Lu et al. (2020c)	Aerospace Basalt Industrial Co., Ltd. (Sichuan, China) TuoXin	BFRP	6.0	Epoxy	NCE 2+Simulated seawater (IMMR)	40	30	5	103.2	5	70.1	
427	Lu et al. (2020c)	Aerospace Basalt Industrial Co., Ltd. (Sichuan, China) TuoXin	BFRP	6.0	Epoxy	NCE 2+Simulated seawater (IMMR)	40	90	5	78.4	5	59.1	
428	Lu et al. (2020c)	Aerospace Basalt Industrial Co., Ltd. (Sichuan, China) TuoXin	BFRP	6.0	Epoxy	NCE 2+Simulated seawater (IMMR)	40	180	5	68.7	5	55.6	
429	Lu et al. (2020c)	Aerospace Basalt Industrial Co., Ltd. (Sichuan, China) TuoXin	BFRP	6.0	Epoxy	NCE 2+Simulated seawater (IMMR)	40	360	5	62.1	5	41.1	
430	Lu et al. (2020c)	Aerospace Basalt Industrial Co., Ltd.	BFRP	6.0	Epoxy	NCE 2+Alkaline solution (IMMR)	40	30	5	92.6	5	77.4	

			(Sichuan, China)										
431	Lu et al. (2020c)		TuoXin Aerospace Basalt Industrial Co., Ltd. (Sichuan, China)	BFRP	6.0	Epoxy	NCE 2+Alkaline solution (IMMR)	40	90	5	83.9	5	68.7
432	Lu et al. (2020c)		TuoXin Aerospace Basalt Industrial Co., Ltd. (Sichuan, China)	BFRP	6.0	Epoxy	NCE 2+Alkaline solution (IMMR)	40	180	5	68.2	5	54.1
433	Lu et al. (2020c)		TuoXin Aerospace Basalt Industrial Co., Ltd. (Sichuan, China)	BFRP	6.0	Epoxy	NCE 2+Alkaline solution (IMMR)	40	360	5	67.6	5	36.1
434	Lu et al. (2021a)		Nanjing Fenghui Composite Material Co. Ltd (China)	GFRP	11.2	Vinylester	Control	20	0	NA	NA	6	100.0
435	Lu et al. (2021a)		Nanjing Fenghui Composite Material Co. Ltd (China)	GFRP	11.2	Vinylester	Alkaline solution (IMMR)	20	12	NA	NA	6	103.1
436	Lu et al. (2021a)		Nanjing Fenghui Composite Material Co. Ltd (China)	GFRP	11.2	Vinylester	Alkaline solution (IMMR)	20	36	NA	NA	6	66.6
437	Lu et al. (2021a)		Nanjing Fenghui Composite Material Co. Ltd (China)	GFRP	11.2	Vinylester	Alkaline solution (IMMR)	20	72	NA	NA	6	65.9
438	Lu et al. (2021a)		Nanjing Fenghui Composite Material Co. Ltd (China)	GFRP	11.2	Vinylester	Saline solution (IMMR)	20	12	NA	NA	6	108.2
439	Lu et al. (2021a)		Nanjing Fenghui Composite Material Co. Ltd (China)	GFRP	11.2	Vinylester	Saline solution (IMMR)	20	36	NA	NA	6	81.7
440	Lu et al. (2021a)		Nanjing Fenghui Composite Material Co. Ltd (China)	GFRP	11.2	Vinylester	Saline solution (IMMR)	20	72	NA	NA	6	82.0
441	Lu et al. (2021a)		Nanjing Fenghui Composite Material Co. Ltd (China)	GFRP	11.2	Vinylester	Water (IMMR)	20	12	NA	NA	6	115.1
442	Lu et al. (2021a)		Nanjing Fenghui Composite Material Co. Ltd (China)	GFRP	11.2	Vinylester	Water (IMMR)	20	36	NA	NA	6	88.9
443	Lu et al. (2021a)		Nanjing Fenghui Composite Material Co. Ltd (China)	GFRP	11.2	Vinylester	Water (IMMR)	20	72	NA	NA	6	83.7
444	Lu et al. (2021a)		Nanjing Fenghui Composite Material Co. Ltd (China)	GFRP	15.6	Vinylester	Control	20	0	NA	NA	6	100.0

445	Lu et al. (2021a)	Nanjing Fenghui Composite Material Co. Ltd (China)	GFRP	15.6	Vinylester	Alkaline solution (IMMR)	20	12	NA	NA	6	93.4
446	Lu et al. (2021a)	Nanjing Fenghui Composite Material Co. Ltd (China)	GFRP	15.6	Vinylester	Alkaline solution (IMMR)	20	36	NA	NA	6	80.5
447	Lu et al. (2021a)	Nanjing Fenghui Composite Material Co. Ltd (China)	GFRP	15.6	Vinylester	Alkaline solution (IMMR)	20	72	NA	NA	6	78.9
448	Lu et al. (2021a)	Nanjing Fenghui Composite Material Co. Ltd (China)	GFRP	15.6	Vinylester	Saline solution (IMMR)	20	12	NA	NA	6	96.3
449	Lu et al. (2021a)	Nanjing Fenghui Composite Material Co. Ltd (China)	GFRP	15.6	Vinylester	Saline solution (IMMR)	20	36	NA	NA	6	93.6
450	Lu et al. (2021a)	Nanjing Fenghui Composite Material Co. Ltd (China)	GFRP	15.6	Vinylester	Saline solution (IMMR)	20	72	NA	NA	6	90.4
451	Lu et al. (2021a)	Nanjing Fenghui Composite Material Co. Ltd (China)	GFRP	15.6	Vinylester	Water (IMMR)	20	12	NA	NA	6	95.7
452	Lu et al. (2021a)	Nanjing Fenghui Composite Material Co. Ltd (China)	GFRP	15.6	Vinylester	Water (IMMR)	20	36	NA	NA	6	83.2
453	Lu et al. (2021a)	Nanjing Fenghui Composite Material Co. Ltd (China)	GFRP	15.6	Vinylester	Water (IMMR)	20	72	NA	NA	6	84.4
454	Lu et al. (2021c)	Tuo Xin Aerospace Basalt Industrial Co., Ltd. (Chengdu City, China)	BFRP	12.0	Epoxy	Control	26	0	NA	NA	3	100.0
455	Lu et al. (2021c)	Tuo Xin Aerospace Basalt Industrial Co., Ltd. (Chengdu City, China)	BFRP	12.0	Epoxy	Alkaline solution (IMMR)	26	30	NA	NA	3	96.5
456	Lu et al. (2021c)	Tuo Xin Aerospace Basalt Industrial Co., Ltd. (Chengdu City, China)	BFRP	12.0	Epoxy	Alkaline solution (IMMR)	26	90	NA	NA	3	92.5
457	Lu et al. (2021c)	Tuo Xin Aerospace Basalt Industrial Co., Ltd. (Chengdu City, China)	BFRP	12.0	Epoxy	Alkaline solution (IMMR)	26	270	NA	NA	3	82.6
458	Lu et al. (2021c)	Tuo Xin Aerospace Basalt Industrial Co., Ltd. (Chengdu City,	BFRP	12.0	Epoxy	Alkaline solution (IMMR)	40	30	NA	NA	3	91.8

		China)										
459	Lu et al. (2021c)	Tuo Xin Aerospace Basalt Industrial Co., Ltd. (Chengdu City, China)	BFRP	12.0	Epoxy	Alkaline solution (IMMR)	40	90	NA	NA	3	91.2
460	Lu et al. (2021c)	Tuo Xin Aerospace Basalt Industrial Co., Ltd. (Chengdu City, China)	BFRP	12.0	Epoxy	Alkaline solution (IMMR)	40	270	NA	NA	3	81.1
461	Lu et al. (2021c)	Tuo Xin Aerospace Basalt Industrial Co., Ltd. (Chengdu City, China)	BFRP	12.0	Epoxy	Alkaline solution (IMMR)	60	30	NA	NA	3	93.7
462	Lu et al. (2021c)	Tuo Xin Aerospace Basalt Industrial Co., Ltd. (Chengdu City, China)	BFRP	12.0	Epoxy	Alkaline solution (IMMR)	60	90	NA	NA	3	97.4
463	Lu et al. (2021c)	Tuo Xin Aerospace Basalt Industrial Co., Ltd. (Chengdu City, China)	BFRP	12.0	Epoxy	Alkaline solution (IMMR)	60	270	NA	NA	3	57.0
464	Lu et al. (2021c)	Tuo Xin Aerospace Basalt Industrial Co., Ltd. (Chengdu City, China)	BFRP	12.0	Epoxy	Simulated seawater (IMMR)	26	30	NA	NA	3	92.9
465	Lu et al. (2021c)	Tuo Xin Aerospace Basalt Industrial Co., Ltd. (Chengdu City, China)	BFRP	12.0	Epoxy	Simulated seawater (IMMR)	26	90	NA	NA	3	97.6
466	Lu et al. (2021c)	Tuo Xin Aerospace Basalt Industrial Co., Ltd. (Chengdu City, China)	BFRP	12.0	Epoxy	Simulated seawater (IMMR)	26	270	NA	NA	3	92.2
467	Lu et al. (2021c)	Tuo Xin Aerospace Basalt Industrial Co., Ltd. (Chengdu City, China)	BFRP	12.0	Epoxy	Simulated seawater (IMMR)	40	30	NA	NA	3	93.7
468	Lu et al. (2021c)	Tuo Xin Aerospace Basalt Industrial Co., Ltd. (Chengdu City, China)	BFRP	12.0	Epoxy	Simulated seawater (IMMR)	40	90	NA	NA	3	97.4
469	Lu et al. (2021c)	Tuo Xin Aerospace Basalt Industrial Co., Ltd. (Chengdu City, China)	BFRP	12.0	Epoxy	Simulated seawater (IMMR)	40	270	NA	NA	3	91.0
470	Lu et al.	Tuo Xin Aerospace	BFRP	12.0	Epoxy	Simulated seawater (IMMR)	60	30	NA	NA	3	97.8

	(2021c)	Basalt Industrial Co., Ltd. (Chengdu City, China)										
471	Lu et al. (2021c)	Tuo Xin Aerospace Basalt Industrial Co., Ltd. (Chengdu City, China)	BFRP	12.0	Epoxy	Simulated seawater (IMMR)	60	90	NA	NA	3	83.7
472	Lu et al. (2021c)	Tuo Xin Aerospace Basalt Industrial Co., Ltd. (Chengdu City, China)	BFRP	12.0	Epoxy	Simulated seawater (IMMR)	60	270	NA	NA	3	72.6
473	Lu et al. (2022a)	Harbin FRP Institute Co., Ltd. (Harbin, China)	GFRP	8.0	Epoxy	Control	20	0	NA	NA	10	100.0
474	Lu et al. (2022a)	Harbin FRP Institute Co., Ltd. (Harbin, China)	GFRP	8.0	Epoxy	Simulated seawater (IMMR)	20	30	NA	NA	10	98.8
475	Lu et al. (2022a)	Harbin FRP Institute Co., Ltd. (Harbin, China)	GFRP	8.0	Epoxy	Simulated seawater (IMMR)	20	60	NA	NA	10	101.3
476	Lu et al. (2022a)	Harbin FRP Institute Co., Ltd. (Harbin, China)	GFRP	8.0	Epoxy	Simulated seawater (IMMR)	20	90	NA	NA	10	88.0
477	Lu et al. (2022a)	Harbin FRP Institute Co., Ltd. (Harbin, China)	GFRP	8.0	Epoxy	Simulated seawater (IMMR)	20	180	NA	NA	10	86.5
478	Lu et al. (2022a)	Harbin FRP Institute Co., Ltd. (Harbin, China)	GFRP	8.0	Epoxy	Simulated seawater (IMMR)	40	30	NA	NA	10	102.0
479	Lu et al. (2022a)	Harbin FRP Institute Co., Ltd. (Harbin, China)	GFRP	8.0	Epoxy	Simulated seawater (IMMR)	40	60	NA	NA	10	107.3
480	Lu et al. (2022a)	Harbin FRP Institute Co., Ltd. (Harbin, China)	GFRP	8.0	Epoxy	Simulated seawater (IMMR)	40	90	NA	NA	10	86.8
481	Lu et al. (2022a)	Harbin FRP Institute Co., Ltd. (Harbin, China)	GFRP	8.0	Epoxy	Simulated seawater (IMMR)	40	180	NA	NA	10	86.5
482	Lu et al. (2022a)	Harbin FRP Institute Co., Ltd. (Harbin, China)	GFRP	8.0	Epoxy	Simulated seawater (IMMR)	60	30	NA	NA	10	104.8
483	Lu et al. (2022a)	Harbin FRP Institute Co., Ltd. (Harbin, China)	GFRP	8.0	Epoxy	Simulated seawater (IMMR)	60	60	NA	NA	10	108.9
484	Lu et al. (2022a)	Harbin FRP Institute Co., Ltd. (Harbin,	GFRP	8.0	Epoxy	Simulated seawater (IMMR)	60	90	NA	NA	10	90.6

			China)										
485	Lu et al. (2022a)		Harbin FRP Institute Co., Ltd. (Harbin, China)	GFRP	8.0	Epoxy	Simulated seawater (IMMR)	60	180	NA	NA	10	85.2
486	Lu et al. (2022a)		Harbin FRP Institute Co., Ltd. (Harbin, China)	GFRP	8.0	Epoxy	Water (IMMR)	60	30	NA	NA	10	102.6
487	Lu et al. (2022a)		Harbin FRP Institute Co., Ltd. (Harbin, China)	GFRP	8.0	Epoxy	Water (IMMR)	60	60	NA	NA	10	86.1
488	Lu et al. (2022a)		Harbin FRP Institute Co., Ltd. (Harbin, China)	GFRP	8.0	Epoxy	Water (IMMR)	60	90	NA	NA	10	81.4
489	Lu et al. (2022a)		Harbin FRP Institute Co., Ltd. (Harbin, China)	GFRP	8.0	Epoxy	Water (IMMR)	60	180	NA	NA	10	82.3
490	Lu et al. (2022a)		TuoXin Aerospace Basalt Industrial Co., Ltd. (Sichuan, China)	BFRP	8.0	Epoxy	Control	20	0	NA	NA	10	100.0
491	Lu et al. (2022a)		TuoXin Aerospace Basalt Industrial Co., Ltd. (Sichuan, China)	BFRP	8.0	Epoxy	Simulated seawater (IMMR)	20	30	NA	NA	10	98.5
492	Lu et al. (2022a)		TuoXin Aerospace Basalt Industrial Co., Ltd. (Sichuan, China)	BFRP	8.0	Epoxy	Simulated seawater (IMMR)	20	60	NA	NA	10	105.6
493	Lu et al. (2022a)		TuoXin Aerospace Basalt Industrial Co., Ltd. (Sichuan, China)	BFRP	8.0	Epoxy	Simulated seawater (IMMR)	20	90	NA	NA	10	86.7
494	Lu et al. (2022a)		TuoXin Aerospace Basalt Industrial Co., Ltd. (Sichuan, China)	BFRP	8.0	Epoxy	Simulated seawater (IMMR)	20	180	NA	NA	10	86.7
495	Lu et al. (2022a)		TuoXin Aerospace Basalt Industrial Co., Ltd. (Sichuan, China)	BFRP	8.0	Epoxy	Simulated seawater (IMMR)	40	30	NA	NA	10	99.5
496	Lu et al. (2022a)		TuoXin Aerospace Basalt Industrial Co., Ltd. (Sichuan, China)	BFRP	8.0	Epoxy	Simulated seawater (IMMR)	40	60	NA	NA	10	105.3
497	Lu et al. (2022a)		TuoXin Aerospace Basalt Industrial Co., Ltd. (Sichuan, China)	BFRP	8.0	Epoxy	Simulated seawater (IMMR)	40	90	NA	NA	10	88.6
498	Lu et al. (2022a)		TuoXin Aerospace Basalt Industrial Co., Ltd. (Sichuan, China)	BFRP	8.0	Epoxy	Simulated seawater (IMMR)	40	180	NA	NA	10	82.5
499	Lu et al. (2022a)		TuoXin Aerospace Basalt Industrial Co., Ltd. (Sichuan, China)	BFRP	8.0	Epoxy	Simulated seawater (IMMR)	60	30	NA	NA	10	99.5

500	Lu et al. (2022a)	TuoXin Aerospace Basalt Industrial Co., Ltd. (Sichuan, China)	BFRP	8.0	Epoxy	Simulated seawater (IMMR)	60	60	NA	NA	10	98.8
501	Lu et al. (2022a)	TuoXin Aerospace Basalt Industrial Co., Ltd. (Sichuan, China)	BFRP	8.0	Epoxy	Simulated seawater (IMMR)	60	90	NA	NA	10	79.3
502	Lu et al. (2022a)	TuoXin Aerospace Basalt Industrial Co., Ltd. (Sichuan, China)	BFRP	8.0	Epoxy	Simulated seawater (IMMR)	60	180	NA	NA	10	75.1
503	Lu et al. (2022a)	TuoXin Aerospace Basalt Industrial Co., Ltd. (Sichuan, China)	BFRP	8.0	Epoxy	Water (IMMR)	60	30	NA	NA	10	106.2
504	Lu et al. (2022a)	TuoXin Aerospace Basalt Industrial Co., Ltd. (Sichuan, China)	BFRP	8.0	Epoxy	Water (IMMR)	60	60	NA	NA	10	94.4
505	Lu et al. (2022a)	TuoXin Aerospace Basalt Industrial Co., Ltd. (Sichuan, China)	BFRP	8.0	Epoxy	Water (IMMR)	60	90	NA	NA	10	76.7
506	Lu et al. (2022a)	TuoXin Aerospace Basalt Industrial Co., Ltd. (Sichuan, China)	BFRP	8.0	Epoxy	Water (IMMR)	60	180	NA	NA	10	76.7
507	Lu et al. (2022b)	Shenzhen Haichuan New Material Technology (Shenzhen, China)	GFRP	6.0	Epoxy-vinyl	Control	RT	0	NA	100.0	NA	100.0
508	Lu et al. (2022b)	Shenzhen Haichuan New Material Technology (Shenzhen, China)	GFRP	6.0	Epoxy-vinyl	SWSSCE+Simulated seawater (IMMR)	RT	30	NA	84.6	NA	87.6
509	Lu et al. (2022b)	Shenzhen Haichuan New Material Technology (Shenzhen, China)	GFRP	6.0	Epoxy-vinyl	SWSSCE+Simulated seawater (IMMR)	RT	60	NA	73.5	NA	86.7
510	Lu et al. (2022b)	Shenzhen Haichuan New Material Technology (Shenzhen, China)	GFRP	6.0	Epoxy-vinyl	SWSSCE+Simulated seawater (IMMR)	RT	120	NA	70.0	NA	68.6
511	Lu et al. (2022b)	Shenzhen Haichuan New Material Technology (Shenzhen, China)	GFRP	6.0	Epoxy-vinyl	SWSSCE+Simulated seawater (IMMR)	40	30	NA	77.5	NA	73.5
512	Lu et al. (2022b)	Shenzhen Haichuan New Material Technology (Shenzhen, China)	GFRP	6.0	Epoxy-vinyl	SWSSCE+Simulated seawater (IMMR)	40	60	NA	60.9	NA	66.1
513	Lu et al.	Shenzhen Haichuan	GFRP	6.0	Epoxy-vinyl	SWSSCE+Simulated seawater	40	120	NA	58.9	NA	46.7

	(2022b)	New Material Technology (Shenzhen, China)				(IMMR)						
514	Lu et al. (2022b)	Shenzhen Haichuan New Material Technology (Shenzhen, China)	GFRP	6.0	Epoxy-vinyl	SWSSCE+Simulated seawater (IMMR)	60	30	NA	73.0	NA	73.9
515	Lu et al. (2022b)	Shenzhen Haichuan New Material Technology (Shenzhen, China)	GFRP	6.0	Epoxy-vinyl	SWSSCE+Simulated seawater (IMMR)	60	60	NA	54.9	NA	55.8
516	Lu et al. (2022b)	Shenzhen Haichuan New Material Technology (Shenzhen, China)	GFRP	6.0	Epoxy-vinyl	SWSSCE+Simulated seawater (IMMR)	60	120	NA	55.4	NA	30.6
517	Lu et al. (2022b)	Shenzhen Haichuan New Material Technology (Shenzhen, China)	GFRP	6.0	Epoxy-vinyl	SL (20%fu)+SWSSCE+Simulated seawater (IMMR)	RT	30	NA	87.6	NA	90.5
518	Lu et al. (2022b)	Shenzhen Haichuan New Material Technology (Shenzhen, China)	GFRP	6.0	Epoxy-vinyl	SL (20%fu)+SWSSCE+Simulated seawater (IMMR)	RT	60	NA	81.0	NA	88.8
519	Lu et al. (2022b)	Shenzhen Haichuan New Material Technology (Shenzhen, China)	GFRP	6.0	Epoxy-vinyl	SL (20%fu)+SWSSCE+Simulated seawater (IMMR)	RT	120	NA	66.9	NA	66.1
520	Lu et al. (2022b)	Shenzhen Haichuan New Material Technology (Shenzhen, China)	GFRP	6.0	Epoxy-vinyl	SL (20%fu)+SWSSCE+Simulated seawater (IMMR)	40	30	NA	87.6	NA	73.5
521	Lu et al. (2022b)	Shenzhen Haichuan New Material Technology (Shenzhen, China)	GFRP	6.0	Epoxy-vinyl	SL (20%fu)+SWSSCE+Simulated seawater (IMMR)	40	60	NA	63.4	NA	50.4
522	Lu et al. (2022b)	Shenzhen Haichuan New Material Technology (Shenzhen, China)	GFRP	6.0	Epoxy-vinyl	SL (20%fu)+SWSSCE+Simulated seawater (IMMR)	40	120	NA	45.3	NA	47.9
523	Lu et al. (2022b)	Shenzhen Haichuan New Material Technology (Shenzhen, China)	GFRP	6.0	Epoxy-vinyl	SL (20%fu)+SWSSCE+Simulated seawater (IMMR)	60	30	NA	63.9	NA	45.0
524	Lu et al. (2022b)	Shenzhen Haichuan New Material Technology	GFRP	6.0	Epoxy-vinyl	SL (20%fu)+SWSSCE+Simulated seawater (IMMR)	60	60	NA	64.9	NA	53.3

		(Shenzhen, China)										
525	Lu et al. (2022b)	Shenzhen Haichuan New Material Technology (Shenzhen, China)	GFRP	6.0	Epoxy-vinyl	SL (20%fu)+SWSSCE+Simulated seawater (IMMR)	60	120	NA	49.8	NA	38.0
526	Lu et al. (2022b)	Shenzhen Haichuan New Material Technology (Shenzhen, China)	GFRP	6.0	Epoxy-vinyl	SL (40%fu)+SWSSCE+Simulated seawater (IMMR)	RT	30	NA	82.2	NA	81.4
527	Lu et al. (2022b)	Shenzhen Haichuan New Material Technology (Shenzhen, China)	GFRP	6.0	Epoxy-vinyl	SL (40%fu)+SWSSCE+Simulated seawater (IMMR)	RT	60	NA	64.6	NA	50.0
528	Lu et al. (2022b)	Shenzhen Haichuan New Material Technology (Shenzhen, China)	GFRP	6.0	Epoxy-vinyl	SL (40%fu)+SWSSCE+Simulated seawater (IMMR)	RT	120	NA	73.2	NA	62.8
529	Lu et al. (2022b)	Shenzhen Haichuan New Material Technology (Shenzhen, China)	GFRP	6.0	Epoxy-vinyl	SL (40%fu)+SWSSCE+Simulated seawater (IMMR)	40	30	NA	72.1	NA	62.8
530	Lu et al. (2022b)	Shenzhen Haichuan New Material Technology (Shenzhen, China)	GFRP	6.0	Epoxy-vinyl	SL (40%fu)+SWSSCE+Simulated seawater (IMMR)	40	60	NA	59.1	NA	52.0
531	Lu et al. (2022b)	Shenzhen Haichuan New Material Technology (Shenzhen, China)	GFRP	6.0	Epoxy-vinyl	SL (40%fu)+SWSSCE+Simulated seawater (IMMR)	40	120	NA	50.1	NA	54.9
532	Lu et al. (2022b)	Shenzhen Haichuan New Material Technology (Shenzhen, China)	GFRP	6.0	Epoxy-vinyl	SL (40%fu)+SWSSCE+Simulated seawater (IMMR)	60	30	NA	72.7	NA	54.5
533	Lu et al. (2022b)	Shenzhen Haichuan New Material Technology (Shenzhen, China)	GFRP	6.0	Epoxy-vinyl	SL (40%fu)+SWSSCE+Simulated seawater (IMMR)	60	60	NA	52.6	NA	47.5
534	Lu et al. (2022b)	Shenzhen Haichuan New Material Technology (Shenzhen, China)	GFRP	6.0	Epoxy-vinyl	SL (40%fu)+SWSSCE+Simulated seawater (IMMR)	60	120	NA	52.1	NA	37.2
535	Manalo et al. (2020)	Pultrall Inc. (Thetford Mines, QC, Canada)	GFRP	9.5	Vinylester	Control	23	0	NA	NA	6	100.0
536	Manalo et al. (2020)	Pultrall Inc. (Thetford Mines, QC, Canada)	GFRP	9.5	Vinylester	Water (IMMR)	23	28	NA	NA	6	86.0
537	Manalo et al.	Pultrall Inc. (Thetford	GFRP	9.5	Vinylester	Water (IMMR)	23	56	NA	NA	6	68.0

	(2020)	Mines, QC, Canada)										
538	Manalo et al. (2020)	Pultrall Inc. (Thetford Mines, QC, Canada)	GFRP	9.5	Vinylester	Water (IMMR)	23	112	NA	NA	6	48.0
539	Manalo et al. (2020)	Pultrall Inc. (Thetford Mines, QC, Canada)	GFRP	9.5	Vinylester	Water (IMMR)	60	28	NA	NA	6	76.0
540	Manalo et al. (2020)	Pultrall Inc. (Thetford Mines, QC, Canada)	GFRP	9.5	Vinylester	Water (IMMR)	60	56	NA	NA	6	57.0
541	Manalo et al. (2020)	Pultrall Inc. (Thetford Mines, QC, Canada)	GFRP	9.5	Vinylester	Water (IMMR)	60	112	NA	NA	6	41.0
542	Manalo et al. (2020)	Pultrall Inc. (Thetford Mines, QC, Canada)	GFRP	9.5	Vinylester	Water (IMMR)	80	28	NA	NA	6	68.0
543	Manalo et al. (2020)	Pultrall Inc. (Thetford Mines, QC, Canada)	GFRP	9.5	Vinylester	Water (IMMR)	80	56	NA	NA	6	48.0
544	Manalo et al. (2020)	Pultrall Inc. (Thetford Mines, QC, Canada)	GFRP	9.5	Vinylester	Water (IMMR)	80	112	NA	NA	6	29.0
545	Manalo et al. (2020)	Pultrall Inc. (Thetford Mines, QC, Canada)	GFRP	9.5	Vinylester	Simulated seawater (IMMR)	23	28	NA	NA	6	94.0
546	Manalo et al. (2020)	Pultrall Inc. (Thetford Mines, QC, Canada)	GFRP	9.5	Vinylester	Simulated seawater (IMMR)	23	56	NA	NA	6	81.0
547	Manalo et al. (2020)	Pultrall Inc. (Thetford Mines, QC, Canada)	GFRP	9.5	Vinylester	Simulated seawater (IMMR)	23	112	NA	NA	6	69.0
548	Manalo et al. (2020)	Pultrall Inc. (Thetford Mines, QC, Canada)	GFRP	9.5	Vinylester	Simulated seawater (IMMR)	60	28	NA	NA	6	90.0
549	Manalo et al. (2020)	Pultrall Inc. (Thetford Mines, QC, Canada)	GFRP	9.5	Vinylester	Simulated seawater (IMMR)	60	56	NA	NA	6	71.0
550	Manalo et al. (2020)	Pultrall Inc. (Thetford Mines, QC, Canada)	GFRP	9.5	Vinylester	Simulated seawater (IMMR)	60	112	NA	NA	6	54.0
551	Manalo et al. (2020)	Pultrall Inc. (Thetford Mines, QC, Canada)	GFRP	9.5	Vinylester	Simulated seawater (IMMR)	80	28	NA	NA	6	85.0
552	Manalo et al. (2020)	Pultrall Inc. (Thetford Mines, QC, Canada)	GFRP	9.5	Vinylester	Simulated seawater (IMMR)	80	56	NA	NA	6	64.0
553	Manalo et al. (2020)	Pultrall Inc. (Thetford Mines, QC, Canada)	GFRP	9.5	Vinylester	Simulated seawater (IMMR)	80	112	NA	NA	6	43.0
554	Manalo et al. (2020)	Pultrall Inc. (Thetford Mines, QC, Canada)	GFRP	9.5	Vinylester	Alkaline solution (IMMR)	23	28	NA	NA	6	81.0
555	Manalo et al. (2020)	Pultrall Inc. (Thetford Mines, QC, Canada)	GFRP	9.5	Vinylester	Alkaline solution (IMMR)	23	56	NA	NA	6	58.0
556	Manalo et al. (2020)	Pultrall Inc. (Thetford Mines, QC, Canada)	GFRP	9.5	Vinylester	Alkaline solution (IMMR)	23	112	NA	NA	6	38.0
557	Manalo et al. (2020)	Pultrall Inc. (Thetford Mines, QC, Canada)	GFRP	9.5	Vinylester	Alkaline solution (IMMR)	60	28	NA	NA	6	63.0
558	Manalo et al. (2020)	Pultrall Inc. (Thetford Mines, QC, Canada)	GFRP	9.5	Vinylester	Alkaline solution (IMMR)	60	56	NA	NA	6	47.0
559	Manalo et al. (2020)	Pultrall Inc. (Thetford Mines, QC, Canada)	GFRP	9.5	Vinylester	Alkaline solution (IMMR)	60	112	NA	NA	6	30.0
560	Manalo et al.	Pultrall Inc. (Thetford	GFRP	9.5	Vinylester	Alkaline solution (IMMR)	80	28	NA	NA	6	52.0

	(2020)	Mines, QC, Canada)										
561	Manalo et al. (2020)	Pultrall Inc. (Thetford Mines, QC, Canada)	GFRP	9.5	Vinylester	Alkaline solution (IMMR)	80	56	NA	NA	6	38.0
562	Manalo et al. (2020)	Pultrall Inc. (Thetford Mines, QC, Canada)	GFRP	9.5	Vinylester	Alkaline solution (IMMR)	80	112	NA	NA	6	23.0
563	Manalo et al. (2020)	Pultrall Inc. (Thetford Mines, QC, Canada)	GFRP	9.5	Vinylester	NCE+Water (IMMR)	23	28	NA	NA	6	92.0
564	Manalo et al. (2020)	Pultrall Inc. (Thetford Mines, QC, Canada)	GFRP	9.5	Vinylester	NCE+Water (IMMR)	23	56	NA	NA	6	90.0
565	Manalo et al. (2020)	Pultrall Inc. (Thetford Mines, QC, Canada)	GFRP	9.5	Vinylester	NCE+Water (IMMR)	23	112	NA	NA	6	88.0
566	Manalo et al. (2020)	Pultrall Inc. (Thetford Mines, QC, Canada)	GFRP	9.5	Vinylester	NCE+Water (IMMR)	60	28	NA	NA	6	89.0
567	Manalo et al. (2020)	Pultrall Inc. (Thetford Mines, QC, Canada)	GFRP	9.5	Vinylester	NCE+Water (IMMR)	60	56	NA	NA	6	86.0
568	Manalo et al. (2020)	Pultrall Inc. (Thetford Mines, QC, Canada)	GFRP	9.5	Vinylester	NCE+Water (IMMR)	60	112	NA	NA	6	83.0
569	Manalo et al. (2020)	Pultrall Inc. (Thetford Mines, QC, Canada)	GFRP	9.5	Vinylester	NCE+Water (IMMR)	80	28	NA	NA	6	79.0
570	Manalo et al. (2020)	Pultrall Inc. (Thetford Mines, QC, Canada)	GFRP	9.5	Vinylester	NCE+Water (IMMR)	80	56	NA	NA	6	76.0
571	Manalo et al. (2020)	Pultrall Inc. (Thetford Mines, QC, Canada)	GFRP	9.5	Vinylester	NCE+Water (IMMR)	80	112	NA	NA	6	70.0
572	Manalo et al. (2020)	Pultrall Inc. (Thetford Mines, QC, Canada)	GFRP	9.5	Vinylester	NCE+Simulated seawater (IMMR)	23	28	NA	NA	6	96.0
573	Manalo et al. (2020)	Pultrall Inc. (Thetford Mines, QC, Canada)	GFRP	9.5	Vinylester	NCE+Simulated seawater (IMMR)	23	56	NA	NA	6	93.0
574	Manalo et al. (2020)	Pultrall Inc. (Thetford Mines, QC, Canada)	GFRP	9.5	Vinylester	NCE+Simulated seawater (IMMR)	23	112	NA	NA	6	91.0
575	Manalo et al. (2020)	Pultrall Inc. (Thetford Mines, QC, Canada)	GFRP	9.5	Vinylester	NCE+Simulated seawater (IMMR)	60	28	NA	NA	6	93.0
576	Manalo et al. (2020)	Pultrall Inc. (Thetford Mines, QC, Canada)	GFRP	9.5	Vinylester	NCE+Simulated seawater (IMMR)	60	56	NA	NA	6	90.0
577	Manalo et al. (2020)	Pultrall Inc. (Thetford Mines, QC, Canada)	GFRP	9.5	Vinylester	NCE+Simulated seawater (IMMR)	60	112	NA	NA	6	87.0
578	Manalo et al. (2020)	Pultrall Inc. (Thetford Mines, QC, Canada)	GFRP	9.5	Vinylester	NCE+Simulated seawater (IMMR)	80	28	NA	NA	6	86.0
579	Manalo et al. (2020)	Pultrall Inc. (Thetford Mines, QC, Canada)	GFRP	9.5	Vinylester	NCE+Simulated seawater (IMMR)	80	56	NA	NA	6	84.0
580	Manalo et al. (2020)	Pultrall Inc. (Thetford Mines, QC, Canada)	GFRP	9.5	Vinylester	NCE+Simulated seawater (IMMR)	80	112	NA	NA	6	81.0
581	Manalo et al. (2020)	Pultrall Inc. (Thetford Mines, QC, Canada)	GFRP	9.5	Vinylester	NCE+Alkaline solution (IMMR)	23	28	NA	NA	6	87.0
582	Manalo et al. (2020)	Pultrall Inc. (Thetford Mines, QC, Canada)	GFRP	9.5	Vinylester	NCE+Alkaline solution (IMMR)	23	56	NA	NA	6	84.0
583	Manalo et al.	Pultrall Inc. (Thetford	GFRP	9.5	Vinylester	NCE+Alkaline solution	23	112	NA	NA	6	80.0

	(2020)	Mines, QC, Canada)				(IMMR)							
584	Manalo et al. (2020)	Pultrall Inc. (Thetford Mines, QC, Canada)	GFRP	9.5	Vinylester	NCE+Alkaline solution (IMMR)	60	28	NA	NA	6	79.0
585	Manalo et al. (2020)	Pultrall Inc. (Thetford Mines, QC, Canada)	GFRP	9.5	Vinylester	NCE+Alkaline solution (IMMR)	60	56	NA	NA	6	76.0
586	Manalo et al. (2020)	Pultrall Inc. (Thetford Mines, QC, Canada)	GFRP	9.5	Vinylester	NCE+Alkaline solution (IMMR)	60	112	NA	NA	6	73.0
587	Manalo et al. (2020)	Pultrall Inc. (Thetford Mines, QC, Canada)	GFRP	9.5	Vinylester	NCE+Alkaline solution (IMMR)	80	28	NA	NA	6	75.0
588	Manalo et al. (2020)	Pultrall Inc. (Thetford Mines, QC, Canada)	GFRP	9.5	Vinylester	NCE+Alkaline solution (IMMR)	80	56	NA	NA	6	71.0
589	Manalo et al. (2020)	Pultrall Inc. (Thetford Mines, QC, Canada)	GFRP	9.5	Vinylester	NCE+Alkaline solution (IMMR)	80	112	NA	NA	6	68.0
590	Micelli and Nanni (2004)	NA	GFRP	6.4	Polyester	Control	22	0	NA	NA	6	100.0
591	Micelli and Nanni (2004)	NA	GFRP	6.4	Polyester	Alkaline solution (IMMR)	22	42	NA	NA	6	94.4
592	Micelli and Nanni (2004)	NA	GFRP	6.4	Polyester	Alkaline solution (IMMR)	60	21	NA	NA	6	17.2
593	Micelli and Nanni (2004)	NA	GFRP	6.4	Polyester	Alkaline solution (IMMR)	60	42	NA	NA	6	9.6
594	Micelli and Nanni (2004)	NA	GFRP	6.4	Polyester	FT+HT+RH+UV	-18-4/16-49	NA	NA	NA	6	100.0
595	Micelli and Nanni (2004)	NA	CFRP	8.3	Modified epoxy	Control	22	0	NA	NA	6	100.0
596	Micelli and Nanni (2004)	NA	CFRP	8.3	Modified epoxy	Alkaline solution (IMMR)	22	42	NA	NA	6	100.4
597	Micelli and Nanni (2004)	NA	CFRP	8.3	Modified epoxy	Alkaline solution (IMMR)	60	21	NA	NA	6	77.5
598	Micelli and Nanni (2004)	NA	CFRP	8.3	Modified epoxy	Alkaline solution (IMMR)	60	42	NA	NA	6	63.6
599	Micelli and Nanni (2004)	NA	CFRP	8.3	Modified epoxy	FT+HT+RH+UV	-18-4/16-49	NA	NA	NA	6	100.4
600	Micelli and Nanni (2004)	NA	CFRP	8.0	Modified epoxy	Control	22	0	NA	NA	6	100.0
601	Micelli and Nanni (2004)	NA	CFRP	8.0	Modified epoxy	Alkaline solution (IMMR)	22	42	NA	NA	6	100.0
602	Micelli and Nanni (2004)	NA	CFRP	8.0	Modified epoxy	Alkaline solution (IMMR)	60	21	NA	NA	6	80.9
603	Micelli and Nanni (2004)	NA	CFRP	8.0	Modified epoxy	Alkaline solution (IMMR)	60	42	NA	NA	6	64.8
604	Micelli and Nanni (2004)	NA	CFRP	8.0	Modified epoxy	FT+HT+RH+UV	-18-4/16-49	NA	NA	NA	6	100.0
605	Micelli and Nanni (2004)	NA	CFRP	7.9	Epoxy	Control	22	0	NA	NA	6	100.0
606	Micelli and	NA	CFRP	7.9	Modified epoxy	Alkaline solution (IMMR)	22	42	NA	NA	6	100.0

607	Nanni (2004) Micelli and Nanni (2004)	NA	CFRP	7.9	Modified epoxy	Alkaline solution (IMMR)	60	21	NA	NA	6	98.7
608	Micelli and Nanni (2004)	NA	CFRP	7.9	Modified epoxy	Alkaline solution (IMMR)	60	42	NA	NA	6	85.6
609	Micelli and Nanni (2004)	NA	CFRP	7.9	Modified epoxy	FT+HT+RH+UV	-18-4/16-49	NA	NA	NA	6	100.0
610	Morales et al. (2021)	NA	GFRP	9.5	Vinylester	Control	25	0	5	100.0	5	100.0
611	Morales et al. (2021)	NA	GFRP	9.5	Vinylester	SWCE 1+Seawater (IMMR)	60	30	4	97.9	4	97.9
612	Morales et al. (2021)	NA	GFRP	9.5	Vinylester	SWCE 1+Seawater (IMMR)	60	180	4	97.2	4	96.3
613	Morales et al. (2021)	NA	GFRP	9.5	Vinylester	SWCE 1+Seawater (IMMR)	60	360	4	96.6	4	96.8
614	Morales et al. (2021)	NA	GFRP	9.5	Vinylester	SWCE 1+Seawater (IMMR)	60	720	4	91.6	4	94.8
615	Morales et al. (2021)	NA	GFRP	9.5	Vinylester	SWCE 2+Seawater (IMMR)	60	30	4	95.7	4	100.8
616	Morales et al. (2021)	NA	GFRP	9.5	Vinylester	SWCE 2+Seawater (IMMR)	60	180	4	94.9	4	104.1
617	Morales et al. (2021)	NA	GFRP	9.5	Vinylester	SWCE 2+Seawater (IMMR)	60	360	4	96.9	4	99.2
618	Morales et al. (2021)	NA	GFRP	9.5	Vinylester	SWCE 2+Seawater (IMMR)	60	720	4	92.2	4	97.9
619	Pan and Yan (2021)	Harbin FRP Institute Co., Ltd. (Harbin, China)	GFRP	8.0	Epoxy	Control	21	0	NA	NA	4	100.0
620	Pan and Yan (2021)	Harbin FRP Institute Co., Ltd. (Harbin, China)	GFRP	8.0	Epoxy	Alkaline solution (IMMR)	21	30	NA	NA	4	101.5
621	Pan and Yan (2021)	Harbin FRP Institute Co., Ltd. (Harbin, China)	GFRP	8.0	Epoxy	Alkaline solution (IMMR)	21	70	NA	NA	4	113.1
622	Pan and Yan (2021)	Harbin FRP Institute Co., Ltd. (Harbin, China)	GFRP	8.0	Epoxy	Alkaline solution (IMMR)	21	100	NA	NA	4	99.1
623	Pan and Yan (2021)	Harbin FRP Institute Co., Ltd. (Harbin, China)	GFRP	8.0	Epoxy	Alkaline solution (IMMR)	21	140	NA	NA	4	96.7
624	Pan and Yan (2021)	Harbin FRP Institute Co., Ltd. (Harbin, China)	GFRP	8.0	Epoxy	Alkaline solution (IMMR)	40	30	NA	NA	4	101.1
625	Pan and Yan (2021)	Harbin FRP Institute Co., Ltd. (Harbin, China)	GFRP	8.0	Epoxy	Alkaline solution (IMMR)	40	70	NA	NA	4	86.3

626	Pan and Yan (2021)	Harbin FRP Institute Co., Ltd. (Harbin, China)	GFRP	8.0	Epoxy	Alkaline solution (IMMR)	40	100	NA	NA	4	69.1
627	Pan and Yan (2021)	Harbin FRP Institute Co., Ltd. (Harbin, China)	GFRP	8.0	Epoxy	Alkaline solution (IMMR)	40	140	NA	NA	4	29.0
628	Pan and Yan (2021)	Harbin FRP Institute Co., Ltd. (Harbin, China)	GFRP	8.0	Epoxy	Alkaline solution (IMMR)	60	30	NA	NA	4	95.7
629	Pan and Yan (2021)	Harbin FRP Institute Co., Ltd. (Harbin, China)	GFRP	8.0	Epoxy	Alkaline solution (IMMR)	60	70	NA	NA	4	62.7
630	Pan and Yan (2021)	Harbin FRP Institute Co., Ltd. (Harbin, China)	GFRP	8.0	Epoxy	Alkaline solution (IMMR)	60	100	NA	NA	4	53.4
631	Pan and Yan (2021)	Harbin FRP Institute Co., Ltd. (Harbin, China)	GFRP	8.0	Epoxy	Alkaline solution (IMMR)	60	140	NA	NA	4	42.7
632	Quagliarini et al. (2016)	NA	BFRP	8.0	Vinylester	Control	NA	0	NA	NA	3	100.0
633	Quagliarini et al. (2016)	NA	BFRP	8.0	Vinylester	Water (IMMR)	60	21	NA	NA	3	94.8
634	Quagliarini et al. (2016)	NA	BFRP	8.0	Vinylester	Saline solution (IMMR)	60	21	NA	NA	3	92.7
635	Rolland et al. (2021)	Pultrall Inc. (Thetford Mines, QC, Canada)	GFRP	12.7	Vinylester	Control	20	0	NA	NA	3	100.0
636	Rolland et al. (2021)	Pultrall Inc. (Thetford Mines, QC, Canada)	GFRP	12.7	Vinylester	Alkaline solution (IMMR)	20	120	NA	NA	3	103.8
637	Rolland et al. (2021)	Pultrall Inc. (Thetford Mines, QC, Canada)	GFRP	12.7	Vinylester	Alkaline solution (IMMR)	20	240	NA	NA	3	109.4
638	Rolland et al. (2021)	Pultrall Inc. (Thetford Mines, QC, Canada)	GFRP	12.7	Vinylester	Alkaline solution (IMMR)	40	120	NA	NA	3	103.9
639	Rolland et al. (2021)	Pultrall Inc. (Thetford Mines, QC, Canada)	GFRP	12.7	Vinylester	Alkaline solution (IMMR)	40	240	NA	NA	3	114.5
640	Rolland et al. (2021)	Pultrall Inc. (Thetford Mines, QC, Canada)	GFRP	12.7	Vinylester	Alkaline solution (IMMR)	60	120	NA	NA	3	116.7
641	Rolland et al. (2021)	Pultrall Inc. (Thetford Mines, QC, Canada)	GFRP	12.7	Vinylester	Alkaline solution (IMMR)	60	240	NA	NA	3	94.6
642	Rolland et al. (2021)	Pultrall Inc. (Thetford Mines, QC, Canada)	GFRP	12.7	Vinylester	NCE+Alkaline solution (IMMR)	20	120	NA	NA	3	95.1
643	Rolland et al. (2021)	Pultrall Inc. (Thetford Mines, QC, Canada)	GFRP	12.7	Vinylester	NCE+Alkaline solution (IMMR)	20	240	NA	NA	3	95.1
644	Rolland et al. (2021)	Pultrall Inc. (Thetford Mines, QC, Canada)	GFRP	12.7	Vinylester	NCE+Alkaline solution (IMMR)	40	120	NA	NA	3	97.2
645	Rolland et al. (2021)	Pultrall Inc. (Thetford Mines, QC, Canada)	GFRP	12.7	Vinylester	NCE+Alkaline solution (IMMR)	40	240	NA	NA	3	91.4

646	Rolland et al. (2021)	Pultrall Inc. (Thetford Mines, QC, Canada)	GFRP	12.7	Vinylester	NCE+Alkaline solution (IMMR)	60	120	NA	NA	3	97.5
647	Rolland et al. (2021)	Pultrall Inc. (Thetford Mines, QC, Canada)	GFRP	12.7	Vinylester	NCE+Alkaline solution (IMMR)	60	240	NA	NA	3	102.1
648	Rolland et al. (2021)	Pultrall Inc. (Thetford Mines, QC, Canada)	GFRP	12.7	Vinylester	NCE+HT	40	120	NA	NA	3	89.8
649	Rolland et al. (2021)	Pultrall Inc. (Thetford Mines, QC, Canada)	GFRP	12.7	Vinylester	NCE+HT	40	240	NA	NA	3	90.9
650	Rolland et al. (2021)	Pultrall Inc. (Thetford Mines, QC, Canada)	GFRP	12.7	Vinylester	NCE+HT	60	120	NA	NA	3	94.3
651	Rolland et al. (2021)	Pultrall Inc. (Thetford Mines, QC, Canada)	GFRP	12.7	Vinylester	NCE+HT	60	240	NA	NA	3	94.8
652	Ruiz Emparanza et al. (2022)	NA	GFRP	10.0	Vinylester	Control	23	0	5	100.0	5	100.0
653	Ruiz Emparanza et al. (2022)	NA	GFRP	10.0	Vinylester	Seawater (IMMR)	23	60	3	96.8	3	103.5
654	Ruiz Emparanza et al. (2022)	NA	GFRP	10.0	Vinylester	Seawater (IMMR)	23	120	3	99.8	3	102.2
655	Ruiz Emparanza et al. (2022)	NA	GFRP	10.0	Vinylester	Seawater (IMMR)	23	210	3	95.7	3	100.9
656	Ruiz Emparanza et al. (2022)	NA	GFRP	10.0	Vinylester	Seawater (IMMR)	23	365	3	99.1	3	100.9
657	Ruiz Emparanza et al. (2022)	NA	GFRP	10.0	Vinylester	Seawater (IMMR)	40	60	3	98.3	3	100.5
658	Ruiz Emparanza et al. (2022)	NA	GFRP	10.0	Vinylester	Seawater (IMMR)	40	120	3	93.5	3	102.7
659	Ruiz Emparanza et al. (2022)	NA	GFRP	10.0	Vinylester	Seawater (IMMR)	40	210	3	84.1	3	101.8
660	Ruiz Emparanza et al. (2022)	NA	GFRP	10.0	Vinylester	Seawater (IMMR)	40	365	3	89.3	3	105.7
661	Ruiz Emparanza et al. (2022)	NA	GFRP	10.0	Vinylester	Seawater (IMMR)	60	60	3	89.3	3	104.0
662	Ruiz Emparanza et al. (2022)	NA	GFRP	10.0	Vinylester	Seawater (IMMR)	60	120	3	75.1	3	103.5
663	Ruiz	NA	GFRP	10.0	Vinylester	Seawater (IMMR)	60	210	3	83.4	3	104.0

	Emparanza et al. (2022)												
664	Ruiz Emparanza et al. (2022)	NA	GFRP	10.0	Vinylester	Seawater (IMMR)	60	365	3	83.4	3	104.8	
665	Ruiz Emparanza et al. (2022)	NA	GFRP	10.0	Vinylester	Control	23	0	5	100.0	5	100.0	
666	Ruiz Emparanza et al. (2022)	NA	GFRP	10.0	Vinylester	Seawater (IMMR)	23	60	3	105.8	3	103.5	
667	Ruiz Emparanza et al. (2022)	NA	GFRP	10.0	Vinylester	Seawater (IMMR)	23	120	3	103.2	3	102.2	
668	Ruiz Emparanza et al. (2022)	NA	GFRP	10.0	Vinylester	Seawater (IMMR)	23	210	3	93.5	3	103.5	
669	Ruiz Emparanza et al. (2022)	NA	GFRP	10.0	Vinylester	Seawater (IMMR)	23	365	3	95.7	3	100.1	
670	Ruiz Emparanza et al. (2022)	NA	GFRP	10.0	Vinylester	Seawater (IMMR)	40	60	3	94.2	3	110.5	
671	Ruiz Emparanza et al. (2022)	NA	GFRP	10.0	Vinylester	Seawater (IMMR)	40	120	3	90.5	3	111.3	
672	Ruiz Emparanza et al. (2022)	NA	GFRP	10.0	Vinylester	Seawater (IMMR)	40	210	3	83.7	3	107.9	
673	Ruiz Emparanza et al. (2022)	NA	GFRP	10.0	Vinylester	Seawater (IMMR)	40	365	3	90.5	3	105.7	
674	Ruiz Emparanza et al. (2022)	NA	GFRP	10.0	Vinylester	Seawater (IMMR)	60	60	3	90.1	3	103.5	
675	Ruiz Emparanza et al. (2022)	NA	GFRP	10.0	Vinylester	Seawater (IMMR)	60	120	3	92.3	3	113.1	
676	Ruiz Emparanza et al. (2022)	NA	GFRP	10.0	Vinylester	Seawater (IMMR)	60	210	3	78.1	3	99.6	
677	Ruiz Emparanza et al. (2022)	NA	GFRP	10.0	Vinylester	Seawater (IMMR)	60	365	3	83.0	3	88.8	
678	Ruiz Emparanza et	NA	GFRP	10.0	Vinylester	Control	23	0	5	100.0	5	100.0	

	al. (2022)												
679	Ruiz Emparanza et al. (2022)	NA	GFRP	10.0	Vinylester	Seawater (IMMR)	23	60	3	105.8	3	103.5	
680	Ruiz Emparanza et al. (2022)	NA	GFRP	10.0	Vinylester	Seawater (IMMR)	23	120	3	103.2	3	102.2	
681	Ruiz Emparanza et al. (2022)	NA	GFRP	10.0	Vinylester	Seawater (IMMR)	23	210	3	93.5	3	103.5	
682	Ruiz Emparanza et al. (2022)	NA	GFRP	10.0	Vinylester	Seawater (IMMR)	23	365	3	95.7	3	100.1	
683	Ruiz Emparanza et al. (2022)	NA	GFRP	10.0	Vinylester	Seawater (IMMR)	40	60	3	94.2	3	110.5	
684	Ruiz Emparanza et al. (2022)	NA	GFRP	10.0	Vinylester	Seawater (IMMR)	40	120	3	90.5	3	111.3	
685	Ruiz Emparanza et al. (2022)	NA	GFRP	10.0	Vinylester	Seawater (IMMR)	40	210	3	83.7	3	107.9	
686	Ruiz Emparanza et al. (2022)	NA	GFRP	10.0	Vinylester	Seawater (IMMR)	40	365	3	90.5	3	105.7	
687	Ruiz Emparanza et al. (2022)	NA	GFRP	10.0	Vinylester	Seawater (IMMR)	60	60	3	90.1	3	103.5	
688	Ruiz Emparanza et al. (2022)	NA	GFRP	10.0	Vinylester	Seawater (IMMR)	60	120	3	92.3	3	113.1	
689	Ruiz Emparanza et al. (2022)	NA	GFRP	10.0	Vinylester	Seawater (IMMR)	60	210	3	78.1	3	99.6	
690	Ruiz Emparanza et al. (2022)	NA	GFRP	10.0	Vinylester	Seawater (IMMR)	60	365	3	83.0	3	88.8	
691	Ruiz Emparanza et al. (2022)	NA	GFRP	10.0	Vinylester	Control	23	0	5	100.0	5	100.0	
692	Ruiz Emparanza et al. (2022)	NA	GFRP	10.0	Vinylester	Seawater (IMMR)	23	60	3	97.2	3	99.2	
693	Ruiz Emparanza et al. (2022)	NA	GFRP	10.0	Vinylester	Seawater (IMMR)	23	120	3	99.8	3	92.7	

694	Ruiz Emparanza et al. (2022)	NA	GFRP	10.0	Vinylester	Seawater (IMMR)	23	210	3	105.0	3	93.1
695	Ruiz Emparanza et al. (2022)	NA	GFRP	10.0	Vinylester	Seawater (IMMR)	23	365	3	99.1	3	100.5
696	Ruiz Emparanza et al. (2022)	NA	GFRP	10.0	Vinylester	Seawater (IMMR)	60	60	3	86.0	3	103.1
697	Ruiz Emparanza et al. (2022)	NA	GFRP	10.0	Vinylester	Seawater (IMMR)	60	120	3	85.2	3	98.8
698	Ruiz Emparanza et al. (2022)	NA	GFRP	10.0	Vinylester	Seawater (IMMR)	60	210	3	85.2	3	97.0
699	Ruiz Emparanza et al. (2022)	NA	GFRP	10.0	Vinylester	Seawater (IMMR)	60	365	3	83.0	3	97.0
700	Ruiz Emparanza et al. (2022)	NA	GFRP	10.0	Epoxy	Control	23	0	5	100.0	5	100.0
701	Ruiz Emparanza et al. (2022)	NA	GFRP	10.0	Epoxy	Seawater (IMMR)	23	60	3	91.6	3	95.3
702	Ruiz Emparanza et al. (2022)	NA	GFRP	10.0	Epoxy	Seawater (IMMR)	23	120	3	91.6	3	90.1
703	Ruiz Emparanza et al. (2022)	NA	GFRP	10.0	Epoxy	Seawater (IMMR)	23	210	3	104.3	3	105.7
704	Ruiz Emparanza et al. (2022)	NA	GFRP	10.0	Epoxy	Seawater (IMMR)	23	365	3	99.8	3	99.2
705	Ruiz Emparanza et al. (2022)	NA	GFRP	10.0	Epoxy	Seawater (IMMR)	60	60	3	97.6	3	100.9
706	Ruiz Emparanza et al. (2022)	NA	GFRP	10.0	Epoxy	Seawater (IMMR)	60	120	3	99.8	3	100.9
707	Ruiz Emparanza et al. (2022)	NA	GFRP	10.0	Epoxy	Seawater (IMMR)	60	210	3	99.8	3	96.6
708	Ruiz Emparanza et al. (2022)	NA	GFRP	10.0	Epoxy	Seawater (IMMR)	60	365	3	97.9	3	99.6
709	Ruiz	NA	GFRP	10.0	Vinylester	Control	23	0	5	100.0	5	100.0

	Emparanza et al. (2022)													
710	Ruiz Emparanza et al. (2022)	NA		GFRP	10.0	Vinylester	Seawater (IMMR)	23	60	3	92.0	3	97.9	
711	Ruiz Emparanza et al. (2022)	NA		GFRP	10.0	Vinylester	Seawater (IMMR)	23	120	3	95.7	3	98.8	
712	Ruiz Emparanza et al. (2022)	NA		GFRP	10.0	Vinylester	Seawater (IMMR)	23	210	3	102.8	3	96.6	
713	Ruiz Emparanza et al. (2022)	NA		GFRP	10.0	Vinylester	Seawater (IMMR)	23	365	3	99.4	3	98.3	
714	Ruiz Emparanza et al. (2022)	NA		GFRP	10.0	Vinylester	Seawater (IMMR)	60	60	3	91.2	3	102.7	
715	Ruiz Emparanza et al. (2022)	NA		GFRP	10.0	Vinylester	Seawater (IMMR)	60	120	3	97.6	3	98.8	
716	Ruiz Emparanza et al. (2022)	NA		GFRP	10.0	Vinylester	Seawater (IMMR)	60	210	3	97.6	3	92.3	
717	Ruiz Emparanza et al. (2022)	NA		GFRP	10.0	Vinylester	Seawater (IMMR)	60	365	3	95.7	3	94.9	
718	Sawpan (2019)	Pultron Limited	Composites (New Zealand)	GFRP	20.0	Vinylester	Control	23	0	4	100.0	5	100.0	
719	Sawpan (2019)	Pultron Limited	Composites (New Zealand)	GFRP	20.0	Vinylester	HT	55	240	4	105.2	5	103.5	
720	Sawpan (2019)	Pultron Limited	Composites (New Zealand)	GFRP	20.0	Vinylester	HT	55	600	4	106.0	5	106.1	
721	Sawpan (2019)	Pultron Limited	Composites (New Zealand)	GFRP	20.0	Vinylester	HT	75	240	4	105.3	5	104.9	
722	Sawpan (2019)	Pultron Limited	Composites (New Zealand)	GFRP	20.0	Vinylester	HT	75	600	4	107.7	5	106.9	
723	Sawpan (2019)	Pultron Limited	Composites (New Zealand)	GFRP	20.0	Vinylester	Seawater (IMMR)	23	240	4	99.7	5	99.0	
724	Sawpan (2019)	Pultron Limited	Composites (New	GFRP	20.0	Vinylester	Seawater (IMMR)	23	600	4	99.8	5	101.6	

		Zealand)											
725	Sawpan (2019)	Pultron Limited Zealand)	Composites (New	GFRP	20.0	Vinylester	Seawater (IMMR)	55	240	4	96.2	5	99.8
726	Sawpan (2019)	Pultron Limited Zealand)	Composites (New	GFRP	20.0	Vinylester	Seawater (IMMR)	55	600	4	95.6	5	102.6
727	Sawpan (2019)	Pultron Limited Zealand)	Composites (New	GFRP	20.0	Vinylester	Seawater (IMMR)	75	240	4	93.6	5	97.9
728	Sawpan (2019)	Pultron Limited Zealand)	Composites (New	GFRP	20.0	Vinylester	Seawater (IMMR)	75	600	4	91.8	5	95.5
729	Sawpan (2021)	Pultron Limited Zealand)	Composites (New	GFRP	20.0	Vinylester	Control	23	0	4	100.0	5	100.0
730	Sawpan (2021)	Pultron Limited Zealand)	Composites (New	GFRP	20.0	Vinylester	HT	55	240	4	105.3	5	103.4
731	Sawpan (2021)	Pultron Limited Zealand)	Composites (New	GFRP	20.0	Vinylester	HT	55	600	4	106.0	5	106.0
732	Sawpan (2021)	Pultron Limited Zealand)	Composites (New	GFRP	20.0	Vinylester	HT	55	900	4	107.1	5	105.3
733	Sawpan (2021)	Pultron Limited Zealand)	Composites (New	GFRP	20.0	Vinylester	HT	55	1080	4	103.9	5	107.3
734	Sawpan (2021)	Pultron Limited Zealand)	Composites (New	GFRP	20.0	Vinylester	HT	75	240	4	105.4	5	104.5
735	Sawpan (2021)	Pultron Limited Zealand)	Composites (New	GFRP	20.0	Vinylester	HT	75	600	4	107.8	5	106.6
736	Sawpan (2021)	Pultron Limited Zealand)	Composites (New	GFRP	20.0	Vinylester	HT	75	900	4	108.5	5	106.4
737	Sawpan (2021)	Pultron Limited Zealand)	Composites (New	GFRP	20.0	Vinylester	HT	75	1080	4	104.2	5	108.7
738	Sawpan (2021)	Pultron Limited Zealand)	Composites (New	GFRP	20.0	Vinylester	Seawater (IMMR)	23	240	4	99.8	5	99.3
739	Sawpan (2021)	Pultron Limited Zealand)	Composites (New	GFRP	20.0	Vinylester	Seawater (IMMR)	23	600	4	99.8	5	101.3

740	Sawpan (2021)	Pultron Limited Zealand)	Composites (New	GFRP	20.0	Vinylester	Seawater (IMMR)	23	900	4	98.0	5	99.0
741	Sawpan (2021)	Pultron Limited Zealand)	Composites (New	GFRP	20.0	Vinylester	Seawater (IMMR)	23	1080	4	95.1	5	101.9
742	Sawpan (2021)	Pultron Limited Zealand)	Composites (New	GFRP	20.0	Vinylester	Seawater (IMMR)	55	240	4	96.3	5	99.7
743	Sawpan (2021)	Pultron Limited Zealand)	Composites (New	GFRP	20.0	Vinylester	Seawater (IMMR)	55	600	4	95.6	5	102.1
744	Sawpan (2021)	Pultron Limited Zealand)	Composites (New	GFRP	20.0	Vinylester	Seawater (IMMR)	55	900	4	92.4	5	101.3
745	Sawpan (2021)	Pultron Limited Zealand)	Composites (New	GFRP	20.0	Vinylester	Seawater (IMMR)	55	1080	4	91.9	5	102.6
746	Sawpan (2021)	Pultron Limited Zealand)	Composites (New	GFRP	20.0	Vinylester	Seawater (IMMR)	75	240	4	93.6	5	97.7
747	Sawpan (2021)	Pultron Limited Zealand)	Composites (New	GFRP	20.0	Vinylester	Seawater (IMMR)	75	600	4	91.9	5	94.7
748	Sawpan (2021)	Pultron Limited Zealand)	Composites (New	GFRP	20.0	Vinylester	Seawater (IMMR)	75	900	4	89.3	5	96.4
749	Sawpan (2021)	Pultron Limited Zealand)	Composites (New	GFRP	20.0	Vinylester	Seawater (IMMR)	75	1080	4	88.5	5	87.2
750	Silva et al. (2022）	NA		CFRP	3.0	Epoxy	Control	30	0	NA	NA	5	100.0
751	Silva et al. (2022）	NA		CFRP	3.0	Epoxy	Water (IMMR)	60	63	NA	NA	5	96.6
752	Silva et al. (2022）	NA		CFRP	3.0	Epoxy	Water (IMMR)	60	125	NA	NA	5	83.6
753	Silva et al. (2022）	NA		CFRP	3.0	Epoxy	Simulated seawater (IMMR)	60	63	NA	NA	5	93.2
754	Silva et al. (2022）	NA		CFRP	3.0	Epoxy	Simulated seawater (IMMR)	60	125	NA	NA	5	87.4
755	Silva et al. (2022）	NA		CFRP	3.0	Epoxy	UV+Water-spray	30/63	63	NA	NA	5	105.3
756	Silva et al. (2022）	NA		CFRP	3.0	Epoxy	UV+Water-spray	30/63	125	NA	NA	5	101.9
757	Silva et al.	NA		CFRP	3.0	Vinylester	Control	30	0	NA	NA	5	100.0

	(2022）											
758	Silva et al. (2022）	NA	CFRP	3.0	Vinylester	Water (IMMR)	60	63	NA	NA	5	75.1
759	Silva et al. (2022）	NA	CFRP	3.0	Vinylester	Water (IMMR)	60	125	NA	NA	5	66.2
760	Silva et al. (2022）	NA	CFRP	3.0	Vinylester	Simulated seawater (IMMR)	60	63	NA	NA	5	69.7
761	Silva et al. (2022）	NA	CFRP	3.0	Vinylester	Simulated seawater (IMMR)	60	125	NA	NA	5	71.1
762	Silva et al. (2022）	NA	CFRP	3.0	Vinylester	UV+Water-spray	30/63	63	NA	NA	5	103.5
763	Silva et al. (2022）	NA	CFRP	3.0	Vinylester	UV+Water-spray	30/63	125	NA	NA	5	92.0
764	Starkova et al. (2021)	Sireg s.r.l. and ATP s.r.l. (Italy)	CFRP	8.0	Vinylester/epoxy-vinylester	Control	20	0	NA	NA	6	100.0
765	Starkova et al. (2021)	Sireg s.r.l. and ATP s.r.l. (Italy)	CFRP	8.0	Vinylester/epoxy-vinylester	Saline solution (IMMR)	20	2555	NA	NA	6	90.6
766	Starkova et al. (2021)	Sireg s.r.l. and ATP s.r.l. (Italy)	CFRP	8.0	Vinylester/epoxy-vinylester	Saline solution (IMMR)	20	5475	NA	NA	6	84.6
767	Starkova et al. (2021)	Sireg s.r.l. and ATP s.r.l. (Italy)	AFRP	5.0	Vinylester/epoxy-vinylester	Control	20	0	NA	NA	6	100.0
768	Starkova et al. (2021)	Sireg s.r.l. and ATP s.r.l. (Italy)	AFRP	5.0	Vinylester/epoxy-vinylester	Saline solution (IMMR)	20	2555	NA	NA	6	47.9
769	Starkova et al. (2021)	Sireg s.r.l. and ATP s.r.l. (Italy)	AFRP	5.0	Vinylester/epoxy-vinylester	Saline solution (IMMR)	20	5475	NA	NA	6	48.6
770	Starkova et al. (2021)	Sireg s.r.l. and ATP s.r.l. (Italy)	GFRP	5.0	Vinylester/epoxy-vinylester	Control	20	0	NA	NA	6	100.0
771	Starkova et al. (2021)	Sireg s.r.l. and ATP s.r.l. (Italy)	GFRP	5.0	Vinylester/epoxy-vinylester	Saline solution (IMMR)	20	1460	NA	NA	6	71.6
772	Starkova et al. (2021)	Sireg s.r.l. and ATP s.r.l. (Italy)	GFRP	5.0	Vinylester/epoxy-vinylester	Saline solution (IMMR)	20	4380	NA	NA	6	72.3
773	Starkova et al. (2021)	Sireg s.r.l. and ATP s.r.l. (Italy)	GFRP	8.0	Vinylester/epoxy-vinylester	Control	20	0	NA	NA	6	100.0
774	Starkova et al. (2021)	Sireg s.r.l. and ATP s.r.l. (Italy)	GFRP	8.0	Vinylester/epoxy-vinylester	Saline solution (IMMR)	20	1460	NA	NA	6	105.8
775	Starkova et al. (2021)	Sireg s.r.l. and ATP s.r.l. (Italy)	GFRP	8.0	Vinylester/epoxy-vinylester	Saline solution (IMMR)	20	4380	NA	NA	6	100.0
776	Sun et al. (2023)	NA	GFRP	6.0	Epoxy	Control	NA	0	NA	NA	5	100.0
777	Sun et al. (2023)	NA	GFRP	6.0	Epoxy	Alkaline solution (IMMR)	NA	300	NA	NA	5	77.2
778	Sun et al. (2023)	NA	GFRP	6.0	Epoxy	Alkaline solution (IMMR)	NA	300	NA	NA	5	75.3
779	Sun et al. (2023)	NA	GFRP	6.0	Epoxy	Alkaline solution (IMMR)	NA	300	NA	NA	5	74.4

780	Sun et al. (2023)	NA	GFRP	6.0	Epoxy	Alkaline solution (IMMR)	NA	300	NA	NA	5	70.5
781	Sun et al. (2023)	NA	GFRP	6.0	Epoxy	Alkaline solution (IMMR)	NA	300	NA	NA	5	69.6
782	Sun et al. (2023)	NA	GFRP	6.0	Epoxy	Alkaline solution (IMMR)	NA	300	NA	NA	5	63.7
783	Sun et al. (2023)	NA	GFRP	6.0	Epoxy	Control	NA	0	NA	NA	5	100.0
784	Sun et al. (2023)	NA	GFRP	6.0	Epoxy	Alkaline solution (IMMR)	NA	300	NA	NA	5	71.1
785	Sun et al. (2023)	NA	GFRP	6.0	Epoxy	Alkaline solution (IMMR)	NA	300	NA	NA	5	71.6
786	Sun et al. (2023)	NA	GFRP	6.0	Epoxy	Alkaline solution (IMMR)	NA	300	NA	NA	5	71.4
787	Sun et al. (2023)	NA	GFRP	6.0	Epoxy	Alkaline solution (IMMR)	NA	300	NA	NA	5	70.8
788	Sun et al. (2023)	NA	GFRP	6.0	Epoxy	Alkaline solution (IMMR)	NA	300	NA	NA	5	70.2
789	Sun et al. (2023)	NA	GFRP	6.0	Epoxy	Alkaline solution (IMMR)	NA	300	NA	NA	5	65.9
790	Sun et al. (2023)	NA	GFRP	6.0	Epoxy	Control	NA	0	NA	NA	5	100.0
791	Sun et al. (2023)	NA	GFRP	6.0	Epoxy	Alkaline solution (IMMR)	NA	300	NA	NA	5	73.8
792	Sun et al. (2023)	NA	GFRP	6.0	Epoxy	Alkaline solution (IMMR)	NA	300	NA	NA	5	74.5
793	Sun et al. (2023)	NA	GFRP	6.0	Epoxy	Alkaline solution (IMMR)	NA	300	NA	NA	5	74.5
794	Sun et al. (2023)	NA	GFRP	6.0	Epoxy	Alkaline solution (IMMR)	NA	300	NA	NA	5	73.4
795	Sun et al. (2023)	NA	GFRP	6.0	Epoxy	Alkaline solution (IMMR)	NA	300	NA	NA	5	72.7
796	Sun et al. (2023)	NA	GFRP	6.0	Epoxy	Alkaline solution (IMMR)	NA	300	NA	NA	5	70.7
797	Sun et al. (2023)	NA	GFRP	6.0	Epoxy	Control	NA	0	NA	NA	5	100.0
798	Sun et al. (2023)	NA	GFRP	6.0	Epoxy	Alkaline solution (IMMR)	NA	300	NA	NA	5	71.6
799	Sun et al. (2023)	NA	GFRP	6.0	Epoxy	Alkaline solution (IMMR)	NA	300	NA	NA	5	70.2
800	Sun et al. (2023)	NA	GFRP	6.0	Epoxy	Alkaline solution (IMMR)	NA	300	NA	NA	5	69.2
801	Sun et al. (2023)	NA	GFRP	6.0	Epoxy	Alkaline solution (IMMR)	NA	300	NA	NA	5	67.8
802	Sun et al. (2023)	NA	GFRP	6.0	Epoxy	Alkaline solution (IMMR)	NA	300	NA	NA	5	65.0

803	Sun et al. (2023)	NA	GFRP	6.0	Epoxy	Alkaline solution (IMMR)	NA	300	NA	NA	5	62.5
804	Wang et al. (2017a)	Jiangsu Green Materials Vally New Material T&D Co., Ltd (Nanjing, China)/*/Harbin FRP Institute (Harbin, China)	BFRP	6.0	Epoxy	Control	25	0	NA	NA	15	100.0
805	Wang et al. (2017a)	Jiangsu Green Materials Vally New Material T&D Co., Ltd (Nanjing, China)/*/Harbin FRP Institute (Harbin, China)	BFRP	6.0	Epoxy	SWSSC solution 1 (IMMR)	25	21	NA	NA	3	96.6
806	Wang et al. (2017a)	Jiangsu Green Materials Vally New Material T&D Co., Ltd (Nanjing, China)/*/Harbin FRP Institute (Harbin, China)	BFRP	6.0	Epoxy	SWSSC solution 1 (IMMR)	25	42	NA	NA	3	92.2
807	Wang et al. (2017a)	Jiangsu Green Materials Vally New Material T&D Co., Ltd (Nanjing, China)/*/Harbin FRP Institute (Harbin, China)	BFRP	6.0	Epoxy	SWSSC solution 1 (IMMR)	25	63	NA	NA	3	89.0
808	Wang et al. (2017a)	Jiangsu Green Materials Vally New Material T&D Co., Ltd (Nanjing, China)/*/Harbin FRP Institute (Harbin, China)	BFRP	6.0	Epoxy	SWSSC solution 1 (IMMR)	25	84	NA	NA	3	87.0
809	Wang et al. (2017a)	Jiangsu Green Materials Vally New Material T&D Co., Ltd (Nanjing, China)/*/Harbin FRP Institute (Harbin, China)	BFRP	6.0	Epoxy	SWSSC solution 1 (IMMR)	40	21	NA	NA	3	89.5
810	Wang et al. (2017a)	Jiangsu Green Materials Vally New	BFRP	6.0	Epoxy	SWSSC solution 1 (IMMR)	40	42	NA	NA	3	76.7

		Material T&D Co., Ltd (Nanjing, China)/*/Harbin FRP Institute (Harbin, China)										
811	Wang et al. (2017a)	Jiangsu Green Materials Vally New Material T&D Co., Ltd (Nanjing, China)/*/Harbin FRP Institute (Harbin, China)	BFRP	6.0	Epoxy	SWSSC solution 1 (IMMR)	40	63	NA	NA	3	35.2
812	Wang et al. (2017a)	Jiangsu Green Materials Vally New Material T&D Co., Ltd (Nanjing, China)/*/Harbin FRP Institute (Harbin, China)	BFRP	6.0	Epoxy	SWSSC solution 1 (IMMR)	40	84	NA	NA	3	15.2
813	Wang et al. (2017a)	Jiangsu Green Materials Vally New Material T&D Co., Ltd (Nanjing, China)/*/Harbin FRP Institute (Harbin, China)	BFRP	6.0	Epoxy	SWSSC solution 1 (IMMR)	55	21	NA	NA	3	54.7
814	Wang et al. (2017a)	Jiangsu Green Materials Vally New Material T&D Co., Ltd (Nanjing, China)/*/Harbin FRP Institute (Harbin, China)	BFRP	6.0	Epoxy	SWSSC solution 1 (IMMR)	55	42	NA	NA	3	18.8
815	Wang et al. (2017a)	Jiangsu Green Materials Vally New Material T&D Co., Ltd (Nanjing, China)/*/Harbin FRP Institute (Harbin, China)	BFRP	6.0	Epoxy	SWSSC solution 1 (IMMR)	55	63	NA	NA	3	0.6
816	Wang et al. (2017a)	Jiangsu Green Materials Vally New Material T&D Co., Ltd (Nanjing, China)/*/Harbin FRP Institute (Harbin,	BFRP	6.0	Epoxy	SWSSC solution 1 (IMMR)	55	84	NA	NA	3	0.2

		China)										
817	Wang et al. (2017a)	Jiangsu Green Materials Vally New Material T&D Co., Ltd (Nanjing, China)/*/Harbin FRP Institute (Harbin, China)	BFRP	6.0	Epoxy	SWSSC solution 2 (IMMR)	25	21	NA	NA	3	93.3
818	Wang et al. (2017a)	Jiangsu Green Materials Vally New Material T&D Co., Ltd (Nanjing, China)/*/Harbin FRP Institute (Harbin, China)	BFRP	6.0	Epoxy	SWSSC solution 2 (IMMR)	25	42	NA	NA	3	96.6
819	Wang et al. (2017a)	Jiangsu Green Materials Vally New Material T&D Co., Ltd (Nanjing, China)/*/Harbin FRP Institute (Harbin, China)	BFRP	6.0	Epoxy	SWSSC solution 2 (IMMR)	25	63	NA	NA	3	92.8
820	Wang et al. (2017a)	Jiangsu Green Materials Vally New Material T&D Co., Ltd (Nanjing, China)/*/Harbin FRP Institute (Harbin, China)	BFRP	6.0	Epoxy	SWSSC solution 2 (IMMR)	25	84	NA	NA	3	93.0
821	Wang et al. (2017a)	Jiangsu Green Materials Vally New Material T&D Co., Ltd (Nanjing, China)/*/Harbin FRP Institute (Harbin, China)	BFRP	6.0	Epoxy	SWSSC solution 2 (IMMR)	40	21	NA	NA	3	91.9
822	Wang et al. (2017a)	Jiangsu Green Materials Vally New Material T&D Co., Ltd (Nanjing, China)/*/Harbin FRP Institute (Harbin, China)	BFRP	6.0	Epoxy	SWSSC solution 2 (IMMR)	40	42	NA	NA	3	93.7
823	Wang et al. (2017a)	Jiangsu Green Materials Vally New Material T&D Co.,	BFRP	6.0	Epoxy	SWSSC solution 2 (IMMR)	40	63	NA	NA	3	87.2

		Ltd (Nanjing, China)/*/Harbin FRP Institute (Harbin, China)										
824	Wang et al. (2017a)	Jiangsu Green Materials Vally New Material T&D Co., Ltd (Nanjing, China)/*/Harbin FRP Institute (Harbin, China)	BFRP	6.0	Epoxy	SWSSC solution 2 (IMMR)	40	84	NA	NA	3	87.2
825	Wang et al. (2017a)	Jiangsu Green Materials Vally New Material T&D Co., Ltd (Nanjing, China)/*/Harbin FRP Institute (Harbin, China)	BFRP	6.0	Epoxy	SWSSC solution 2 (IMMR)	55	21	NA	NA	3	89.2
826	Wang et al. (2017a)	Jiangsu Green Materials Vally New Material T&D Co., Ltd (Nanjing, China)/*/Harbin FRP Institute (Harbin, China)	BFRP	6.0	Epoxy	SWSSC solution 2 (IMMR)	55	42	NA	NA	3	81.8
827	Wang et al. (2017a)	Jiangsu Green Materials Vally New Material T&D Co., Ltd (Nanjing, China)/*/Harbin FRP Institute (Harbin, China)	BFRP	6.0	Epoxy	SWSSC solution 2 (IMMR)	55	63	NA	NA	3	60.5
828	Wang et al. (2017a)	Jiangsu Green Materials Vally New Material T&D Co., Ltd (Nanjing, China)/*/Harbin FRP Institute (Harbin, China)	BFRP	6.0	Epoxy	SWSSC solution 2 (IMMR)	55	84	NA	NA	3	49.6
829	Wang et al. (2017a)	NA	CFRP	5.8	Epoxy	Control	25	0	NA	NA	15	100.0
830	Wang et al. (2017a)	NA	CFRP	5.8	Epoxy	SWSSC solution 1 (IMMR)	25	21	NA	NA	3	96.2
831	Wang et al. (2017a)	NA	CFRP	5.8	Epoxy	SWSSC solution 1 (IMMR)	25	42	NA	NA	3	93.4
832	Wang et al.	NA	CFRP	5.8	Epoxy	SWSSC solution 1 (IMMR)	25	63	NA	NA	3	93.4

	(2017a)											
833	Wang et al. (2017a)	NA	CFRP	5.8	Epoxy	SWSSC solution 1 (IMMR)	25	84	NA	NA	3	93.1
834	Wang et al. (2017a)	NA	CFRP	5.8	Epoxy	SWSSC solution 1 (IMMR)	40	21	NA	NA	3	86.7
835	Wang et al. (2017a)	NA	CFRP	5.8	Epoxy	SWSSC solution 1 (IMMR)	40	42	NA	NA	3	82.9
836	Wang et al. (2017a)	NA	CFRP	5.8	Epoxy	SWSSC solution 1 (IMMR)	40	63	NA	NA	3	76.1
837	Wang et al. (2017a)	NA	CFRP	5.8	Epoxy	SWSSC solution 1 (IMMR)	40	84	NA	NA	3	34.1
838	Wang et al. (2017a)	NA	CFRP	5.8	Epoxy	SWSSC solution 1 (IMMR)	55	21	NA	NA	3	83.9
839	Wang et al. (2017a)	NA	CFRP	5.8	Epoxy	SWSSC solution 1 (IMMR)	55	42	NA	NA	3	64.0
840	Wang et al. (2017a)	NA	CFRP	5.8	Epoxy	SWSSC solution 1 (IMMR)	55	63	NA	NA	3	42.9
841	Wang et al. (2017a)	NA	CFRP	5.8	Epoxy	SWSSC solution 1 (IMMR)	55	84	NA	NA	3	3.1
842	Wang et al. (2017a)	NA	CFRP	5.8	Epoxy	SWSSC solution 2 (IMMR)	25	21	NA	NA	3	95.3
843	Wang et al. (2017a)	NA	CFRP	5.8	Epoxy	SWSSC solution 2 (IMMR)	25	42	NA	NA	3	96.7
844	Wang et al. (2017a)	NA	CFRP	5.8	Epoxy	SWSSC solution 2 (IMMR)	25	63	NA	NA	3	90.8
845	Wang et al. (2017a)	NA	CFRP	5.8	Epoxy	SWSSC solution 2 (IMMR)	25	84	NA	NA	3	94.1
846	Wang et al. (2017a)	NA	CFRP	5.8	Epoxy	SWSSC solution 2 (IMMR)	40	21	NA	NA	3	90.5
847	Wang et al. (2017a)	NA	CFRP	5.8	Epoxy	SWSSC solution 2 (IMMR)	40	42	NA	NA	3	82.9
848	Wang et al. (2017a)	NA	CFRP	5.8	Epoxy	SWSSC solution 2 (IMMR)	40	63	NA	NA	3	80.1
849	Wang et al. (2017a)	NA	CFRP	5.8	Epoxy	SWSSC solution 2 (IMMR)	40	84	NA	NA	3	84.6
850	Wang et al. (2017a)	NA	CFRP	5.8	Epoxy	SWSSC solution 2 (IMMR)	55	21	NA	NA	3	82.5
851	Wang et al. (2017a)	NA	CFRP	5.8	Epoxy	SWSSC solution 2 (IMMR)	55	42	NA	NA	3	79.4
852	Wang et al. (2017a)	NA	CFRP	5.8	Epoxy	SWSSC solution 2 (IMMR)	55	63	NA	NA	3	81.8
853	Wang et al. (2017a)	NA	CFRP	5.8	Epoxy	SWSSC solution 2 (IMMR)	55	84	NA	NA	3	61.1
854	Wang et al. (2017a)	Harbin FRP Institute (Harbin, China)	GFRP	6.3	Epoxy	Control	25	0	NA	NA	15	100.0
855	Wang et al.	Harbin FRP Institute	GFRP	6.3	Epoxy	SWSSC solution 1 (IMMR)	25	21	NA	NA	3	98.4

	(2017a)	(Harbin, China)										
856	Wang et al. (2017a)	Harbin FRP Institute (Harbin, China)	GFRP	6.3	Epoxy	SWSSC solution 1 (IMMR)	25	42	NA	NA	3	100.0
857	Wang et al. (2017a)	Harbin FRP Institute (Harbin, China)	GFRP	6.3	Epoxy	SWSSC solution 1 (IMMR)	25	63	NA	NA	3	95.1
858	Wang et al. (2017a)	Harbin FRP Institute (Harbin, China)	GFRP	6.3	Epoxy	SWSSC solution 1 (IMMR)	25	84	NA	NA	3	94.3
859	Wang et al. (2017a)	Harbin FRP Institute (Harbin, China)	GFRP	6.3	Epoxy	SWSSC solution 1 (IMMR)	40	21	NA	NA	3	88.4
860	Wang et al. (2017a)	Harbin FRP Institute (Harbin, China)	GFRP	6.3	Epoxy	SWSSC solution 1 (IMMR)	40	42	NA	NA	3	82.7
861	Wang et al. (2017a)	Harbin FRP Institute (Harbin, China)	GFRP	6.3	Epoxy	SWSSC solution 1 (IMMR)	40	63	NA	NA	3	81.9
862	Wang et al. (2017a)	Harbin FRP Institute (Harbin, China)	GFRP	6.3	Epoxy	SWSSC solution 1 (IMMR)	40	84	NA	NA	3	75.7
863	Wang et al. (2017a)	Harbin FRP Institute (Harbin, China)	GFRP	6.3	Epoxy	SWSSC solution 1 (IMMR)	55	21	NA	NA	3	81.4
864	Wang et al. (2017a)	Harbin FRP Institute (Harbin, China)	GFRP	6.3	Epoxy	SWSSC solution 1 (IMMR)	55	42	NA	NA	3	72.9
865	Wang et al. (2017a)	Harbin FRP Institute (Harbin, China)	GFRP	6.3	Epoxy	SWSSC solution 1 (IMMR)	55	63	NA	NA	3	58.4
866	Wang et al. (2017a)	Harbin FRP Institute (Harbin, China)	GFRP	6.3	Epoxy	SWSSC solution 1 (IMMR)	55	84	NA	NA	3	42.1
867	Wang et al. (2017a)	Harbin FRP Institute (Harbin, China)	GFRP	6.3	Epoxy	SWSSC solution 2 (IMMR)	25	21	NA	NA	3	98.2
868	Wang et al. (2017a)	Harbin FRP Institute (Harbin, China)	GFRP	6.3	Epoxy	SWSSC solution 2 (IMMR)	25	42	NA	NA	3	91.2
869	Wang et al. (2017a)	Harbin FRP Institute (Harbin, China)	GFRP	6.3	Epoxy	SWSSC solution 2 (IMMR)	25	63	NA	NA	3	93.8
870	Wang et al. (2017a)	Harbin FRP Institute (Harbin, China)	GFRP	6.3	Epoxy	SWSSC solution 2 (IMMR)	25	84	NA	NA	3	93.5
871	Wang et al. (2017a)	Harbin FRP Institute (Harbin, China)	GFRP	6.3	Epoxy	SWSSC solution 2 (IMMR)	40	21	NA	NA	3	85.8
872	Wang et al. (2017a)	Harbin FRP Institute (Harbin, China)	GFRP	6.3	Epoxy	SWSSC solution 2 (IMMR)	40	42	NA	NA	3	85.3
873	Wang et al. (2017a)	Harbin FRP Institute (Harbin, China)	GFRP	6.3	Epoxy	SWSSC solution 2 (IMMR)	40	63	NA	NA	3	87.9
874	Wang et al. (2017a)	Harbin FRP Institute (Harbin, China)	GFRP	6.3	Epoxy	SWSSC solution 2 (IMMR)	40	84	NA	NA	3	82.9
875	Wang et al. (2017a)	Harbin FRP Institute (Harbin, China)	GFRP	6.3	Epoxy	SWSSC solution 2 (IMMR)	55	21	NA	NA	3	87.1
876	Wang et al. (2017a)	Harbin FRP Institute (Harbin, China)	GFRP	6.3	Epoxy	SWSSC solution 2 (IMMR)	55	42	NA	NA	3	83.2
877	Wang et al. (2017a)	Harbin FRP Institute (Harbin, China)	GFRP	6.3	Epoxy	SWSSC solution 2 (IMMR)	55	63	NA	NA	3	85.8
878	Wang et al.	Harbin FRP Institute	GFRP	6.3	Epoxy	SWSSC solution 2 (IMMR)	55	84	NA	NA	3	80.4

	(2017a)	(Harbin, China)											
879	Wang et al. (2022)	Dextra Co., ltd (Dongguan, China)	GFRP	9.5	Vinylester	Control	23	0	NA	NA	5	100.0	
880	Wang et al. (2022)	Dextra Co., ltd (Dongguan, China)	GFRP	9.5	Vinylester	Water (IMMR)	23	45	NA	NA	5	99.8	
881	Wang et al. (2022)	Dextra Co., ltd (Dongguan, China)	GFRP	9.5	Vinylester	Water (IMMR)	23	90	NA	NA	5	99.8	
882	Wang et al. (2022)	Dextra Co., ltd (Dongguan, China)	GFRP	9.5	Vinylester	Water (IMMR)	23	180	NA	NA	5	99.8	
883	Wang et al. (2022)	Dextra Co., ltd (Dongguan, China)	GFRP	9.5	Vinylester	Water (IMMR)	23	270	NA	NA	5	95.1	
884	Wang et al. (2022)	Dextra Co., ltd (Dongguan, China)	GFRP	9.5	Vinylester	Water (IMMR)	23	360	NA	NA	5	96.9	
885	Wang et al. (2022)	Dextra Co., ltd (Dongguan, China)	GFRP	9.5	Vinylester	Water (IMMR)	40	45	NA	NA	5	101.0	
886	Wang et al. (2022)	Dextra Co., ltd (Dongguan, China)	GFRP	9.5	Vinylester	Water (IMMR)	40	90	NA	NA	5	99.2	
887	Wang et al. (2022)	Dextra Co., ltd (Dongguan, China)	GFRP	9.5	Vinylester	Water (IMMR)	40	180	NA	NA	5	98.6	
888	Wang et al. (2022)	Dextra Co., ltd (Dongguan, China)	GFRP	9.5	Vinylester	Water (IMMR)	40	270	NA	NA	5	95.7	
889	Wang et al. (2022)	Dextra Co., ltd (Dongguan, China)	GFRP	9.5	Vinylester	Water (IMMR)	40	360	NA	NA	5	95.7	
890	Wang et al. (2022)	Dextra Co., ltd (Dongguan, China)	GFRP	9.5	Vinylester	Water (IMMR)	60	45	NA	NA	5	100.4	
891	Wang et al. (2022)	Dextra Co., ltd (Dongguan, China)	GFRP	9.5	Vinylester	Water (IMMR)	60	90	NA	NA	5	96.9	
892	Wang et al. (2022)	Dextra Co., ltd (Dongguan, China)	GFRP	9.5	Vinylester	Water (IMMR)	60	180	NA	NA	5	99.2	
893	Wang et al. (2022)	Dextra Co., ltd (Dongguan, China)	GFRP	9.5	Vinylester	Water (IMMR)	60	270	NA	NA	5	95.1	
894	Wang et al. (2022)	Dextra Co., ltd (Dongguan, China)	GFRP	9.5	Vinylester	Water (IMMR)	60	360	NA	NA	5	96.3	
895	Wang et al. (2022)	Dextra Co., ltd (Dongguan, China)	GFRP	9.5	Vinylester	Alkaline solution 1 (IMMR)	23	45	NA	NA	5	100.4	
896	Wang et al. (2022)	Dextra Co., ltd (Dongguan, China)	GFRP	9.5	Vinylester	Alkaline solution 1 (IMMR)	23	90	NA	NA	5	99.8	
897	Wang et al. (2022)	Dextra Co., ltd (Dongguan, China)	GFRP	9.5	Vinylester	Alkaline solution 1 (IMMR)	23	180	NA	NA	5	99.8	
898	Wang et al. (2022)	Dextra Co., ltd (Dongguan, China)	GFRP	9.5	Vinylester	Alkaline solution 1 (IMMR)	23	270	NA	NA	5	95.1	
899	Wang et al. (2022)	Dextra Co., ltd (Dongguan, China)	GFRP	9.5	Vinylester	Alkaline solution 1 (IMMR)	23	360	NA	NA	5	95.1	
900	Wang et al. (2022)	Dextra Co., ltd (Dongguan, China)	GFRP	9.5	Vinylester	Alkaline solution 1 (IMMR)	40	45	NA	NA	5	98.6	
901	Wang et al.	Dextra Co., ltd	GFRP	9.5	Vinylester	Alkaline solution 1 (IMMR)	40	90	NA	NA	5	98.0	

	(2022)	(Dongguan, China)											
902	Wang et al. (2022)	Dextra Co., ltd (Dongguan, China)	GFRP	9.5	Vinylester	Alkaline solution 1 (IMMR)	40	180	NA	NA	5	97.4
903	Wang et al. (2022)	Dextra Co., ltd (Dongguan, China)	GFRP	9.5	Vinylester	Alkaline solution 1 (IMMR)	40	270	NA	NA	5	96.3
904	Wang et al. (2022)	Dextra Co., ltd (Dongguan, China)	GFRP	9.5	Vinylester	Alkaline solution 1 (IMMR)	40	360	NA	NA	5	95.1
905	Wang et al. (2022)	Dextra Co., ltd (Dongguan, China)	GFRP	9.5	Vinylester	Alkaline solution 1 (IMMR)	60	45	NA	NA	5	101.0
906	Wang et al. (2022)	Dextra Co., ltd (Dongguan, China)	GFRP	9.5	Vinylester	Alkaline solution 1 (IMMR)	60	90	NA	NA	5	96.3
907	Wang et al. (2022)	Dextra Co., ltd (Dongguan, China)	GFRP	9.5	Vinylester	Alkaline solution 1 (IMMR)	60	180	NA	NA	5	99.8
908	Wang et al. (2022)	Dextra Co., ltd (Dongguan, China)	GFRP	9.5	Vinylester	Alkaline solution 1 (IMMR)	60	270	NA	NA	5	96.3
909	Wang et al. (2022)	Dextra Co., ltd (Dongguan, China)	GFRP	9.5	Vinylester	Alkaline solution 1 (IMMR)	60	360	NA	NA	5	96.3
910	Wang et al. (2022)	Dextra Co., ltd (Dongguan, China)	GFRP	9.5	Vinylester	Alkaline solution 2 (IMMR)	23	45	NA	NA	5	101.6
911	Wang et al. (2022)	Dextra Co., ltd (Dongguan, China)	GFRP	9.5	Vinylester	Alkaline solution 2 (IMMR)	23	90	NA	NA	5	97.4
912	Wang et al. (2022)	Dextra Co., ltd (Dongguan, China)	GFRP	9.5	Vinylester	Alkaline solution 2 (IMMR)	23	180	NA	NA	5	98.0
913	Wang et al. (2022)	Dextra Co., ltd (Dongguan, China)	GFRP	9.5	Vinylester	Alkaline solution 2 (IMMR)	23	270	NA	NA	5	95.7
914	Wang et al. (2022)	Dextra Co., ltd (Dongguan, China)	GFRP	9.5	Vinylester	Alkaline solution 2 (IMMR)	23	360	NA	NA	5	96.9
915	Wang et al. (2022)	Dextra Co., ltd (Dongguan, China)	GFRP	9.5	Vinylester	Alkaline solution 2 (IMMR)	40	45	NA	NA	5	99.2
916	Wang et al. (2022)	Dextra Co., ltd (Dongguan, China)	GFRP	9.5	Vinylester	Alkaline solution 2 (IMMR)	40	90	NA	NA	5	96.3
917	Wang et al. (2022)	Dextra Co., ltd (Dongguan, China)	GFRP	9.5	Vinylester	Alkaline solution 2 (IMMR)	40	180	NA	NA	5	99.8
918	Wang et al. (2022)	Dextra Co., ltd (Dongguan, China)	GFRP	9.5	Vinylester	Alkaline solution 2 (IMMR)	40	270	NA	NA	5	95.7
919	Wang et al. (2022)	Dextra Co., ltd (Dongguan, China)	GFRP	9.5	Vinylester	Alkaline solution 2 (IMMR)	40	360	NA	NA	5	95.7
920	Wang et al. (2022)	Dextra Co., ltd (Dongguan, China)	GFRP	9.5	Vinylester	Alkaline solution 2 (IMMR)	60	45	NA	NA	5	98.0
921	Wang et al. (2022)	Dextra Co., ltd (Dongguan, China)	GFRP	9.5	Vinylester	Alkaline solution 2 (IMMR)	60	90	NA	NA	5	96.3
922	Wang et al. (2022)	Dextra Co., ltd (Dongguan, China)	GFRP	9.5	Vinylester	Alkaline solution 2 (IMMR)	60	180	NA	NA	5	98.6
923	Wang et al. (2022)	Dextra Co., ltd (Dongguan, China)	GFRP	9.5	Vinylester	Alkaline solution 2 (IMMR)	60	270	NA	NA	5	96.3
924	Wang et al.	Dextra Co., ltd	GFRP	9.5	Vinylester	Alkaline solution 2 (IMMR)	60	360	NA	NA	5	96.9

	(2022)	(Dongguan, China)										
925	Wang et al. (2022)	Dextra Co., ltd (Dongguan, China)	GFRP	9.5	Vinylester	Alkaline solution 3 (IMMR)	23	45	NA	NA	5	101.0
926	Wang et al. (2022)	Dextra Co., ltd (Dongguan, China)	GFRP	9.5	Vinylester	Alkaline solution 3 (IMMR)	23	90	NA	NA	5	96.3
927	Wang et al. (2022)	Dextra Co., ltd (Dongguan, China)	GFRP	9.5	Vinylester	Alkaline solution 3 (IMMR)	23	180	NA	NA	5	98.6
928	Wang et al. (2022)	Dextra Co., ltd (Dongguan, China)	GFRP	9.5	Vinylester	Alkaline solution 3 (IMMR)	23	270	NA	NA	5	95.7
929	Wang et al. (2022)	Dextra Co., ltd (Dongguan, China)	GFRP	9.5	Vinylester	Alkaline solution 3 (IMMR)	23	360	NA	NA	5	96.3
930	Wang et al. (2022)	Dextra Co., ltd (Dongguan, China)	GFRP	9.5	Vinylester	Alkaline solution 3 (IMMR)	40	45	NA	NA	5	101.0
931	Wang et al. (2022)	Dextra Co., ltd (Dongguan, China)	GFRP	9.5	Vinylester	Alkaline solution 3 (IMMR)	40	90	NA	NA	5	95.1
932	Wang et al. (2022)	Dextra Co., ltd (Dongguan, China)	GFRP	9.5	Vinylester	Alkaline solution 3 (IMMR)	40	180	NA	NA	5	98.6
933	Wang et al. (2022)	Dextra Co., ltd (Dongguan, China)	GFRP	9.5	Vinylester	Alkaline solution 3 (IMMR)	40	270	NA	NA	5	95.1
934	Wang et al. (2022)	Dextra Co., ltd (Dongguan, China)	GFRP	9.5	Vinylester	Alkaline solution 3 (IMMR)	40	360	NA	NA	5	96.9
935	Wang et al. (2022)	Dextra Co., ltd (Dongguan, China)	GFRP	9.5	Vinylester	Alkaline solution 3 (IMMR)	60	45	NA	NA	5	101.6
936	Wang et al. (2022)	Dextra Co., ltd (Dongguan, China)	GFRP	9.5	Vinylester	Alkaline solution 3 (IMMR)	60	90	NA	NA	5	99.8
937	Wang et al. (2022)	Dextra Co., ltd (Dongguan, China)	GFRP	9.5	Vinylester	Alkaline solution 3 (IMMR)	60	180	NA	NA	5	98.0
938	Wang et al. (2022)	Dextra Co., ltd (Dongguan, China)	GFRP	9.5	Vinylester	Alkaline solution 3 (IMMR)	60	270	NA	NA	5	96.9
939	Wang et al. (2022)	Dextra Co., ltd (Dongguan, China)	GFRP	9.5	Vinylester	Alkaline solution 3 (IMMR)	60	360	NA	NA	5	96.3
940	Won and Park (2006)	NA	CFRP	9.0	Vinylester	Control	NA	0	NA	NA	6	100.0
941	Won and Park (2006)	NA	CFRP	9.0	Vinylester	Alkaline solution (IMMR)	60	50	NA	NA	6	87.2
942	Won and Park (2006)	NA	CFRP	9.0	Vinylester	Acid solution (IMMR)	60	50	NA	NA	6	87.5
943	Won and Park (2006)	NA	CFRP	9.0	Vinylester	Saline solution 1 (IMMR)	60	50	NA	NA	6	88.3
944	Won and Park (2006)	NA	CFRP	9.0	Vinylester	Water (IMMR)	60	50	NA	NA	6	91.7
945	Won and Park (2006)	NA	CFRP	9.0	Vinylester	Water (WD)	23/60	50	NA	NA	6	89.4
946	Won and Park (2006)	NA	CFRP	9.0	Vinylester	HT	60	50	NA	NA	6	94.0
947	Won and Park	NA	CFRP	9.0	Vinylester	Water (FT)	-18/4	50	NA	NA	6	86.4

	(2006)												
948	Won and Park (2006)	NA		CFRP	9.0	Vinylester	Saline solution 2 (IMMR)	23	50	NA	NA	6	88.7
949	Won and Park (2006)	NA		CFRP	9.0	Vinylester	Saline solution 3 (IMMR)	23	50	NA	NA	6	87.2
950	Won and Park (2006)	NA		GFRP	9.0	Vinylester	Control	NA	0	NA	NA	6	100.0
951	Won and Park (2006)	NA		GFRP	9.0	Vinylester	Alkaline solution (IMMR)	60	50	NA	NA	6	60.4
952	Won and Park (2006)	NA		GFRP	9.0	Vinylester	Saline solution 1 (IMMR)	60	50	NA	NA	6	55.1
953	Won and Park (2006)	NA		GFRP	9.0	Vinylester	Acid solution (IMMR)	60	50	NA	NA	6	73.2
954	Won and Park (2006)	NA		GFRP	9.0	Vinylester	Water (IMMR)	60	50	NA	NA	6	72.1
955	Won and Park (2006)	NA		GFRP	9.0	Vinylester	Water (WD)	23/60	50	NA	NA	6	81.5
956	Won and Park (2006)	NA		GFRP	9.0	Vinylester	HT	60	50	NA	NA	6	83.4
957	Won and Park (2006)	NA		GFRP	9.0	Vinylester	Water (FT)	-18/4	50	NA	NA	6	75.8
958	Won and Park (2006)	NA		GFRP	9.0	Vinylester	Saline solution 2 (IMMR)	23	50	NA	NA	6	80.4
959	Won and Park (2006)	NA		GFRP	9.0	Vinylester	Saline solution 3 (IMMR)	23	50	NA	NA	6	81.9
960	Won et al. (2013)	Hughes Company NE, USA)	Brothers (Seward,	GFRP	6.0	Vinylester	Control	NA	0	NA	NA	NA	100.0
961	Won et al. (2013)	Hughes Company NE, USA)	Brothers (Seward,	GFRP	6.0	Vinylester	Saline solution 1 (IMMR)	60	50	NA	NA	NA	81.4
962	Won et al. (2013)	Hughes Company NE, USA)	Brothers (Seward,	GFRP	6.0	Vinylester	Saline solution 2 (IMMR)	20	50	NA	NA	NA	82.7
963	Won et al. (2013)	Hughes Company NE, USA)	Brothers (Seward,	GFRP	6.0	Vinylester	Saline solution 3 (IMMR)	20	50	NA	NA	NA	82.7
964	Won et al. (2013)	Hughes Company NE, USA)	Brothers (Seward,	GFRP	6.0	Vinylester	Saline solution 1 (WD)	20/60	50	NA	NA	NA	79.1
965	Won et al. (2013)	Hughes Company NE, USA)	Brothers (Seward,	GFRP	6.0	Vinylester	Saline solution 4 (FT)	-10/20	50	NA	NA	NA	67.6
966	Wu et al. (2014)	NA		BFRP	12.0	Vinylester	Control	NA	0	NA	NA	5	100.0
967	Wu et al.	NA		BFRP	12.0	Vinylester	Alkaline solution (IMMR)	55	21	NA	NA	5	87.3

	(2014)												
968	Wu et al. (2014)	NA	BFRP	12.0	Vinylester	Alkaline solution (IMMR)	55	42	NA	NA	5	86.7	
969	Wu et al. (2014)	NA	BFRP	12.0	Vinylester	Alkaline solution (IMMR)	55	63	NA	NA	5	85.0	
970	Xie et al. (2022)	NA	BFRP	6.0	Epoxy	Control	26	0	5	100.0	5	100.0	
971	Xie et al. (2022)	NA	BFRP	6.0	Epoxy	Alkaline solution (IMMR)	26	15	5	87.5	5	100.0	
972	Xie et al. (2022)	NA	BFRP	6.0	Epoxy	Alkaline solution (IMMR)	26	30	5	99.0	5	77.3	
973	Xie et al. (2022)	NA	BFRP	6.0	Epoxy	Alkaline solution (IMMR)	26	90	5	80.5	5	66.6	
974	Xie et al. (2022)	NA	BFRP	6.0	Epoxy	Alkaline solution (IMMR)	26	180	5	69.6	5	70.1	
975	Xie et al. (2022)	NA	BFRP	6.0	Epoxy	Alkaline solution (IMMR)	26	360	5	67.3	5	20.1	
976	Xie et al. (2022)	NA	BFRP	6.0	Epoxy	Alkaline solution (IMMR)	26	540	5	65.4	5	16.0	
977	Xie et al. (2022)	NA	BFRP	6.0	Epoxy	Alkaline solution (IMMR)	40	15	5	87.5	5	92.5	
978	Xie et al. (2022)	NA	BFRP	6.0	Epoxy	Alkaline solution (IMMR)	40	30	5	91.4	5	88.2	
979	Xie et al. (2022)	NA	BFRP	6.0	Epoxy	Alkaline solution (IMMR)	40	90	5	71.8	5	54.8	
980	Xie et al. (2022)	NA	BFRP	6.0	Epoxy	Alkaline solution (IMMR)	40	180	5	58.7	5	53.7	
981	Xie et al. (2022)	NA	BFRP	6.0	Epoxy	Alkaline solution (IMMR)	40	360	5	62.2	5	26.5	
982	Xie et al. (2022)	NA	BFRP	6.0	Epoxy	Alkaline solution (IMMR)	40	540	5	62.2	5	12.3	
983	Xie et al. (2022)	NA	BFRP	6.0	Epoxy	Alkaline solution (IMMR)	60	15	5	87.8	5	97.9	
984	Xie et al. (2022)	NA	BFRP	6.0	Epoxy	Alkaline solution (IMMR)	60	30	5	91.4	5	85.0	
985	Xie et al. (2022)	NA	BFRP	6.0	Epoxy	Alkaline solution (IMMR)	60	90	5	68.0	5	60.7	
986	Xie et al. (2022)	NA	BFRP	6.0	Epoxy	Alkaline solution (IMMR)	60	180	5	49.7	5	32.1	
987	Xie et al. (2022)	NA	BFRP	6.0	Epoxy	Alkaline solution (IMMR)	60	360	5	50.3	5	2.7	
988	Xie et al. (2022)	NA	BFRP	6.0	Epoxy	Alkaline solution (IMMR)	60	540	5	51.0	5	1.6	
989	Xie et al. (2022)	NA	BFRP	6.0	Epoxy	Artifical seawater (IMMR)	26	15	5	85.3	5	66.3	
990	Xie et al.	NA	BFRP	6.0	Epoxy	Artifical seawater (IMMR)	26	30	5	88.1	5	64.4	

	(2022)												
991	Xie et al. (2022)	NA	BFRP	6.0	Epoxy	Artifical seawater (IMMR)	26	90	5	86.5	5	96.0
992	Xie et al. (2022)	NA	BFRP	6.0	Epoxy	Artifical seawater (IMMR)	26	180	5	76.6	5	84.0
993	Xie et al. (2022)	NA	BFRP	6.0	Epoxy	Artifical seawater (IMMR)	26	360	5	88.1	5	77.0
994	Xie et al. (2022)	NA	BFRP	6.0	Epoxy	Artifical seawater (IMMR)	26	540	5	91.4	5	74.1
995	Xie et al. (2022)	NA	BFRP	6.0	Epoxy	Artifical seawater (IMMR)	40	15	5	83.0	5	98.4
996	Xie et al. (2022)	NA	BFRP	6.0	Epoxy	Artifical seawater (IMMR)	40	30	5	90.1	5	89.0
997	Xie et al. (2022)	NA	BFRP	6.0	Epoxy	Artifical seawater (IMMR)	40	90	5	95.8	5	88.0
998	Xie et al. (2022)	NA	BFRP	6.0	Epoxy	Artifical seawater (IMMR)	40	180	5	46.5	5	61.8
999	Xie et al. (2022)	NA	BFRP	6.0	Epoxy	Artifical seawater (IMMR)	40	360	5	68.0	5	50.8
1000	Xie et al. (2022)	NA	BFRP	6.0	Epoxy	Artifical seawater (IMMR)	40	540	5	68.9	5	32.6
1001	Xie et al. (2022)	NA	BFRP	6.0	Epoxy	Artifical seawater (IMMR)	60	15	5	77.6	5	100.0
1002	Xie et al. (2022)	NA	BFRP	6.0	Epoxy	Artifical seawater (IMMR)	60	30	5	83.7	5	90.4
1003	Xie et al. (2022)	NA	BFRP	6.0	Epoxy	Artifical seawater (IMMR)	60	90	5	74.4	5	64.4
1004	Xie et al. (2022)	NA	BFRP	6.0	Epoxy	Artifical seawater (IMMR)	60	180	5	62.5	5	43.1
1005	Xie et al. (2022)	NA	BFRP	6.0	Epoxy	Artifical seawater (IMMR)	60	360	5	53.2	5	15.0
1006	Xie et al. (2022)	NA	BFRP	6.0	Epoxy	Artifical seawater (IMMR)	60	540	5	55.1	5	5.6
1007	Xie et al. (2022)	NA	BFRP	6.0	Epoxy	Tap water (IMMR)	26	15	5	99.4	5	99.7
1008	Xie et al. (2022)	NA	BFRP	6.0	Epoxy	Tap water (IMMR)	26	30	5	91.4	5	85.3
1009	Xie et al. (2022)	NA	BFRP	6.0	Epoxy	Tap water (IMMR)	26	90	5	89.4	5	91.2
1010	Xie et al. (2022)	NA	BFRP	6.0	Epoxy	Tap water (IMMR)	26	180	5	79.5	5	95.2
1011	Xie et al. (2022)	NA	BFRP	6.0	Epoxy	Tap water (IMMR)	26	360	5	81.7	5	84.5
1012	Xie et al. (2022)	NA	BFRP	6.0	Epoxy	Tap water (IMMR)	26	540	5	93.3	5	78.6
1013	Xie et al.	NA	BFRP	6.0	Epoxy	Tap water (IMMR)	40	15	5	67.3	5	68.7

	(2022)												
1014	Xie et al. (2022)	NA	BFRP	6.0	Epoxy	Tap water (IMMR)	40	30	5	89.4	5	96.5
1015	Xie et al. (2022)	NA	BFRP	6.0	Epoxy	Tap water (IMMR)	40	90	5	76.0	5	94.4
1016	Xie et al. (2022)	NA	BFRP	6.0	Epoxy	Tap water (IMMR)	40	180	5	82.1	5	86.9
1017	Xie et al. (2022)	NA	BFRP	6.0	Epoxy	Tap water (IMMR)	40	360	5	84.6	5	76.7
1018	Xie et al. (2022)	NA	BFRP	6.0	Epoxy	Tap water (IMMR)	40	540	5	97.4	5	77.3
1019	Xie et al. (2022)	NA	BFRP	6.0	Epoxy	Tap water (IMMR)	60	15	5	92.3	5	97.9
1020	Xie et al. (2022)	NA	BFRP	6.0	Epoxy	Tap water (IMMR)	60	30	5	78.2	5	69.0
1021	Xie et al. (2022)	NA	BFRP	6.0	Epoxy	Tap water (IMMR)	60	90	5	81.1	5	82.1
1022	Xie et al. (2022)	NA	BFRP	6.0	Epoxy	Tap water (IMMR)	60	180	5	72.8	5	54.8
1023	Xie et al. (2022)	NA	BFRP	6.0	Epoxy	Tap water (IMMR)	60	360	5	78.9	5	43.1
1024	Xie et al. (2022)	NA	BFRP	6.0	Epoxy	Tap water (IMMR)	60	540	5	68.3	5	33.4
1025	Xie et al. (2022)	NA	BFRP	6.0	Epoxy	SWSSCE 1+Alkaline solution (IMMR)	26	15	5	85.3	5	73.8
1026	Xie et al. (2022)	NA	BFRP	6.0	Epoxy	SWSSCE 1+Alkaline solution (IMMR)	26	30	5	80.5	5	71.7
1027	Xie et al. (2022)	NA	BFRP	6.0	Epoxy	SWSSCE 1+Alkaline solution (IMMR)	26	90	5	70.5	5	57.5
1028	Xie et al. (2022)	NA	BFRP	6.0	Epoxy	SWSSCE 1+Alkaline solution (IMMR)	26	180	5	53.2	5	47.9
1029	Xie et al. (2022)	NA	BFRP	6.0	Epoxy	SWSSCE 1+Alkaline solution (IMMR)	26	360	5	70.8	5	24.1
1030	Xie et al. (2022)	NA	BFRP	6.0	Epoxy	SWSSCE 1+Alkaline solution (IMMR)	26	540	5	60.6	5	23.3
1031	Xie et al. (2022)	NA	BFRP	6.0	Epoxy	SWSSCE 1+Alkaline solution (IMMR)	40	15	5	90.7	5	79.4
1032	Xie et al. (2022)	NA	BFRP	6.0	Epoxy	SWSSCE 1+Alkaline solution (IMMR)	40	30	5	94.6	5	71.9
1033	Xie et al. (2022)	NA	BFRP	6.0	Epoxy	SWSSCE 1+Alkaline solution (IMMR)	40	90	5	85.6	5	55.1
1034	Xie et al. (2022)	NA	BFRP	6.0	Epoxy	SWSSCE 1+Alkaline solution (IMMR)	40	180	5	54.5	5	46.3
1035	Xie et al. (2022)	NA	BFRP	6.0	Epoxy	SWSSCE 1+Alkaline solution (IMMR)	40	360	5	55.5	5	11.5
1036	Xie et al.	NA	BFRP	6.0	Epoxy	SWSSCE 1+Alkaline solution	40	540	5	55.8	5	5.4

	(2022)						(IMMR)						
1037	Xie et al. (2022)	NA	BFRP	6.0	Epoxy	SWSSCE (IMMR)	1+Alkaline solution	60	15	5	79.2	5	84.5
1038	Xie et al. (2022)	NA	BFRP	6.0	Epoxy	SWSSCE (IMMR)	1+Alkaline solution	60	30	5	82.4	5	69.0
1039	Xie et al. (2022)	NA	BFRP	6.0	Epoxy	SWSSCE (IMMR)	1+Alkaline solution	60	90	5	63.5	5	42.3
1040	Xie et al. (2022)	NA	BFRP	6.0	Epoxy	SWSSCE (IMMR)	1+Alkaline solution	60	180	5	42.0	5	16.0
1041	Xie et al. (2022)	NA	BFRP	6.0	Epoxy	SWSSCE (IMMR)	1+Alkaline solution	60	360	5	53.5	5	0.8
1042	Xie et al. (2022)	NA	BFRP	6.0	Epoxy	SWSSCE (IMMR)	1+Alkaline solution	60	540	5	37.8	5	1.1
1043	Xie et al. (2022)	NA	BFRP	6.0	Epoxy	SWSSCE (IMMR)	1+Artifical seawater	26	15	5	97.4	5	88.5
1044	Xie et al. (2022)	NA	BFRP	6.0	Epoxy	SWSSCE (IMMR)	1+Artifical seawater	26	30	5	90.4	5	86.6
1045	Xie et al. (2022)	NA	BFRP	6.0	Epoxy	SWSSCE (IMMR)	1+Artifical seawater	26	90	5	76.3	5	77.3
1046	Xie et al. (2022)	NA	BFRP	6.0	Epoxy	SWSSCE (IMMR)	1+Artifical seawater	26	180	5	64.7	5	68.5
1047	Xie et al. (2022)	NA	BFRP	6.0	Epoxy	SWSSCE (IMMR)	1+Artifical seawater	26	360	5	70.2	5	58.0
1048	Xie et al. (2022)	NA	BFRP	6.0	Epoxy	SWSSCE (IMMR)	1+Artifical seawater	26	540	5	83.3	5	49.2
1049	Xie et al. (2022)	NA	BFRP	6.0	Epoxy	SWSSCE (IMMR)	1+Artifical seawater	40	15	5	84.9	5	83.2
1050	Xie et al. (2022)	NA	BFRP	6.0	Epoxy	SWSSCE (IMMR)	1+Artifical seawater	40	30	5	77.6	5	82.6
1051	Xie et al. (2022)	NA	BFRP	6.0	Epoxy	SWSSCE (IMMR)	1+Artifical seawater	40	90	5	83.3	5	80.8
1052	Xie et al. (2022)	NA	BFRP	6.0	Epoxy	SWSSCE (IMMR)	1+Artifical seawater	40	180	5	71.2	5	67.7
1053	Xie et al. (2022)	NA	BFRP	6.0	Epoxy	SWSSCE (IMMR)	1+Artifical seawater	40	360	5	68.9	5	46.0
1054	Xie et al. (2022)	NA	BFRP	6.0	Epoxy	SWSSCE (IMMR)	1+Artifical seawater	40	540	5	74.0	5	42.0
1055	Xie et al. (2022)	NA	BFRP	6.0	Epoxy	SWSSCE (IMMR)	1+Artifical seawater	60	15	5	90.1	5	86.4
1056	Xie et al. (2022)	NA	BFRP	6.0	Epoxy	SWSSCE (IMMR)	1+Artifical seawater	60	30	5	93.3	5	86.1
1057	Xie et al. (2022)	NA	BFRP	6.0	Epoxy	SWSSCE (IMMR)	1+Artifical seawater	60	90	5	77.2	5	65.0
1058	Xie et al. (2022)	NA	BFRP	6.0	Epoxy	SWSSCE (IMMR)	1+Artifical seawater	60	180	5	54.8	5	55.9
1059	Xie et al.	NA	BFRP	6.0	Epoxy	SWSSCE	1+Artifical seawater	60	360	5	57.4	5	20.3

	(2022)						(IMMR)						
1060	Xie et al. (2022)	NA	BFRP	6.0	Epoxy	SWSSCE (IMMR)	1+Artifical seawater	60	540	5	62.2	5	16.3
1061	Xie et al. (2022)	NA	BFRP	6.0	Epoxy	SWSSCE (IMMR)	1+Distilled water	26	15	5	96.2	5	81.6
1062	Xie et al. (2022)	NA	BFRP	6.0	Epoxy	SWSSCE (IMMR)	1+Distilled water	26	30	5	83.0	5	77.0
1063	Xie et al. (2022)	NA	BFRP	6.0	Epoxy	SWSSCE (IMMR)	1+Distilled water	26	90	5	91.7	5	68.2
1064	Xie et al. (2022)	NA	BFRP	6.0	Epoxy	SWSSCE (IMMR)	1+Distilled water	26	180	5	78.5	5	62.3
1065	Xie et al. (2022)	NA	BFRP	6.0	Epoxy	SWSSCE (IMMR)	1+Distilled water	26	360	5	61.5	5	50.0
1066	Xie et al. (2022)	NA	BFRP	6.0	Epoxy	SWSSCE (IMMR)	1+Distilled water	26	540	5	81.4	5	52.4
1067	Xie et al. (2022)	NA	BFRP	6.0	Epoxy	SWSSCE (IMMR)	1+Distilled water	40	15	5	92.3	5	71.7
1068	Xie et al. (2022)	NA	BFRP	6.0	Epoxy	SWSSCE (IMMR)	1+Distilled water	40	30	5	99.0	5	74.9
1069	Xie et al. (2022)	NA	BFRP	6.0	Epoxy	SWSSCE (IMMR)	1+Distilled water	40	90	5	87.8	5	73.5
1070	Xie et al. (2022)	NA	BFRP	6.0	Epoxy	SWSSCE (IMMR)	1+Distilled water	40	180	5	57.1	5	63.9
1071	Xie et al. (2022)	NA	BFRP	6.0	Epoxy	SWSSCE (IMMR)	1+Distilled water	40	360	5	71.8	5	46.5
1072	Xie et al. (2022)	NA	BFRP	6.0	Epoxy	SWSSCE (IMMR)	1+Distilled water	40	540	5	67.6	5	50.0
1073	Xie et al. (2022)	NA	BFRP	6.0	Epoxy	SWSSCE (IMMR)	1+Distilled water	60	15	5	81.1	5	75.4
1074	Xie et al. (2022)	NA	BFRP	6.0	Epoxy	SWSSCE (IMMR)	1+Distilled water	60	30	5	93.6	5	73.3
1075	Xie et al. (2022)	NA	BFRP	6.0	Epoxy	SWSSCE (IMMR)	1+Distilled water	60	90	5	54.2	5	57.8
1076	Xie et al. (2022)	NA	BFRP	6.0	Epoxy	SWSSCE (IMMR)	1+Distilled water	60	180	5	57.4	5	56.4
1077	Xie et al. (2022)	NA	BFRP	6.0	Epoxy	SWSSCE (IMMR)	1+Distilled water	60	360	5	61.2	5	30.5
1078	Xie et al. (2022)	NA	BFRP	6.0	Epoxy	SWSSCE (IMMR)	1+Distilled water	60	540	5	62.2	5	23.8
1079	Xie et al. (2022)	NA	BFRP	6.0	Epoxy	SWSSCE (IMMR)	2+Alkaline solution	26	15	5	87.8	5	58.6
1080	Xie et al. (2022)	NA	BFRP	6.0	Epoxy	SWSSCE (IMMR)	2+Alkaline solution	26	30	5	88.5	5	60.2
1081	Xie et al. (2022)	NA	BFRP	6.0	Epoxy	SWSSCE (IMMR)	2+Alkaline solution	26	90	5	75.3	5	54.0
1082	Xie et al.	NA	BFRP	6.0	Epoxy	SWSSCE	2+Alkaline solution	26	180	5	52.6	5	30.2

	(2022)						(IMMR)						
1083	Xie et al. (2022)	NA	BFRP	6.0	Epoxy	SWSSCE (IMMR)	2+Alkaline solution	26	360	5	52.2	5	14.2
1084	Xie et al. (2022)	NA	BFRP	6.0	Epoxy	SWSSCE (IMMR)	2+Alkaline solution	26	540	5	57.4	5	4.3
1085	Xie et al. (2022)	NA	BFRP	6.0	Epoxy	SWSSCE (IMMR)	2+Alkaline solution	40	15	5	72.4	5	75.9
1086	Xie et al. (2022)	NA	BFRP	6.0	Epoxy	SWSSCE (IMMR)	2+Alkaline solution	40	30	5	82.1	5	61.2
1087	Xie et al. (2022)	NA	BFRP	6.0	Epoxy	SWSSCE (IMMR)	2+Alkaline solution	40	90	5	68.0	5	44.9
1088	Xie et al. (2022)	NA	BFRP	6.0	Epoxy	SWSSCE (IMMR)	2+Alkaline solution	40	180	5	44.2	5	18.5
1089	Xie et al. (2022)	NA	BFRP	6.0	Epoxy	SWSSCE (IMMR)	2+Alkaline solution	40	360	5	37.2	5	4.0
1090	Xie et al. (2022)	NA	BFRP	6.0	Epoxy	SWSSCE (IMMR)	2+Alkaline solution	40	540	5	53.2	5	2.1
1091	Xie et al. (2022)	NA	BFRP	6.0	Epoxy	SWSSCE (IMMR)	2+Alkaline solution	60	15	5	84.9	5	57.5
1092	Xie et al. (2022)	NA	BFRP	6.0	Epoxy	SWSSCE (IMMR)	2+Alkaline solution	60	30	5	73.1	5	50.8
1093	Xie et al. (2022)	NA	BFRP	6.0	Epoxy	SWSSCE (IMMR)	2+Alkaline solution	60	90	5	53.5	5	23.5
1094	Xie et al. (2022)	NA	BFRP	6.0	Epoxy	SWSSCE (IMMR)	2+Alkaline solution	60	180	5	37.5	5	2.4
1095	Xie et al. (2022)	NA	BFRP	6.0	Epoxy	SWSSCE (IMMR)	2+Alkaline solution	60	360	5	34.9	5	0.8
1096	Xie et al. (2022)	NA	BFRP	6.0	Epoxy	SWSSCE (IMMR)	2+Alkaline solution	60	540	5	35.3	5	0.8
1097	Xie et al. (2022)	NA	BFRP	6.0	Epoxy	SWSSCE (IMMR)	2+Artifical seawater	26	15	5	85.9	5	58.8
1098	Xie et al. (2022)	NA	BFRP	6.0	Epoxy	SWSSCE (IMMR)	2+Artifical seawater	26	30	5	78.5	5	60.4
1099	Xie et al. (2022)	NA	BFRP	6.0	Epoxy	SWSSCE (IMMR)	2+Artifical seawater	26	90	5	71.2	5	58.8
1100	Xie et al. (2022)	NA	BFRP	6.0	Epoxy	SWSSCE (IMMR)	2+Artifical seawater	26	180	5	57.7	5	39.0
1101	Xie et al. (2022)	NA	BFRP	6.0	Epoxy	SWSSCE (IMMR)	2+Artifical seawater	26	360	5	65.7	5	38.5
1102	Xie et al. (2022)	NA	BFRP	6.0	Epoxy	SWSSCE (IMMR)	2+Artifical seawater	26	540	5	67.0	5	39.6
1103	Xie et al. (2022)	NA	BFRP	6.0	Epoxy	SWSSCE (IMMR)	2+Artifical seawater	40	15	5	91.4	5	74.1
1104	Xie et al. (2022)	NA	BFRP	6.0	Epoxy	SWSSCE (IMMR)	2+Artifical seawater	40	30	5	90.7	5	64.7
1105	Xie et al.	NA	BFRP	6.0	Epoxy	SWSSCE	2+Artifical seawater	40	90	5	86.9	5	50.3

	(2022)						(IMMR)						
1106	Xie et al. (2022)	NA	BFRP	6.0	Epoxy	SWSSCE (IMMR)	2+Artifical seawater	40	180	5	53.9	5	32.9
1107	Xie et al. (2022)	NA	BFRP	6.0	Epoxy	SWSSCE (IMMR)	2+Artifical seawater	40	360	5	59.0	5	12.3
1108	Xie et al. (2022)	NA	BFRP	6.0	Epoxy	SWSSCE (IMMR)	2+Artifical seawater	40	540	5	60.9	5	12.6
1109	Xie et al. (2022)	NA	BFRP	6.0	Epoxy	SWSSCE (IMMR)	2+Artifical seawater	60	15	5	80.8	5	60.7
1110	Xie et al. (2022)	NA	BFRP	6.0	Epoxy	SWSSCE (IMMR)	2+Artifical seawater	60	30	5	76.0	5	57.0
1111	Xie et al. (2022)	NA	BFRP	6.0	Epoxy	SWSSCE (IMMR)	2+Artifical seawater	60	90	5	70.2	5	35.3
1112	Xie et al. (2022)	NA	BFRP	6.0	Epoxy	SWSSCE (IMMR)	2+Artifical seawater	60	180	5	48.4	5	23.5
1113	Xie et al. (2022)	NA	BFRP	6.0	Epoxy	SWSSCE (IMMR)	2+Artifical seawater	60	360	5	46.8	5	5.4
1114	Xie et al. (2022)	NA	BFRP	6.0	Epoxy	SWSSCE (IMMR)	2+Artifical seawater	60	540	5	47.8	5	1.9
1115	Xie et al. (2022)	NA	BFRP	6.0	Epoxy	SWSSCE (IMMR)	2+Distilled water	26	15	5	104.8	5	60.2
1116	Xie et al. (2022)	NA	BFRP	6.0	Epoxy	SWSSCE (IMMR)	2+Distilled water	26	30	5	89.4	5	59.9
1117	Xie et al. (2022)	NA	BFRP	6.0	Epoxy	SWSSCE (IMMR)	2+Distilled water	26	90	5	95.2	5	57.8
1118	Xie et al. (2022)	NA	BFRP	6.0	Epoxy	SWSSCE (IMMR)	2+Distilled water	26	180	5	57.1	5	29.1
1119	Xie et al. (2022)	NA	BFRP	6.0	Epoxy	SWSSCE (IMMR)	2+Distilled water	26	360	5	58.7	5	31.0
1120	Xie et al. (2022)	NA	BFRP	6.0	Epoxy	SWSSCE (IMMR)	2+Distilled water	26	540	5	55.8	5	15.5
1121	Xie et al. (2022)	NA	BFRP	6.0	Epoxy	SWSSCE (IMMR)	2+Distilled water	40	15	5	89.4	5	70.6
1122	Xie et al. (2022)	NA	BFRP	6.0	Epoxy	SWSSCE (IMMR)	2+Distilled water	40	30	5	88.8	5	64.4
1123	Xie et al. (2022)	NA	BFRP	6.0	Epoxy	SWSSCE (IMMR)	2+Distilled water	40	90	5	58.0	5	49.2
1124	Xie et al. (2022)	NA	BFRP	6.0	Epoxy	SWSSCE (IMMR)	2+Distilled water	40	180	5	48.7	5	24.6
1125	Xie et al. (2022)	NA	BFRP	6.0	Epoxy	SWSSCE (IMMR)	2+Distilled water	40	360	5	54.2	5	6.2
1126	Xie et al. (2022)	NA	BFRP	6.0	Epoxy	SWSSCE (IMMR)	2+Distilled water	40	540	5	54.5	5	7.5
1127	Xie et al. (2022)	NA	BFRP	6.0	Epoxy	SWSSCE (IMMR)	2+Distilled water	60	15	5	76.6	5	54.3
1128	Xie et al.	NA	BFRP	6.0	Epoxy	SWSSCE	2+Distilled water	60	30	5	90.4	5	52.9

	(2022)						(IMMR)						
1129	Xie et al. (2022)	NA	BFRP	6.0	Epoxy	SWSSCE 2+Distilled water (IMMR)	60	90	5	74.7	5	23.8	
1130	Xie et al. (2022)	NA	BFRP	6.0	Epoxy	SWSSCE 2+Distilled water (IMMR)	60	180	5	45.2	5	17.7	
1131	Xie et al. (2022)	NA	BFRP	6.0	Epoxy	SWSSCE 2+Distilled water (IMMR)	60	360	5	45.8	5	11.0	
1132	Xie et al. (2022)	NA	BFRP	6.0	Epoxy	SWSSCE 2+Distilled water (IMMR)	60	540	5	46.8	5	5.1	
1133	Xie et al. (2022)	NA	BFRP	6.0	Epoxy	Alkaline solution (IMMR)	26	540	NA	NA	5	15.8	
1134	Xie et al. (2022)	NA	BFRP	6.0	Epoxy	Alkaline solution (IMMR)	40	540	NA	NA	5	10.7	
1135	Xie et al. (2022)	NA	BFRP	6.0	Epoxy	Alkaline solution (IMMR)	60	540	NA	NA	5	1.3	
1136	Xie et al. (2022)	NA	BFRP	6.0	Epoxy	Artifical seawater (IMMR)	26	540	NA	NA	5	75.7	
1137	Xie et al. (2022)	NA	BFRP	6.0	Epoxy	Artifical seawater (IMMR)	40	540	NA	NA	5	30.0	
1138	Xie et al. (2022)	NA	BFRP	6.0	Epoxy	Artifical seawater (IMMR)	60	540	NA	NA	5	4.8	
1139	Xie et al. (2022)	NA	BFRP	6.0	Epoxy	Tap water (IMMR)	26	540	NA	NA	5	80.8	
1140	Xie et al. (2022)	NA	BFRP	6.0	Epoxy	Tap water (IMMR)	40	540	NA	NA	5	78.1	
1141	Xie et al. (2022)	NA	BFRP	6.0	Epoxy	Tap water (IMMR)	60	540	NA	NA	5	35.0	
1142	Xie et al. (2022)	NA	BFRP	6.0	Epoxy	NCE 1+Alkaline solution (IMMR)	26	540	NA	NA	5	48.9	
1143	Xie et al. (2022)	NA	BFRP	6.0	Epoxy	NCE 1+Alkaline solution (IMMR)	40	540	NA	NA	5	37.2	
1144	Xie et al. (2022)	NA	BFRP	6.0	Epoxy	NCE 1+Alkaline solution (IMMR)	60	540	NA	NA	5	2.4	
1145	Xie et al. (2022)	NA	BFRP	6.0	Epoxy	NCE 1+Artifical seawater (IMMR)	26	540	NA	NA	5	61.5	
1146	Xie et al. (2022)	NA	BFRP	6.0	Epoxy	NCE 1+Artifical seawater (IMMR)	40	540	NA	NA	5	51.9	
1147	Xie et al. (2022)	NA	BFRP	6.0	Epoxy	NCE 1+Artifical seawater (IMMR)	60	540	NA	NA	5	34.0	
1148	Xie et al. (2022)	NA	BFRP	6.0	Epoxy	NCE 1+Distilled water (IMMR)	26	540	NA	NA	5	68.2	
1149	Xie et al. (2022)	NA	BFRP	6.0	Epoxy	NCE 1+Distilled water (IMMR)	40	540	NA	NA	5	61.2	
1150	Xie et al. (2022)	NA	BFRP	6.0	Epoxy	NCE 1+Distilled water (IMMR)	60	540	NA	NA	5	46.5	
1151	Xie et al.	NA	BFRP	6.0	Epoxy	NCE 2+Alkaline solution	26	540	NA	NA	5	30.8	

	(2022)					(IMMR)						
1152	Xie et al. (2022)	NA	BFRP	6.0	Epoxy	NCE 2+Alkaline solution (IMMR)	40	540	NA	NA	5	27.3
1153	Xie et al. (2022)	NA	BFRP	6.0	Epoxy	NCE 2+Alkaline solution (IMMR)	60	540	NA	NA	5	2.9
1154	Xie et al. (2022)	NA	BFRP	6.0	Epoxy	NCE 2+Artifical seawater (IMMR)	26	540	NA	NA	5	45.7
1155	Xie et al. (2022)	NA	BFRP	6.0	Epoxy	NCE 2+Artifical seawater (IMMR)	40	540	NA	NA	5	53.2
1156	Xie et al. (2022)	NA	BFRP	6.0	Epoxy	NCE 2+Artifical seawater (IMMR)	60	540	NA	NA	5	29.1
1157	Xie et al. (2022)	NA	BFRP	6.0	Epoxy	NCE 2+Distilled water (IMMR)	26	540	NA	NA	5	50.8
1158	Xie et al. (2022)	NA	BFRP	6.0	Epoxy	NCE 2+Distilled water (IMMR)	40	540	NA	NA	5	51.3
1159	Xie et al. (2022)	NA	BFRP	6.0	Epoxy	NCE 2+Distilled water (IMMR)	60	540	NA	NA	5	46.3
1160	Yi et al. (2021)	Jiangsu Green Materials Vally New Material T&D Co., Ltd (Nanjing, China)	BFRP	8.0	Epoxy	Control	25	0	4	100.0	5	100.0
1161	Yi et al. (2021)	Jiangsu Green Materials Vally New Material T&D Co., Ltd (Nanjing, China)	BFRP	8.0	Epoxy	SWSSC solution 1 (IMMR)	25	30	4	95.2	5	85.4
1162	Yi et al. (2021)	Jiangsu Green Materials Vally New Material T&D Co., Ltd (Nanjing, China)	BFRP	8.0	Epoxy	SWSSC solution 1 (IMMR)	25	60	4	95.6	5	90.0
1163	Yi et al. (2021)	Jiangsu Green Materials Vally New Material T&D Co., Ltd (Nanjing, China)	BFRP	8.0	Epoxy	SWSSC solution 1 (IMMR)	25	90	4	94.0	5	86.2
1164	Yi et al. (2021)	Jiangsu Green Materials Vally New Material T&D Co., Ltd (Nanjing, China)	BFRP	8.0	Epoxy	SWSSC solution 1 (IMMR)	40	30	4	76.8	5	86.8
1165	Yi et al. (2021)	Jiangsu Green Materials Vally New Material T&D Co., Ltd (Nanjing, China)	BFRP	8.0	Epoxy	SWSSC solution 1 (IMMR)	40	60	4	82.4	5	81.8
1166	Yi et al. (2021)	Jiangsu Green Materials Vally New Material T&D Co., Ltd (Nanjing, China)	BFRP	8.0	Epoxy	SWSSC solution 1 (IMMR)	40	90	4	79.2	5	76.4
1167	Yi et al. (2021)	Jiangsu Green	BFRP	8.0	Epoxy	SWSSC solution 1 (IMMR)	55	30	4	85.1	5	76.3

		Materials Vally New Material T&D Co., Ltd (Nanjing, China)										
1168	Yi et al. (2021)	Jiangsu Green Materials Vally New Material T&D Co., Ltd (Nanjing, China)	BFRP	8.0	Epoxy	SWSSC solution 1 (IMMR)	55	60	4	84.3	5	57.5
1169	Yi et al. (2021)	Jiangsu Green Materials Vally New Material T&D Co., Ltd (Nanjing, China)	BFRP	8.0	Epoxy	SWSSC solution 1 (IMMR)	55	90	4	69.9	5	42.2
1170	Yi et al. (2021)	Jiangsu Green Materials Vally New Material T&D Co., Ltd (Nanjing, China)	BFRP	8.0	Epoxy	SWSSC solution 2 (IMMR)	25	30	4	103.2	5	90.8
1171	Yi et al. (2021)	Jiangsu Green Materials Vally New Material T&D Co., Ltd (Nanjing, China)	BFRP	8.0	Epoxy	SWSSC solution 2 (IMMR)	25	60	4	104.0	5	91.5
1172	Yi et al. (2021)	Jiangsu Green Materials Vally New Material T&D Co., Ltd (Nanjing, China)	BFRP	8.0	Epoxy	SWSSC solution 2 (IMMR)	25	90	4	96.8	5	93.5
1173	Yi et al. (2021)	Jiangsu Green Materials Vally New Material T&D Co., Ltd (Nanjing, China)	BFRP	8.0	Epoxy	SWSSC solution 2 (IMMR)	40	30	4	86.8	5	88.8
1174	Yi et al. (2021)	Jiangsu Green Materials Vally New Material T&D Co., Ltd (Nanjing, China)	BFRP	8.0	Epoxy	SWSSC solution 2 (IMMR)	40	60	4	88.4	5	89.2
1175	Yi et al. (2021)	Jiangsu Green Materials Vally New Material T&D Co., Ltd (Nanjing, China)	BFRP	8.0	Epoxy	SWSSC solution 2 (IMMR)	40	90	4	84.0	5	95.0
1176	Yi et al. (2021)	Jiangsu Green Materials Vally New Material T&D Co., Ltd (Nanjing, China)	BFRP	8.0	Epoxy	SWSSC solution 2 (IMMR)	55	30	4	89.6	5	91.2
1177	Yi et al. (2021)	Jiangsu Green Materials Vally New Material T&D Co., Ltd (Nanjing, China)	BFRP	8.0	Epoxy	SWSSC solution 2 (IMMR)	55	60	4	79.9	5	92.4
1178	Yi et al. (2021)	Jiangsu Green Materials Vally New Material T&D Co.,	BFRP	8.0	Epoxy	SWSSC solution 2 (IMMR)	55	90	4	71.9	5	85.5

		Ltd (Nanjing, China)										
1179	Yi et al. (2021)	Jiangsu Green Materials Vally New Material T&D Co., Ltd (Nanjing, China)	BFRP	8.0	Epoxy	SWSSC solution 3 (IMMR)	25	30	4	103.6	5	86.5
1180	Yi et al. (2021)	Jiangsu Green Materials Vally New Material T&D Co., Ltd (Nanjing, China)	BFRP	8.0	Epoxy	SWSSC solution 3 (IMMR)	25	60	4	102.0	5	86.9
1181	Yi et al. (2021)	Jiangsu Green Materials Vally New Material T&D Co., Ltd (Nanjing, China)	BFRP	8.0	Epoxy	SWSSC solution 3 (IMMR)	25	90	4	96.0	5	90.4
1182	Yi et al. (2021)	Jiangsu Green Materials Vally New Material T&D Co., Ltd (Nanjing, China)	BFRP	8.0	Epoxy	SWSSC solution 3 (IMMR)	40	30	4	93.6	5	86.5
1183	Yi et al. (2021)	Jiangsu Green Materials Vally New Material T&D Co., Ltd (Nanjing, China)	BFRP	8.0	Epoxy	SWSSC solution 3 (IMMR)	40	60	4	88.0	5	95.3
1184	Yi et al. (2021)	Jiangsu Green Materials Vally New Material T&D Co., Ltd (Nanjing, China)	BFRP	8.0	Epoxy	SWSSC solution 3 (IMMR)	40	90	4	81.6	5	90.3
1185	Yi et al. (2021)	Jiangsu Green Materials Vally New Material T&D Co., Ltd (Nanjing, China)	BFRP	8.0	Epoxy	SWSSC solution 3 (IMMR)	55	30	4	90.0	5	92.0
1186	Yi et al. (2021)	Jiangsu Green Materials Vally New Material T&D Co., Ltd (Nanjing, China)	BFRP	8.0	Epoxy	SWSSC solution 3 (IMMR)	55	60	4	81.1	5	89.7
1187	Yi et al. (2021)	Jiangsu Green Materials Vally New Material T&D Co., Ltd (Nanjing, China)	BFRP	8.0	Epoxy	SWSSC solution 3 (IMMR)	55	90	4	75.9	5	89.3
1188	Yi et al. (2022b)	Green Material Valley (GMV) New Material Technology Co., Ltd. (Zhenjiang, China)	BFRP	8.0	Epoxy	Control	25	0	NA	NA	4	100.0
1189	Yi et al. (2022b)	Green Material Valley (GMV) New Material Technology Co., Ltd. (Zhenjiang, China)	BFRP	8.0	Epoxy	SWSSC solution 1 (IMMR)	25	180	NA	NA	4	83.3
1190	Yi et al.	Green Material Valley	BFRP	8.0	Epoxy	SWSSC solution 1 (IMMR)	40	180	NA	NA	4	66.9

	(2022b)	(GMV) New Material Technology Co., Ltd. (Zhenjiang, China)										
1191	Yi et al. (2022b)	Green Material Valley (GMV) New Material Technology Co., Ltd. (Zhenjiang, China)	BFRP	8.0	Epoxy	SWSSC solution 1 (IMMR)	55	180	NA	NA	4	17.3
1192	Yi et al. (2022b)	Green Material Valley (GMV) New Material Technology Co., Ltd. (Zhenjiang, China)	BFRP	8.0	Epoxy	SWSSC solution 2 (IMMR)	25	180	NA	NA	4	84.7
1193	Yi et al. (2022b)	Green Material Valley (GMV) New Material Technology Co., Ltd. (Zhenjiang, China)	BFRP	8.0	Epoxy	SWSSC solution 2 (IMMR)	40	180	NA	NA	4	78.5
1194	Yi et al. (2022b)	Green Material Valley (GMV) New Material Technology Co., Ltd. (Zhenjiang, China)	BFRP	8.0	Epoxy	SWSSC solution 2 (IMMR)	55	180	NA	NA	4	76.5
1195	Yi et al. (2022b)	Green Material Valley (GMV) New Material Technology Co., Ltd. (Zhenjiang, China)	BFRP	8.0	Epoxy	SWSSC solution 3 (IMMR)	25	180	NA	NA	4	88.1
1196	Yi et al. (2022b)	Green Material Valley (GMV) New Material Technology Co., Ltd. (Zhenjiang, China)	BFRP	8.0	Epoxy	SWSSC solution 3 (IMMR)	40	180	NA	NA	4	84.4
1197	Yi et al. (2022b)	Green Material Valley (GMV) New Material Technology Co., Ltd. (Zhenjiang, China)	BFRP	8.0	Epoxy	SWSSC solution 3 (IMMR)	55	180	NA	NA	4	76.8
1198	Yi et al. (2022b)	Green Material Valley (GMV) New Material Technology Co., Ltd. (Zhenjiang, China)	BFRP	8.0	Epoxy	SWSSCE 1+Simulated seawater (IMMR)	25	90	NA	NA	4	89.5
1199	Yi et al. (2022b)	Green Material Valley (GMV) New Material Technology Co., Ltd. (Zhenjiang, China)	BFRP	8.0	Epoxy	SWSSCE 1+Simulated seawater (IMMR)	25	180	NA	NA	4	80.3
1200	Yi et al. (2022b)	Green Material Valley (GMV) New Material Technology Co., Ltd. (Zhenjiang, China)	BFRP	8.0	Epoxy	SWSSCE 1+Simulated seawater (IMMR)	25	240	NA	NA	4	81.3
1201	Yi et al. (2022b)	Green Material Valley (GMV) New Material Technology Co., Ltd.	BFRP	8.0	Epoxy	SWSSCE 1+Simulated seawater (IMMR)	40	90	NA	NA	4	77.5

			(Zhenjiang, China)										
1202	Yi et al. (2022b)		Green Material Valley (GMV) New Material Technology Co., Ltd. (Zhenjiang, China)	BFRP	8.0	Epoxy	SWSSCE seawater (IMMR)	1+Simulated	40	180	NA	NA	4	70.9
1203	Yi et al. (2022b)		Green Material Valley (GMV) New Material Technology Co., Ltd. (Zhenjiang, China)	BFRP	8.0	Epoxy	SWSSCE seawater (IMMR)	1+Simulated	40	240	NA	NA	4	63.1
1204	Yi et al. (2022b)		Green Material Valley (GMV) New Material Technology Co., Ltd. (Zhenjiang, China)	BFRP	8.0	Epoxy	SWSSCE seawater (IMMR)	1+Simulated	55	90	NA	NA	4	68.4
1205	Yi et al. (2022b)		Green Material Valley (GMV) New Material Technology Co., Ltd. (Zhenjiang, China)	BFRP	8.0	Epoxy	SWSSCE seawater (IMMR)	1+Simulated	55	180	NA	NA	4	53.0
1206	Yi et al. (2022b)		Green Material Valley (GMV) New Material Technology Co., Ltd. (Zhenjiang, China)	BFRP	8.0	Epoxy	SWSSCE seawater (IMMR)	1+Simulated	55	240	NA	NA	4	42.0
1207	Yi et al. (2022b)		Green Material Valley (GMV) New Material Technology Co., Ltd. (Zhenjiang, China)	BFRP	8.0	Epoxy	SWSSCE seawater (IMMR)	2+Simulated	25	90	NA	NA	4	87.9
1208	Yi et al. (2022b)		Green Material Valley (GMV) New Material Technology Co., Ltd. (Zhenjiang, China)	BFRP	8.0	Epoxy	SWSSCE seawater (IMMR)	2+Simulated	25	180	NA	NA	4	92.8
1209	Yi et al. (2022b)		Green Material Valley (GMV) New Material Technology Co., Ltd. (Zhenjiang, China)	BFRP	8.0	Epoxy	SWSSCE seawater (IMMR)	2+Simulated	25	240	NA	NA	4	86.1
1210	Yi et al. (2022b)		Green Material Valley (GMV) New Material Technology Co., Ltd. (Zhenjiang, China)	BFRP	8.0	Epoxy	SWSSCE seawater (IMMR)	2+Simulated	40	90	NA	NA	4	80.3
1211	Yi et al. (2022b)		Green Material Valley (GMV) New Material Technology Co., Ltd. (Zhenjiang, China)	BFRP	8.0	Epoxy	SWSSCE seawater (IMMR)	2+Simulated	40	180	NA	NA	4	77.8
1212	Yi et al. (2022b)		Green Material Valley (GMV) New Material Technology Co., Ltd. (Zhenjiang, China)	BFRP	8.0	Epoxy	SWSSCE seawater (IMMR)	2+Simulated	40	240	NA	NA	4	87.8
1213	Yi et al.		Green Material Valley	BFRP	8.0	Epoxy	SWSSCE	2+Simulated	55	90	NA	NA	4	86.4

	(2022b)		(GMV) New Material Technology Co., Ltd. (Zhenjiang, China)				seawater (IMMR)							
1214	Yi et al. (2022b)		Green Material Valley (GMV) New Material Technology Co., Ltd. (Zhenjiang, China)	BFRP	8.0	Epoxy	SWSSCE seawater (IMMR)	2+Simulated	55	180	NA	NA	4	80.6
1215	Yi et al. (2022b)		Green Material Valley (GMV) New Material Technology Co., Ltd. (Zhenjiang, China)	BFRP	8.0	Epoxy	SWSSCE seawater (IMMR)	2+Simulated	55	240	NA	NA	4	87.6
1216	Yi et al. (2022b)		Green Material Valley (GMV) New Material Technology Co., Ltd. (Zhenjiang, China)	BFRP	8.0	Epoxy	SWSSCE seawater (IMMR)	3+Simulated	25	90	NA	NA	4	91.7
1217	Yi et al. (2022b)		Green Material Valley (GMV) New Material Technology Co., Ltd. (Zhenjiang, China)	BFRP	8.0	Epoxy	SWSSCE seawater (IMMR)	3+Simulated	25	180	NA	NA	4	86.5
1218	Yi et al. (2022b)		Green Material Valley (GMV) New Material Technology Co., Ltd. (Zhenjiang, China)	BFRP	8.0	Epoxy	SWSSCE seawater (IMMR)	3+Simulated	25	240	NA	NA	4	88.5
1219	Yi et al. (2022b)		Green Material Valley (GMV) New Material Technology Co., Ltd. (Zhenjiang, China)	BFRP	8.0	Epoxy	SWSSCE seawater (IMMR)	3+Simulated	40	90	NA	NA	4	86.0
1220	Yi et al. (2022b)		Green Material Valley (GMV) New Material Technology Co., Ltd. (Zhenjiang, China)	BFRP	8.0	Epoxy	SWSSCE seawater (IMMR)	3+Simulated	40	180	NA	NA	4	79.3
1221	Yi et al. (2022b)		Green Material Valley (GMV) New Material Technology Co., Ltd. (Zhenjiang, China)	BFRP	8.0	Epoxy	SWSSCE seawater (IMMR)	3+Simulated	40	240	NA	NA	4	86.1
1222	Yi et al. (2022b)		Green Material Valley (GMV) New Material Technology Co., Ltd. (Zhenjiang, China)	BFRP	8.0	Epoxy	SWSSCE seawater (IMMR)	3+Simulated	55	90	NA	NA	4	85.9
1223	Yi et al. (2022b)		Green Material Valley (GMV) New Material Technology Co., Ltd. (Zhenjiang, China)	BFRP	8.0	Epoxy	SWSSCE seawater (IMMR)	3+Simulated	55	180	NA	NA	4	80.7
1224	Yi et al. (2022b)		Green Material Valley (GMV) New Material Technology Co., Ltd.	BFRP	8.0	Epoxy	SWSSCE seawater (IMMR)	3+Simulated	55	240	NA	NA	4	84.0

			(Zhenjiang, China)										
1225	Yu et al. (2021)	Harbin FRP Institute Co., Ltd. (Harbin, China)	GFRP	8.0	Epoxy	Control	21	0	NA	NA	4	100.0
1226	Yu et al. (2021)	Harbin FRP Institute Co., Ltd. (Harbin, China)	GFRP	8.0	Epoxy	Alkaline solution (IMMR)	21	30	NA	NA	4	104.0
1227	Yu et al. (2021)	Harbin FRP Institute Co., Ltd. (Harbin, China)	GFRP	8.0	Epoxy	Alkaline solution (IMMR)	21	70	NA	NA	4	116.5
1228	Yu et al. (2021)	Harbin FRP Institute Co., Ltd. (Harbin, China)	GFRP	8.0	Epoxy	Alkaline solution (IMMR)	21	100	NA	NA	4	98.8
1229	Yu et al. (2021)	Harbin FRP Institute Co., Ltd. (Harbin, China)	GFRP	8.0	Epoxy	Alkaline solution (IMMR)	21	140	NA	NA	4	101.4
1230	Yu et al. (2021)	Harbin FRP Institute Co., Ltd. (Harbin, China)	GFRP	8.0	Epoxy	Alkaline solution (IMMR)	40	30	NA	NA	4	100.9
1231	Yu et al. (2021)	Harbin FRP Institute Co., Ltd. (Harbin, China)	GFRP	8.0	Epoxy	Alkaline solution (IMMR)	40	70	NA	NA	4	86.4
1232	Yu et al. (2021)	Harbin FRP Institute Co., Ltd. (Harbin, China)	GFRP	8.0	Epoxy	Alkaline solution (IMMR)	40	100	NA	NA	4	69.7
1233	Yu et al. (2021)	Harbin FRP Institute Co., Ltd. (Harbin, China)	GFRP	8.0	Epoxy	Alkaline solution (IMMR)	40	140	NA	NA	4	22.4
1234	Yu et al. (2021)	Harbin FRP Institute Co., Ltd. (Harbin, China)	GFRP	8.0	Epoxy	Alkaline solution (IMMR)	60	30	NA	NA	4	95.7
1235	Yu et al. (2021)	Harbin FRP Institute Co., Ltd. (Harbin, China)	GFRP	8.0	Epoxy	Alkaline solution (IMMR)	60	70	NA	NA	4	62.4
1236	Yu et al. (2021)	Harbin FRP Institute Co., Ltd. (Harbin, China)	GFRP	8.0	Epoxy	Alkaline solution (IMMR)	60	100	NA	NA	4	61.4
1237	Yu et al. (2021)	Harbin FRP Institute Co., Ltd. (Harbin, China)	GFRP	8.0	Epoxy	Alkaline solution (IMMR)	60	140	NA	NA	4	40.6
1238	Yu et al. (2021)	Harbin FRP Institute Co., Ltd. (Harbin, China)	GFRP	8.0	Epoxy	Alkaline solution (IMMR)	21	30	NA	NA	4	102.1
1239	Yu et al. (2021)	Harbin FRP Institute Co., Ltd. (Harbin, China)	GFRP	8.0	Epoxy	Alkaline solution (IMMR)	21	70	NA	NA	4	106.2

1240	Yu et al. (2021)	Harbin FRP Institute Co., Ltd. (Harbin, China)	GFRP	8.0	Epoxy	Alkaline solution (IMMR)	21	100	NA	NA	4	106.2
1241	Yu et al. (2021)	Harbin FRP Institute Co., Ltd. (Harbin, China)	GFRP	8.0	Epoxy	Alkaline solution (IMMR)	21	140	NA	NA	4	104.1
1242	Yu et al. (2021)	Harbin FRP Institute Co., Ltd. (Harbin, China)	GFRP	8.0	Epoxy	Alkaline solution (IMMR)	40	30	NA	NA	4	108.2
1243	Yu et al. (2021)	Harbin FRP Institute Co., Ltd. (Harbin, China)	GFRP	8.0	Epoxy	Alkaline solution (IMMR)	40	70	NA	NA	4	99.0
1244	Yu et al. (2021)	Harbin FRP Institute Co., Ltd. (Harbin, China)	GFRP	8.0	Epoxy	Alkaline solution (IMMR)	40	100	NA	NA	4	104.1
1245	Yu et al. (2021)	Harbin FRP Institute Co., Ltd. (Harbin, China)	GFRP	8.0	Epoxy	Alkaline solution (IMMR)	40	140	NA	NA	4	109.3
1246	Yu et al. (2021)	Harbin FRP Institute Co., Ltd. (Harbin, China)	GFRP	8.0	Epoxy	Alkaline solution (IMMR)	60	30	NA	NA	4	93.9
1247	Yu et al. (2021)	Harbin FRP Institute Co., Ltd. (Harbin, China)	GFRP	8.0	Epoxy	Alkaline solution (IMMR)	60	70	NA	NA	4	108.2
1248	Yu et al. (2021)	Harbin FRP Institute Co., Ltd. (Harbin, China)	GFRP	8.0	Epoxy	Alkaline solution (IMMR)	60	100	NA	NA	4	89.8
1249	Yu et al. (2021)	Harbin FRP Institute Co., Ltd. (Harbin, China)	GFRP	8.0	Epoxy	Alkaline solution (IMMR)	60	140	NA	NA	4	94.9
1250	Yu et al. (2021)	Harbin FRP Institute Co., Ltd. (Harbin, China)	GFRP	8.0	Epoxy	Water (IMMR)	21	30	NA	NA	4	102.5
1251	Yu et al. (2021)	Harbin FRP Institute Co., Ltd. (Harbin, China)	GFRP	8.0	Epoxy	Water (IMMR)	21	70	NA	NA	4	101.0
1252	Yu et al. (2021)	Harbin FRP Institute Co., Ltd. (Harbin, China)	GFRP	8.0	Epoxy	Water (IMMR)	21	100	NA	NA	4	108.0
1253	Yu et al. (2021)	Harbin FRP Institute Co., Ltd. (Harbin, China)	GFRP	8.0	Epoxy	Water (IMMR)	21	140	NA	NA	4	101.5
1254	Yu et al. (2021)	Harbin FRP Institute Co., Ltd. (Harbin, China)	GFRP	8.0	Epoxy	Water (IMMR)	40	30	NA	NA	4	101.0
1255	Yu et al.	Harbin FRP Institute	GFRP	8.0	Epoxy	Water (IMMR)	40	70	NA	NA	4	102.0

	(2021)	Co., Ltd. (Harbin, China)										
1256	Yu et al. (2021)	Harbin FRP Institute Co., Ltd. (Harbin, China)	GFRP	8.0	Epoxy	Water (IMMR)	40	100	NA	NA	4	99.0
1257	Yu et al. (2021)	Harbin FRP Institute Co., Ltd. (Harbin, China)	GFRP	8.0	Epoxy	Water (IMMR)	40	140	NA	NA	4	104.5
1258	Yu et al. (2021)	Harbin FRP Institute Co., Ltd. (Harbin, China)	GFRP	8.0	Epoxy	Water (IMMR)	60	30	NA	NA	4	99.5
1259	Yu et al. (2021)	Harbin FRP Institute Co., Ltd. (Harbin, China)	GFRP	8.0	Epoxy	Water (IMMR)	60	70	NA	NA	4	103.0
1260	Yu et al. (2021)	Harbin FRP Institute Co., Ltd. (Harbin, China)	GFRP	8.0	Epoxy	Water (IMMR)	60	100	NA	NA	4	100.5
1261	Yu et al. (2021)	Harbin FRP Institute Co., Ltd. (Harbin, China)	GFRP	8.0	Epoxy	Water (IMMR)	60	140	NA	NA	4	102.5
1262	Zhou et al. (2023)	Green Material Valley (GMV) New Material Technology Co., Ltd. (Zhenjiang, China)	BFRP	8.0	Epoxy	Control	25	0	NA	NA	4	100.0
1263	Zhou et al. (2023)	Green Material Valley (GMV) New Material Technology Co., Ltd. (Zhenjiang, China)	BFRP	8.0	Epoxy	SWSSCE+Simulated seawater (IMMR)	25	60	NA	NA	4	91.1
1264	Zhou et al. (2023)	Green Material Valley (GMV) New Material Technology Co., Ltd. (Zhenjiang, China)	BFRP	8.0	Epoxy	SWSSCE+Simulated seawater (IMMR)	25	120	NA	NA	4	84.0
1265	Zhou et al. (2023)	Green Material Valley (GMV) New Material Technology Co., Ltd. (Zhenjiang, China)	BFRP	8.0	Epoxy	SWSSCE+Simulated seawater (IMMR)	25	180	NA	NA	4	81.1
1266	Zhou et al. (2023)	Green Material Valley (GMV) New Material Technology Co., Ltd. (Zhenjiang, China)	BFRP	8.0	Epoxy	SWSSCE+Simulated seawater (IMMR)	40	60	NA	NA	4	85.0
1267	Zhou et al. (2023)	Green Material Valley (GMV) New Material Technology Co., Ltd. (Zhenjiang, China)	BFRP	8.0	Epoxy	SWSSCE+Simulated seawater (IMMR)	40	120	NA	NA	4	75.0
1268	Zhou et al. (2023)	Green Material Valley (GMV) New Material	BFRP	8.0	Epoxy	SWSSCE+Simulated seawater (IMMR)	40	180	NA	NA	4	69.0

		Technology Co., Ltd. (Zhenjiang, China)										
1269	Zhou et al. (2023)	Green Material Valley (GMV) New Material Technology Co., Ltd. (Zhenjiang, China)	BFRP	8.0	Epoxy	SWSSCE+Simulated seawater (IMMR)	55	60	NA	NA	4	75.0
1270	Zhou et al. (2023)	Green Material Valley (GMV) New Material Technology Co., Ltd. (Zhenjiang, China)	BFRP	8.0	Epoxy	SWSSCE+Simulated seawater (IMMR)	55	120	NA	NA	4	64.6
1271	Zhou et al. (2023)	Green Material Valley (GMV) New Material Technology Co., Ltd. (Zhenjiang, China)	BFRP	8.0	Epoxy	SWSSCE+Simulated seawater (IMMR)	55	180	NA	NA	4	60.0

Notes:
(1) IMMR = Immersion; WD = Wet-dry cycle; FT = Freeze-thaw cycle; HT = High temperature; RT= Room temperature; RH = Relative humidity; UV = Ultraviolet radiation; SL = Sustained load;
(2) NC = Normal concrete; SWC = Seawater concrete; SWSSC = Seawater sea-sand concrete; NCE = Normal concrete-embedded; SWCE= Seawater concrete-embedded; SWSSCE = Sea water sea-sand concrete-embedded;
(3) f_u is the ultimate tensile strength of FRP bars;
(4) Control = Unconditioned specimens without environmental exposure and time aging effect;
(5) NA = Not applicable.

Table A3 AAT database for flexural properties of FRP bars

No.	Reference	FRP properties				Environmental condition	Temperature (℃)	Exposure duration (d)	Specimen number (pcs)	Flexural strength retention (%)	Flexural elastic modulus retention (%)
		Manufacturer	Type	Bar diameter (mm)	Resin type						
1	Ali et al. (2019)	Pultrall Inc. (Thetford Mines, QC, Canada)	BFRP	19.0	Vinylester	Control	22	0	6	100.0	100.0
2	Ali et al. (2019)	Pultrall Inc. (Thetford Mines, QC, Canada)	BFRP	19.0	Vinylester	Alkaline solution (IMMR)	22	42	6	99.1	99.7
3	Ali et al. (2019)	Pultrall Inc. (Thetford Mines, QC, Canada)	BFRP	19.0	Vinylester	Alkaline solution (IMMR)	22	125	6	91.0	99.2
4	Ali et al. (2019)	Pultrall Inc. (Thetford Mines, QC, Canada)	BFRP	19.0	Vinylester	Alkaline solution (IMMR)	22	208	6	82.7	98.7
5	Ali et al. (2019)	Pultrall Inc. (Thetford Mines, QC, Canada)	BFRP	19.0	Vinylester	Alkaline solution (IMMR)	40	42	6	98.9	99.5
6	Ali et al. (2019)	Pultrall Inc. (Thetford Mines, QC, Canada)	BFRP	19.0	Vinylester	Alkaline solution (IMMR)	40	125	6	90.7	99.4
7	Ali et al. (2019)	Pultrall Inc. (Thetford Mines, QC, Canada)	BFRP	19.0	Vinylester	Alkaline solution (IMMR)	40	208	6	81.6	98.6
8	Ali et al. (2019)	Pultrall Inc. (Thetford Mines, QC, Canada)	BFRP	19.0	Vinylester	Alkaline solution (IMMR)	60	42	6	98.3	98.2
9	Ali et al. (2019)	Pultrall Inc. (Thetford Mines, QC, Canada)	BFRP	19.0	Vinylester	Alkaline solution (IMMR)	60	125	6	90.4	95.7
10	Ali et al. (2019)	Pultrall Inc. (Thetford Mines, QC, Canada)	BFRP	19.0	Vinylester	Alkaline solution (IMMR)	60	208	6	80.9	91.7
11	Ali et al. (2020)	Galen LLC (Russia)	BFRP	9.5	Vinylester	Control	NA	0	4	100.0	100.0
12	Ali et al. (2020)	Galen LLC (Russia)	BFRP	9.5	Vinylester	Alkaline solution (IMMR)	60	90	4	80.0	97.2
13	Ali et al. (2020)	Galen LLC (Russia)	BFRP	12.7	Vinylester	Control	NA	0	4	100.0	100.0
14	Ali et al. (2020)	Galen LLC (Russia)	BFRP	12.7	Vinylester	Alkaline solution (IMMR)	60	90	4	73.2	91.0
15	Ali et al. (2020)	Galen LLC (Russia)	BFRP	15.9	Vinylester	Control	NA	0	4	100.0	100.0
16	Ali et al. (2020)	Galen LLC (Russia)	BFRP	15.9	Vinylester	Alkaline solution (IMMR)	60	90	4	81.6	99.2
17	Ali et al. (2020)	Galen LLC (Russia)	BFRP	19.0	Vinylester	Control	NA	0	4	100.0	100.0
18	Ali et al. (2020)	Galen LLC (Russia)	BFRP	19.0	Vinylester	Alkaline solution (IMMR)	60	90	4	89.5	96.1
19	Ali et al. (2020)	Galen LLC (Russia)	BFRP	25.0	Vinylester	Control	NA	0	4	100.0	100.0
20	Ali et al. (2020)	Galen LLC (Russia)	BFRP	25.0	Vinylester	Alkaline solution (IMMR)	60	90	4	91.3	98.5
21	Arczewska et al. (2021)	Pultrall Inc. (Thetford Mines, QC, Canada)	GFRP	12.7	NA	Control	NA	0	4	100.0	NA
22	Arczewska et al. (2021)	Pultrall Inc. (Thetford Mines, QC, Canada)	GFRP	12.7	NA	Alkaline solution (IMMR)	50	30	4	95.0	NA

23	Arczewska et al. (2021)	Pultrall Inc. (Thetford Mines, QC, Canada)	GFRP	12.7	NA	Alkaline (IMMR)	solution	50	90	4	90.0	NA
24	Arczewska et al. (2021)	Pultrall Inc. (Thetford Mines, QC, Canada)	GFRP	12.7	NA	Alkaline (IMMR)	solution	50	150	4	88.4	NA
25	Arczewska et al. (2021)	Pultrall Inc. (Thetford Mines, QC, Canada)	GFRP	12.7	NA	Alkaline (IMMR)	solution	60	30	4	89.8	NA
26	Arczewska et al. (2021)	Pultrall Inc. (Thetford Mines, QC, Canada)	GFRP	12.7	NA	Alkaline (IMMR)	solution	60	90	4	85.6	NA
27	Arczewska et al. (2021)	Pultrall Inc. (Thetford Mines, QC, Canada)	GFRP	12.7	NA	Alkaline (IMMR)	solution	60	150	4	82.1	NA
28	Arczewska et al. (2021)	Pultrall Inc. (Thetford Mines, QC, Canada)	GFRP	12.7	NA	Alkaline (IMMR)	solution	70	30	4	84.8	NA
29	Arczewska et al. (2021)	Pultrall Inc. (Thetford Mines, QC, Canada)	GFRP	12.7	NA	Alkaline (IMMR)	solution	70	90	4	78.7	NA
30	Arczewska et al. (2021)	Pultrall Inc. (Thetford Mines, QC, Canada)	GFRP	12.7	NA	Alkaline (IMMR)	solution	70	150	4	74.2	NA
31	Arczewska et al. (2021)	Pultrall Inc. (Thetford Mines, QC, Canada)	GFRP	15.9	NA	Control		NA	0	4	100.0	NA
32	Arczewska et al. (2021)	Pultrall Inc. (Thetford Mines, QC, Canada)	GFRP	15.9	NA	Alkaline (IMMR)	solution	50	30	4	96.5	NA
33	Arczewska et al. (2021)	Pultrall Inc. (Thetford Mines, QC, Canada)	GFRP	15.9	NA	Alkaline (IMMR)	solution	50	90	4	93.3	NA
34	Arczewska et al. (2021)	Pultrall Inc. (Thetford Mines, QC, Canada)	GFRP	15.9	NA	Alkaline (IMMR)	solution	50	150	4	89.3	NA
35	Arczewska et al. (2021)	Pultrall Inc. (Thetford Mines, QC, Canada)	GFRP	15.9	NA	Alkaline (IMMR)	solution	60	30	4	92.5	NA
36	Arczewska et al. (2021)	Pultrall Inc. (Thetford Mines, QC, Canada)	GFRP	15.9	NA	Alkaline (IMMR)	solution	60	90	4	86.2	NA
37	Arczewska et al. (2021)	Pultrall Inc. (Thetford Mines, QC, Canada)	GFRP	15.9	NA	Alkaline (IMMR)	solution	60	150	4	83.2	NA
38	Arczewska et al. (2021)	Pultrall Inc. (Thetford Mines, QC, Canada)	GFRP	15.9	NA	Alkaline (IMMR)	solution	70	30	4	88.0	NA
39	Arczewska et al. (2021)	Pultrall Inc. (Thetford Mines, QC, Canada)	GFRP	15.9	NA	Alkaline (IMMR)	solution	70	90	4	80.8	NA
40	Arczewska et al. (2021)	Pultrall Inc. (Thetford Mines, QC, Canada)	GFRP	15.9	NA	Alkaline (IMMR)	solution	70	150	4	77.2	NA
41	Arczewska et al. (2021)	Schoeck Inc. (Canada)	GFRP	12.0	NA	Control		NA	0	4	100.0	NA
42	Arczewska et al. (2021)	Schoeck Inc. (Canada)	GFRP	12.0	NA	Alkaline (IMMR)	solution	50	30	4	96.1	NA
43	Arczewska et al. (2021)	Schoeck Inc. (Canada)	GFRP	12.0	NA	Alkaline (IMMR)	solution	50	90	4	94.4	NA
44	Arczewska et al. (2021)	Schoeck Inc. (Canada)	GFRP	12.0	NA	Alkaline (IMMR)	solution	50	150	4	92.3	NA
45	Arczewska et al. (2021)	Schoeck Inc. (Canada)	GFRP	12.0	NA	Alkaline (IMMR)	solution	60	30	4	93.2	NA

46	Arczewska et al. (2021)	Schoeck Inc. (Canada)	GFRP	12.0	NA	Alkaline solution (IMMR)	60	90	4	88.7	NA
47	Arczewska et al. (2021)	Schoeck Inc. (Canada)	GFRP	12.0	NA	Alkaline solution (IMMR)	60	150	4	86.4	NA
48	Arczewska et al. (2021)	Schoeck Inc. (Canada)	GFRP	12.0	NA	Alkaline solution (IMMR)	70	30	4	89.3	NA
49	Arczewska et al. (2021)	Schoeck Inc. (Canada)	GFRP	12.0	NA	Alkaline solution (IMMR)	70	90	4	83.4	NA
50	Arczewska et al. (2021)	Schoeck Inc. (Canada)	GFRP	12.0	NA	Alkaline solution (IMMR)	70	150	4	78.8	NA
51	Arczewska et al. (2021)	Schoeck Inc. (Canada)	GFRP	16.0	NA	Control	NA	0	4	100.0	NA
52	Arczewska et al. (2021)	Schoeck Inc. (Canada)	GFRP	16.0	NA	Alkaline solution (IMMR)	50	30	4	97.5	NA
53	Arczewska et al. (2021)	Schoeck Inc. (Canada)	GFRP	16.0	NA	Alkaline solution (IMMR)	50	90	4	95.7	NA
54	Arczewska et al. (2021)	Schoeck Inc. (Canada)	GFRP	16.0	NA	Alkaline solution (IMMR)	50	150	4	94.0	NA
55	Arczewska et al. (2021)	Schoeck Inc. (Canada)	GFRP	16.0	NA	Alkaline solution (IMMR)	60	30	4	94.6	NA
56	Arczewska et al. (2021)	Schoeck Inc. (Canada)	GFRP	16.0	NA	Alkaline solution (IMMR)	60	90	4	91.1	NA
57	Arczewska et al. (2021)	Schoeck Inc. (Canada)	GFRP	16.0	NA	Alkaline solution (IMMR)	60	150	4	89.8	NA
58	Arczewska et al. (2021)	Schoeck Inc. (Canada)	GFRP	16.0	NA	Alkaline solution (IMMR)	70	30	4	90.8	NA
59	Arczewska et al. (2021)	Schoeck Inc. (Canada)	GFRP	16.0	NA	Alkaline solution (IMMR)	70	90	4	84.6	NA
60	Arczewska et al. (2021)	Schoeck Inc. (Canada)	GFRP	16.0	NA	Alkaline solution (IMMR)	70	150	4	81.2	NA
61	Ashrafi et al. (2018)	Armastek (Russia)	GFRP	6.0	Epoxy	Control	NA	0	3	100.0	NA
62	Ashrafi et al. (2018)	Armastek (Russia)	GFRP	6.0	Epoxy	UV radiation+Water vapor condensation	/	42	3	91.0	NA
63	Ashrafi et al. (2018)	Armastek (Russia)	GFRP	6.0	Epoxy	UV radiation+Water vapor condensation	/	83	3	90.0	NA
64	Ashrafi et al. (2018)	Armastek (Russia)	GFRP	6.0	Epoxy	UV radiation+Water vapor condensation	/	125	3	83.0	NA
65	Ashrafi et al. (2018)	Armastek (Russia)	GFRP	10.0	Epoxy	Control	NA	0	3	100.0	NA
66	Ashrafi et al. (2018)	Armastek (Russia)	GFRP	10.0	Epoxy	UV radiation+Water vapor condensation	/	42	3	93.0	NA
67	Ashrafi et al. (2018)	Armastek (Russia)	GFRP	10.0	Epoxy	UV radiation+Water vapor condensation	/	83	3	93.0	NA
68	Ashrafi et al. (2018)	Armastek (Russia)	GFRP	10.0	Epoxy	UV radiation+Water vapor condensation	/	125	3	92.0	NA

69	Ashrafi et al. (2018)	Armastek (Russia)	GFRP	14.0	Epoxy	Control	NA	0	3	100.0	NA
70	Ashrafi et al. (2018)	Armastek (Russia)	GFRP	14.0	Epoxy	UV radiation+Water vapor condensation	/	42	3	101.0	NA
71	Ashrafi et al. (2018)	Armastek (Russia)	GFRP	14.0	Epoxy	UV radiation+Water vapor condensation	/	83	3	98.0	NA
72	Ashrafi et al. (2018)	Armastek (Russia)	GFRP	14.0	Epoxy	UV radiation+Water vapor condensation	/	125	3	97.0	NA
73	Benmokrane et al. (2015)	NA	BFRP	6.0	Epoxy	Control	NA	0	6	100.0	100.0
74	Benmokrane et al. (2015)	NA	BFRP	6.0	Epoxy	Alkaline solution (IMMR)	60	42	6	84.0	96.0
75	Benmokrane et al. (2015)	NA	BFRP	6.0	Epoxy	Alkaline solution (IMMR)	60	125	6	72.0	96.0
76	Benmokrane et al. (2015)	NA	BFRP	6.0	Epoxy	Alkaline solution (IMMR)	60	208	6	61.0	86.0
77	Benmokrane et al. (2015)	NA	BFRP	6.0	Vinylester	Control	NA	0	6	100.0	100.0
78	Benmokrane et al. (2015)	NA	BFRP	6.0	Vinylester	Alkaline solution (IMMR)	60	42	6	98.0	95.0
79	Benmokrane et al. (2015)	NA	BFRP	6.0	Vinylester	Alkaline solution (IMMR)	60	125	6	73.0	89.0
80	Benmokrane et al. (2015)	NA	BFRP	6.0	Vinylester	Alkaline solution (IMMR)	60	208	6	63.0	84.0
81	Benmokrane et al. (2015)	NA	GFRP	6.0	Vinylester	Control	NA	0	6	100.0	100.0
82	Benmokrane et al. (2015)	NA	GFRP	6.0	Vinylester	Alkaline solution (IMMR)	60	42	6	96.0	93.0
83	Benmokrane et al. (2015)	NA	GFRP	6.0	Vinylester	Alkaline solution (IMMR)	60	125	6	100.0	89.0
84	Benmokrane et al. (2015)	NA	GFRP	6.0	Vinylester	Alkaline solution (IMMR)	60	208	6	93.0	81.0
85	Benmokrane et al. (2017a)	Firep International AG (Switzerland)	GFRP	12.0	Polyester	Control	NA	0	6	100.0	100.0
86	Benmokrane et al. (2017a)	Firep International AG (Switzerland)	GFRP	12.0	Polyester	Alkaline solution (IMMR)	60	42	6	98.5	96.7
87	Benmokrane et al. (2017a)	Firep International AG (Switzerland)	GFRP	12.0	Polyester	Alkaline solution (IMMR)	60	125	6	81.7	94.9
88	Benmokrane et al. (2017a)	Firep International AG (Switzerland)	GFRP	12.0	Polyester	Alkaline solution (IMMR)	60	208	6	75.0	89.3
89	Benmokrane et al. (2017a)	Firep International AG (Switzerland)	GFRP	12.0	Vinylester	Control	NA	0	6	100.0	100.0
90	Benmokrane et al. (2017a)	Firep International AG (Switzerland)	GFRP	12.0	Vinylester	Alkaline solution (IMMR)	60	42	6	98.4	96.5
91	Benmokrane et al. (2017a)	Firep International AG (Switzerland)	GFRP	12.0	Vinylester	Alkaline solution (IMMR)	60	125	6	88.9	92.2

92	Benmokrane et al. (2017a)	Firep International AG (Switzerland)	GFRP	12.0	Vinylester	Alkaline solution (IMMR)	60	208	6	82.8	88.2
93	Benmokrane et al. (2017a)	Firep International AG (Switzerland)	GFRP	12.0	Epoxy	Control	NA	0	6	100.0	100.0
94	Benmokrane et al. (2017a)	Firep International AG (Switzerland)	GFRP	12.0	Epoxy	Alkaline solution (IMMR)	60	42	6	91.9	95.5
95	Benmokrane et al. (2017a)	Firep International AG (Switzerland)	GFRP	12.0	Epoxy	Alkaline solution (IMMR)	60	125	6	82.7	93.0
96	Benmokrane et al. (2017a)	Firep International AG (Switzerland)	GFRP	12.0	Epoxy	Alkaline solution (IMMR)	60	208	6	77.0	87.4
97	Benmokrane et al. (2017b)	Pultrall Inc. (Thetford Mines, QC, Canada)	GFRP	9.5	Vinylester	Control	23	0	6	100.0	NA
98	Benmokrane et al. (2017b)	Pultrall Inc. (Thetford Mines, QC, Canada)	GFRP	9.5	Vinylester	Alkaline solution (IMMR)	60	90	6	88.7	NA
99	Benmokrane et al. (2017b)	Pultrall Inc. (Thetford Mines, QC, Canada)	GFRP	12.7	Vinylester	Control	23	0	6	100.0	NA
100	Benmokrane et al. (2017b)	Pultrall Inc. (Thetford Mines, QC, Canada)	GFRP	12.7	Vinylester	Alkaline solution (IMMR)	60	90	6	91.7	NA
101	Benmokrane et al. (2017b)	Pultrall Inc. (Thetford Mines, QC, Canada)	GFRP	15.9	Vinylester	Control	23	0	6	100.0	NA
102	Benmokrane et al. (2017b)	Pultrall Inc. (Thetford Mines, QC, Canada)	GFRP	15.9	Vinylester	Alkaline solution (IMMR)	60	90	6	94.5	NA
103	Benmokrane et al. (2017b)	Pultrall Inc. (Thetford Mines, QC, Canada)	GFRP	25.4	Vinylester	Control	23	0	6	100.0	NA
104	Benmokrane et al. (2017b)	Pultrall Inc. (Thetford Mines, QC, Canada)	GFRP	25.4	Vinylester	Alkaline solution (IMMR)	60	90	6	97.5	NA
105	Fergani et al. (2018)	NA	GFRP	8.0	Vinylester	Control	20	0	5	100.0	100.0
106	Fergani et al. (2018)	NA	GFRP	8.0	Vinylester	Alkaline solution (IMMR)	20	270	3	87.9	104.0
107	Fergani et al. (2018)	NA	GFRP	8.0	Vinylester	Alkaline solution (IMMR)	40	270	3	94.7	104.1
108	Fergani et al. (2018)	NA	GFRP	8.0	Vinylester	Alkaline solution (IMMR)	60	270	3	83.6	100.4
109	Fergani et al. (2018)	NA	GFRP	8.0	Vinylester	SL (3000με)+Alkaline solution (IMMR)	20	270	3	95.5	100.4
110	Fergani et al. (2018)	NA	GFRP	8.0	Vinylester	SL (3000με)+Alkaline solution (IMMR)	40	270	3	84.6	103.2
111	Fergani et al. (2018)	NA	GFRP	8.0	Vinylester	SL (3000με)+Alkaline solution (IMMR)	60	270	3	83.7	95.2
112	Fergani et al. (2018)	NA	GFRP	8.0	Vinylester	Water (IMMR)	20	270	3	99.4	107.0
113	Fergani et al. (2018)	NA	GFRP	8.0	Vinylester	Water (IMMR)	40	270	3	96.9	112.2
114	Fergani et al. (2018)	NA	GFRP	8.0	Vinylester	Water (IMMR)	60	270	3	82.2	101.1

115	Fergani et al. (2018)	NA	GFRP	8.0	Vinylester	SL (3000με)+Water (IMMR)	20	270	3	97.3	100.9
116	Fergani et al. (2018)	NA	GFRP	8.0	Vinylester	SL (3000με)+Water (IMMR)	40	270	3	77.0	117.6
117	Fergani et al. (2018)	NA	GFRP	8.0	Vinylester	SL (3000με)+Water (IMMR)	60	270	3	77.0	104.7
118	Lu et al. (2020b)	TuoXin Aerospace Basalt Industrial Co., Ltd. (Sichuan, China)	BFRP	8.0	Epoxy	Control	23	0	5	100.0	100.0
119	Lu et al. (2020b)	TuoXin Aerospace Basalt Industrial Co., Ltd. (Sichuan, China)	BFRP	8.0	Epoxy	Simulated seawater (IMMR)	23	15	5	99.0	117.8
120	Lu et al. (2020b)	TuoXin Aerospace Basalt Industrial Co., Ltd. (Sichuan, China)	BFRP	8.0	Epoxy	Simulated seawater (IMMR)	23	30	5	102.4	109.3
121	Lu et al. (2020b)	TuoXin Aerospace Basalt Industrial Co., Ltd. (Sichuan, China)	BFRP	8.0	Epoxy	Simulated seawater (IMMR)	23	60	5	105.2	125.3
122	Lu et al. (2020b)	TuoXin Aerospace Basalt Industrial Co., Ltd. (Sichuan, China)	BFRP	8.0	Epoxy	Simulated seawater (IMMR)	23	180	5	110.7	108.9
123	Lu et al. (2020b)	TuoXin Aerospace Basalt Industrial Co., Ltd. (Sichuan, China)	BFRP	8.0	Epoxy	Simulated seawater (IMMR)	23	360	5	75.3	55.1
124	Lu et al. (2020b)	TuoXin Aerospace Basalt Industrial Co., Ltd. (Sichuan, China)	BFRP	8.0	Epoxy	Simulated seawater (IMMR)	40	15	5	91.8	84.0
125	Lu et al. (2020b)	TuoXin Aerospace Basalt Industrial Co., Ltd. (Sichuan, China)	BFRP	8.0	Epoxy	Simulated seawater (IMMR)	40	30	5	94.2	105.3
126	Lu et al. (2020b)	TuoXin Aerospace Basalt Industrial Co., Ltd. (Sichuan, China)	BFRP	8.0	Epoxy	Simulated seawater (IMMR)	40	60	5	103.4	128.4
127	Lu et al. (2020b)	TuoXin Aerospace Basalt Industrial Co., Ltd. (Sichuan, China)	BFRP	8.0	Epoxy	Simulated seawater (IMMR)	40	180	5	103.8	107.1
128	Lu et al. (2020b)	TuoXin Aerospace Basalt Industrial Co., Ltd. (Sichuan, China)	BFRP	8.0	Epoxy	Simulated seawater (IMMR)	40	360	5	58.8	47.6
129	Lu et al. (2020b)	TuoXin Aerospace Basalt Industrial Co., Ltd. (Sichuan, China)	BFRP	8.0	Epoxy	Simulated seawater (IMMR)	60	15	5	87.6	84.4
130	Lu et al. (2020b)	TuoXin Aerospace Basalt Industrial Co., Ltd. (Sichuan, China)	BFRP	8.0	Epoxy	Simulated seawater (IMMR)	60	30	5	84.9	101.8
131	Lu et al. (2020b)	TuoXin Aerospace Basalt	BFRP	8.0	Epoxy	Simulated seawater	60	60	5	94.5	125.3

		Industrial Co., Ltd. (Sichuan, China)				(IMMR)					
132	Lu et al. (2020b)	TuoXin Aerospace Basalt Industrial Co., Ltd. (Sichuan, China)	BFRP	8.0	Epoxy	Simulated seawater (IMMR)	60	180	5	84.2	100.4
133	Lu et al. (2020b)	TuoXin Aerospace Basalt Industrial Co., Ltd. (Sichuan, China)	BFRP	8.0	Epoxy	Simulated seawater (IMMR)	60	360	5	18.6	9.3
134	Lu et al. (2020b)	TuoXin Aerospace Basalt Industrial Co., Ltd. (Sichuan, China)	BFRP	8.0	Epoxy	NCE+Simulated seawater (IMMR)	23	15	5	108.6	107.1
135	Lu et al. (2020b)	TuoXin Aerospace Basalt Industrial Co., Ltd. (Sichuan, China)	BFRP	8.0	Epoxy	NCE+Simulated seawater (IMMR)	23	30	5	107.6	106.7
136	Lu et al. (2020b)	TuoXin Aerospace Basalt Industrial Co., Ltd. (Sichuan, China)	BFRP	8.0	Epoxy	NCE+Simulated seawater (IMMR)	23	60	5	105.2	112.0
137	Lu et al. (2020b)	TuoXin Aerospace Basalt Industrial Co., Ltd. (Sichuan, China)	BFRP	8.0	Epoxy	NCE+Simulated seawater (IMMR)	23	180	5	85.2	96.9
138	Lu et al. (2020b)	TuoXin Aerospace Basalt Industrial Co., Ltd. (Sichuan, China)	BFRP	8.0	Epoxy	NCE+Simulated seawater (IMMR)	23	360	5	51.5	29.8
139	Robert et al. (2010)	NA	GFRP	9.5	Vinylester	Control	23	0	6	100.0	NA
140	Robert et al. (2010)	NA	GFRP	9.5	Vinylester	Water (IMMR)	23	40	6	96.6	NA
141	Robert et al. (2010)	NA	GFRP	9.5	Vinylester	Water (IMMR)	23	100	6	94.8	NA
142	Robert et al. (2010)	NA	GFRP	9.5	Vinylester	Water (IMMR)	23	120	6	92.1	NA
143	Robert et al. (2010)	NA	GFRP	9.5	Vinylester	Water (IMMR)	40	40	6	94.4	NA
144	Robert et al. (2010)	NA	GFRP	9.5	Vinylester	Water (IMMR)	40	100	6	91.3	NA
145	Robert et al. (2010)	NA	GFRP	9.5	Vinylester	Water (IMMR)	40	120	6	89.2	NA
146	Robert et al. (2010)	NA	GFRP	9.5	Vinylester	Water (IMMR)	60	40	6	87.8	NA
147	Robert et al. (2010)	NA	GFRP	9.5	Vinylester	Water (IMMR)	60	100	6	84.8	NA
148	Robert et al. (2010)	NA	GFRP	9.5	Vinylester	Water (IMMR)	60	120	6	81.3	NA
149	Robert et al. (2010)	NA	GFRP	9.5	Vinylester	Water (IMMR)	80	40	6	80.0	NA
150	Robert et al.	NA	GFRP	9.5	Vinylester	Water (IMMR)	80	100	6	63.1	NA

	(2010)														
151	Robert et al. (2010)		NA			GFRP	9.5	Vinylester	Water (IMMR)		80	120	6	54.2	NA
152	Wang et al. (2022)		Dextra Co., ltd (Dongguan, China)			GFRP	9.5	Vinylester	Control		23	0	5	100.0	100.0
153	Wang et al. (2022)		Dextra Co., ltd (Dongguan, China)			GFRP	9.5	Vinylester	Water (IMMR)		23	45	5	97.3	103.3
154	Wang et al. (2022)		Dextra Co., ltd (Dongguan, China)			GFRP	9.5	Vinylester	Water (IMMR)		23	90	5	101.4	103.3
155	Wang et al. (2022)		Dextra Co., ltd (Dongguan, China)			GFRP	9.5	Vinylester	Water (IMMR)		23	180	5	97.3	101.5
156	Wang et al. (2022)		Dextra Co., ltd (Dongguan, China)			GFRP	9.5	Vinylester	Water (IMMR)		23	270	5	100.8	103.9
157	Wang et al. (2022)		Dextra Co., ltd (Dongguan, China)			GFRP	9.5	Vinylester	Water (IMMR)		23	360	5	99.0	101.5
158	Wang et al. (2022)		Dextra Co., ltd (Dongguan, China)			GFRP	9.5	Vinylester	Water (IMMR)		40	45	5	96.1	100.3
159	Wang et al. (2022)		Dextra Co., ltd (Dongguan, China)			GFRP	9.5	Vinylester	Water (IMMR)		40	90	5	93.2	102.7
160	Wang et al. (2022)		Dextra Co., ltd (Dongguan, China)			GFRP	9.5	Vinylester	Water (IMMR)		40	180	5	96.1	105.1
161	Wang et al. (2022)		Dextra Co., ltd (Dongguan, China)			GFRP	9.5	Vinylester	Water (IMMR)		40	270	5	99.0	103.3
162	Wang et al. (2022)		Dextra Co., ltd (Dongguan, China)			GFRP	9.5	Vinylester	Water (IMMR)		40	360	5	99.0	101.5
163	Wang et al. (2022)		Dextra Co., ltd (Dongguan, China)			GFRP	9.5	Vinylester	Water (IMMR)		60	45	5	95.0	101.5
164	Wang et al. (2022)		Dextra Co., ltd (Dongguan, China)			GFRP	9.5	Vinylester	Water (IMMR)		60	90	5	101.4	100.9
165	Wang et al. (2022)		Dextra Co., ltd (Dongguan, China)			GFRP	9.5	Vinylester	Water (IMMR)		60	180	5	96.1	105.7
166	Wang et al. (2022)		Dextra Co., ltd (Dongguan, China)			GFRP	9.5	Vinylester	Water (IMMR)		60	270	5	99.6	102.1
167	Wang et al. (2022)		Dextra Co., ltd (Dongguan, China)			GFRP	9.5	Vinylester	Water (IMMR)		60	360	5	99.0	103.9
168	Wang et al. (2022)		Dextra Co., ltd (Dongguan, China)			GFRP	9.5	Vinylester	Alkaline solution (IMMR)	1	23	45	5	102.5	102.7
169	Wang et al. (2022)		Dextra Co., ltd (Dongguan, China)			GFRP	9.5	Vinylester	Alkaline solution (IMMR)	1	23	90	5	96.7	102.1
170	Wang et al. (2022)		Dextra Co., ltd (Dongguan, China)			GFRP	9.5	Vinylester	Alkaline solution (IMMR)	1	23	180	5	104.3	103.9
171	Wang et al. (2022)		Dextra Co., ltd (Dongguan, China)			GFRP	9.5	Vinylester	Alkaline solution (IMMR)	1	23	270	5	99.6	103.9
172	Wang et al. (2022)		Dextra Co., ltd (Dongguan, China)			GFRP	9.5	Vinylester	Alkaline solution (IMMR)	1	23	360	5	98.5	101.5
173	Wang et al.		Dextra Co., ltd (Dongguan,			GFRP	9.5	Vinylester	Alkaline solution	1	40	45	5	103.1	100.3

	(2022)			China)						(IMMR)							
174	Wang (2022)	et	al.	Dextra China)	Co.,	ltd	(Dongguan,	GFRP	9.5	Vinylester	Alkaline (IMMR)	solution	1	40	90	5	100.2	100.3
175	Wang (2022)	et	al.	Dextra China)	Co.,	ltd	(Dongguan,	GFRP	9.5	Vinylester	Alkaline (IMMR)	solution	1	40	180	5	93.8	99.7
176	Wang (2022)	et	al.	Dextra China)	Co.,	ltd	(Dongguan,	GFRP	9.5	Vinylester	Alkaline (IMMR)	solution	1	40	270	5	99.6	101.5
177	Wang (2022)	et	al.	Dextra China)	Co.,	ltd	(Dongguan,	GFRP	9.5	Vinylester	Alkaline (IMMR)	solution	1	40	360	5	100.8	103.3
178	Wang (2022)	et	al.	Dextra China)	Co.,	ltd	(Dongguan,	GFRP	9.5	Vinylester	Alkaline (IMMR)	solution	1	60	45	5	97.3	100.9
179	Wang (2022)	et	al.	Dextra China)	Co.,	ltd	(Dongguan,	GFRP	9.5	Vinylester	Alkaline (IMMR)	solution	1	60	90	5	99.0	99.7
180	Wang (2022)	et	al.	Dextra China)	Co.,	ltd	(Dongguan,	GFRP	9.5	Vinylester	Alkaline (IMMR)	solution	1	60	180	5	103.1	106.3
181	Wang (2022)	et	al.	Dextra China)	Co.,	ltd	(Dongguan,	GFRP	9.5	Vinylester	Alkaline (IMMR)	solution	1	60	270	5	100.8	105.1
182	Wang (2022)	et	al.	Dextra China)	Co.,	ltd	(Dongguan,	GFRP	9.5	Vinylester	Alkaline (IMMR)	solution	1	60	360	5	99.0	99.7
183	Wang (2022)	et	al.	Dextra China)	Co.,	ltd	(Dongguan,	GFRP	9.5	Vinylester	Alkaline (IMMR)	solution	2	23	45	5	104.3	99.1
184	Wang (2022)	et	al.	Dextra China)	Co.,	ltd	(Dongguan,	GFRP	9.5	Vinylester	Alkaline (IMMR)	solution	2	23	90	5	104.3	102.1
185	Wang (2022)	et	al.	Dextra China)	Co.,	ltd	(Dongguan,	GFRP	9.5	Vinylester	Alkaline (IMMR)	solution	2	23	180	5	97.9	103.9
186	Wang (2022)	et	al.	Dextra China)	Co.,	ltd	(Dongguan,	GFRP	9.5	Vinylester	Alkaline (IMMR)	solution	2	23	270	5	99.0	102.1
187	Wang (2022)	et	al.	Dextra China)	Co.,	ltd	(Dongguan,	GFRP	9.5	Vinylester	Alkaline (IMMR)	solution	2	23	360	5	99.6	103.3
188	Wang (2022)	et	al.	Dextra China)	Co.,	ltd	(Dongguan,	GFRP	9.5	Vinylester	Alkaline (IMMR)	solution	2	40	45	5	101.4	96.1
189	Wang (2022)	et	al.	Dextra China)	Co.,	ltd	(Dongguan,	GFRP	9.5	Vinylester	Alkaline (IMMR)	solution	2	40	90	5	105.4	100.3
190	Wang (2022)	et	al.	Dextra China)	Co.,	ltd	(Dongguan,	GFRP	9.5	Vinylester	Alkaline (IMMR)	solution	2	40	180	5	101.4	99.7
191	Wang (2022)	et	al.	Dextra China)	Co.,	ltd	(Dongguan,	GFRP	9.5	Vinylester	Alkaline (IMMR)	solution	2	40	270	5	97.3	102.7
192	Wang (2022)	et	al.	Dextra China)	Co.,	ltd	(Dongguan,	GFRP	9.5	Vinylester	Alkaline (IMMR)	solution	2	40	360	5	99.0	99.1
193	Wang (2022)	et	al.	Dextra China)	Co.,	ltd	(Dongguan,	GFRP	9.5	Vinylester	Alkaline (IMMR)	solution	2	60	45	5	100.8	100.9
194	Wang (2022)	et	al.	Dextra China)	Co.,	ltd	(Dongguan,	GFRP	9.5	Vinylester	Alkaline (IMMR)	solution	2	60	90	5	97.9	103.3
195	Wang (2022)	et	al.	Dextra China)	Co.,	ltd	(Dongguan,	GFRP	9.5	Vinylester	Alkaline (IMMR)	solution	2	60	180	5	99.0	105.7
196	Wang	et	al.	Dextra	Co.,	ltd	(Dongguan,	GFRP	9.5	Vinylester	Alkaline	solution	2	60	270	5	100.2	103.3

	(2022)			China)							(IMMR)						
197	Wang (2022)	et	al.	Dextra China)	Co.,	ltd	(Dongguan,	GFRP	9.5	Vinylester	Alkaline (IMMR)	solution	2	60	360	5	98.5	102.1
198	Wang (2022)	et	al.	Dextra China)	Co.,	ltd	(Dongguan,	GFRP	9.5	Vinylester	Alkaline (IMMR)	solution	3	23	45	5	99.6	103.3
199	Wang (2022)	et	al.	Dextra China)	Co.,	ltd	(Dongguan,	GFRP	9.5	Vinylester	Alkaline (IMMR)	solution	3	23	90	5	104.3	102.7
200	Wang (2022)	et	al.	Dextra China)	Co.,	ltd	(Dongguan,	GFRP	9.5	Vinylester	Alkaline (IMMR)	solution	3	23	180	5	102.0	103.9
201	Wang (2022)	et	al.	Dextra China)	Co.,	ltd	(Dongguan,	GFRP	9.5	Vinylester	Alkaline (IMMR)	solution	3	23	270	5	99.0	101.5
202	Wang (2022)	et	al.	Dextra China)	Co.,	ltd	(Dongguan,	GFRP	9.5	Vinylester	Alkaline (IMMR)	solution	3	23	360	5	100.2	100.3
203	Wang (2022)	et	al.	Dextra China)	Co.,	ltd	(Dongguan,	GFRP	9.5	Vinylester	Alkaline (IMMR)	solution	3	40	45	5	100.2	100.3
204	Wang (2022)	et	al.	Dextra China)	Co.,	ltd	(Dongguan,	GFRP	9.5	Vinylester	Alkaline (IMMR)	solution	3	40	90	5	97.3	100.9
205	Wang (2022)	et	al.	Dextra China)	Co.,	ltd	(Dongguan,	GFRP	9.5	Vinylester	Alkaline (IMMR)	solution	3	40	180	5	100.2	102.7
206	Wang (2022)	et	al.	Dextra China)	Co.,	ltd	(Dongguan,	GFRP	9.5	Vinylester	Alkaline (IMMR)	solution	3	40	270	5	100.8	99.1
207	Wang (2022)	et	al.	Dextra China)	Co.,	ltd	(Dongguan,	GFRP	9.5	Vinylester	Alkaline (IMMR)	solution	3	40	360	5	100.2	102.1
208	Wang (2022)	et	al.	Dextra China)	Co.,	ltd	(Dongguan,	GFRP	9.5	Vinylester	Alkaline (IMMR)	solution	3	60	45	5	100.2	102.7
209	Wang (2022)	et	al.	Dextra China)	Co.,	ltd	(Dongguan,	GFRP	9.5	Vinylester	Alkaline (IMMR)	solution	3	60	90	5	98.5	102.7
210	Wang (2022)	et	al.	Dextra China)	Co.,	ltd	(Dongguan,	GFRP	9.5	Vinylester	Alkaline (IMMR)	solution	3	60	180	5	97.3	100.3
211	Wang (2022)	et	al.	Dextra China)	Co.,	ltd	(Dongguan,	GFRP	9.5	Vinylester	Alkaline (IMMR)	solution	3	60	270	5	98.5	100.3
212	Wang (2022)	et	al.	Dextra China)	Co.,	ltd	(Dongguan,	GFRP	9.5	Vinylester	Alkaline (IMMR)	solution	3	60	360	5	100.2	102.1

Notes:
(1) IMMR = Immersion; UV = Ultraviolet radiation; SL = Sustained load;
(2) NC = Normal concrete; NCE = Normal concrete-embedded;
(3) Control = Unconditioned specimens without environmental exposure and time aging effect;
(4) NA = Not applicable.

Table B1 AAT database for bond properties of FRP bars in concrete

No.	Reference	FRP properties					Concrete type	Environmental condition	Temperature (℃)	Exposure duration (d)	Specimen number (pcs)	Bond strength retention (%)
		Manufacturer	Type	Bar diameter (mm)	Resin type	Surface characteristics						
1	Abbasi and Hogg (2005)	Hughes Brothers Company (Seward, NE, USA)	GFRP	12.7	Polyester	HW+S	NC	Water (IMMR)	RT	30	5	NA
2	Abbasi and Hogg (2005)	Hughes Brothers Company (Seward, NE, USA)	GFRP	12.7	Polyester	HW+S	NC	Water (IMMR)	RT	120	5	NA
3	Abbasi and Hogg (2005)	Hughes Brothers Company (Seward, NE, USA)	GFRP	12.7	Polyester	HW+S	NC	Water (IMMR)	RT	240	5	NA
4	Abbasi and Hogg (2005)	Hughes Brothers Company (Seward, NE, USA)	GFRP	12.7	Polyester	HW+S	NC	Water (IMMR)+HT	RT+40	30+NA	5	NA
5	Abbasi and Hogg (2005)	Hughes Brothers Company (Seward, NE, USA)	GFRP	12.7	Polyester	HW+S	NC	Water (IMMR)+HT	RT+40	120+NA	5	NA
6	Abbasi and Hogg (2005)	Hughes Brothers Company (Seward, NE, USA)	GFRP	12.7	Polyester	HW+S	NC	Water (IMMR)+HT	RT+40	240+NA	5	NA
7	Abbasi and Hogg (2005)	Hughes Brothers Company (Seward, NE, USA)	GFRP	12.7	Polyester	HW+S	NC	Water (IMMR)+HT	RT+60	30+NA	5	NA
8	Abbasi and Hogg (2005)	Hughes Brothers Company (Seward, NE, USA)	GFRP	12.7	Polyester	HW+S	NC	Water (IMMR)+HT	RT+60	120+NA	5	NA
9	Abbasi and Hogg (2005)	Hughes Brothers Company (Seward, NE, USA)	GFRP	12.7	Polyester	HW+S	NC	Water (IMMR)+HT	RT+60	240+NA	5	NA
10	Abbasi and Hogg (2005)	Hughes Brothers Company (Seward, NE, USA)	GFRP	12.7	Polyester	HW+S	NC	Water (IMMR)+HT	RT+80	30+NA	5	NA
11	Abbasi and Hogg (2005)	Hughes Brothers Company (Seward, NE, USA)	GFRP	12.7	Polyester	HW+S	NC	Water (IMMR)+HT	RT+80	120+NA	5	NA
12	Abbasi and Hogg (2005)	Hughes Brothers Company (Seward, NE, USA)	GFRP	12.7	Polyester	HW+S	NC	Water (IMMR)+HT	RT+80	240+NA	5	NA
13	Abbasi and Hogg (2005)	Hughes Brothers Company (Seward, NE, USA)	GFRP	12.7	Polyester	HW+S	NC	Alkaline solution (IMMR)	RT	30	5	NA

14	Abbasi and Hogg (2005)	Hughes Brothers Company (Seward, NE, USA)	GFRP	12.7	Polyester	HW+S	NC	Alkaline solution (IMMR)	RT	120	5	NA
15	Abbasi and Hogg (2005)	Hughes Brothers Company (Seward, NE, USA)	GFRP	12.7	Polyester	HW+S	NC	Alkaline solution (IMMR)	RT	240	5	NA
16	Abbasi and Hogg (2005)	Hughes Brothers Company (Seward, NE, USA)	GFRP	12.7	Polyester	HW+S	NC	Alkaline solution (IMMR)+HT	RT+40	30+NA	5	NA
17	Abbasi and Hogg (2005)	Hughes Brothers Company (Seward, NE, USA)	GFRP	12.7	Polyester	HW+S	NC	Alkaline solution (IMMR)+HT	RT+40	120+NA	5	NA
18	Abbasi and Hogg (2005)	Hughes Brothers Company (Seward, NE, USA)	GFRP	12.7	Polyester	HW+S	NC	Alkaline solution (IMMR)+HT	RT+40	240+NA	5	NA
19	Abbasi and Hogg (2005)	Hughes Brothers Company (Seward, NE, USA)	GFRP	12.7	Polyester	HW+S	NC	Alkaline solution (IMMR)+HT	RT+60	30+NA	5	NA
20	Abbasi and Hogg (2005)	Hughes Brothers Company (Seward, NE, USA)	GFRP	12.7	Polyester	HW+S	NC	Alkaline solution (IMMR)+HT	RT+60	120+NA	5	NA
21	Abbasi and Hogg (2005)	Hughes Brothers Company (Seward, NE, USA)	GFRP	12.7	Polyester	HW+S	NC	Alkaline solution (IMMR)+HT	RT+60	240+NA	5	NA
22	Abbasi and Hogg (2005)	Hughes Brothers Company (Seward, NE, USA)	GFRP	12.7	Polyester	HW+S	NC	Alkaline solution (IMMR)+HT	RT+80	30+NA	5	NA
23	Abbasi and Hogg (2005)	Hughes Brothers Company (Seward, NE, USA)	GFRP	12.7	Polyester	HW+S	NC	Alkaline solution (IMMR)+HT	RT+80	120+NA	5	NA
24	Abbasi and Hogg (2005)	Hughes Brothers Company (Seward, NE, USA)	GFRP	12.7	Polyester	HW+S	NC	Alkaline solution (IMMR)+HT	RT+80	240+NA	5	NA
25	Altalmas et al. (2015)	Magmatech	BFRP	12.0	NA	HW+S	HSC	Control	NA	0	5	100.0
26	Altalmas et al. (2015)	Pultron	GFRP	12.0	NA	R	HSC	Control	NA	0	3	100.0
27	Altalmas et al. (2015)	Magmatech	BFRP	12.0	NA	HW+S	HSC	Acid solution (IMMR)	60	30	3	83.4
28	Altalmas et al. (2015)	Magmatech	BFRP	12.0	NA	HW+S	HSC	Acid solution (IMMR)	60	60	3	82.3
29	Altalmas et al. (2015)	Magmatech	BFRP	12.0	NA	HW+S	HSC	Acid solution (IMMR)	60	90	3	81.7
30	Altalmas et al. (2015)	Pultron	GFRP	12.0	NA	R	HSC	Acid solution (IMMR)	60	30	3	108.6
31	Altalmas et al.	Pultron	GFRP	12.0	NA	R	HSC	Acid solution (IMMR)	60	60	3	92.3

	(2015)											
32	Altalmas et al. (2015)	Pultron	GFRP	12.0	NA	R	HSC	Acid solution (IMMR)	60	90	3	82.5
33	Altalmas et al. (2015)	Magmatech	BFRP	12.0	NA	HW+S	HSC	Alkaline solution (IMMR)	60	30	3	94.2
34	Altalmas et al. (2015)	Magmatech	BFRP	12.0	NA	HW+S	HSC	Alkaline solution (IMMR)	60	60	3	95.3
35	Altalmas et al. (2015)	Magmatech	BFRP	12.0	NA	HW+S	HSC	Alkaline solution (IMMR)	60	90	3	87.4
36	Altalmas et al. (2015)	Pultron	GFRP	12.0	NA	R	HSC	Alkaline solution (IMMR)	60	30	3	101.8
37	Altalmas et al. (2015)	Pultron	GFRP	12.0	NA	R	HSC	Alkaline solution (IMMR)	60	60	3	99.4
38	Altalmas et al. (2015)	Pultron	GFRP	12.0	NA	R	HSC	Alkaline solution (IMMR)	60	90	3	98.6
39	Altalmas et al. (2015)	Magmatech	BFRP	12.0	NA	HW+S	HSC	Saline solution (IMMR)	60	30	3	87.5
40	Altalmas et al. (2015)	Magmatech	BFRP	12.0	NA	HW+S	HSC	Saline solution (IMMR)	60	60	3	92.2
41	Altalmas et al. (2015)	Magmatech	BFRP	12.0	NA	HW+S	HSC	Saline solution (IMMR)	60	90	3	85.8
42	Altalmas et al. (2015)	Pultron	GFRP	12.0	NA	R	HSC	Saline solution (IMMR)	60	30	3	100.2
43	Altalmas et al. (2015)	Pultron	GFRP	12.0	NA	R	HSC	Saline solution (IMMR)	60	60	3	99.0
44	Altalmas et al. (2015)	Pultron	GFRP	12.0	NA	R	HSC	Saline solution (IMMR)	60	90	3	95.9
45	Alves et al. (2011)	Pultrall Inc. Canada	GFRP	15.9	Vinylester	S	NC	Control	NA	0	1	100.0
46	Alves et al. (2011)	Pultrall Inc. Canada	GFRP	15.9	Vinylester	S	NC	Control	NA	0	1	100.0
47	Alves et al. (2011)	Pultrall Inc. Canada	GFRP	15.9	Vinylester	S	NC	Control	NA	0	1	100.0
48	Alves et al. (2011)	Pultrall Inc. Canada	GFRP	18.9	Vinylester	S	NC	Control	NA	0	1	100.0
49	Alves et al. (2011)	Pultrall Inc. Canada	GFRP	18.9	Vinylester	S	NC	Control	NA	0	1	100.0
50	Alves et al. (2011)	Pultrall Inc. Canada	GFRP	18.9	Vinylester	S	NC	Control	NA	0	1	100.0
51	Alves et al. (2011)	Pultrall Inc. Canada	GFRP	15.9	Vinylester	S	NC	SL (30% fu)+FT	-30~20	125	1	144.0
52	Alves et al. (2011)	Pultrall Inc. Canada	GFRP	15.9	Vinylester	S	NC	SL (30% fu)+FT	-30~20	125	1	145.5
53	Alves et al. (2011)	Pultrall Inc. Canada	GFRP	15.9	Vinylester	S	NC	SL (30% fu)+FT	-30~20	125	1	125.9
54	Alves et al.	Pultrall Inc. Canada	GFRP	18.9	Vinylester	S	NC	SL (30% fu)+FT	-30~20	125	1	90.6

	(2011)											
55	Alves et al. (2011)	Pultrall Inc. Canada	GFRP	18.9	Vinylester	S	NC	SL (30% fu)+FT	-30~20	125	1	94.6
56	Alves et al. (2011)	Pultrall Inc. Canada	GFRP	18.9	Vinylester	S	NC	SL (30% fu)+FT	-30~20	125	1	126.0
57	Al-Zahrani et al. (2002)	NA	GFRP	10.0	Urethane modified vinylester	NA	NC	Control	NA	0	NA	100.0
58	Al-Zahrani et al. (2002)	NA	GFRP	10.0	Urethane modified vinylester	NA	NC	Seawater (IMMR)	22	90	NA	84.4
59	Al-Zahrani et al. (2002)	NA	GFRP	10.0	Urethane modified vinylester	NA	NC	Seawater (IMMR)	22	180	NA	98.5
60	Al-Zahrani et al. (2002)	NA	GFRP	10.0	Urethane modified vinylester	NA	NC	Saline solution (IMMR)	22	90	NA	103.0
61	Al-Zahrani et al. (2002)	NA	GFRP	10.0	Urethane modified vinylester	NA	NC	Saline solution (IMMR)	22	180	NA	117.8
62	Bank et al. (1998)	NA	GFRP	12.7	Polyester	Plain	NC	Reference	21	84	3	NA
63	Bank et al. (1998)	NA	GFRP	12.7	Vinylester	Plain	NC	Reference	21	84	3	NA
64	Bank et al. (1998)	NA	GFRP	12.7	Vinylester	HW	NC	Reference	21	84	3	NA
65	Bank et al. (1998)	NA	GFRP	12.7	Polyester	HW+S	NC	Reference	21	84	3	NA
66	Bank et al. (1998)	NA	GFRP	12.7	Polyester	Plain	NC	Water (IMMR)	80	14	3	NA
67	Bank et al. (1998)	NA	GFRP	12.7	Vinylester	Plain	NC	Water (IMMR)	80	14	3	NA
68	Bank et al. (1998)	NA	GFRP	12.7	Vinylester	HW	NC	Water (IMMR)	80	14	3	NA
69	Bank et al. (1998)	NA	GFRP	12.7	Polyester	HW+S	NC	Water (IMMR)	80	14	3	NA
70	Bank et al. (1998)	NA	GFRP	12.7	Polyester	Plain	NC	Water (IMMR)	80	84	3	NA
71	Bank et al. (1998)	NA	GFRP	12.7	Vinylester	Plain	NC	Water (IMMR)	80	84	3	NA
72	Bank et al. (1998)	NA	GFRP	12.7	Vinylester	HW	NC	Water (IMMR)	80	84	3	NA
73	Bank et al. (1998)	NA	GFRP	12.7	Polyester	HW+S	NC	Water (IMMR)	80	84	3	NA
74	Bazli et al. (2017)	NA	GFRP	8.0	Vinylester	R	NC	Water (IMMR)	RT	150	3	100.0
75	Bazli et al. (2017)	NA	GFRP	8.0	Vinylester	R	NC	Water (IMMR)	RT	150	3	100.0
76	Bazli et al. (2017)	NA	GFRP	8.0	Vinylester	R	NC	Seawater (IMMR)	20	150	3	91.3
77	Bazli et al. (2017)	NA	GFRP	8.0	Vinylester	R	NC	Seawater (IMMR)	40	150	3	97.4
78	Bazli et al. (2017)	NA	GFRP	8.0	Vinylester	R	NC	Seawater (IMMR)	60	150	3	99.2
79	Bazli et al. (2017)	NA	GFRP	8.0	Vinylester	R	HSC	Seawater (IMMR)	20	150	3	92.9
80	Bazli et al. (2017)	NA	GFRP	8.0	Vinylester	R	NC	Seawater (IMMR)	40	150	3	92.5
81	Bazli et al. (2017)	NA	GFRP	8.0	Vinylester	R	NC	Seawater (IMMR)	60	150	3	91.9
82	Bazli et al. (2017)	NA	GFRP	8.0	Vinylester	R	NC	Seawater (WD)	RT	150	3	95.0
83	Bazli et al. (2017)	NA	GFRP	8.0	Vinylester	R	NC	Seawater (WD)	RT	150	3	93.8
84	Bazli et al. (2017)	NA	GFRP	8.0	Vinylester	R	NC	Alkaline solution (IMMR)	RT	150	3	89.8
85	Bazli et al. (2017)	NA	GFRP	8.0	Vinylester	R	NC	Alkaline solution (IMMR)	RT	150	3	87.7

86	Bazli et al. (2017)	NA	GFRP	8.0	Vinylester	R	NC	Alkaline solution (IMMR)	RT	150	3	92.9
87	Bazli et al. (2017)	NA	GFRP	8.0	Vinylester	R	HSC	Alkaline solution (IMMR)	RT	150	3	89.3
88	Bazli et al. (2017)	NA	GFRP	8.0	Vinylester	R	HSC	Alkaline solution (IMMR)	RT	150	3	90.1
89	Bazli et al. (2017)	NA	GFRP	8.0	Vinylester	R	NC	Alkaline solution (IMMR)	RT	150	3	90.9
90	Bazli et al. (2017)	NA	GFRP	8.0	Vinylester	R	NC	Acid solution (IMMR)	RT	150	3	84.3
91	Bazli et al. (2017)	NA	GFRP	8.0	Vinylester	R	NC	Acid solution (IMMR)	RT	150	3	87.5
92	Bazli et al. (2017)	NA	GFRP	8.0	Vinylester	R	NC	Acid solution (IMMR)	RT	150	3	90.0
93	Bazli et al. (2017)	NA	GFRP	8.0	Vinylester	R	NC	Acid solution (IMMR)	RT	150	3	91.0
94	Belarbi and Wang (2012)	NA	CFRP	13.0	Epoxy modified vinylester	Plain	NC	Control	NA	0	3	100.0
95	Belarbi and Wang (2012)	NA	GFRP	13.0	Epoxy modified vinylester	HW+S	NC	Control	NA	0	3	100.0
96	Belarbi and Wang (2012)	NA	GFRP	25.0	Epoxy modified vinylester	HW+S	NC	Control	NA	0	3	100.0
97	Belarbi and Wang (2012)	NA	CFRP	13.0	Epoxy modified vinylester	Plain	NC	Saline solution (FT)+Temperature cycles	-20~60	100	3	77.3
98	Belarbi and Wang (2012)	NA	GFRP	13.0	Epoxy modified vinylester	HW+S	NC	Saline solution (FT)+Temperature cycles	-20~60	100	3	43.6
99	Belarbi and Wang (2012)	NA	GFRP	25.0	Epoxy modified vinylester	HW+S	NC	Saline solution (FT)+Temperature cycles	-20~60	100	3	96.4
100	Calvet et al. (2015)	Pultrall Inc. Canada	CFRP	6.4	Vinylester	S	NC	FT	-20~20	5	5	NA
101	Calvet et al. (2015)	Pultrall Inc. Canada	CFRP	12.7	Vinylester	S	NC	FT	-20~20	5	5	NA
102	Calvet et al. (2015)	Marshall Composite Technologies LLC, Salem, Oregon, USA	CFRP	9.5	Urethane modified vinylester	R	NC	FT	-20~20	5	5	NA
103	Calvet et al. (2015)	Sika SAU, Quart de Poblet, Valencia, Spain	CFRP	9.5	Epoxy	D+T	NC	FT	-20~20	5	5	NA
104	Calvet et al. (2015)	Pultrall Inc. Canada	CFRP	6.4	Vinylester	S	NC	HT	5	2	5	NA
105	Calvet et al. (2015)	Pultrall Inc. Canada	CFRP	6.4	Vinylester	S	NC	HT	20	2	5	NA
106	Calvet et al. (2015)	Pultrall Inc. Canada	CFRP	6.4	Vinylester	S	NC	HT	40	2	5	NA
107	Calvet et al.	Pultrall Inc. Canada	CFRP	6.4	Vinylester	S	NC	HT	80	2	5	NA

	(2015)												
108	Calvet et al. (2015)	Pultrall Inc. Canada	CFRP	12.7	Vinylester	S	NC	HT	5	2	5	NA
109	Calvet et al. (2015)	Pultrall Inc. Canada	CFRP	12.7	Vinylester	S	NC	HT	20	2	5	NA
110	Calvet et al. (2015)	Pultrall Inc. Canada	CFRP	12.7	Vinylester	S	NC	HT	40	2	5	NA
111	Calvet et al. (2015)	Pultrall Inc. Canada	CFRP	12.7	Vinylester	S	NC	HT	80	2	5	NA
112	Calvet et al. (2015)	Marshall Composite Technologies LLC, Salem, Oregon, USA	CFRP	9.5	Urethane modified vinylester	R	NC	HT	5	2	5	NA
113	Calvet et al. (2015)	Marshall Composite Technologies LLC, Salem, Oregon, USA	CFRP	9.5	Urethane modified vinylester	R	NC	HT	20	2	5	NA
114	Calvet et al. (2015)	Marshall Composite Technologies LLC, Salem, Oregon, USA	CFRP	9.5	Urethane modified vinylester	R	NC	HT	40	2	5	NA
115	Calvet et al. (2015)	Marshall Composite Technologies LLC, Salem, Oregon, USA	CFRP	9.5	Urethane modified vinylester	R	NC	HT	80	2	5	NA
116	Calvet et al. (2015)	Sika SAU, Quart de Poblet, Valencia, Spain	CFRP	9.5	Epoxy	D+T	NC	HT	5	2	5	NA
117	Calvet et al. (2015)	Sika SAU, Quart de Poblet, Valencia, Spain	CFRP	9.5	Epoxy	D+T	NC	HT	20	2	5	NA
118	Calvet et al. (2015)	Sika SAU, Quart de Poblet, Valencia, Spain	CFRP	9.5	Epoxy	D+T	NC	HT	40	2	5	NA
119	Calvet et al. (2015)	Sika SAU, Quart de Poblet, Valencia, Spain	CFRP	9.5	Epoxy	D+T	NC	HT	80	2	5	NA
120	Chang et al. (2021)	Huyu Glass Fiber reinforced Polymer Products Co., Ltd., Nantong, China	GFRP	12.0	Vinylester	R	SWSSC	Control	NA	0	3	100.0
121	Chang et al. (2021)	Huyu Glass Fiber reinforced Polymer Products Co., Ltd., Nantong, China	GFRP	16.0	Vinylester	R	SWSSC	Control	NA	0	3	100.0
122	Chang et al. (2021)	Huyu Glass Fiber reinforced Polymer Products Co., Ltd., Nantong, China	GFRP	12.0	Vinylester	R	SWSSC	Seawater (IMMR)	25	90	3	104.8
123	Chang et al. (2021)	Huyu Glass Fiber reinforced Polymer Products Co., Ltd., Nantong, China	GFRP	12.0	Vinylester	R	SWSSC	Seawater (IMMR)	25	180	3	97.7
124	Chang et al.	Huyu Glass Fiber	GFRP	12.0	Vinylester	R	SWSSC	Seawater (IMMR)	25	270	3	92.6

	(2021)	reinforced Polymer Products Co., Ltd., Nantong, China											
125	Chang et al. (2021)	Huyu Glass Fiber reinforced Polymer Products Co., Ltd., Nantong, China	GFRP	16.0	Vinylester	R	SWSSC	Seawater (IMMR)	25	90	3	104.9
126	Chang et al. (2021)	Huyu Glass Fiber reinforced Polymer Products Co., Ltd., Nantong, China	GFRP	16.0	Vinylester	R	SWSSC	Seawater (IMMR)	25	180	3	112.9
127	Chang et al. (2021)	Huyu Glass Fiber reinforced Polymer Products Co., Ltd., Nantong, China	GFRP	16.0	Vinylester	R	SWSSC	Seawater (IMMR)	25	270	3	115.7
128	Chang et al. (2021)	Huyu Glass Fiber reinforced Polymer Products Co., Ltd., Nantong, China	GFRP	12.0	Vinylester	R	SWSSC	SL (25%fu)+Seawater (IMMR)	25	90	3	103.0
129	Chang et al. (2021)	Huyu Glass Fiber reinforced Polymer Products Co., Ltd., Nantong, China	GFRP	12.0	Vinylester	R	SWSSC	SL (25%fu)+Seawater (IMMR)	25	180	3	96.9
130	Chang et al. (2021)	Huyu Glass Fiber reinforced Polymer Products Co., Ltd., Nantong, China	GFRP	12.0	Vinylester	R	SWSSC	SL (25%fu)+Seawater (IMMR)	25	270	3	89.1
131	Chang et al. (2021)	Huyu Glass Fiber reinforced Polymer Products Co., Ltd., Nantong, China	GFRP	16.0	Vinylester	R	SWSSC	SL (25%fu)+Seawater (IMMR)	25	90	3	103.3
132	Chang et al. (2021)	Huyu Glass Fiber reinforced Polymer Products Co., Ltd., Nantong, China	GFRP	16.0	Vinylester	R	SWSSC	SL (25%fu)+Seawater (IMMR)	25	180	3	109.8
133	Chang et al. (2021)	Huyu Glass Fiber reinforced Polymer Products Co., Ltd., Nantong, China	GFRP	16.0	Vinylester	R	SWSSC	SL (25%fu)+Seawater (IMMR)	25	270	3	113.6
134	Chen et al. (2007)	Hughes Brothers Company (Seward, NE, USA)	GFRP	9.5	Vinylester	HW+S	NC	Reference	RT	60	2	100.0
135	Chen et al. (2007)	Hughes Brothers Company (Seward, NE, USA)	GFRP	12.7	Vinylester	HW+S	NC	Reference	RT	60	2	100.0
136	Chen et al. (2007)	Hughes Brothers	GFRP	9.5	Vinylester	HW+S	NC	Alkaline solution	60	60	2	87.7

		Company (Seward, NE, USA)						(IMMR)				
137	Chen et al. (2007)	Hughes Brothers Company (Seward, NE, USA)	GFRP	12.7	Vinylester	HW+S	NC	Alkaline solution (IMMR)	60	60	2	86.0
138	Dai et al. (2023)	NA	BFRP	12.0	NA	R	SWSSC	Control	RT	0	3	100.0
139	Dai et al. (2023)	NA	BFRP	12.0	NA	R	SWSSC	Saline solution (WD)	30	60	3	102.3
140	Dai et al. (2023)	NA	BFRP	12.0	NA	R	SWSSC	Saline solution (WD)	30	120	3	98.2
141	Dai et al. (2023)	NA	BFRP	12.0	NA	R	SWSSC	Saline solution (WD)	30	180	3	90.0
142	Dai et al. (2023)	NA	BFRP	12.0	NA	R	SWSSC	Saline solution (WD)	45	60	3	101.8
143	Dai et al. (2023)	NA	BFRP	12.0	NA	R	SWSSC	Saline solution (WD)	45	120	3	96.2
144	Dai et al. (2023)	NA	BFRP	12.0	NA	R	SWSSC	Saline solution (WD)	45	180	3	86.8
145	Dai et al. (2023)	NA	BFRP	12.0	NA	R	SWSSC	Saline solution (WD)	60	60	3	100.3
146	Dai et al. (2023)	NA	BFRP	12.0	NA	R	SWSSC	Saline solution (WD)	60	120	3	86.0
147	Dai et al. (2023)	NA	BFRP	12.0	NA	R	SWSSC	Saline solution (WD)	60	180	3	76.9
148	Dai et al. (2023)	NA	BFRP	12.0	NA	R	SWSSC	Saline solution (WD)	45	180	3	101.8
149	Dai et al. (2023)	NA	BFRP	12.0	NA	R	SWSSC	Saline solution (WD)	45	180	3	86.2
150	Dai et al. (2023)	NA	BFRP	12.0	NA	R	SWSSC	Saline solution (WD)	45	180	3	84.3
151	Dai et al. (2023)	NA	BFRP	12.0	NA	R	SWSSC	Saline solution (WD)	45	180	3	114.7
152	Dai et al. (2023)	NA	BFRP	12.0	NA	R	SWSSC	Saline solution (WD)	30	180	3	123.5
153	Dai et al. (2023)	NA	BFRP	12.0	NA	R	SWSSC	Saline solution (WD)	30	180	3	110.0
154	Dai et al. (2023)	NA	BFRP	12.0	NA	R	SWSSC	Saline solution (WD)	30	180	3	76.5
155	Davalos et al. (2008)	Hughes Brothers Company (Seward, NE, USA)	GFRP	9.5	Vinylester	HW+S	HSC	Control	NA	0	3	100.0
156	Davalos et al. (2008)	Hughes Brothers Company (Seward, NE, USA)	GFRP	12.7	Vinylester	HW+S	HSC	Control	NA	0	3	100.0
157	Davalos et al. (2008)	Hughes Brothers Company (Seward, NE, USA)	GFRP	9.5	Vinylester	S	HSC	Control	NA	0	3	100.0
158	Davalos et al. (2008)	Hughes Brothers Company (Seward, NE, USA)	CFRP	9.0	Epoxy	S	HSC	Control	NA	0	3	100.0
159	Davalos et al. (2008)	Hughes Brothers Company (Seward, NE, USA)	GFRP	9.5	Vinylester	HW+S	HSC	Water (IMMR)	RT	90	3	84.7
160	Davalos et al. (2008)	Hughes Brothers Company (Seward, NE, USA)	GFRP	12.7	Vinylester	HW+S	HSC	Water (IMMR)	RT	90	3	99.8
161	Davalos et al. (2008)	Hughes Brothers Company (Seward, NE, USA)	GFRP	9.5	Vinylester	S	HSC	Water (IMMR)	RT	90	3	80.4
162	Davalos et al. (2008)	Hughes Brothers Company (Seward, NE, USA)	CFRP	9.0	Epoxy	S	HSC	Water (IMMR)	RT	90	3	92.9

163	Davalos et al. (2008)	Hughes Brothers Company (Seward, NE, USA)	GFRP	9.5	Vinylester	HW+S	NC	Water (IMMR)	60	90	3	91.6
164	Davalos et al. (2008)	Hughes Brothers Company (Seward, NE, USA)	GFRP	12.7	Vinylester	HW+S	NC	Water (IMMR)	60	90	3	97.2
165	Davalos et al. (2008)	Hughes Brothers Company (Seward, NE, USA)	GFRP	9.5	Vinylester	S	NC	Water (IMMR)	60	90	3	94.6
166	Davalos et al. (2008)	Hughes Brothers Company (Seward, NE, USA)	CFRP	9.0	Epoxy	S	NC	Water (IMMR)	60	90	3	90.0
167	Davalos et al. (2008)	Hughes Brothers Company (Seward, NE, USA)	GFRP	9.5	Vinylester	HW+S	HSC	Temperature cycle	-20~60	30	3	82.4
168	Davalos et al. (2008)	Hughes Brothers Company (Seward, NE, USA)	GFRP	12.7	Vinylester	HW+S	HSC	Temperature cycle	-20~60	30	3	90.0
169	Davalos et al. (2008)	Hughes Brothers Company (Seward, NE, USA)	GFRP	9.5	Vinylester	S	HSC	Temperature cycle	-20~60	30	3	82.4
170	Davalos et al. (2008)	Hughes Brothers Company (Seward, NE, USA)	CFRP	9.0	Epoxy	S	HSC	Temperature cycle	-20~60	30	3	95.6
171	Dong et al. (2016)	Zhejiang GBF Basalt Fiber Co., Ltd., Hengdian, China	BFRP	8.0	Vinylester	R	NC	Control	NA	0	3	100.0
172	Dong et al. (2016)	Zhejiang GBF Basalt Fiber Co., Ltd., Hengdian, China	BFRP	8.0	Vinylester	S	NC	Control	NA	0	3	100.0
173	Dong et al. (2016)	Zhejiang GBF Basalt Fiber Co., Ltd., Hengdian, China	BFRP	8.0	Epoxy	R	NC	Control	NA	0	3	100.0
174	Dong et al. (2016)	Taishan Fiberglass Inc. Tai'an, China	GFRP	8.0	Vinylester	R	NC	Control	NA	0	3	100.0
175	Dong et al. (2016)	Zhongfu Shenying Carbon Fiber Co., Ltd., Lianyungang, China	CFRP	8.0	Epoxy	R	NC	Control	NA	0	3	100.0
176	Dong et al. (2016)	Zhejiang GBF Basalt Fiber Co., Ltd., Hengdian, China	BFRP	8.0	Vinylester	R	NC	Simulated seawater (IMMR)	25	30	3	103.0
177	Dong et al. (2016)	Zhejiang GBF Basalt Fiber Co., Ltd., Hengdian, China	BFRP	8.0	Vinylester	R	NC	Simulated seawater (IMMR)	25	45	3	106.7
178	Dong et al. (2016)	Zhejiang GBF Basalt Fiber Co., Ltd., Hengdian,	BFRP	8.0	Vinylester	R	NC	Simulated seawater (IMMR)	25	60	3	94.0

179	Dong et al. (2016)			China Zhejiang GBF Basalt Fiber Co., Ltd., Hengdian, China	BFRP	8.0	Vinylester	R	NC	Simulated (IMMR)	seawater	40	15	3	97.7
180	Dong et al. (2016)			Zhejiang GBF Basalt Fiber Co., Ltd., Hengdian, China	BFRP	8.0	Vinylester	R	NC	Simulated (IMMR)	seawater	40	30	3	98.7
181	Dong et al. (2016)			Zhejiang GBF Basalt Fiber Co., Ltd., Hengdian, China	BFRP	8.0	Vinylester	R	NC	Simulated (IMMR)	seawater	40	45	3	94.1
182	Dong et al. (2016)			Zhejiang GBF Basalt Fiber Co., Ltd., Hengdian, China	BFRP	8.0	Vinylester	R	NC	Simulated (IMMR)	seawater	40	60	3	91.0
183	Dong et al. (2016)			Zhejiang GBF Basalt Fiber Co., Ltd., Hengdian, China	BFRP	8.0	Vinylester	R	NC	Simulated (IMMR)	seawater	55	30	3	94.1
184	Dong et al. (2016)			Zhejiang GBF Basalt Fiber Co., Ltd., Hengdian, China	BFRP	8.0	Vinylester	R	NC	Simulated (IMMR)	seawater	55	45	3	87.5
185	Dong et al. (2016)			Zhejiang GBF Basalt Fiber Co., Ltd., Hengdian, China	BFRP	8.0	Vinylester	R	NC	Simulated (IMMR)	seawater	55	60	3	87.1
186	Dong et al. (2016)			Zhejiang GBF Basalt Fiber Co., Ltd., Hengdian, China	BFRP	8.0	Vinylester	S	NC	Simulated (IMMR)	seawater	40	15	3	119.1
187	Dong et al. (2016)			Zhejiang GBF Basalt Fiber Co., Ltd., Hengdian, China	BFRP	8.0	Vinylester	S	NC	Simulated (IMMR)	seawater	40	30	3	190.0
188	Dong et al. (2016)			Zhejiang GBF Basalt Fiber Co., Ltd., Hengdian, China	BFRP	8.0	Vinylester	S	NC	Simulated (IMMR)	seawater	40	45	3	139.5
189	Dong et al. (2016)			Zhejiang GBF Basalt Fiber Co., Ltd., Hengdian, China	BFRP	8.0	Vinylester	S	NC	Simulated (IMMR)	seawater	40	60	3	135.9
190	Dong et al. (2016)			Zhejiang GBF Basalt Fiber Co., Ltd., Hengdian, China	BFRP	8.0	Epoxy	R	NC	Simulated (IMMR)	seawater	40	15	3	107.4
191	Dong et al. (2016)			Zhejiang GBF Basalt Fiber Co., Ltd., Hengdian, China	BFRP	8.0	Epoxy	R	NC	Simulated (IMMR)	seawater	40	30	3	99.9
192	Dong et al. (2016)			Zhejiang GBF Basalt Fiber Co., Ltd., Hengdian, China	BFRP	8.0	Epoxy	R	NC	Simulated (IMMR)	seawater	40	45	3	103.2
193	Dong et al. (2016)			Zhejiang GBF Basalt Fiber Co., Ltd., Hengdian, China	BFRP	8.0	Epoxy	R	NC	Simulated (IMMR)	seawater	40	60	3	101.4

194	Dong et al. (2016)	Taishan Fiberglass Inc. Tai'an, China	GFRP	8.0	Vinylester	R	NC	Simulated (IMMR)	seawater	40	15	3	102.6
195	Dong et al. (2016)	Taishan Fiberglass Inc. Tai'an, China	GFRP	8.0	Vinylester	R	NC	Simulated (IMMR)	seawater	40	30	3	94.4
196	Dong et al. (2016)	Taishan Fiberglass Inc. Tai'an, China	GFRP	8.0	Vinylester	R	NC	Simulated (IMMR)	seawater	40	45	3	107.1
197	Dong et al. (2016)	Taishan Fiberglass Inc. Tai'an, China	GFRP	8.0	Vinylester	R	NC	Simulated (IMMR)	seawater	40	60	3	92.9
198	Dong et al. (2016)	Zhongfu Shenying Carbon Fiber Co., Ltd., Lianyungang, China	CFRP	8.0	Epoxy	R	NC	Simulated (IMMR)	seawater	25	30	3	101.5
199	Dong et al. (2016)	Zhongfu Shenying Carbon Fiber Co., Ltd., Lianyungang, China	CFRP	8.0	Epoxy	R	NC	Simulated (IMMR)	seawater	25	45	3	110.0
200	Dong et al. (2016)	Zhongfu Shenying Carbon Fiber Co., Ltd., Lianyungang, China	CFRP	8.0	Epoxy	R	NC	Simulated (IMMR)	seawater	40	15	3	105.6
201	Dong et al. (2016)	Zhongfu Shenying Carbon Fiber Co., Ltd., Lianyungang, China	CFRP	8.0	Epoxy	R	NC	Simulated (IMMR)	seawater	40	30	3	120.4
202	Dong et al. (2016)	Zhongfu Shenying Carbon Fiber Co., Ltd., Lianyungang, China	CFRP	8.0	Epoxy	R	NC	Simulated (IMMR)	seawater	40	45	3	NA
203	Dong et al. (2016)	Zhongfu Shenying Carbon Fiber Co., Ltd., Lianyungang, China	CFRP	8.0	Epoxy	R	NC	Simulated (IMMR)	seawater	55	30	3	98.7
204	Dong et al. (2016)	Zhongfu Shenying Carbon Fiber Co., Ltd., Lianyungang, China	CFRP	8.0	Epoxy	R	NC	Simulated (IMMR)	seawater	55	45	3	101.2
205	Dong et al. (2018b)	Zhejiang GBF Basalt Fiber Co., Ltd., Hengdian, China	BFRP	13.0	Vinylester	R	SSC	Control		NA	0	3	100.0
206	Dong et al. (2018b)	Zhejiang GBF Basalt Fiber Co., Ltd., Hengdian, China	BFRP	13.0	Vinylester	R	SSC	Simulated (IMMR)	seawater	50	90	3	91.6
207	Dong et al. (2018b)	Zhejiang GBF Basalt Fiber Co., Ltd., Hengdian, China	BFRP	13.0	Vinylester	R	SSC	Simulated (IMMR)	seawater	50	180	3	79.9
208	Dong et al. (2018b)	Zhejiang GBF Basalt Fiber Co., Ltd., Hengdian, China	BFRP	13.0	Vinylester	R	SSC	Simulated (IMMR)	seawater	50	270	3	78.4
209	Dong et al. (2018b)	Zhejiang GBF Basalt Fiber Co., Ltd., Hengdian, China	BFRP	13.0	Vinylester	R	SSC	Simulated (WD)	seawater	40	90	3	87.3
210	Dong et al. (2018b)	Zhejiang GBF Basalt Fiber Co., Ltd., Hengdian,	BFRP	13.0	Vinylester	R	SSC	Simulated (WD)	seawater	40	180	3	104.7

211	Dong et al. (2018b)	China Zhejiang GBF Basalt Fiber Co., Ltd., Hengdian, China	BFRP	13.0	Vinylester	R	SSC	Simulated seawater (WD)	40	270	3	92.0
212	El Refai et al. (2015)	Magmatech and Sudaglass	BFRP	12.0	NA	HW	NC	Control	NA	0	3	100.0
213	El Refai et al. (2015)	Magmatech and Sudaglass	BFRP	12.0	NA	HW+S	NC	Control	NA	0	5	100.0
214	El Refai et al. (2015)	Pultron	GFRP	12.0	NA	R	NC	Control	NA	0	3	100.0
215	El Refai et al. (2015)	Magmatech and Sudaglass	BFRP	12.0	NA	HW	NC	Water (IMMR)	RT	90	3	94.7
216	El Refai et al. (2015)	Magmatech and Sudaglass	BFRP	12.0	NA	HW+S	NC	Water (IMMR)	RT	90	3	87.1
217	El Refai et al. (2015)	Pultron	GFRP	12.0	NA	R	NC	Water (IMMR)	RT	90	3	101.6
218	El Refai et al. (2015)	Magmatech and Sudaglass	BFRP	12.0	NA	HW	NC	Simulated seawater (IMMR)	60	90	3	94.8
219	El Refai et al. (2015)	Magmatech and Sudaglass	BFRP	12.0	NA	HW+S	NC	Simulated seawater (IMMR)	60	90	3	85.8
220	El Refai et al. (2015)	Pultron	GFRP	12.0	NA	R	NC	Simulated seawater (IMMR)	60	90	3	95.9
221	El Refai et al. (2015)	Magmatech and Sudaglass	BFRP	12.0	NA	HW	NC	HT	80	90	3	117.0
222	El Refai et al. (2015)	Magmatech and Sudaglass	BFRP	12.0	NA	HW+S	NC	HT	80	90	3	96.4
223	El Refai et al. (2015)	Pultron	GFRP	12.0	NA	R	NC	HT	80	90	3	112.8
224	El Refai et al. (2015)	Magmatech and Sudaglass	BFRP	12.0	NA	HW	NC	HT+Water (IMMR)	80+RT	60+30	3	102.0
225	El Refai et al. (2015)	Magmatech and Sudaglass	BFRP	12.0	NA	HW+S	NC	HT+Water (IMMR)	80+RT	60+30	3	91.6
226	El Refai et al. (2015)	Pultron	GFRP	12.0	NA	R	NC	HT+Water (IMMR)	80+RT	60+30	3	108.4
227	El Refai et al. (2015)	Magmatech and Sudaglass	BFRP	12.0	NA	HW	NC	HT+Simulated seawater (IMMR)	80+60	60+30	3	103.5
228	El Refai et al. (2015)	Magmatech and Sudaglass	BFRP	12.0	NA	HW+S	NC	HT+Simulated seawater (IMMR)	80+60	60+30	3	68.9
229	El Refai et al. (2015)	Pultron	GFRP	12.0	NA	R	NC	HT+Simulated seawater (IMMR)	80+60	60+30	3	102.2
230	Feng et al. (2024)	Green Materials Valley	BFRP	8.0	Epoxy	S	SWSSC	Simulated seawater (IMMR)	55	0	3	100.0
231	Feng et al. (2024)	Green Materials Valley	BFRP	8.0	Epoxy	S	SWSSC	Simulated seawater (IMMR)	55	60	3	79.0
232	Feng et al. (2024)	Green Materials Valley	BFRP	8.0	Epoxy	S	SWSSC	Simulated seawater (IMMR)	55	120	3	70.0

233	Feng et al. (2024)	Green Materials Valley	BFRP	8.0	Epoxy	S	SWSSC	Simulated (IMMR)	seawater	55	180	3	49.5
234	Feng et al. (2024)	Green Materials Valley	BFRP	8.0	Epoxy	R	SWSSC	Simulated (IMMR)	seawater	55	0	3	100.0
235	Feng et al. (2024)	Green Materials Valley	BFRP	8.0	Epoxy	R	SWSSC	Simulated (IMMR)	seawater	55	60	3	68.0
236	Feng et al. (2024)	Green Materials Valley	BFRP	8.0	Epoxy	R	SWSSC	Simulated (IMMR)	seawater	55	120	3	44.4
237	Feng et al. (2024)	Green Materials Valley	BFRP	8.0	Epoxy	R	SWSSC	Simulated (IMMR)	seawater	55	180	3	37.0
238	Feng et al. (2024)	Green Materials Valley	BFRP	8.0	Epoxy	HW	SWSSC	Simulated (IMMR)	seawater	55	0	3	100.0
239	Feng et al. (2024)	Green Materials Valley	BFRP	8.0	Epoxy	HW	SWSSC	Simulated (IMMR)	seawater	55	60	3	72.9
240	Feng et al. (2024)	Green Materials Valley	BFRP	8.0	Epoxy	HW	SWSSC	Simulated (IMMR)	seawater	55	120	3	49.1
241	Feng et al. (2024)	Green Materials Valley	BFRP	8.0	Epoxy	HW	SWSSC	Simulated (IMMR)	seawater	55	180	3	29.6
242	Galati et al. (2004)	Hughes Brothers Company (Seward, NE, USA)	GFRP	9.5	NA	HW+S	NC	Control		NA	0	3	100.0
243	Galati et al. (2004)	Hughes Brothers Company (Seward, NE, USA)	GFRP	9.5	NA	HW+S	NC	Control		NA	0	3	100.0
244	Galati et al. (2004)	Hughes Brothers Company (Seward, NE, USA)	GFRP	9.5	NA	HW+S	NC	Control		NA	0	3	100.0
245	Galati et al. (2004)	Hughes Brothers Company (Seward, NE, USA)	GFRP	9.5	NA	HW+S	NC	Control		NA	0	3	100.0
246	Galati et al. (2004)	Hughes Brothers Company (Seward, NE, USA)	GFRP	9.5	NA	HW+S	NC	Control		NA	0	3	100.0
247	Galati et al. (2004)	Hughes Brothers Company (Seward, NE, USA)	GFRP	9.5	NA	HW+S	NC	Control		NA	0	3	100.0
248	Galati et al. (2004)	Hughes Brothers Company (Seward, NE, USA)	GFRP	9.5	NA	HW+S	NC	HT		70	8.3	3	97.4
249	Galati et al. (2004)	Hughes Brothers Company (Seward, NE, USA)	GFRP	9.5	NA	HW+S	NC	HT		70	8.3	3	97.4
250	Galati et al. (2004)	Hughes Brothers Company (Seward, NE, USA)	GFRP	9.5	NA	HW+S	NC	HT		70	8.3	3	96.7
251	Galati et al.	Hughes Brothers	GFRP	9.5	NA	HW+S	NC	HT		70	8.3	3	84.0

	(2004)	Company (Seward, NE, USA)												
252	Galati et al. (2004)	Hughes Brothers Company (Seward, NE, USA)	GFRP	9.5	NA	HW+S	NC	HT		70	8.3	3	104.7	
253	Galati et al. (2004)	Hughes Brothers Company (Seward, NE, USA)	GFRP	9.5	NA	HW+S	NC	HT		70	8.3	3	88.4	
254	Hassan et al. (2016)	ASA.TEC GMBH (Austria)	BFRP	12.0	Vinylester	R	NC	Control		23	0	5	100.0	
255	Hassan et al. (2016)	ASA.TEC GMBH (Austria)	BFRP	12.0	Vinylester	R	NC	Alkaline (IMMR)	solution	40	45	5	95.7	
256	Hassan et al. (2016)	ASA.TEC GMBH (Austria)	BFRP	12.0	Vinylester	R	NC	Alkaline (IMMR)	solution	40	90	5	85.9	
257	Hassan et al. (2016)	ASA.TEC GMBH (Austria)	BFRP	12.0	Vinylester	R	NC	Alkaline (IMMR)	solution	40	180	5	80.7	
258	Hassan et al. (2016)	ASA.TEC GMBH (Austria)	BFRP	12.0	Vinylester	R	NC	Alkaline (IMMR)	solution	50	45	5	124.7	
259	Hassan et al. (2016)	ASA.TEC GMBH (Austria)	BFRP	12.0	Vinylester	R	NC	Alkaline (IMMR)	solution	50	90	5	119.0	
260	Hassan et al. (2016)	ASA.TEC GMBH (Austria)	BFRP	12.0	Vinylester	R	NC	Alkaline (IMMR)	solution	50	180	5	116.3	
261	Hassan et al. (2016)	ASA.TEC GMBH (Austria)	BFRP	12.0	Vinylester	R	NC	Alkaline (IMMR)	solution	60	45	5	125.6	
262	Hassan et al. (2016)	ASA.TEC GMBH (Austria)	BFRP	12.0	Vinylester	R	NC	Alkaline (IMMR)	solution	60	90	5	123.8	
263	Hassan et al. (2016)	ASA.TEC GMBH (Austria)	BFRP	12.0	Vinylester	R	NC	Alkaline (IMMR)	solution	60	180	5	118.8	
264	Hussain et al. (2022)	Hengshui Aoliadne trading Co. Ltd., Hengshui. China	BFRP	12.7	Polyester	R	HSC	Reference		NA	30	2	100.0	
265	Hussain et al. (2022)	Hengshui Aoliadne trading Co. Ltd., Hengshui. China	BFRP	12.7	Polyester	R	HSC	Reference		NA	30	2	100.0	
266	Hussain et al. (2022)	Hengshui Aoliadne trading Co. Ltd., Hengshui. China	BFRP	12.7	Polyester	R	HSC	Reference		NA	30	2	100.0	
267	Hussain et al. (2022)	Hengshui Aoliadne trading Co. Ltd., Hengshui. China	BFRP	15.9	Polyester	R	HSC	Reference		NA	30	2	100.0	
268	Hussain et al. (2022)	Hengshui Aoliadne trading Co. Ltd., Hengshui. China	BFRP	15.9	Polyester	R	HSC	Reference		NA	30	2	100.0	
269	Hussain et al. (2022)	Hengshui Aoliadne trading Co. Ltd., Hengshui. China	BFRP	15.9	Polyester	R	HSC	Reference		NA	30	2	100.0	

270	Hussain et al. (2022)			Hengshui trading Co. Hengshui. China	Aoliadne Ltd.,	BFRP	19.0	Polyester	R	HSC	Reference		NA	30	2	100.0
271	Hussain et al. (2022)			Hengshui trading Co. Hengshui. China	Aoliadne Ltd.,	BFRP	19.0	Polyester	R	HSC	Reference		NA	30	2	100.0
272	Hussain et al. (2022)			Hengshui trading Co. Hengshui. China	Aoliadne Ltd.,	BFRP	19.0	Polyester	R	HSC	Reference		NA	30	2	100.0
273	Hussain et al. (2022)			Hengshui trading Co. Hengshui. China	Aoliadne Ltd.,	BFRP	12.7	Polyester	R	HSC	Alkaline (IMMR)	solution	RT	90	2	84.2
274	Hussain et al. (2022)			Hengshui trading Co. Hengshui. China	Aoliadne Ltd.,	BFRP	12.7	Polyester	R	HSC	Alkaline (IMMR)	solution	RT	90	2	83.3
275	Hussain et al. (2022)			Hengshui trading Co. Hengshui. China	Aoliadne Ltd.,	BFRP	15.9	Polyester	R	HSC	Alkaline (IMMR)	solution	RT	90	2	84.1
276	Hussain et al. (2022)			Hengshui trading Co. Hengshui. China	Aoliadne Ltd.,	BFRP	15.9	Polyester	R	HSC	Alkaline (IMMR)	solution	RT	90	2	80.4
277	Hussain et al. (2022)			Hengshui trading Co. Hengshui. China	Aoliadne Ltd.,	BFRP	15.9	Polyester	R	HSC	Alkaline (IMMR)	solution	RT	90	2	81.9
278	Hussain et al. (2022)			Hengshui trading Co. Hengshui. China	Aoliadne Ltd.,	BFRP	19.0	Polyester	R	HSC	Alkaline (IMMR)	solution	RT	90	2	80.4
279	Hussain et al. (2022)			Hengshui trading Co. Hengshui. China	Aoliadne Ltd.,	BFRP	19.0	Polyester	R	HSC	Alkaline (IMMR)	solution	RT	90	2	79.4
280	Hussain et al. (2022)			Hengshui trading Co. Hengshui. China	Aoliadne Ltd.,	BFRP	19.0	Polyester	R	HSC	Alkaline (IMMR)	solution	RT	90	2	81.1
281	Hussain et al. (2022)			Hengshui trading Co. Hengshui. China	Aoliadne Ltd.,	BFRP	19.0	Polyester	R	HSC	Alkaline (IMMR)	solution	RT	90	2	80.5
282	Hussain et al. (2022)			Hengshui trading Co. Hengshui. China	Aoliadne Ltd.,	BFRP	12.7	Polyester	R	HSC	Simulated (IMMR)	seawater	RT	90	2	87.5
283	Hussain et al. (2022)			Hengshui trading Co. Hengshui. China	Aoliadne Ltd.,	BFRP	12.7	Polyester	R	HSC	Simulated (IMMR)	seawater	RT	90	2	88.3
284	Hussain et al. (2022)			Hengshui trading Co. Hengshui. China	Aoliadne Ltd.,	BFRP	15.9	Polyester	R	HSC	Simulated (IMMR)	seawater	RT	90	2	82.1
285	Hussain et al.			Hengshui	Aoliadne	BFRP	15.9	Polyester	R	HSC	Simulated	seawater	RT	90	2	87.5

	(2022)	trading Co. Ltd., Hengshui. China							(IMMR)				
286	Hussain et al. (2022)	Hengshui Aoliadne trading Co. Ltd., Hengshui. China	BFRP	15.9	Polyester	R	HSC	Simulated seawater (IMMR)	RT	90	2	85.5
287	Hussain et al. (2022)	Hengshui Aoliadne trading Co. Ltd., Hengshui. China	BFRP	19.0	Polyester	R	HSC	Simulated seawater (IMMR)	RT	90	2	84.9
288	Hussain et al. (2022)	Hengshui Aoliadne trading Co. Ltd., Hengshui. China	BFRP	19.0	Polyester	R	HSC	Simulated seawater (IMMR)	RT	90	2	82.6
289	Hussain et al. (2022)	Hengshui Aoliadne trading Co. Ltd., Hengshui. China	BFRP	19.0	Polyester	R	HSC	Simulated seawater (IMMR)	RT	90	2	83.3
290	Hussain et al. (2022)	Hengshui Aoliadne trading Co. Ltd., Hengshui. China	BFRP	19.0	Polyester	R	HSC	Simulated seawater (IMMR)	RT	90	2	82.5
291	Kazemi et al. (2022)	NA	GFRP	10.0	Epoxy	S	NC	Reference	25	250	3	100.0
292	Kazemi et al. (2022)	NA	GFRP	10.0	Epoxy	S	NC	Water (IMMR)	25	250	3	105.2
293	Kazemi et al. (2022)	NA	GFRP	10.0	Epoxy	S	NC	Simulated seawater (IMMR)	25	250	3	98.2
294	Kazemi et al. (2022)	NA	GFRP	10.0	Epoxy	S	NC	Simulated seawater (WD)	25	250	3	96.7
295	Kazemi et al. (2022)	NA	GFRP	10.0	Epoxy	S	SWC	Reference	25	250	3	100.0
296	Kazemi et al. (2022)	NA	GFRP	10.0	Epoxy	S	SWC	Water (IMMR)	25	250	3	113.4
297	Kazemi et al. (2022)	NA	GFRP	10.0	Epoxy	S	SWC	Simulated seawater (IMMR)	25	250	3	80.4
298	Kazemi et al. (2022)	NA	GFRP	10.0	Epoxy	S	SWC	Simulated seawater (WD)	25	250	3	91.8
299	Khanfour and El Refai (2017)	NA	BFRP	8.0	NA	S	NC	Control	RT	0	3	100.0
300	Khanfour and El Refai (2017)	NA	BFRP	10.0	NA	S	NC	Control	RT	0	3	100.0
301	Khanfour and El Refai (2017)	NA	BFRP	12.0	NA	S	NC	Control	RT	0	3	100.0
302	Khanfour and El Refai (2017)	NA	BFRP	8.0	NA	S	NC	FT	-25~15	50	3	103.6
303	Khanfour and El Refai (2017)	NA	BFRP	10.0	NA	S	NC	FT	-25~15	50	3	109.6
304	Khanfour and El Refai (2017)	NA	BFRP	12.0	NA	S	NC	FT	-25~15	50	3	134.0
305	Khanfour and El	NA	BFRP	8.0	NA	S	NC	FT	-25~15	100	3	112.7

	Refai (2017)											
306	Khanfour and El Refai (2017)	NA	BFRP	10.0	NA	S	NC	FT	-25~15	100	3	101.2
307	Khanfour and El Refai (2017)	NA	BFRP	12.0	NA	S	NC	FT	-25~15	100	3	104.1
308	Khanfour and El Refai (2017)	NA	BFRP	8.0	NA	S	NC	LT	-20	10	3	94.0
309	Khanfour and El Refai (2017)	NA	BFRP	10.0	NA	S	NC	LT	-20	10	3	90.4
310	Khanfour and El Refai (2017)	NA	BFRP	12.0	NA	S	NC	LT	-20	10	3	108.8
311	Khatibmasjedi et al. (2020)	NA	GFRP	15.8	Vinylester	HW	NC	Control	NA	0	NA	100.0
312	Khatibmasjedi et al. (2020)	NA	GFRP	15.8	Vinylester	HW	NC	Seawater (IMMR)	60	360	NA	100.0
313	Khatibmasjedi et al. (2020)	NA	GFRP	15.8	Vinylester	HW	NC	Seawater (IMMR)	60	540	NA	116.7
314	Khatibmasjedi et al. (2020)	NA	GFRP	15.8	Vinylester	HW	NC	Seawater (IMMR)	60	720	NA	106.8
315	Khatibmasjedi et al. (2020)	NA	GFRP	15.8	Vinylester	HW	SWC	Control	NA	0	NA	100.0
316	Khatibmasjedi et al. (2020)	NA	GFRP	15.8	Vinylester	HW	SWC	Seawater (IMMR)	60	360	NA	104.8
317	Khatibmasjedi et al. (2020)	NA	GFRP	15.8	Vinylester	HW	SWC	Seawater (IMMR)	60	540	NA	97.6
318	Khatibmasjedi et al. (2020)	NA	GFRP	15.8	Vinylester	HW	SWC	Seawater (IMMR)	60	720	NA	88.6
319	Kim and Chai (2020)	NA	GFRP	13.0	Vinylester	HW	NC	Control	23	0	3	100.0
320	Kim and Chai (2020)	NA	BFRP	10.0	Epoxy	NA	NC	Control	23	0	3	100.0
321	Kim and Chai (2020)	NA	GFRP	13.0	Vinylester	HW	NC	Saline solution (IMMR)	RT	14	3	89.9
322	Kim and Chai (2020)	NA	GFRP	13.0	Vinylester	HW	NC	Saline solution (IMMR)	RT	28	3	83.3
323	Kim and Chai (2020)	NA	GFRP	13.0	Vinylester	HW	NC	Saline solution (IMMR)	RT	42	3	78.9
324	Kim and Chai (2020)	NA	GFRP	13.0	Vinylester	HW	NC	Saline solution (IMMR)	RT	56	3	67.9
325	Kim and Chai (2020)	NA	GFRP	13.0	Vinylester	HW	NC	Saline solution (IMMR)	RT	70	3	54.9
326	Kim and Chai (2020)	NA	BFRP	10.0	Epoxy	NA	NC	Saline solution (IMMR)	RT	14	3	92.8
327	Kim and Chai (2020)	NA	BFRP	10.0	Epoxy	NA	NC	Saline solution (IMMR)	RT	28	3	92.6
328	Kim and Chai	NA	BFRP	10.0	Epoxy	NA	NC	Saline solution	RT	42	3	88.2

	(2020)							(IMMR)					
329	Kim and Chai (2020)	NA	BFRP	10.0	Epoxy	NA	NC	Saline (IMMR)	solution	RT	56	3	82.3
330	Kim and Chai (2020)	NA	BFRP	10.0	Epoxy	NA	NC	Saline (IMMR)	solution	RT	70	3	80.7
331	Li et al. (2023)	NA	BFRP	8.0	Epoxy	R	SWSSC	Control		RT	0	3	100.0
332	Li et al. (2023)	NA	BFRP	8.0	Epoxy	R	SWSSC	Simulated (IMMR)	seawater	25	90 d	3	108.3
333	Li et al. (2023)	NA	BFRP	8.0	Epoxy	R	SWSSC	Simulated (IMMR)	seawater	25	180 d	3	98.1
334	Li et al. (2023)	NA	BFRP	8.0	Epoxy	R	SWSSC	Simulated (IMMR)	seawater	25	270 d	3	93.6
335	Li et al. (2023)	NA	BFRP	8.0	Epoxy	R	SWSSC	Simulated (IMMR)	seawater	55	90 d	3	89.9
336	Li et al. (2023)	NA	BFRP	8.0	Epoxy	R	SWSSC	Simulated (IMMR)	seawater	55	180 d	3	83.7
337	Li et al. (2023)	NA	BFRP	8.0	Epoxy	R	SWSSC	Simulated (IMMR)	seawater	55	270 d	3	75.6
338	Lu et al. (2021c)	Tuo Xin Aerospace Basalt Industrial Co., Ltd., Chengdu, China	BFRP	12.0	Epoxy	S	NC	Control		RT	0	3	100.0
339	Lu et al. (2021c)	Tuo Xin Aerospace Basalt Industrial Co., Ltd., Chengdu, China	BFRP	12.0	Epoxy	S	NC	Alkaline (IMMR)	solution	26	30	3	87.0
340	Lu et al. (2021c)	Tuo Xin Aerospace Basalt Industrial Co., Ltd., Chengdu, China	BFRP	12.0	Epoxy	S	NC	Alkaline (IMMR)	solution	26	90	3	77.0
341	Lu et al. (2021c)	Tuo Xin Aerospace Basalt Industrial Co., Ltd., Chengdu, China	BFRP	12.0	Epoxy	S	NC	Alkaline (IMMR)	solution	26	180	3	45.5
342	Lu et al. (2021c)	Tuo Xin Aerospace Basalt Industrial Co., Ltd., Chengdu, China	BFRP	12.0	Epoxy	S	NC	Alkaline (IMMR)	solution	40	30	3	72.0
343	Lu et al. (2021c)	Tuo Xin Aerospace Basalt Industrial Co., Ltd., Chengdu, China	BFRP	12.0	Epoxy	S	NC	Alkaline (IMMR)	solution	40	90	3	54.0
344	Lu et al. (2021c)	Tuo Xin Aerospace Basalt Industrial Co., Ltd., Chengdu, China	BFRP	12.0	Epoxy	S	NC	Alkaline (IMMR)	solution	40	180	3	49.0
345	Lu et al. (2021c)	Tuo Xin Aerospace Basalt Industrial Co., Ltd., Chengdu, China	BFRP	12.0	Epoxy	S	NC	Alkaline (IMMR)	solution	60	30	3	45.0
346	Lu et al. (2021c)	Tuo Xin Aerospace Basalt Industrial Co., Ltd., Chengdu, China	BFRP	12.0	Epoxy	S	NC	Alkaline (IMMR)	solution	60	90	3	28.0
347	Lu et al. (2021c)	Tuo Xin Aerospace Basalt	BFRP	12.0	Epoxy	S	NC	Alkaline	solution	60	180	3	31.0

		Industrial Co., Ltd., Chengdu, China						(IMMR)					
348	Lu et al. (2021c)	Tuo Xin Aerospace Basalt Industrial Co., Ltd., Chengdu, China	BFRP	12.0	Epoxy	S	NC	Simulated (IMMR)	seawater	26	30	3	78.0
349	Lu et al. (2021c)	Tuo Xin Aerospace Basalt Industrial Co., Ltd., Chengdu, China	BFRP	12.0	Epoxy	S	NC	Simulated (IMMR)	seawater	26	90	3	69.0
350	Lu et al. (2021c)	Tuo Xin Aerospace Basalt Industrial Co., Ltd., Chengdu, China	BFRP	12.0	Epoxy	S	HSC	Simulated (IMMR)	seawater	26	180	3	58.0
351	Lu et al. (2021c)	Tuo Xin Aerospace Basalt Industrial Co., Ltd., Chengdu, China	BFRP	12.0	Epoxy	S	NC	Simulated (IMMR)	seawater	26	360	3	65.0
352	Lu et al. (2021c)	Tuo Xin Aerospace Basalt Industrial Co., Ltd., Chengdu, China	BFRP	12.0	Epoxy	S	NC	Simulated (IMMR)	seawater	40	30	3	72.0
353	Lu et al. (2021c)	Tuo Xin Aerospace Basalt Industrial Co., Ltd., Chengdu, China	BFRP	12.0	Epoxy	S	NC	Simulated (IMMR)	seawater	40	90	3	53.0
354	Lu et al. (2021c)	Tuo Xin Aerospace Basalt Industrial Co., Ltd., Chengdu, China	BFRP	12.0	Epoxy	S	HSC	Simulated (IMMR)	seawater	40	180	3	51.0
355	Lu et al. (2021c)	Tuo Xin Aerospace Basalt Industrial Co., Ltd., Chengdu, China	BFRP	12.0	Epoxy	S	HSC	Simulated (IMMR)	seawater	40	360	3	57.0
356	Lu et al. (2021c)	Tuo Xin Aerospace Basalt Industrial Co., Ltd., Chengdu, China	BFRP	12.0	Epoxy	S	NC	Simulated (IMMR)	seawater	60	30	3	52.0
357	Lu et al. (2021c)	Tuo Xin Aerospace Basalt Industrial Co., Ltd., Chengdu, China	BFRP	12.0	Epoxy	S	NC	Simulated (IMMR)	seawater	60	90	3	49.0
358	Lu et al. (2021c)	Tuo Xin Aerospace Basalt Industrial Co., Ltd., Chengdu, China	BFRP	12.0	Epoxy	S	NC	Simulated (IMMR)	seawater	60	180	3	45.0
359	Lu et al. (2021c)	Tuo Xin Aerospace Basalt Industrial Co., Ltd., Chengdu, China	BFRP	12.0	Epoxy	S	NC	Simulated (IMMR)	seawater	60	360	3	29.0
360	Nassar et al. (2022)	NA	GFRP	9.4	NA	S	NC	Control		20	0	4	NA
361	Nassar et al. (2022)	NA	GFRP	9.4	Epoxy	S	NC	Control		20	0	4	NA
362	Nassar et al. (2022)	NA	GFRP	9.4	NA	S	NC	Control		20	0	4	NA
363	Nassar et al. (2022)	NA	GFRP	9.4	Epoxy	S	NC	Control		20	0	4	NA

364	Nassar et al. (2022)	NA	GFRP	9.4	NA	S	NC	Water (IMMR)	60	21	3	NA
365	Nassar et al. (2022)	NA	GFRP	9.4	Epoxy	S	NC	Water (IMMR)	60	21	3	NA
366	Nassar et al. (2022)	NA	GFRP	9.4	NA	S	NC	Water (IMMR)	60	21	3	NA
367	Nassar et al. (2022)	NA	GFRP	9.4	Epoxy	S	NC	Water (IMMR)	60	21	3	NA
368	Robert and Benmokrane (2010)	Pultrall Inc. Canada	GFRP	19.0	Vinylester	S	NC	Control	23	180	5	100.0
369	Robert and Benmokrane (2010)	Pultrall Inc. Canada	GFRP	19.0	Vinylester	S	NC	Water (IMMR)	23	60	5	100.0
370	Robert and Benmokrane (2010)	Pultrall Inc. Canada	GFRP	19.0	Vinylester	S	NC	Water (IMMR)	23	120	5	96.0
371	Robert and Benmokrane (2010)	Pultrall Inc. Canada	GFRP	19.0	Vinylester	S	NC	Water (IMMR)	23	180	5	94.0
372	Robert and Benmokrane (2010)	Pultrall Inc. Canada	GFRP	19.0	Vinylester	S	NC	Water (IMMR)	40	60	5	99.3
373	Robert and Benmokrane (2010)	Pultrall Inc. Canada	GFRP	19.0	Vinylester	S	NC	Water (IMMR)	40	120	5	95.3
374	Robert and Benmokrane (2010)	Pultrall Inc. Canada	GFRP	19.0	Vinylester	S	NC	Water (IMMR)	40	180	5	93.3
375	Robert and Benmokrane (2010)	Pultrall Inc. Canada	GFRP	19.0	Vinylester	S	NC	Water (IMMR)	50	60	5	97.3
376	Robert and Benmokrane (2010)	Pultrall Inc. Canada	GFRP	19.0	Vinylester	S	NC	Water (IMMR)	50	120	5	94.0
377	Robert and Benmokrane (2010)	Pultrall Inc. Canada	GFRP	19.0	Vinylester	S	NC	Water (IMMR)	50	180	5	92.0
378	Rolland et al. (2021)	Pultrall Inc. Canada	GFRP	12.7	Vinylester	S	NC	Control	20	0	4	100.0
379	Rolland et al. (2021)	Pultrall Inc. Canada	GFRP	12.7	Vinylester	S	NC	Alkaline solution (IMMR)	20	120	4	117.1
380	Rolland et al. (2021)	Pultrall Inc. Canada	GFRP	12.7	Vinylester	S	NC	Alkaline solution (IMMR)	20	240	4	116.5
381	Rolland et al. (2021)	Pultrall Inc. Canada	GFRP	12.7	Vinylester	S	NC	Alkaline solution (IMMR)	40	120	4	134.0

382	Rolland et al. (2021)	Pultrall Inc. Canada	GFRP	12.7	Vinylester	S	NC	Alkaline solution (IMMR)	40	240	4	116.9
383	Rolland et al. (2021)	Pultrall Inc. Canada	GFRP	12.7	Vinylester	S	NC	Alkaline solution (IMMR)	60	120	4	111.0
384	Rolland et al. (2021)	Pultrall Inc. Canada	GFRP	12.7	Vinylester	S	NC	Alkaline solution (IMMR)	60	240	4	120.8
385	Rolland et al. (2021)	Pultrall Inc. Canada	GFRP	12.7	Vinylester	S	NC	HT	40	120	4	130.7
386	Rolland et al. (2021)	Pultrall Inc. Canada	GFRP	12.7	Vinylester	S	NC	HT	40	240	4	114.4
387	Rolland et al. (2021)	Pultrall Inc. Canada	GFRP	12.7	Vinylester	S	NC	HT	60	120	4	150.7
388	Rolland et al. (2021)	Pultrall Inc. Canada	GFRP	12.7	Vinylester	S	NC	HT	60	240	4	123.1
389	Ruiz Emparanza et al. (2018)	NA	GFRP	10.0	NA	HW+S	NC	Control	NA	0	3	100.0
390	Ruiz Emparanza et al. (2018)	NA	GFRP	10.0	NA	HW	NC	Control	NA	0	3	100.0
391	Ruiz Emparanza et al. (2018)	NA	GFRP	10.0	NA	R	NC	Control	NA	0	3	100.0
392	Ruiz Emparanza et al. (2018)	NA	GFRP	10.0	NA	HW+S	NC	Seawater (IMMR)	23	60	3	80.1
393	Ruiz Emparanza et al. (2018)	NA	GFRP	10.0	NA	HW+S	NC	Seawater (IMMR)	23	120	3	85.3
394	Ruiz Emparanza et al. (2018)	NA	GFRP	10.0	NA	HW+S	NC	Seawater (IMMR)	40	60	3	100.3
395	Ruiz Emparanza et al. (2018)	NA	GFRP	10.0	NA	HW+S	NC	Seawater (IMMR)	40	120	3	79.8
396	Ruiz Emparanza et al. (2018)	NA	GFRP	10.0	NA	HW+S	NC	Seawater (IMMR)	60	60	3	88.6
397	Ruiz Emparanza et al. (2018)	NA	GFRP	10.0	NA	HW+S	NC	Seawater (IMMR)	60	120	3	86.2
398	Ruiz Emparanza et al. (2018)	NA	GFRP	10.0	NA	HW	NC	Seawater (IMMR)	23	60	3	86.7
399	Ruiz Emparanza et al. (2018)	NA	GFRP	10.0	NA	HW	NC	Seawater (IMMR)	23	120	3	106.1
400	Ruiz Emparanza et al. (2018)	NA	GFRP	10.0	NA	HW	NC	Seawater (IMMR)	40	60	3	89.8
401	Ruiz Emparanza et al. (2018)	NA	GFRP	10.0	NA	HW	NC	Seawater (IMMR)	40	120	3	104.7
402	Ruiz Emparanza et al. (2018)	NA	GFRP	10.0	NA	HW	NC	Seawater (IMMR)	60	60	3	96.9
403	Ruiz Emparanza et al. (2018)	NA	GFRP	10.0	NA	HW	NC	Seawater (IMMR)	60	120	3	91.5
404	Ruiz Emparanza et al. (2018)	NA	GFRP	10.0	NA	R	NC	Seawater (IMMR)	23	60	3	83.6

405	Ruiz Emparanza et al. (2018)	NA	GFRP	10.0	NA	R	NC	Seawater (IMMR)	23	120	3	95.2
406	Ruiz Emparanza et al. (2018)	NA	GFRP	10.0	NA	R	NC	Seawater (IMMR)	40	60	3	93.0
407	Ruiz Emparanza et al. (2018)	NA	GFRP	10.0	NA	R	NC	Seawater (IMMR)	40	120	3	88.3
408	Ruiz Emparanza et al. (2018)	NA	GFRP	10.0	NA	R	NC	Seawater (IMMR)	60	60	3	92.4
409	Ruiz Emparanza et al. (2018)	NA	GFRP	10.0	NA	R	NC	Seawater (IMMR)	60	120	3	89.5
410	Ruiz Emparanza et al. (2022)	NA	GFRP	10.2	Vinylester	HW+S	NC	Control	NA	0	5	100.0
411	Ruiz Emparanza et al. (2022)	NA	GFRP	10.5	Vinylester	G	NC	Control	NA	0	5	100.0
412	Ruiz Emparanza et al. (2022)	NA	GFRP	10.1	Vinylester	R	NC	Control	NA	0	5	100.0
413	Ruiz Emparanza et al. (2022)	NA	GFRP	10.7	Vinylester	HM+S	NC	Control	NA	0	5	100.0
414	Ruiz Emparanza et al. (2022)	NA	GFRP	10.8	Epoxy	G	NC	Control	NA	0	5	100.0
415	Ruiz Emparanza et al. (2022)	NA	GFRP	10.3	Vinylester	HW+S	NC	Control	NA	0	5	100.0
416	Ruiz Emparanza et al. (2022)	NA	GFRP	10.2	Vinylester	HW+S	NC	Seawater (IMMR)	23	60	3	81.0
417	Ruiz Emparanza et al. (2022)	NA	GFRP	10.2	Vinylester	HW+S	NC	Seawater (IMMR)	23	120	3	86.0
418	Ruiz Emparanza et al. (2022)	NA	GFRP	10.2	Vinylester	HW+S	NC	Seawater (IMMR)	23	210	3	92.0
419	Ruiz Emparanza et al. (2022)	NA	GFRP	10.2	Vinylester	HW+S	NC	Seawater (IMMR)	23	360	3	96.0
420	Ruiz Emparanza et al. (2022)	NA	GFRP	10.5	Vinylester	G	NC	Seawater (IMMR)	23	60	3	91.0
421	Ruiz Emparanza et al. (2022)	NA	GFRP	10.5	Vinylester	G	NC	Seawater (IMMR)	23	120	3	106.0
422	Ruiz Emparanza et al. (2022)	NA	GFRP	10.5	Vinylester	G	NC	Seawater (IMMR)	23	210	3	93.0
423	Ruiz Emparanza et al. (2022)	NA	GFRP	10.5	Vinylester	G	NC	Seawater (IMMR)	23	360	3	104.0
424	Ruiz Emparanza et al. (2022)	NA	GFRP	10.1	Vinylester	R	NC	Seawater (IMMR)	23	60	3	94.0
425	Ruiz Emparanza et al. (2022)	NA	GFRP	10.1	Vinylester	R	NC	Seawater (IMMR)	23	120	3	95.0
426	Ruiz Emparanza et al. (2022)	NA	GFRP	10.1	Vinylester	R	NC	Seawater (IMMR)	23	210	3	82.0
427	Ruiz Emparanza et al. (2022)	NA	GFRP	10.1	Vinylester	R	NC	Seawater (IMMR)	23	360	3	97.0

428	Ruiz Emparanza et al. (2022)	NA	GFRP	10.7	Vinylester	HM+S	NC	Seawater (IMMR)	23	60	3	107.0
429	Ruiz Emparanza et al. (2022)	NA	GFRP	10.7	Vinylester	HM+S	NC	Seawater (IMMR)	23	120	3	108.0
430	Ruiz Emparanza et al. (2022)	NA	GFRP	10.7	Vinylester	HM+S	NC	Seawater (IMMR)	23	210	3	108.0
431	Ruiz Emparanza et al. (2022)	NA	GFRP	10.7	Vinylester	HM+S	NC	Seawater (IMMR)	23	360	3	93.0
432	Ruiz Emparanza et al. (2022)	NA	GFRP	10.8	Epoxy	G	NC	Seawater (IMMR)	23	60	3	109.0
433	Ruiz Emparanza et al. (2022)	NA	GFRP	10.8	Epoxy	G	NC	Seawater (IMMR)	23	120	3	97.0
434	Ruiz Emparanza et al. (2022)	NA	GFRP	10.8	Epoxy	G	NC	Seawater (IMMR)	23	210	3	106.0
435	Ruiz Emparanza et al. (2022)	NA	GFRP	10.8	Epoxy	G	NC	Seawater (IMMR)	23	360	3	95.0
436	Ruiz Emparanza et al. (2022)	NA	GFRP	10.3	Vinylester	HW+S	NC	Seawater (IMMR)	23	60	3	104.0
437	Ruiz Emparanza et al. (2022)	NA	GFRP	10.3	Vinylester	HW+S	NC	Seawater (IMMR)	23	120	3	94.0
438	Ruiz Emparanza et al. (2022)	NA	GFRP	10.3	Vinylester	HW+S	NC	Seawater (IMMR)	23	210	3	105.0
439	Ruiz Emparanza et al. (2022)	NA	GFRP	10.3	Vinylester	HW+S	NC	Seawater (IMMR)	23	360	3	91.0
440	Ruiz Emparanza et al. (2022)	NA	GFRP	10.2	Vinylester	HW+S	NC	Seawater (IMMR)	40	60	3	100.0
441	Ruiz Emparanza et al. (2022)	NA	GFRP	10.2	Vinylester	HW+S	NC	Seawater (IMMR)	40	120	3	80.0
442	Ruiz Emparanza et al. (2022)	NA	GFRP	10.2	Vinylester	HW+S	NC	Seawater (IMMR)	40	210	3	93.0
443	Ruiz Emparanza et al. (2022)	NA	GFRP	10.2	Vinylester	HW+S	NC	Seawater (IMMR)	40	360	3	86.0
444	Ruiz Emparanza et al. (2022)	NA	GFRP	10.5	Vinylester	G	NC	Seawater (IMMR)	40	60	3	90.0
445	Ruiz Emparanza et al. (2022)	NA	GFRP	10.5	Vinylester	G	NC	Seawater (IMMR)	40	120	3	103.0
446	Ruiz Emparanza et al. (2022)	NA	GFRP	10.5	Vinylester	G	NC	Seawater (IMMR)	40	210	3	87.0
447	Ruiz Emparanza et al. (2022)	NA	GFRP	10.5	Vinylester	G	NC	Seawater (IMMR)	40	360	3	97.0
448	Ruiz Emparanza et al. (2022)	NA	GFRP	10.1	Vinylester	R	NC	Seawater (IMMR)	40	60	3	93.0
449	Ruiz Emparanza et al. (2022)	NA	GFRP	10.1	Vinylester	R	NC	Seawater (IMMR)	40	120	3	88.0
450	Ruiz Emparanza et al. (2022)	NA	GFRP	10.1	Vinylester	R	NC	Seawater (IMMR)	40	210	3	78.0

451	Ruiz Emparanza et al. (2022)	NA	GFRP	10.1	Vinylester	R	NC	Seawater (IMMR)	40	360	3	90.0
452	Ruiz Emparanza et al. (2022)	NA	GFRP	10.2	Vinylester	HW+S	NC	Seawater (IMMR)	60	60	3	89.0
453	Ruiz Emparanza et al. (2022)	NA	GFRP	10.2	Vinylester	HW+S	NC	Seawater (IMMR)	60	120	3	86.0
454	Ruiz Emparanza et al. (2022)	NA	GFRP	10.2	Vinylester	HW+S	NC	Seawater (IMMR)	60	210	3	94.0
455	Ruiz Emparanza et al. (2022)	NA	GFRP	10.2	Vinylester	HW+S	NC	Seawater (IMMR)	60	360	3	88.0
456	Ruiz Emparanza et al. (2022)	NA	GFRP	10.5	Vinylester	G	NC	Seawater (IMMR)	60	60	3	97.0
457	Ruiz Emparanza et al. (2022)	NA	GFRP	10.5	Vinylester	G	NC	Seawater (IMMR)	60	120	3	91.0
458	Ruiz Emparanza et al. (2022)	NA	GFRP	10.5	Vinylester	G	NC	Seawater (IMMR)	60	210	3	83.0
459	Ruiz Emparanza et al. (2022)	NA	GFRP	10.5	Vinylester	G	NC	Seawater (IMMR)	60	360	3	93.0
460	Ruiz Emparanza et al. (2022)	NA	GFRP	10.1	Vinylester	R	NC	Seawater (IMMR)	60	60	3	92.0
461	Ruiz Emparanza et al. (2022)	NA	GFRP	10.1	Vinylester	R	NC	Seawater (IMMR)	60	120	3	89.0
462	Ruiz Emparanza et al. (2022)	NA	GFRP	10.1	Vinylester	R	NC	Seawater (IMMR)	60	210	3	82.0
463	Ruiz Emparanza et al. (2022)	NA	GFRP	10.1	Vinylester	R	NC	Seawater (IMMR)	60	360	3	97.0
464	Ruiz Emparanza et al. (2022)	NA	GFRP	10.7	Vinylester	HM+S	NC	Seawater (IMMR)	60	60	3	101.0
465	Ruiz Emparanza et al. (2022)	NA	GFRP	10.7	Vinylester	HM+S	NC	Seawater (IMMR)	60	120	3	98.0
466	Ruiz Emparanza et al. (2022)	NA	GFRP	10.7	Vinylester	HM+S	NC	Seawater (IMMR)	60	210	3	104.0
467	Ruiz Emparanza et al. (2022)	NA	GFRP	10.7	Vinylester	HM+S	NC	Seawater (IMMR)	60	360	3	97.0
468	Ruiz Emparanza et al. (2022)	NA	GFRP	10.8	Epoxy	G	NC	Seawater (IMMR)	60	60	3	105.0
469	Ruiz Emparanza et al. (2022)	NA	GFRP	10.8	Epoxy	G	NC	Seawater (IMMR)	60	120	3	103.0
470	Ruiz Emparanza et al. (2022)	NA	GFRP	10.8	Epoxy	G	NC	Seawater (IMMR)	60	210	3	107.0
471	Ruiz Emparanza et al. (2022)	NA	GFRP	10.8	Epoxy	G	NC	Seawater (IMMR)	60	360	3	98.0
472	Ruiz Emparanza et al. (2022)	NA	GFRP	10.3	Vinylester	HW+S	NC	Seawater (IMMR)	60	60	3	101.0
473	Ruiz Emparanza et al. (2022)	NA	GFRP	10.3	Vinylester	HW+S	NC	Seawater (IMMR)	60	120	3	100.0

474	Ruiz Emparanza et al. (2022)	NA	GFRP	10.3	Vinylester	HW+S	NC	Seawater (IMMR)	60	210	3	111.0
475	Ruiz Emparanza et al. (2022)	NA	GFRP	10.3	Vinylester	HW+S	NC	Seawater (IMMR)	60	360	3	92.0
476	Sreehari and Kavitha (2020)	NA	BFRP	10.0	NA	R	NC	Control	NA	0	NA	100.0
477	Sreehari and Kavitha (2020)	NA	BFRP	12.0	NA	R	NC	Control	NA	0	NA	100.0
478	Sreehari and Kavitha (2020)	NA	BFRP	20.0	NA	R	NC	Control	NA	0	NA	100.0
479	Sreehari and Kavitha (2020)	NA	BFRP	10.0	NA	R	NC	Control	NA	0	NA	100.0
480	Sreehari and Kavitha (2020)	NA	BFRP	12.0	NA	R	NC	Control	NA	0	NA	100.0
481	Sreehari and Kavitha (2020)	NA	BFRP	20.0	NA	R	NC	Control	NA	0	NA	100.0
482	Sreehari and Kavitha (2020)	NA	BFRP	10.0	NA	R	NC	Control	NA	0	NA	100.0
483	Sreehari and Kavitha (2020)	NA	BFRP	12.0	NA	R	NC	Control	NA	0	NA	100.0
484	Sreehari and Kavitha (2020)	NA	BFRP	20.0	NA	R	NC	Control	NA	0	NA	100.0
485	Sreehari and Kavitha (2020)	NA	BFRP	10.0	NA	R	NC	Acid solution (IMMR)	NA	28	NA	153.9
486	Sreehari and Kavitha (2020)	NA	BFRP	12.0	NA	R	NC	Acid solution (IMMR)	NA	28	NA	126.3
487	Sreehari and Kavitha (2020)	NA	BFRP	20.0	NA	R	NC	Acid solution (IMMR)	NA	28	NA	129.2
488	Sreehari and Kavitha (2020)	NA	BFRP	10.0	NA	R	NC	Acid solution (IMMR)	NA	28	NA	148.3
489	Sreehari and Kavitha (2020)	NA	BFRP	12.0	NA	R	NC	Acid solution (IMMR)	NA	28	NA	132.1
490	Sreehari and Kavitha (2020)	NA	BFRP	20.0	NA	R	NC	Acid solution (IMMR)	NA	28	NA	128.1
491	Sreehari and Kavitha (2020)	NA	BFRP	10.0	NA	R	NC	Acid solution (IMMR)	NA	28	NA	134.3
492	Sreehari and Kavitha (2020)	NA	BFRP	12.0	NA	R	NC	Acid solution (IMMR)	NA	28	NA	117.9
493	Sreehari and Kavitha (2020)	NA	BFRP	20.0	NA	R	NC	Acid solution (IMMR)	NA	28	NA	105.5
494	Sreehari and Kavitha (2020)	NA	BFRP	10.0	NA	R	NC	Acid solution (IMMR)	NA	56	NA	93.0
495	Sreehari and Kavitha (2020)	NA	BFRP	12.0	NA	R	NC	Acid solution (IMMR)	NA	56	NA	82.8
496	Sreehari and Kavitha (2020)	NA	BFRP	20.0	NA	R	NC	Acid solution (IMMR)	NA	56	NA	80.0

497	Sreehari and Kavitha (2020)	NA	BFRP	10.0	NA	R	NC	Acid solution (IMMR)	NA	56	NA	98.6
498	Sreehari and Kavitha (2020)	NA	BFRP	12.0	NA	R	NC	Acid solution (IMMR)	NA	56	NA	85.2
499	Sreehari and Kavitha (2020)	NA	BFRP	20.0	NA	R	NC	Acid solution (IMMR)	NA	56	NA	87.5
500	Sreehari and Kavitha (2020)	NA	BFRP	10.0	NA	R	NC	Acid solution (IMMR)	NA	56	NA	93.3
501	Sreehari and Kavitha (2020)	NA	BFRP	12.0	NA	R	NC	Acid solution (IMMR)	NA	56	NA	76.5
502	Sreehari and Kavitha (2020)	NA	BFRP	20.0	NA	R	NC	Acid solution (IMMR)	NA	56	NA	75.2
503	Su et al. (2022)	Jiangsu GMV Co., Ltd., China	BFRP	12.0	Epoxy	R	SWSSC	Control	RT	0	3	100.0
504	Su et al. (2022)	Jiangsu GMV Co., Ltd., China	BFRP	10.0	Epoxy	S	SWSSC	Control	RT	0	3	100.0
505	Su et al. (2022)	Jiangsu GMV Co., Ltd., China	BFRP	12.0	Epoxy	R	SWSSC	Simulated seawater (WD)	55	90	3	71.7
506	Su et al. (2022)	Jiangsu GMV Co., Ltd., China	BFRP	12.0	Epoxy	R	SWSSC	Simulated seawater (WD)	55	180	3	77.5
507	Su et al. (2022)	Jiangsu GMV Co., Ltd., China	BFRP	12.0	Epoxy	R	SWSSC	Simulated seawater (WD)	55	270	3	71.7
508	Su et al. (2022)	Jiangsu GMV Co., Ltd., China	BFRP	10.0	Epoxy	S	SWSSC	Simulated seawater (WD)	55	90	3	81.1
509	Su et al. (2022)	Jiangsu GMV Co., Ltd., China	BFRP	10.0	Epoxy	S	SWSSC	Simulated seawater (WD)	55	180	3	77.8
510	Su et al. (2022)	Jiangsu GMV Co., Ltd., China	BFRP	10.0	Epoxy	S	SWSSC	Simulated seawater (WD)	55	270	3	76.7
511	Taha and Alnahhal (2021)	NA	BFRP	10.0	Vinylester	HW	NC	Control	NA	0	3	100.0
512	Taha and Alnahhal (2021)	NA	BFRP	10.0	Vinylester	HW	NC	Simulated seawater (IMMR)	35	30	3	72.7
513	Taha and Alnahhal (2021)	NA	BFRP	10.0	Vinylester	HW	NC	Simulated seawater (IMMR)	35	60	3	83.0
514	Taha and Alnahhal (2021)	NA	BFRP	10.0	Vinylester	HW	NC	Simulated seawater (IMMR)	35	90	3	92.4
515	Taha and Alnahhal (2021)	NA	BFRP	10.0	Vinylester	HW	NC	Simulated seawater (IMMR)	60	30	3	102.0
516	Taha and Alnahhal (2021)	NA	BFRP	10.0	Vinylester	HW	NC	Simulated seawater (IMMR)	60	60	3	92.6
517	Taha and Alnahhal (2021)	NA	BFRP	10.0	Vinylester	HW	NC	Simulated seawater (IMMR)	60	90	3	89.6
518	Taha et al. (2020)	NA	BFRP	10.0	Vinylester	HW	NC	Control	NA	0	3	100.0
519	Taha et al. (2020)	NA	BFRP	10.0	Vinylester	HW	NC	Simulated seawater (IMMR)	35	30	3	72.7
520	Taha et al. (2020)	NA	BFRP	10.0	Vinylester	HW	NC	Simulated seawater	35	60	3	83.0

521	Taha et al. (2020)	NA	BFRP	10.0	Vinylester	HW	NC	(IMMR) Simulated seawater (IMMR)	35	90	3	92.4
522	Taha et al. (2020)	NA	BFRP	10.0	Vinylester	HW	NC	Simulated seawater (IMMR)	60	30	3	102.0
523	Taha et al. (2020)	NA	BFRP	10.0	Vinylester	HW	NC	Simulated seawater (IMMR)	60	60	3	92.6
524	Taha et al. (2020)	NA	BFRP	10.0	Vinylester	HW	NC	Simulated seawater (IMMR)	60	90	3	89.6
525	Won and Park (2006)	NA	CFRP	9.0	Vinylester	R	NC	Control	NA	0	NA	100.0
526	Won and Park (2006)	NA	GFRP	9.0	Vinylester	R	NC	Control	NA	0	NA	100.0
527	Won and Park (2006)	NA	CFRP	9.0	Vinylester	R	NC	Alkaline solution (IMMR)	60	50	NA	66.4
528	Won and Park (2006)	NA	GFRP	9.0	Vinylester	R	NC	Alkaline solution (IMMR)	60	50	NA	42.0
529	Won and Park (2006)	NA	CFRP	9.0	Vinylester	R	NC	Acid solution (IMMR)	60	50	NA	64.4
530	Won and Park (2006)	NA	GFRP	9.0	Vinylester	R	NC	Acid solution (IMMR)	60	50	NA	48.5
531	Won and Park (2006)	NA	CFRP	9.0	Vinylester	R	NC	Saline solution (IMMR)	60	50	NA	62.8
532	Won and Park (2006)	NA	GFRP	9.0	Vinylester	R	NC	Saline solution (IMMR)	60	50	NA	48.3
533	Won and Park (2006)	NA	CFRP	9.0	Vinylester	R	NC	Water (IMMR)	60	50	NA	71.5
534	Won and Park (2006)	NA	GFRP	9.0	Vinylester	R	NC	Water (IMMR)	60	50	NA	51.0
535	Won and Park (2006)	NA	CFRP	9.0	Vinylester	R	NC	Water (WD)	23~60	25	NA	84.5
536	Won and Park (2006)	NA	GFRP	9.0	Vinylester	R	NC	Water (WD)	23~60	25	NA	82.7
537	Won and Park (2006)	NA	CFRP	9.0	Vinylester	R	NC	HT	60	50	NA	92.8
538	Won and Park (2006)	NA	GFRP	9.0	Vinylester	R	NC	HT	60	50	NA	84.5
539	Won and Park (2006)	NA	CFRP	9.0	Vinylester	R	NC	FT	-18~4	50	NA	78.4
540	Won and Park (2006)	NA	GFRP	9.0	Vinylester	R	NC	FT	-18~4	50	NA	78.1
541	Won and Park (2006)	NA	CFRP	9.0	Vinylester	R	NC	Saline solution (IMMR)	RT	50	NA	79.9
542	Won and Park (2006)	NA	GFRP	9.0	Vinylester	R	NC	Saline solution (IMMR)	RT	50	NA	71.2
543	Won and Park	NA	CFRP	9.0	Vinylester	R	NC	Saline solution	RT	50	NA	76.2

	(2006)							(IMMR)				
544	Won and Park (2006)	NA	GFRP	9.0	Vinylester	R	NC	Saline solution (IMMR)	RT	50	NA	75.5
545	Won et al. (2013)	Hughes Brothers Company (Seward, NE, USA)	GFRP	6.0	Vinylester	HW	NC	Control	NA	0	NA	100.0
546	Won et al. (2013)	Hughes Brothers Company (Seward, NE, USA)	GFRP	6.0	Vinylester	HW	NC	Saline solution 1 (IMMR)	60	50	NA	54.0
547	Won et al. (2013)	Hughes Brothers Company (Seward, NE, USA)	GFRP	6.0	Vinylester	HW	NC	Saline solution 2 (IMMR)	20	50	NA	81.0
548	Won et al. (2013)	Hughes Brothers Company (Seward, NE, USA)	GFRP	6.0	Vinylester	HW	NC	Saline solution 3 (IMMR)	20	50	NA	78.0
549	Won et al. (2013)	Hughes Brothers Company (Seward, NE, USA)	GFRP	6.0	Vinylester	HW	NC	Saline solution (WD)	20/60	50	NA	78.0
550	Won et al. (2013)	Hughes Brothers Company (Seward, NE, USA)	GFRP	6.0	Vinylester	HW	NC	Saline solution (FT)	-10/20	50	NA	78.0
551	Wu et al. (2016)	Zhejiang Jinshi Basalt Fiber Co., Ltd., China	BFRP	8.0	Vinylester	R	NC	Control	NA	0	3	100.0
552	Wu et al. (2016)	Zhejiang Jinshi Basalt Fiber Co., Ltd., China	BFRP	8.0	Vinylester	R	NC	Simulated seawater (IMMR)	25	30	3	102.9
553	Wu et al. (2016)	Zhejiang Jinshi Basalt Fiber Co., Ltd., China	BFRP	8.0	Vinylester	R	NC	Simulated seawater (IMMR)	25	45	3	106.7
554	Wu et al. (2016)	Zhejiang Jinshi Basalt Fiber Co., Ltd., China	BFRP	8.0	Vinylester	R	NC	Simulated seawater (IMMR)	25	60	3	94.2
555	Wu et al. (2016)	Zhejiang Jinshi Basalt Fiber Co., Ltd., China	BFRP	8.0	Vinylester	R	NC	Simulated seawater (IMMR)	40	30	3	98.6
556	Wu et al. (2016)	Zhejiang Jinshi Basalt Fiber Co., Ltd., China	BFRP	8.0	Vinylester	R	NC	Simulated seawater (IMMR)	40	45	3	94.2
557	Wu et al. (2016)	Zhejiang Jinshi Basalt Fiber Co., Ltd., China	BFRP	8.0	Vinylester	R	NC	Simulated seawater (IMMR)	40	60	3	90.9
558	Wu et al. (2016)	Zhejiang Jinshi Basalt Fiber Co., Ltd., China	BFRP	8.0	Vinylester	R	NC	Simulated seawater (IMMR)	55	30	3	94.2
559	Wu et al. (2016)	Zhejiang Jinshi Basalt Fiber Co., Ltd., China	BFRP	8.0	Vinylester	R	NC	Simulated seawater (IMMR)	55	45	3	87.5
560	Wu et al. (2016)	Zhejiang Jinshi Basalt Fiber Co., Ltd., China	BFRP	8.0	Vinylester	R	NC	Simulated seawater (IMMR)	55	60	3	87.0
561	Xiong et al. (2022)	NA	BFRP	8.0	NA	R	SWSSC	Control	NA	0	3	100.0
562	Xiong et al. (2022)	NA	BFRP	10.0	NA	R	SWSSC	Control	NA	0	3	100.0
563	Xiong et al.	NA	BFRP	12.0	NA	R	SWSSC	Control	NA	0	3	100.0

	(2022)												
564	Xiong et al. (2022)	NA	BFRP	10.0	NA	R	SWSSC	Control	NA	0	3	100.0	
565	Xiong et al. (2022)	NA	BFRP	10.0	NA	R	SWSSC	Control	NA	0	3	100.0	
566	Xiong et al. (2022)	NA	BFRP	8.0	NA	R	SWSSC	Temperature cycle	25~60	22.5	3	82.7	
567	Xiong et al. (2022)	NA	BFRP	10.0	NA	R	SWSSC	Temperature cycle	25~60	22.5	3	NA	
568	Xiong et al. (2022)	NA	BFRP	12.0	NA	R	SWSSC	Temperature cycle	25~60	22.5	3	96.4	
569	Xiong et al. (2022)	NA	BFRP	10.0	NA	R	SWSSC	Temperature cycle	25~60	22.5	3	NA	
570	Xiong et al. (2022)	NA	BFRP	10.0	NA	R	SWSSC	Temperature cycle	25~60	22.5	3	NA	
571	Xiong et al. (2022)	NA	BFRP	10.0	NA	R	SWSSC	Temperature cycle	25~60	7.5	3	NA	
572	Xiong et al. (2022)	NA	BFRP	10.0	NA	R	SWSSC	Temperature cycle	25~60	15	3	NA	
573	Xiong et al. (2022)	NA	BFRP	10.0	NA	R	SWSSC	Temperature cycle	25~60	30	3	NA	
574	Xiong et al. (2022)	NA	BFRP	10.0	NA	R	SWSSC	Temperature cycle	25~60	37.5	3	NA	
575	Xiong et al. (2022)	NA	BFRP	10.0	NA	R	SWSSC	Temperature cycle	25~40	22.5	3	NA	
576	Xiong et al. (2022)	NA	BFRP	10.0	NA	R	SWSSC	Temperature cycle	25~80	22.5	3	NA	
577	Yan and Lin (2017)	Hughes Brothers Company (Seward, NE, USA)	GFRP	12.7	Vinylester	HW+S	NC	Control	NA	0	3	100.0	
578	Yan and Lin (2017)	Hughes Brothers Company (Seward, NE, USA)	GFRP	12.7	Vinylester	HW+S	NC	Saline solution (IMMR)	50	30	3	95.6	
579	Yan and Lin (2017)	Hughes Brothers Company (Seward, NE, USA)	GFRP	12.7	Vinylester	HW+S	NC	Saline solution (IMMR)	50	45	3	92.7	
580	Yan and Lin (2017)	Hughes Brothers Company (Seward, NE, USA)	GFRP	12.7	Vinylester	HW+S	NC	Saline solution (IMMR)	50	60	3	90.7	
581	Yan and Lin (2017)	Hughes Brothers Company (Seward, NE, USA)	GFRP	12.7	Vinylester	HW+S	NC	Saline solution (IMMR)	70	30	3	93.2	
582	Yan and Lin (2017)	Hughes Brothers Company (Seward, NE, USA)	GFRP	12.7	Vinylester	HW+S	NC	Saline solution (IMMR)	70	45	3	89.3	
583	Yan and Lin	Hughes Brothers	GFRP	12.7	Vinylester	HW+S	NC	Saline solution	70	60	3	88.0	

	(2017)	Company (Seward, NE, USA)						(IMMR)				
584	Yan et al. (2017)	Hughes Brothers Company (Seward, NE, USA)	GFRP	12.7	Vinylester	HW+S	NC	Control	25	0	3	100.0
585	Yan et al. (2017)	Hughes Brothers Company (Seward, NE, USA)	GFRP	12.7	Vinylester	HW+S	NC	Control	25	0	3	100.0
586	Yan et al. (2017)	Hughes Brothers Company (Seward, NE, USA)	GFRP	12.7	Vinylester	HW+S	NC	Control	25	0	3	100.0
587	Yan et al. (2017)	Hughes Brothers Company (Seward, NE, USA)	GFRP	12.7	Vinylester	HW+S	NC	Water (FT)	-18~4	15.6	2	88.5
588	Yan et al. (2017)	Hughes Brothers Company (Seward, NE, USA)	GFRP	12.7	Vinylester	HW+S	NC	Water (FT)	-18~4	15.6	3	96.9
589	Yang et al. (2017)	NA	BFRP	8.0	Epoxy	HW+S	NC	Control	NA	0	NA	100.0
590	Yang et al. (2017)	NA	BFRP	20.0	Epoxy	HW+S	NC	Control	NA	0	NA	100.0
591	Yang et al. (2017)	NA	BFRP	25.0	Epoxy	HW+S	NC	Control	NA	0	NA	100.0
592	Yang et al. (2017)	NA	BFRP	NA	Epoxy	HW+S	NC	Control	NA	0	NA	100.0
593	Yang et al. (2017)	NA	BFRP	NA	Epoxy	HW+S	NC	Control	NA	0	NA	100.0
594	Yang et al. (2017)	NA	BFRP	NA	Epoxy	HW+S	NC	Control	NA	0	NA	100.0
595	Yang et al. (2017)	NA	BFRP	8.0	Epoxy	HW+S	NC	Simulated seawater (IMMR)	40	60	NA	92.4
596	Yang et al. (2017)	NA	BFRP	8.0	Epoxy	HW+S	NC	Simulated seawater (IMMR)	40	90	NA	88.9
597	Yang et al. (2017)	NA	BFRP	25.0	Epoxy	HW+S	NC	Simulated seawater (IMMR)	40	60	NA	93.0
598	Yang et al. (2017)	NA	BFRP	25.0	Epoxy	HW+S	NC	Simulated seawater (IMMR)	40	90	NA	82.8
599	Yang et al. (2017)	NA	BFRP	20.0	Epoxy	HW+S	NC	Simulated seawater (IMMR)	40	90	NA	94.5
600	Yang et al. (2017)	NA	BFRP	NA	Epoxy	HW+S	NC	Simulated seawater (IMMR)	40	90	NA	95.6
601	Yang et al. (2017)	NA	BFRP	NA	Epoxy	HW+S	NC	Simulated seawater (IMMR)	40	90	NA	97.4
602	Yang et al. (2017)	NA	BFRP	NA	Epoxy	HW+S	NC	Simulated seawater (IMMR)	40	90	NA	96.2
603	Zheng et al. (2020)	NA	GFRP	11.2	Vinylester	R	NC	Control	NA	0	3	100.0
604	Zheng et al. (2020)	NA	GFRP	11.2	Epoxy	R	NC	Control	NA	0	3	100.0
605	Zheng et al. (2020)	NA	GFRP	11.2	Vinylester	R	NC	Water (IMMR)	RT	150	3	85.4
606	Zheng et al.	NA	GFRP	11.2	Vinylester	R	NC	Water (IMMR)	RT	210	3	73.5

	(2020)											
607	Zheng et al. (2020)	NA	GFRP	11.2	Vinylester	R	NC	Water (IMMR)	RT	270	3	73.0
608	Zheng et al. (2020)	NA	GFRP	11.2	Epoxy	R	NC	Water (IMMR)	RT	150	3	81.4
609	Zheng et al. (2020)	NA	GFRP	11.2	Epoxy	R	NC	Water (IMMR)	RT	210	3	71.3
610	Zheng et al. (2020)	NA	GFRP	11.2	Epoxy	R	NC	Water (IMMR)	RT	270	3	68.7
611	Zheng et al. (2020)	NA	GFRP	11.2	Vinylester	R	NC	Saline solution (IMMR)	RT	150	3	79.7
612	Zheng et al. (2020)	NA	GFRP	11.2	Vinylester	R	NC	Saline solution (IMMR)	RT	210	3	64.5
613	Zheng et al. (2020)	NA	GFRP	11.2	Vinylester	R	NC	Saline solution (IMMR)	RT	270	3	58.8
614	Zheng et al. (2020)	NA	GFRP	11.2	Epoxy	R	NC	Saline solution (IMMR)	RT	150	3	70.2
615	Zheng et al. (2020)	NA	GFRP	11.2	Epoxy	R	NC	Saline solution (IMMR)	RT	210	3	55.1
616	Zheng et al. (2020)	NA	GFRP	11.2	Epoxy	R	NC	Saline solution (IMMR)	RT	270	3	37.9
617	Zheng et al. (2020)	NA	GFRP	11.2	Vinylester	R	NC	Alkaline solution (IMMR)	RT	150	3	88.9
618	Zheng et al. (2020)	NA	GFRP	11.2	Vinylester	R	NC	Alkaline solution (IMMR)	RT	210	3	71.2
619	Zheng et al. (2020)	NA	GFRP	11.2	Vinylester	R	NC	Alkaline solution (IMMR)	RT	270	3	61.9
620	Zheng et al. (2020)	NA	GFRP	11.2	Epoxy	R	NC	Alkaline solution (IMMR)	RT	150	3	66.8
621	Zheng et al. (2020)	NA	GFRP	11.2	Epoxy	R	NC	Alkaline solution (IMMR)	RT	210	3	59.9
622	Zheng et al. (2020)	NA	GFRP	11.2	Epoxy	R	NC	Alkaline solution (IMMR)	RT	270	3	58.7
623	Zhou et al. (2011)	NA	GFRP	17.0	Polyester	R	NC	Reference	20	30	3	100.0
624	Zhou et al. (2011)	NA	GFRP	17.0	Polyester	R	NC	Reference	20	45	3	100.0
625	Zhou et al. (2011)	NA	GFRP	17.0	Polyester	R	NC	Reference	20	60	3	100.0
626	Zhou et al. (2011)	NA	GFRP	17.0	Polyester	R	NC	Reference	20	75	3	100.0
627	Zhou et al. (2011)	NA	GFRP	17.0	Polyester	R	NC	Water (IMMR)	20	30	3	89.8
628	Zhou et al. (2011)	NA	GFRP	17.0	Polyester	R	NC	Water (IMMR)	20	45	3	89.3
629	Zhou et al. (2011)	NA	GFRP	17.0	Polyester	R	NC	Water (IMMR)	20	60	3	95.9
630	Zhou et al. (2011)	NA	GFRP	17.0	Polyester	R	NC	Water (IMMR)	20	75	3	95.8
631	Zhou et al. (2011)	NA	GFRP	17.0	Polyester	R	NC	Acid solution (IMMR)	20	30	3	90.3
632	Zhou et al. (2011)	NA	GFRP	17.0	Polyester	R	NC	Acid solution (IMMR)	20	45	3	82.6
633	Zhou et al. (2011)	NA	GFRP	17.0	Polyester	R	NC	Acid solution (IMMR)	20	60	3	83.2
634	Zhou et al. (2011)	NA	GFRP	17.0	Polyester	R	NC	Acid solution (IMMR)	20	75	3	77.9
635	Zhou et al. (2011)	NA	GFRP	17.0	Polyester	R	NC	Acid solution (IMMR)	20	30	3	91.1

636	Zhou et al. (2011)	NA	GFRP	17.0	Polyester	R	NC	Acid solution (IMMR)	20	45	3	90.7
637	Zhou et al. (2011)	NA	GFRP	17.0	Polyester	R	NC	Acid solution (IMMR)	20	60	3	86.6
638	Zhou et al. (2011)	NA	GFRP	17.0	Polyester	R	NC	Acid solution (IMMR)	20	75	3	83.9
639	Zhou et al. (2011)	NA	GFRP	17.0	Polyester	R	NC	Acid solution (IMMR)	20	30	3	95.9
640	Zhou et al. (2011)	NA	GFRP	17.0	Polyester	R	NC	Acid solution (IMMR)	20	45	3	91.3
641	Zhou et al. (2011)	NA	GFRP	17.0	Polyester	R	NC	Acid solution (IMMR)	20	60	3	88.3
642	Zhou et al. (2011)	NA	GFRP	17.0	Polyester	R	NC	Acid solution (IMMR)	20	75	3	86.2
643	Zhou et al. (2012)	NA	GFRP	17.0	Polyester	R	NC	Reference	20	30	3	100.0
644	Zhou et al. (2012)	NA	GFRP	17.0	Polyester	R	NC	Reference	20	60	3	100.0
645	Zhou et al. (2012)	NA	GFRP	17.0	Polyester	R	NC	Reference	20	90	3	100.0
646	Zhou et al. (2012)	NA	GFRP	17.0	Polyester	R	NC	Water (IMMR)	20	30	3	89.8
647	Zhou et al. (2012)	NA	GFRP	17.0	Polyester	R	NC	Water (IMMR)	20	60	3	96.0
648	Zhou et al. (2012)	NA	GFRP	17.0	Polyester	R	NC	Water (IMMR)	20	90	3	104.1
649	Zhou et al. (2012)	NA	GFRP	17.0	Polyester	R	NC	Alkaline solution (IMMR)	20	30	3	98.5
650	Zhou et al. (2012)	NA	GFRP	17.0	Polyester	R	NC	Alkaline solution (IMMR)	20	60	3	100.5
651	Zhou et al. (2012)	NA	GFRP	17.0	Polyester	R	NC	Alkaline solution (IMMR)	20	90	3	113.1
652	Zhou et al. (2012)	NA	GFRP	17.0	Polyester	R	NC	Saline solution (IMMR)	20	30	3	95.2
653	Zhou et al. (2012)	NA	GFRP	17.0	Polyester	R	NC	Saline solution (IMMR)	20	60	3	92.7
654	Zhou et al. (2012)	NA	GFRP	17.0	Polyester	R	NC	Saline solution (IMMR)	20	90	3	108.4
655	Zhou et al. (2012)	NA	GFRP	17.0	Polyester	R	NC	Acid solution (IMMR)	20	30	3	90.3
656	Zhou et al. (2012)	NA	GFRP	17.0	Polyester	R	NC	Acid solution (IMMR)	20	60	3	83.2
657	Zhou et al. (2012)	NA	GFRP	17.0	Polyester	R	NC	Acid solution (IMMR)	20	90	3	79.6

Notes:
(1) IMMR = Immersion; WD = Wet-dry cycle; FT = Freeze-thaw cycle; HT = High temperature; LT = Low temperature; RT = Room temperature; SL = Sustained load;
(2) NC = Normal concrete; SWC = Seawater concrete; SSC = Sea and concrete; SWSSC = Seawater sea-sand concrete; HSC = High strength concrete;
(3) S = Sand coated; G = Grooved; HM = Helically mesh; HW = Helically wrapped; R = Ribbed; D+T = Deformed and textured;
(4) f_u is the ultimate tensile strength of FRP bars;
(5) Control = Unconditioned specimens without environmental exposure and time aging effect; Reference = Unconditioned specimens without environmental exposure but with time aging effect;
(6) NA = Not applicable.

Table C1 AAT database for flexural behavior of FRP-reinforced concrete beams

No.	Reference	FRP properties				Concrete type	Environmental condition	Temperature (℃)	Exposure duration (d)	Specimen number (pcs)	Ultimate load retention (%)
		Manufacturer	Type	Tensile bar diameter (mm)	Resin type						
1	Almusallam and Al-Salloum (2006)	NA	GFRP	10.0	Vinylester	NC	Control	RT	0	1	100.0
2	Almusallam and Al-Salloum (2006)	NA	GFRP	10.0	Vinylester	NC	Water (IMMR)	40	240	1	87.5
3	Almusallam and Al-Salloum (2006)	NA	GFRP	10.0	Vinylester	NC	SL (20-25% fu)+Water (IMMR)	40	240	1	69.4
4	Almusallam and Al-Salloum (2006)	NA	GFRP	10.0	Vinylester	NC	Seawater (IMMR)	40	240	1	73.6
5	Almusallam and Al-Salloum (2006)	NA	GFRP	10.0	Vinylester	NC	SL (20-25% fu)+Seawater (IMMR)	40	240	1	75.0
6	Almusallam and Al-Salloum (2006)	NA	GFRP	10.0	Vinylester	NC	Seawater (WD)	40	240	1	79.2
7	Almusallam and Al-Salloum (2006)	NA	GFRP	10.0	Vinylester	NC	SL (20-25% fu)+Seawater (WD)	40	240	1	66.7
8	Al-Salloum and Almusallam (2007)	NA	GFRP	10.0	NA	NC	SL (23% fu)	RT	300	2	NA
9	Al-Salloum and Almusallam (2007)	NA	GFRP	10.0	NA	NC	SL (23% fu)+Water (IMMR)	40	300	2	NA
10	Al-Salloum and Almusallam (2007)	NA	GFRP	10.0	NA	NC	SL (23% fu)+Seawater (IMMR)	40	300	2	NA
11	Al-Salloum and Almusallam (2007)	NA	GFRP	10.0	NA	NC	SL (23% fu)+Seawater (WD)	40	300	2	NA
12	Dong et al. (2018)	Zhejiang GBF Basalt Fiber Co., Ltd., Hengdian, China	BFRP	13.0	Vinylester	SWSSC	Control	NA	0	1	100.0
13	Dong et al. (2018)	Zhejiang GBF Basalt Fiber Co., Ltd., Hengdian, China	BFRP	13.0	Vinylester	SWSSC	Simulated seawater (IMMR)	50	90	1	102.5
14	Dong et al. (2018)	Zhejiang GBF Basalt Fiber Co., Ltd., Hengdian, China	BFRP	13.0	Vinylester	SWSSC	Simulated seawater (IMMR)	50	180	1	88.5
15	Dong et al. (2018)	Zhejiang GBF Basalt Fiber Co., Ltd., Hengdian, China	BFRP	13.0	Vinylester	SWSSC	Simulated seawater (IMMR)	50	270	1	78.8
16	Dong et al. (2018)	Zhejiang GBF Basalt Fiber Co., Ltd., Hengdian, China	BFRP	13.0	Vinylester	SWSSC	Simulated seawater (WD)	40	90	1	110.1
17	Dong et al. (2018)	Zhejiang GBF Basalt Fiber Co., Ltd.,	BFRP	13.0	Vinylester	SWSSC	Simulated seawater (WD)	40	180	1	105.4

18	Dong et al. (2018)	Hengdian, China Zhejiang GBF Basalt Fiber Co., Ltd., Hengdian, China	BFRP	13.0	Vinylester	SWSSC	Simulated seawater (WD)	40	270	1	101.5
19	Dong et al. (2018)	NA	BFRP	8.0	Vinylester	NC	Control	NA	0	2	100.0
20	Dong et al. (2018)	NA	BFRP	8.0	Vinylester	NC	SL (30 kN)+Simulated seawater (WD)	20~35	180	2	77.6
21	Dong et al. (2018)	NA	BFRP	8.0	Vinylester	NC	SL (30 kN)+Simulated seawater (WD)	20~35	270	2	66.7
22	Dong et al. (2018)	NA	BFRP	8.0	Vinylester	NC	SL (30 kN)+Simulated seawater (WD)	20~35	360	2	58.0
23	Dong et al. (2020)	Jiangsu Hengshen Co, Ltd., China	CFRP	8.0	NA	SWSSC	Control	NA	0	1	100.0
24	Dong et al. (2020)	Jiangsu Hengshen Co, Ltd., China	CFRP	8.0	NA	SWSSC	Simulated seawater (IMMR)	50	90	1	91.3
25	Dong et al. (2020)	Jiangsu Hengshen Co, Ltd., China	CFRP	8.0	NA	SWSSC	Simulated seawater (IMMR)	50	180	1	84.3
26	Dong et al. (2020)	Jiangsu Hengshen Co, Ltd., China	CFRP	8.0	NA	SWSSC	Simulated seawater (IMMR)	50	270	1	69.7
27	Dong et al. (2020)	Jiangsu Hengshen Co, Ltd., China	CFRP	8.0	NA	SWSSC	Simulated seawater (WD)	40	90	1	105.4
28	Dong et al. (2020)	Jiangsu Hengshen Co, Ltd., China	CFRP	8.0	NA	SWSSC	Simulated seawater (WD)	40	180	1	87.0
29	Dong et al. (2020)	Jiangsu Hengshen Co, Ltd., China	CFRP	8.0	NA	SWSSC	Simulated seawater (WD)	40	270	1	97.8
30	Fergani et al. (2018)	NA	GFRP	8.0	Vinylester	NC	Reference	20	270	2	100.0
31	Fergani et al. (2018)	NA	GFRP	8.0	Vinylester	NC	SL(3000 microstrain)	20	270	2	80.3
32	Fergani et al. (2018)	NA	GFRP	8.0	Vinylester	NC	SL(3000 microstrain)+Water (IMMR)	60	270	2	88.0
33	Fergani et al. (2018)	NA	GFRP	8.0	Vinylester	NC	SL(5000 microstrain)+Water (IMMR)	60	270	2	87.0
34	Khanfour and El Refai (2017)	NA	BFRP	8.0	NA	NC	Control	RT	0	1	100.0
35	Khanfour and El Refai (2017)	NA	BFRP	8.0	NA	NC	Control	RT	0	1	100.0
36	Khanfour and El Refai (2017)	NA	BFRP	8.0	NA	NC	Control	RT	0	1	100.0
37	Khanfour and El Refai (2017)	NA	BFRP	8.0	NA	NC	FT	-25~15	100	1	98.7
38	Khanfour and El Refai (2017)	NA	BFRP	8.0	NA	NC	FT	-25~15	100	1	103.6
39	Khanfour and El Refai (2017)	NA	BFRP	8.0	NA	NC	FT	-25~15	100	1	91.6
40	Khanfour and El Refai (2017)	NA	BFRP	10.0	NA	NC	Control	RT	0	1	100.0
41	Khanfour and El	NA	BFRP	10.0	NA	NC	Control	RT	0	1	100.0

	Refai (2017)										
42	Khanfour and El Refai (2017)	NA	BFRP	10.0	NA	NC	Control	RT	0	1	100.0
43	Khanfour and El Refai (2017)	NA	BFRP	10.0	NA	NC	FT	-25~15	100	1	100.0
44	Khanfour and El Refai (2017)	NA	BFRP	10.0	NA	NC	FT	-25~15	100	1	103.9
45	Khanfour and El Refai (2017)	NA	BFRP	10.0	NA	NC	FT	-25~15	100	1	86.8
46	Laoubi et al. (2006)	Pulturall Inc	GFRP	9.5	Vinylester	NC	Reference	RT	50	1	100.0
47	Laoubi et al. (2006)	Pulturall Inc	GFRP	9.5	Vinylester	NC	Reference	RT	100	1	100.0
48	Laoubi et al. (2006)	Pulturall Inc	GFRP	9.5	Vinylester	NC	Reference	RT	180	1	100.0
49	Laoubi et al. (2006)	Pulturall Inc	GFRP	9.5	Vinylester	NC	SL (27%fu)	RT	50	2	96.0
50	Laoubi et al. (2006)	Pulturall Inc	GFRP	9.5	Vinylester	NC	SL (27%fu)	RT	100	2	95.7
51	Laoubi et al. (2006)	Pulturall Inc	GFRP	9.5	Vinylester	NC	SL (27%fu)	RT	180	2	106.8
52	Laoubi et al. (2006)	Pulturall Inc	GFRP	9.5	Vinylester	NC	FT	-20~+20	50	2	105.4
53	Laoubi et al. (2006)	Pulturall Inc	GFRP	9.5	Vinylester	NC	FT	-20~+20	100	2	99.0
54	Laoubi et al. (2006)	Pulturall Inc	GFRP	9.5	Vinylester	NC	FT	-20~+20	180	2	102.9
55	Laoubi et al. (2006)	Pulturall Inc	GFRP	9.5	Vinylester	NC	SL (27%fu)+FT	-20~+20	50	2	98.1
56	Laoubi et al. (2006)	Pulturall Inc	GFRP	9.5	Vinylester	NC	SL (27%fu)+FT	-20~+20	100	2	94.6
57	Laoubi et al. (2006)	Pulturall Inc	GFRP	9.5	Vinylester	NC	SL (27%fu)+FT	-20~+20	180	2	105.4
58	Liang and Yin (2022)	NA	BFRP	12.0	Vinylester	NC	Control	35	0	1	100.0
59	Liang and Yin (2022)	NA	BFRP	12.0	Vinylester	NC	Simulated seawater (IMMR)	35	90	1	100.0
60	Lu et al. (2023)	Tuo Xin Aerospace Basalt Industrial Co., ltd.	BFRP	8.0	Epoxy	SWSSC	Control	RT	0	3	100.0
61	Lu et al. (2023)	Tuo Xin Aerospace Basalt Industrial Co., ltd.	BFRP	8.0	Epoxy	SWSSC	Simulated seawater (IMMR)	RT	180	1	62.9
62	Lu et al. (2023)	Tuo Xin Aerospace Basalt Industrial Co., ltd.	BFRP	8.0	Epoxy	SWSSC	Simulated seawater (IMMR)	RT	360	1	46.6
63	Lu et al. (2023)	Tuo Xin Aerospace Basalt Industrial Co., ltd.	BFRP	8.0	Epoxy	SWSSC	Water (IMMR)	RT	180	2	74.3
64	Lu et al. (2023)	Tuo Xin Aerospace Basalt Industrial Co., ltd.	BFRP	8.0	Epoxy	SWSSC	Water (IMMR)	RT	360	2	41.8
65	Mukherjee and Arwikar (2005)	NA	GFRP	9.5	Vinylester	NC	Control	NA	0	1	100.0
66	Mukherjee and Arwikar (2005)	NA	GFRP	9.5	Vinylester	NC	Control	NA	0	1	100.0
67	Mukherjee and Arwikar (2005)	NA	GFRP	9.5	Vinylester	NC	Control	NA	0	1	100.0
68	Mukherjee and Arwikar (2005)	NA	GFRP	9.5	Vinylester	NC	Control	NA	0	1	100.0
69	Mukherjee and Arwikar (2005)	NA	GFRP	9.5	Vinylester	NC	Water (IMMR)	60	90	1	140.2
70	Mukherjee and	NA	GFRP	9.5	Vinylester	NC	Water (IMMR)	60	90	1	129.2

	Arwikar (2005)										
71	Mukherjee and Arwikar (2005)	NA	GFRP	9.5	Vinylester	NC	Water (IMMR)	60	90	1	120.5
72	Mukherjee and Arwikar (2005)	NA	GFRP	9.5	Vinylester	NC	Water (IMMR)	60	90	1	141.6
73	Mukherjee and Arwikar (2005)	NA	GFRP	9.5	Vinylester	NC	Water (IMMR)	60	180	1	157.7
74	Mukherjee and Arwikar (2005)	NA	GFRP	9.5	Vinylester	NC	Water (IMMR)	60	180	1	126.6
75	Mukherjee and Arwikar (2005)	NA	GFRP	9.5	Vinylester	NC	Water (IMMR)	60	180	1	147.7
76	Mukherjee and Arwikar (2005)	NA	GFRP	9.5	Vinylester	NC	Water (IMMR)	60	180	1	117.3
77	Mukherjee and Arwikar (2005)	NA	GFRP	9.5	Vinylester	NC	Water (IMMR)	60	360	1	130.5
78	Mukherjee and Arwikar (2005)	NA	GFRP	9.5	Vinylester	NC	Water (IMMR)	60	360	1	135.4
79	Mukherjee and Arwikar (2005)	NA	GFRP	9.5	Vinylester	NC	Water (IMMR)	60	360	1	120.5
80	Mukherjee and Arwikar (2005)	NA	GFRP	9.5	Vinylester	NC	Water (IMMR)	60	360	1	111.4
81	Park et al. (2014)	Hughes Brothers Company (Seward, NE, USA)	GFRP	13.0	Vinylester	NC	Control	NA	0	3	100.0
82	Park et al. (2014)	Hughes Brothers Company (Seward, NE, USA)	GFRP	16.0	Vinylester	NC	Control	NA	0	3	100.0
83	Park et al. (2014)	Hughes Brothers Company (Seward, NE, USA)	GFRP	13.0	Vinylester	NC	Control	NA	0	3	100.0
84	Park et al. (2014)	Hughes Brothers Company (Seward, NE, USA)	GFRP	16.0	Vinylester	NC	Control	NA	0	3	100.0
85	Park et al. (2014)	Hughes Brothers Company (Seward, NE, USA)	GFRP	13.0	Vinylester	NC	SL (30% Ultimate load)+{Saline solution (IMMR) for 72 h}+HT	47	300	3	90.9
86	Park et al. (2014)	Hughes Brothers Company (Seward, NE, USA)	GFRP	16.0	Vinylester	NC	SL (30% Ultimate load)+{Saline solution (IMMR) for 72 h}+HT	47	300	3	90.7
87	Park et al. (2014)	Hughes Brothers Company (Seward, NE, USA)	GFRP	13.0	Vinylester	NC	SL (30% Ultimate load)+{Saline solution (IMMR) for 72 h}+HT	47	300	3	99.6
88	Park et al. (2014)	Hughes Brothers Company (Seward, NE, USA)	GFRP	16.0	Vinylester	NC	SL (30% Ultimate load)+{Saline solution (IMMR) for 72 h}+HT	47	300	3	95.4
89	Rajput and Sharma	NA	GFRP	12.0	Epoxy	NC	Reference	27	30	3	NA

	(2017)										
90	Rajput and Sharma (2017)	NA	GFRP	12.0	Epoxy	NC	Saline solution (WD)	45	30	3	NA
91	Rajput and Sharma (2017)	NA	GFRP	12.0	Epoxy	NC	Alkaline solution (IMMR)	60	30	3	NA
92	Ren et al. (2024)	NA	GFRP	8.0	NA	NC	Reference	15-20	365	1	100.0
93	Ren et al. (2024)	NA	GFRP	8.0	NA	NC	SL(100% Crack load)+Temperature cycles	2-35	365	1	118.8
94	Ren et al. (2024)	NA	GFRP	8.0	NA	NC	SL(200% Crack load)+Temperature cycles	2-35	365	1	118.9
95	Ren et al. (2024)	NA	GFRP	8.0	NA	SWSSC	Reference	15-20	365	1	100.0
96	Ren et al. (2024)	NA	GFRP	8.0	NA	SWSSC	SL(100% Crack load)+Temperature cycles	2-35	365	1	110.8
97	Ren et al. (2024)	NA	GFRP	8.0	NA	SWSSC	SL(200% Crack load)+Temperature cycles	2-35	365	1	103.4
98	Sen et al. (1998)	NA	CFRP	6.2	Epoxy	NC	Control	NA	0	3	100.0
99	Sen et al. (1998)	NA	CFRP	6.2	Epoxy	NC	SL (45% fu)+Saline solution (WD)	NA	180	2	97.6
100	Sen et al. (1998)	NA	CFRP	6.2	Epoxy	NC	SL (45% fu)+Saline solution (WD)	NA	360	2	101.0
101	Sen et al. (1998)	NA	CFRP	6.2	Epoxy	NC	SL (45% fu)+Saline solution (WD)	NA	540	2	95.7
102	Sen et al. (1998)	NA	CFRP	6.2	Epoxy	NC	SL (45% fu)+Saline solution (WD)	NA	720	2	87.0
103	Sen et al. (1998)	NA	CFRP	6.2	Epoxy	NC	SL (45% fu)+Saline solution (WD)	NA	1080	2	96.6
104	Sen et al. (1999)	NA	CFRP	6.2	Epoxy	NC	Control	NA	0	3	100.0
105	Sen et al. (1999)	NA	CFRP	6.2	Epoxy	NC	SL (45% fu)+Saline solution (WD)	RT (Dry)/60(Wet)	42	3	97.6
106	Sen et al. (1999)	NA	CFRP	6.2	Epoxy	NC	SL (45% fu)+Saline solution (WD)	RT (Dry)/60(Wet)	270	2	99.0
107	Sen et al. (1999)	NA	CFRP	6.2	Epoxy	NC	SL (45% fu)+Saline solution (WD)	RT (Dry)/60(Wet)	420	2	103.9
108	Sen et al. (1999)	NA	CFRP	6.2	Epoxy	NC	SL (45% fu)+Saline solution (WD)	RT (Dry)/60(Wet)	630	2	97.1
109	Sen et al. (1999)	NA	CFRP	6.2	Epoxy	NC	SL (45% fu)+Saline solution (WD)	RT (Dry)/60(Wet)	990	3	95.2
110	Su et al. (2022)	Jiangsu GMV Co., Ltd., China	BFRP	12.0	Epoxy	SWSSC	Control	RT	0	1	100.0
111	Su et al. (2022)	Jiangsu GMV Co., Ltd., China	BFRP	12.0	Epoxy	SWSSC	Control	RT	0	1	100.0
112	Su et al. (2022)	Jiangsu GMV Co., Ltd., China	BFRP	12.0	Epoxy	SWSSC	Control	RT	0	1	100.0
113	Su et al. (2022)	Jiangsu GMV Co., Ltd., China	BFRP	12.0	Epoxy	SWSSC	Simulated seawater (WD)	55	90	1	91.3
114	Su et al. (2022)	Jiangsu GMV Co., Ltd.,	BFRP	12.0	Epoxy	SWSSC	Simulated seawater (WD)	55	180	1	82.2

115	Su et al. (2022)	China Jiangsu GMV Co., Ltd., China	BFRP	12.0	Epoxy	SWSSC	Simulated seawater (WD)	55	270	1	85.5
116	Su et al. (2022)	Jiangsu GMV Co., Ltd., China	BFRP	12.0	Epoxy	SWSSC	Simulated seawater (WD)	55	90	1	89.6
117	Su et al. (2022)	Jiangsu GMV Co., Ltd., China	BFRP	12.0	Epoxy	SWSSC	Simulated seawater (WD)	55	180	1	84.6
118	Su et al. (2022)	Jiangsu GMV Co., Ltd., China	BFRP	12.0	Epoxy	SWSSC	Simulated seawater (WD)	55	270	1	83.6
119	Su et al. (2022)	Jiangsu GMV Co., Ltd., China	BFRP	12.0	Epoxy	SWSSC	Simulated seawater (WD)	55	90	1	93.4
120	Su et al. (2022)	Jiangsu GMV Co., Ltd., China	BFRP	12.0	Epoxy	SWSSC	Simulated seawater (WD)	55	180	1	79.8
121	Su et al. (2022)	Jiangsu GMV Co., Ltd., China	BFRP	12.0	Epoxy	SWSSC	Simulated seawater (WD)	55	270	1	84.8
122	Tannous and Saadatmanesh (1998)	NA	GFRP	10.0	Polyester	NC	Reference	RT	365	1	100.0
123	Tannous and Saadatmanesh (1998)	NA	GFRP	10.0	Vinylester	NC	Reference	RT	365	1	100.0
124	Tannous and Saadatmanesh (1998)	NA	GFRP	10.0	Polyester	NC	Saline solution (IMMR)	RT	365	1	97.7
125	Tannous and Saadatmanesh (1998)	NA	GFRP	10.0	Polyester	NC	Saline solution (IMMR)	RT	730	1	93.1
126	Tannous and Saadatmanesh (1998)	NA	GFRP	10.0	Polyester	NC	Saline solution (IMMR)	RT	365	1	94.0
127	Tannous and Saadatmanesh (1998)	NA	GFRP	10.0	Polyester	NC	Saline solution (IMMR)	RT	730	1	90.2
128	Tannous and Saadatmanesh (1998)	NA	GFRP	10.0	Vinylester	NC	Saline solution (IMMR)	RT	365	1	90.8
129	Tannous and Saadatmanesh (1998)	NA	GFRP	10.0	Vinylester	NC	Saline solution (IMMR)	RT	730	1	87.3
130	Tannous and Saadatmanesh (1998)	NA	GFRP	10.0	Vinylester	NC	Saline solution (IMMR)	RT	365	1	92.9
131	Tannous and Saadatmanesh (1998)	NA	GFRP	10.0	Vinylester	NC	Saline solution (IMMR)	RT	730	1	87.1
132	Wang and Belarbi	NA	GFRP	13.0	Epoxy	NC	Control	NA	0	2	100.0

	(2013)				modified vinylester						
133	Wang and Belarbi (2013)	NA	GFRP	25.0	Epoxy modified vinylester	NC	Control	NA	0	2	100.0
134	Wang and Belarbi (2013)	NA	CFRP	13.0	Epoxy modified vinylester	NC	Control	NA	0	2	100.0
135	Wang and Belarbi (2013)	NA	GFRP	13.0	Epoxy modified vinylester	NC	Saline solution (FT)+Temperature cycles	-20~60	100	2	96.2
136	Wang and Belarbi (2013)	NA	GFRP	25.0	Epoxy modified vinylester	NC	Saline solution (FT)+Temperature cycles	-20~60	100	2	84.3
137	Wang and Belarbi (2013)	NA	CFRP	13.0	Epoxy modified vinylester	NC	Saline solution (FT)+Temperature cycles	-20~60	100	2	93.4
138	Wang et al. (2023)	Shenzhen Haichuan New Material Technology Co., Ltd.	GFRP	14.0	Vinylester	SWSSC	SL (40 kN)+Simulated seawater (WD)	25 (Dry)/40(Wet)	0	1	100.0
139	Wang et al. (2023)	Shenzhen Haichuan New Material Technology Co., Ltd.	GFRP	14.0	Vinylester	SWSSC	SL (40 kN)+Simulated seawater (WD)	25 (Dry)/40(Wet)	90	1	103.4
140	Wang et al. (2023)	Shenzhen Haichuan New Material Technology Co., Ltd.	GFRP	14.0	Vinylester	SWSSC	SL (40 kN)+Simulated seawater (WD)	25 (Dry)/40(Wet)	180	1	100.0
141	Wang et al. (2023)	Shenzhen Haichuan New Material Technology Co., Ltd.	GFRP	14.0	Vinylester	SWSSC	SL (40 kN)+Simulated seawater (WD)	25 (Dry)/40(Wet)	270	1	100.0
142	Wang et al. (2023)	Shenzhen Haichuan New Material Technology Co., Ltd.	GFRP	14.0	Vinylester	SWSSC	SL (40 kN)+Simulated seawater (WD)	25 (Dry)/40(Wet)	0	1	100.0
143	Wang et al. (2023)	Shenzhen Haichuan New Material Technology Co., Ltd.	GFRP	14.0	Vinylester	SWSSC	SL (40 kN)+Simulated seawater (WD)	25 (Dry)/40(Wet)	90	1	106.9
144	Wang et al. (2023)	Shenzhen Haichuan New Material Technology Co., Ltd.	GFRP	14.0	Vinylester	SWSSC	SL (40 kN)+Simulated seawater (WD)	25 (Dry)/40(Wet)	180	1	96.2
145	Wang et al. (2023)	Shenzhen Haichuan New Material Technology Co., Ltd.	GFRP	14.0	Vinylester	SWSSC	SL (40 kN)+Simulated seawater (WD)	25 (Dry)/40(Wet)	270	1	98.8

Notes:
(1) IMMR = Immersion; WD = Wet-dry cycle; FT = Freeze-thaw cycle; HT = High temperature; RT = Room temperature; SL = Sustained load;
(2) NC = Normal concrete; SWSSC = Seawater sea-sand concrete;
(3) f_u is the ultimate tensile strength of FRP bars;
(4) Control = Unconditioned specimens without environmental exposure and time aging effect; Reference = Unconditioned specimens without environmental exposure but with time aging effect;

(5) NA = Not applicable.

APPENDIX B
DATABASE FOR FIELD EXPOSURE TESTS

The results of field exposure tests for FRP bars, FRP bar-to-concrete bonded joints, and FRP-reinforced concrete beams, collected from the existing literature, are respectively summarized in Tables D1-D3, E and F, as follows.

Table D1 FET database for tensile properties of FRP bars

No.	Reference	FRP properties				Environmental condition	Temperature (℃)	Exposure duration (d)	Specimen number (pcs)	Tensile strength retention (%)	Tensile elastic modulus retention (%)
		Manufacturer	Type	Bar diameter (mm)	Resin type						
1	Al-Khafaji et al. (2021)	NA	GFRP	16.0	Vinylester	Control	NA	0	10	100.00	100.0
2	Al-Khafaji et al. (2021)	NA	GFRP	16.0	Vinylester	NCE+Field	NA	5475~7300	9	92.84	106.1
3	Al-Salloum et al. (2013)	NA	GFRP	12.0	Vinylester	Reference	23	180	5	100.00	100.0
4	Al-Salloum et al. (2013)	NA	GFRP	12.0	Vinylester	Field	9~45	180	5	99.66	97.0
5	Al-Salloum et al. (2013)	NA	GFRP	12.0	Vinylester	Field	9~45	180	5	99.80	98.9
6	Al-Salloum et al. (2013)	NA	GFRP	12.0	Vinylester	Reference	23	360	5	100.00	100.0
7	Al-Salloum et al. (2013)	NA	GFRP	12.0	Vinylester	Field	9~45	360	5	99.59	99.7
8	Al-Salloum et al. (2013)	NA	GFRP	12.0	Vinylester	Field	9~45	360	5	99.46	97.8
9	Al-Salloum et al. (2013)	NA	GFRP	12.0	Vinylester	Reference	23	540	5	100.00	100.0
10	Al-Salloum et al. (2013)	NA	GFRP	12.0	Vinylester	Field	9~45	540	5	99.46	99.7
11	Al-Salloum et al. (2013)	NA	GFRP	12.0	Vinylester	Field	9~45	540	5	99.46	99.0
12	Al-Zahrani et al. (2002)	NA	GFRP	10.0	Modified vinylester	Control	22	0	NA	100.00	100.0
13	Al-Zahrani et al. (2002)	NA	GFRP	10.0	Modified vinylester	Field	NA	90	NA	100.46	93.4
14	Al-Zahrani et al. (2002)	NA	GFRP	10.0	Modified vinylester	Field	NA	180	NA	100.80	91.7
15	Bakis et al. (2005)	Hughes Brothers Company (Seward, NE, USA)	GFRP	10.2	Vinylester	Control	23	0	3-6	100.00	100.0
16	Bakis et al. (2005)	Hughes Brothers Company (Seward, NE, USA)	GFRP	10.2	Vinylester	Pre-cracks+SL (20%Mu)+NCE+Field	-15~30	360	3-6	97.67	111.0
17	Bakis et al. (2005)	Hughes Brothers Company (Seward, NE, USA)	GFRP	10.2	Vinylester	Pre-cracks+SL (20%Mu)+NCE+Field	-15~30	1080	3-6	96.74	110.1
18	Chen et al. (2022)	Chengxinda Glass Fiber Factory, China	GFRP	14.0	Epoxy	Control	15~30	0	NA	100.00	NA
19	Chen et al. (2022)	Chengxinda Glass Fiber Factory, China	GFRP	14.0	Epoxy	Field (Tidal)	15~30	180	NA	76.36	NA
20	Chen et al.	Chengxinda Glass Fiber	GFRP	14.0	Epoxy	Field (Tidal)	15~30	270	NA	69.89	NA

	(2022)	Factory, China									
21	Lu et al. (2020b)	TuoXin Aerospace Basalt Industrial Co., Ltd. (Sichuan, China)	BFRP	8.0	Epoxy	Control	23	0	5	100.00	100.0
22	Lu et al. (2020b)	TuoXin Aerospace Basalt Industrial Co., Ltd. (Sichuan, China)	BFRP	8.0	Epoxy	Field (Seawater IMMR)	0.9~24	180	5	98.39	97.8
23	Lu et al. (2020b)	TuoXin Aerospace Basalt Industrial Co., Ltd. (Sichuan, China)	BFRP	8.0	Epoxy	Field (Seawater IMMR)	0.9~24	360	5	88.76	86.8
24	Lu et al. (2020b)	TuoXin Aerospace Basalt Industrial Co., Ltd. (Sichuan, China)	BFRP	8.0	Epoxy	NCE+Field (Seawater IMMR)	0.9~24	180	5	73.49	90.8
25	Lu et al. (2020b)	TuoXin Aerospace Basalt Industrial Co., Ltd. (Sichuan, China)	BFRP	8.0	Epoxy	NCE+Field (Seawater IMMR)	0.9~24	360	5	64.26	80.7
26	Lu et al. (2023b)	Nanjing Fenghui Composite Material Co. Ltd (China)	GFRP	11.2	Vinylester	Control	25	0	3	100.00	NA
27	Lu et al. (2023b)	Nanjing Fenghui Composite Material Co. Ltd (China)	GFRP	11.2	Vinylester	NCE+Field	Ave. 15.6	366	3	97.80	NA
28	Lu et al. (2023b)	Nanjing Fenghui Composite Material Co. Ltd (China)	GFRP	11.2	Vinylester	Pre-cracks+SL (15-20%fu)+NCE+Field	Ave. 15.6	366	6	92.80	NA
29	Morales et al. (2021)	NA	GFRP	9.5	Vinylester	Control	NA	0	5	100.00	100.0
30	Morales et al. (2021)	NA	GFRP	9.5	Vinylester	SWCE 1+Field	Ave. 25	30	3	99.86	105.9
31	Morales et al. (2021)	NA	GFRP	9.5	Vinylester	SWCE 1+Field	Ave. 25	180	3	96.69	98.1
32	Morales et al. (2021)	NA	GFRP	9.5	Vinylester	SWCE 1+Field	Ave. 25	360	3	100.53	96.7
33	Morales et al. (2021)	NA	GFRP	9.5	Vinylester	SWCE 1+Field	Ave. 25	720	3	98.60	99.9
34	Morales et al. (2021)	NA	GFRP	9.5	Vinylester	SWCE 2+Field	Ave. 25	30	3	85.45	99.6
35	Morales et al. (2021)	NA	GFRP	9.5	Vinylester	SWCE 2+Field	Ave. 25	180	3	88.87	98.8
36	Morales et al. (2021)	NA	GFRP	9.5	Vinylester	SWCE 2+Field	Ave. 25	360	3	88.67	101.9
37	Morales et al. (2021)	NA	GFRP	9.5	Vinylester	SWCE 2+Field	Ave. 25	720	3	81.51	98.1
38	Mukherjee and Arwikar (2005)	NA	GFRP	9.5	Vinylester	Control	NA	0	NA	100.00	NA
39	Mukherjee and Arwikar (2005)	NA	GFRP	9.5	Vinylester	Pre-cracks+SL (20%Mu)+NCE+Field	10~38	540	NA	65.43	NA
40	Mukherjee and Arwikar (2005)	NA	GFRP	9.5	Vinylester	Pre-cracks+SL (20%Mu)+NCE+Field	10~38	900	NA	61.40	NA

41	Trejo et al. (2011)	NA	GFRP	16.0	Polyester	Control	NA	0	10	100.00	NA
42	Trejo et al. (2011)	NA	GFRP	16.0	Polyester	Preloaded+NCE+Field	5~40	2555	15	87.16	NA
43	Trejo et al. (2011)	NA	GFRP	16.0	Vinylester	Control	NA	0	5	100.00	NA
44	Trejo et al. (2011)	NA	GFRP	16.0	Vinylester	Preloaded+NCE+Field	5~40	2555	35	88.32	NA
45	Trejo et al. (2011)	NA	GFRP	16.0	Vinylester	Control	NA	0	5	100.00	NA
46	Trejo et al. (2011)	NA	GFRP	16.0	Vinylester	Preloaded+NCE+Field	5~40	2555	30	73.89	NA
47	Trejo et al. (2011)	NA	GFRP	19.0	Polyester	Control	NA	0	10	100.00	NA
48	Trejo et al. (2011)	NA	GFRP	19.0	Polyester	Preloaded+NCE+Field	5~40	2555	33	92.73	NA
49	Trejo et al. (2011)	NA	GFRP	19.0	Vinylester	Control	NA	0	10	100.00	NA
50	Trejo et al. (2011)	NA	GFRP	19.0	Vinylester	Preloaded+NCE+Field	5~40	2555	29	79.34	NA
51	Trejo et al. (2011)	NA	GFRP	19.0	Vinylester	Control	NA	0	10	100.00	NA
52	Trejo et al. (2011)	NA	GFRP	19.0	Vinylester	Preloaded+NCE+Field	5~40	2555	18	78.50	NA

Notes:
(1) IMMR = Immersion; SL = Sustained load;
(2) NCE = Normal concrete-embedded; SWCE= Seawater concrete-embedded;
(3) f_u is the ultimate tensile strength of FRP bars; M_u is the ultimate moment measured in the beam tests;
(4) Control = Unconditioned specimens without environmental exposure and time aging effect; Reference = Unconditioned specimens without environmental exposure but with time aging effect;
(5) NA = Not applicable.

Table D2 FET database for shear properties of FRP bars

No.	Reference	FRP properties				Environmental condition	Temperature (℃)	Exposure duration (d)	Specimen number (pcs)	Transverse shear strength retention (%)	Specimen number (pcs)	Interlaminar shear strength retention (%)
		Manufacturer	Type	Bar diameter (mm)	Resin type							
1	Al-Khafaji et al. (2021)	NA	GFRP	22.0	NA	Control	NA	0	NA	NA	3	100.0
2	Al-Khafaji et al. (2021)	NA	GFRP	22.0	NA	NCE+Field	NA	5475~7300	NA	NA	3	79.3
3	Al-Khafaji et al. (2021)	NA	GFRP	19.0	NA	Control	NA	0	NA	NA	3	100.0
4	Al-Khafaji et al. (2021)	NA	GFRP	19.0	NA	NCE+Field	NA	5475-7300	NA	NA	3	95.7
5	Al-Khafaji et al. (2021)	NA	GFRP	19.0	Vinylester	Control	NA	0	NA	NA	3	100.0
6	Al-Khafaji et al. (2021)	NA	GFRP	19.0	Vinylester	NCE+Field	NA	5475-7300	NA	NA	3	63.8
7	Al-Khafaji et al. (2021)	NA	GFRP	10.0	Polyester	Control	NA	0	NA	NA	3	100.0
8	Al-Khafaji et al. (2021)	NA	GFRP	10.0	Polyester	NCE+Field	NA	5475-7300	NA	NA	3	100.0
9	Al-Khafaji et al. (2021)	NA	GFRP	16.0	Vinylester	Control	NA	0	NA	NA	3	100.0
10	Al-Khafaji et al. (2021)	NA	GFRP	16.0	Vinylester	NCE+Field	NA	5475-7300	NA	NA	3	111.9
11	Al-Khafaji et al. (2021)	NA	GFRP	16.0	Vinylester	Control	NA	0	NA	NA	3	100.0
12	Al-Khafaji et al. (2021)	NA	GFRP	16.0	Vinylester	NCE+Field	NA	5475-7300	NA	NA	3	100.0
13	Al-Khafaji et al. (2021)	NA	GFRP	19.0	Vinylester	Control	NA	0	NA	NA	3	100.0
14	Al-Khafaji et al. (2021)	NA	GFRP	19.0	Vinylester	NCE+Field	NA	5475-7300	NA	NA	3	78.7
15	Al-Khafaji et al. (2021)	NA	GFRP	13.0	NA	Control	NA	0	NA	NA	3	100.0
16	Al-Khafaji et al. (2021)	NA	GFRP	13.0	NA	NCE+Field	NA	5475-7300	NA	NA	3	93.6
17	Al-Khafaji et al. (2021)	NA	GFRP	19.0	NA	Control	NA	0	NA	NA	3	100.0
18	Al-Khafaji et al. (2021)	NA	GFRP	19.0	NA	NCE+Field	NA	5475-7300	NA	NA	3	100.0
19	Al-Khafaji et al. (2021)	NA	GFRP	6.4	Polyester	Control	NA	0	NA	NA	3	100.0
20	Al-Khafaji et al.	NA	GFRP	6.4	Polyester	NCE+Field	NA	5475-7300	NA	NA	3	94.3

	(2021)											
21	Al-Zahrani (2024)	NA	GFRP	130.	Modified vinylester	Control	NA	0	5	100.0	5	100.0
22	Al-Zahrani (2024)	NA	GFRP	13.0	Modified vinylester	NCE+Field (Tidal)	2.2~49.6	~7300	5	82.5	5	84.4
23	Al-Zahrani (2024)	NA	GFRP	13.2	Vinylester	Control	NA	0	5	100.0	5	100.0
24	Al-Zahrani (2024)	NA	GFRP	13.2	Vinylester	NCE+Field (Tidal)	2.2~49.6	~7300	5	79.4	5	78.1
25	Benmokrane et al. (2018)	Pultrall Inc. (Thetford Mines, QC, Canada)	GFRP	15.9	Vinylester	Control	NA	0	NA	NA	5	100.0
26	Benmokrane et al. (2018)	Pultrall Inc. (Thetford Mines, QC, Canada)	GFRP	15.9	Vinylester	NCE+Field	-30~30	~4015	NA	NA	2	86.4
27	Feng et al. (2023)	Green Material Valley (GMV) New Material Technology Co., Ltd. (Zhenjiang, China)	BFRP	8.0	Epoxy	Control	NA	0	NA	NA	5	100.0
28	Feng et al. (2023)	Green Material Valley (GMV) New Material Technology Co., Ltd. (Zhenjiang, China)	BFRP	8.0	Epoxy	Field (Tidal)	Ave. 9.8	180	NA	NA	5	92.7
29	Feng et al. (2023)	Green Material Valley (GMV) New Material Technology Co., Ltd. (Zhenjiang, China)	BFRP	8.0	Epoxy	Field (Tidal)	Ave. 9.8	180	NA	NA	5	72.5
30	Feng et al. (2023)	Green Material Valley (GMV) New Material Technology Co., Ltd. (Zhenjiang, China)	BFRP	8.0	Epoxy	SWSSCE 1+Field (Tidal)	Ave. 9.8	180	NA	NA	5	97.2
31	Feng et al. (2023)	Green Material Valley (GMV) New Material Technology Co., Ltd. (Zhenjiang, China)	BFRP	8.0	Epoxy	SWSSCE 2+Field (Tidal)	Ave. 9.8	180	NA	NA	5	85.4
32	Gooranorimi and Nanni (2017)	Hughes Brothers Company (Seward, NE, USA)	GFRP	15.9	Vinylester	Control	NA	0	NA	NA	10	100.0
33	Gooranorimi and Nanni (2017)	Hughes Brothers Company (Seward, NE, USA)	GFRP	15.9	Vinylester	NCE+Field	-6~35	~5475	NA	NA	1	104.4
34	Gooranorimi and Nanni (2017)	Hughes Brothers Company (Seward, NE, USA)	GFRP	19.0	Vinylester	Control	NA	0	NA	NA	10	100.0
35	Gooranorimi and Nanni (2017)	Hughes Brothers Company (Seward, NE, USA)	GFRP	19.0	Vinylester	NCE+Field	-6~35	~5475	NA	NA	1	76.1
36	Lu et al.	TuoXin Aerospace Basalt	BFRP	8.0	Epoxy	Control	23	0	5	100.0	NA	NA

	(2020b)	Industrial Co., Ltd. (Sichuan, China)										
37	Lu et al. (2020b)	TuoXin Aerospace Basalt Industrial Co., Ltd. (Sichuan, China)	BFRP	8.0	Epoxy	Field (Seawater IMMR)	0.9~24	180	5	112.4	NA	NA
38	Lu et al. (2020b)	TuoXin Aerospace Basalt Industrial Co., Ltd. (Sichuan, China)	BFRP	8.0	Epoxy	Field (Seawater IMMR)	0.9~24	360	5	71.1	NA	NA
39	Lu et al. (2020b)	TuoXin Aerospace Basalt Industrial Co., Ltd. (Sichuan, China)	BFRP	8.0	Epoxy	NCE+Field (Seawater IMMR)	0.9~24	180	5	98.3	NA	NA
40	Lu et al. (2020b)	TuoXin Aerospace Basalt Industrial Co., Ltd. (Sichuan, China)	BFRP	8.0	Epoxy	NCE+Field (Seawater IMMR)	0.9~24	360	5	64.6	NA	NA
41	Morales et al. (2021)	NA	GFRP	9.5	Vinylester	Control	NA	0	5	100.0	5	100.0
42	Morales et al. (2021)	NA	GFRP	9.5	Vinylester	SWCE 1+Field	Ave. 25	30	4	93.4	4	98.1
43	Morales et al. (2021)	NA	GFRP	9.5	Vinylester	SWCE 1+Field	Ave. 25	180	4	94.9	4	100.8
44	Morales et al. (2021)	NA	GFRP	9.5	Vinylester	SWCE 1+Field	Ave. 25	360	4	98.4	4	97.2
45	Morales et al. (2021)	NA	GFRP	9.5	Vinylester	SWCE 1+Field	Ave. 25	720	4	98.4	4	98.8
46	Morales et al. (2021)	NA	GFRP	9.5	Vinylester	SWCE 2+Field	Ave. 25	30	4	97.0	4	106.4
47	Morales et al. (2021)	NA	GFRP	9.5	Vinylester	SWCE 2+Field	Ave. 25	180	4	99.5	4	103.2
48	Morales et al. (2021)	NA	GFRP	9.5	Vinylester	SWCE 2+Field	Ave. 25	360	4	97.1	4	101.5
49	Morales et al. (2021)	NA	GFRP	9.5	Vinylester	SWCE 2+Field	Ave. 25	720	4	98.4	4	100.8
50	Ramanathan et al. (2021)	NA	GFRP	16.0	Epoxy	Control	NA	0	NA	NA	NA	100.0
51	Ramanathan et al. (2021)	NA	GFRP	16.0	Epoxy	NCE+Field	NA	~6570	NA	NA	NA	70.0
52	Ramanathan et al. (2021)	NA	GFRP	16.0	Epoxy	Control	NA	0	NA	NA	NA	100.0
53	Ramanathan et al. (2021)	NA	GFRP	16.0	Epoxy	NCE+Field	NA	~6570	NA	NA	NA	62.0

Notes:
(1) IMMR = Immersion;
(2) NCE = Normal concrete-embedded; SWCE = Seawater concrete-embedded; SWSSCE = Seawater sea-sand concrete-embedded;
(3) Control = Unconditioned specimens without environmental exposure and time aging effect;
(4) NA = Not applicable.

Table D3 FET database for flexural properties of FRP bars

No.	Reference	FRP properties				Environmental condition	Temperature (°C)	Exposure duration (d)	Specimen number (pcs)	Flexural strength retention (%)	Flexural elastic modulus retention (%)
		Manufacturer	Type	Bar diameter (mm)	Resin type						
1	Lu et al. (2020b)	TuoXin Aerospace Basalt Industrial Co., Ltd. (Sichuan, China)	BFRP	8.0	Epoxy	Control	23	0	5	100.00	100.0
2	Lu et al. (2020b)	TuoXin Aerospace Basalt Industrial Co., Ltd. (Sichuan, China)	BFRP	8.0	Epoxy	Field (Seawater IMMR)	0.9~24	180	5	112.37	116.4
3	Lu et al. (2020b)	TuoXin Aerospace Basalt Industrial Co., Ltd. (Sichuan, China)	BFRP	8.0	Epoxy	Field (Seawater IMMR)	0.9~24	360	5	71.13	49.3
4	Lu et al. (2020b)	TuoXin Aerospace Basalt Industrial Co., Ltd. (Sichuan, China)	BFRP	8.0	Epoxy	NCE+Field (Seawater IMMR)	0.9~24	180	5	98.28	76.4
5	Lu et al. (2020b)	TuoXin Aerospace Basalt Industrial Co., Ltd. (Sichuan, China)	BFRP	8.0	Epoxy	NCE+Field (Seawater IMMR)	0.9~24	360	5	64.60	51.6

Notes:
(1) IMMR = Immersion;
(2) NCE = Normal concrete-embedded;
(3) Control = Unconditioned specimens without environmental exposure and time aging effect;
(4) NA = Not applicable.

Table E1 FET database for bond properties of FRP bars in concrete

No.	Reference	FRP properties					Concrete type	Environmental condition	Temperature (℃)	Exposure duration (d)	Specimen number (pcs)	Bond strength retention (%)
		Manufacturer	Type	Bar diameter (mm)	Resin type	Surface characteristics						
1	Al-Tamimi et al. (2014)	Pultron Composites	GFRP	13.0	Synthetic	R	NC	Reference	23	60	2	100.0
2	Al-Tamimi et al. (2014)	Pultron Composites	GFRP	13.0	Synthetic	R	NC	Reference	23	90	2	100.0
3	Al-Tamimi et al. (2014)	Pultron Composites	GFRP	13.0	Synthetic	R	NC	Direct sun exposure	NA	60	2	95.0
4	Al-Tamimi et al. (2014)	Pultron Composites	GFRP	13.0	Synthetic	R	NC	Direct sun exposure	NA	90	2	104.4

Notes:
(1) NC = Normal concrete;
(2) R = Ribbed;
(3) Reference = Unconditioned specimens without environmental exposure but with time aging effect;
(4) NA = Not applicable.

Table F1 FET database for flexural behavior of FRP-reinforced concrete beams

No.	Reference	FRP properties				Concrete type	Environmental condition	Temperature (℃)	Exposure duration (d)	Specimen number (pcs)	Ultimate load retention (%)
		Manufacturer	Type	Tensile bar diameter (mm)	Resin type						
1	Alkhraisha et al. (2020)	Galen (Russia)	BFRP	8.0	NA	NC	Control	NA	0	1	100.0
2	Alkhraisha et al. (2020)	Galen (Russia)	BFRP	16.0	NA	NC	Control	NA	0	1	100.0
3	Alkhraisha et al. (2020)	Galen (Russia)	BFRP	8.0	NA	NC	Field	15~40	450	1	101.9
4	Alkhraisha et al. (2020)	Galen (Russia)	BFRP	12.0	NA	NC	Field	15~40	450	1	NA
5	Alkhraisha et al. (2020)	Galen (Russia)	BFRP	12.0	NA	NC	Field	15~40	450	1	NA
6	Alkhraisha et al. (2020)	Galen (Russia)	BFRP	16.0	NA	NC	Field	15~40	450	1	107.4
7	Chang et al. (2022)	NA	GFRP	16.0	Vinylester	SWSSC	Control	20	0	2	100.0
8	Chang et al. (2022)	NA	GFRP	16.0	Vinylester	SWSSC	SL (25%/40% Mu)+Field (Seawater IMMR)	20	90	1	99.9
9	Chang et al. (2022)	NA	GFRP	16.0	Vinylester	SWSSC	SL (25%/40% Mu)+Field (Seawater IMMR)	20	90	1	104.8
10	Chang et al. (2022)	NA	GFRP	16.0	Vinylester	SWSSC	SL (25%/40% Mu)+Field (Seawater IMMR)	20	90	1	109.2
11	Chang et al. (2022)	NA	GFRP	16.0	Vinylester	SWSSC	SL (25%/40% Mu)+Field (Seawater IMMR)	20	180	1	88.0
12	Chang et al. (2022)	NA	GFRP	16.0	Vinylester	SWSSC	SL (25%/40% Mu)+Field (Seawater IMMR)	20	180	1	85.5
13	Chang et al. (2022)	NA	GFRP	16.0	Vinylester	SWSSC	SL (25%/40% Mu)+Field (Seawater IMMR)	20	180	1	83.2
14	Chang et al. (2022)	NA	GFRP	16.0	Vinylester	SWSSC	SL (25%/40% Mu)+Field (Seawater IMMR)	20	270	2	77.1
15	Chang et al. (2022)	NA	GFRP	16.0	Vinylester	SWSSC	SL (25%/40% Mu)+Field (Seawater IMMR)	20	270	1	70.4
16	Chang et al. (2022)	NA	GFRP	16.0	Vinylester	SWSSC	SL (25%/40% Mu)+Field (Seawater IMMR)	20	270	2	60.2
17	Chen et al. (2022)	Chengxinda Glass Fiber Factory, China	GFRP	14.0	Epoxy	SWSSC	Reference	15~30	270	1	100.0
18	Chen et al. (2022)	Chengxinda Glass Fiber Factory, China	GFRP	14.0	Epoxy	SWSSC	Field (Atmosphere)	15~30	270	1	128.0
19	Chen et al. (2022)	Chengxinda Glass Fiber Factory, China	GFRP	14.0	Epoxy	SWSSC	Field (Salt spray)	15~30	270	1	87.0
20	Chen et al. (2022)		GFRP	14.0	Epoxy	SWSSC	Field (Tidal)	15~30	90	1	NA
21	Chen et al. (2022)		GFRP	14.0	Epoxy	SWSSC	Field (Tidal)	15~30	180	1	NA
22	Chen et al. (2022)		GFRP	14.0	Epoxy	SSC	Field (Tidal)	15~30	270	1	86.0

23	Chen et al. (2022)		GFRP	14.0	Epoxy	SWC	Field (Tidal)	15~30	270	1	123.4
24	Chen et al. (2022)		GFRP	14.0	Epoxy	SWSSC	Field (Tidal)	15~30	270	1	116.2
25	Esmaeili et al. (2020)	NA	GFRP	12.7	Vinylester	NC	Reference	23	360	3	100.0
26	Esmaeili et al. (2020)	NA	GFRP	12.7	Vinylester	NC	SL (40%fu)+Field	-25~35	~3600	3	80.5
27	Mukherjee and Arwikar (2005)	NA	GFRP	9.5	Vinylester	NC	Control	NA	0	1	100.0
28	Mukherjee and Arwikar (2005)	NA	GFRP	9.5	Vinylester	NC	Control	NA	0	1	100.0
29	Mukherjee and Arwikar (2005)	NA	GFRP	9.5	Vinylester	NC	Control	NA	0	1	100.0
30	Mukherjee and Arwikar (2005)	NA	GFRP	9.5	Vinylester	NC	Control	NA	0	1	100.0
31	Mukherjee and Arwikar (2005)	NA	GFRP	9.5	Vinylester	NC	Field	10~38	540	1	153.8
32	Mukherjee and Arwikar (2005)	NA	GFRP	9.5	Vinylester	NC	Field	10~38	540	1	168.1
33	Mukherjee and Arwikar (2005)	NA	GFRP	9.5	Vinylester	NC	Field	10~38	900	1	150.0
34	Mukherjee and Arwikar (2005)	NA	GFRP	9.5	Vinylester	NC	Field	10~38	900	1	160.0
35	Ren et al. (2024)	NA	GFRP	8.0	NA	NC	Reference	15~20	365	1	100.0
36	Ren et al. (2024)	NA	GFRP	8.0	NA	SWSSC	Reference	15~20	365	1	100.0
37	Ren et al. (2024)	NA	GFRP	8.0	NA	NC	SL (100%Pc)+Field	15~30	365	1	117.7
38	Ren et al. (2024)	NA	GFRP	8.0	NA	NC	SL (200%Pc)+Field	15~30	365	1	120.7
39	Ren et al. (2024)	NA	GFRP	8.0	NA	SWSSC	SL (100%Pc)+Field	15~30	365	1	103.7
40	Ren et al. (2024)	NA	GFRP	8.0	NA	SWSSC	SL (200%Pc)+Field	15~30	365	1	76.7
41	Ren et al. (2021)	NA	BFRP	8.0	NA	NC	Field	15~30	90	1	NA
42	Ren et al. (2021)	NA	BFRP	8.0	NA	NC	Field	15~30	180	1	NA
43	Ren et al. (2021)	NA	BFRP	8.0	NA	NC	Field	15~30	360	1	NA
44	Ren et al. (2021)	NA	BFRP	8.0	NA	SSC	Field	15~30	90	1	NA
45	Ren et al. (2021)	NA	BFRP	8.0	NA	SSC	Field	15~30	180	1	NA
46	Ren et al. (2021)	NA	BFRP	8.0	NA	SSC	Field	15~30	360	1	NA
47	Ren et al. (2021)	NA	BFRP	8.0	NA	SWSSC	Field	15~30	90	1	NA
48	Ren et al. (2021)	NA	BFRP	8.0	NA	SWSSC	Field	15~30	180	1	NA
49	Ren et al. (2021)	NA	BFRP	8.0	NA	SWSSC	Field	15~30	360	1	NA
50	Ren et al. (2021)	NA	GFRP	8.0	NA	NC	Field	15~30	90	1	NA
51	Ren et al. (2021)	NA	GFRP	8.0	NA	NC	Field	15~30	180	1	NA
52	Ren et al. (2021)	NA	GFRP	8.0	NA	NC	Field	15~30	360	1	NA
53	Ren et al. (2021)	NA	GFRP	8.0	NA	SSC	Field	15~30	90	1	NA
54	Ren et al. (2021)	NA	GFRP	8.0	NA	SSC	Field	15~30	180	1	NA
55	Ren et al. (2021)	NA	GFRP	8.0	NA	SSC	Field	15~30	360	1	NA
56	Ren et al. (2021)	NA	GFRP	8.0	NA	SWSSC	Field	15~30	90	1	NA
57	Ren et al. (2021)	NA	GFRP	8.0	NA	SWSSC	Field	15~30	180	1	NA
58	Ren et al. (2021)	NA	GFRP	8.0	NA	SWSSC	Field	15~30	360	1	NA

Notes:
(1) IMMR = Immersion; SL = Sustained load;
(2) NC = Normal concrete; SSC = Sea and concrete; SWC = Seawater concrete; SWSSC = Seawater sea-sand concrete;
(3) f_u is the ultimate tensile strength of FRP bars; M_u is the ultimate moment measured in the beam tests; P_c is the cracking load of the beams;
(4) Control = Unconditioned specimens without environmental exposure and time aging effect; Reference = Unconditioned specimens without environmental exposure but with time aging effect;
(5) NA = Not applicable.